

Cooperative Institute for Mesoscale Meteorological Studies

Annual Report

Prepared for the
National Oceanic and Atmospheric Administration
Office of Oceanic and Atmospheric Research

Cooperative Agreement NA16OAR4320115

Fiscal Year – 2018

Cover image – Example of design process from a group participating in the August 2017 Hazardous Weather Testbed workshop. Similar graphics and design elements were provided by all groups. The workshop culminated in the development of prototypes based on individual groups designs. Feedback and ideas from the participating NWS forecasters will ultimately prioritize Multi-Radar Multi-Sensor (MRMS) design and implementation. For more on this project, “Integration of the Geostationary Lightning Mapper with Ground-based Lightning Detection Systems for National Weather Service Operations,” led by Kristin Calhoun, Darrel Kingfield, and Tiffany Meyer (CIMMS at NSSL), see pages 344-345.

Table of Contents

Introduction	4
General Description of CIMMS and its Core Activities	4
Management of CIMMS, including Mission and Vision Statements, and Organizational Structure	5
Executive Summary Listing of Activities during FY2018	6
Distribution of NOAA Funding by CIMMS Task and Research Theme	12
CIMMS Executive Board and Assembly of Fellows Meeting Dates and Membership	13
General Description of Task I Expenditures	15
Research Performance	16
Theme 1 – Weather Radar Research and Development	16
Theme 2 – Stormscale and Mesoscale Modeling Research and Development	137
Theme 3 – Forecast and Warning Improvements Research and Development	239
Theme 4 – Impacts of Climate Change Related to Extreme Weather Events	374
Theme 5 – Societal and Socioeconomic Impacts of High Impact Weather Systems	380
Public Affairs and Outreach	396
Appendix A – Awards and Honors	402
Appendix B – Publication Summary	404
Appendix C – Personnel Summary – NOAA Funded Research Only	405
Appendix D – Compilation of CIMMS-Related Publications FY 2018	406
Appendix E – NOAA Competitive Award Recipient Reports	413

**COOPERATIVE INSTITUTE FOR MESOSCALE METEOROLOGICAL STUDIES
THE UNIVERSITY OF OKLAHOMA**

**Annual Report of Research Progress Under
Cooperative Agreement NA16OAR4320115
During the 2017 Fiscal Year: July 1, 2017–June 30, 2018**

Greg McFarquhar, Director
Randy Peppler, Associate Director
Tracy Reinke, Executive Director of Finance and Operations
Sebastian Torres, Assistant Director for NOAA Relations

INTRODUCTION

General Description of CIMMS and its Core Activities

The Cooperative Institute for Mesoscale Meteorological Studies (CIMMS) was established in 1978 as a cooperative program between the National Oceanic and Atmospheric Administration (NOAA) and The University of Oklahoma (OU). CIMMS provides a mechanism to link the scientific and technical resources of OU and NOAA to create a center of research excellence in weather radar, stormscale meteorological phenomena, regional climate variations, and related subject areas – all with the goal of helping to produce better forecasts and warnings that save lives and protect property.

CIMMS promotes cooperation and collaboration on problems of mutual interest among university researchers and the NOAA Office of Oceanic and Atmospheric Research (OAR) National Severe Storms Laboratory (NSSL), National Weather Service (NWS) Radar Operations Center (ROC) for the WSR-88D (NEXRAD) Program, NWS NCEP (National Centers for Environmental Prediction) Storm Prediction Center (SPC), NWS Warning Decision Training Division (WDTD), NWS Norman Forecast Office (OUN), NWS Training Center (NWSTC) in Kansas City, Missouri, and NOAA Air Resources Laboratory Atmospheric Turbulence and Diffusion Division (ATDD) in Oak Ridge, Tennessee.

CIMMS research contributes to the NOAA mission through improvement of the observation, analysis, understanding, and prediction of weather elements and systems and climate anomalies ranging in size from cloud nuclei to multi-state areas. Advances in observational and analytical techniques lead to improvements in understanding of the evolution and structure of these phenomena. Understanding provides the foundation for more accurate prediction of hazardous weather and anomalous regional climate. Better prediction contributes to improved social and economic welfare. Because small-, meso-, and regional-scale phenomena are also important causes and manifestations of climate, CIMMS research is contributing to improved understanding of the global climate system and regional climate variability and change. CIMMS promotes research collaboration between scientists at OU and NOAA by providing a center where government and

academic scientists may work together to learn about and apply their knowledge of stormscale weather and regional-scale climate processes.

CIMMS is part of the National Weather Center, a unique confederation of federal, state, and OU organizations that work together in partnership to improve understanding of the Earth's atmosphere. Recognized for its collective expertise in severe weather, many of the research and development activities of the Center have served society by improving weather observing and forecasting, and thus have contributed to reductions in loss of life and property.

In addition to CIMMS, National Weather Center organizations include:

- NOAA OAR National Severe Storms Laboratory (NSSL)
- NOAA NWS Warning Decision Training Division (WDTD)
- NOAA NWS NCEP Storm Prediction Center (SPC)
- NOAA NWS Radar Operations Center (ROC)
- NOAA NWS Norman Forecast Office (OUN)
- Oklahoma Climatological Survey (OCS)
- OU Center for Analysis and Prediction of Storms (CAPS)
- OU Advanced Radar Research Center (ARRC)
- OU College of Atmospheric and Geographic Sciences
- OU School of Meteorology
- OU Department of Geography and Environmental Sustainability

CIMMS concentrates its research and outreach efforts and resources on the following principal themes: (1) weather radar research and development, (2) stormscale and mesoscale modeling research and development, (3) forecast and warning improvements research and development, (4) impacts of climate change related to extreme weather events, and (5) societal and socioeconomic impacts of high impact weather systems.

This report describes NOAA-funded research and outreach progress made by CIMMS scientists at OU and those assigned to our collaborating NOAA units under cooperative agreement NA16OAR4320115 during 1 July 2017 through 30 June 2018. Publications written, awards received, and employee and funding statistics are presented in Appendices.

Management of CIMMS, including Mission and Vision Statements, and Organizational Structure

An Executive Board and Council of Fellows help advise CIMMS.

The CIMMS Executive Board is to meet quarterly to provide advice and recommendations to the Director of CIMMS regarding appointments, procedures, and policies; to review and adopt bylaws; and to periodically review the accomplishments and progress of the technical and scientific programs and projects of the CIMMS.

The Council of Fellows meets as needed and is composed of a cross-section of local and national scientists who have expertise relevant to the research themes of CIMMS and are actively involved in the programs and projects of CIMMS. Appointment as a Fellow, by the CIMMS Executive Board, is normally for a two-year term, and reappointment is possible. Appointments may be made for a shorter period of time or on a part-time basis with the concurrence of the appointee and the CIMMS Executive Board. Fellows will review and suggest modifications of bylaws, participate in reviews of CIMMS activities, and elect two of their number to serve on the Executive Board. The Executive Board appoints Fellows.

The Mission and Vision Statements of CIMMS are as follows:

Mission – *To promote collaborative research among University and NOAA scientists on problems of mutual interest to improve basic understanding and to help produce better forecasts and warnings that save lives and property*

Vision – *A center of research excellence in mesoscale meteorology and related topics, fostering vibrant University-NOAA collaborations*

The organizational structure of CIMMS in FY18 included: Director (Greg McFarquhar), Associate Director (Randy Peppler), Executive Director of Finance and Operations Director (Tracy Reinke), Assistant Director for NOAA Relations (Sebastian Torres), Account and Budget Representative (Jamie Foucher), and Staff Assistants (Tanya Riley and Missy Coulson). Scientists, students, and post-docs are housed on the OU campus in its National Weather Center (NWC), at the NWSTC in Kansas City, and at ATDD in Oak Ridge. Some CIMMS undergraduate students have duty stations off-campus at ROC in Norman.

Executive Summary Listing of Activities during FY2018

Theme 1 – Weather Radar Research and Development

At the very center of NOAA's mission are the objectives of achieving a "reduced loss of life, property, and disruption from high-impact weather events", "improved transportation efficiency and safety", and "improved freshwater resource management" (NOAA's *Next Generation Strategic Plan*, Long-Term Goal: Weather Ready Nation, pp. 10-14, December 2010). The weather systems involved include severe thunderstorms, tornadoes, tropical storms and hurricanes, and winter cyclones. Those systems produce the high intensity precipitation, strong winds, flooding, lightning strikes, freezing rain, and large snow accumulations that damage property, cost lives, disrupt transportation, and cause other economic dislocation. Reduction of these adverse impacts can result from the availability and use of accurate forecasts of the above weather systems and their associated phenomena, for future periods ranging from several days down to a few minutes. One of the essential starting points for developing those forecasts is the detailed observation of the present state of the atmosphere.

For almost 60 years, remote sensing via weather radar has been a vital source of the necessary observations. The present national weather radar system (WSR-88D) uses reflectivity and Doppler velocity measurements to document the location and movement of the above weather systems, and indicate the time evolution of their precipitation intensity and wind strength. However, this radar system soon will be as old (30 years) as the chronologically and technologically ancient system (WSR-57) that it replaced in 1988. This situation has two crucial implications for NOAA's continued pursuit of its above objectives to achieve a "reduced loss of life, property, and disruption from high impact weather events", "improved transportation efficiency and safety", and "improved freshwater management". First, NOAA and its partners must complete the recently initiated development of the new Multi-Function Phased Array Radar (MPAR) system that will replace the WSR-88D and is incorporating all relevant technological advances during the last 20+ years. Second, since completion of this development activity will require another 7-12 years at its current rate of progression, the ongoing current WSR-88D upgrades (especially Dual-Polarization) must be brought to fruition as soon as possible.

During the past year, research was conducted on:

- ***NSSL Project 1 – Advancements in Weather Radar***
 - WSR-88D Improvements
 - Dual-Polarization
 - MPAR Meteorology
 - MPAR Engineering
- ***NSSL Project 2 – Hydrometeorology Research***
- ***CIMMS Task III Projects***
 - ARRC Demonstrator Development Activities for the MPAR Program: CPPAR and Horus
 - Spectrum Efficient National Surveillance Radar (SENSR) – Development of the All-Digital Horus Demonstrator
 - Spectrum Efficient National Surveillance Radar (SENSR) – ARRC Risk Reduction Activities
 - Polarimetric Phased Array Radar Research in Support for MPAR Strategy – Continued

Theme 2 – Stormscale and Mesoscale Modeling Research and Development

Research and development for stormscale and mesoscale modeling are essential for NOAA's aforementioned objectives. Use of stormscale and mesoscale models is a major ingredient of the forecasting and nowcasting procedures for high impact weather events, and is expected to grow in the future. The initialization of those prediction models is depending increasingly on wind and other observations from the current weather radar systems. This dependence also is anticipated to expand and therefore is

a principal motivation for the weather radar research and development proposed above -- to improve the initialization and hence performance of the prediction models. At the center of this radar-modeling interface is the manner in which radar data are ingested into the models, especially in combination with measurements from other platforms (e.g., satellite, rawinsonde, surface) via “assimilation” procedures. In addition to their predictive roles, stormscale and mesoscale models also are used extensively in a research mode to understand better the behavior of weather systems on those scales. The atmospheric processes that receive particular attention in these simulations include mesoscale dynamics, convective initiation, cloud dynamics and microphysics, and the precipitation process. Also investigated is the sensitivity of the simulation results to the data assimilation procedures. The ultimate goal of such stormscale and mesoscale simulation research is to improve the performance of the operational forecasting models.

During the past year, research was conducted on:

- ***NSSL Project 3 – Numerical Modeling and Data Assimilation***
- ***NSSL Project 4 – Hydrologic Modeling Research***
- ***NSSL Project 7 – Synoptic, Mesoscale and Stormscale Processes Associated with Hazardous Weather***
- ***CIMMS Task III Projects***
 - Probabilistic Precipitation Rate Estimates from GOES-R for Hydrologic Applications
 - Post-Processing of Solid-State Polarimetric Weather Radar Data for Hydrology
 - Using Total Lightning Data from GLM/GOES-R to Improve Real-Time Tropical Cyclone Genesis and Intensity Forecasts
 - Lightning Mapper Array Operation in Oklahoma and South Texas to Aid Verification and Application Research for the GOES-R and GOES-S GLMs
 - Ensemble Kalman Filter and Hybrid Data Assimilation for Convective-Scale “Warn-on Forecast”
 - MPAR Targeting Observation Research for WoF
 - GSI-based Dual Resolution EnVar Data Assimilation for Convective-Scale “Warn-on Forecast”
 - Assimilation of High Resolution GOES-R ABI Infrared Water Vapor and Cloud Sensitive Radiances Using the GSI-based Hybrid Ensemble-Variational Data Assimilation System to Improve Convection Initiation Forecast

Theme 3 – Forecast and Warning Improvements Research and Development

It is under this theme that the results of the research and development from the two preceding themes are integrated and converted into improved weather forecasts and warnings disseminated to the U.S. public. The ultimate outcome is to provide NWS forecasters routinely with enhanced information on which to base their forecasts. Two areas of highly innovative activity, anchored within the Hazardous Weather Testbed (HWT), dominate this effort – the Experimental Forecasting Program and the Experimental Warning Program. Activity within this theme also is dominated by the training activities of CIMMS scientists at the Warning Decision Training Branch.

During the past year, research and training were conducted on:

- ***NSSL Project 5 – Hazardous Weather Testbed***
- ***NSSL Project 6 – Development of Technologies and Techniques in Support of Warnings***
- ***ROC Project 10 – Analysis of Dual Polarized Weather Radar Observations of Severe Convective Storms to Understand Severe Storm Processes and Improve Warning Decision Support***
- ***SPC Project 11 – Advancing Science to Improve Knowledge of Mesoscale Hazardous Weather***
- ***WDTD Project 12 – Warning Decision-Making Research and Training***
- ***OST Project 13 and 15 – Research on Integration and Use of Multi-Sensor Information for Severe Weather Warning Operations***
- ***NWSTC Project 14 – Forecast Systems Optimization and Decision Support Services Research Simulation and Training***
- ***ARL Project 15 – Weather and Climate Change Monitoring and Research Support of the Atmospheric Turbulence and Diffusion Division of NOAA's Air Resources Laboratory***
- ***CIMMS Task III Projects***
 - Utilizing Sub-Flash Properties of GLM to Monitor Convective Intensity with Probabilistic Guidance
 - Integration of the Geostationary Lightning Mapper with Ground-based Lightning Detection Systems for National Weather Service Operations
 - Development of an Archival System for the Integration of High Resolution GOES-R, Radar and Lightning Data for Improving Severe Weather Forecasting and Warning Capabilities
 - National Sea Grant Weather & Climate Extension Specialist Activities

- Enhancement and Evaluation of NGGPS Model FV3 at Convection-Allowing Resolutions through Hazardous Weather Testbed Spring Experiment towards Accelerated Operational Implementation of FV3 for Mesoscale Applications
- Assimilation of High-Frequency GOES-R Geostationary Lightning Mapper (GLM) Flash Extent Density Data in GSI-Based EnKF and Hybrid for Improving Convective Scale Weather Predictions
- Advanced Data Assimilation and Prediction Research for Convective-Scale “Warn-on-Forecast”
- Impact of Assimilating Polarimetric Phased Array Radar Observations on Convective-scale Numerical Weather Prediction Model for Severe Weather Forecasts
- Mobile Radar Operations to Support VORTEX-SE
- VORTEX-SE Operations Risk Reduction Exercise (ORRE 2018) for Non-Classic Tornadoic Storms and Environmental Heterogeneity
- Three-Dimensional Profiling of the Severe Weather Environment

Theme 4 – Impacts of Climate Change Related to Extreme Weather Events

Here, we are concerned with the regional and global climate system context of mesoscale and stormscale weather variability, and especially the functioning of what now is termed the weather-climate interface. The genesis and trends of extreme events are of particular interest, given society’s current concerns about climate maintenance and change. The optimum path forward will require an appropriate combination of observational (using fine resolution data) and modeling (emphasizing convection) research. This theme also addresses the NOAA objective of achieving “improved scientific understanding of the changing climate system and its impacts” and “assessments of current and future states of the climate system that identify potential impacts and inform science, services, and stewardship decisions” (*NOAA’s Next Generation Strategic Plan*, Long-Term Goal: Climate Adaptation and Mitigation, pp. 5-10, December 2010).

During the past year, research and outreach were conducted on:

- **CIMMS Task III Project**
 - The Assimilation, Analysis, and Dissemination of Pacific Rain Gauge Data (PACRAIN)

Theme 5 – Societal and Socioeconomic Impacts of High Impact Weather Systems

This theme contributes to several of NOAA’s objectives - - providing “mitigation and adaptation choices supported by sustained, reliable, and timely climate services”; achieving “a climate-literate public that understands its vulnerabilities to a changing climate and makes informed decisions”; and furnishing “services meeting the evolving demands of regional stakeholders” (*NOAA’s Next-Generation Strategic Plan*, Long-Term Goal: Climate Adaptation and Mitigation, pp. 5-10, December 2010). Much of the

effort here is motivated and fed by results obtained under the Forecast and Warning Improvements and Extreme Weather-Climate Change Impacts themes that, in turn, are built around the core of the more basic Weather Radar and Stormscale/Mesoscale Modeling Research and Development. The goal here is to facilitate the mitigation (enhancement) of the adverse (beneficial) social and socioeconomic impacts of high-impact weather systems and regional/seasonal-scale climate variations. Thus, our contributions to this theme are part of NOAA's crucial ultimate interface with society, and therefore will reflect the continuing and increasing involvement of social scientists.

During the past year, research and outreach were conducted on:

- ***NSSL Project 8 – Warning Process Evolution and Effective Communication to the Public***
- ***NSSL Project 9 – Evaluating the Impact of New Technologies, Data, and Information in the Operational Forecasting Environment***
- ***CIMMS Task III Projects***
 - Development of a Digital Collaboration Environment for The Alliance for Integrative Approaches to Extreme Environmental Events, Phase I: Scoping and Functional Requirements Development
 - Coping with Drought: Building Resilience to Drought
 - Baseline of Public Responsiveness to Uncertainty in Forecasts

Public Affairs and Outreach

CIMMS education and outreach activities help NOAA achieve its objectives of providing “an engaged and educated public with an improved capacity to make scientifically informed environmental decisions” and making “full and effective use of international partnerships and policy leadership to achieve NOAA’s mission objectives” (NOAA’s *Next Generation Strategic Plan*, Engagement Enterprise Objective, pp. 30-32, December 2010). CIMMS location and role within the OU-NOAA National Weather Center (NWC) has embedded it within a wide-ranging and ongoing set of education and outreach activities that will draw continuously on the knowledge developed within the five above research themes. Those activities (a) involve local and national outreach to the general public, (b) extend across all levels of formal education, and (c) provide post-doctoral and professional development opportunities for individuals in careers related to the atmospheric sciences.

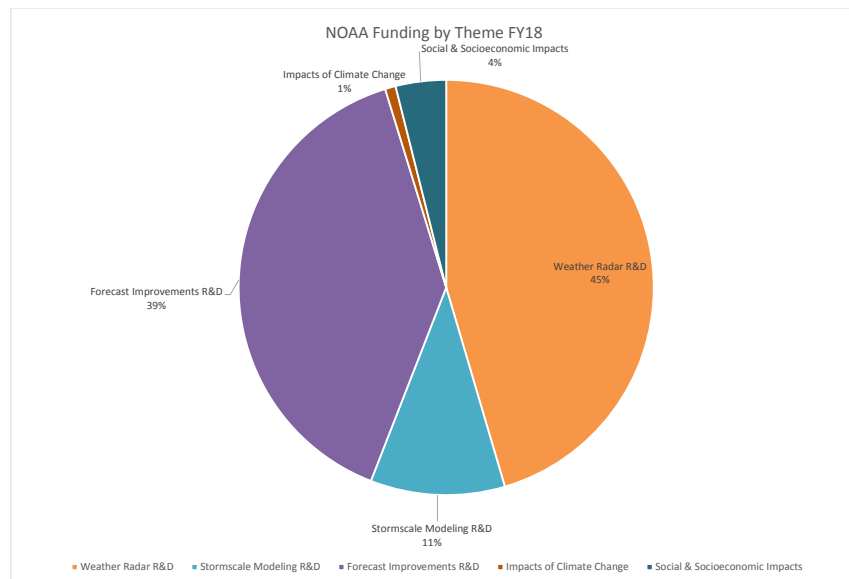
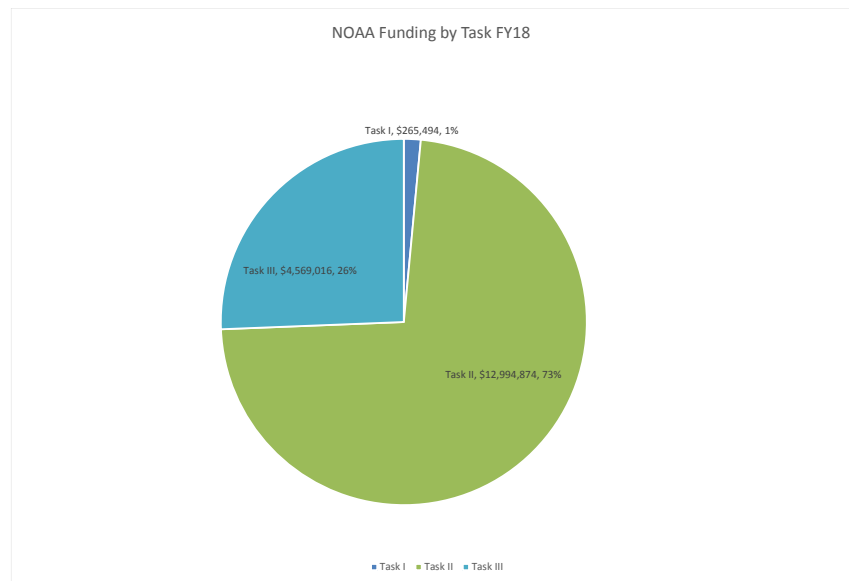
During the past year, public affairs and outreach activities included:

- NOAA Partners and CIMMS Communications, Public Affairs, and Outreach
- CIMMS Staff Outreach at WDTD

Awards and Honors

- See Appendix A.

Distribution of NOAA Funding by CIMMS Task and Research Theme



CIMMS Executive Board and Council of Fellows Meeting Dates and Membership

An Executive Board meeting was held on May 1, 2018. Membership was:

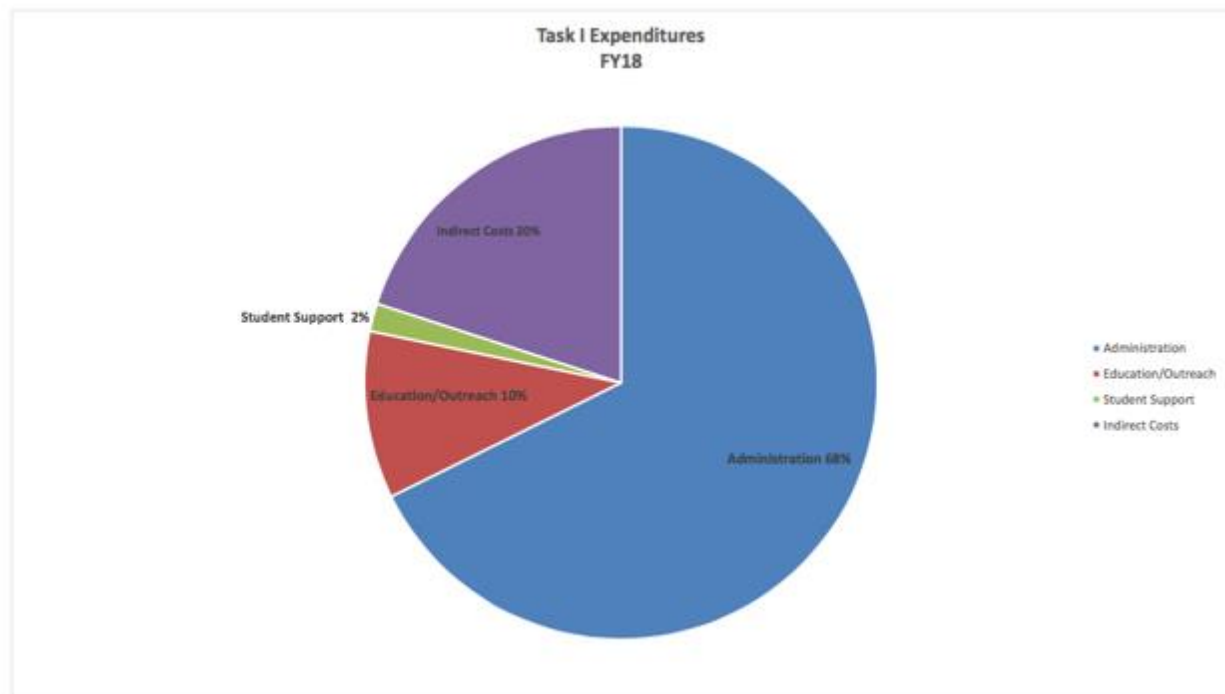
- Dr. Greg McFarquhar (Chair), Director, CIMMS, and Professor, School of Meteorology, OU
- Dr. Robert Palmer, Associate Vice President for Research, Executive Director, ARRC, and Professor and Tommy C. Craighead Chair, School of Meteorology, OU (Provost designated)
- Dr. Carol Silva, Director, CRCM, and Associate Professor of Political Science, OU (Provost designated)
- Dr. Kirsten de Beurs, Chair and Associate Professor, Department of Geography and Environmental Sustainability, OU (Provost designated)
- Mr. Lans Rothfusz, Deputy Director, NSSL (OAR designated)
- Vacant (OAR designated)
- Mr. Richard Murnan, Radar Operations Center Applications Branch (NWS designated)
- Vacant (NWS designated)
- Dr. Boon Leng Cheong, Research Scientist, ARRC (Elected from Council of Fellows)
- Dr. Ming Xue, Director, CAPS, and Professor and Weathernews Chair, School of Meteorology, OU (Elected from Council of Fellows)
- Mr. David Andra, Meteorologist-in-Charge, Norman NWS WFO (*ex-officio* member)
- Dr. Steven Koch, Director, NSSL (*ex-officio* member)
- Mr. Ed Mahoney, Director, WDTD (*ex-officio* member)
- Dr. Russell Schneider, Director, SPC (*ex-officio* member)
- Mr. Terry Clark, Director, ROC (*ex-officio* member)
- Mr. John Ogren, Director, NWSTC, and Chief Learning Officer, NWS (*ex-officio* member)
- Dr. David Parsons, Chair, OU School of Meteorology, Associate Director, CAPS, and Mark and Kandi McCasland Professor of Meteorology (*ex-officio* member)
- Dr. Berrien Moore, Dean, OU College of Atmospheric and Geographic Sciences, OU Vice President, Weather & Climate Programs, School of Meteorology Chesapeake Energy Corporation Chair in Climate Studies, and Director, National Weather Center (*ex-officio* member)

No Council of Fellows meetings took place during the fiscal year. Membership was:

- Dr. Jeffrey B. Basara, Associate Professor of Meteorology, OU
- Dr. Michael I. Biggerstaff, Professor of Meteorology, OU
- Dr. Howard B. Bluestein, George Lynn Cross Research Professor of Meteorology, OU
- Dr. Keith Brewster, Senior Scientist and Associate Director, CAPS, OU
- Dr. Harold E. Brooks, Research Meteorologist and Team Leader, Mesoscale Applications Group, NSSL, and Adjunct Professor of Meteorology, OU
- Dr. Frederick H. Carr, Professor of Meteorology OU
- Dr. Steven Cavallo, Assistant Professor of Meteorology, OU
- Dr. Boon Leng Cheong, Research Scientist, ARRC, OU
- Dr. Phillip Chilson, Professor of Meteorology, OU
- Dr. Adam J. Clark, Research Meteorologist, NSSL
- Mr. Terrence Clark, Director, ROC
- Dr. Michael Coniglio, Research Scientist, NSSL
- Dr. Kirsten de Beurs, Chair and Associate Professor of Geography and Environmental Sustainability, OU
- Dr. Richard J. Doviak, Senior Engineer, Doppler Radar and Remote Sensing Research Group, NSSL, and Affiliate Professor of Meteorology and of Electrical and Computer Engineering, OU
- Dr. Kelvin K. Droegemeier, Vice President for Research and Regents' Professor, OU
- Dr. Claude E. Duchon, Emeritus Professor of Meteorology, OU
- Dr. Chris Fiebrich, Associate Director, OCS
- Dr. Jack Friedman, Research Scientist, CASR, OU
- Dr. Caleb Fulton, Assistant Professor of Electrical and Computer Engineering, OU
- Dr. Jidong Gao, Research Scientist, NSSL
- Dr. Nathan Goodman, Associate Professor of Electrical and Computer Engineering, and Director of Research, ARRC, OU
- Dr. J.J. Gourley, Research Scientist, NSSL
- Dr. Pamela Heinzelman, Chief, Forecasting Research & Development Division, NSSL

- Mr. Kurt Hondl, Research Meteorologist, NSSL
- Dr. Yang Hong, Associate Professor of Civil Engineering and Environmental Sciences, OU
- Mr. Ken Howard, Research Meteorologist, NSSL
- Mr. Michael Jain, Acting Chief, Radar Research & Development Division, NSSL
- Dr. Hank Jenkins-Smith, Associate Director, CASR, and Professor of Political Science, OU
- Dr. Israel Jirak, Science and Operations Officer, SPC
- Dr. Petra Klein, E. K. Gaylord Presidential Professor and Associate Professor of Meteorology, OU
- Dr. James F. Kimpel, Director, Emeritus NSSL, and Emeritus Professor of Meteorology, OU
- Dr. Kevin Kloesel, Director, OCS, and Associate Professor of Meteorology, OU
- Dr. Steven Koch, Director, NSSL
- Dr. Fanyou Kong, Research Scientist, CAPS, OU
- Dr. Daphne LaDue, Research Scientist, CAPS, OU
- Dr. S. Lakshmivaran, George Lynn Cross Research Professor of Computer Science, OU
- Dr. Donald R. MacGorman, Research Physicist, Convective Weather Research Group, NSSL, and Affiliate Professor of Meteorology and of Physics and Astronomy, OU
- Mr. Ed Mahoney, Chief, WDTD
- Dr. Edward Mansell, Research Scientist, NSSL
- Dr. Patrick Marsh, Techniques Development Meteorologist, SPC
- Dr. Elinor Martin, Assistant Professor of Meteorology, OU
- Dr. Amy McGovern, Associate Professor of Computer Science, OU
- Dr. Renee McPherson, Director of Research, South Central Climate Adaptation Science Center, and Associate Professor of Geography and Environmental Sustainability, OU
- Dr. Berrien Moore III, Vice President for Weather and Climate Programs, Dean, College of Atmospheric and Geographic Sciences, Director, National Weather Center, and Chesapeake Professor of Meteorology, OU
- Mr. Richard Murnan, Radar Meteorologist, ROC
- Mr. John Ogren, Chief Learning Officer, NWS
- Dr. Robert D. Palmer, Associate Vice President for Research, Executive Director, ARRC, and Tommy Craighead Chair and Professor of Meteorology, and OU
- Dr. David Parsons, Director, School of Meteorology, Mark and Kandi McCasland Professor of Meteorology, OU
- Dr. Robert Rabin, Research Scientist, NSSL
- Dr. Michael B. Richman, E. K. Gaylord Presidential Professor of Meteorology, OU
- Mr. Lans Rothfusz, Deputy Director, NSSL
- Dr. Jessica Ruyle, Assistant Professor of Electrical and Computer Engineering, OU
- Dr. Jorge Salazar-Cerreno, Assistant Professor of Electrical and Computer Engineering, OU
- Dr. Russell Schneider, Director, SPC
- Dr. Mark Shafer, Director of Climate Services, OCS, and Assistant Professor of Geography and Environmental Sustainability, OU
- Dr. Alan M. Shapiro, American Airlines Professor and President's Associates Presidential Professor of Meteorology, OU
- Dr. Hjalti Sigmarsson, Assistant Professor of Electrical and Computer Engineering, OU
- Dr. Carol Silva, Director, CRCM, and Professor of Political Science, OU
- Dr. Paul Spicer, Professor of Anthropology, OU
- Dr. David Turner, Research Scientist, Global Systems Division, ESRL
- Dr. Xuguang Wang, Associate Professor of Meteorology, and Presidential Research Professor, OU
- Dr. Louis J. Wicker, Research Meteorologist, Convective Weather Research Group, NSSL, and Affiliate Associate Professor of Meteorology, OU
- Dr. Qin Xu, Research Meteorologist, Models and Assimilation Team, NSSL, and Affiliate Professor of Meteorology, OU
- Dr. Ming Xue, Director, CAPS, and Professor of Meteorology, OU
- Dr. Mark Yeary, Professor of Electrical and Computer Engineering, OU
- Dr. Tian-You Yu, Director of Operations, ARRC, and Professor of Electrical and Computer Engineering, OU
- Dr. Guifu Zhang, Professor of Meteorology, OU
- Dr. Jian Zhang, Research Hydrometeorologist, NSSL
- Dr. Yan Zhang, Associate Professor of Electrical and Computer Engineering, OU
- Dr. Conrad Ziegler, Research Meteorologist, Models and Assimilation Team, NSSL
- Dr. Dusan S. Zrnica, Senior Engineer and Group Leader, Doppler Radar and Remote Sensing Research Group, NSSL, and Affiliate Professor of Meteorology and of Electrical and Computer Engineering, OU

General Description of Task I Expenditures



RESEARCH PERFORMANCE

Theme 1 – Weather Radar Research and Development

NSSL Project 1 – Advancements in Weather Radar

NOAA Technical Leads: Michael Jain and Dusan Zrnic (NSSL)

NOAA Strategic Goal 2 – *Weather-Ready Nation – Society is Prepared for and Responds to Weather-Related Events*

Funding Type: CIMMS Task II

1. WSR-88D Improvements

Overall Objectives

Conduct research and development to provide improvements to the NWS operational radar (WSR-88D), exploring ways to improve the detection of hazardous weather and the quality of weather radar data.

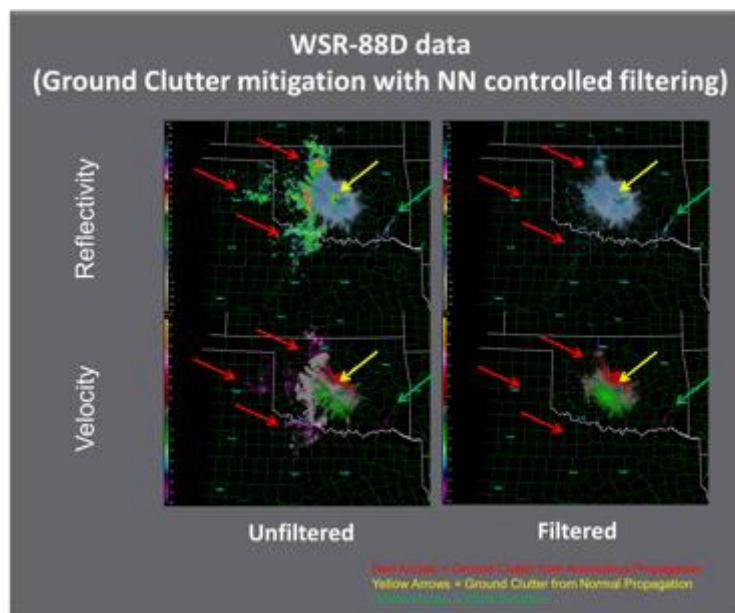
Accomplishments

a. Ground Clutter Mitigation - CLEAN-AP™/WET

David Warde and Sebastián Torres (CIMMS at NSSL)

A common dilemma in obtaining good-quality meteorological-variable estimates using Doppler weather radar is the application (or misapplication) of ground clutter filters (GCF) to mitigate contamination from ground returns. The problem of applying the GCF becomes very complex considering the dynamic atmospheric effects on radar beam propagation. Automation of clutter maps (i.e., automated identification of clutter contaminated regions) to control the application of the GCF allows for adapting to the weather/clutter environment while still mitigating the ground clutter contamination that obscures weather estimates. The goal of this project is to develop efficient techniques that provide both automated detection and application of ground clutter filtering. The Weather Environment Thresholding (WET) and the Clutter Environment Analysis using Adaptive Processing (CLEAN-AP™) filter are two techniques for automatic detection and mitigation of ground clutter contamination developed by CIMMS personnel. We had previously shown the clutter detection and mitigation performance of the CLEAN-AP™ filter using time-series data from the national network of weather surveillance radars (WSR-88D), the dual-polarized (DP) KOUN and OU Prime radars, and the NWRT PAR. The WET algorithm is used to enhance the automated ground clutter mitigation capability of CLEAN-AP™ by removing uncontaminated weather regions from filter consideration, especially when weather signals are near zero velocity. Both techniques were transferred to the ROC for implementation and testing on the WSR-88D system.

During FY18, we compared level II output using WET/CLEAN-AP with level II output supplied by the ROC using CMD/GMAP, the current WSR-88D ground clutter mitigation scheme. Our analysis showed clutter mitigation was comparable for clear weather regions with some minor differences where WET/CLEAN-AP outperformed CMD/GMAP in weather regions. Although WET/CLEAN-AP performed well, there were small regions of false detection by WET in the weather region. At the ROC's suggestion, we are modifying the WET algorithm to allow integration at an earlier stage of the WSR-88D DSP. Consequently, we simplified the logical architecture of WET and are evaluating the use of circular statistics to improve its performance. To exemplify the use of circular statistics, we developed a simple neural network that utilized circular statistics to classify individual range bins as clutter, weather, or noise. The identified clutter bins were used to create a clutter map that was then applied to the data to activate clutter filtering using CLEAN-AP on several WSR-88D data sets. The results show that the circular statistics provide valuable information for clutter/weather identification. Figure 1 shows unfiltered/filtered reflectivity and velocity fields from the NSSL WSR-88D testbed (KOUN) where a strong inversion to the west of the radar caused a large area of ground clutter contamination (red arrows). The unfiltered images (left two panels) show the extent of the ground clutter contamination where high reflectivity (top panel) and near zero velocity (bottom panel) obscured the clear air echoes. The filtered images (right two panels) show that the ground clutter was properly identified by the neural network and the ground clutter was removed by the filter. Also, clutter contamination due to normal-propagation and weak weather signals (green arrows) were properly handled.



Unfiltered (left panels) and filtered (right panels) of reflectivity (top panels) and velocity (bottom panels) PPI from NSSL WSR-88D testbed (KOUN). The filtered PPI fields were processed using a newly developed neural network to identify clutter contamination and CLEAN-AP™ to mitigate the ground clutter contamination. Ground clutter is shown to be properly mitigated in both anomalous propagation (red arrows) and normal propagation (yellow arrows) regions while weak weather signals (green arrows) were properly identified and not filtered.

b. Range and Velocity Ambiguity Mitigation: Staggered PRT

David Warde and Sebastián Torres (CIMMS at NSSL)

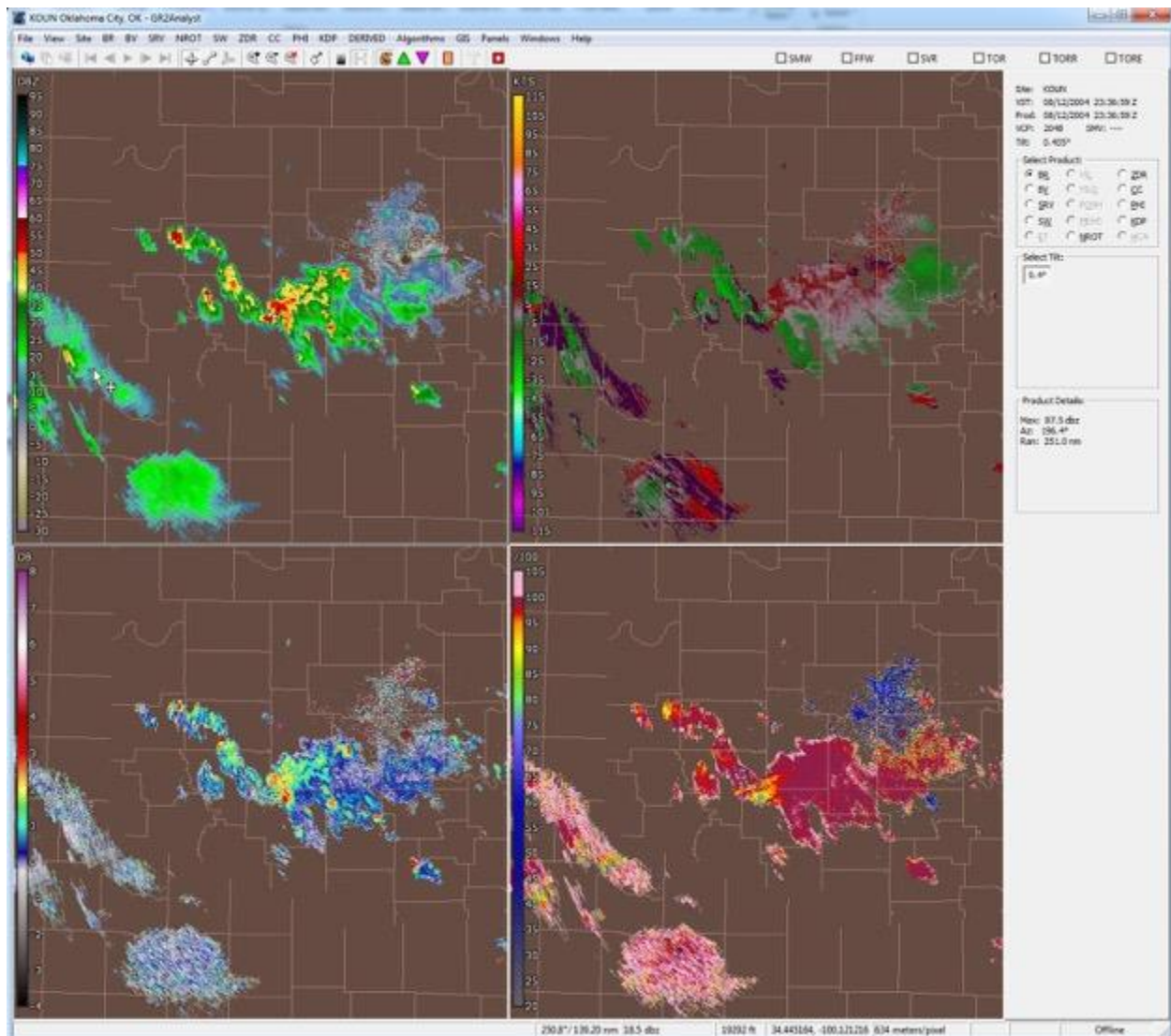
In pulsed Doppler weather radars, the range and Doppler velocity ambiguity problems are coupled so that trying to alleviate one of them worsens the other. Special techniques are necessary to resolve both range and velocity ambiguities to the levels required for the efficient observation of severe weather. Efforts in this area are expected to culminate in significantly improved WSR-88D data quality when implemented on the Radar Data Acquisition sub-system. The increased data quality will result in an improved ability for the WSR-88D to detect severe weather, flash floods, winter storms, and provide aviation forecasts. Over the last decade, two techniques have emerged as viable candidates to address the mitigation of range and velocity ambiguities in the WSR-88D, thus reducing the amount of purple haze obscuration currently encountered during the observation of severe phenomena. These are: systematic phase coding (SZ-2) and staggered pulse repetition time (SPRT). The two techniques are complementary since they offer advantages at specific elevation angles; hence, they can be simultaneously incorporated into the same volume coverage pattern. The first stage of upgrades that implemented SZ-2 is now complete and has been operational with great success for a number of years. The second stage of NEXRAD upgrades dealing with range and velocity ambiguities involves the operational implementation of SPRT. For ground clutter filtering SPRT data, we developed a novel spectral processing SPRT algorithm that incorporates the mature CLEAN-AP filter, range-overlaid recovery, dual polarization and dual polarization with generalized PRT ratios.

We transferred the Staggered PRT algorithm with upgrades to include improved spectrum width computations and are currently supporting the implementation, integration, validation, and testing of the SPRT processing mode for the WSR-88D network of radars. Analysis of level II output observed in the SPRT processing mode from KOUN indicated better performance over batch mode processing in many aspects such as increased coverage for all fields (both due to no overlaid echoes and increased detectability at range), dual polarization and reflectivity fields with better quality, and, of course, larger maximum unambiguous velocity. Test results showed that clutter mitigation using CLEAN-APTM in SPRT is performing well, providing about 50 dB of clutter suppression. An area of concern is the unexpected increase in velocity dealiasing errors possibly related to the coherency issues with the WSR-88D system reported in the FY17 CIMMS report. It is worth noting that the dealiasing errors appear to be correctable in the post-processed (level III) products using our suggested changes to the 2D-velocity-dealiasing algorithm. Still, the ROC would like us to continue to pursue the mitigation of dealiasing errors using other signal processing techniques. Accordingly, we are currently investigating reducing the variance of the velocity difference transfer function which may allow a signal processing solution to improve the velocity field.

c. Range-and-Velocity Ambiguity Mitigation: SZ-2

Sebastian Torres and David Warde (CIMMS at NSSL)

The SZ-2 algorithm was developed in the late 1990s and was transferred to the WSR-88D over a decade ago. Over time, it has gained popularity among NWS forecasters, especially in widespread weather situations where accurate Doppler velocity measurements are needed. Since then, the WSR-88D signal processor has undergone a series of functional upgrades, some of which required extensive modifications to the original SZ-2 algorithm. For example, the dual-polarization upgrade of the network led to significant changes to the signal processor and required extension of the original single-polarization SZ-2 algorithm to support dual-polarization operations. Other signal processing techniques aimed at improving data quality such as Coherency-Based Thresholding (CBT) and the hybrid spectrum-width estimator also required modifications to the SZ-2 algorithm. Throughout the years, these algorithmic modifications were documented in a differential manner (these were referred to as “delta” documents) to the point that the full algorithm description could only be grasped by looking at three different documents. Because of this, the development of new techniques for improving data quality (e.g., CLEAN-AP and Weather Environment Thresholding - WET), and a need to re-validate the operational implementation of SZ-2 (after undergoing a series of updates), we developed a fresh implementation and delivered the corresponding algorithm description to the Radar Operations Center (ROC) in 2017. This document contains the dual-polarization SZ-2 algorithm with modifications required to integrate the Hybrid Spectrum Width, WET, and CLEAN-AP algorithms. In 2018, a revised algorithm description was developed and delivered to the ROC. This version is functionally equivalent to the algorithm delivered in 2017, but it uses the GMAP ground clutter filter instead of CLEAN-AP and WET. This latest document will be useful to ROC engineers as they test their implementation of the improved SZ-2 algorithm with the existing clutter-mitigation solution (CMD and GMAP) without having to integrate it with CLEAN-AP and WET. Finally, in preparation for future signal processing upgrades, we developed and tested a proof-of-concept implementation of the SZ-2 algorithm that works with the dual-polarization Hybrid-Scan Estimators (HSE) and with range-oversampling processing. An example of data processed with the updated dual-polarimetric SZ-2 algorithm is shown in the figure below.



Reflectivity (top left), Doppler velocity (top right), differential reflectivity (bottom left), and correlation coefficient (bottom right) corresponding to phase-coded, range-oversampled data collected with the KOUN radar on 8 Aug 2004.

d. Improved Radar Data Quality Control - Range-Doppler Spectral Analysis

David Warde (CIMMS at NSSL)

Quality-control techniques come into play when radar data fails to meet expected performance metrics (e.g., large variance of estimates or excessive clutter contamination). As such, they are designed to preserve good-quality data and remove (censor) bad- or dubious-quality data. Currently, the system relies on thresholds conceived during the single-polarization era (e.g., the polarimetric variables on split cuts are censored based on the SNR using the reflectivity SNR threshold).

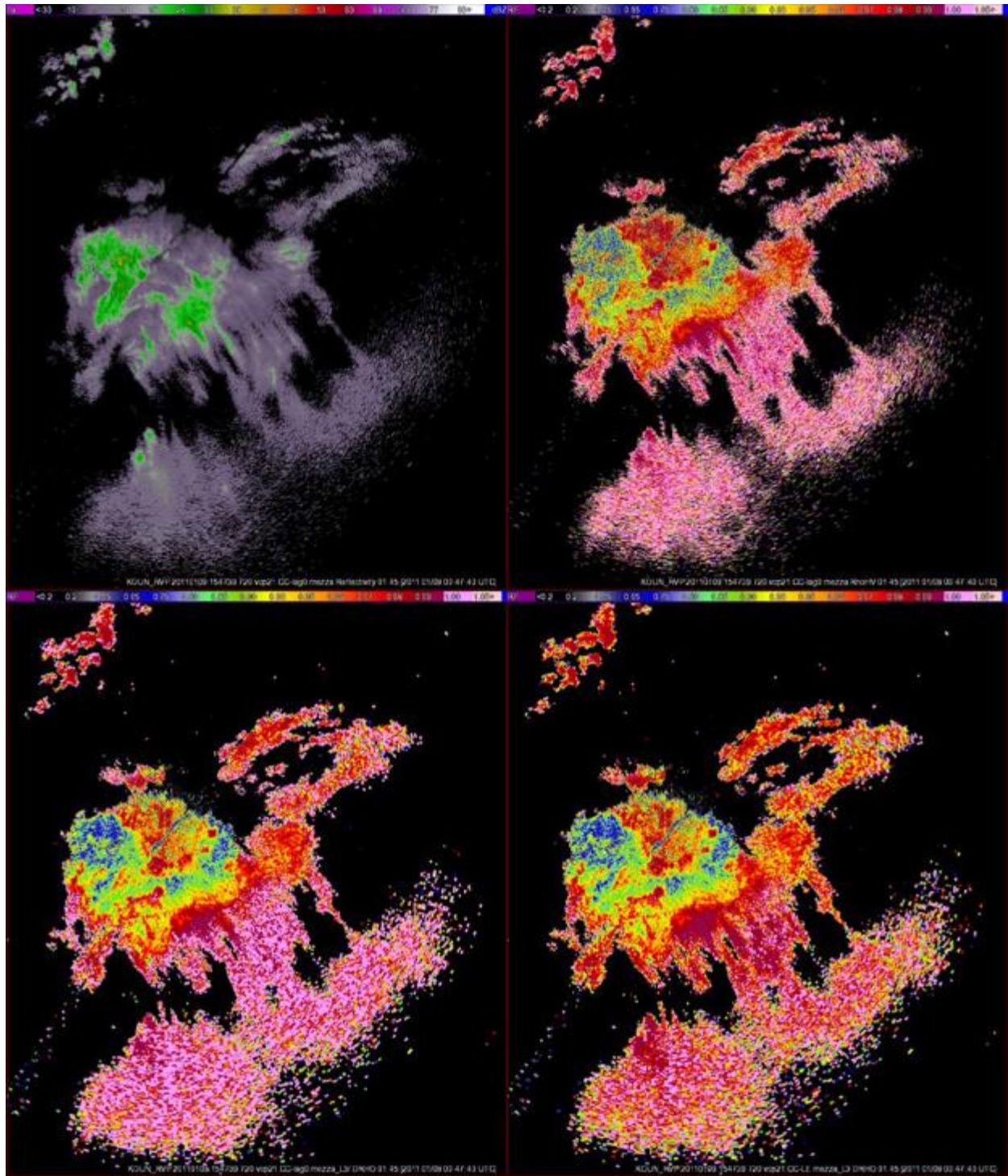
For our purposes, the Range-Doppler spectrum is the two-dimensional Doppler spectra formed from the Fourier transform of a set of time series and placed consecutively based on range. This two-dimensional view of the power-weighted velocity with respect to range has been shown to help mitigate artifacts in the meteorological estimates (i.e., Nai et al. 2013). Similarly, a novel spectral representation for staggered PRT sequences using the generalized autocorrelation spectral density (ASD) was formulated, and spectral dealiasing techniques were applied to extend the Nyquist co-interval of these spectra. These new spectra were combined into a range-Doppler spectrum, and spatial dealiasing (i.e., along range) of catastrophic errors were attempted using a median filter. The result was only moderately successful and therefore was abandoned.

e. Correlation Coefficient Estimation

Igor Ivić (CIMMS at NSSL)

The co-polar correlation coefficient (CC) is one of the three polarimetric variables being produced by the WSR-88D. CC aids in the recognition of types of radar echoes and in the separation of returns from rain and snow. The latter requires precise measurements of CC in areas with low and moderate signal-to-noise ratios (SNR). Unfortunately, correlation coefficient estimates are unusable when they become larger than one, which is common when the number of samples per dwell is small and in areas with SNR less than ~15 dB. In addition, the current CC estimator is positively biased, especially when the number of samples per dwell is small. To mitigate these issues, a novel correlation coefficient estimation technique is being developed that has the potential of producing less biased estimates. Mitigating the CC bias will result in the more accurate estimates which will improve polarimetric recognition of echoes. It will also reduce the number of invalid estimates, which cannot be used for classification. The improved CC estimator will provide improved accuracy while being computationally viable for operational implementation on the WSR-88D.

During FY18, the algorithm was improved to reduce the size of the look-up table. Also, the effects of the improved CC estimator application on the Level III data (which are produced from the base Level II products by applying spatial averaging) were examined using the Warning Decision Support System -- Integrated Information (WDSS-II) tool as a proxy for Advanced Weather Interactive Processing System (AWIPS).



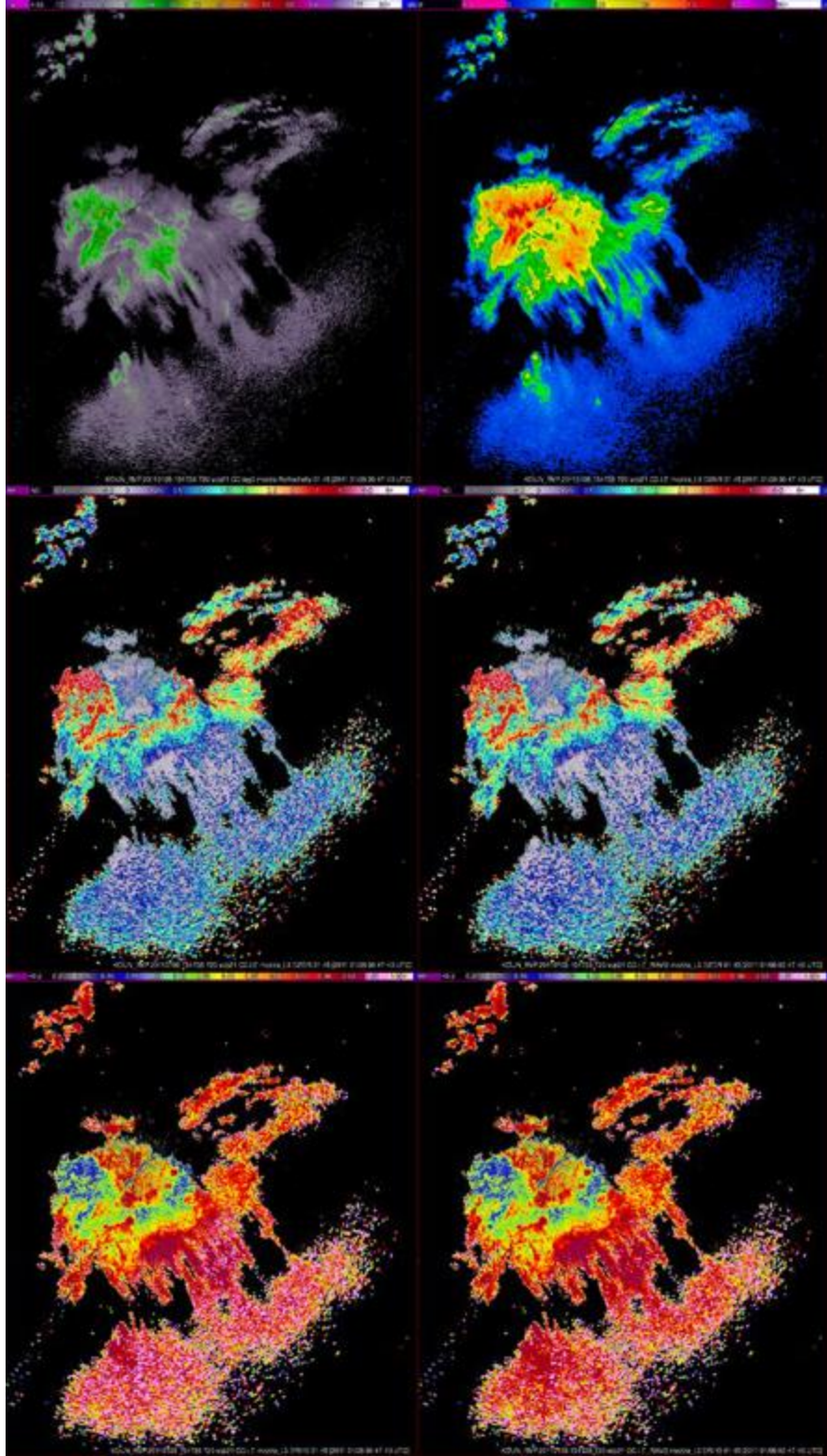
Comparison between Level-III CC fields produced using the legacy estimator (bottom left) and the improved CC estimation technique (bottom right). The field on the right exhibits a visibly reduced number of invalid estimates (shown in pink). The top panels show the corresponding reflectivity (left) and the legacy estimator (right) Level-II fields.

f. Polarimetric Variable Improvement by Trading Spatial Resolution for Quality at Low-to-Moderate SNRs

Igor Ivić (CIMMS at NSSL)

Standard deviations of all weather radar products are affected negatively by the decrease of Signal-to-Noise Ratio (SNR). But, while this effect is moderate in the estimates of Doppler moments, it is far more visible in the estimates of polarimetric variables as an increased noisiness of fields in the areas of low-to-moderate SNR (e.g., below ~15 dB). Consequently, the recognition of weather features may be impaired in the areas where echoes are weak. This provides an incentive to improve the fields of polarimetric variables in these areas. Because polarimetric variable gradients are smaller at low-to-moderate SNRs, it is possible to decrease noisiness by applying averaging in range in those areas without degradation to the range resolution of meteorological features. On the network of WSR-88D radars, such an approach is already implemented in the case of differential phase. Similar results may be achieved by applying a running average filter in range to produce improved fields of differential reflectivity and correlation coefficient.

In FY18, the effects of the range averaging application on the Level III data (which are produced from the base Level II products by applying spatial averaging) were examined using the Warning Decision Support System -- Integrated Information (WDSS-II) tool as proxy for Advanced Weather Interactive Processing System (AWIPS). This work is ongoing.



Reflectivity (top left panel) and SNR (top right panel) fields. Original (middle left panel) and range averaged (middle right panel) differential reflectivity Level III fields. Original (bottom left panel) and range averaged (bottom right panel) correlation coefficient Level III fields.

g. Hybrid Scan Estimator

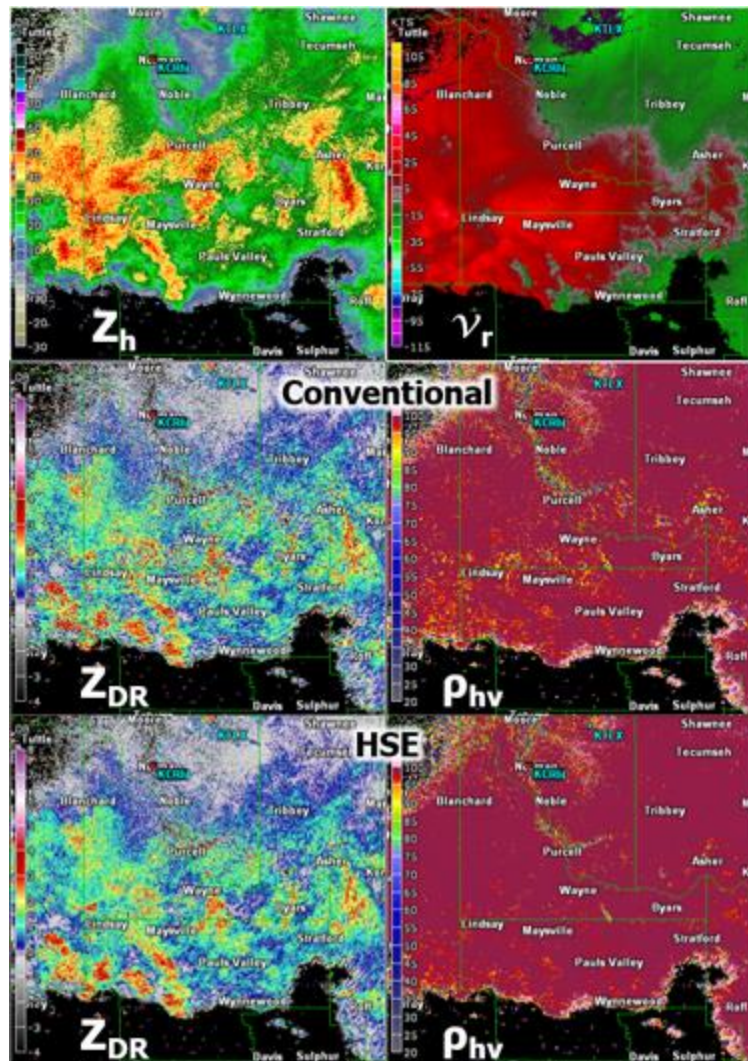
David Schwartzman, Sebastián Torres, and David Warde (CIMMS at NSSL)

At the lowest elevation levels where increased range coverage is required, Volume Coverage Patterns (VCPs) used by the WSR-88D utilize split cuts. To help mitigate range and velocity ambiguities, the same elevation angle is scanned twice using two different pulse repetition times (PRT). In other words, split cuts are used to maximize the spatial coverage of data through a surveillance scan with a long PRT and also to reduce the occurrence of velocity aliasing through a Doppler scan with a short PRT. Reflectivity (Z) and polarimetric variables are currently obtained from the surveillance scan; whereas, Doppler velocity (v_r) and spectrum width (σ_v) are obtained from the Doppler scan. While not currently used, polarimetric variables estimated using data from the Doppler scan could result in better estimates than those from the surveillance scan. This could happen under several conditions: (a) when dwell times in the Doppler scan are longer than those in the surveillance scan, (b) at low-to-medium Signal-to-Noise Ratio (SNR) when the larger number of samples may help reduce statistical fluctuations, (c) for wide spectrum widths, or (d) in the case of ground-clutter contamination for which a larger number of samples typically results in improved mitigation. The goal of this work is to provide an algorithm that selects polarimetric variables with better statistical properties from either the surveillance or Doppler scan for conventional and phase coded (SZ-2) VCPs.

The Hybrid-Scan Estimator (HSE) algorithm has been improved significantly over time by evaluating its performance on different types of weather (e.g., convective and stratiform) and by taking into consideration valuable feedback provided by meteorologists. For example, an apparent data-quality gap was sometimes created using HSE during widespread weather cases near the unambiguous range of the Doppler scan. Even though the initial implementation of HSE provides the ‘best achievable’ data quality, we understand that this gap could affect some algorithms that generate Level-III products. To mitigate this, we explored several range weighting schemes that favor the selection of estimates from the surveillance scan near the end of the Doppler scan’s first trip. Even though this slightly degrades the quality of polarimetric estimates (by using lower quality data from the surveillance scan), it blends the sharp change in data quality that exists between the Doppler and Surveillance scan data. However, since the data-quality gap only becomes apparent in widespread weather cases, we made the weighting scheme dependent on the detection of overlaid echoes. That is, if the Doppler-scan data are unfolded to the second trip (i.e., no overlaid data), then the unweighted HSE is used to maximize the data quality improvement without creating visual artifacts on the data. This is mostly beneficial in convective weather cases.

Following the modifications to the HSE algorithm, we verified the hypothesis that HSE would not impact the Hydrometeor Classification Algorithm (HCA), a Level-III product that provides the distribution of hydrometeor types in the scan. Several cases were processed with the Radar Product Generation (RPG) software using both the

conventional method (i.e., no HSE) and with the HSE-based method for polarimetric estimates. A qualitative comparison between polarimetric variables obtained using both methods is shown in the figure below. It can be seen that the HSE estimates are less noisy and that data quality has generally improved. No significant differences were observed in the produced HCA fields as expected. It is noted that by feeding Level-III algorithms with more accurate HSE estimates, the Level-III products will have higher quality.



Qualitative comparison between polarimetric variables obtained using the conventional method (middle row) and the HSE method (bottom row). Reflectivity and radial velocity (top row) are shown for reference. Data was collected by the KOUN radar on 07 June 2018 using VCP 212 (17:33:46 Z).

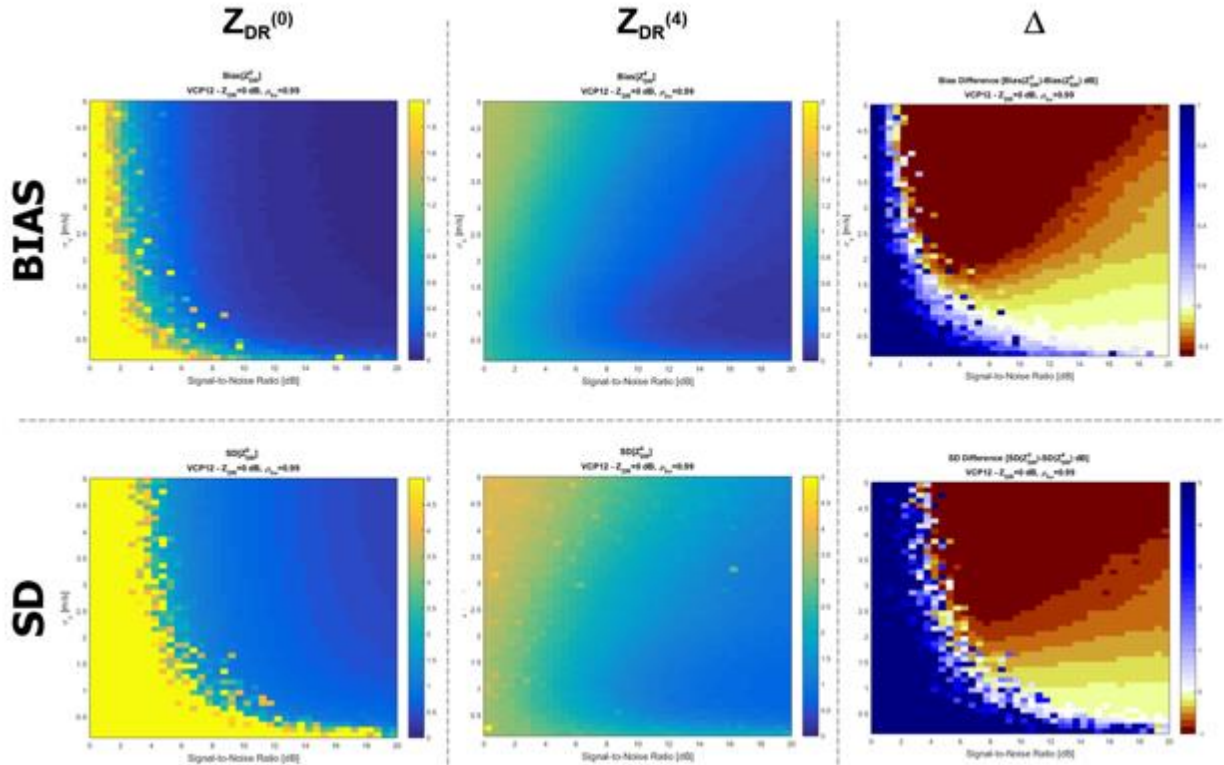
h. Hybrid Differential Reflectivity Estimator

David Schwartzman and David Warde (CIMMS at NSSL)

One of the three polarimetric variables generated by the WSR-88D radar network is differential reflectivity or Z_{DR} . Differential reflectivity is a measure of the reflectivity-

weighted axis ratio (or shape) of the hydrometeors, and it is calculated by taking the logarithmic ratio of signal powers from the horizontal (H) and vertical (V) channels. Since the natural shape of precipitating liquid hydrometeors is oblate (due to gravity and drag forces), we typically measure Z_{DR} values in the range from -1 dB to 4 dB. Because Z_{DR} is a ratio, it is very sensitive to measurement errors and can be significantly biased due to noise, especially at low Signal-to-Noise Ratios (SNR). Even though this is greatly mitigated by the new radial-by-radial noise estimator, there are still opportunities for further enhancements. Due to the importance of providing the most accurate differential reflectivity estimates possible to forecasters and meteorologists, researchers have suggested alternative Z_{DR} estimators which are less sensitive to noise. Specifically, estimators that use lags other than lag-0 are free from influence of noise and are therefore more robust at lower SNRs. In this project, we are exploring hybrid differential-reflectivity estimators that use several correlation lags: 0 at medium-to-high SNRs and 1 or 2 at low-to-medium SNRs.

This year we implemented the lag-1 and lag-2 Z_{DR} estimators. Through extensive simulations, we obtained tables with statistical properties of these estimators, specifically, their bias and standard deviation for typical weather signal characteristics (σ_v varying from 0.5 to 5 m/s, ρ_{hv} from 0.90 to 0.99, and *true* Z_{DR} from -1 to 4 dB). Comparing these tables to the corresponding ones from the traditional lag-0 estimator revealed there could be some improvement. We designed an algorithm that used these lookup tables to choose the estimator with the best statistical properties from the lag-0, lag-1, or lag-2 Z_{DR} estimators. Through the integration of this algorithm in our signal processor, we processed real data cases to evaluate the performance. Overall, the hybrid estimator performs better than the lag-0 estimator. The figure below shows the bias, standard deviation, and their difference as a function of the SNR and the spectrum width for the traditional lag-0 and the lag-4 Z_{DR} estimators.



Bias, standard deviation, and Δ (difference of bias, or standard deviation) as a function of SNR and spectrum width for the traditional lag-0 and the lag-4 Z_{DR} estimators.

i. Range Oversampling Techniques

Sebastián Torres, Christopher Curtis, and Igor Ivić (CIMMS at NSSL)

Obtaining radar data at faster rates can improve the ability of forecasters to observe rapidly evolving weather phenomena. When increasing data rates, the conventional trade-off involves sacrificing either spatial coverage or data precision. With range oversampling, it is possible to add a new dimension to this trade-off: signal processing. Range oversampling allows us to either obtain data twice as fast with variances similar to conventional processing or improve data quality without sacrificing update time or spatial coverage. This type of processing has been used to significantly reduce update times on the National Weather Radar Testbed (NWRT) Phased Array Radar (PAR) and to improve polarimetric data quality on a NEXRAD research radar (KOUN).

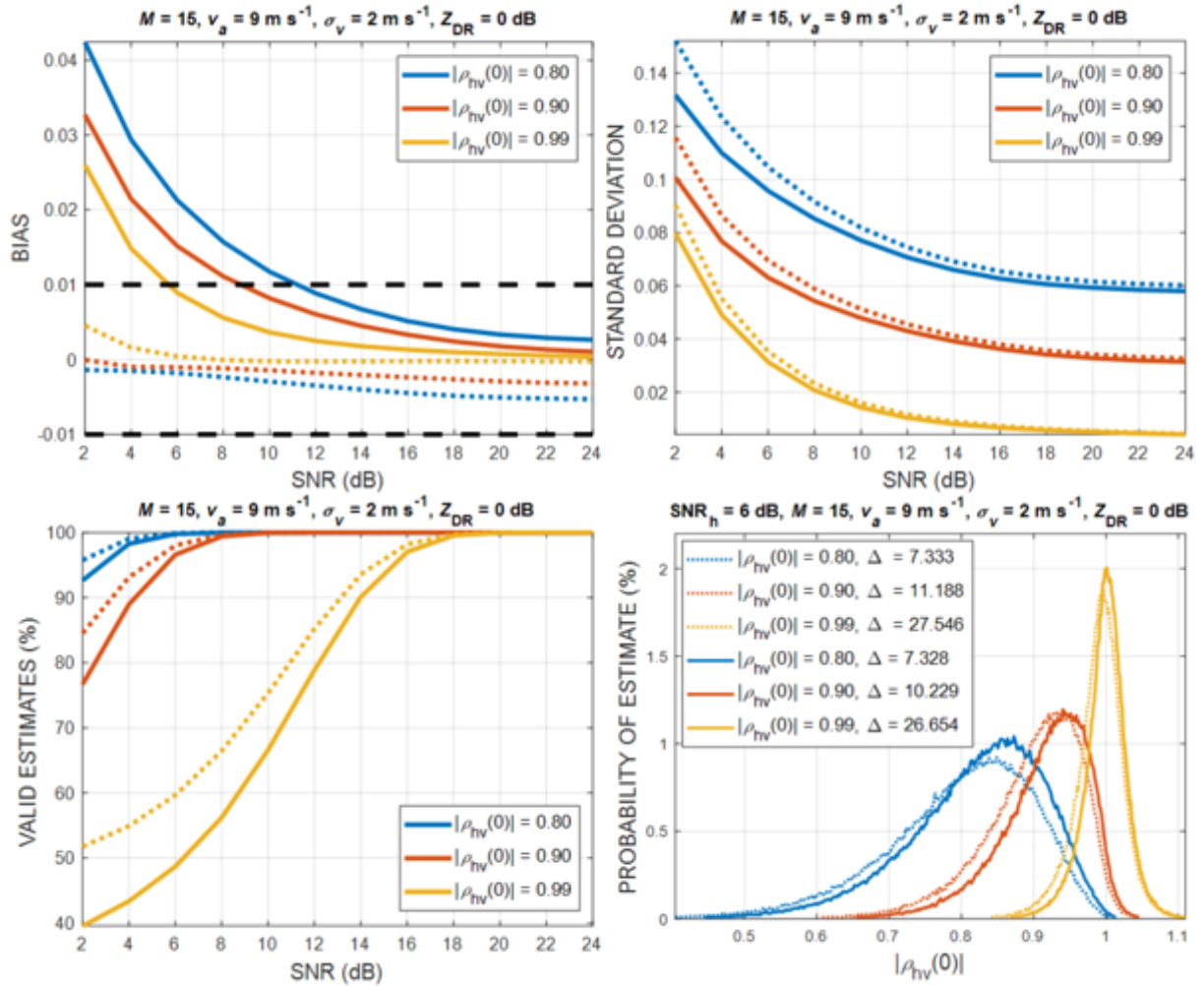
In FY18, work was started on integrating range oversampling processing with a new staggered PRT mode for the MATLAB digital signal processor (DSP). This mode is based directly on the SPRT Algorithm Description Document that was previously provided to the Radar Operations Center. The mode is being designed to take into account some of the capabilities of the most recent MATLAB DSP.

We also began some research on the effects of the IF filter bandwidth on the performance of adaptive pseudowhitening. Originally, it was recommended that the IF

filter bandwidth be opened up to ensure that the noise was nearly uncorrelated in range. Some initial research showed that it may be advantageous to use a narrower filter bandwidth to reduce the amount of noise. We developed a simulator to test the performance of different filter bandwidths based on the FIR filters used by the Vaisala hardware.

We continued to work on integrating range oversampling processing with the new correlation coefficient estimator described in subsection (d). This estimator has less bias than the conventional lag-0 estimator and provides more valid estimates. We want to keep the advantages of this new estimator and also use range oversampling processing to lower the variance. We tried to modify the lookup tables used in the new estimator for adaptive pseudowhitening, but there were some problems with the initial approach. We are now trying a couple of new approaches to possibly combine lag-0 and lag-1 estimators and also to review some of the component estimators of the new correlation coefficient estimator. The analytical formulas for one of the estimators which comprise the new CC hybrid estimator for the non-oversampled data were revisited and modified to accommodate adaptive pseudowhitening. The results obtained using the simulated time series in the case of a rectangular pulse and window with an oversampling factor of 4 indicate reduced bias with respect to the legacy CC estimator even without correction using the pre-computed lookup tables. Additional work to modify the analytical formulas for other estimators and combine them into a single estimation technique is planned. We also plan to evaluate the estimator performance for a realistic non-rectangular transmit pulse.

In addition to our research, we also continued to work with Radar Operations Center engineers to determine how best to implement range oversampling processing on the NEXRAD network. Vaisala has provided new software to allow the collection of data with four-times oversampling even for the longest pulse repetition times.



Biases (top left panel), standard deviations (top right panel), percentage of valid estimates (bottom left panel), and probability of estimates (bottom right panel) for the legacy lag-0 estimator (full lines) and one of the estimators which comprise the new CC hybrid estimator (dotted lines). The results are produced for the rectangular pulse, Meza window and an oversampling factor of 4. The symbol Δ (in the bottom right panel) denotes the percentage of estimates that fall within ± 0.01 of the true value.

j. Hardware and Software Development and Maintenance for KOUN and Mobile Radars

Mike Schmidt, Allen Zahrai, Eddie Forren, Stephen Gregg, David Schwartzman, and Charles Kuster (CIMMS at NSSL)

NSSL maintains several radar assets used by researchers, including both mobile radars and NSSL's research and development WSR-88D, KOUN. In addition to their use as meteorological and hydrological research instruments, these radar assets also serve as testbeds for technological research. Technologies prototyped on KOUN in particular are directly applicable to the WSR-88D network. Maintenance and continual improvement of

these assets is essential to providing high quality instruments for new research and for supporting NSSL's commitment to R2O.

Work on the shared software baseline between the Advanced Technology Demonstrator and KOUN continued this past year, and KOUN data playback and processing was supported by tweaking and running the old 32-bit version of the software baseline. The 64-bit software baseline was used briefly to convert archive-I KOUN data into MATLAB pulse groups and to process IQ data in an attempt to support Jeff Snyder's efforts with the HSE algorithm. This brief test confirmed that some small part of the 64-bit baseline still works with KOUN data, but further testing and processing for the HSE algorithm did not occur because of the demands of the ATD project. As the ATD goes online this year, there may be an opportunity to do more extensive testing of the 64-bit software for KOUN DSP processing.

The complete teardown and rebuild of Mike Biggerstaff's OU-SR1 mobile radar was completed. This included the design and implementation of a new dual-polarized radar and the specification of required parts and subsystems. We also configured, developed and tested a Vaisala Sigmet RVP-900 data acquisition and signal processing system for the SR1. The pedestal for SR1 came with a new antenna drive system, but we decided to change it back to the older system that we were using on the other trucks so we would not have to spend time developing new software. We have had to replace the AC units on both transmitter cabinets of SR1 and SR2. In the rebuild of SR1, we also added a rooftop AC unit for the cab of the truck. SR1 is still in the testing stages at this time. Some repairs to the antenna drive system of SR2 were made.

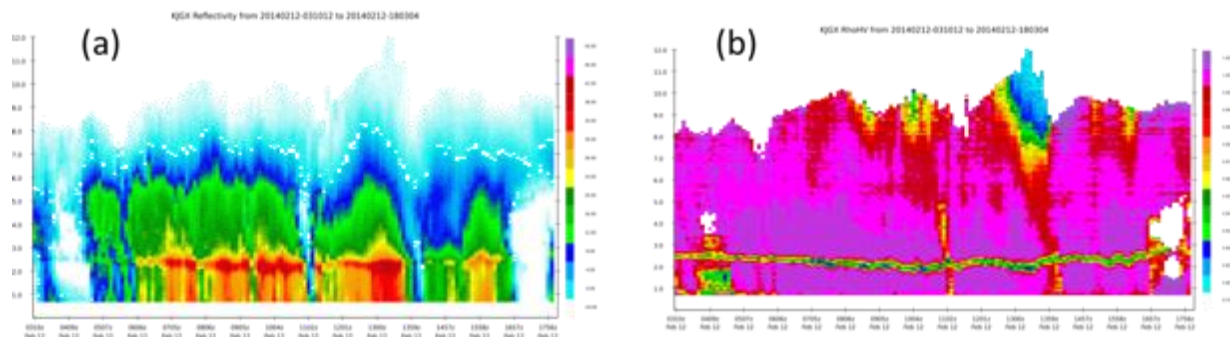
We had to replace the transmitter AC unit on NOXP. We made some wiring changes to NOXP to make it more compatible with SR1 and SR2. The changes were made in the hopes of trying to keep all the mobile radars as similar as possible in wiring and software configurations.

k. Generating QVP Products as Part of a Prototype WSR-88D Operational Software

John Krause (CIMMS at NSSL)

Quasi-vertical profiles (QVP) were first introduced by Ryzhkov, et al. in 2016 and have been a part of NSSL's research code base since their inception. In 2017, we continued moving this unique product toward possible use in operations. The product represents evolution of vertical structure of the storm in a height vs time format. Previously, most radar data were traditionally displayed in the PPI or RHI formats and looped in a sequence to show time evolution. The figure below was automatically generated by our prototype pre-production code base in C and C++. The results have been compared to the research code and found to be comparable. The real time prototype environment can now easily generate QVP plots of any radar variable for any radar in the US. This step forward allows us to explore and promote the unique value of QVP plots for forecasting and research. The new code allows generating these plots reliably and

efficiently. We have also worked to transfer the Column Vertical Profile (CVP) technique (which is an extension of QVP) from our research portfolio into prototype code for testing and evaluating in 2018.



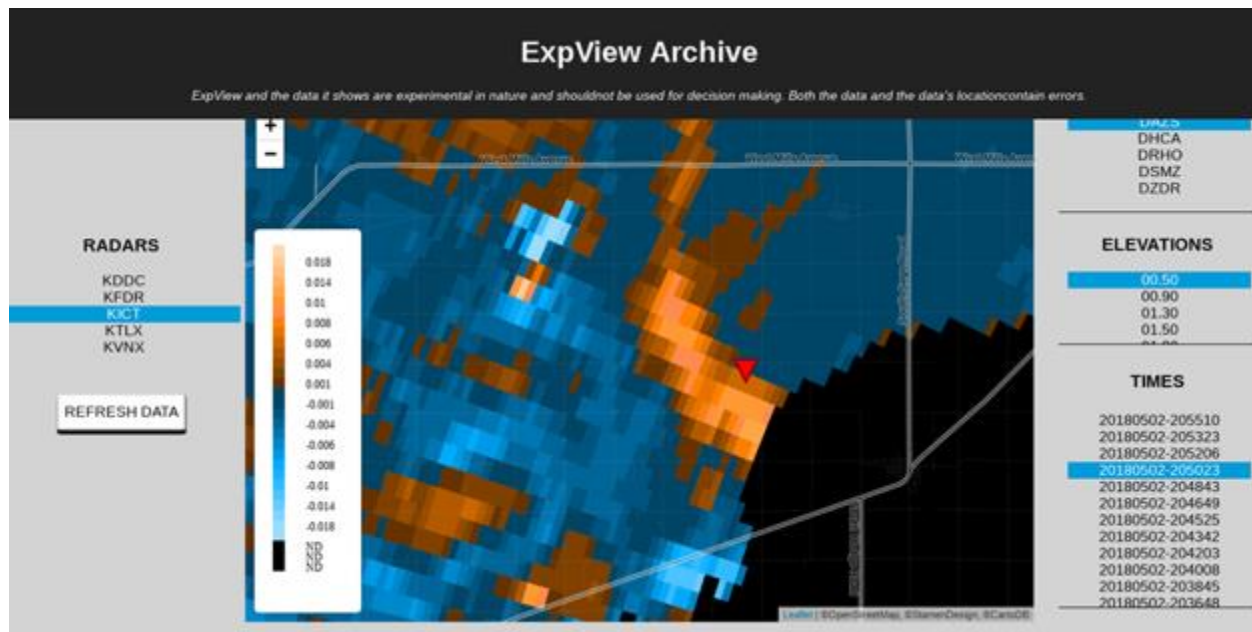
Automatically generated QVPs (quasi-vertical profiles) of a) radar reflectivity and b) cross-correlation coefficient from the KJGX WSR-88D radar for a 15 hour period starting at 03 UTC on February 12, 2014

I. Using Cloud Computing to Run Experimental Algorithms in Real Time

John Krause (CIMMS at NSSL)

A cloud computing proposal (DDRF) was funded by NSSL and its goal was “to develop experience and knowledge in cloud computing”. This was accomplished by creating and running a limited set of radar algorithms on the Amazon Web Services (AWS) cloud computing platform. In the course of this project, we were able to run the azimuthal shear (AS) and Tornado Debris Signature detection (TDS) algorithms on the AWS platform in real time using data from 1-6 radars. The AS product has been used by others previously, but it generally has not been widely viewed in real time. In the latest version of the TDS algorithm developed by J. Snyder, the AS field is used as a key input. Both the AS and HCA (with TDS) products are developmentally mature and are under consideration for inclusion on the ORPG. During the course of the evaluation of the TDS algorithm, we developed an icon- or object-based module that allows displaying TDS detections atop other radar fields. An example is the figure below.

Initial project challenges included learning how to use AWS for computing and display purposes. The data that were used had to be viewable by NSSL/CIMMS and other NOAA personnel and partners (e.g., ROC personnel) locally as well as remotely (e.g., in the NOAA headquarters). In addition, the experimental data and algorithm output were not to be exposed to the public since these are considerable experimental data. We were able to configure AWS to achieve an appropriate data security level which allowed remote views of the data and limited the exposure of the data only to those with valid NOAA email accounts. The visual output itself was presented by a web application written in JavaScript and operated from the secure (internal) portion of the NSSL website.

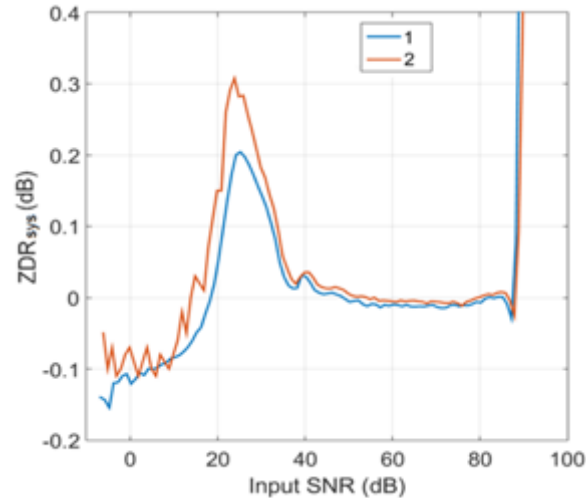


A screenshot of the ExpView javascript display developed to show experimental products in real time. The background example shown (in orange and blue) is the Azimuthal Shear from the KICT WSR-88D radar (Tulsa, OK) on May 2, 2018 at 2050 UTC. Also displayed is the TDS (Tornado Debris Signature) detected by the improved HCA (Hydrometeor Classification Algorithm) as a red triangle in the center of the image.

m. Absolute Calibration of Differential Reflectivity

Valery Melnikov (CIMMS at NSSL)

Reflectivity (Z) and differential reflectivity (Z_{DR}) are used in radar quantitative precipitation measurements. Accurate measurements of Z_{DR} are ensured by a special calibration routine controlling the system Z_{DR} bias (Z_{DRsys}) is obtained. According to the WSR-88D's specifications, Z_{DRsys} should be obtained with the accuracy of 0.1 dB. Currently, Z_{DRsys} is considered constant in a full dynamic range of received radar signals. Z_{DRsys} is sensitive to linearity of a radar receiver. Our recent measurements reveal the dependency of Z_{DRsys} on the intensity of input radar signals or signal-to-noise ratio (SNR). An example of such dependence is presented in Fig. 1c. It is obvious that Z_{DRsys} is not constant and changes by about 0.3-0.4 dB with varying SNR well exceeding the tolerance in the WSR-88D radar specification. i.e., variations in Z_{DRsys} are larger than 0.1 dB desired for ZDR measurements. Such variability must be accounted for in radar measurements. Recommendations on how to mitigate this artifact have been provided to the Radar Operation Center.



The magnitude of ZDR_{sys} as a function of the power of input signal (SNR) on the KJIM WSR-88D radar. Curves '1' and '2' were obtained on 06/04/2018 and 06/06/2018 respectively.

Publications

Curtis, C. D., and S. M. Torres, 2017: Adaptive range oversampling processing for nontraditional radar-variable estimators. *Journal of Atmospheric and Oceanic Technology*, **34**, 1607–1623.
 Warde, D. A., and S. M. Torres, 2017: Spectrum width estimation using matched autocorrelations. *IEEE GRSL*, **14**, 1661-1664.

2. Dual-Polarization

Overall Objectives

Use dual-polarization radars for quantitative precipitation estimation, hydrometeor classification, and investigation of microphysical processes in clouds and precipitation.

Accomplishments

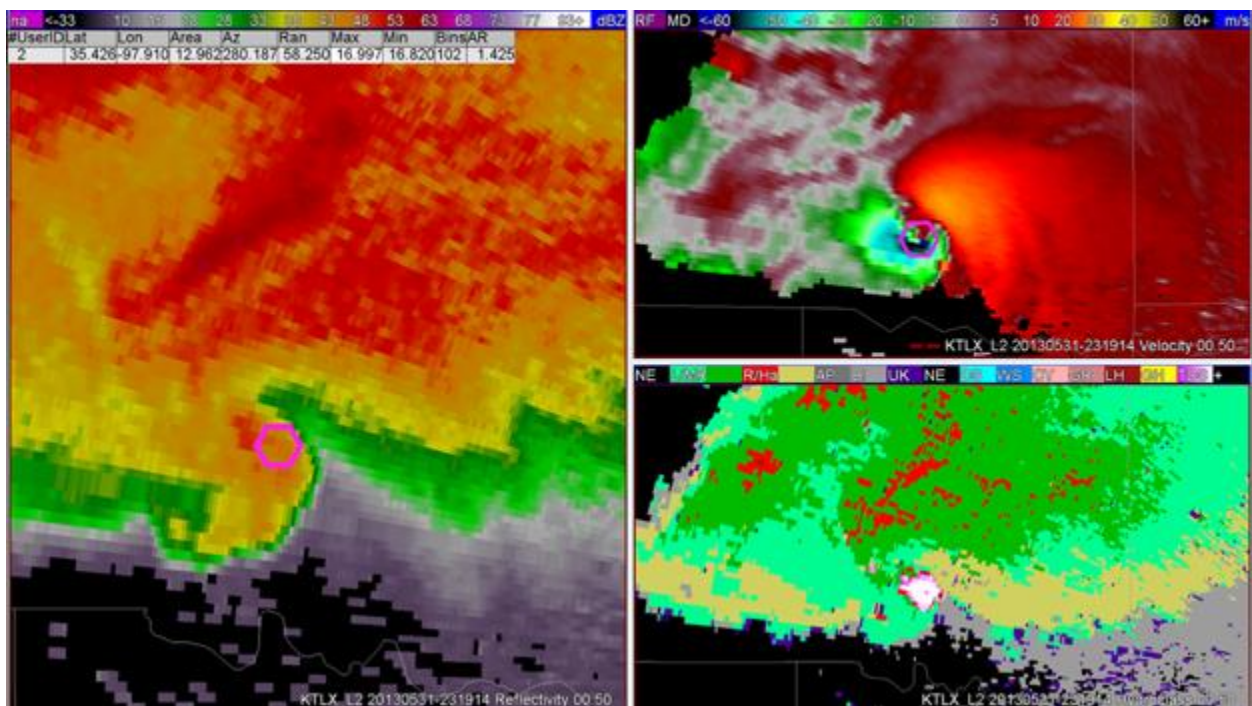
a. Developing an Object-Based Tornado Debris Signature Detection Algorithm

Jeff Snyder (NSSL), John Krause (CIMMS at NSSL), and Arthur Witt (NSSL)

The relatively unique scattering characteristics of debris lofted by tornadoes can be identified and subsequently used by meteorologists to confirm that a tornado is occurring. Past studies have noted that the tornado debris signature (TDS) occurs more commonly with strong and violent tornadoes (e.g., EF2 and higher). The hydrometeor classification algorithm (HCA) with TDS detection first described in Snyder and Ryzhkov (2015) has undergone further development in the past several years, and a substantial effort was made during the July 2017 – June 2018 reporting period to assess how well the algorithm worked. A total of 628 PPIs covering 18 events were examined, from which 1648 TDS “clusters” were identified, composed of 41422 range gates classified as TDS. Although the algorithm was designed with the aim of minimizing false alarms, the verification indicate that many false alarms remained, though we suspect that most would be easily discounted by trained meteorologists familiar with radar data and

severe storms. For example, most of the false alarms were small in size, had lower maximum aggregation values, tended to be highly non-circular when viewed on a standard PPI, and usually occurred away from locations where strong tornadoes are usually observed. The most common source of alarms was ground clutter contamination.

To improve the performance of automated TDS detection, a new object-based algorithm was designed. The base of this algorithm is the TDS-enabled HCA. Clusters of TDS-classified gates are extracted by the HCA, and a series of thresholds are applied. The thresholds were determined subjectively, though computer-driven optimization techniques are being explored. This object-based algorithm tends to eliminate the vast majority of the false alarms present in the raw HCA output while maintaining most of the correct hits. Output from this object-based algorithm can be displayed on top of other relevant data (e.g., radial velocity and reflectivity; Fig 2a) to reduce the need for the user to examine yet another two-dimensional product (HCA) during critical severe weather operations when time is often very limited. In addition, the ability to display icons associated with the new algorithm directly atop other radar fields may improve the ability of a trained user to quickly determine the legitimacy of a detection based upon geospatial information (e.g., the location of the detection relative to other storm structures).



3-Panel plot of Z (left), V (upper-right), and HCA output (lower-right) from the KTLX radar on 31 May 2013. The magenta pentagon in Z and V denotes the approximate location of the qualified TDS centroid. Two other much smaller areas preliminarily classified TDS may be seen in the HCA output, but the object-based algorithm disqualified them because they didn't pass several thresholds (e.g., too small size, maximum aggregation value too low, etc.).

b. Hail and Updraft Detection by Polarimetric Radar

Jeff Snyder (NSSL) and John Krause (CIMMS at NSSL)

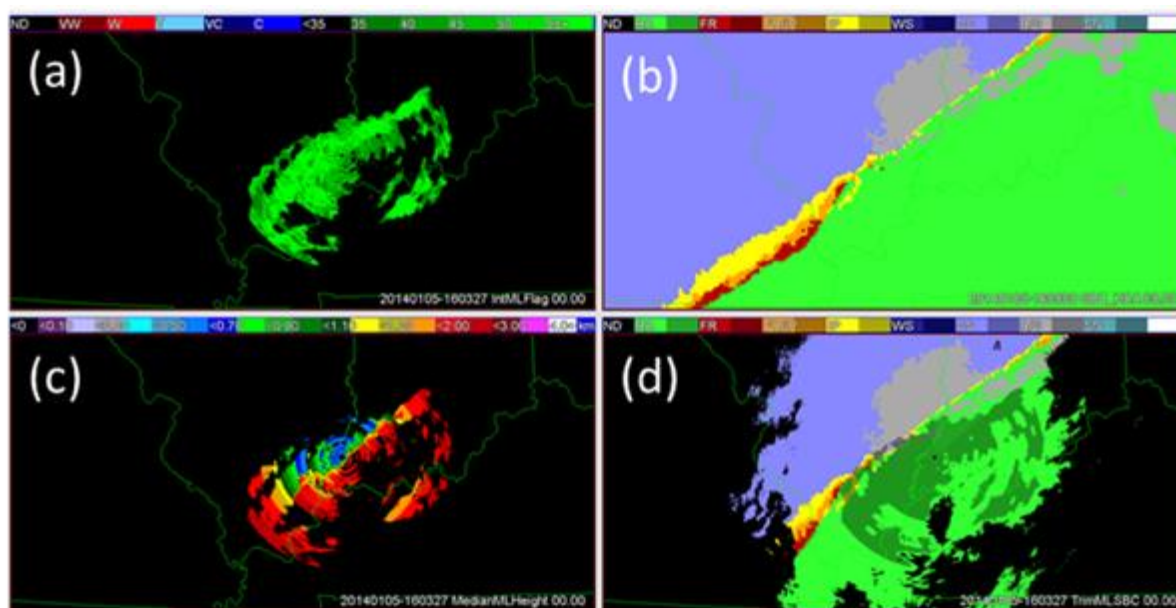
Polarimetric radar has proven useful for improving hail detection (e.g., Ryzhov et al. 2013a,b; Ortega et al. 2014) and for enhancing our ability to identify the location of convective storm updrafts (e.g., Snyder et al. 2015, among many others). During the 2018 fiscal year, algorithms were developed to retrieve Z_{DR} and Depolarization Ratio (DR) column characteristics similar to those based on the original Z_{DR} column algorithm described in Snyder et al. (2013). The new algorithms can operate on either a latitude-longitude-height grid or on the native polar grid and are designed to run quickly. Z_{DR} and DR columns are currently being examined with hail reports collected by SHAVE in an effort to determine the relationship between large hail and these polarimetric signatures associated with updraft location and intensity. In addition, a series of other potentially relevant polarimetric quantities such as minimum Z_{DR} and ρ_{hv} at -20°C , -30°C , and -40°C heights are being investigated for their relationship to hail size and location. We hypothesize that areas of negative Z_{DR} and reduced ρ_{hv} within the updraft of strong convective storms are associated with large hail and may be used to improve hail sizing algorithms such as the Hail Size Discrimination Algorithm (HSDA), though structural changes are needed within the HCA and HSDA to use this information. A detailed, manual inspection of these products is ongoing and will be completed during the 2019 fiscal year.

c. Development and Testing of New Algorithms for the WSR-88D that Combine Polarimetric Radar Data with Model Output to Determine Melting Layer Coverage and Surface-based Precipitation Types in Winter Storms

Terry Schuur, John Krause, and Alexander Ryzhkov (CIMMS at NSSL)

The classification of cold-season precipitation type at the surface is complicated by the broad range of precipitation types that might result from processes that occur below the height of the radar's lowest elevation sweep. For example, a shallow layer of subfreezing air near the surface might lead to either a complete refreezing of drops (ice pellets) or refreezing upon contact with the surface (freezing rain). Both of these precipitation types are difficult to determine using radar data alone, and may not be observed at all at distances > 50 km from the radar. This deficiency has motivated the development of two new algorithms: the 1) surface Hydrometeor Classification Algorithm (sHCA), in which thermodynamic output from a numerical model is used to produce a surface-based precipitation type (referred to as the Spectral Bin Classifier, or SBC), and 2) the Hybrid Melting Layer Detection Algorithm (HMLDA), in which thermodynamic output from a numerical model is combined with polarimetric WSR-88D radar observations from all elevation angles are used to produce a melting layer (ML) coverage map. When warranted by the observations, the ML coverage map can then be used to modify the SBC "background classification".

Since radar-based reclassification in the sHCA largely depends upon accurate detection of the ML, considerable effort in the past year has focused on evaluating and improving the performance of the HMLDA. This work included refining adjustable parameters in the algorithm, investigating techniques to fill gaps that can occur in the ML coverage map when WSR-88D elevation angles are widely spaced, and improving a median ML height product. While challenges still remain with the full integration of the HMLDA product into the sHCA, we have found that the HMLDA product overlaid on surface precipitation type from the SBC can, by itself, serve as a stand-alone product that provides value-added information to forecasters. In particular, the HMLDA has proven to be particularly adept at tracking the leading boundary of an elevated warm layer in transitional winter weather events, which can provide good situational awareness to forecasters during transitional winter weather events. An example of such an event is shown in the figure below.



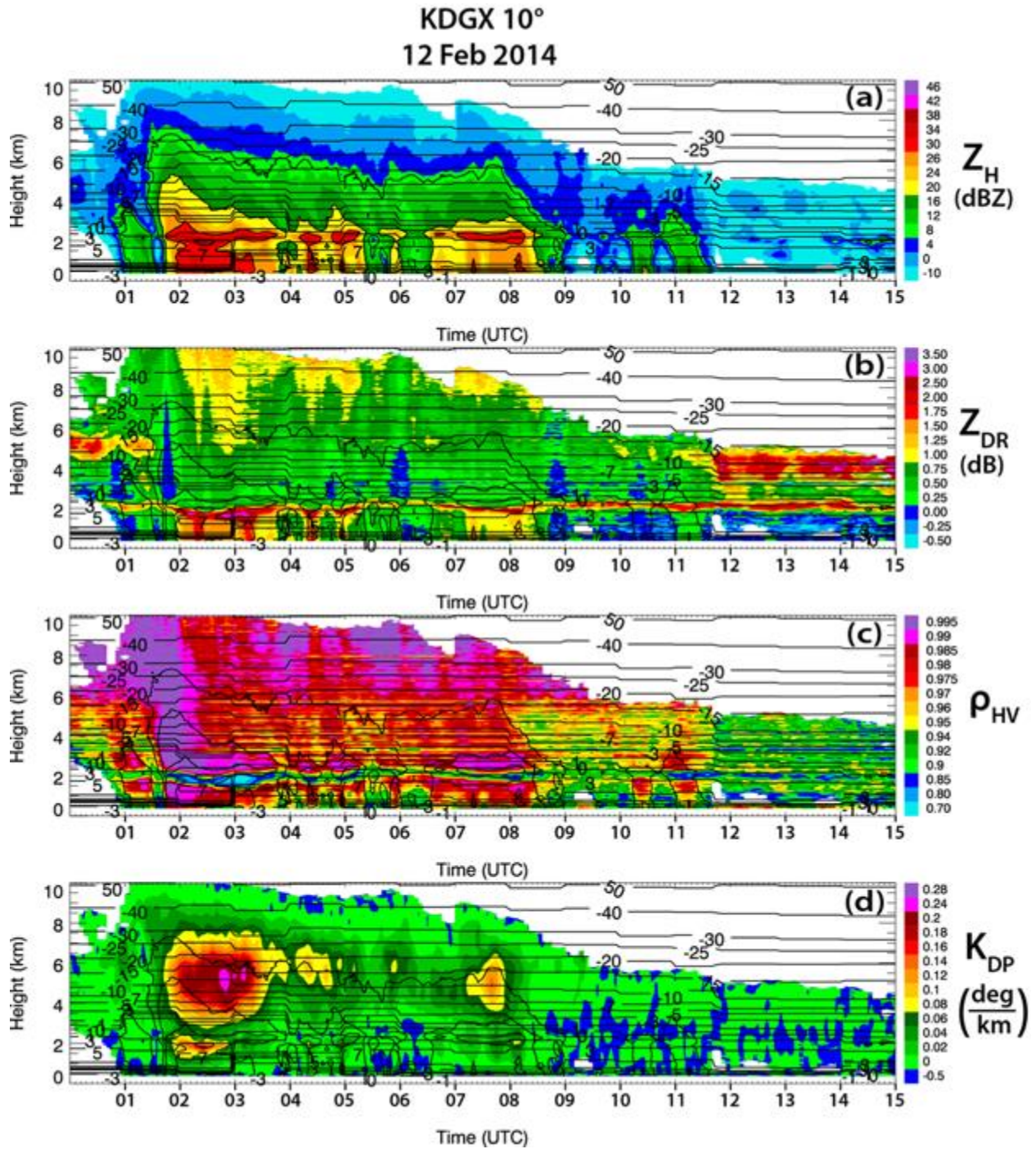
Evansville, IN WSR-88D (KVWX) (a) HMLDA melting layer (ML) coverage product, (b) Spectral Bin Classifier (SBC) surface classification, (c) HMLDA median ML height product, and (d) radar filtered SBC product with melting layer product from (a) overlaid at 1603 UTC on 05 January 2014. The overlaid ML coverage product and median ML height product for this case both show good agreement with the model-based SBC classifier. For other events (not shown), disagreement between the observed, radar-based ML products and model-based surface precipitation type provide forecasters with evidence that the model-based classification must be adjusted.

d. A Polarimetric Analysis of Ice Microphysical Processes in Snow Using Quasi-Vertical Profiles

Erica Griffin, Terry Schuur, and Alexander Ryzhkov (CIMMS at NSSL)

Investigating the polarimetric and thermodynamic characteristics of winter precipitation is necessary to further our understanding of the microphysical processes within winter storms, as well as to improve their representation in numerical models. This study implements a new quasi-vertical profile (QVP) methodology to investigate the microphysical evolution and significance of intriguing winter polarimetric signatures and their statistical correlations, observed in a selection of winter events. QVPs of transitional stratiform and pure snow precipitation were analyzed at high elevation angles (i.e., 9.9°-19.5°) using data from S-band WSR-88Ds, alongside their corresponding environmental thermodynamic HRRR model analyses

In particular, QVPs of K_{DP} and Z_{DR} were implemented to demonstrate their value in interpreting ice processes in the upper levels of storms. Several fascinating and repetitive signatures were observed. The most striking feature was maximum Z_{DR} (up to 6 dB) in the dendritic growth layer (DGL) occurring near the -10 dBZ Z_H contour within low K_{DP} and during shallower and warmer cloud tops. Conversely, maximum K_{DP} (up to $0.3^\circ \text{ km}^{-1}$) in the DGL was found to occur within low Z_{DR} and during taller and colder cloud tops. Essentially, Z_{DR} and K_{DP} in the DGL are anti-correlated and strongly depend on cloud top temperature. Analyses also show correlations indicating larger Z_{DR} within lower Z_H in the DGL, and larger K_{DP} within greater Z_H in the DGL. The QVP results can be attributed to distinct polarimetric radar characteristics of isometric (I type) and dendritic (D type) ice particles. We advocate that the regions of high Z_{DR} are dominated by D-type ice, whereas the regions of high K_{DP} are overwhelmed with the I-type ice, which does not exclude the presence of D-type ice crystals as well. In other words, the high Z_{DR} regions are likely dominated by growth of a mixture of highly oblate dendrites and/or hexagonal plates, or prolate needles. Regions of high K_{DP} are expected to be overwhelmed with snow aggregates and crystals with irregular or nearly spherical shapes, seeded at cloud tops.

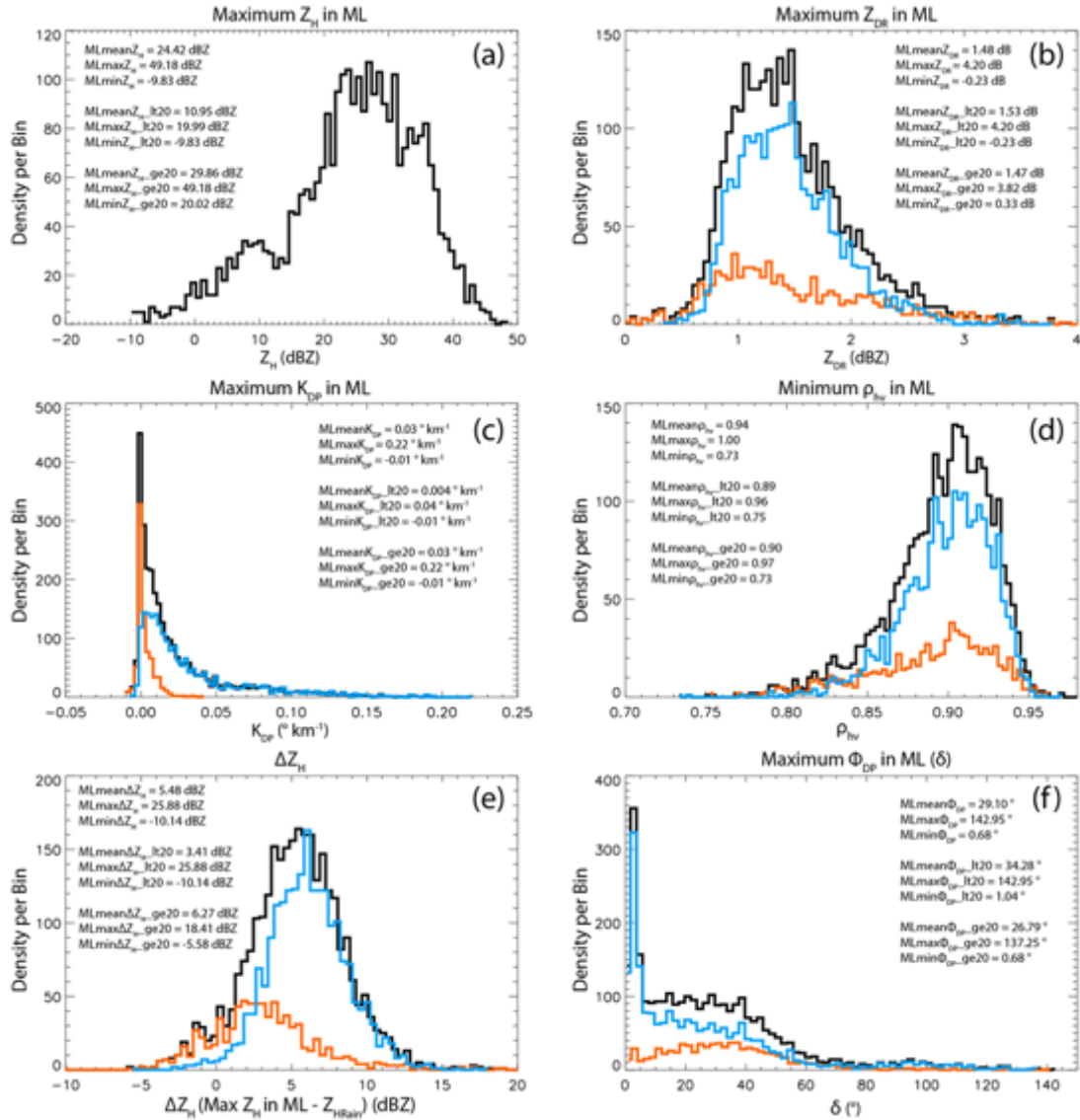


QVPs of a) Z_H , b) Z_{DR} , c) ρ_{HV} , and d) K_{DP} , for KDGX from 0006 through 1500 UTC on 12 Feb 2014, at 10° elevation. Contours of HRRR model wet-bulb temperature (°C) are overlaid in each plot. Also, Z_H is contoured at 10, 20, 30, and 40 dBZ.

e. Polarimetric Characteristics of the Melting Layer at S Band Retrieved from Quasi-Vertical Profiles

Erica Griffin, Terry Schuur, and Alexander Ryzhkov (CIMMS at NSSL)

Having a complete understanding of the polarimetric characteristics above, within, and below the melting layer is crucial towards developing techniques to mitigate rainfall overestimation in regions where the radar's beam intersects the bright band. In this study, quasi-vertical profiles (QVPs) obtained from a large-scale database of U.S. WSR-88D radar data were used to document the polarimetric characteristics of the melting layer (ML) in cold-season storms with high vertical resolution and accuracy. A polarimetric technique to define the top and bottom of the ML was first introduced. Using the QVPs, statistical relationships were then developed to gain insight into the evolution of microphysical processes above, within, and below the ML, leading to a statistical polarimetric model of the ML that reveals characteristics that reflectivity data alone are not able to provide, particularly in regions of weak Z_H . Results reveal strong positive correlation between Z_H in rain (i.e., 0.3 km below ML) and Z_H in snow (i.e., 0.3 km above ML) and between maximum Z_{DR} in the ML and Z_{DR} in rain. Strong positive correlation is also observed between maximum K_{DP} and maximum Z_H in the ML. Strong negative correlation occurs between maximum Z_{DR} and minimum ρ_{hv} in the ML and between minimum ρ_{hv} in the ML and the corresponding enhancement of Z_H (i.e., $\Delta Z = Z_{Hmax} - Z_{Hrain}$). Quantifying the $\Delta Z(\min(\rho_{hv}))$ dependence is crucial for implementation of a polarimetric vertical profiles of rain (PVPR) technique designed to mitigate the impact of the ML contamination on QPE. The evidence of very large Z_{DR} (up to 4 dB) associated with lower Z_H (-10 to 20 dBZ) in the ML is documented in the situations when pristine, nonaggregated ice falls through it.



Composite histograms of a) maximum Z_H in the ML (dBZ), b) maximum Z_{DR} in the ML (dB), c) maximum K_{DP} in the ML (° km⁻¹), d) minimum ρ_{hv} in the ML, e) ΔZ_H (i.e., Z_H in ML - Z_H in rain; dBZ), and f) maximum Φ_{DP} (i.e., δ ; °) in the ML, for the 33 QVP ML events. Mean, maximum, and minimum values are indicated in each panel.

f. Ice Microphysical Retrievals Using Polarimetric Radar Data

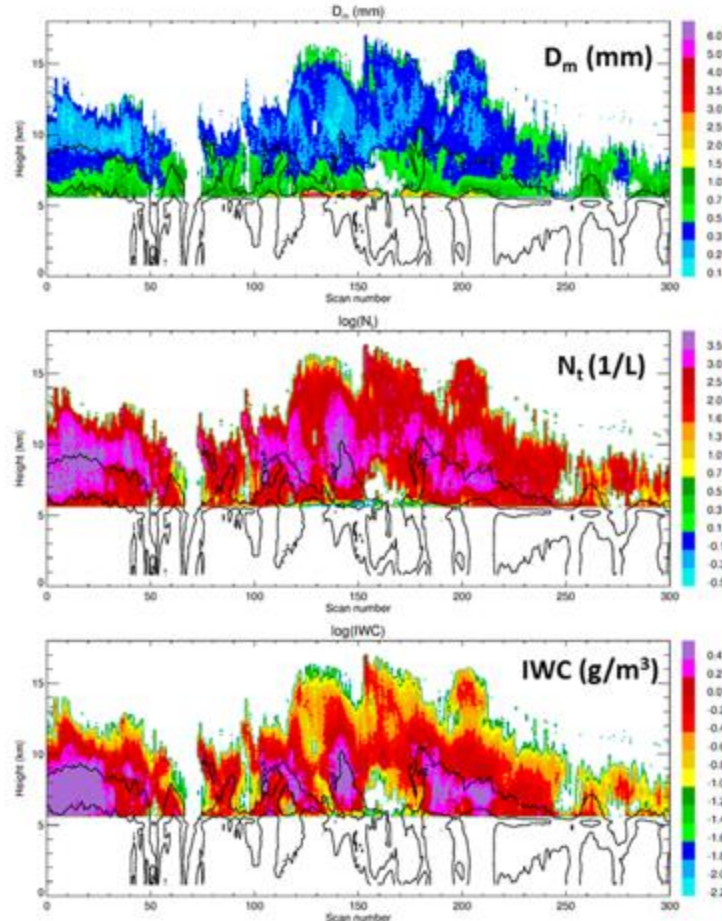
Alexander Ryzhkov, Petar Bukovcic, and Amanda Murphy (CIMMS at NSSL)

A novel polarimetric radar method for size distribution retrievals of ice and estimation of ice water content (IWC) has been developed. The technique is based on the combination of three radar variables: radar reflectivity Z , differential reflectivity Z_{DR} (or reflectivity difference Z_{DP}), and specific differential phase K_{DP} . The latter plays a particularly important role because it is proportional to the first moment of size distribution in ice and, therefore, is very sensitive to ice particles of small sizes. It is

demonstrated that the estimates of the mean volume diameter D_m , total concentration N_t , and IWC of ice particles obtained from Z and the ratio of Z_{DP} and K_{DP} are robust with respect to the diversity of ice habits, their shapes, orientations, density, and size distributions.

It is instrumental to use new methodologies for processing and displaying polarimetric radar data such as quasi-vertical profiles (QVP) and columnar vertical profiles (CVP) to ensure appropriate quality of the K_{DP} and Z_{DP} measurements for reliable retrievals. Comparisons of the radar-retrieved size distribution parameters of ice with their in situ aircraft measurements in midlatitude MCSs show good agreement between the two.

Preliminary testing of the suggested technique using the WSR-88D radar data collected in hurricanes Irene, Harvey, and Irma reveals extreme concentrations of very small ice with significant IWC that is almost an order of magnitude higher than the one estimated from conventional Z – IWC relations. Vertical distribution of D_m , N_t , and IWC above the freezing level in the hurricane Irene represented in a height vs time format is displayed in the figure below.



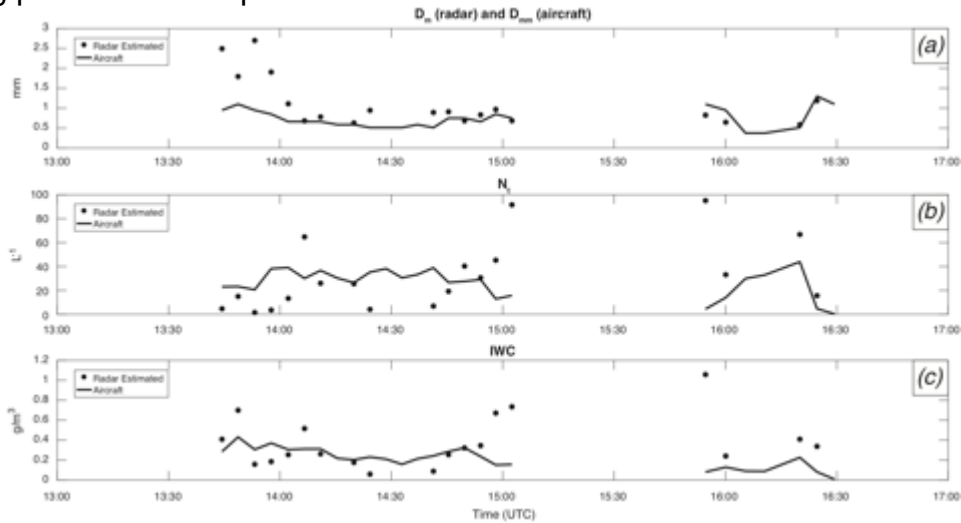
Vertical cross-sections of the mean volume diameter D_m , total number concentration N_t , and ice water content IWC above the freezing level retrieved from the QVP data collected in the hurricane Irene on 27 August 2011. The N_t and IWC contours are in logarithmic steps. Overlaid are contours of $Z = 10, 20$, and 30 dBZ.

g. A Microphysical Analysis of the Stratiform Rain Region of Mesoscale Convective Systems Using Polarimetric Radar and In Situ Aircraft Measurements

Amanda Murphy and Alexander Ryzhkov (CIMMS at NSSL), and Greg McFarquhar (CIMMS at OU)

For the first time, a direct comparison of polarimetric radar data and in situ aircraft measurements has been performed in the stratiform parts of MCSs to test a novel polarimetric technique for ice microphysical retrievals. Such a task required development of a special methodology for processing radar data and comparing them with the aircraft observations. In this study, a new radar data processing technique, the column-vertical profile (CVP) technique, is introduced. In situ aircraft microphysical data from two flights during the MC3E and PECAN campaigns were analyzed as the UND Citation and P-3 aircraft flew within the stratiform rain regions of four MCSs. The vertical profiles of polarimetric radar variables and radar-retrieved parameters of size distribution (SD) of ice are associated with a vertical column that follows the aircraft track. The retrieved parameters of SD include particles' mean volume diameter (D_m), total number concentration (N_t), and ice water content (IWC).

Fig. 2g shows point-by-point collocation of ice microphysical retrieval data to aircraft in situ data for a mesoscale convective system sampled during the MC3E campaign on May 20, 2011. Points represent radar microphysical retrievals, and the lines represent aircraft in situ data for collocated times and three-dimensional locations. The results of the radar – aircraft comparison are promising. A large majority of the points (greater than or equal to 68% of all points on each panel) have less than a 100% error when compared to the aircraft in situ data, which is the upper limit for propagated uncertainty of imaging probes for both particle size and concentration.



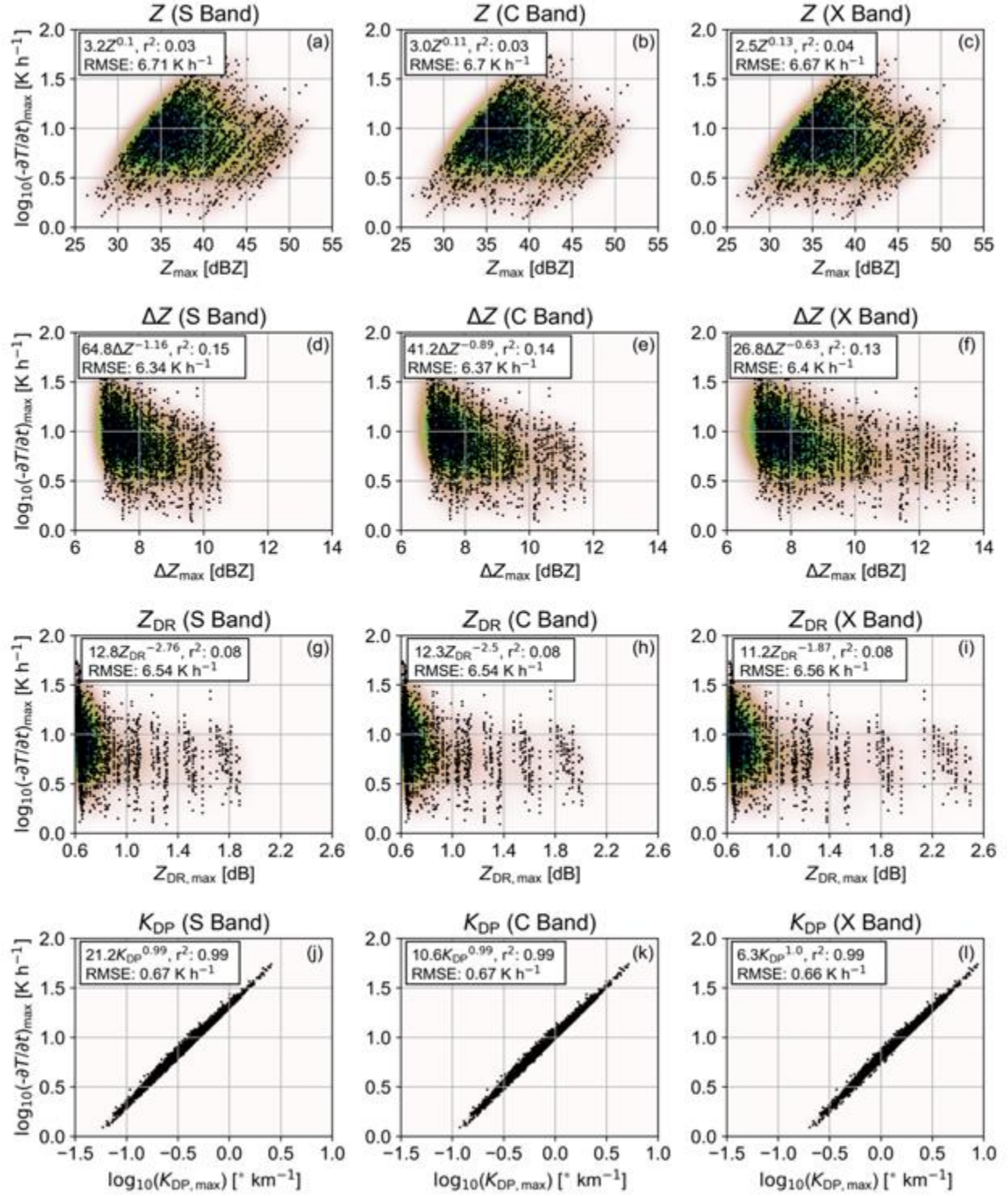
Collocated aircraft in situ data (solid line) and ice microphysical retrievals of moving CVP data (dots) collected on May 20, 2011. Panels are of (a) D_m (radar) and median mass diameter (D_{mm} , aircraft), (b) N_t , and (c) IWC. The height of the melting layer was subjectively determined to be 4.5 km, and data collected below that level are not shown. Units are (a) mm, (b) L^{-1} , and (c) g/m^3 .

h. Spectral Bin Modeling Studies of Polarimetric Thermodynamic Retrievals

Jacob Carlin and Alexander Ryzhkov (CIMMS at NSSL)

Latent heating and cooling associated with hydrometeor phase changes can have significant effects across a wide range of temporal and spatial scales. A number of techniques have been developed to estimate latent heating and cooling rates in precipitation systems from radar reflectivity and derived wind fields. However, the discovery of numerous polarimetric signatures associated with distinct microphysical processes and the added microphysical information they contain suggest the potential for improved estimates of latent heating and cooling rates using radar polarimetry.

Using a suite of models with spectral bin microphysics coupled to a polarimetric radar operator, the potential for estimating heating rates within convective updrafts, cooling rates within convective downdrafts, and cooling rates within the melting layer in stratiform precipitation using polarimetric radar data is examined. Results from Hebrew University Cloud Model simulations suggest a reliable relation between Z_{DR} column characteristics (e.g., height) and the vertical profile of latent heating within and above the column that can be used to construct a look-up table. A one-dimensional model of melting snow was used to model the bright band characteristics for a wide array ($n = 2700$) of characteristic snow size distributions (based on reported in situ observations), environmental lapse rates and humidity profiles, and radar wavelengths. While the maximum Z , Z_{DR} , and ΔZ in the bright band contained little to no information about the maximum cooling rate within the melting layer, the maximum K_{DP} was found to be highly correlated with the concurrent cooling rate across environments and wavelengths. Work is ongoing to establish the existence and nature of relations between the polarimetric variables and cooling rates within convective downdrafts due to the sublimation, melting, and evaporation using an analogous one-dimensional model of melting hail and graupel.



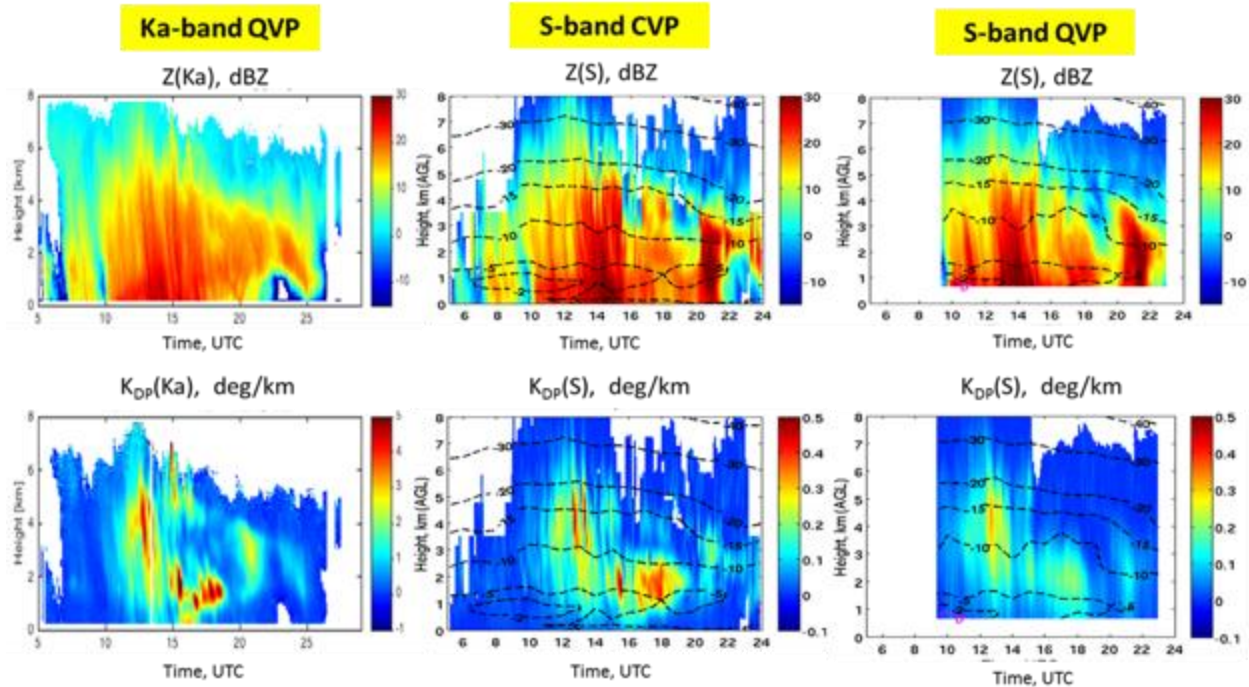
Comparison of maximum (a-c) Z [dBZ], (d-f) ΔZ [dBZ], (g-i) Z_{DR} [dB], and (j-l) $\log_{10}(K_{\text{DP}})$ [$^{\circ} \text{ km}^{-1}$] and the maximum cooling rate (expressed in $\log_{10}(-\partial T/\partial t)$) for a lapse rate of $6.0^{\circ} \text{ C km}^{-1}$ and a relative humidity gradient of $-3.0\% ^{\circ} \text{ C}^{-1}$ at S, C, and X bands.

i. Exploring Synergy Among Polarimetric, Multi-Frequency, and Doppler Radar Measurements to Provide Information About Microphysical and Kinematic Processes in Ice and Mixed-Phase Clouds

Alexander Ryzhkov and Pengfei Zhang (CIMMS at NSSL)

CIMMS researchers collaborate with the radar group at the Stony Brook University (SBU) to explore the synergy between polarimetric, multi-frequency, and Doppler radar measurements to provide information about microphysical and kinematic processes in winter storms. Observations of a number of winter storm events in the US Northeast using the operational KOKX WSR-88D radar and the research Ka-band scanning polarimetric radar (KASPR) belonging to SBU have been performed during the 2017 – 2018 winter season. Novel methodologies to process and display polarimetric radar data such as Quasi-Vertical Profiles (QVP) and Columnar Vertical Profiles (CVP) have been utilized to reveal temporal evolution of polarimetric radar variables in a storm cycle and to match the measurements by the two different radars operating at different wavelengths and separated by the distance 22 km.

An example of comparison of the QVP and CVP Z and K_{DP} products obtained from the KASPR and KOKX data respectively is illustrated in the figure below. Direct comparison of the Ka-band QVP and S-band CVP data exhibits a close match of the K_{DP} values scaled by the radar wavelength ratio (which indicates predominantly Rayleigh – type scattering at Ka-band) and a general consistency of the Z measurements at both wavelengths except for the periods when the Parsivel disdrometer detects very large snowflakes responsible for a noticeable difference in Z (i.e., dual-wavelength ratio). This demonstrates that the QVP/CVP approach to generate and display multi-frequency dual-polarization radar data *effectively mitigates the problem of beam matching for the radars operating at different wavelengths*.

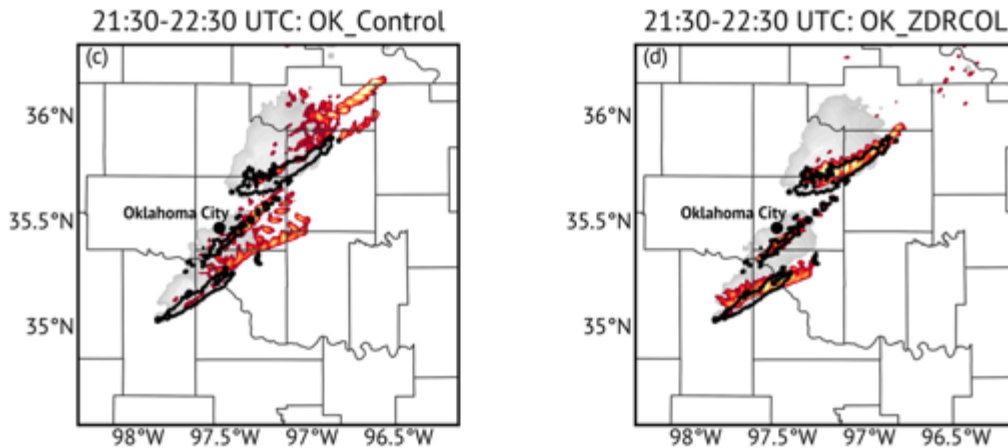


Comparative analysis of the Ka-band and S-band Z and K_{DP} measured by KASPR and KOKX during snowfall event on 4 January 2018. Left panels: QVPs of Z and K_{DP} retrieved from the KASPR data at elevation 15°. Middle panels: CVPs of Z and K_{DP} obtained from the KOKX data in a column with horizontal size 20 km x 20° centered at KASPR. Right panels: QVPs of Z and K_{DP} retrieved from the KOKX data. Overlaid are the isotherms retrieved from the RAP model.

j. Assimilation of Z_{DR} Columns into Storm-Scale Models

Jacob Carlin (CIMMS at NSSL), Jeff Snyder (NSSL), and Alexander Ryzhkov (CIMMS at NSSL)

Weather radar data is a primary source of information for assimilation into storm-scale models. One common method for accomplishing this is using a cloud analysis approach, which employs empirical rules for reflectivity (Z) to insert hydrometeors and temperature and moisture increments to aid the spin-up of convection in the model. Differential reflectivity (Z_{DR}) columns are ubiquitous polarimetric signatures that serve as indicators for updrafts in deep moist convection but have yet to be utilized for assimilation into storm-scale models. Predicated on the use of Z_{DR} columns as proxies for updrafts, the Advanced Regional Prediction System (ARPS) cloud analysis was modified to assimilate Z_{DR} columns by inserting increments of temperature and moisture where Z_{DR} columns are detected. Studies were performed for two real cases (the 19 May 2013 tornado outbreak in central Oklahoma and the 25 May 2016 tornadic supercell in north-central Kansas) in which the short-term forecasts from the original reflectivity-based cloud analysis were compared to those that assimilated Z_{DR} column information. Positive impacts were observed for both cases through the duration of each 1-h forecast period, including a reduction in analyzed spurious convection, better forecasts of mesocyclone path compared to observed rotation tracks, and improved quantitative verification scores.

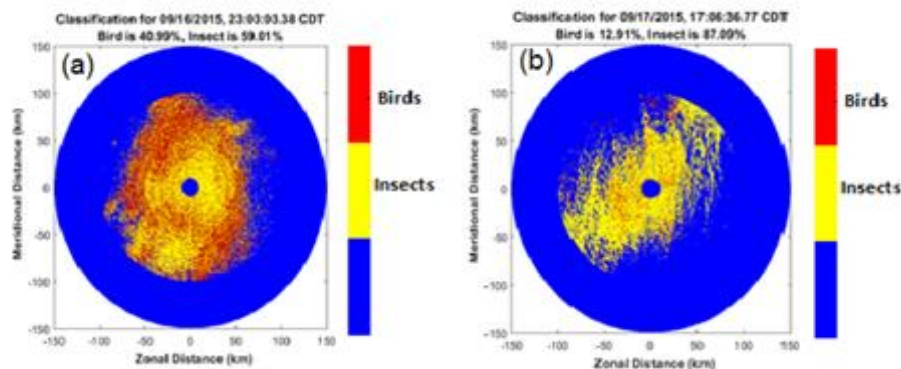


Comparison of 1-h 1-6 km updraft helicity forecasts (reds) and observed MRMS rotation tracks (0.01 s^{-1} , black contours) from the (left) original cloud analysis and the (right) cloud analysis with Z_{DR} column assimilation for the 19 May 2013 case.

k. Discrimination Between Radar Echoes from Birds and Insects Using Polarimetric Radar

Valery Melnikov and Precious Jatau (CIMMS at NSSL)

Flying birds are a hazard for aviation. It is important to detect birds near the aircraft routes. The WSR-88D can detect a small single bird at distances up to 100 km from the radar. “Clear air” radar echoes are originated from birds and insects. Insects are not a hazard for aviation, therefore an algorithm is needed to distinguish radar echoes from birds and insects. To separate bird echoes, all dual-polarization radar parameters have been used along with their spatial texture. A fuzzy logic algorithm has been developed using these radar variables. Some results are shown in the figure below. Panel (a) shows mostly birds in the atmosphere on September 16, 2015 at about midnight whereas panel (b) shows the results for the next day at about 5 pm when insects dominate radar echoes. The images have been obtained using data from the operational KTLX WSR-88D radar.



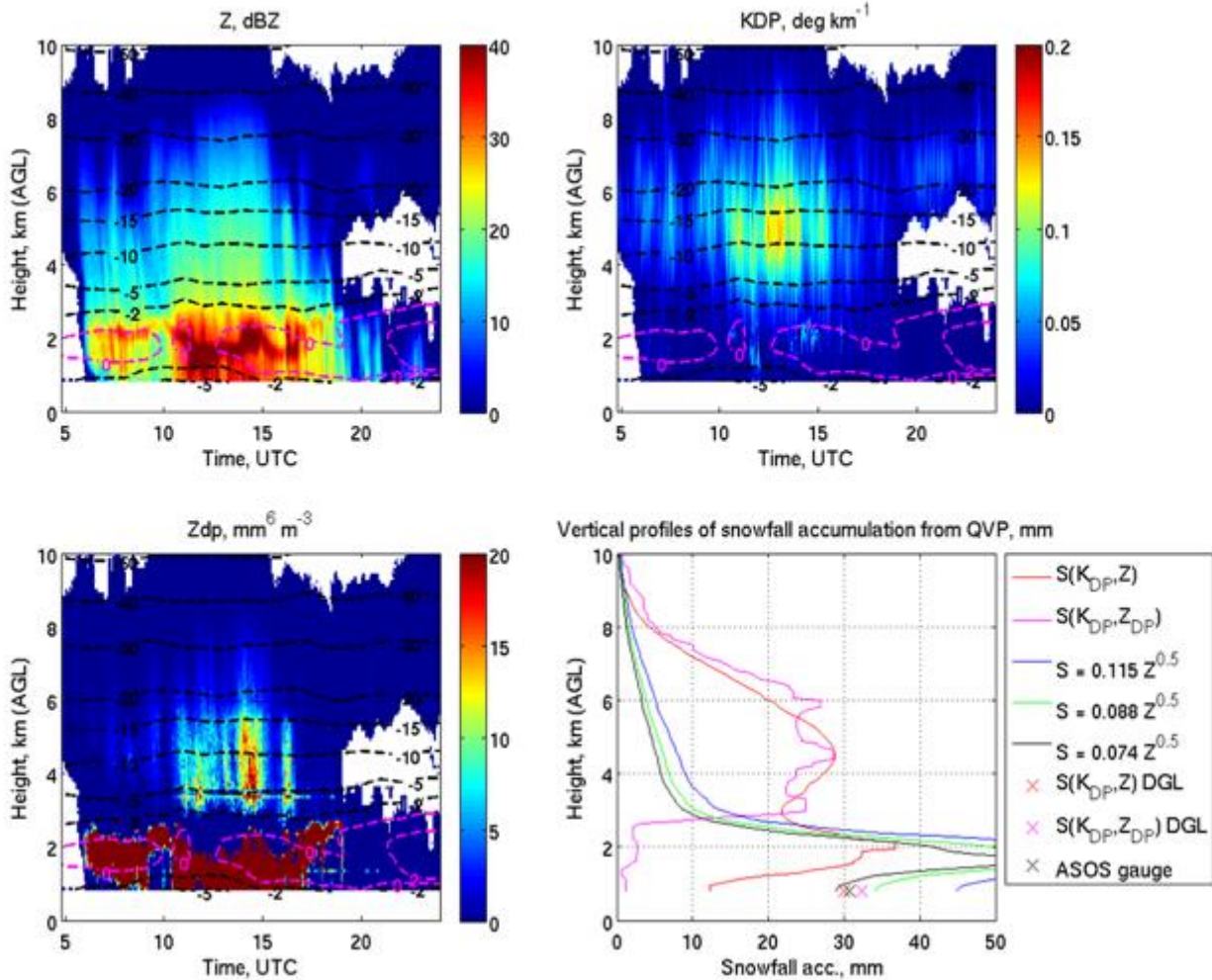
Results of radar echo classification for two days of observations.

I. Polarimetric Measurements of Snow

Petar Bukovcic and Alexander Ryzhkov (CIMMS at NSSL)

Tremendous variability of snow particle size distributions (PSDs), shape, orientation, crystal habits, density, water content, etc. makes radar measurements of snow extremely challenging. Thus, quantitative precipitation estimation (QPE) of snow with radar is very difficult. Snow estimations with standard $S(Z)$ relations are unreliable, moreover, ground measurements of snow liquid-water equivalent S are often unsatisfactory. Although significant strides in identification of snow with polarimetric radar have been made in the past, not much work on the polarimetric snow estimation has been done. For the same reflectivity factor, radar estimates using the standard $S(Z)$ relations (Z is usually proportional to S^2) exhibit roughly an order of magnitude difference in snowfall amounts.

We use extensive snow disdrometer data – measured snow particle size distributions (PSD's), collected in central Oklahoma from late 2006 until early 2015, to derive polarimetric relations for liquid-water equivalent snow rate S using specific differential phase K_{DP} and reflectivity Z , in a form of bivariate power-law relation $S = \gamma K_{DP}^\alpha Z^\beta$. We also use theoretical simulations to derive $S(K_{DP}, Z, Z_{DP})$ relation for the exponential snow size distribution. Our proposed methodology is applicable to the cloud depth from the ice crystal forming region through aggregation, which in winter storms often extends down to the ground. We submit that over such layer the flux of ice water is constant. The bulk of precipitation (80-90% of total precipitation) is formed within the dendritic growth layer (DGL, -20°C to -10°C), where K_{DP} , and to some extent, Z_{DP} , exhibit the most pronounced signatures. We are trying to utilize this K_{DP}/Z_{DP} feature to relate the values of S obtained within the DGL to the in situ measurements on the ground through the aid of the Quasi Vertical Profile (QVP) methodology. As an example, the QVPs from the KCAE WSR-88D (19.5 deg) of Z , K_{DP} , Z_{DP} and vertical profiles of snow accumulation obtained from QVP of snowfall rate S are presented in the figure below. Both $S(K_{DP}, Z)$ and $S(K_{DP}, Z, Z_{DP})$ show very promising results within the DGL, with the accumulation estimate close to the ground measurements.



QVPs of a) Z in dBZ, b) K_{DP} in deg km^{-1} , c) Z_{DP} in $\text{mm}^6 \text{m}^{-3}$, KCAE, 19.5 deg elevation angle, Columbia SC, 12 February 2014. The black dashed lines are isotherms (RAP model), where the temperatures above the 0°C are highlighted in magenta; d) vertical profiles of total snowfall accumulation obtained from KCAE 19.5 deg QVPs using various $S(Z)$ s, $S(K_{DP}, Z)$ and $S(K_{DP}, Z, Z_{DP})$ relations. The black cross (X) represents collocated reference ground measurement of snow liquid-water equivalent presented at the lowest snowfall accumulation height; red and magenta crosses are estimates of snowfall accumulation from $S(K_{DP}, Z)$ and $S(K_{DP}, Z, Z_{DP})$ using the $\max(K_{DP})$ value from the DGL (-20°C to -10°C).

Publications

- Bluestein, H. B., K. J. Thiem, J. C. Snyder, and J. B. Houser, 2018: The multiple-vortex structure of the El Reno, Oklahoma tornado on 31 May 2013. *Monthly Weather Review*, **146**, 2486–2502.
- Bukovcic, P., A. Ryzhkov, D. Zrnica, and G. Zhang, 2018: Polarimetric radar relations for quantification of snow based on the disdrometer data. *Journal of Applied Meteorology and Climatology*, **57**, 103 – 120.
- Carlin, J., J. Gao, J. Snyder, and A. Ryzhkov, 2017: Assimilation of Z_{DR} columns for improving the spin-up and forecast of convective storms in storm-scale models: Proof-of-concept experiments. *Monthly Weather Review*, **145**, 5033 – 5057.
- Cocks, S., Y. Wang, L. Tang, A. Ryzhkov, P. Zhang, J. Zhang, and K. Howard, 2018: A prototype quantitative precipitation estimation algorithm for operational S-band polarimetric radar utilizing

- specific attenuation and specific differential phase: Part II – Case study analysis and performance verification. *Journal of Hydrometeorology*, accepted pending revision.
- Griffin, C. B., C. C. Weiss, A. E. Reinhart, J. C. Snyder, H. B. Bluestein, J. Wurman, and K. A. Kosiba, 2018: In situ and radar observations of the low reflectivity ribbon in supercells during VORTEX2. *Monthly Weather Review*, **146**, 307 – 327.
- Griffin, E., T. Schuur, and A. Ryzhkov, 2018: A polarimetric analysis of ice microphysical processes in snow, using quasi-vertical profiles. *Journal of Applied Meteorology and Climatology*, **57**, 31 – 50.
- Hu, J., D. Rosenfeld, D. Zrnic, E. Williams, P. Zhang, J. Snyder, R. Orville, A. Ryzhkov, E. Hashimshoni, R. Zhang, R. Weitz, 2018: Multiple convective cell identification and tracking algorithm for documenting time-height evolution of polarimetric radar variables and lightning properties. *Journal of Applied Meteorology and Climatology*, accepted pending revision.
- Iltoviz, E., A. Khain, A. Ryzhkov, and J. Snyder, 2018: Relationship between hail microphysics, aerosols, and Z_{DR} columns. *Journal of the Atmospheric Sciences*, **75**, 1755 - 1781.
- Kuster, C. M., P. L. Heinselman, J. C. Snyder, K. A. Wilson, D. A. Spehger, and J. E. Hocker, 2017: An evaluation of radar-based tornado track estimation products by Oklahoma public safety officials. *Weather and Forecasting*, **32**, 1711 – 1726.
- Oue, M., P. Kollias, A. Ryzhkov, and E. Luke, 2018: Towards exploring the synergy between cloud radar polarimetry and Doppler spectral analysis in deep cold precipitating systems in the Arctic. *Journal of Geophysical Research: Atmospheres*, **123**, 2797 – 2815.
- Wienhoff, Z., H. B. Bluestein, L. J. Wicker, J. C. Snyder, A. Shapiro, C. K. Potvin, J. B. Houser, and D. W. Reif, 2018: Applications of a spatially variable advection correction technique for temporal correction of dual-Doppler analyses of tornadic supercells. *Monthly Weather Review*, **146**, 2949–2971.
- Witt, A., D. W. Burgess, A. Seimon, J. T. Allen, J. C. Snyder, and H. B. Bluestein, 2018: Rapid-scan radar observations of an Oklahoma tornadic hailstorm producing extremely large hail. *Monthly Weather Review*, in press.
- Wang, Y., S. Cocks, L. Tang, A. Ryzhkov, P. Zhang, J. Zhang, and K. Howard, 2018: A prototype quantitative precipitation estimation algorithm for operational S-band polarimetric radar utilizing specific attenuation and specific differential phase: Part I – Algorithm description and initial results. *Journal of Hydrometeorology*, accepted pending revision.

Awards

Mercator Fellowship (Germany) – **Alexander Ryzhkov**

3. MPAR Meteorology

Overall Objectives

Advance scientific understanding of storms and evaluate operational benefits provided by rapid-scan radar data.

Accomplishments

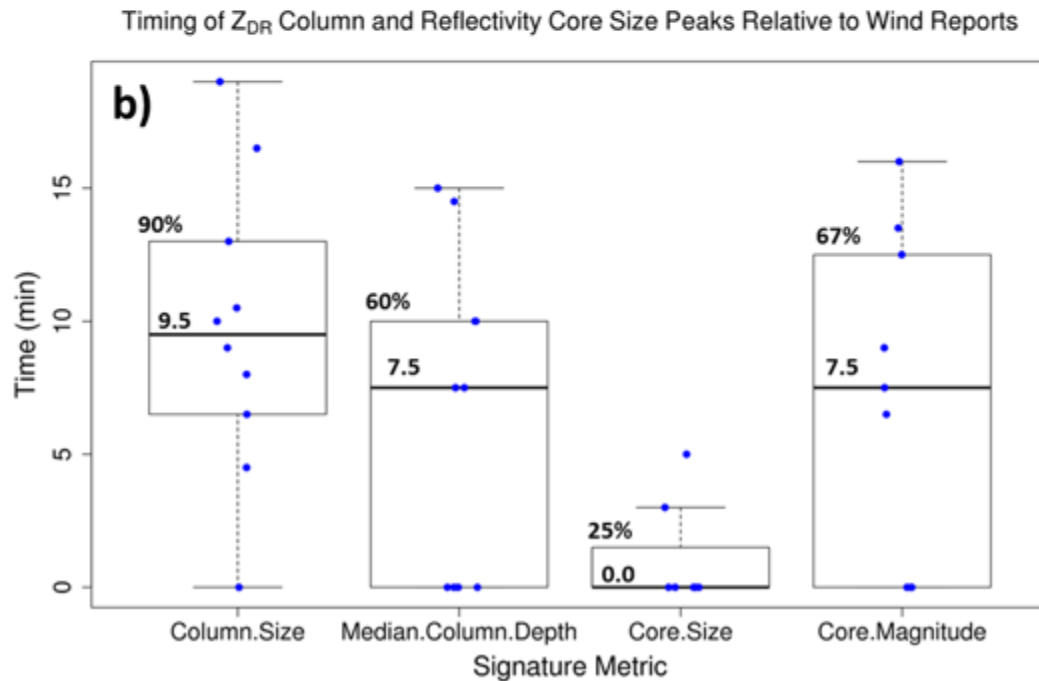
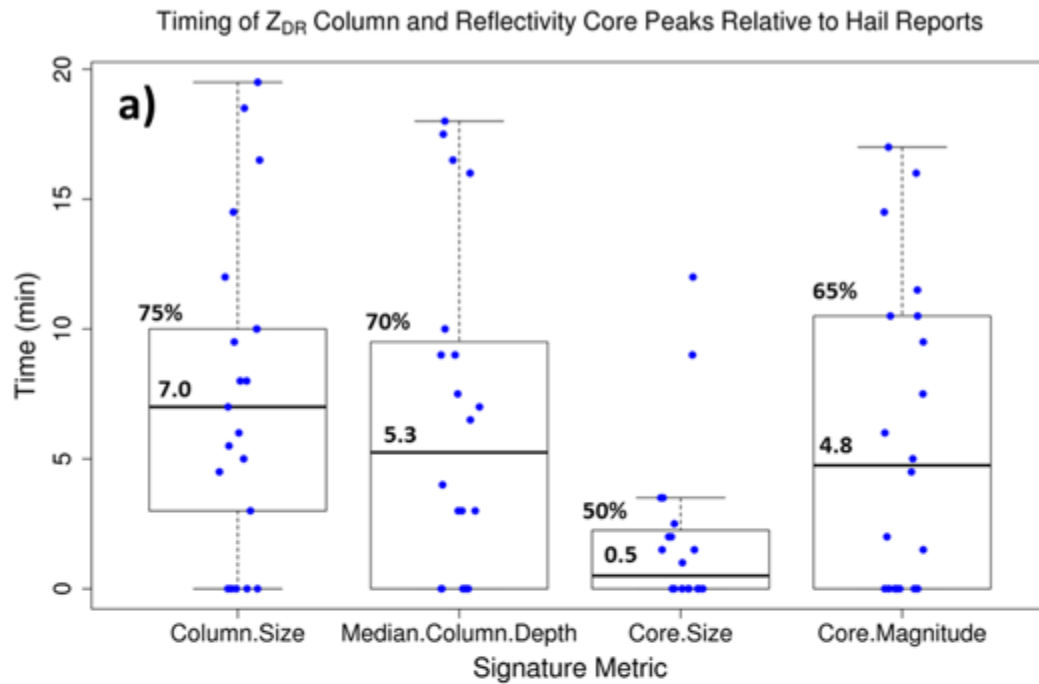
a. Rapid-Scan Radar Observations of Z_{DR} Column Depth and its Potential Use During the Warning Decision Process

Charles Kuster, Terry Schuur, Jeff Brogden, and Robert Toomey (CIMMS at NSSL), Jeffrey Snyder and Pam Heinselman (NSSL)

With the recent dual-polarization upgrade of the National Weather Service (NWS) radar network, new data is now available to NWS forecasters. One new signature forecasters can see is the Z_{DR} column, which is an indicator of thunderstorm updraft location and magnitude. To examine the evolution of this potentially useful signature, we used a

research Weather Surveillance Radar-1988 Doppler radar located in Norman, Oklahoma (KOUN) to collect rapid-update volumetric data of severe and nonsevere thunderstorms using 90-degree sector scans. Our analysis considered 15 of these rapid-update cases.

In an effort to better integrate Z_{DR} columns into existing NWS forecaster conceptual models, Z_{DR} column depth size and magnitude were compared to -20°C reflectivity cores, mesocyclone intensity, and local storm reports for 43 different storms ranging from tornadic supercells to nonsevere single cells. Over 1400 radar volume scans were included in the analysis, which has revealed that 1) there is a statistically significant difference between the Z_{DR} column depth size and magnitude of severe and nonsevere storms but not between tornadic and nontornadic supercells, 2) Z_{DR} column depth tends to evolve prior to -20°C reflectivity and therefore provides slightly longer lead time for severe wind and hail reports, and 3) rapid-update volumetric radar data samples trends in Z_{DR} column depth evolution more completely and up to four minutes earlier than traditional-update data (5–6 min volumes), which can provide forecasters with additional lead time prior to severe wind and hail reports.

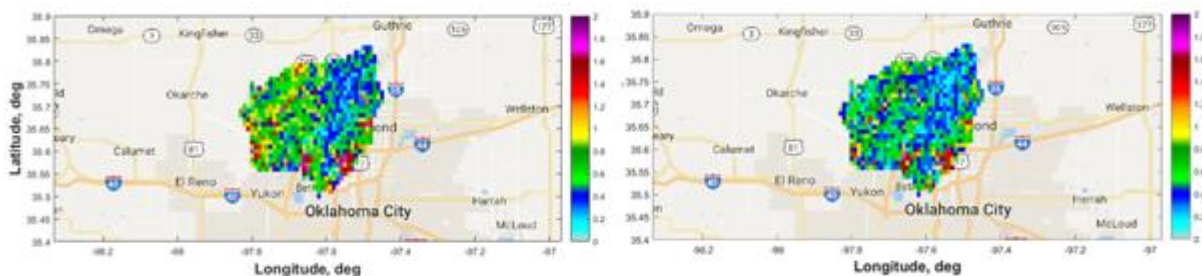


Box and whisker plot showing timing of radar metric peaks (i.e., local maxima) prior to a) severe hail reports and b) severe wind reports. Median value and percentage of reports preceded by a peak in each signature metric are annotated. The middle black line indicates the median value, box edges indicate the lower and upper quartiles (i.e., interquartile range), and whiskers indicate the minimum and maximum values (excluding outliers). Blue dots indicate timing data for each severe-weather report used to create the plot.

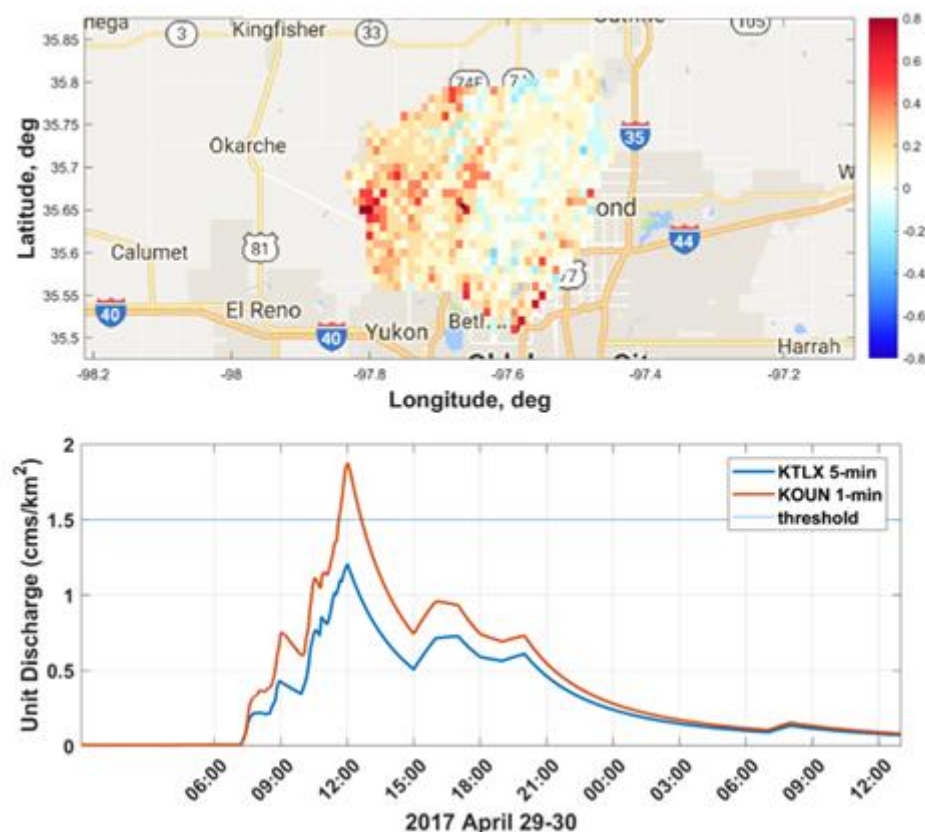
b. Evaluate the Operational Benefits of Higher Temporal Resolution Data on Flash Flooding Early Warning Using Rapid-Scan KOUN Dual-Polarization Data Sets

Berry Wen, Terry Schuur, and Charles Kuster (CIMMS at NSSL)

Conventional WSR-88D radars provide rainfall intensities at approximately five minute intervals, therefore often missing peak rainfall rates in severe weather events that evolve rapidly. In order to evaluate the potential ability of higher temporal resolution data to provide improved flash flood warnings, Ensemble Framework for Flash Flood Forecasting (EF5) hydrologic model simulations were conducted using rapid-scan KOUN dual-polarization data collected during the April 29, 2017 flash flooding event over the Cottonwood Creek watershed near Seward, OK. In order to test the influence of different temporal-spatial precipitation data on flash flooding simulation, the rapid-scan KOUN data were reconstructed to different temporal and spatial resolutions that matched the mainstream remote sensing Quantitative Precipitation Estimation (QPE) products, such as the conventional 5-min resolution provided by operational WSR-88D radars. The results showed that the runoff generated by rapid-scan KOUN QPE at 1-min temporal resolution better matched stream gauge observations than that generated by 5-min QPE. Furthermore, the unit runoff using KOUN revealed higher maximum values, thereby indicating the ability of high temporal resolution data to better capture flash flooding.



The maximum unit runoff simulated using (left panel) rapid-scan KOUN 1-min QPE; and (right panel) standard 5-min QPE over Cottonwood Creek watershed near Seward, OK.



Upper panel, difference of maximum unit flow between KOUN and KTLX; Lower panel, time series of unit runoff from the location indicated as a black point in the Upper panel figure.

c. Examining Benefits of Rapid-Update Radar Data and Tornado Track Estimation Products to Emergency Managers

Charles Kuster, Katie Wilson, and Terry Schuur (CIMMS at NSSL), Jeffrey Snyder and Pam Heinselman (NSSL), Doug Speheger (NWS), and James Hocker (OCS)

Emergency managers are an important end user of radar data and radar-based products. Based on results from research conducted in FY17 and published in October 2017 (Kuster et al. 2017), more specific surveys were created to obtain emergency manager feedback on various tornado track estimation products and determine if radar update time impacted use of these products. Surveys were given at three different emergency manager meetings across the state of Oklahoma. Participants indicated that filtering lower values of azimuthal shear from the rotation track product would be useful for short-lived tornadoes produced by quasi linear convective systems, but not for other longer-lived tornadoes. Participants also indicated a strong preference for tornado track estimation products created using rapid-update data primarily because the product was more complete and easier to use.

d. Collection of Rapid-Scan KOUN Dual-Polarization Data in Support of MPAR and WoF Studies.

Charles Kuster, Terry Schuur, and Berry Wen (CIMMS at NSSL)

One of the primary objectives of the MPAR Meteorology project is to evaluate potential operational benefits provided by rapid-scan radar data. While considerable previous research that has already been conducted using data collected at a single polarization, however, much has yet to be learned of the operational advantages provided by rapid-scan dual-polarization radar data. As we await the delivery and installation of the Advanced Technology Demonstrator (ATD), which will provide a first ever opportunity to collect rapid-scan dual-polarization radar data with a phased-array antenna, we have therefore been focusing our data collection efforts on the collection of sector scan (thereby providing 1-2 minute updates) dual-polarization data sets by the KOUN WSR-88D radar. In the past year, rapid-scan KOUN data sets were collected for 10 weather events. These included flash flood/heavy rain events, downburst events, severe hail events, quasi-linear convective systems that produced weak tornadoes, and a winter precipitation event that exhibited a broad region of transitional winter weather. In addition to providing additional data sets that can be used to evaluate the operational advantages provided by rapid-scan radar, the data collected as part of this ongoing effort will also be used to support Warn-on-Forecast (WoF) studies and, eventually, to assist in the evaluation of ATD data quality.

Publications

Kuster, C. M., P. L. Heinselman, J. C. Snyder, K. A. Wilson, D. A. Speheger, and J. E. Hocker, 2017: An evaluation of radar-based tornado track estimation products by Oklahoma public safety officials. *Weather and Forecasting*, **32**, 1711–1726.

4. MPAR Engineering

Objectives

Continue research and development in collaboration with NSSL and other government, industry, and university partners to determine the usefulness of phased array radars (PAR) for meteorological observations in a multifunction environment. The National Weather Radar Testbed Phased-Array Radar (NWRT/PAR) in Norman, OK was the first of its kind to study meteorological applications of this technology. The facility is currently being upgraded to take advantage of modern PAR technology and to add a dual-polarization capability. Theoretical, simulation, and experimental studies are being conducted to determine the feasibility of dual-polarized phased-array antenna systems along with the applications of using the radar for multiple functions (e.g., aircraft and weather surveillance). Other areas of research and development include the design of adaptive scanning techniques, the refinement of radar functional requirements, and the evaluation of advanced digital signal processing techniques.

Accomplishments

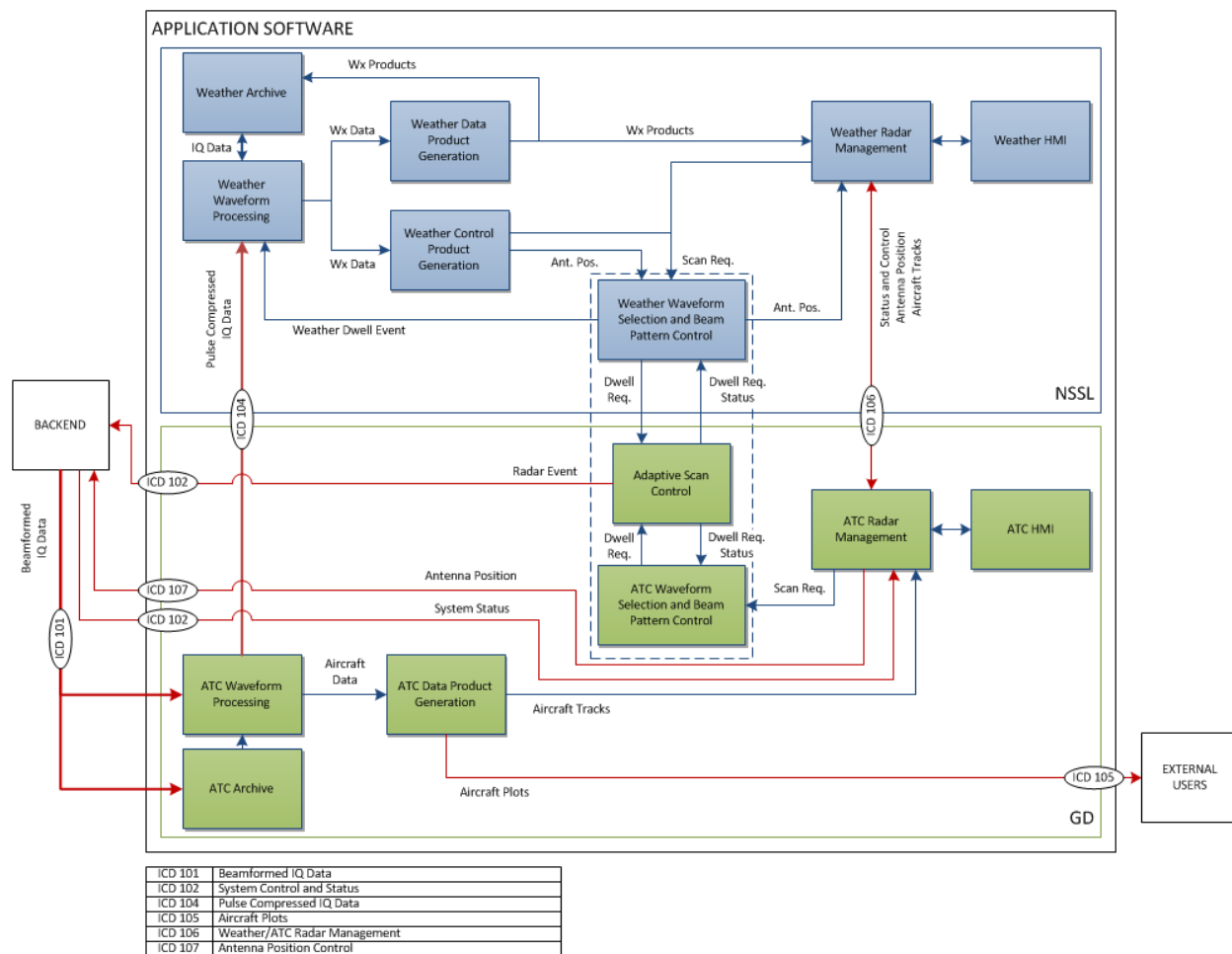
a. MPAR Advanced Technology Demonstrator (ATD)

Christopher Curtis, Eddie Forren, Stephen Gregg, Igor Ivić, David Schwartzman, Christopher Schwarz, Sebastián Torres, and Allen Zahrai, (CIMMS at NSSL), Mark Benner, Kurt Hondl, Micheal Shattuck, and Danny Wasielewski (NSSL), and other government, industry, and university collaborators.

Developed in support of the Multifunction Phased-Array Radar (MPAR) program, the Advanced Technology Demonstrator (ATD) has replaced the legacy SPY-1A antenna at the NWRT with an S-Band, 4-m diameter, dual-polarization, active phased array. The system's operating capabilities are intended to serve as a basis for ongoing engineering and meteorological research at CIMMS and NSSL. The ATD leverages several prior investments in order to provide a flexible, useful system while striving to keep cost and risk low. The antenna system is based around tile-able array panels developed under the MPAR Government Proof-of-Concept Technology Risk Reduction Program carried out by MIT/Lincoln Laboratory. The receiver and exciter electronics leverage work done by General Dynamics Mission Systems (GD) for the United States Navy in support of the Air and Missile Defense Radar development. The radar control system leverages the work done by GD for the Office of Naval Research under the Digital Array Radar and Affordable Common Radar Architecture (ACRA) programs. Finally, the weather signal processor (including the inter-process-communication infrastructure, system control and monitoring, techniques, and algorithms) leverages the work done by CIMMS and NSSL for the legacy NWRT/PAR. Accomplishments by CIMMS staff in three main areas are described next: programmatic, application software, and facilities.

Programmatic Support. We supported programmatic ATD efforts by actively participating in planning and design meetings, by providing input to scheduling decisions, outlining and reviewing system requirements and system design documents, and supporting programmatic milestones such as periodic design review meetings.

Application Software. We continued leading the Application Software portion of the ATD, which involves software developers and engineers from CIMMS and GD. The required functionality of the Application Software includes generating weather- and aircraft-surveillance products, providing scan control and high-level radar control, system status monitoring, and archiving and display of data and products. The goal for the design of the Application Software is to maximally leverage legacy NWRT and ACRA software to reduce risk. The figure below shows the functional architecture of the ATD Application Software and delineates responsibilities between the CIMMS/NSSL (blue) and GD (green) teams.



Block diagram of the application software for the ATD. The application software integrates legacy and new software developed by CIMMS/NSSL (blue blocks) and GD (green blocks).

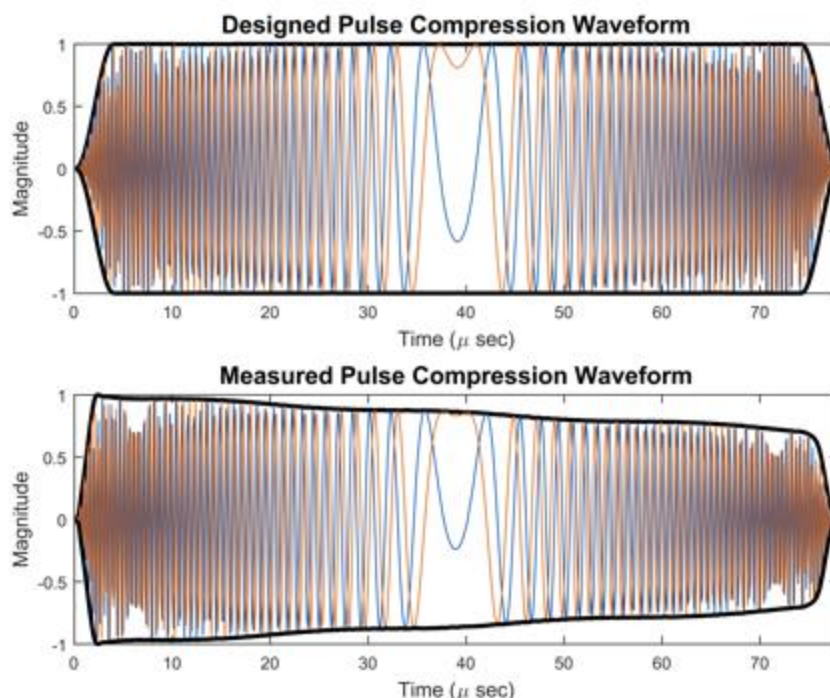
Because the NSSL/GD Application Software baseline is built from of two pre-existing software baselines (each with over 500,000 lines of C, C++, and Java source code), a significant portion of the effort in FY18 was related to finding and fixing software bugs, re-working various portions of the software infrastructure, improving the stability and integration between the two baselines, and dealing with building and configuration issues. Other work included updating the Weather Digital Signal Processing (DSP) software to support new acquisition modes, connecting GD's calibration scanning capabilities to NSSL's weather processing chain, implementing a product database server to support generation of calibration products by MATLAB algorithms, defining and integrating new calibration metadata into the Weather DSP chain, and significantly improving the appearance and functionality of NSSL's Human-Machine Interface (HMI).

An important milestone was accomplished at the end of FY18: we were able to run end-to-end Application Software tests in multifunction mode (Weather and Aircraft surveillance) using the actual Backend hardware at GD. In addition, we ran many long tests using simulated backend data on the development system at NSSL. These tests allowed us to measure memory and bandwidth consumption of the Application Software

across the many nodes in the system. Also, they helped expose several software stability issues that were fixed, leading to more robust data transfers between the Backend and the Application Software sub-systems and between the GD and NSSL portions of the Application Software.

During this reporting period, we also continued to develop the weather signal processing capabilities for the ATD. A new mode for the MATLAB DSP was developed to capture all of the functions needed for the initial testing of the system. This includes the triple-PRF mode and several modifications to simplify and streamline the code. The real-time DSP was also updated to reflect these changes, and another round of validation was performed to ensure that the real-time and MATLAB implementations matched. Methods for calibrating the dual polarization radar variables were developed, and plans were made to implement these methods in the DSP.

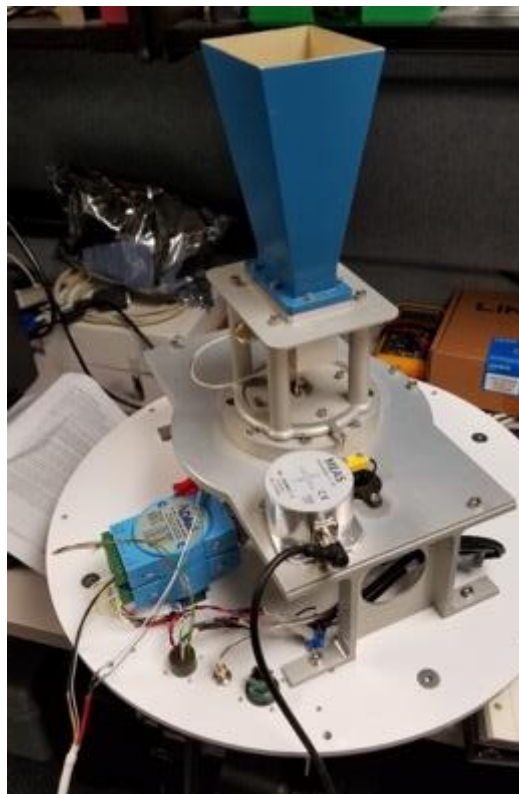
We also spent significant time on developing software to support calibration of the ATD. We created a plan for implementing the calibration “recipes” that have been proposed, some internally and others by collaborators. This includes the infrastructure to get data into MATLAB routines that calculate appropriate calibration values. We continued to use the real-time weather-processing thread that was developed last year and were able to test both phase-coding and spoiled-beam processing. Finally, we analyzed and tested the pulse compression waveforms for weather data collection during the near-field testing of the ATD antenna.



Comparison of a designed pulse compression waveform to the actual waveform measured during the near-field testing of the ATD antenna.

Facilities. In FY18, we managed and developed the contract vehicle for installation of the ATD and the ATD calibration tower. We also worked with General Dynamics in assisting with installation and maintenance of the Application Software development system at NSSL. Further work included the design, acquisition, and fabrication of the ATD calibration tower system and circuits. We also assisted NSSL engineers with the development of the ATD calibration tower controller software. This software is responsible for sending and receiving messages between the Weather and ATC HMI's and the calibration tower.

Additionally, we developed and deployed a data management plan for the ATD. During this process, details such as the architecture for the flow of data, data format, and archive location were ironed out.



Picture of the horn that is controlled by the ATD calibration tower controller software.

b. MPAR Dual Polarization Demonstrator

Igor Ivić, Christopher Schwarz, and Allen Zahrai (CIMMS at NSSL), and Rafael Mendoza and Daniel Wasielewski (NSSL)

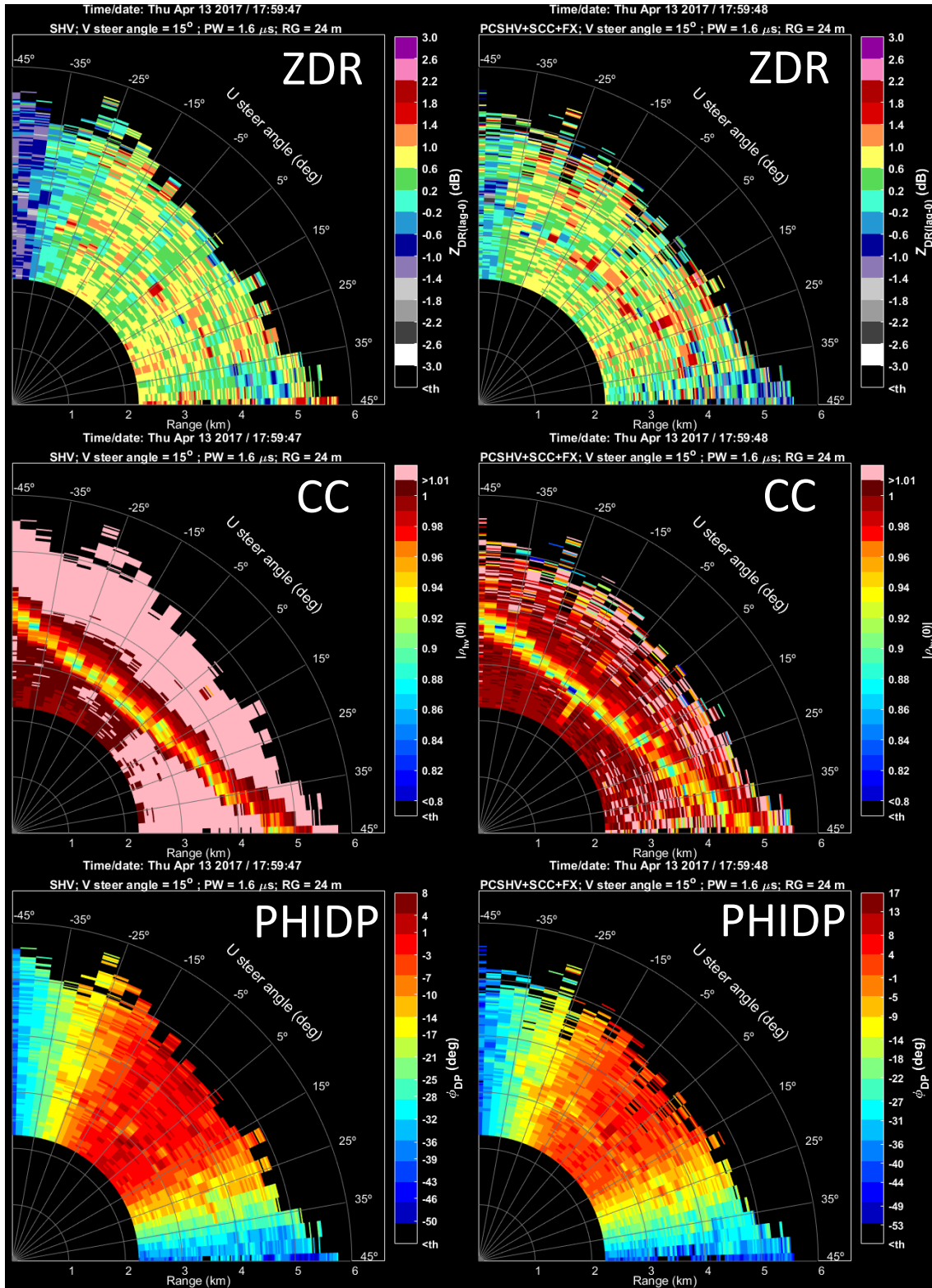
The goal of this project is to evaluate the performance of polarimetric planar phased array technology with respect to the national weather mission. For this purpose, NSSL and the FAA commissioned the construction of a 10-panel, mobile, polarimetric, phased-array system (referred to as the Ten Panel Demonstrator or TPD) by

MIT/Lincoln Laboratory to be used as an evaluation platform to assess the polarimetric performance of the planar phased array technology. A test plan was developed that exercises the capabilities of the demonstration system, which focuses on absolute and relative accuracy measurements. Absolute measurements resolve the system's capability to accurately identify hydrometeors, while relative measurements examine the correct calibration of the system as well as off-broadside cross-polarization impacts. Analyses of the TPD performance have played an important role in defining the expected performance of future systems, including the replacement of the SPY-1A antenna on the NWRT PAR (see the previous project). Thus, the TPD has been an essential tool for the experimental evaluation of the phased array polarimetric performance. Having addressed the most pressing reliability issues with the TPD in FY 16, numerous data sets with the antenna pointing at vertical incidence (i.e., birdbath) were collected in FY17. The array characterization results indicated a strong cross coupling between the horizontal (H) and vertical (V) channels, which exceeds the levels predicted by the theoretical analysis and simulations. During this time, several weather events occurred that prompted the deployment of the 10-panel Demonstrator for data collection testing purposes.



Deployment of the 10-panel Demonstrator up at Max Westheimer Airport on 03 May 2018 during morning convection.

Application of pulse-to-pulse phase coding produced results with visible differences compared to those from non-phase coded data. These differences indicated a reduction of cross coupling as predicted by the analytical derivations and simulations. In FY18, a spectral domain filtering method was developed using the TPD data. This method removes the portion of the cross-coupled signal that is left intact by the original pulse-to-pulse phase coding application (it operates in time domain only) and improves the performance of pulse-to-pulse phase coding. Also, TPD data was used to test the novel time domain approach that combines the phase coded samples to improve performance for small Nyquist velocities (i.e., when spectral domain filtering is not viable).



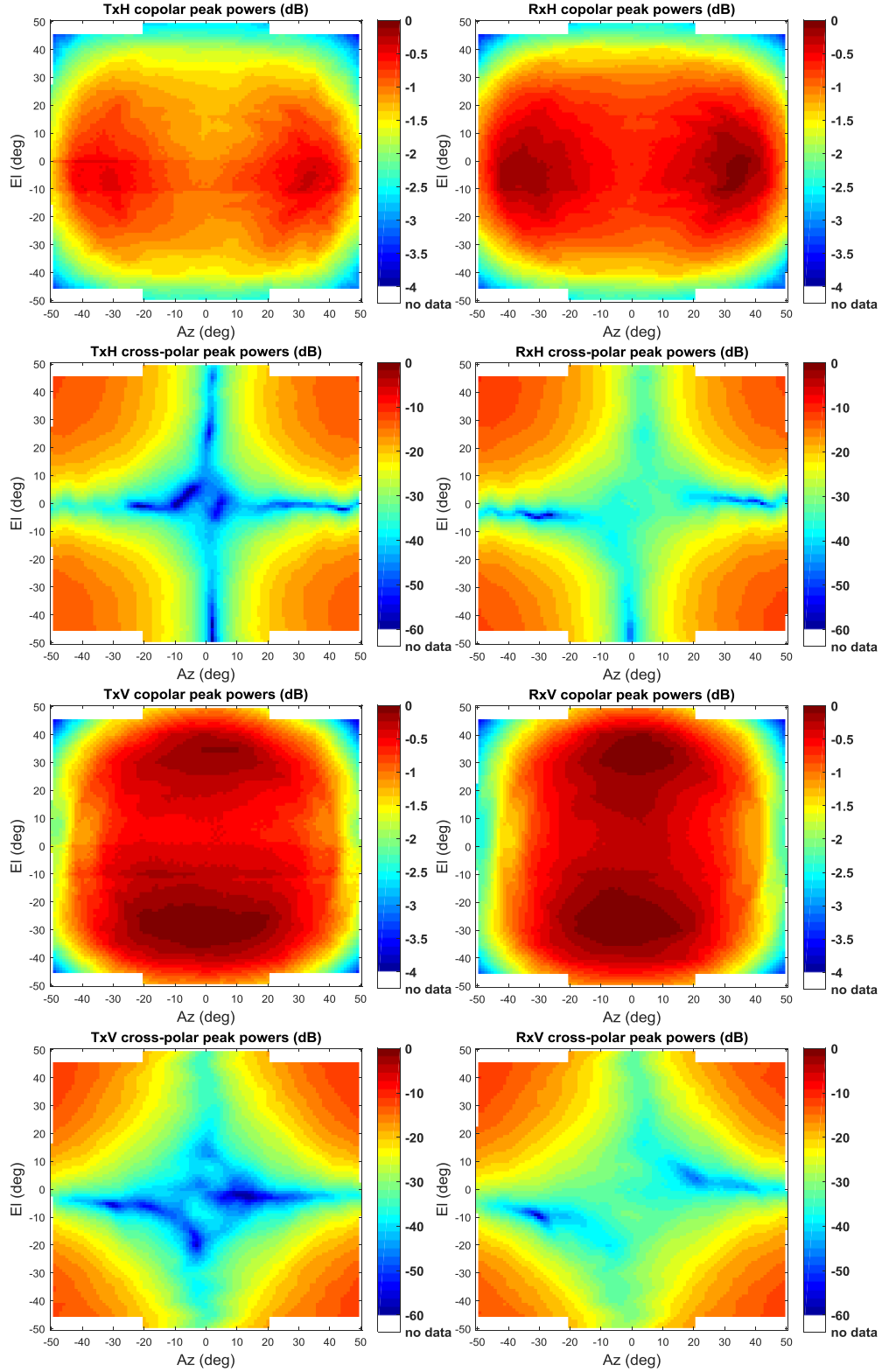
Non-phase-coded (left panels) vs. phase-coded (right panels) data collected with the TPD to demonstrate the advantages of using pulse-to-pulse phase coding to improve the quality of polarimetric data with phased array radar.

c. PAR Dual Polarization

Igor Ivić and Djordje Mirković (CIMMS at NSSL), and Dusan Zrnić (NSSL)

Search for novel methods to improve the polarimetric performance of phased array radars (PAR) is an important part of the effort to determine their usefulness for meteorological observations. In that regard, creating controlled realistic environment in which these methods can be tested is essential. The first step towards this goal is obtaining realistic antenna radiation patterns. This can be achieved using simulations or via measurements. The patterns alone, however, do not provide direct information about the ensuing errors in radar measurements. Hence, a method using a specific set of analytical formulas was developed to compute the biases of polarimetric variable estimates from radiation patterns. Also, a method to produce the simulated weather-like time series which account for polarimetric PAR (PPAR) effects (i.e., cross coupling and antenna gain variations with beam steering) was developed. It achieves this by combining the simulated weather-like time series (which do not account for PPAR effects) and the radiation patterns. Consequently, this method provides for evaluation of standard deviations as well as biases via Monte-Carlo simulations. Both methods, however, depend on the accuracy of computed or measured radiation patterns to produce valid results.

In FY18, extensive measurements were performed by engineers at MIT Lincoln Laboratory while the Advanced Technology Demonstrator (ATD) antenna was in the near-field chamber. Through a collaborative effort between Lincoln Laboratory and CIMMS, the measured data were processed to produce far-field ATD antenna patterns, which were used to assess the ATD polarimetric performance. It is unlikely, though, that the near-field measurements will be adequate for the ATD weather calibration. For this purpose, a tower with the horn antenna will be installed near the ATD site. It will be used to measure the peaks of the ATD antenna patterns on transmit and receive, which will be used to perform the ATD calibration functions. However, the limited accuracy of beam peak measurements will affect calibration quality. Due to its critical importance, an extensive investigation of beam peak measurement aspects was conducted in FY18 and will continue in FY19. As part of this research, an elaborate mathematical mechanism is being developed to support these measurements.



Co-polar and cross-polar transmit (left panels) and receive (right panels) beam peak powers measured in the near-field for the horizontal (top two rows) and vertical (bottom two rows) channels.

d. PAR Computational Electromagnetic Modeling (CEM)

Djordje Mirković (CIMMS at NSSL) and Dusan Zrnić (NSSL)

In FY18, a fully functional and automated model of the Ten Panel Demonstrator (TPD) radar was developed and simulated with beam steering in the horizontal cardinal plane. The TPD was simulated in two set-ups: with and without radome cover. These simulations were of specific interest as they confirmed the hypothesis that a flat radome cover on top of the TPD antenna caused a differential-phase bias in polarimetric measurements. Such finding was also confirmed at X-band with the U. Mass' polarimetric phased array radar. Prior to these findings, a complete validation of the CEM software tools was conducted in collaboration with NSSL and OU Advanced Radar Research Center (ARRC) engineers: CEM results using the single panel model compared favorably with measurements of the real panel in the ARRC's anechoic chamber.

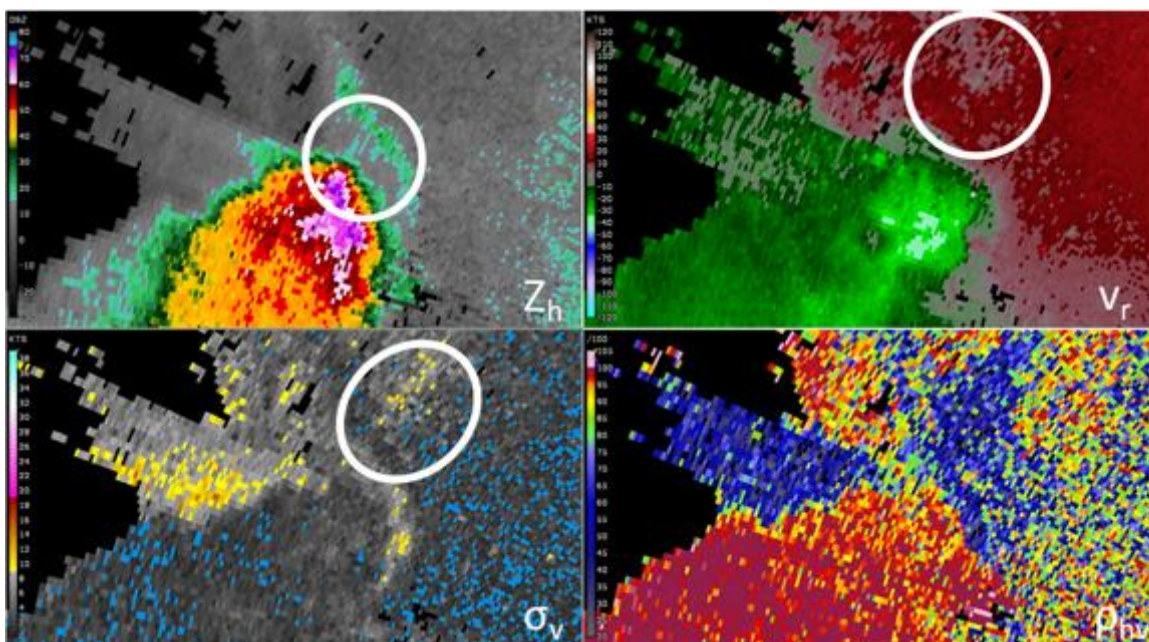
e. SENSR Data Quality Simulations

Feng Nai, Jami Boettcher, Christopher Curtis, David Schwartzman, and Sebastián Torres (CIMMS at NSSL)

The Spectrum Efficient National Surveillance Radar (SENSR) program is an opportunity to integrate weather and aircraft surveillance capabilities by replacing the aging networks of federally owned, fixed, ground-based radar systems, while making at least 30 MHz of bandwidth in the L band available for auction in 2024. One promising candidate to meet the demanding SENSR requirements is a multifunction phased-array radar (MPAR). To provide information to the NOAA/National Weather Service (NWS) about SENSR system requirements for weather surveillance missions, we developed a data quality simulator to qualitatively assess the impacts of specific cost-driving requirements on NWS mission-critical weather features that affect warning decision making. To show the impacts on data quality from modifying the system requirements, we used the Signal Processing And Radar Characteristic (SPARC) simulator to simulate realistic radar data as if they were obtained with radar systems with different design and performance requirements. A library of weather events with different types of weather features was generated and maintained to provide cases for the data quality simulations.

During FY18, we completed the preliminary analysis of the impacts of azimuthal sidelobes on data quality. In the study, 16 azimuthal antenna radiation patterns with varying sidelobe levels were simulated for each of 9 cases involving strong reflectivity gradients. By comparing across all cases, we arrived at an antenna radiation pattern with azimuthal sidelobes that did not meet the SENSR preliminary requirements, yet were still acceptable for NWS mission-critical decision making. The threshold of acceptable was based on forecaster decision making in real-time warning operations. The analysis of these particular cases suggests that it may be possible to relax the antenna radiation pattern requirements in the azimuthal direction for SENSR without

impacting the NWS mission. However, a more comprehensive study involving all stakeholders would be needed to determine new requirements. A preliminary report has been submitted based on these results. The figure below shows an example of simulated radar data that was classified in the acceptable category. Other requirements, such as range sidelobes and sensitivity, were also studied using simulations.



Example of acceptable simulated reflectivity (Z_h), radial velocity (V_r), spectrum width (σ_v), and correlation coefficient (ρ_{hv}) of a storm that was observed by KBGM at 23:50Z on 3 May 2012 at 0.9° elevation. The sidelobe contaminations present (in the circled area) do not negatively impact forecaster interpretation of the radar data.

f. SENSR Command and Control Simulations

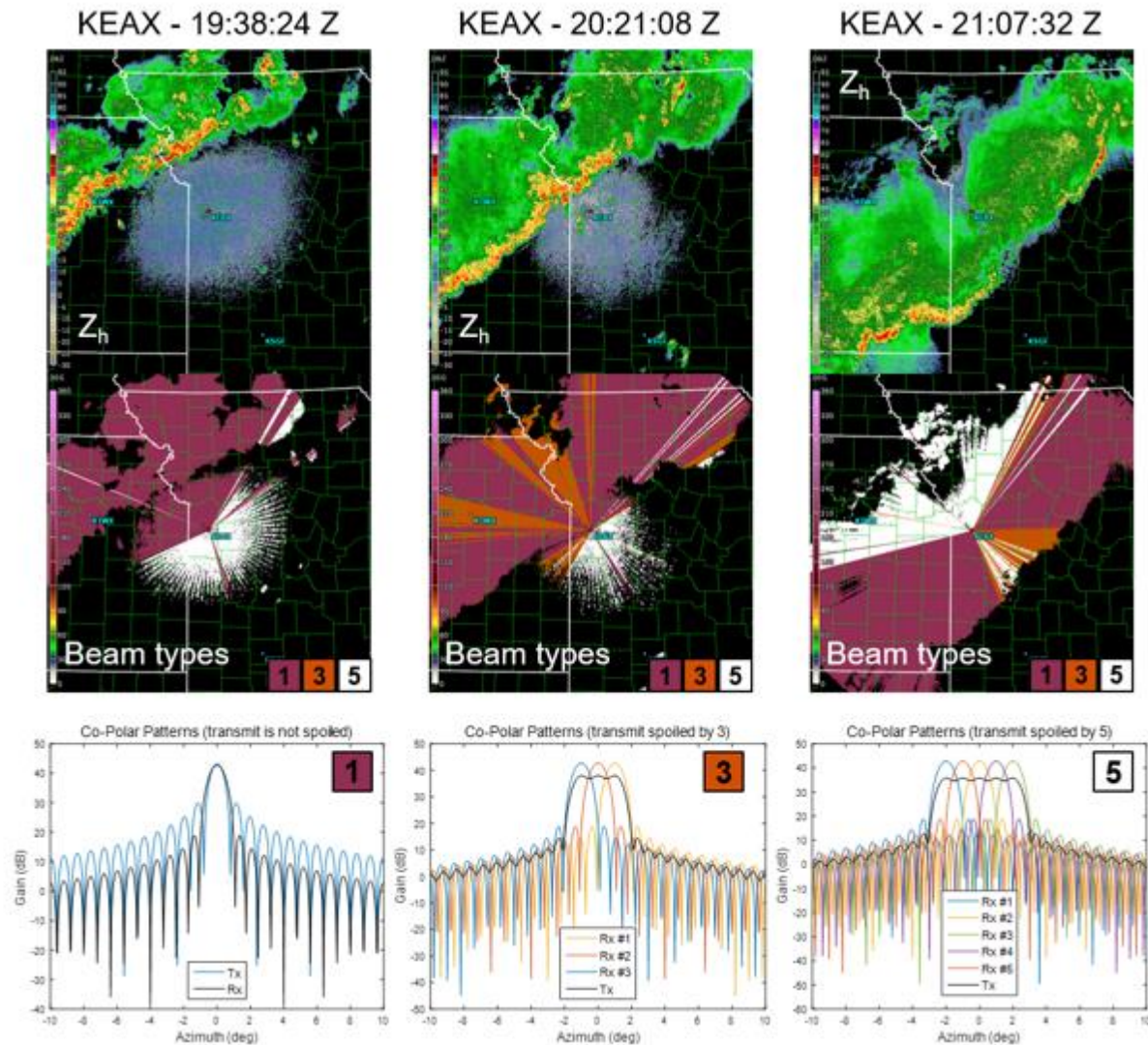
Sebastián Torres and David Schwartzman (CIMMS at NSSL)

The Spectrum Efficient National Surveillance Radar (SENSR) program aims to replace weather and aircraft surveillance capabilities for the aging networks of federally owned, fixed, ground-based radar systems and to make at least 30 MHz of bandwidth in the L band available for auction by 2024. A multi-agency study is being conducted to assess the feasibility of reallocating radar frequencies currently in the L band while addressing cross-agency mission efficiency. One promising candidate to meet the demanding SENSR requirements is a multifunction phased-array radar (MPAR). Implementing the NOAA/National Weather Service (NWS) weather-surveillance function using an MPAR lowers maintenance costs, while introducing new capabilities and tradeoffs that depend on the architecture, geometry, and other system design choices. At the core of an MPAR design are the spatial and temporal sampling requirements for the different functions, which can be met with a combination of radar architecture and concept of operations. Unfortunately, a system that would meet the most demanding requirements for all functions at all times would be prohibitively expensive. Load-shedding algorithms

have to be investigated to find optimum adaptive-scan tradeoffs that minimize the operational impact when not meeting one or more requirements. As such, a well-designed concept of operations exploits the PAR beam agility to surveil the atmosphere using focused and tailored scan strategies, a process commonly referred to as adaptive scanning. Defining rules for adaptive scanning is a complex process; it depends not only on the type and location of storms but also on their temporal evolution. Because data quality, spatial coverage, and temporal resolution are coupled, improving one or more of these inevitably results in a degradation of one or more of the others.

During FY18, we developed a closed-loop command-and-control framework that produces realistic time-series dual-polarization weather radar data. The simulation framework ingests archived radar-variable data from the National Centers for Environmental Information (NCEI) and simulates complex received radar signals for any combination of radar system characteristics and concept of operations. These simulated signals can be processed using conventional and advanced digital signal processing (DSP) techniques to drive different adaptive-scanning algorithms, which dynamically define the scan to be used in the next cycle. The radar-variable data produced by the signal processor using adaptive scanning can be evaluated to assess the operational benefits of different command-and-control schemes. This framework enables the demonstration that it is possible to provide accurate mission-critical weather radar data to NWS forecasters when there are multiple functions competing for radar time.

At the core of the command-and-control simulator is the adaptive scanning algorithm, which was also our focus during FY18. The goal of this algorithm is to dictate how to scan the atmosphere such that other functions can be accommodated in the radar timeline while preserving weather features of interest. There are several ways of reducing the scan time, all of which inevitably degrade the data quality. For an initial demonstration, we chose using spoiled transmit beams as way to reduce the scan time with a relatively low impact on data quality. We applied a load-shedding algorithm that adaptively spoils the transmit beam to process a convective precipitation case originally observed by the Kansas City WSR-88D. Selected time-steps of reflectivity fields and their associated scans are shown in the figure below. Preliminary results indicate that it is possible to meet SENSR's temporal resolution requirements by using adaptive beam spoiling.



Command-and-control simulation for a convective storm in the Kansas City metro area on 6 July 2015. The scan is driven by an adaptive scanning algorithm that selects a type of beam (pencil beam, or beam spoiled by a factor of 3, or beam spoiled by a factor of 5) for different storm regions. Using this scanning strategy, the scan time is reduced by a factor of 2, which would allow other functions to occupy more radar time.

Publications

Ivić, I. R., 2018: Effects of phase coding on Doppler spectra in PPAR weather radar. *IEEE Transactions on Geoscience and Remote Sensing*, **56**, 2043–2065.

Awards

2018 OAR Distinguished Career Award Recipient – **Allen Zahrai**

NSSL Project 2 – Hydrometeorology Research

NOAA Technical Leads: Kenneth Howard and Jian Zhang (NSSL)

NOAA Strategic Goal 2 – *Weather-Ready Nation – Society is Prepared for and Responds to Weather-Related Events*

Funding Type: CIMMS Task II

General Objectives

The hydrometeorology research objectives center on dual-polarized radar research and quantitative precipitation estimations (QPEs). The following are specific objectives:

- Dual-polarized Radar Coverage in Terminal Airspaces and its Effect on Interpretation of Winter Weather Signatures: Current Capabilities and Future Recommendations
- Development of a Probabilistic Subfreezing Road Temperature Nowcast Using Machine Learning
- Alamosa, CO Mobile Radar Deployment and Analysis
- Implementing a new Surface Hydrometeor Classification Scheme in MRMS
- Meteorological Phenomena Identification near the Ground (mPING)
- mPING Random Forest Research
- MRMS Data Quality Control
- Quality Controlling Weather Radar through Hardware Variables
- Advancements in Quality Control of Gauge Observations in the MRMS System
- Feasibility Study for Real-Time Gauge Correction for Wind Undercatch
- MRMS Support for Cloud Detection Algorithm
- Evaluation of Short-Term Model QPF and Satellite QPE Data
- Automated Tropical Trigger Guidance for Dual Pol QPE
- Development and Verification of New QPE Algorithm to Estimate Rainfall
- Evaluating MRMS Operational Dual Pol Quantitative Precipitation Estimates from April 2017 – March 2018
- Assessment of Radar Only QPE in the Hawaiian Islands
- Blending Various Precipitations from Observational and Modeling Platforms to Generate a Multi-Sensor Merged QPE
- Implementation of Advanced Multi-Sensor Analysis and Data Fusion Algorithm for Real-time High-Resolution Quantitative Precipitation Estimation
- MRMS Experimental Testbed for Operational Products (METOP)
- Hydromet Viewer for Salt River Project
- Web Tool Suite for the Radar Operations Center
- QVS Work for the vMRMS system hosted in Norman and Operational Version at the NCO
- Operational Implementation of the Multi-Radar Multi-Sensor System v11.5
- NSSL's Virtual Multi-Radar Multi-Sensor (VMRMS)

Accomplishments

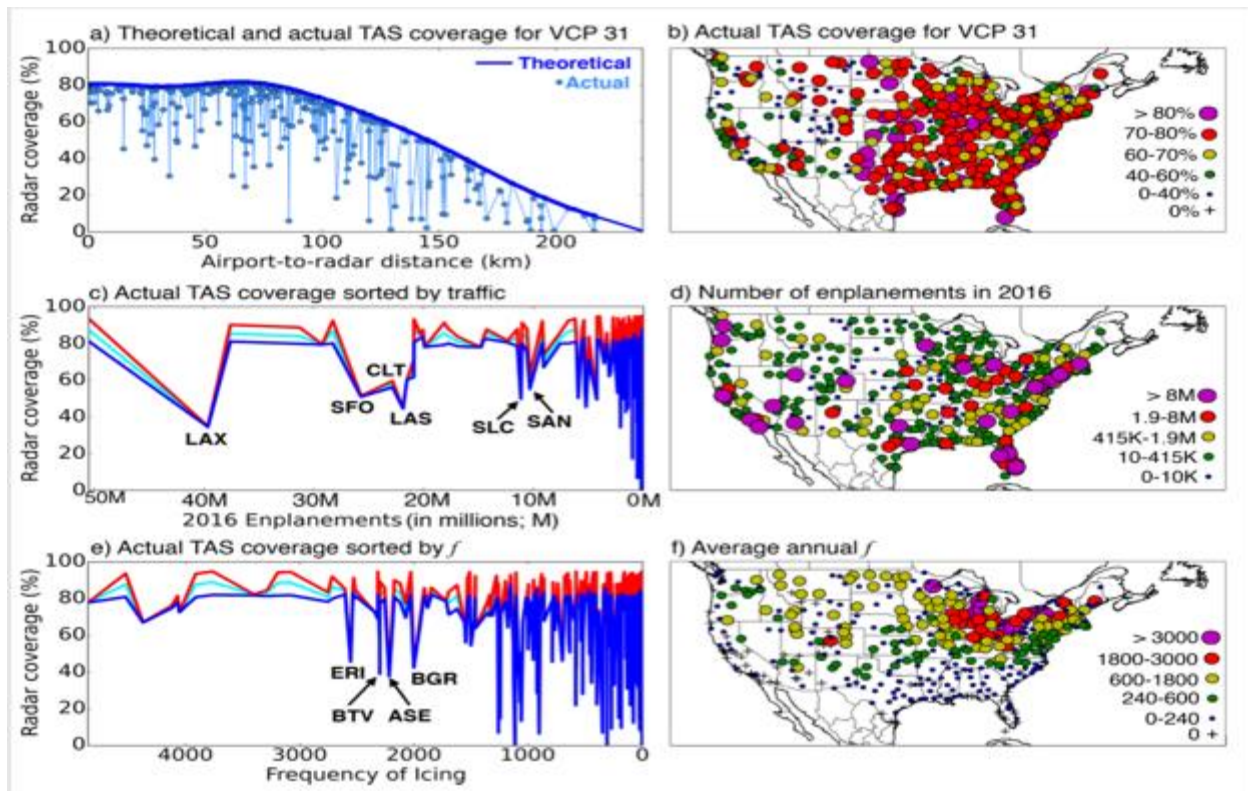
1. Dual-Polarized Radar Coverage in Terminal Airspaces and its Effect on Interpretation of Winter Weather Signatures: Current Capabilities and Future Recommendations

Heather Reeves (CIMMS at NSSL)

This is a feasibility study on the use of dual-polarized radars to infer icing in Terminal Air Spaces TASs of commercial airports. The amount/quality of coverage in each TAS is quantified as a function of its location, traffic, and vulnerability to icing. Though there are some exceptions, most high-traffic or high-icing airports have comparatively good coverage. A major limitation for icing detection is anomalous propagation as most events had an inversion below the top of the TAS. This leads to overestimates in the elevation where icing layers exist and significant contamination from ground clutter. The effects of beam broadening on the radar's ability to resolve key microphysical signatures shows that at most airports dendrite growth and melting can only be resolved in part of the TAS part of the time.

Because most airports have coverage from multiple radars, use of a three-dimensional mosaic was investigated. This does partly mitigate some resolution issues, but the maxima within individual layers are somewhat reduced in the interpolation process. Also, there can be a gap in coverage between the ground and the lowest vertical layer in the mosaic leading to an absence of data in the near-ground environment.

A series of recommendations are made to address the concerns raised by this investigation. These include using only icing tops (not bottoms) to identify areas of icing, use of data mining to retrieve precipitation echo in the presence of ground clutter, and including the beamwidth in radar mosaics. This project is ongoing.



The (a) theoretical and actual TAS coverage sorted by A2R, (c,e), the actual TAS coverage sorted by the number of annual enplanements and frequency of icing f , (b,d,f) spatial distributions of the TAS coverage, number of enplanements, and average annual f . The line colors in (c,d) correspond to different VCP modes.

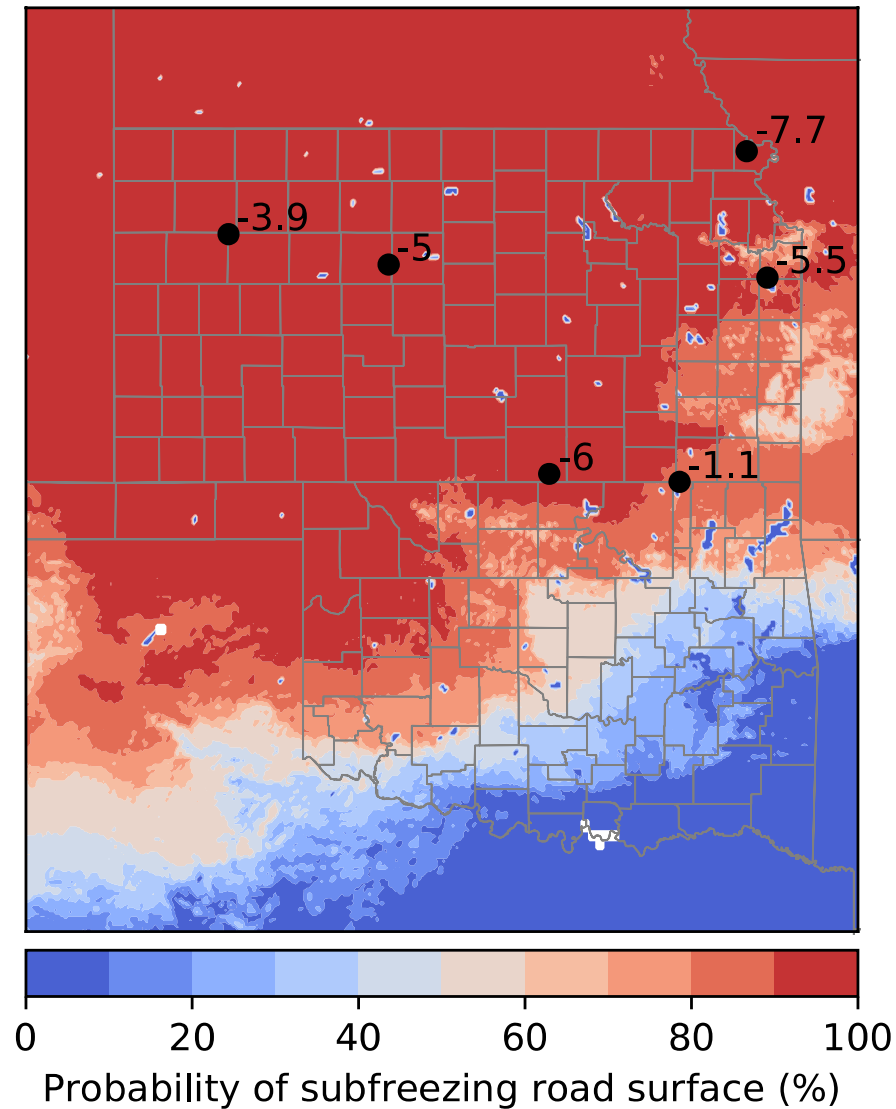
2. Development of a Probabilistic Subfreezing Road Temperature Nowcast Using Machine Learning

Shawn Handler and Heather Reeves (CIMMS at NSSL)

On average, 5,897 lives are lost each year in car accidents caused by adverse weather conditions. It would be beneficial for the NWS to have a tool for predicting the road temperature in a timely manner such that they can more confidently communicate risks, including accumulating snow or ice accretion, to the public. Since NWP models do not explicitly forecast the temperature of the road, we propose a model which outputs a 1-hr probabilistic short-term forecast indicating the likelihood the temperature of a road surface is at or below freezing (0°C). The probabilistic road temperature model is developed using machine learning, specifically using a random forest. The random forest is trained using various surface-based variables from the 02-hour HRRR forecast along with analyses from the Multi-Radar/Multi-Sensor (MRMS) reflectivity mosaics and QPE products. The observed road surface temperature provided by Road Weather Information System (RWIS) sites serve as verification.

Preliminary results are encouraging with an average Brier Skill Score (BSS) of 0.71 and an area under the receiver operating characteristics curve statistic of 0.976. Obtaining

an accurate and reliable prediction of the road temperature is the first step in preventing weather-related road fatalities. This project is ongoing.



1-hr probabilistic output from the random forest for 08 UTC 07 April 2018 over Kansas and Oklahoma. Contoured is the probability of a subfreezing road surface. Overlaid black circles represent sample RWIS site locations with numeric values representing the observed road temperature (°C).

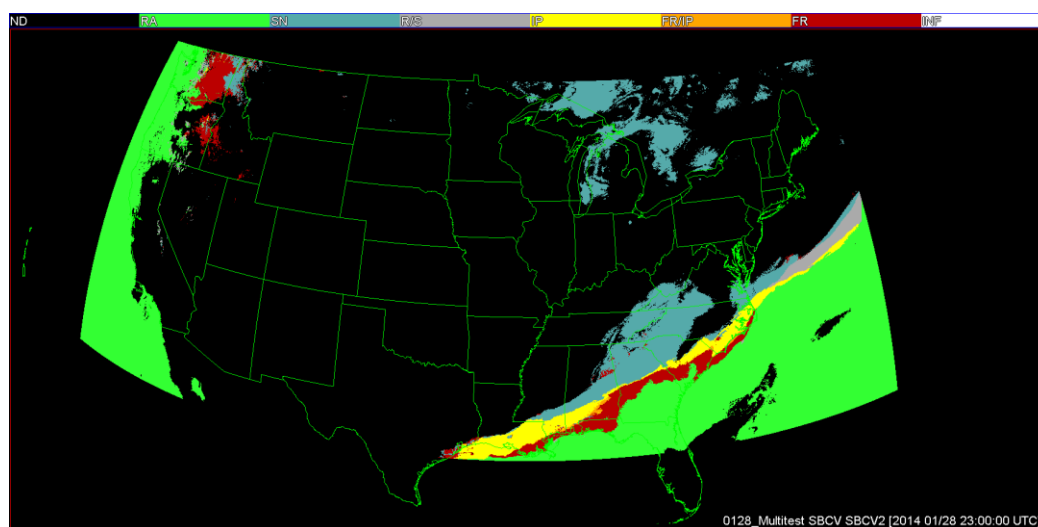
3. Implementing a New Surface Hydrometeor Classification Scheme in MRMS

Andrew Rosenow, Heather Reeves, Stephen Cocks, Carrie Langston, Steven Martinaitis, Karen Cooper, and John Krause (CIMMS at NSSL)

Diagnosing and forecasting surface precipitation type during the cold season remains a challenge operationally. To that end, a new surface precipitation type algorithm, the Spectral Bin Classifier (SBC) was developed and tested at CIMMS/NSSL. After the successful previous testing of the algorithm, it is being implemented in the Multi Radar/Multi Sensor (MRMS) suite. Work in the past year has included porting the algorithm into C++, integrating the C++ code within the MRMS framework, and testing the C++ code output for both scientific and technical performance with various case studies.

The new version of the algorithm is significantly faster than the original code, and is capable of being run operationally. The testing performed as part of code development has resulted in improvements in the algorithm. An example of output from the SBC is included as Figure #. The colors represent categories of surface precipitation type diagnosed by the SBC algorithm from a surface cyclone across the southeastern United States. The classification is performed using numerical model fields from the High Resolution Rapid Refresh model. The SBC did a good job capturing the location and width of the transition from rain to snow across the region in this case and others examined (not shown).

The SBC module is in the process of being onboarded into the experimental MRMS system run at NSSL for testing this winter. The work on this task is ongoing.



Spectral Bin Classifier output for 2300 UTC 28 January, 2014. The colors indicate the diagnosed surface precipitation type: green is rain, red is freezing rain, orange is a freezing rain/ice pellet mix, yellow is ice pellets, cyan is snow, and gray is a rain/snow mix.

4. Alamosa, CO Mobile Radar Deployment and Analysis

Andrew Rosenow and José Meitín (CIMMS at NSSL), and Kenneth Howard (NSSL)

This task concludes work performed during the previous year. The NOXP and PX-1000 mobile radars were deployed in Alamosa, Colorado from December 2016 to April 2017. The purpose of the data collection was to determine the ability to improve quantitative precipitation estimation (QPE) in a region without adequate radar coverage. In addition to calculating QPEs, NOXP captured a scientifically significant event as a snow squall traversed the San Luis Valley essentially undetected by the operational radar network.

Work during this year focused on completing the analysis of data collected on the snow squall event and publishing the results. The final report to the funding agencies was delivered at the beginning of this reporting period. After completion of this report, a formal publication was written up on a snow squall event. This paper was published in Monthly Weather Review. Finally, results from this work was presented at two major conferences, the 38th American Meteorological Society Conference on Radar Meteorology in Chicago, IL, and the 98th American Meteorological Society Annual Meeting in Austin, TX. Work on this task has been completed.

5. Meteorological Phenomena Identification near the Ground (mPING)

Kim Elmore and Jeff Brogden (CIMMS at NSSL)

The meteorological Phenomena Identification near the Ground (mPING) app has received nearly 1.7 million reports since its beginning on 19 December 2012. Since the application program interface (API) was included within Weather Decision Technology's RadarScope in early 2017, a steady one third of all the reports received by mPING come from RadarScope. Our analysis shows that these are in addition to what mPING would normally receive and that submissions from the mPING app remain steady.

In addition, mPING has now been active for over five years. A climatology of winter precipitation type has been produced by merging mPING observations with ASOS observations. For ice pellets, mPING is the only widespread, reliable observation source. Thus a short term climatology of ice pellet hours per year (as well as hours per month) has been produced. When freezing rain is considered, inclusion of mPING observations nearly doubles the total number of hours per year in some areas, and increase it by 50% in others. For snow, including mPING reports increases the total number of hours of snow by 15% to 30%, depending on the area. These climatologies are important for assessing effects on transportation systems and aid in planning for mitigation of winter weather. This project is ongoing.

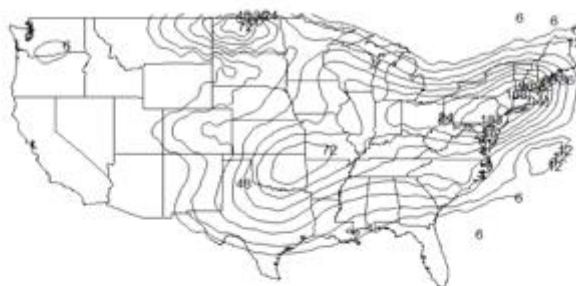
6. mPING Random Forest Research

Kim Elmore and John Krause (CIMMS at NSSL)

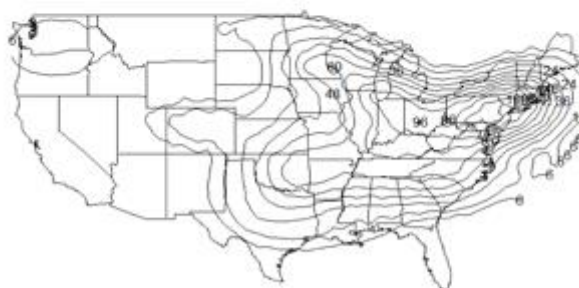
The random forest performed poorly in the last test, where it was trained on the RAP model output on one year and tested on the following year, during which period the RAP model remained unchanged. Fairly strong evidence points to insufficient variety exists in the training data over a period a single season. There exists five years of mPING observation data. Thus, to get a longer training period, reforecasts of the five years of mPING data will be conducted and those five years used as training data. The trained model will then be tested on the sixth year.

We expect that the random forest performance will increase when using a longer training period, which will provide ample evidence that machine learning algorithms for winter precipitation type must be trained on more than one season using a stationary (unchanged) numerical weather prediction model so as to capture the necessary variety needed for good generalization. This project is ongoing.

mPING plus ASOS Hours of Freezing Rain per Year per 34500 sq km



mPING plus ASOS Hours of Ice Pellets per Year per 34500 sq km

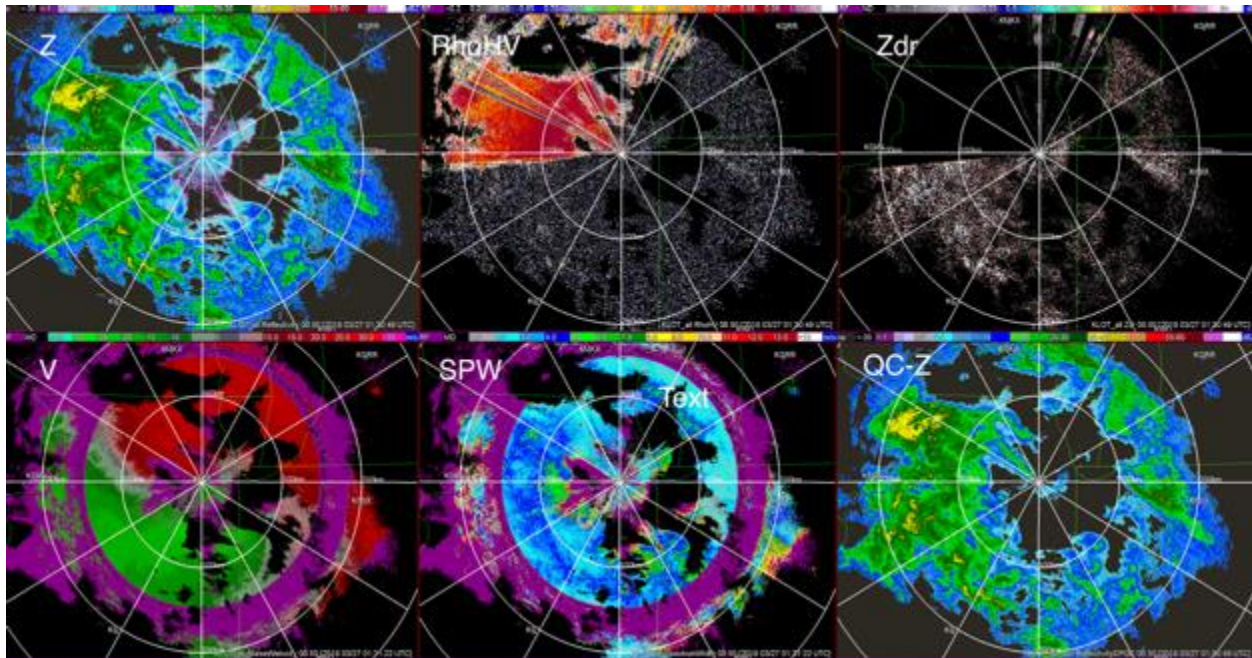


Average number of hours of freezing rain per year (top) and ice pellets per year (bottom) based on combined mPING and ASOS reports for the months November through March during the five year period 2013 through 2017.

7. MRMS Data Quality Control

Lin Tang and Carrie Langston (CIMMS at NSSL), and Jian Zhang and Kenneth Howard (NSSL)

The quality control (QC) process of radar data in the multi-radar-multi-sensor system has been continuously improved to ensure its robust performance in various weather scenarios through real-time observation and users' feedbacks. The updates in QC module applied in S-band dual-polarization WSR-88D radars include 1) support refinements of QC other than hydro-applications (e.g., severe weather and aviation), 2) addition of supplemental single polarization QC during the hardware failure, where Fig shows one example of the QC updates. The figure shows the performance of the QC addition when dual polarization variables are contaminated. The QC updates in C-band single-polarization Canadian radars include 1) the blockage updates and 2) addition of volume coverage pattern. These QC updates were implemented in the operational MRMS system after real-time testing. This project is on-going.



The addition of sqc takes QC task in the dpQC algorithm when dual polarization variables are contaminated. The six subfigures are from UTC 01:30 on March 27, 2018 observed by KLOT: Z, RhoHV, Zdr, AliasedVelocity, SpectrumWidth, and the Quality controlled Z correspondingly, as indicated at the top-left corner in each subfigure.

8. *Advancements in Quality Control of Gauge Observations in the MRMS System*

Steven Martinaitis, Carrie Langston, and Stephen Cocks (CIMMS at NSSL), and Jian Zhang and Kenneth Howard (NSSL)

Surface gauge observations are regarded as “ground truth” when used to verify and calibrate radar-derived quantitative precipitation estimates (QPE). However, gauges not properly vetted by a quality control (QC) procedure can introduce erroneous statistical results and bias calibration. Continued advancements were made to the precipitation gauge ingest and QC algorithms to allow for a greater quantity of gauges to undergo a more complex QC and to modify decision-tree logic in the executable coding.

One primary update for the QC algorithm for the MRMS system included dynamic outlier bounds for hourly gauge observations. Internal studies showed that using fixed outlier curves for rain were not optimal given the tendency for radar to overshoot key precipitation features at farther ranges. This led to likely correct gauge observations being failed by the QC algorithm. To mitigate this issue, the outlier curves are dynamically adjusted based on the Radar Quality Index (RQI) product, where the outlier bounds become less strict as RQI decreases. Additional logic updates included the utilization of both satellite-derived QPE and numerical weather prediction (NWP) quantitative precipitation forecasts (QPFs) to QC gauges outside of optimal radar coverage areas. This includes fail-safes for when either or both of the non-radar observation platforms are unavailable.

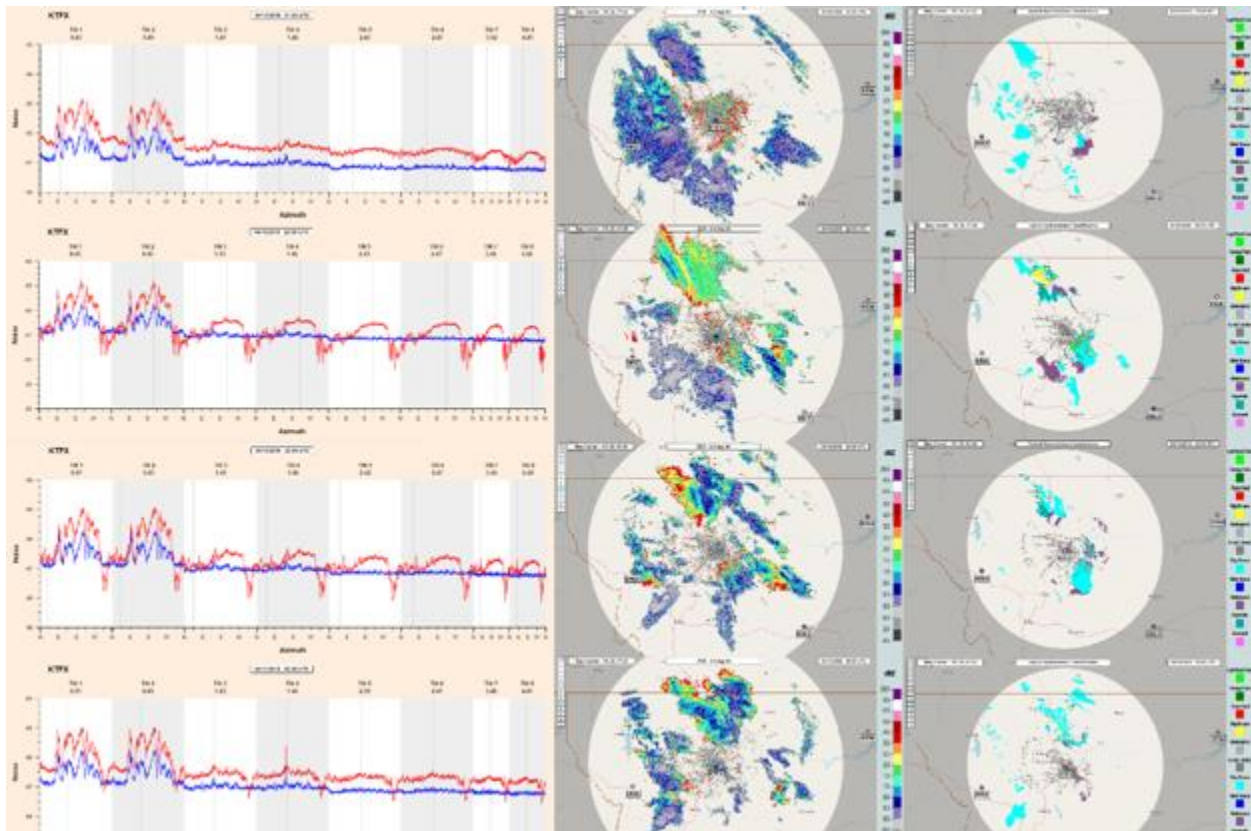
Continuing long-term collaboration between the National Severe Storms Laboratory (NSSL) and other National Oceanic and Atmospheric Administration (NOAA) partners will address continued collection and QC of gauge observations and metadata. This project is ongoing.

9. *Quality Controlling Weather Radar through Hardware Variables*

Micheal Simpson, Brian Kaney, and Lin Tang (CIMMS at NSSL)

Quality controlling weather radars, in general, is through post-processing of the raw data retrieved by the system. This implies that the hardware is in perfect condition and that there are no issues contaminating the underlying data. However, during the winter of 2017/2018, Portland, OR (KRTX) exhibited reflectivity and differential reflectivity degradation. This was due, primarily, from a sharp reduction in the horizontal and vertical noise caused by the Azimuthal Rotary joint (ARJ). Due to age and inevitable wear, grinding of the ARJ is translated into electromagnetic signals which deteriorates the quality of the radar products. Therefore, a real-time detection algorithm was developed, tested, and shown to ameliorate these issues through a simple threshold algorithm. Further implementation of the algorithm was necessary to handle the impacts of degraded noise data on the ZDR offset (also referred to as system ZDR; ZDRO). The equation for ZDRO is calculated as: $ZDRO = 2 * SMB + TXB + RXB$, where SMB is the sun measurement bias, TXB is the transmitter bias, and RXB is the receiver bias. Noise

degradation impacts the RXB and, as such, would impact ZDRO. This applies a blanket 'fix' to the ZDR field which, when sufficient degradation has occurred, results in significantly degraded products, particularly ZDR. Due to the particularly severe degradation that can occur, this has been shown to directly impact quality control products (dualpolQC) which, in turn, can impact hydrometeor classifications and, ultimately, quantitative precipitation estimates (QPE's). This project is completed.



Great Falls, MT (KTFX) horizontal (blue) and vertical (red) noise (left column), differential reflectivity at the 0.5 degree elevation scan (middle column), and hydrometeor classification (right column) for 21Z 20180410 (top row), 22Z 20180410 (second-top row), 23Z 20180410 (third-top row), and 00Z 20180412 (bottom row). Note that as the vertical noise becomes degraded, the differential reflectivity and hydrometeor classifications react such that the fields are inaccurate representations of the true values.

10. Feasibility Study for Real-Time Gauge Correction for Wind Undercatch

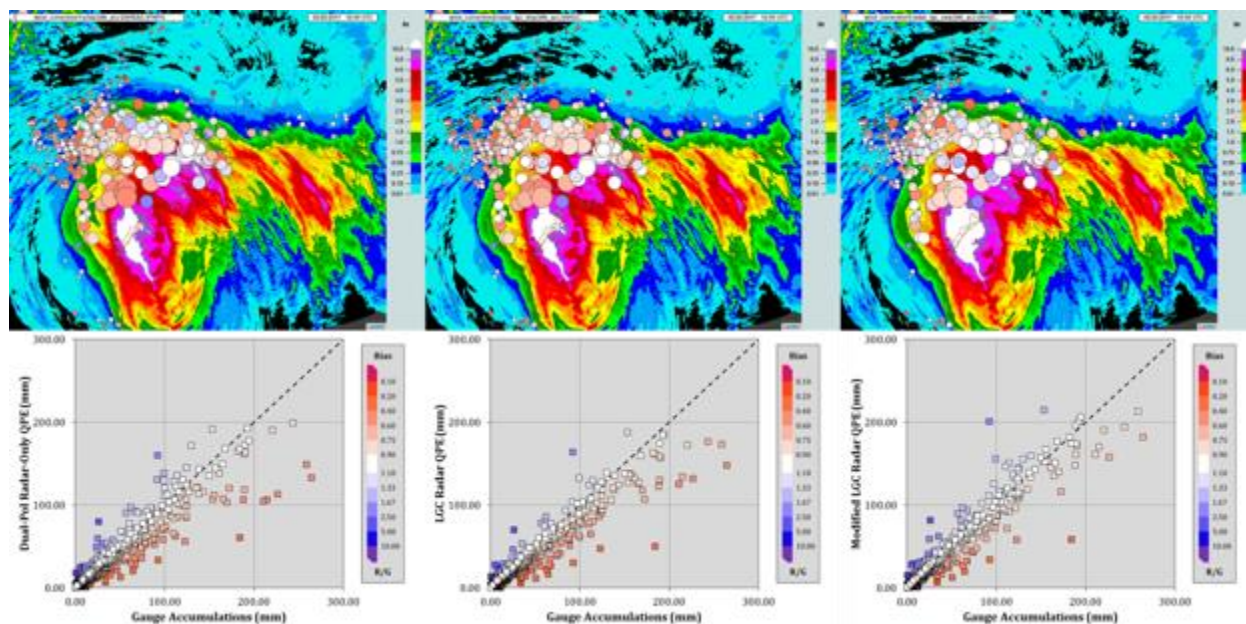
Steven Martinaitis, Andrew Osborne, Micheal Simpson, and Stephen Cocks (CIMMS at NSSL), and Jian Zhang and Kenneth Howard (NSSL)

One of the greatest sources of error with gauge observations is an underestimation of accumulated precipitation from strong winds. Studies have shown that the amount of underestimation by precipitation gauges is typically 2–10% in rain and 10–50% in snow. This wind undercatch has been shown to degrade QPE performance when gauges are

used to bias correct radar-derived quantitative precipitation estimations (QPEs). Past research computed different correction equations based on specific gauge characteristics/instrumentation and at specific temporal periods (e.g., instantaneous, daily); however, no metadata exists on the configurations of the different gauges that are ingested by the Multi-Radar Multi-Sensor (MRMS) system. A feasibility study was conducted to create a generic wind correction scheme for rain and snow on the hourly time scale.

Two equations were generated for both snow and rain precipitation types using previous studies. The wind field used was the 10 m wind speeds from the High Resolution Rapid Refresh (HRRR) model interpolated down to the height of 1.00 m. The hourly gauges were corrected and then ingested by MRMS algorithms to create modified locally gauge-corrected radar QPEs to compare against those created in real-time without any wind correction applied. Three case studies were conducted using the experimental wind correction equations: 1) Hurricane Harvey, 2) synoptic rain/snow event (February 2018), and 3) snow storm (March 2018).

Results showed a marked statistical improvement with all three events over the radar-only and original gauge-corrected radar QPEs. There were also minor impacts on the percentage of gauges that are passed and failed by the gauge QC scheme. The most notable event impacted by the wind correction algorithm was Hurricane Harvey. The adjustment of the gauge values increased the QPE totals by over four inches in some regions over a 72-hour period. This project is ongoing.



24-hour QPE accumulation ending 1200 UTC 26 August 2017 of (left) MRMS experimental dual-pol synthetic radar-only QPE, (center) MRMS locally gauge-corrected radar QPE, and (right) MRMS locally gauge-corrected radar QPE using gauges modified for wind correction.

The top row shows the bubble plot comparing CoCoRaHS gauges with the gridded QPE products, and the bottom row shows the scatterplots of the CoCoRaHS gauges versus the gridded QPE products.

11. MRMS Support for Cloud Detection Algorithms

Andrew Osborne, Lin Tang, Stephen Cocks, and Valery Melnikov (CIMMS at NSSL), and Jian Zhang (NSSL)

The real-time cloud detection capabilities of the WSR-88D radars were tested in MRMS. The algorithm searches for the highest detectable reflectivity echo within the 3D column to determine the cloud top height value at each point. Results from a diverse set of case studies indicate the radars have some capability of detecting non-precipitating clouds, especially those closer to the radar.

The cloud top height values tended to agree with the values from the GOES satellite-based cloud top product used for comparison. Each case did have areas of cloudiness present in the visible satellite and the IR-based cloud top product which went undetected by the radar product. This lack of detectability of non-precipitating clouds is due to the lack of scattering signal available from small droplets especially at far distances from the radar. Also, the Automated Volume Scan Elevation and Termination (AVSET) scanning strategy was inhibiting some of the radars from reaching the higher elevation angles where layers of high clouds were sometimes present. There was also some increase in detection capability noted when the quality control threshold was lowered, although this also caused large areas of non-meteorological echoes to not be removed. This project is completed.

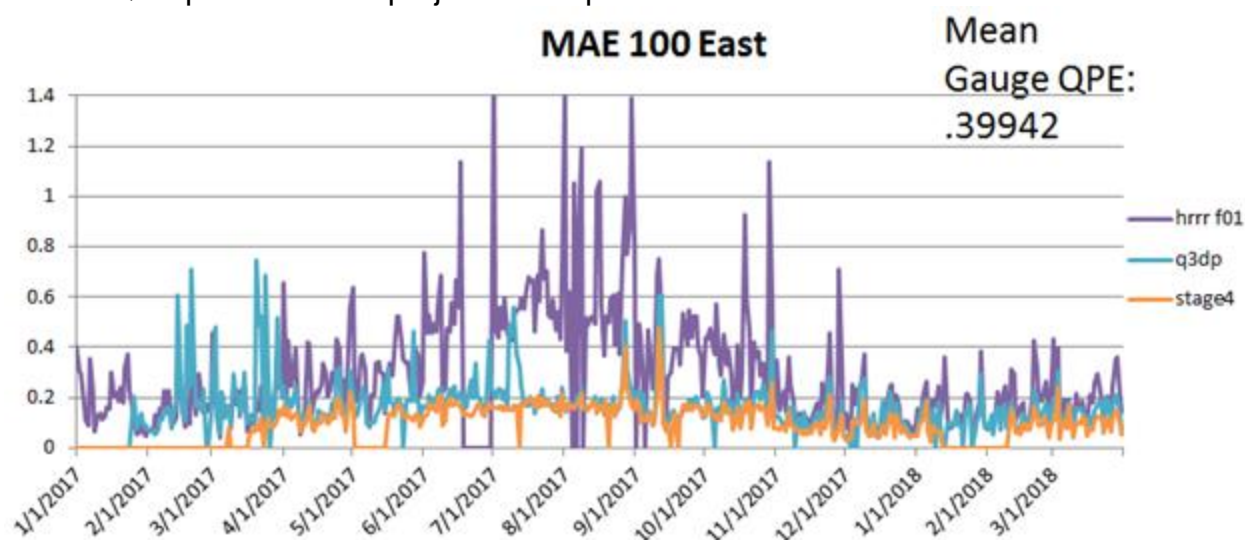
12. Evaluation of Short-Term Model QPF and Satellite QPE Data

Andrew Osborne (CIMMS at NSSL), Jian Zhang (NSSL), Steve Martinaitis (CIMMS at NSSL), and Ken Howard (NSSL)

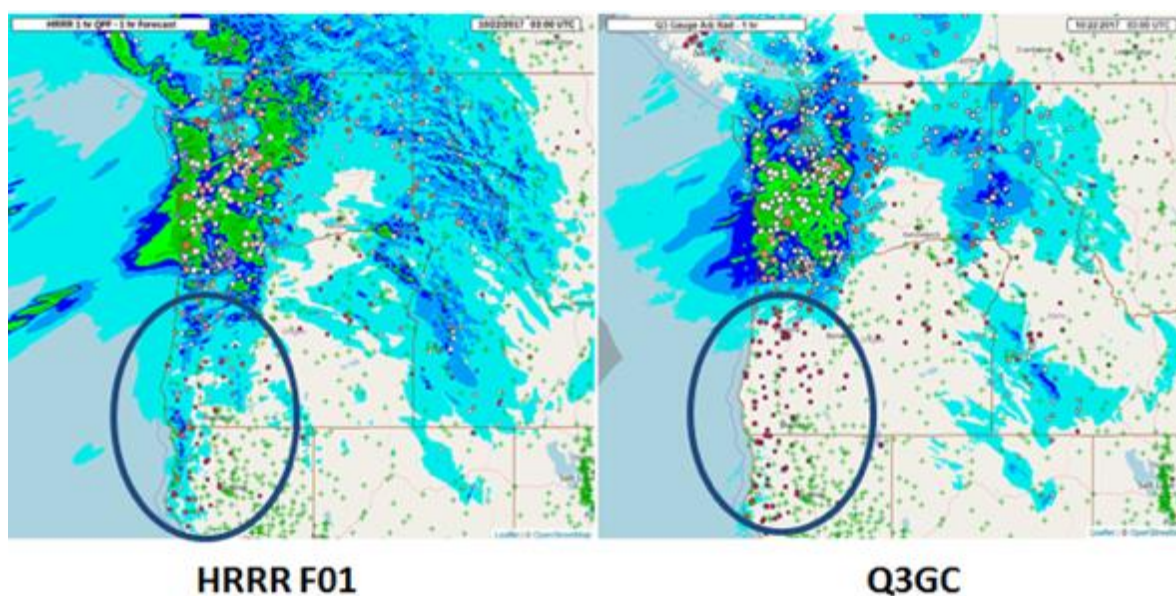
High accuracy QPE is essential for many applications including flash flood prediction, water resource management, and input to hydrological models. The MRMS QPE products use different combinations of radar, gauge, and climatological data. Gaps in radar and gauge coverage (especially prevalent in the western US) can lower the accuracy of the QPE products. Alternate sources of precipitation information include IR satellite and Numerical Weather Prediction (NWP) models. These low latency and continuous coverage sources will be used in a new multi-sensor QPE product. A long term evaluation of the Self-Calibrating Multivariate Precipitation Retrieval (SCaMPR) satellite QPE and High Resolution Rapid Refresh (HRRR) model QPF was needed to determine the uncertainties associated with these new precipitation sources.

Statistical analysis of HRRR QPF compared to gauges indicates a decrease in accuracy in the warmer months, coincident with increased convective precipitation. HRRR has been known to perform better with large scale stratiform precipitation, while struggling with proper placement, coverage, and initiation of convective areas. Individual stratiform and convective events were also examined and the HRRR performance for these was consistent with the long-term statistical analysis with overestimation of convective precipitation and better accuracy in stratiform/ winter precipitation regimes.

The SCaMPR QPE verification indicates low skill compared to the reference datasets. Individual case studies show better accuracy in convective cases compared to stratiform cases. This is expected as the cloud top temperature-rain rate relation used by SCaMPR is most suitable for high, cold cloud tops. Although SCaMPR performs better in convective regimes, there are still some notable issues in convection (false precipitation in anvils areas and lack of detailed structure) which will need to be taken into account before the satellite product can be reliably used to fill in gaps in a multi-sensor QPE product. This project is completed.



Comparison of HRRR QPF, radar-based gauge-corrected QPE, and stage 4 QPE mean absolute error based on 24 hour gauge verification. Spike in HRRR error (purple line) during the summer months is evident.



Verification against hourly QC'ed gauges for 1 hour forecast HRRR 1 hour QPF (left) and radar-based gauge-corrected QPE (right). HRRR adds precipitation in the coverage gap in SW Oregon which matches up well with gauges.

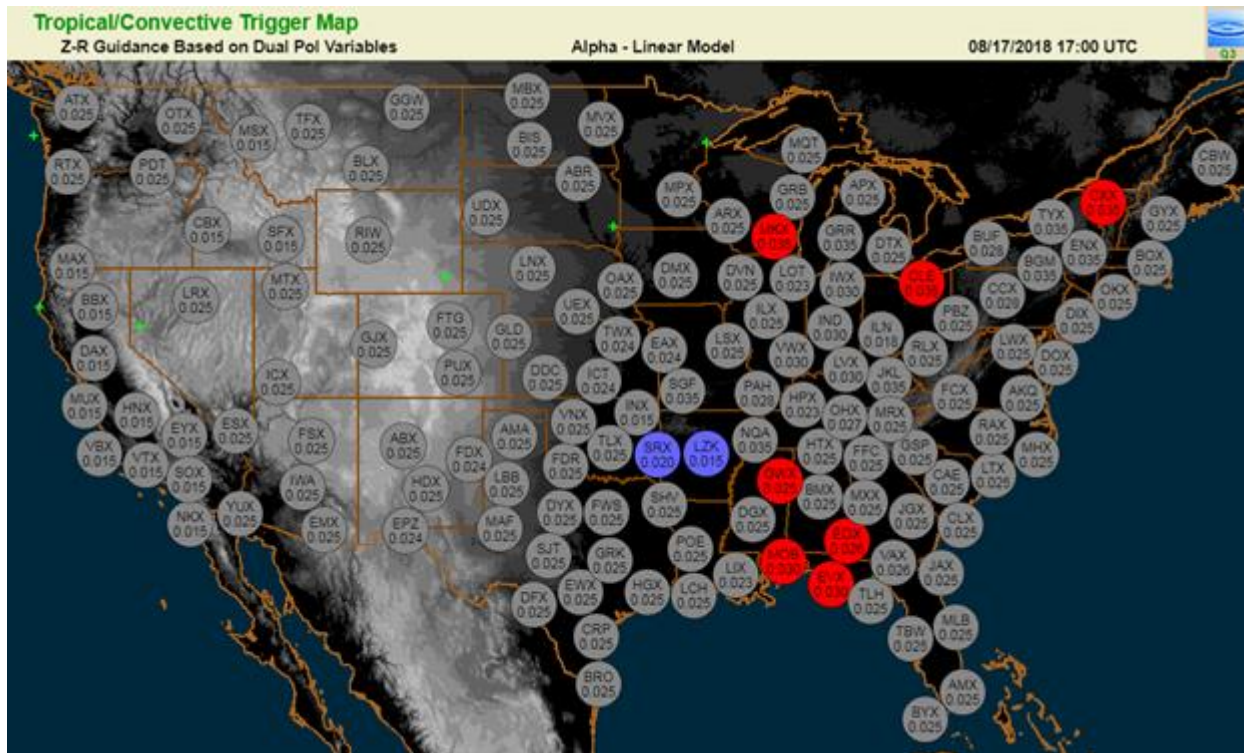
13. Automated Tropical Trigger Guidance for Dual Pol QPE

Andrew Osborne, Steve Cocks, Brian Kaney, and Carrie Langston (CIMMS at NSSL)

There is an option in the open radar product generator (ORPG) for the WSR-88D radars to use either a continental or tropical $R(Z,ZDR)$ relation to generate a dual-pol rain rate. Currently, there is limited guidance available on whether a certain radar domain is experiencing continental (larger drops, less efficient) or tropical precipitation (smaller drops, more efficient). The alpha parameter from the specific attenuation rain rate equation could potentially be used for this purpose. Prior studies have shown alpha tends to be less than .02 when continental rain is occurring, greater than .025 when tropical rain is occurring, and between .02 and .025 when there is a mix between the two regime types.

Several cases were examined to get an idea of the possible accuracy difference when using the alpha parameter guidance. When adjacent radars were in opposite modes sensing the same precipitation area it provided an opportunity to see which rain rate relation was more accurate. This information was then compared to the alpha guidance. There is strong evidence that the tropical rain rate is most accurate when alpha indicates a clearly tropical regime. The continental rate was underestimating the 24 hour accumulation in these cases. For the cases where alpha was predominantly continental, the difference in accuracy between adjacent radars in different modes was not as clear. A likely explanation for this is most of the “continental” alpha cases actually involved convective storms with trailing stratiform regions that were more tropical in nature. Hourly verification showed increased accuracy could be obtained by switching the rain rate relation used at times when alpha makes a clear jump from one regime to the other.

A new QVS level 3 metadata page was developed with the alpha values displayed for each radar. The circle for each radar is shaded either red for tropical, blue for continental, or gray if not enough non-zero Z/ZDR pairs are available to estimate alpha. Discussions are still to be had with the ROC applications team to coordinate the dissemination of the alpha product to field forecasters. This project is ongoing.



Level 3 display indicating the dominant precipitation type occurring over each radar (blue for continental and red for tropical).

14. Development and Verification of New QPE Algorithm to Estimate Rainfall

Stephen Cocks, Lin Tang, Yadong Wang, and Pengfei Zhang (CIMMS at NSSL)

As further discussed in section 16, the project finished a 13 month (April 2017 through April 2018) performance evaluation of the new Q3 Dual Pol (Q3DP) vs. quality controlled CoCoRaHS gauges. The Q3DP results which were also compared to the MRMS Legacy Q3RAD and operational Dual Pol QPEs, was found to show significant progress over the past year. The results continued to indicate the new QPE performed significantly better for moderate to high end precipitation events. The following is a short summary of the work accomplished to date.

Using the same equations of Ryzhkov et al. (2014: their equations 12 – 15), calculation of specific attenuation fields for the purpose of estimating rain requires radial reflectivity (Z) and the span of differential phase (Φ_{DP}) along a radar radial. A critical component to this process is the calculation of the path integrated attenuation which utilizes the parameter α , defined as the ratio of specific attenuation (A) to specific differential phase (K_{dp}). Disdrometer simulations of the parameter α and differential reflectivity (Z_{dr}) indicated the former is inversely proportional to the later. The parameter α could easily be calculated using Z_{dr} if the later was well calibrated to within 0.1 dB; however, this is not the case as calibration challenges for Z_{dr} remain for the NEXRAD network. Hence, α was estimated via the use of a linear model that is dependent upon the slope of Z_{dr}

vs. Z provided there was enough Zdr vs. Z pairs for the radar FOV, of which the initial requirement was set at 30,000 to ensure a stable slope calculation. Since α was calculated for the radar FOV, Zdr vs. Z distribution checks were also made to ensure a fairly broad distribution of precipitation (convective or convective/stratiform) was present. However, if there was very little convection present (few Zdr vs. Z pairs for Z >40 dBZ) then a slope calculation was not made; rather, α was assigned a value representative of stratiform rain (currently set at 0.035). This logic, installed mid-summer last year, was key to reducing underestimates in stratiform rain events that were initially observed in the Spring of 2017.

However, we noticed the new QPE continued to exhibit an underestimate trend in some stratiform rain events. This trend was related to the logic used to carryover the parameter α during periods where *no precipitation or isolated to widely scattered precipitation was present in the radar field of view (FOV)*. Specifically, if the required number of Zdr vs. Z pairs (30,000) was not met a default alpha value of 0.015 (the default convective value) was used in the path integrated attenuation calculation. For some of the light stratiform rain events, where early in the event the threshold for the number of Zdr vs. Z pairs was not met, the default convective alpha value was used to estimate rainfall which resulted in underestimates.

The initial fix for this was to create an additional layer of Zdr vs. Z distribution checks that were used to determine what value of alpha to use when precipitation was not widespread. Code was written to check whether a significant number (100 pairs) of Zdr vs. Z pairs were present for Z \geq 40 dBZ when the threshold for the number of pairs to make a slope estimate of alpha was not met. If met, then isolated to widely scattered convection was likely present and the default convective alpha value was used; if this condition was not met, then the stratiform alpha was applied. Further, we used a time history of alpha (initially set at 3 hours and maintained internally within the algorithm) in order to smooth alpha transitions across the threshold for the required number ZDR vs. Z pairs.

From the evaluation of precipitation events during the 2018 warm season, we noticed that while there was some reduction in underestimates during light rain events (due to the code changes), there were also more overestimates associated with isolated to widely scattered convection. Analysis revealed that some additional fine-tuning was needed to be made within the code for these types of precipitation events. Initial tests using code to mitigate the overestimates showed good results. We are currently in the process of further refining the code changes before we run the new code on the MRMS real-time research testbed. This project is ongoing.

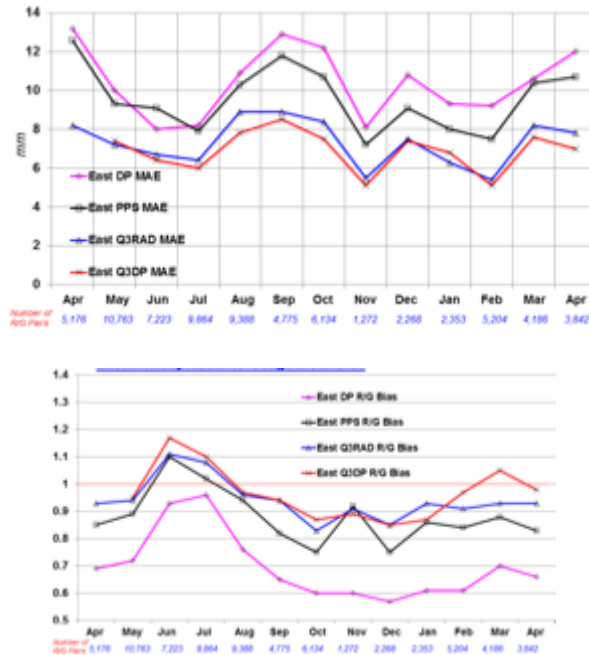
15. Evaluating MRMS Operational Dual Pol Quantitative Precipitation Estimates from April 2017 – March 2018

Stephen Cocks, Steven Martinaitis, Carrie Langston, and Brian Kaney (CIMMS at NSSL)

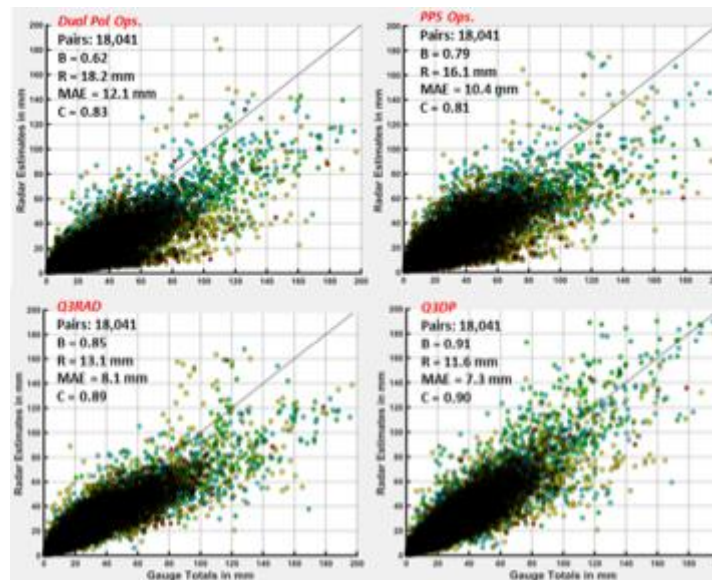
A quantitative evaluation of the operational Dual Pol, the legacy precipitation processing system (PPS), the MRMS Q3 radar only (Q3RAD) and the experimental MRMS Dual Pol (Q3DP) quantitative precipitation estimate (QPE) was conducted for the period between April 2017 and April 2018. The overall goal was to determine whether the operational Dual Pol QPE could replace the legacy PPS within the ORPG while including a newly developed evaporation correction scheme. Comparisons were made to the mosaicked Q3RAD and Q3DP to document the differences with single radar QPE to determine how much more value added was provided by the former vs. the latter.

In addition to the data collected last year (April through July 2017) data has been collected and analyzed for the months of August 2017 through April 2018. Therefore the assessment covers a 13 month period that includes 569 radar precipitation events collected from 111 radars on 219 calendar days. The results indicated Dual Pol QPE during this period exhibited a distinct underestimate bias ratio across the US, primarily due to its performance within stratiform, tropical and mixed convective/tropical rain regimes. Overall, the mosaic QPEs performed much better with lower error, higher correlation and more consistent radar-to-gauge bias ratio than the single radar QPEs. Further, the operational Dual Pol QPEs performance was at times only marginally better than PPS. Using the ROC ZDR calibration charts, used to determine what radars are considered well calibrated with regards to ZDR, an extensive effort was made to separate out that data that was collected from what was considered to be well calibrated radars, where $|Zdr| \leq 0.2$ dB. However, the operational Dual Pol performance did not significantly improve when using data from radars consider calibrated by the ZDR calibration charts.

Smaller samples of continental, stratiform, and tropical rainfall were examined to better understand these results. It was found that in continental events, which were composed of primarily strong to severe convection, that Dual Pol exhibited significantly lower error and a better radar-to-gauge bias ratio than PPS. However, for stratiform and tropical rainfall events the operational Dual Pol exhibited significant underestimates and at times higher error than PPS. Further analysis indicated that the marginal Dual Pol QPE performance was likely related to field of view Zdr fluctuations caused by hardware failures and/or natural phenomena (e.g. such as radome wetting), the currently rain rate relations used by PPS and Dual Pol for stratiform and tropical rainfall, and the forecaster's choice of what rain rate relation to use for a given precipitation event. A detailed report and a possible journal article are in the works. This project is ongoing.



Comparison of Mean Absolute Error (MAE, top) and radar-to-gauge bias ratio (R/G Bias, bottom) for operational Dual Pol, PPS, MRMS Q3RAD, and MRMS Q3DP QPEs for precipitation events East of the Rocky Mountains 13 month study period. The number of radar/gauge pairs for each month were annotated at the bottom of each chart.



Scatter plot comparison between 24 hour operational Dual Pol (top left), PPS (top right), Q3RAD (bottom left) and Q3DP (bottom right) QPE totals versus quality controlled 24 hour CoCoRaHS gauges for rainfall (only) events East of the Rocky Mountains during the cool season (October 2017 – April 2018). 'B' refers to gauge to radar bias where underestimates are < 1.0, 'R' refers to Root Mean Square Error, 'MAE' is Mean Absolute Error and 'C' is correlation coefficient. mPING and model data was used to filter out frozen precipitation events.

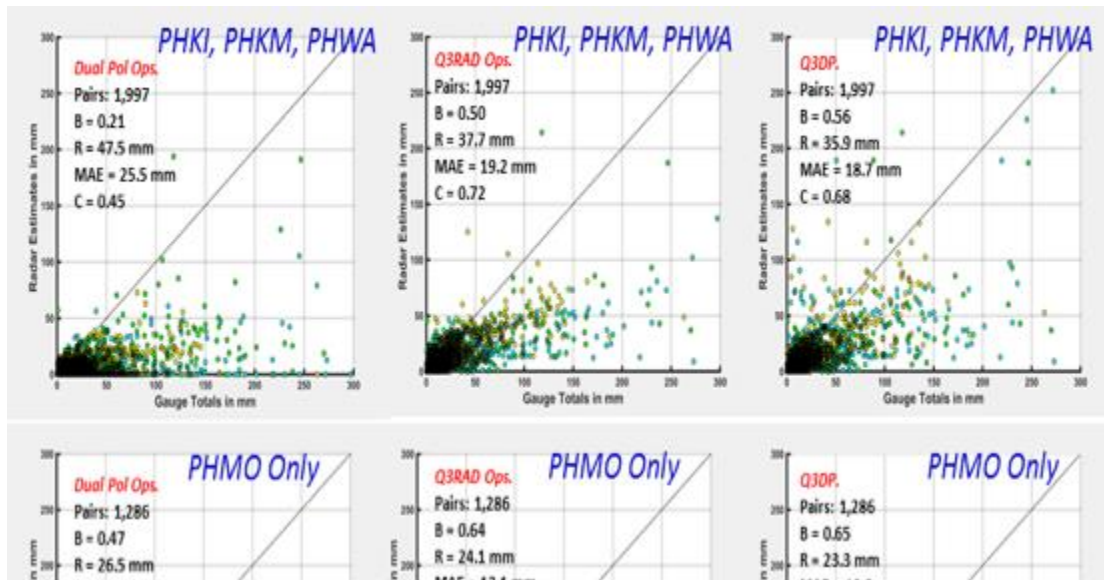
16. Assessment of Radar Only QPE in the Hawaiian Islands

Stephen Cocks and Steven Martinaitis (CIMMS at NSSL)

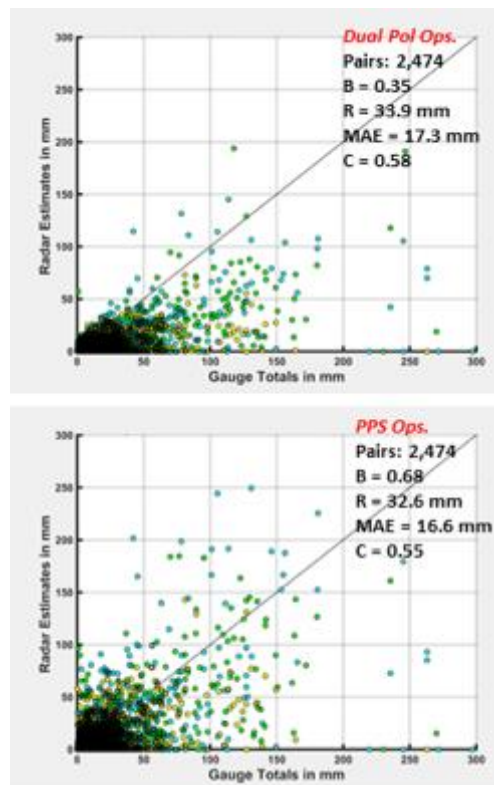
This task was in response to a request by the Honolulu WFO to better understand the performance of the Dual Pol QPE within the Hawaiian Islands. The task focused on the Dual Pol, PPS, R(A) and MRMS Q3RAD QPE performance in the region. Data was collected from 28 calendar days for 59 radar precipitation events from the four operational WSR-88D radars in the region between 24 October 2017 and 11 May used to. The mountainous terrain has an immense impact on the four operational WSR-88D radars hence all the QPEs were significantly impacted although the use of mosaicked radars partially mitigated the impact in the MRMS products. This, along with three of the radars located at significant elevation above sea level, means that radar beam overshoot tropical, low echo centroid, like precipitation systems can easily occur.1e to the substantial impacts from terrain and elevation above sea level, the QPE performance was assessed separately for radars with the most impacts (PHKI, PHKM, PHWA) and PHMO which had the least. The second figure showed the results and one can clearly appreciate the substantial differences in performance between PHMO and the more terrain/elevation impacted radars. For higher impacted radars, Dual Pol exhibited over 100% lower radar-to-gauge underestimate bias ratio (e.g. more underestimates present) and ~25% higher RMSE/MAE error than the mosaicked MRMS QPEs. The reason for the large disparity was due to the use bright band corrected reflectivity and the use of neighboring radars to create a mosaicked QPE field.

For PHMO, the Dual Pol performance results are more comparable with those of Q3RAD and Q3DP. Nonetheless, Dual Pol exhibited a 36% lower radar-to-gauge underestimate bias ratio and at least 10% higher RMSE/MAE than Q3RAD and Q3DP. An interesting observation was that even though Q3DP exhibited overall higher QPE accumulations for gauges > 50 mm it also exhibited more scatter. Analysis is still underway, but it appears that this is due to the use of R(Z) instead of R(A) in areas where radar beam blockage > 90%. For gauges within these regions, the Q3DP accumulation was the same as Q3RAD, which for heavier rainfall was usually an underestimate in tropical precipitation systems. However, in areas where beam blockage < 90% and when heavier rainfall was present Q3DP usually had higher QPE totals. This overall effect can give the appearance of more variability within the Q3 DP scatter plot.

The second figure showed a performance comparison, utilizing all radars, between the operational Dual Pol and available (beginning February 05) PPS QPE. While the PPS QPE was more aggressive than Dual Pol and exhibited a much better radar-to-gauge bias ratio and slightly lower errors, it also exhibited appreciably more scatter. Comparisons of PPS with Q3RAD and Q3DP (not shown) also indicated a much better bias ratio albeit with significantly higher RMSE/MAE error and substantially lower correlation. This project is ongoing.



Scatter plot comparison between 24 hour accumulations of operational Dual Pol (left), Q3RAD (middle) and Q3DP (right) for radars substantially impacted by terrain and radar elevation (top) and PHMO which is the least impacted (bottom). QPE totals were compared to 24 accumulations of quality controlled gauges. 'B' refers to gauge to radar bias where underestimates are < 1.0, 'R' refers to Root Mean Square Error, 'MAE' is Mean Absolute Error and 'C' is correlation coefficient.



Scatter plot comparison between 24 hour accumulations of operational Dual Pol (top) and available PPS (bottom) for the period between February and May 2018.

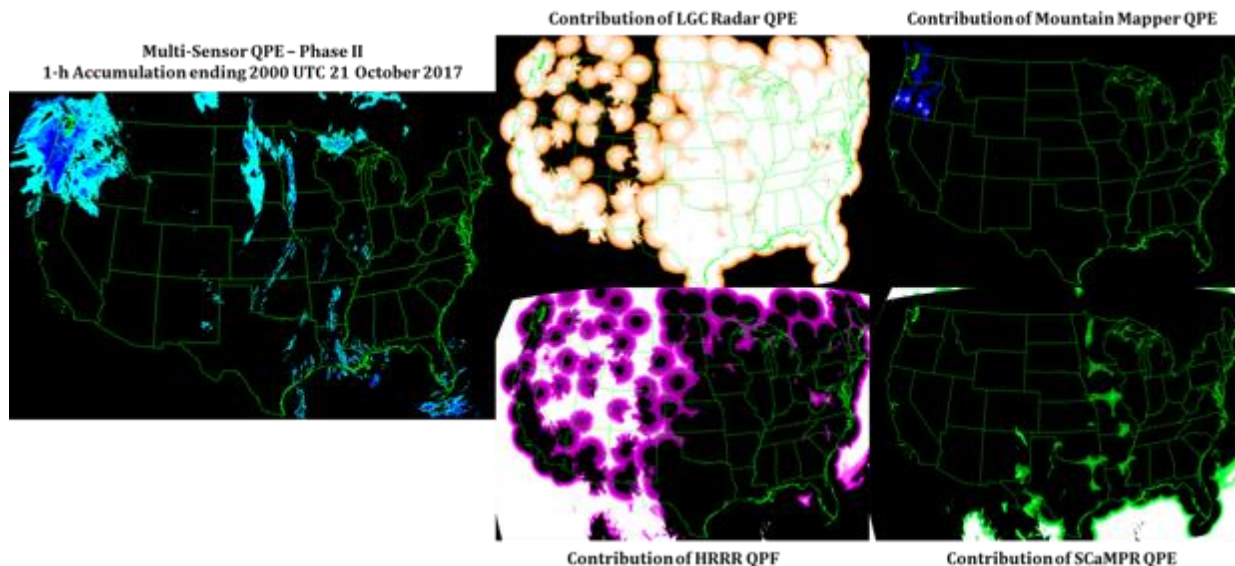
17. Blending Various Precipitations from Observational and Modeling Platforms to Generate a Multi-Sensor Merged QPE

Steven Martinaitis, Andrew Osborne, Micheal Simpson, and Carrie Langston (CIMMS at NSSL), and Jian Zhang and Kenneth Howard (NSSL)

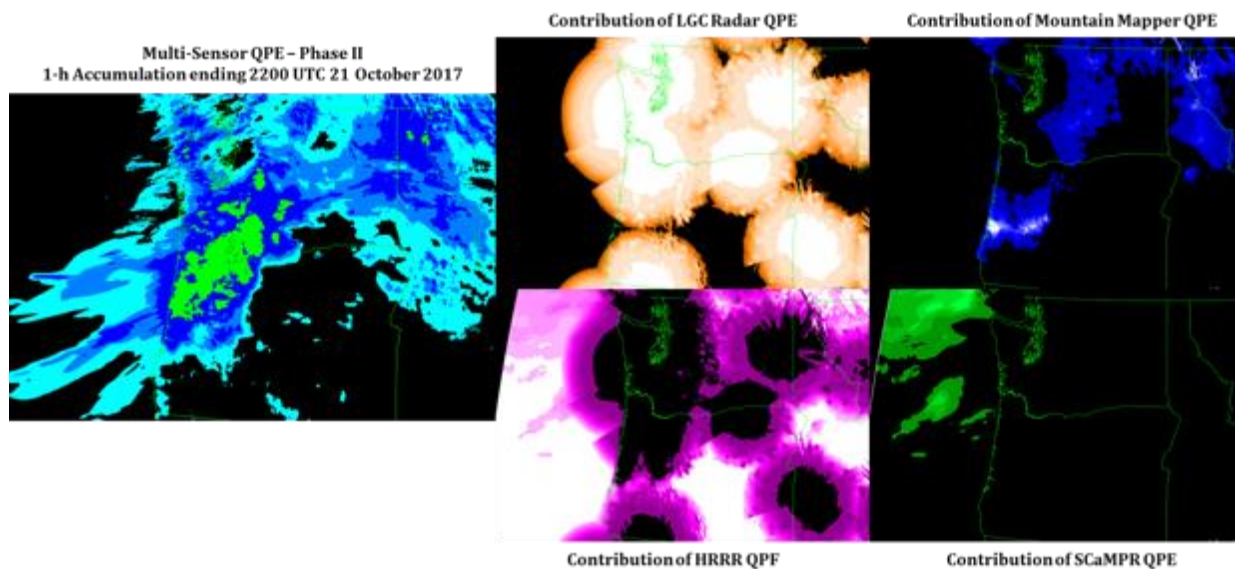
Different sources of QPE have varying strengths and challenges in generating deterministic surface precipitation values. These challenges are magnified in areas lacking observational coverage (e.g., the western United States and Alaska) where there are significant gaps in radar coverage due to less dense coverage and beam blockage from complex terrain along with a sparse network of gauge observations. CIMMS scientists are developing a scheme to merge radar-derived quantitative precipitation estimation (QPE) with gauge observations, satellite-derived QPE, and numerical weather prediction (NWP) quantitative precipitation forecasts (QPFs) to provide a more accurate and comprehensive QPE coverage in the Multi-Radar Multi-Sensor (MRMS) system.

The algorithm for the MRMS Multi-Sensor QPE product for the CONUS uses the radar QPE and a modified Radar Quality Index (RQI) to define where gap-filling QPE would be utilized. The radar coverage within the scheme is dynamic based on environmental characteristics to reduce radar influence in stratiform/snow regimes where overshooting precipitation can be easily done while increasing its use in convective environments. The satellite and NWP sources for gap-filling are also blended based on the environmental parameters for convection versus stratiform/snow. This satellite/NWP combination is then blended with the MRMS Mountain Mapper QPE in regions of complex terrain. This algorithm is being evaluated over numerous cases over the western CONUS. The first set of results show an improvement of QPE coverage and accuracy over all individual precipitation inputs when compared to independent CoCoRaHS gauges.

The MRMS Multi-Sensor QPE product is also being developed for the domains outside of the CONUS (hereinafter denoted as oCONUS). The Hawaii MRMS domain will utilize a combination of the locally gauge-corrected radar QPE with the Mountain Mapper QPE for the initial running of this product. The Hawaii version was tailored to work with the tropical nature of the QPE and the complex terrain resulting in significant radar blockages. Site visits are ongoing to collaborate with the San Juan, Puerto Rico and Anchorage, Alaska offices to design the Multi-Sensor QPE product to be best optimized for their observations sources and needs within the various oCONUS domains. This project is ongoing.



CONUS view of the Multi-Sensor QPE product for the 1-hour period ending 2000 UTC 21 October 2017. The left panel shows the final QPE field. The four-panel on the right shows the contribution of the various fields (clockwise from top-right): locally gauge-corrected radar QPE, Mountain Mapper QPE, SCaMPR satellite QPE, and HRRR QPF.



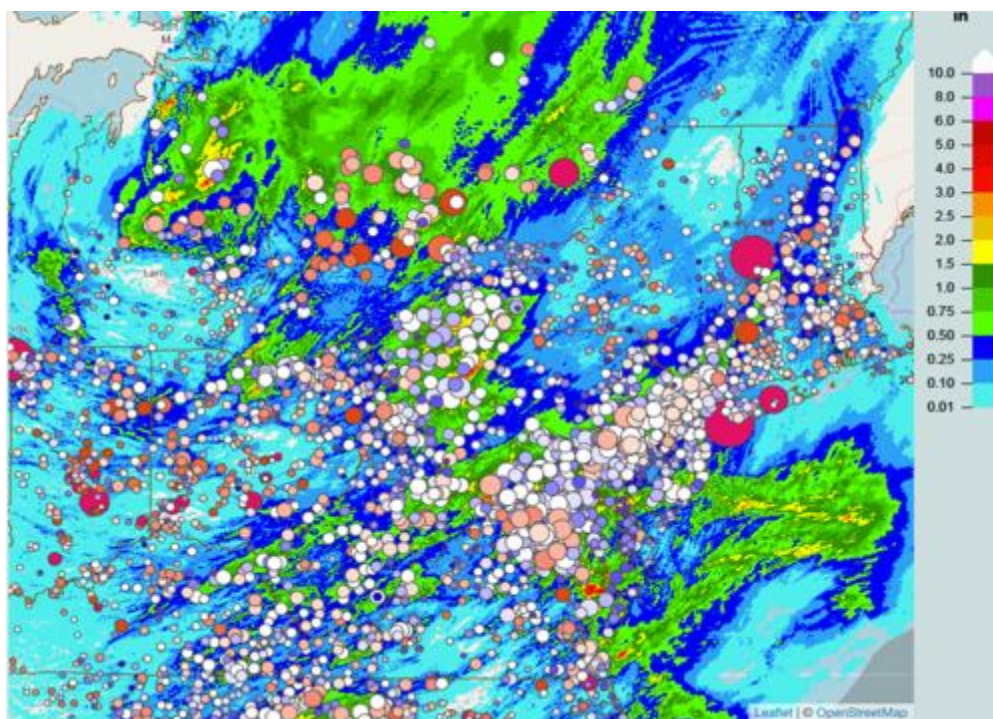
Same as previous image except zoomed in to the Pacific Northwest for the 1-hour period ending 2200 UTC 21 October 2017.

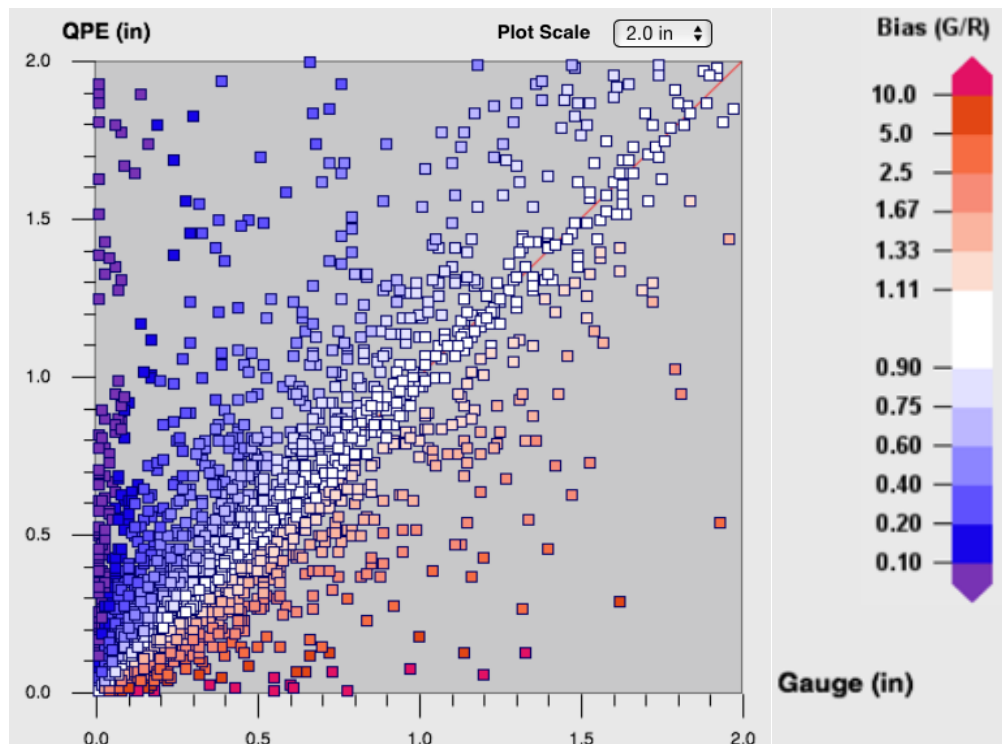
18. Implementation of Advanced Multi-Sensor Analysis and Data Fusion Algorithm for Real-Time High-Resolution Quantitative Precipitation Estimation

Lin Tang (CIMMS at NSSL), Jian Zhang (NSSL), and Carrie Langston and Brian Kaney (CIMMS at NSSL)

The objective of this project is to implement new algorithms from the University of Texas in Arlington (UTA) for multi-sensor quantitative precipitation estimation (QPE) and multi-QPE fusion on the Multi-Radar Multi-Sensor (MRMS) Testbed for future operation at the National Centers for Environmental Prediction Central Operations. These algorithms are proposed to improve the accuracy of high-resolution QPE and water prediction especially for heavy-to-extreme precipitation and severe-to-extreme flooding events.

This project is a collaboration among the University of Oklahoma (OU), UTA, National Severe Storm Laboratory (NSSL), and National Weather Service (NWS). In the past year, the OU and NSSL started with software engineering of algorithm modules from UTA for MRMS. We identified the interface between the algorithm modules and MRMS to perform case testing using selected precipitation events. After the UTA team optimized the algorithms and refined parameters, we conducted algorithm implementation into MRMS testbed. The QPE module uses the MRMS radar-only estimation and quality-controlled hourly gauge data as inputs to deliver the gauge corrected QPE products. Evaluation will be carried out for different types of precipitation events over the CONUS. The figure shows the implemented QPE product and the scattering plot of QPE vs. gauge measurement. This project is on-going.





*Top subfigure: the gauge babble chart on the top of QPE products;
bottom subfigure: scattering plot of QPE estimation and gauge measurement.*

19. MRMS Experimental Testbed for Operational Products (METOP)

Micheal Simpson, Brian Kaney, Steven Martinaitis (CIMMS at NSSL), Jian Zhang, Ken Howard (NSSL) and Heather Grams (ROC)

Accurate high-resolution quantitative precipitation estimation (QPE) at the continental scale is of critical importance to the nation's weather, water and climate services. To address this need, a Multi-Radar Multi-Sensor (MRMS) system was developed at the National Severe Storms Lab of National Oceanic and Atmospheric Administration that integrates radar, gauge, model and satellite data and provides a suite of QPE products at 1-km and 2-min resolution.

MRMS system consists of three components: 1) an operational system, 2) a real-time research system, and 3) an archive testbed. The operational system currently provides instantaneous precipitation rate, type and 1-h to 72-h accumulations for conterminous United States and southern Canada. The research system has the similar hardware infrastructure and data environment as the operational system, but runs newer and more advanced algorithms. The newer algorithms are tested on the research system for robustness and computational efficiency in a pseudo operational environment before they are transitioned into operations. The archive testbed, also called the MRMS Experimental Testbed for Operational Products (METOP), consists of a large database that encompasses a wide range of hydro-climatological and geographical regimes.

METOP is for the testing and refinements of the most advanced radar QPE techniques, which are often developed on specific data from limited times and locations. The archive data includes quality controlled in-situ observations for the validation of the new radar QPE across all seasons and geographic regions. A number of operational QPE products derived from different sensors/models are also included in METOP for the fusion of multiple sources of complementary precipitation information. This project is ongoing.

20. Operational Implementation of the Multi-Radar Multi-Sensor System v11.5

Carrie Langston, Karen Cooper, Jeff Brogden, Robert Toomey, Brian Kaney, Ami Arthur, Travis Smith, Darrel Kingfield, Kiel Ortega, Brandon Smith, Lin Tang, Steven Martinaitis, Youcun Qi, Micheal Simpson, Zac Flamig, and Humberto Vergara-Arrieta (CIMMS at NSSL)

The vast majority of the NSSL's MRMS-related operational onboarding tasks are performed by members of the Analytics and Enterprise Group (AEG). However, many members from many groups contribute to the operational suite by developing new algorithms and improving existing ones. In the Spring of 2018, the Multi-Radar Multi-Sensor (MRMS) system was upgraded from v11.0 to v11.5.4 at the National Centers for Environmental Prediction (NCEP) Central Operations (NCO) as part of the Integrated Dissemination Program (IDP). This was a significant update that incorporated new data streams and many upgrades to existing algorithm suites. The initial code drop for MRMS v11.5 was provided to NCO at the end of the calendar year 2017. Subsequent testing and changes in radar behavior required multiple patches before v11.5 became operational. Below is a summary of updates from v11.0 to v11.5.4.

System-wide Changes

New Inputs

- GOES-16 ABI bands
- Meteorological Assimilation Data Ingest System (MADIS) gauge observations

Handling of New WSR-88D Radar Characteristics

- New Volume Coverage Patterns (VCPs) 35 and 215
- New scan strategy: Mid-Volume Rescan of Low-Level Elevations (MRLE)
- New extra low-level elevation angles for the San Francisco, CA (KMUX) and Cedar City, UT (KICX) radars

Severe Weather Updates

EchoTops

- Updated with improved vertical interpolation when sparse vertical reflectivity profiles exist.

AzShear and RotationTracks

- Updated underlying velocity dealiasing scheme to match the ORPG.

Vertically Integrated Ice (VII)

- Minimum thresholding of VII was reduced from 1 to 0.5 kg*m⁻².

Missing vs. No Data Values

- Missing and No Data values were standardized across much of the severe weather products. Products affected are
 - Low Composite Reflectivity (0-4km)
 - Layer Composite Reflectivity (Low [0-24kft], High[24-60kft], Super[33-60kft])
 - EchoTop (18/30/50/60)
 - AzShear and RotationTracks (all)
 - Thickness/Height of [50dBZ above 0C, 50dBZ above -20C, 60dBZ above 0C, 60dBZ above -20C]
 - VII
 - VIL
 - VILD

Hydromet Updates

Gauge Usage

- Incorporated MADIS's (~9000) gauge observations, which more than doubled MRMS's gauge count.
- Improved quality control especially with regard to identifying outlier gauges.
- Reduced latency of gauge ingest and processing by approximately 20-minutes

Radar Quality Index

- Improvements to spatial continuity

Precip Flag

- Improvements to spatial continuity
- Improvements to tropical rain delineation in western US.

Quantitative Precipitation Estimates (QPEs)

- Radar QPE: Reduced occurrences of a "skipping" pattern that occurred with fast moving rain bands. This was accomplished by taking advantage of more frequent low-level scans (SAILS). Reduced overestimation in warm season when the probability of warm rain processes is low.
- Gauge Corrected QPE, Gauge Only QPE: Improved QPE accuracy as a result of better gauge QC and more gauge observations. Product latency was reduced from approximately 90 to 60-minutes
- Mountain Mapper QPE: Improved QPE accuracy as a result of better gauge QC and more gauge observations. Product latency was reduced from approximately 75 to 65-minutes

Flooded Location and Simulated Hydrographs (FLASH) Updates

All CREST, HP and SAC products

- FLASH's land mask reference data was updated to increase accuracy along the coast.

Max Soil Saturation (CREST, HP, SAC)

- Updates to soil property reference data that improves product performance along the coast and western US.

Average Recurrence Intervals (ARI)

- Updated geolocation information in the GRIB2 header to more correctly display in AWIPS.

AutoNowCaster (ANC) Updates

All products

- Replaced GOES-13 input with GOES-16.

The MRMS on-boarding documentation suite (not including ANC) consists of approximately 210 pages and 3 companion worksheets. To assist NCO with testing and implementing MRMS v11.5.4, three documents were updated/created. A copy of the documentation can be made available if requested.

Build Instructions -- Steps for compiling the various software components of MRMS (updated for v11.5.4)

Update Instructions (new) – Summary of v11.5.4 changes and very specific update instructions organized by update type and then again by virtual machine.

Release Notes (new) – Summary of v11.5.4 updates geared towards communicating important changes to NWS (and other) MRMS users.

The MRMS v11.5.4 work is complete.

In June of 2018, the MRMS v11.5.6 patch was delivered to NCO along with the appropriate documentation and update instructions. The patch was made operational after June 30, 2018. Below is a summary of updates delivered to NCO as part of v11.5.6.

System-wide Changes

Radar Quality Control

- Increased robustness of Canadian radar QC algorithm to better handle the real-time data flow behavior of CONVOL and DOPVOL data.

Handling of New WSR-88D Radar Characteristics

- Improved handling of extra low-level elevation angles in general (no longer radar specific).

Hydromet Updates

XMRG Formatted Products

- Increased robustness of XMRG encoding by reorganizing its associated processing chain.

Model Ingest

- Updated logic for decoding HRRR data to compensate for organizational changes made at NCO.

Flooded Location and Simulated Hydrographs (FLASH) Updates

All Products

- Added logic and scripts to push FLASH products to the Satellite Broadcast Network (SBN). Note the functionality is in place but has not been activated (i.e., flags are turned off for now).

21. NSSL's Virtual Multi-Radar Multi-Sensor (VMRMS)

Karen Cooper, Carrie Langston, Lin Tang, Jeff Brogden, Robert Toomey, Brian Kaney, Ami Arthur, Alicia Keys, Travis Smith, Darrel Kingfield, Kiel Ortega, Brandon Smith, Anthony Reinhart, Steven Martinaitis, Youcun Qi, Micheal Simpson, Andrew Osborne, Shawn Handler, Heather Reeves, Zac Flamig, and Humberto Vergara-Arrieta (CIMMS at NSSL), and NSSL Information Technology Services (AcelInfo Solutions)

A key NSSL strategy to maintain the stability of MRMS for research and operational environments is to host development efforts on a computing infrastructure similar to what is used at NCO. To fill this need, a development and testing system (called VMRMS) is maintained at NSSL. The algorithms and configurations for the next operational MRMS are tested and verified on VMRMS before they're given to NCO. VMRMS also houses experimental products in their earliest stages of development.

Hands-on management of the system is performed almost exclusively by the Analytics and Enterprise Group (AEG) and NSSL ITS. However, many members from many groups contribute to the system by developing new algorithms and improving existing ones.

VMRMS changes in FY18 include the following:

New Algorithms/Products:

- Incorporation of GOES-16, eRAP and GFS data
- New logic and reference information to handle VCPs 35 and 215

- New logic to handle extra low-level scan from KMUX (Dec 2017) and eventually to handle such instances from any radar (Spring 2018).
- 3D ConUS mosaic of radar observation age (Fall 2017).
- 3D ConUS mosaic of spectrum width (Fall 2017)
- Evaporation Correction – online for ConUS in Fall 2017
- Continued expansion of the MRMS product suite for Hawaii – Addition of MADIS gauges for Hawaii, Dualpol RA QPE, Synthetic QPE, Evaporation Correction (Summer 2018)
- Velocity dealiasing -- replaced dealiasing algorithm with new program that matches what's used in the ORPG
- Radar QC – replaced radar QC algorithm used to create input for AzShear / RotationTracks products with new variation of Dualpol QC called “Dualpol QC Light” (Spring 2018)
- New product -- Added processes to crop and convert a subset of products for the HWT experiment (Spring 2018)

Updates

- Gauge Ingest – refined values associated with reports of no rain or missing rain and increased scripts' robustness.
- Gauge QC – bug fixes, added SCaMPR and 1H QPF input to help address areas with low RQI and further refined QC logic
- Dualpol QC – bug fixes, optimization, added logic to mitigate false alarms and contamination from radar hardware failures, added option to relax QC logic for downstream applications that have different QC requirements.
- Canada AP QC – bug fixes, added sea clutter mitigation for WGJ, improved mitigation of residual AP clutter.
- Seamless HSR – many changes including a major rewrite of the algorithm. Highlights include changes to logic to write out products more frequently when SAILS or MRLE are in use, RQI calculation changed from using beam center to beam top, added transition zone for RQI when shifting above/below the freezing level.
- Seamless HSR Mosaic – merger of RQI field updated to use maximum value scheme
- Dualpol RA QPE – bug fixes, added extra logic for high-value Z, better handling of small areas of precipitation, refined handling of various calculations and the use of blockage information.
- Merged QPE – bug fixes, increased influence of Mountain Mapper QPE and modified weight of Radar Only QPE in final QPE field
- AutoNowCaster – updated to use GOES-16 data, internal coding refinements, and increased grid resolution of final products from 5 to 1km.
- Caribbean – added radars in Belize and Sabancuy, Mexico to unQC'd BREF
- Reference data – updated terrain, beam blockages, w2mergercache and wind farm information

Ongoing

- Addition of the new algorithm suite ProbSevere started in FY18 and continues.

In addition to this work, there were ongoing efforts to react to real-time data flow problems. For example, when Chicago's radar had a hardware failure that caused it to send bad dualpol moments, the radar was pulled from VMRMS until it was repaired. There were also ongoing efforts to troubleshoot complex problems with VMRMS's hardware including unexplained CPU bottlenecks and network storage slowdowns. Note, these particular issues seem to be mostly resolved at the time of this report.

VMRMS computing resources increased in FY18. The following list outlines this growth:

- Dell Chassis: increased from 4 to 4.5
- Dell Blade Servers: increased from 24 to 35
- Processor count (CPUs): increased from ~900 to 1312
- CPU capacity: increased from 1.92 to 3.27 THz
- Memory: increased from 9.25 to 13.37 TB
- Storage (NetApp, Network Attached Storage): increased from 40 to 70 TB for real-time data processing. 160 TB was added for onsite archive purposes. The METOP storage remains at 300 TB. Connectivity is 10 GB.
- Virtual machine count: increased from 81 to 90

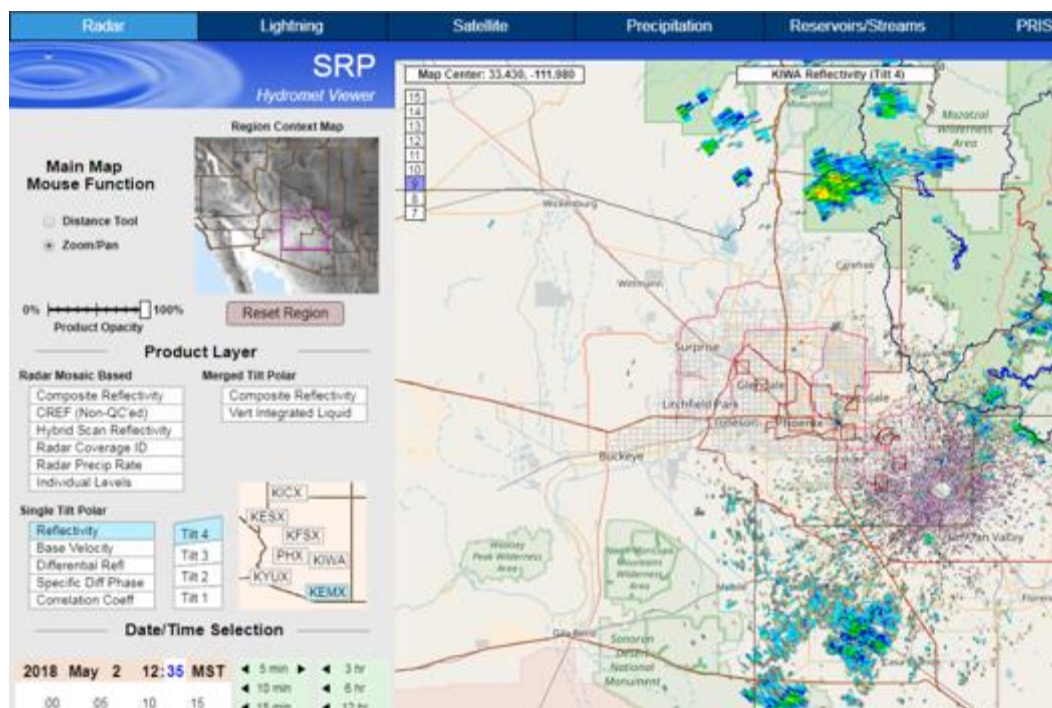
Additionally, the effort to better document the VMRMS system and MRMS in general continues. In February of 2017, a new wiki was configured on an internal NSSL server. When possible, members of AEG (along with SHMG and SCG) are continuing to populate the wiki with a range of basic and detailed information. For example, there are pages defining Volume Coverage Patterns, tracking the status of non-US radars for the Caribbean domain, algorithm specific pages and a change log for all updates made to VMRMS. This wiki is available on NSSL's network only, but excerpts can be made available if requested. Adding to the wiki is an ongoing effort. From FY17 to FY18, the wiki's page count increased by nearly 10-fold and its information volume increased by 800%.

22. Hydromet Viewer for Salt River Project

Brian Kaney, Carrie Langston, and Karen Cooper (CIMMS at NSSL)

The Salt River Project (SRP) water and power utility operate in a very challenging QPE/QPF environment and had the first WSR-88D installation in the mountain west. With significant mountain blockages, complex terrain, large areas of orographically enhanced precipitation, significant winter precipitation from low based clouds, significant summer thunderstorms from high based clouds, and even tropical storm remnants, central Arizona is well suited to test the limits of multi-sensor QPE and the new dual-polarization capabilities in MRMS.

Work this year consisted of maintenance and a small number of bug fixes and user requested improvements. For instance, a drop down text menu of individual radar sites was replaced with buttons laid out on a map background. Other issues involved fixing map background tile sources, TDWR radar site fix, manual override buttons for the satellite looper, and timing issues on the complicated PRISMS mesonet display tool.



Sample image from Salt River Project Hydromet Viewer.

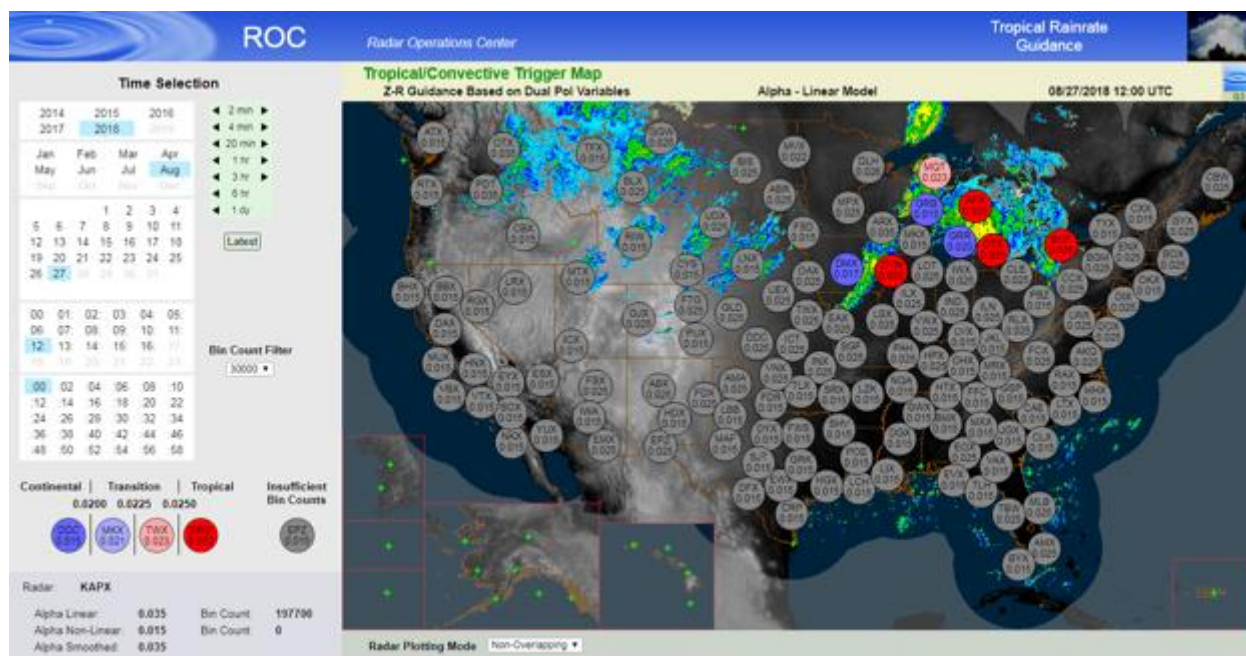
23. Web Tool Suite for the Radar Operations Center

Brian Kaney, Carrie Langston, and Karen Cooper (CIMMS at NSSL)

Our group maintains a suite of tools for the Radar Operations Center (ROC). This FY we saw an increased MOU funding and task list with a wider variety of projects of significance.

A major new web tool added this year is the Tropical Trigger Guidance page. This further extends the science underlying the ZDR vs Z scatterplot web tool from last FY. That tool was a testbed for evaluating a rain rate determination method pioneered by Ryzhkov and Zrnic in the 1990's. The central segment of the ZDR vs Z plot is fit with a straight line with a slope referred to as alpha. The alpha parameter is then used to determine the ZR relation to find rain rates and in particular is proposed as a method to identify when a radar should be finding rain rates using a tropical model. The new web tool highlights, every five minutes, where the rain rate regime is continental, transitional, or tropical across the WSR-88D network.

The next figure shows a screen shot of the web tool. The lower left and right areas of the map show inclusions of sub-maps for Hawaii, Alaska, Guam, Korea, Okinawa, and Puerto Rico. While data for all of these domains outside the CONUS was not fully established by the end of FY 18, their inclusion was part of the current round of work for the ROC. Several older Level 3 Metadata web tools that have existed for the CONUS in years past were also extended to these other domains in this year's work.



Sample image from the Tropical Trigger Guidance web tool created for the Radar Operations Center.

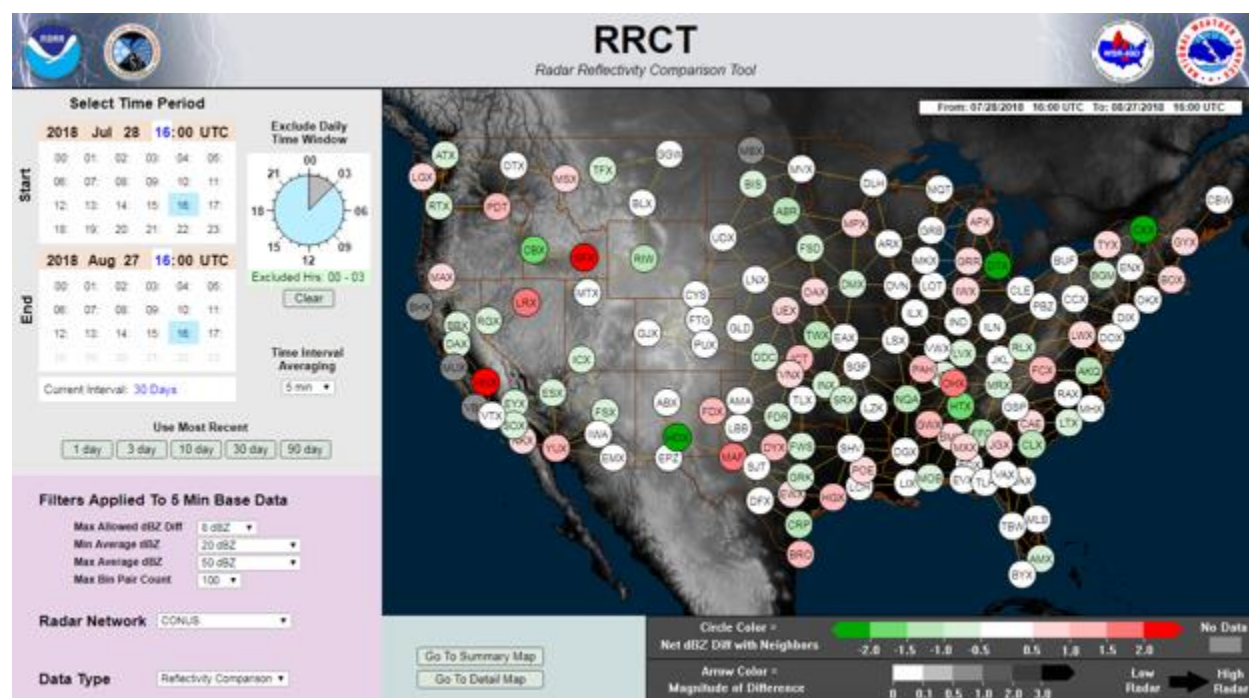
Significant work also occurred on a gauge extraction tool. This will allow users to query the MRMS gauge archive in a variety of ways. Hourly time series or accumulations of various time periods can be requested. The text output can be easily exported to a spread sheet or other programs for analysis. A number of filters can be applied including latitude/longitude bounding box, QC flag status, and completeness of record for accumulation.

Another major project was a redesign of the Radar Reflectivity Comparison Tool (RRCT). This was the last web tool still hosted on OU domain machines. With a code set largely dating back to mostly 2009 and a little 2013, it is also the oldest code of any of our currently active web tools. As such, there was much room for improvement. This work is still on going at the end of FY 18. The main changes are not in the form of completely new features, as these were not requested, but the improvement of existing features. In particular, a completely new layer was added to the back-end that improves the speed of results by a factor of about 10 times. This brings the usefulness of the page into a whole new realm. There are many filters and options on the web tool, but every minor setting change meant 6, 8, 12 seconds waiting for a reload of the new results. This made the page tedious to browse for very long. As the requested time

period of data increased the response time crossed over the line to practical non-usability. To look at one year's run of data meant 1 to 2 minutes refresh for every minor navigational change. One had to have a serious level of interest to keep using this for long at that level of performance.

The new RRCT is lightning fast by comparison. It just takes a second or second and a half for any request to be full-filled for data periods of a few months or less. Even a year's worth of data can now be queried with reload times under 10 seconds.

The older RRCT code set required the user to click a 'Submit' button every time a filter or option was changed. Now a change to a drop down menu or checkbox, or so on, is detected and automatically triggers the change to be reflected on the page output. This makes the new page feel even faster. In a side by side comparison, a new RRCT user is seeing on the screen the end result of an option change before the user on the old RRCT has even clicked the 'Submit' button to start the 8 second wait for new data to reload.



Sample image from the new Radar Reflectivity Comparison Tool (RRCT) web application for the Radar Operations Center in progress.

24. QVS Work for the vMRMS System Hosted in Norman and Operational Version at the NCO

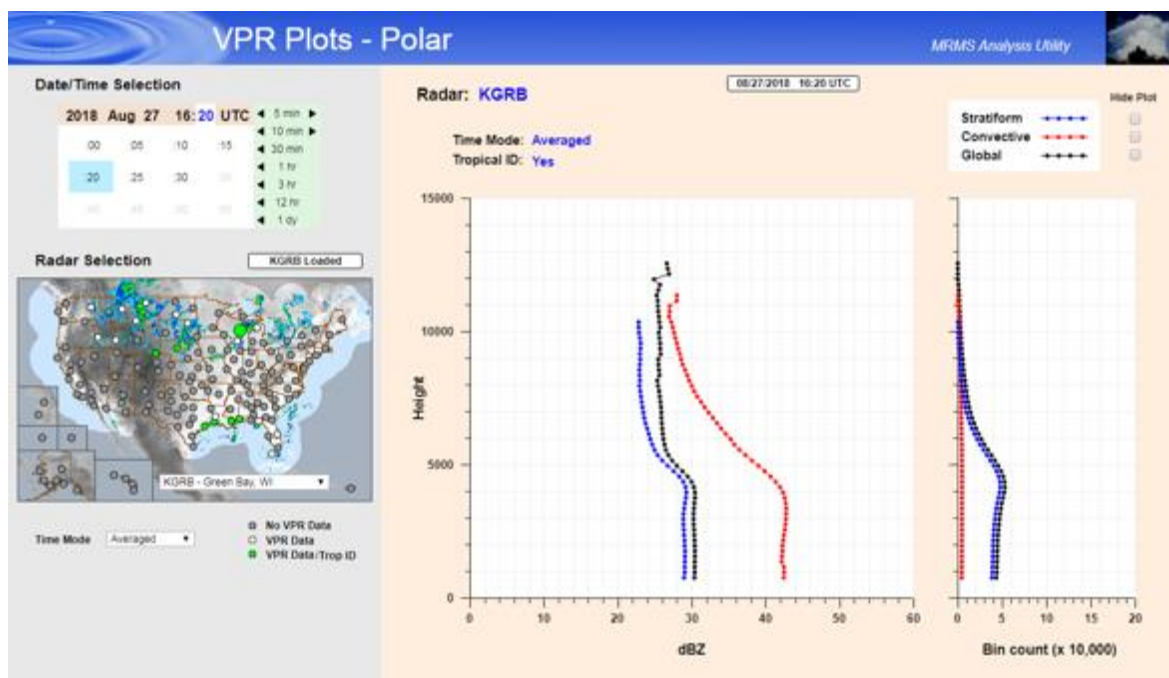
Brian Kaney, Carrie Langston, and Karen Cooper (CIMMS at NSSL)

The QVS acronym originally came from QPE Verification System, where QPE itself stands for Quantitative Precipitation Estimate. Evaluating our precipitation products

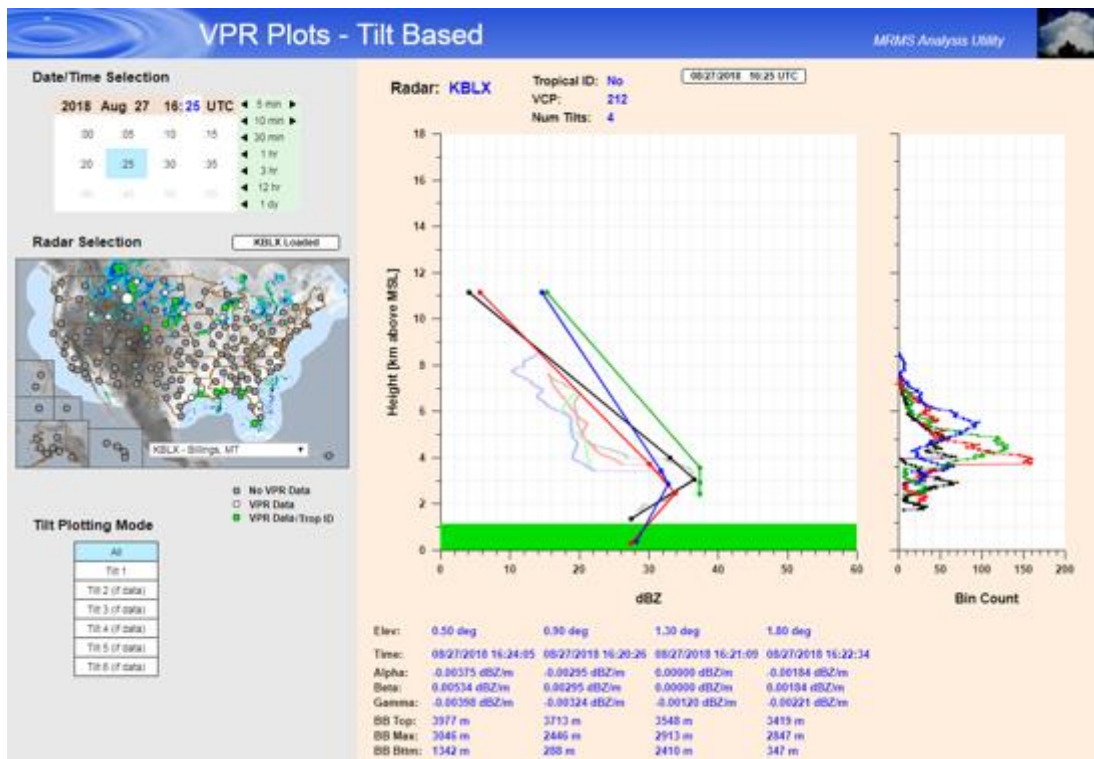
against other fields and ground truth is still a core purpose of the QVS. But as our methods for creating a precipitation field relies on many inputs there are also many variables, fields, and observations that can be brought to bear on post analysis. As such the term QVS has been used for a wide variety of web tools that aid our analyses in many different ways.

The Multi-Radar Multiple-Sensor (MRMS) product suite went into operations a couple years ago and still has a research version running locally in Norman. In FY2017 a major reorganization of this research MRMS system occurred. This included the QVS suite of over two dozen web tools and applications. The QVS system was moved completely from ou.edu domain machines to nssl.noaa.gov domain machines. Along with this went some major changes in the back-end architecture. Some of these changes had to do with security and others performance.

This was a major undertaking last year and continued through-out FY 2018. A number of web tools from the former system went dark for a time and were just revived this fiscal year. Two related tools that were revived (and improved) this FY was the plots for Polar VPR and individual tilt-based VPR's.



Sample image from the Polar VPR Plot generator.

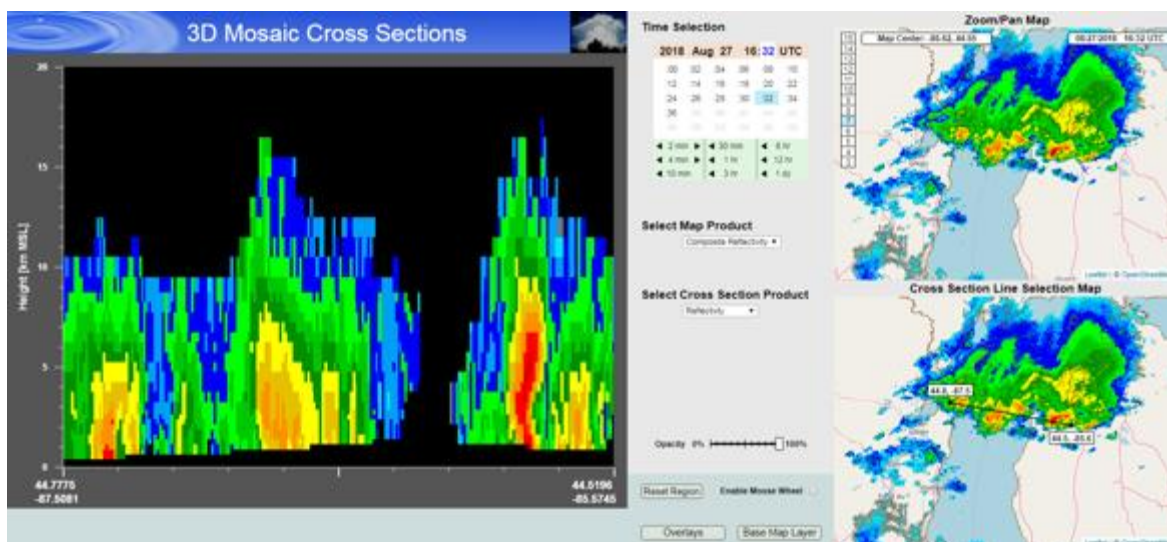


Sample image from the Tilt-Based VPR Plot generator.

Both tools are used extensively within the MRMS research group to assess questions of radar mosaicking and QPE performance. Even though the core features of these web pages are the same as the prior version, the code set has undergone a major revision. The older code reloaded the page from scratch with every change in option. The user would set new options but usually this had to be followed by a click on a 'Submit' button before the changes would be reloaded. The new code only loads the whole page once and then as different navigational options are made the change begins immediately. Either through a call to the server for new data or changes made client-side. Only those portions of the display that need to be change are refreshed. This results in faster and more smoothly performing web tools.

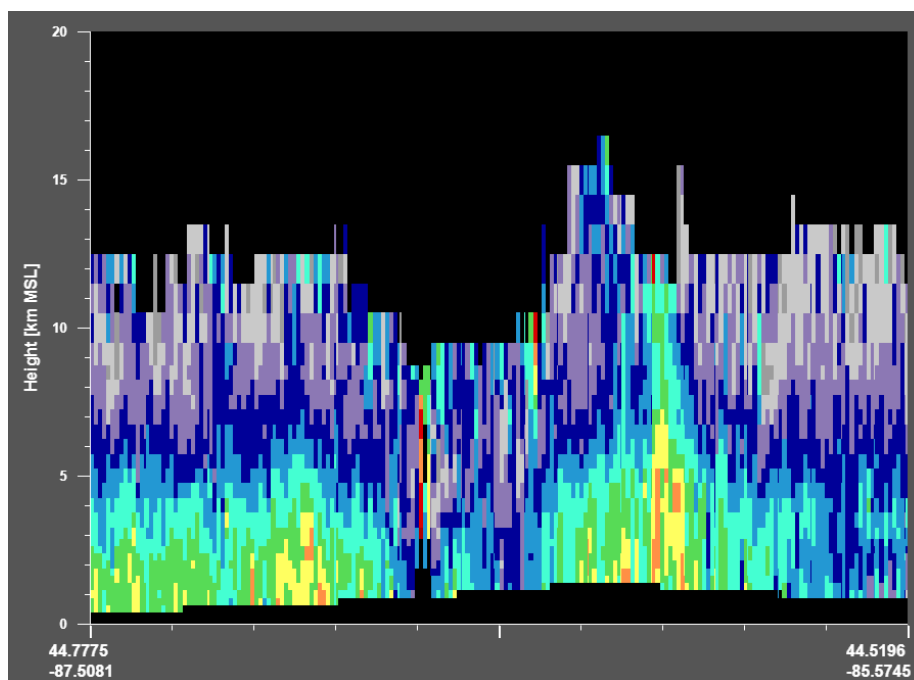
Another important diagnostic for MRMS performance and many other meteorological issues is the 3-D mosaic cross section tool. The old system had the ability for the user to draw an arbitrary line across a data map and see a vertical cross-section of the 3-D mosaic along that line. This tool was unavailable for a while but was revived in FY 18. One challenge was that the new storage of data on the back-end was actually not optimal for doing vertical cross-sections. The old system had a multi-layer file that contained all 31 layers of the mosaic in a single file, but cut into a few tiles to cover the CONUS. Tiles were abandoned as all new files contain the entire CONUS. A single 31 layer file was prohibitive for the whole CONUS so this was split into 31 separate single layer files. Unfortunately, this greatly impacted the performance of extracting the data needed for a vertical cross section. This problem was addressed by dividing the image drawing into four horizontal strips. Each strip is draw by a different server call and as

such they can be launched all at once. Each strip needs to read about 8 layers of data (instead of all 31) and so the performance is much faster again – comparable to the older version of the tool.



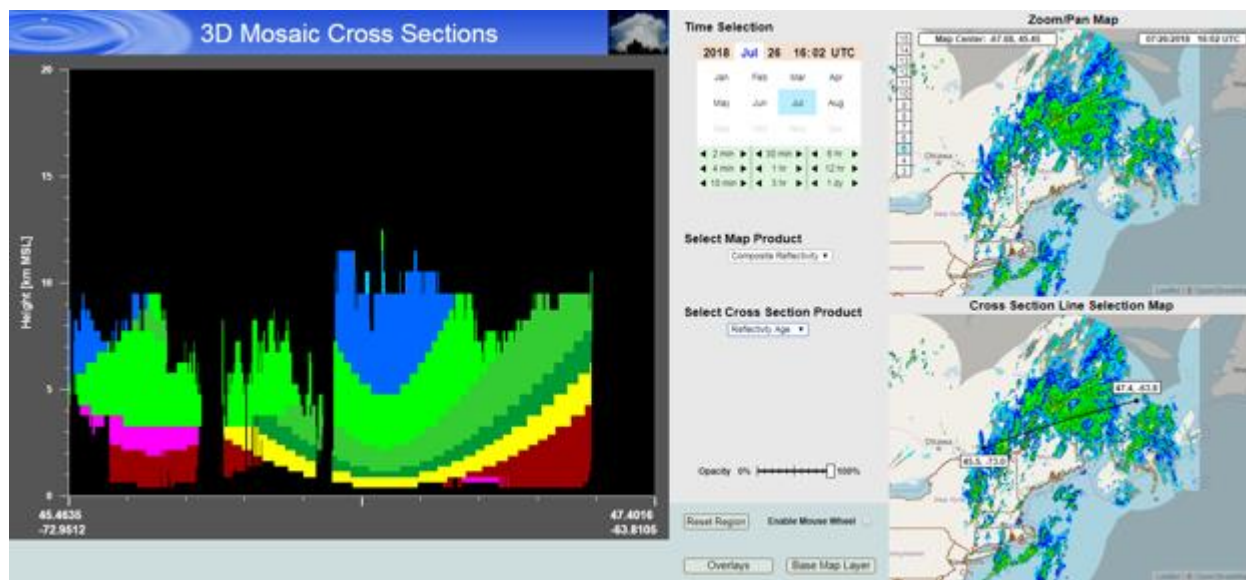
Sample image from the new 3D Cross Section tool revived in FY 2018.

The old tool displayed arbitrary vertical cross sections for the only 3D mosaic we generated at that time, namely radar reflectivity. In the interim however, several new 3D mosaics have been added so a lot more information can be obtained. The new mosaics are mostly related to the new Dual Pol variables. The following image shows an example of just the cross section pane for ZDR.



Sample 3D Cross Section panel of ZDR (Differential Reflectivity) dual pol variable.

Cross sections are also available for KDP, RhoHV, and Spectrum Width. And then a more recent addition, in support of our work for the FAA, was a mosaic showing the age of the data used in the mosaic. This is seen in the image below. Blues and greens are very recent data (1 to 2 minutes old) whereas red and magenta are getting up to 10 or more minutes old. The exact age of different parts of the mosaic is of interest to highly weather dependent users such as the FAA and can play a role in how algorithms calculate radar derived products that use the mosaic as an input.



Reflectivity Age 3D cross section.

The MRMS research group strives to be agile and flexible in terms of which research paths to pursue. It was discovered at one point that the azimuthal radial joint (ARJ) in the WSR-88D fleet was sometime causing issues with the MRMS radar mosaic. Work was done to analyze where and how often this was something of concern. In a relatively short period of time an entire back-end process chain and web tool viewer was developed to address this topic.

A sample screen from this internal diagnostic tool is shown in the next figure. There are many elements. Line plots of the noise in both the vertical and horizontal polarized signals versus azimuth are shown for all tilts in a single volume scan. An azimuthal wedge chart of any bad radials or sector is shown. And a large amount of metadata about the volume scan in table form at the bottom.

CIMMS Task III Project – ARRC R&D Activities for the Multi-Mission Phased Array

- **ARRC Demonstrator Development Activities for the MPAR Program: CPPAR and Horus**
- **Spectrum Efficient National Surveillance Radar (SENSR) – Development of the All-Digital Horus Demonstrator**
- **Spectrum Efficient National Surveillance Radar (SENSR) – ARRC Risk Reduction Activities**

Boon Leng Cheong (ARRC), Caleb Fulton (ARRC/ECE), Robert Palmer (ARRC/School of Meteorology/VPR), Jorge Salazar (ARRC/ECE), Hjalti Sigmarsson (ARRC/ECE), Mark Yeary (ARRC/ECE), Guifu Zhang (ARRC/School of Meteorology), Rockee Zhang (ARRC/ECE), and Tian-You Yu (ARRC/ECE)

NOAA Technical Lead: Kurt Hondl (NSSL)

NOAA Strategic Goal 2 – *Weather Ready Nation: Society is Prepared for and Responds to Weather-Related Events*

Funding Type: CIMMS Task III

General Objectives

Develop several complementary technologies that are essential to the forward progress of multi-mission phased array systems. The projects described below are ongoing.

1. Architecture-Specific System Modeling for Multi-Functional Testbeds

OU POC: Rockee Zhang

Objectives

Develop a unique simulator for future weather radar systems, such as Spectrum-Efficient National Surveillance Radar (SENSR), called PASIM (Phased Array Simulator). Different from previous weather radar simulations, PASIM needs to be a system simulation tool which includes impacts of electronics, time-domain waveforms, and a data quality prediction and analysis tool to support SENSR trade studies.

Accomplishments

PASIM is going to become part of the official release of MATHWORK's MATLAB 2018b+ Phased Array Systems Tool Box, which is based on a series of weather-radar-focused functions developed by the team and is being used by industrial partners who participated in SENSR and other government radar developments. The main technical achievement is the inclusion of multiple system elements written in diversified languages, such as JAVA, C, Python and MATLAB into a data-focused radar design assessment tool, which has the elements of electronics modeling, capabilities of using hardware model parameters from benchtop measurements, waveform and time-domain

radiation/scattering models based on Finite-Difference-Time-Domain (FDTD) solution, and multiple severe weather scenarios for data quality analysis.

2. Blind Range on Pulse Compression Radars

OU POC: Boon Leng Cheong

Objectives

This research project has for objective the development of a novel technique to get rid of the blind region from solid state radars using pulse compression, this progress report presents the last update into this objective. This technique, different from implementations proposed in literature [1, 2] does not require of a different frequency fill pulse.

Accomplishments

An inherit problem with solid state radar is the long waveform required to get back the loss in sensitivity due to the low transmit power. A consequence is a strong leak-through from the transmit signal affecting a portion of the received signal, this portion is called blind region and targets inside this region are usually obscured due to this leak-through. However, the echo from a target is distributed through different samples and is usually processed using pulse compression, then even when the received signal from a target is partially corrupted by this leak-through a portion of this is still unaffected, and this portion is in theory enough to recover the target. That is exactly what is proposed in this study to zero out the leak-through from the transmitted waveform, and thanks to pulse compression and the calculation of a calibration factor, the information inside the blind region can be recovered.

To demonstrate the advantages of this proposed technique compared to regular pulse compression implementation, called conventional techniques, different simulation scenarios has been tested, each one simulating 4 targets, 2 inside and 2 outside the blind region. The difference between each simulation exercise is the transmitted waveform, three different waveforms were used: a non LFM waveform, an LFM waveform and a windowed LFM. The waveforms used are presented in Figure 2.

Results from the simulation are divided in three categories: ideal target, results from conventional technique, and results from the proposed technique. Results are provided in Figures 3 to 5.

Simulation results shows that one of the advantages of this technique is that targets inside blind region are now visible and not obscured by the leak-through. It is also important to mention the importance of the calibration factor to correct for the portion of the waveform missing due to the leak-through in the received waveform.

In general terms, the progress for this quarter and the projections for the next one can be summarize in the following steps:

- Study the effect of zero out the leak-through from the transmit signal. As explained before, blind region is originated due to the leak-through from the transmitter, then if this leak is zero out, the remaining echoes could still be enough to recover the information inside the blind region thanks to pulse compression, during this quarter different experiments has been performed to test this claim, from simulations with different waveforms, to different techniques to zero out and process the remaining data.
- Design and calculate the proper calibration factor. Due to the nature of the technique, return from target inside blind region result affected and some products as the reflectivity and some parameters as the noise level must be calibrated. Calibration factor is different depending on the transmitted waveform and the range gate, and their value depends on how much information remains for the target after a part of the signal has been zero out.
- Test the implementation and study the effect over real data. Simulations confirms the applicability and the advantage of this technique over the conventional technique, next step is to corroborate these results using real data, different examples have been tested and results are being compared to results from the same dataset using both, pulse compression and results using the technique currently implemented in PX-1000, TFM [2]. Preliminary results confirm previous results and confirms the advantage of this technique; however, further analysis is currently being conducted.
- Next quarter will be focused on the improvement of this techniques using real data from PX-1000, some effect usually appears on real data, in consequence, more analysis over different datasets are required, to study and solve them.

3. Analog Interference Mitigation in Future All-Digital Phased Array Radars

OU POC: Hjalti Sigmarsson

Objectives

In this task, the possibility of embedding RF filters into a phased array radar front-end module is being investigated. Substrate-integrated cavity filters are being embedded into the bottom two layers of the antenna stack-up without affecting the antenna performance but still providing significant improvement in the out-of-band interference rejection. The goal is to design filters that operate at 2.85 GHz, cover the entire band of interest from 2.7 to 3 GHz, and add more than 30 dB of additional rejection while maintaining low loss. The full specifications of the filters are shown in Table 1.

Table 1: Filter specifications

Parameter	Target Value
Center Frequency	2.85 GHz
Bandwidth	350 MHz
Fractional BW	12%
Insertion Loss	< 1 dB
Rejection @ $(1 \pm 0.15) f_0$	> 30 dB

Accomplishments

Originally, to meet the desired specifications in Table 1, a fourth-order filter was selected. Last year, an alternative method was pursued. This method consists of cascading a second-order BPF with an elliptic lowpass filter (LPF). One benefit of such an LPF is that it exhibits a very low insertion loss in the passband, while providing a sharp roll-off and a constant attenuation level in its stopband. One concern about using this technique is the total size of the cascade. However, such a cascade can result in a low profile BPF with a wide stopband, provided that each individual filter is designed properly. The structure of a second order evanescent-mode cavity BPF cascaded with an elliptic LPF was shown in last year's report but is included here again for visualization purposes. The structure is shown in Figure 6. The LPF is implemented using non-symmetric stripline technology, which is used in the antenna stack-up. Figure 7 shows the fabricated filter cascade prototypes. Two designs were included in the fabrication run, one that has the individually designed components and one where both filters have been optimized to compensate for the interaction between the two.

The fabricated filter prototype requires 4-mil traces and 4-mil spaces, both of which are pushing the fabrication capabilities of the ARRC to the limits. The connectorized LPF prototype and the measured versus simulated results are shown in Figure 8. Overall, the filter achieved the desired stopband performance, but there is a slight variation in the cutoff frequency. This can be attributed to the fabrication tolerances of the in-house processing. These tolerances are not as big of an issue for state-of-the-art circuit board shops. Therefore, the next revision of the filters will be fabricated by Accurate Circuit Engineering.

4. Exploiting All-Digital Architecture to Meet the MPAR Task Timeline

OU POC: Tian-You Yu

Objectives

- Develop multiple scanning strategies (Volume Coverage Patterns, or VCPs) to meet or exceed the requirements of MPAR/SENSR for spatial resolution, temporal sampling, and data quality
- Demonstrate benefits of using a rapid-scan phased-array radar for weather observations
- Test various VCPs in both a small-scale and large-scale radar simulator
- Assess effects of VCP selection on data quality and error estimates

Accomplishments

For this project, we aim to assess the benefits obtained via use of a rapid and flexible scanning phased-array radar for weather observations. Additionally, multiple radar simulators have been modified and/or developed to assess the qualitative and quantitative impacts of various VCPs. One such simulator is SimRadar, which uses a Large Eddy Simulation (LES) with a domain of approximately 1 km x 1 km to simulate dual-polarization radar returns. This simulator has been modified for the purposes of this project, such that various VCP modes can be supported, rather than simply

scanning at one elevation or one azimuth angle repeatedly. Another radar simulator being developed is RSim, a large-scale radar simulator which uses data from the Weather Research and Forecasting (WRF) model at high spatial resolution to produce simulated radar outputs over a larger domain. This simulator is able to produce simulated polarimetric radar data with various input beam patterns and VCPs.

Within SimRadar, modifications have been made to simulate various scanning strategies. Initially, the program was only capable of performing PPIs or RHIs at one elevation or azimuth angle, respectively. In FY18, a VCP option has been added, and multiple VCPs can be chosen to simulate radar returns. Currently, VCPs 35 and 215 from NEXRAD can be simulated, as well as 2 other “custom” VCPs. Additionally, low-level debris contributions have been suppressed to simulate beam blockage at low levels. For quantitative assessment of the benefits and tradeoffs of each scanning strategy, a tornadic vortex signature and tornadic debris signature (TVS/TDS) detection algorithm is under development and has shown some initial success during testing. The detection latency time for each VCP will be tested for a variety of tornado scanning scenarios at various ranges and various times, to assess how quickly the tornado can be detected via automated algorithms. An example output is shown in Figure 9.

In order to supplement the more quantitative assessment of output from SimRadar, RSim has been developed during FY18 to simulate radar returns from a larger (on the order of 50 km x 50 km x 10 km) domain, where WRF data are input at high spatial resolution. Each radial is simulated independently via a linear time interpolation scheme, and the microphysical fields (rain, ice, snow, and graupel) are used to derive radar variables at each model grid point. These data are then weighted by the radar antenna weighting function to derive the expected radar variables at each range, elevation, and azimuth combination. This simulator will provide complementary information to that from SimRadar, as a variety of weather scenarios can be simulated. An example PPI of horizontal reflectivity factor (Z_H) from a radar with 1-degree beamwidth on both transmit and receive is shown in Figure 10. These data will be used to assess the benefits and limitations of each scanning strategy qualitatively. Examples of how this might be achieved include qualitative assessment of the evolution of the precipitation field and manual detection of Z_{DR} columns.

5. UAS Calibration Receiver: Development and Secondary Use as a Passive Radar for 3D Wind Estimation

OU POC: Robert Palmer

Objectives

The development of practical approaches to high-quality polarimetric phased array radar calibration is a key component of current SENSr efforts. One promising avenue currently being explored is the development of a UAV-based calibration system bearing a dual-polarization antenna and capable of both transmit and receive operation. This solution will require a low-SWaP S-band receiver. An initial prototype of such a receiver has been constructed through combination of an existing ARRC-designed digital

receiver based on the AD9361 with an S-band front end. Efforts have been ongoing to test this hardware through observation of signals transmitted by the WSR-88D, improve the software associated with this system and resolve any performance issues. Further packaging development is needed to reduce the size and weight of this system, but its current performance is encouraging.

Accomplishments

One exciting aspect of the inclusion of a receiver in the calibration hardware package is that it opens up a range of possible research uses of the system that may add additional value to the hardware development work currently underway. Of particular interest is the possibility of operating the calibration receiver as a multistatic radar receiver, with the WSR-88D (and eventually a SENSr system) acting as the transmitter. A network consisting of a transmit radar and 2 or more of these receivers would allow for the direct retrieval of 3-dimensional wind fields without reliance on fluid dynamics assumptions. The value of multistatic radar systems for wind field retrieval has been demonstrated [1], but previous systems of this type have relied on bulky, expensive, GPS-disciplined oscillators and dedicated communications infrastructure between the transmit and receive systems. If, however, synchronization between the two systems could be achieved through careful processing of the direct path transmissions to the receiver, it would allow the calibration receiver to be used for this purpose without modification. That could facilitate an inexpensive but potentially transformative improvement in wind retrieval capabilities with no additional spectrum use.

Before beginning work on development of the signal processing software necessary to implement this idea using the calibration receiver, a multistatic radar system simulator was developed. This simulator ingests numerical weather prediction data, transmitter and receiver parameters, and the geometry of the simulated network. It returns simulated values of received power, SNR, and measured bistatic velocity (Doppler velocities measured by multistatic radar correspond to motion along the bistatic bisector rather than the transmit or receive pointing direction). This simulation software demonstrated that we could expect to obtain useful SNRs from systems with specifications corresponding to the WSR-88D and the calibration receiver.

Next, signal processing software was developed in order to implement this concept using the calibration receiver. Direct path pulses are detected using a CFAR detector and quality-controlled using basic assumptions about PRF. This information is then used to organize the received IQ into a fast-time/slow-time matrix. Next, the frequency offset between the local oscillators (which varies over time) is estimated through the application of pulse-pair processing to the direct-path pulses and is removed from the received signal. While, in reality, this removes the true frequency offset plus or minus some integer multiple of the PRF, this estimate is adequate. Traditional MLE frequency estimation (using the peak frequency bin of the FFT of the received signal) is impractical in realistic scenarios due to multipath effects. The pulse-pair method results in correct Doppler velocity estimates due to aliasing, and a negligible loss in sensitivity for typical weather radar pulse lengths. After the frequency offset removal, standard weather radar signal processing is applied to the resulting data.

This software was then tested, first using returns from ground clutter, and then through actual weather observations. Figure 11 shows a comparison between simultaneous observations collected by the prototype receiver (located on the roof of the Radar Innovations Laboratory) and by KTLX. The data, collected at 14:45 UTC on July 15, 2018, depict some scattered thunderstorms just north of Norman, Oklahoma. The quality of these results appears highly promising.

First, it should be noted that the “blob” connecting the transmitter and receiver is to be expected from bistatic radar images and reflects a loss of spatial resolution in regions near the Tx-Rx baseline. This effect would eventually be mitigated using the spatial diversity afforded by multiple receivers. That said, note the zero or near-zero Doppler velocities associated with ground clutter in contrast with the clear motion indicated for weather regions. Correct Doppler velocities are indicative of quality frequency offset removal, which is potentially the largest challenge associated with this concept. The images from the passive radar also demonstrate reasonable sensitivity, as expected (it is censored at 3 dB SNR).

Future work on this topic will include improved packaging for the receive module, which will be critical for both the calibration and passive radar applications, as well as refinement of transceiver control and signal processing software. Multiple prototype systems will be produced for use both in the calibration application and in collection of multistatic data using multiple passive receivers simultaneously. This will allow for a demonstration of the potential for 3-dimensional wind field retrieval using this hardware.

6. Multi-Channel Digital Equalization to Enable Wideband Digital Arrays

OU POC: Mark Yeary

Objectives

In a digital beamforming system, equalization in the digital domain is utilized to help in calibration and reducing errors induced by the system processing chain. This is done by precisely matching amplitude and phase between elemental channels. Without this critical processing step, the desired beamforming (i.e., main beam and null) of next generation radar systems cannot be achieved. These concepts were demonstrated on data collected from a Horus module.

Accomplishments

To begin, several equalizer algorithms and implementations for next generation radar systems were evaluated using a known data set captured from Horus with a metric known as the channel pair cancelation ratio (CPCR). An equalizer was implemented to process the data and to correct for mismatches using a multi-channel FIR filter. The equalization of channels was based on a reference signal that was either known prior or based on a chosen reference channel (the latter was employed in the results below). Both zero forcing equalization and minimum-mean-square-error (MMSE) equalization were evaluated across the entire band. The data also has a nonlinear relative phase

difference across the band that needed to be corrected as well. The short time Fourier transform (STFT) was used to view the time varying data, as well as compute sets of equalizer coefficients for each stationary segment of data. Additional ways of processing the data and implementing an alternative equalizer algorithm were also studied. It was based on breaking the signal into subbands, equalizing each subband, and reconstructing the wideband signal. A polyphase channelizer with near perfect reconstruction through oversampling was studied and implemented as an efficient way of design. Equalizers were implemented in each subband, and it was shown how the computation of the coefficients is less complex than across the entire band, because inverting a set of small matrices in parallel was less computationally expensive than inverting one large matrix.

Next, the laboratory data are discussed. The multi-channel data captured from Horus was used for evaluating the equalizer. The data contained approximately 62,000 samples by four channels of 125 MSPS (mega samples per second) data received simultaneously. The excitation waveform was a chirp starting at -62 MHz going to +62 MHz over a duration of approximately 500 μ s. This transmit waveform was converted to RF around 2.8 GHz and coupled to the four channels through an RF splitter, analog down converted and digitized. The RF components caused several dB of variance across this bandwidth. Tones caused by artifacts of direct conversion transceivers impacted the received signal as well. Other artifacts included a DC offset caused by LO leakage, finite image rejection, and third-order nonlinearities. Figure 12 depicts the results of our MMSE-based equalization procedure on the data.

Based on the data, a four-channel beamforming environment was created with an interferer and desired signal coming in at specific angles (-15 degrees and +30 degrees, respectively). This was used to show the importance of equalization in forming main lobes and nulls. Additionally, it was shown how a TTD FIR filter and wideband adaptive beamforming FIR filter can be utilized and combined with the equalization FIR filter. The steps taken were: equalization, true-time delay, and linear constrained minimum variance (LCMV) beamforming. Figure 13 shows the results.

In summary: several equalization algorithms were studied, and the MMSE across the full band performed well without the need to cycle through coefficients within a sub-banded architecture. Although the latter is less computationally intensive, the former demonstrated that equalization is needed to form nulls. A journal article is in progress.

7. HFSS Design for Cylindrical Arrays

OU POC: Caleb Fulton

HFSS Design for Cylindrical Array

HFSS is used to simulate a simple cylindrical phased array made up of slot antennas. One element is simulated using master/slave boundary conditions and the results are processed to create an embedded element pattern in MATLAB. This method of simulation is called unit cell analysis. The cylindrical array is designed to be infinitely

long to understand fundamentally how the curvature of the array is dictating the electric and magnetic fields. This physical design can be visualized in Figure 14. The first component in the XZ-plane is the slot antenna. This component is the one closest to the origin. The second component in the XZ-plane is the radiation boundary. The third component in the XZ-plane is the PML, and the final face in the XZ-plane is the end of the air box. The location of the radiation boundary and the PML are moved in the y-direction during the respective simulations.

Simulations

The radius of the cylinder is fixed at one meter while the length from the antenna to the PML is varied, or the length from the antenna to the radiation boundary face is varied. In both cases, the further the radiation boundary and PML were from the antenna, the more the phase mode spectrum acts uncharacteristically. In the first simulation the PML was kept at a 400mm distance from the antenna. The radiation face was varied from 112.5mm to 387.5mm away from the antenna. As the distance between the antenna and the radiation face increases, more phase modes have non-negligible values. Additionally, when there is no radiation face present and the PML is moved away from the antenna, the same phenomenon occurs where phase modes become non-negligible.

For the second simulation, the radiation boundary was fixed at 25mm from the antenna while the distance from the antenna to the PML was varied. The results, shown in Figures 15 and 16, showed the phase mode spectrum and phase modes behaving mostly as expected, meaning the phase modes had negligible values in the same range for each PML placement. However, as seen in Figure 16 and Figure 17, convergence issues did appear significantly around phase modes 17 and 47 when the PML was 50mm or less away from the antenna (and 25mm away from the radiation boundary). Each placement of the PML showed slight non-convergence, the 50mm or less case is being emphasized to show the more exaggerated effects non-convergence has on the E_y patterns. This lack of convergence causes problems in the radiation pattern for the 50mm design. Another simulation of this type was executed to find the approximate length where the convergence issues are no longer present. The distance from the antenna to PML was extended up to 85mm in increments of 5mm. When the PML is 65mm and 70mm away there is a small amount of non-convergence at the specified phase modes, which creates small ripples in the radiation pattern. Once the PML is 80mm away from the antenna the convergence issues are cleaned up and the radiation pattern does not have ripples.

Electric Fields

Finally, the electric fields on the wedge component were observed for different phase modes. The phase modes included are 17, 32, and 47. Phase modes 17 and 47 are included for the same reason as stated above; these are the phase modes where non-convergence begins to appear. Phase mode 32 is included as a baseline, to see that the fields are behaving as expected when the simulation converges at a phase mode. Phase modes 17 and 47 behaved as expected as well for both the 85mm distance and

65mm distance. There were no visible differences between the 65mm and 85mm distances in each respective phase mode.

8. Cylindrical Polarimetric Phased Array Radar Geometry Studies

OU POC: Guifu Zhang

Objectives

The first objective is to identify the best image configuration for the large array of antennas. The image configuration is used for improving the cross-polarization level and increasing the geometrical symmetry of the array antenna. Using image configuration will suppress the cross-polarization level; however, it could cause undesired side lobes in the array radiation pattern.

The second objective is to characterize the co and cross-polarization radiation pattern of multifaceted cylindrical array antenna while the number of columns in each facet is increased. By using the embedded element pattern, the radiation pattern of multifaceted array antenna can be calculated; however, for multifaceted arrays, since the coupling between elements is different compared to a planar array or large cylindrical arrays, the full-wave simulations are preferred. Also, our goal is to calculate the polarimetric biases for different geometries and then determining the maximum number of the columns on each facet.

In the multifaceted cylindrical array antennas shown in Figure 22, the beam steering in azimuth angles is also required. In our simulations, we steered the beam to the angle that has the most asymmetry in terms of array geometry which depends on the number of facets in the 90-degree sector of the cylinder ($\Phi=90/(4 \times N_f)$).

Accomplishments

For the first part of our research, we have studied the image feed method which is widely used for reducing the cross-polarization level of the antenna arrays. The results of our studies show that none of four different 2×2 -element subarray configurations will totally suppress the sidelobe issue of configured arrays. We accurately identified the reasons for the appearance of the sidelobes and proposed the accurate procedure for predicting and reducing the sidelobe level of the large configured array antennas to the desired level. The results of this study are submitted to IEEE Transactions on the Antenna and Propagation journal and are currently under review.

For the second part of our research, we are investigating the effect of the facets on the differential reflectivity (Z_{DR}) bias. To have an accurate calculation and comparison, we are using a cross-dipole antenna and full-wave simulations for characterizing the array radiation pattern. For this study, a 90-degree sector of TMPAR sized multifaceted antenna arrays while the beam pointing angle is steered to the angle in which the array radiation pattern has the most asymmetric form, are simulated. The results are shown in Figure 23.

This study has not been completed yet; however, current simulations results show that up to 16 columns per facet won't significantly affect the polarimetric biases.

9. Characterization of the Impact of a Wet Radome on Polarimetric Phased Array Radars and Feasibility Study for Real-Time Calibration

OU POC: Jorge Salazar

Objectives

This proposed research consists in developing a technique that enables the prediction of the impact of a wet radome over the performance of a dual-polarized active and flat S-band phased array radar system. Recent findings based on experimental results demonstrated that water accumulation on an S-band radome of a radar system degrades polarimetric radar products, especially the differential reflectivity. Our main goal in this research consists in developing a technique that quantifies the differential attenuation of an S-band flat radome as a function of rain rate, tilting angle, and radome condition. This report presents the last stage of the proposed research. It shows the results of the completed analytical model and respective validation using numerical simulations and measured results. The antenna patterns of a dual-polarized active array antenna with a wet radome on an S-band with different water accumulation is discussed.

Two journal papers [1,2] that discuss the proposed techniques for S-band PAR are published in AMS/JTECH and an additional journal paper is in preparation [4] as part of this work. A provisional patent of the real-time characterization of a wet radome was submitted and currently in revision process by the US patent office.

Accomplishments

Measured results of HORUS active antenna array patterns with droplets and rivulets and partial film water during the experiment conducted on April 04, 2018 (see Figures 24, 25 and 26). In this experiment 2x8 elements were excited with T/R modules for e-scanning beam and the antenna elements were terminated. In Figure 24, a) to d) shows the setup of artificial droplets, rivulets and film water on the antenna surface. Since the antenna setup has to be vertical for NF test, a droplet holder (wrap-up plastic) was used to keep the droplets in place. Illustrations from e) to i) shows infrared images to illustrate the water formation (droplets, droplets aligned, rivulets and partial film water). Water formation on S-band radome surface (spherical or flat geometries) degrades differently the attenuation for H- and V-polarizations. Droplets formation are less critical than rivulet and film water. Rivulet formation and film water are real offenders for dual-polarized S-band radars. About 4 dB mismatch was found in the co-polar scanned patterns across 60° scanning range in presence of rivulets and 20 dB mismatch in the cross-polarization. Similarly, for partial film, about 5 dB and 20 dB mismatch were found for co- and cross-polarization respectively.

10. Spectrum Efficient National Surveillance Radar (SENSR) - Development of the All-Digital Horus Demonstrator

OU POCs: Robert Palmer, Caleb Fulton, Jorge Salazar, Hjalti Sigmarsson, and Mark Yeary

Horus Demonstrator

The all-digital Horus demonstrator can be broken into several major subsystems, which are shown in the Figure 27. A brief summary of the progress over the last year is then given for each of these subsystems.

Electronics (Octoblade, Superblade, Digital Bridge)

The Octoblade is a 16-channel, RF-to-digital transceiver, and makes up the heart of the Horus radar. The other major electronics components are the Superblade (power, control) and the Digital Bridge (RapidIO).

- Sent updated BOM to Advanced Assembly for LRU-ADP3 and shipped PCBs. Received first article LRU-ADP3 and performed in-depth test and evaluation (Quad board to FPGA development boards).
- Made detailed harmonic distortion measurements of the GaN front-end (RFE), other candidate mid-layer amp replacements, and the full TX chain. Added low-pass filters to RFE and candidate amplifiers to verify/measure removal of harmonics. Performed high-power testing of low-pass filter with RFE.
- Designed modified RX setup which enables better tradeoff between low-noise and high linearity states. Moved over to AD9371 EVB setup and integrated candidate replacements for TX/RX chains. After some initial hurdles, made several discoveries that clarified almost all of the measurements we have made in the last few weeks.
- Optimized TX and RX performance, verified satisfactory response across frequency and documented everything as much as possible.
- Completed RF midlayer schematic changes to the Quadboard and started to work on layout. Working through change list for other areas of PCB.
- Worked on the layout of the stack-up test board and adding the different geometries of interest. Investigated solderless end-launch connectors and contacted companies about launch geometry.
- The important goal for the next quarter (end of calendar year) is to make significant progress on the design and layout of the FPGA board, which would bring the Octoblade close to completion. Figure 28 shows the Quadboard (top panel) along with a mockup of the FPGA board (bottom panel).

Mechanical (LRU, Truck, Positioner, etc.)

The LRU houses 8 Octoblades and 1 Superblade. It also serves as the conduit for the cooling liquid and provides the overall structural integrity. The truck provides power to the radar and the chiller system and will also allow easy transport for demonstrations and field experiments. The positioner is being designed to allow “birdbath” mode for calibration studies and 360-degree coverage.

- Received as-built models for 1x1 LRU from KCR which include all changes that were made during the fabrication process. KCR pressure tested the three LRU frames with no problems. The three frames are getting some minor tweaks performed at the machine shop prior to heading out for final anodizing.
- Defined the equipment needed in the 1x1 LRU support system enclosure and started ordering components. The support system will play a major role in testing of a complete 1x1 LRU and will enclose the cooling system, power supplies, and computer. A rendering of the support system is shown in Figure 29 with the front and back access doors open. The bulkhead plates will be used to pass cables and fluid to/from the LRU.
- The Horus truck is currently at Real Power in Indiana for the generator install. KCR is getting the final long-lead items on order. The pedestal plates will soon be released to the machine shop. Completed analysis for outrigger load and variable pocketing pedestal
- Started first wave of structural simulations on the latest pedestal design, which includes variable-depth pocketing based on stress distributions. The benefit of constant-depth pocketing is weight-saving and ease of manufacturing. Variable-depth would give us higher strength.
- Worked on system/superblade power supply design. Specified parts, requested quotes, and got technical questions answered.

LRU Antenna/Filter Design & Fabrication

The Horus antenna is an 8x8 dual-pol stacked patch design, which will be affixed to the front of the LRU and will directly connect to the RF connections on the Octoblades. The first design proved to have extremely good performance, and the second generation is being designed to reduce overall cost and increase robustness. The inclusion of filters into the antenna stack-up is also being investigated for future revisions.

- Currently waiting on engineering support for antenna ver-2 fabrication process. This work will begin in October 2018.
- First round of the filter prototype fabrication was completed in June 2018.
- The measured lowpass filters met the isolation specifications of 30 dB at 5 GHz. Overall, the performance was very good, but the fabrication tolerances are causing a slight frequency shift. Next fabrication will be done by a professional circuit board shop.
- The two filters still need to be arranged into the actual antenna stack-up. One filter will be integrated for each polarization. The phase shift from the coaxial feed to the antenna coupling mechanism needs to be carefully matched between the H- and V-channels. The current version of the filter is shown in Figure 30.

Software/Other

The Horus demonstrator is an all-digital polarimetric radar exploiting the latest in COTS digital transceiver technology. As such, software is an integral and extremely important “subsystem” of the radar.

- Developed and tested a packet store and forward block to prevent having to deal with fragmented packets in the FPGAs.
- Completed several software features, including waveform generation, scan counter, and pulse triggering. Reached a point on the Rx beamformer where the core module used to form beams is working as desired. Worked on expanding the comprising piece to form beams for every desired combination of pointing angle, elevation spoil, and azimuth spoil.
- Remodularized packet chain for more robust testbench verification with each new or changed block. Made packet generation code easier to change. Simulated systolic beamformer in context with other blocks with no surprises. Made systolic beamforming (summing network only) work reliably.
- Testing maximum possible RapidIO throughput with current configuration and reliable transport concerns. Considering possible packet stream recovery mechanisms.
- Started work on developing a real-time PPI plotting mode for the Horus GUI. So far, have a plot using Vispy/OpenGL that can draw 100,000 range cells per second at 10 fps with arbitrary beamwidth. Still need to add panning, zooming, and integrate with geomap for the background.
- Created method to propagate user-level scan configuration between FPGAs via RapidIO, including a concrete start time that does not rely on back-and-forth with unsynchronized control computer.
- Started discussions with OU's Office of Export Controls about the commodity jurisdiction process for Horus radar under different software configurations. The hope is to have a version that will not be export controlled.
- No progress on frequency allocation, but Horus is now capable with 2.7-3.1 GHz.

Publications

- Mancini, A., J. L. Salazar, R. M. Lebrón, and B. L. Cheong, 2018: A novel instrument for real-time measurement of attenuation of weather radar radome including its outer surface. Part I: The concept. *Journal of Atmospheric and Oceanic Technology*, **35**, 953–973.
- Mancini, A., J. L. Salazar, R. M. Lebrón, and B. L. Cheong, 2018: A novel instrument for real-time measurement of attenuation of weather radar radome including its outer surface. Part II: Applications. *Journal of Atmospheric and Oceanic Technology*, **35**, 975–991.
- Saeidi-Manesh, H., S. Karimkashi, G. Zhang, and R. J. Doviak, 2017: High-isolation low cross-polarization phased-array antenna for MPAR application. *Radio Science*, **52**, 1544-1557.
- Saeedi, S., and H. H. Sigmarsson, 2018: Miniaturized evanescent-mode cavity SIW bandpass filter with spurious suppression, *IEEE Radio and Wireless Week (RWW)*, January.

Awards

First Place in the student presentation competition at the 34th *Environmental Information Processing Techniques* (EIPT) Conference – **Andrew Mahre**

Patents & Invention Disclosures

"Apparatus and Method for Wet Radome Characterization and Radar Calibration.", U.S. Provisional Patent 62488301, submitted April 21, 2017 – **Jorge L. Salazar-Cerreno, Alessio Mancini and Boon Leng Cheong**

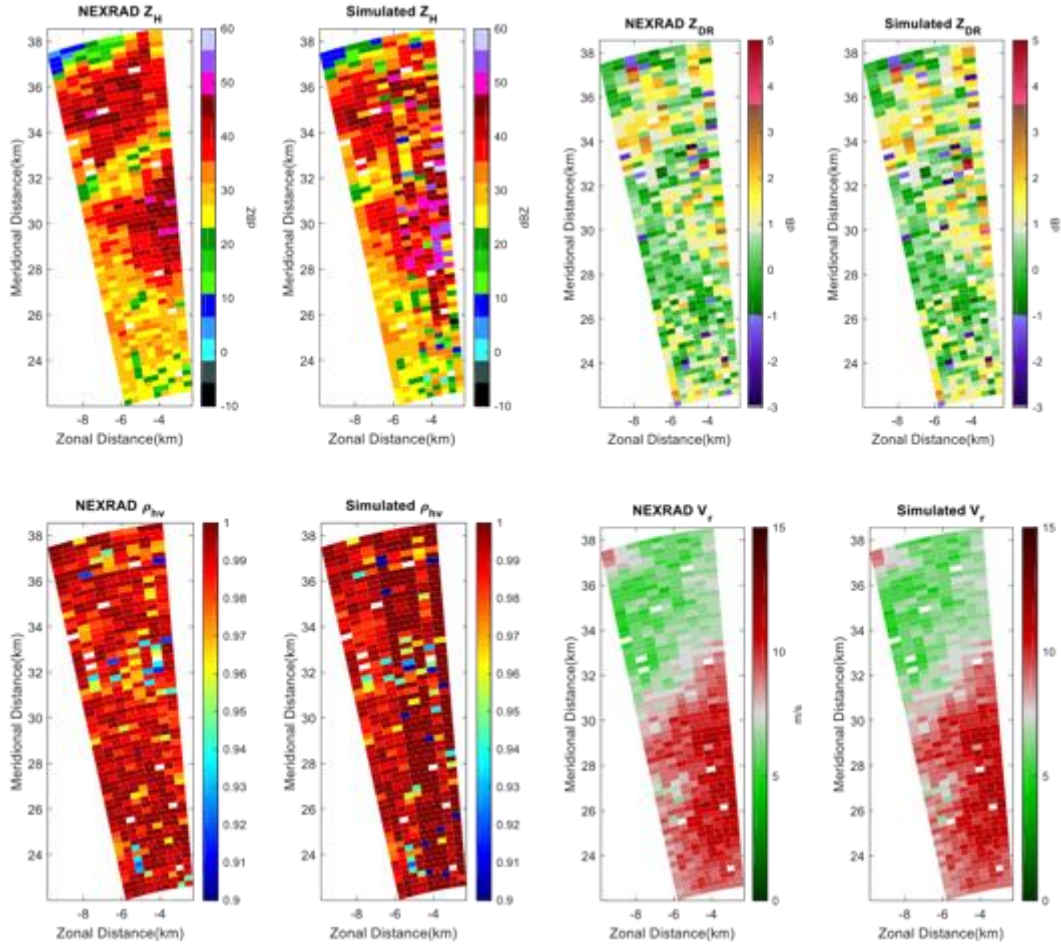


Figure 1: An example of comparison between NEXRAD “Truth Data” moments and the simulated moment data from PASIM output. The tool generates data quality reports (bias and standard deviation) that can be used to evaluate specific system configurations.

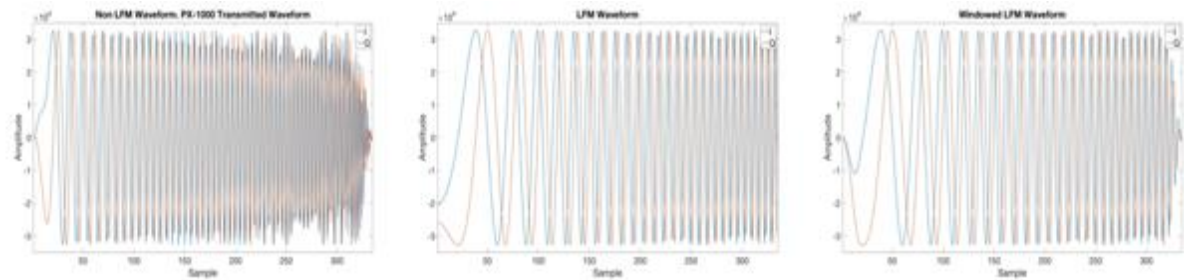


Figure 2: Left panel: Non LFM waveform. Center panel: LFM waveform. Right panel: Windowed LFM waveform.

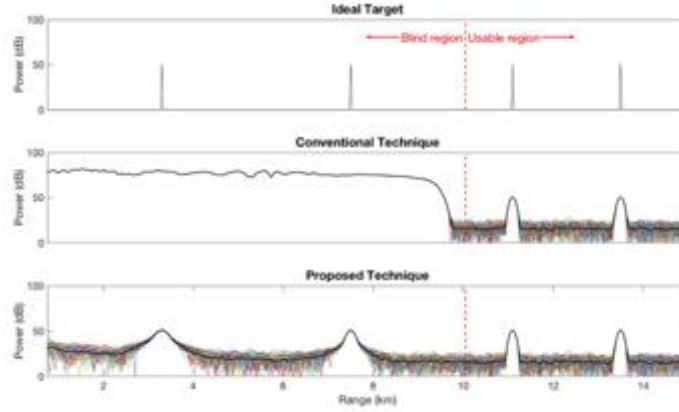


Figure 3: Simulation based on a non LFM waveform. Up panel: Ideal targets. Center panel: Reflectivity from received signal using Conventional method. Down panel: Reflectivity from received signal using Proposed method.

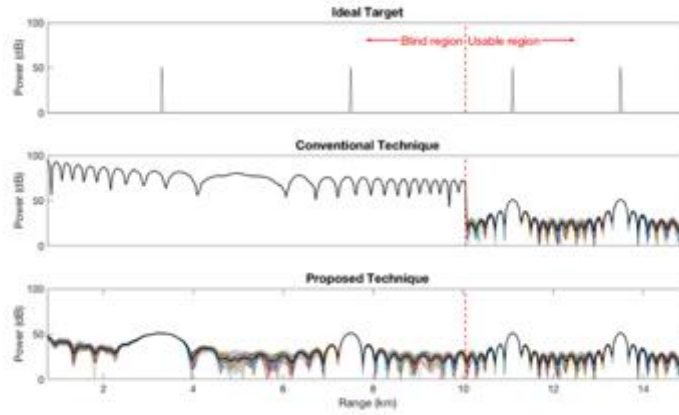


Figure 4: Simulation based on a LFM waveform. Up panel: Ideal targets. Center panel: Reflectivity from received signal using Conventional method. Down panel: Reflectivity from received signal using Proposed method.

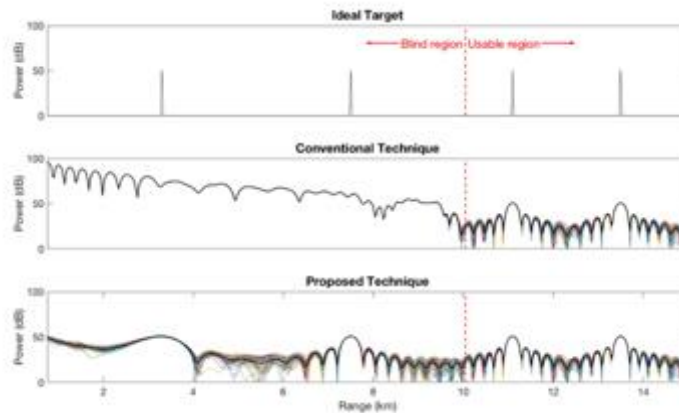


Figure 5: Simulation based on a Windowed LFM waveform. Up panel: Ideal targets. Center panel: Reflectivity from received signal using Conventional method. Down panel: Reflectivity from received signal using Proposed method.

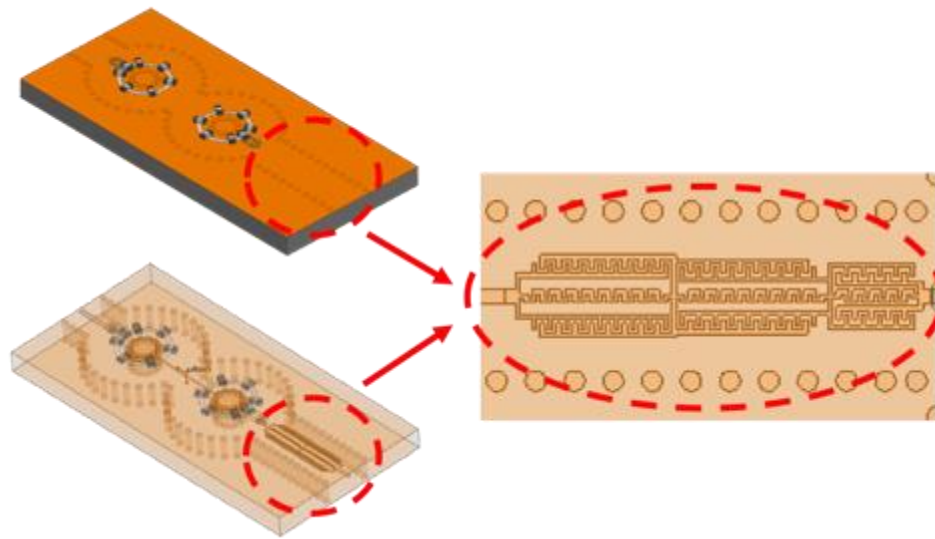


Figure 6: Structure of the integrated filter showing the elliptic LPF cascaded with the substrate-integrated waveguide (SIW), second-order, evanescent-mode-cavity BPF.

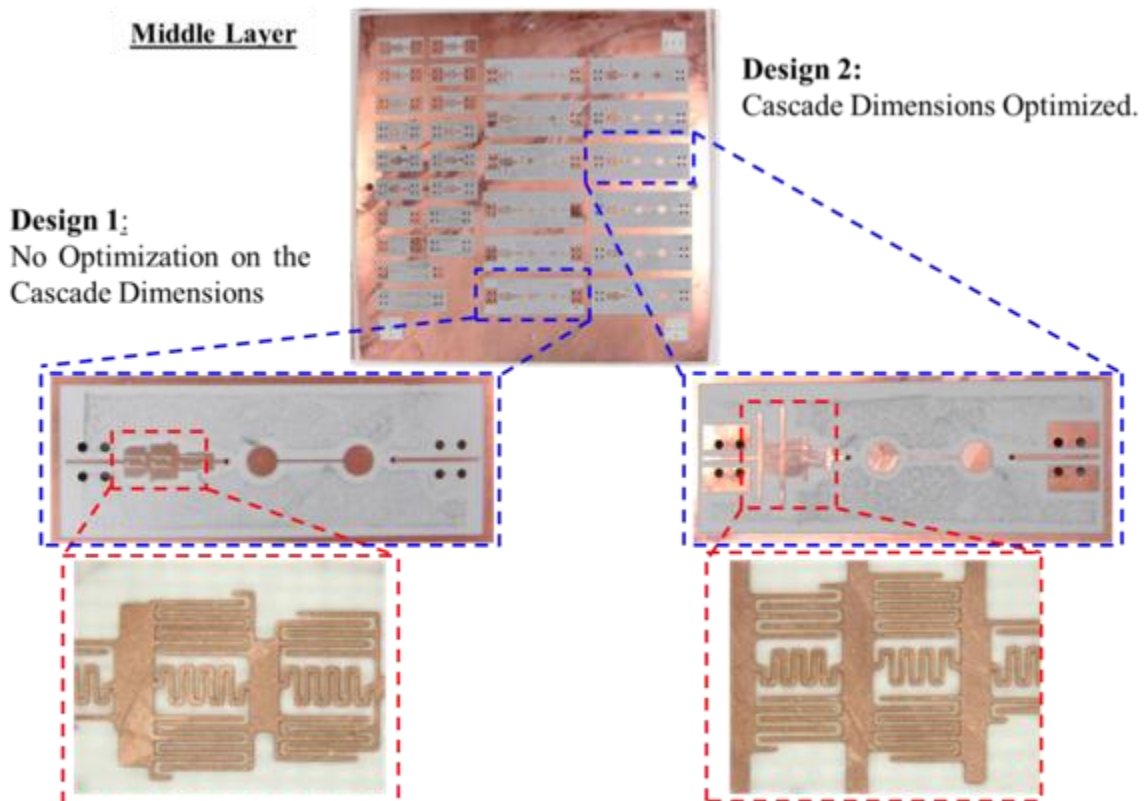


Figure 7: Fabricated BP-LP filter cascade prototypes.

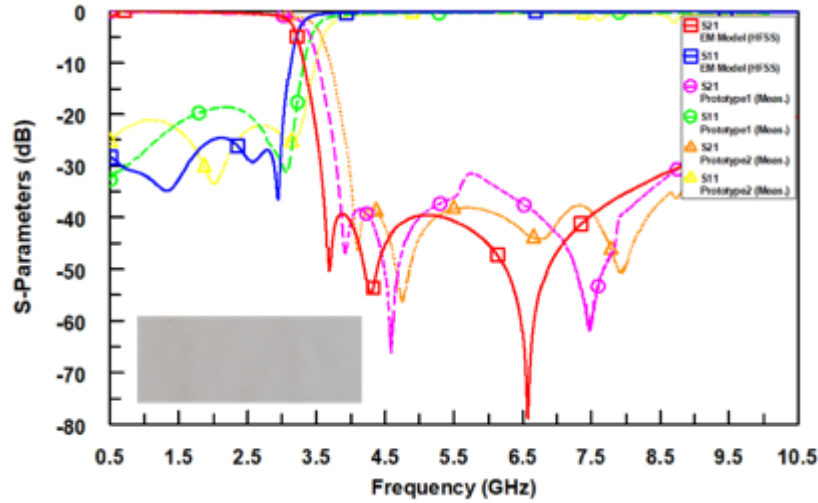


Figure 8: Simulated and measured results of the LPF prototype. The inset shows the final, connectorized prototype.

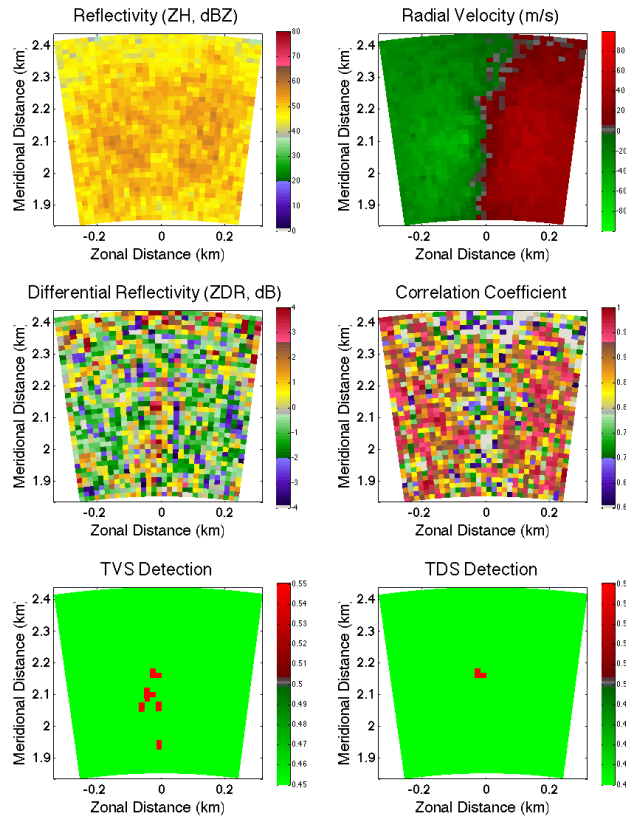


Figure 9: An example output from SimRadar. Clockwise, from top left: reflectivity factor (Z_H), radial velocity (v_r), correlation coefficient (ρ_{hv}), TDS detection, TVS detection, and differential reflectivity (Z_{DR}). The TVS detection algorithm detects azimuthal shear greater than 30 m/s, and the TDS detection algorithm adds the criteria of $\rho_{hv} < 0.825$ to the output from the TVS detection algorithm. In both the TVS and TDS panels, red indicates a positive detection, and green indicates a lack of TVS/TDS.

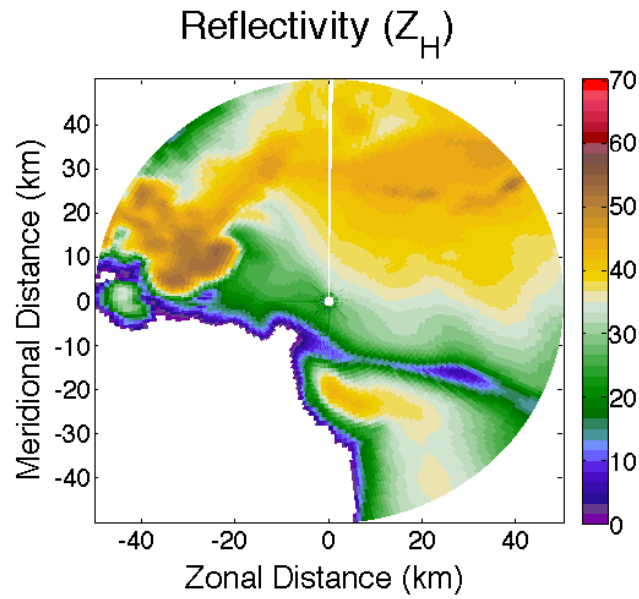


Figure 10: A PPI of horizontal reflectivity factor (Z_H) for a supercell, derived from RSim. This setup assumes a radar scanning at 18 degrees per second at 0.5 degrees in elevation, with a beamwidth on transmit and receive of 1 degree.

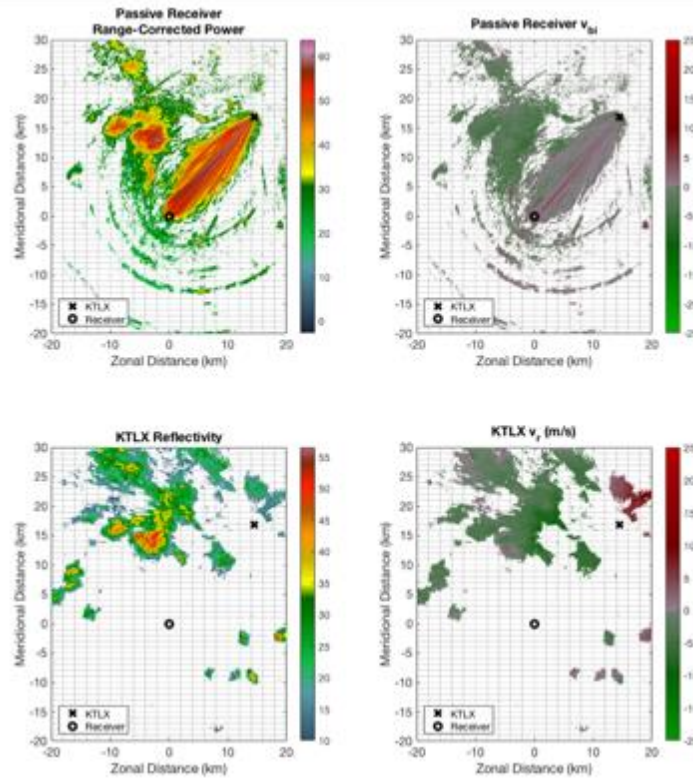


Figure 11: Comparison of weather observations collected using KTLX and the passive receiver. The data were collected at 14:45 UTC on July 15, 2018 and show a group of scattered storms north of Norman, OK. KTLX elevation angle was 1.2°. Passive receiver data was censored at an SNR of 3 dB and KTLX data was censored at a reflectivity of 10 dBZ.

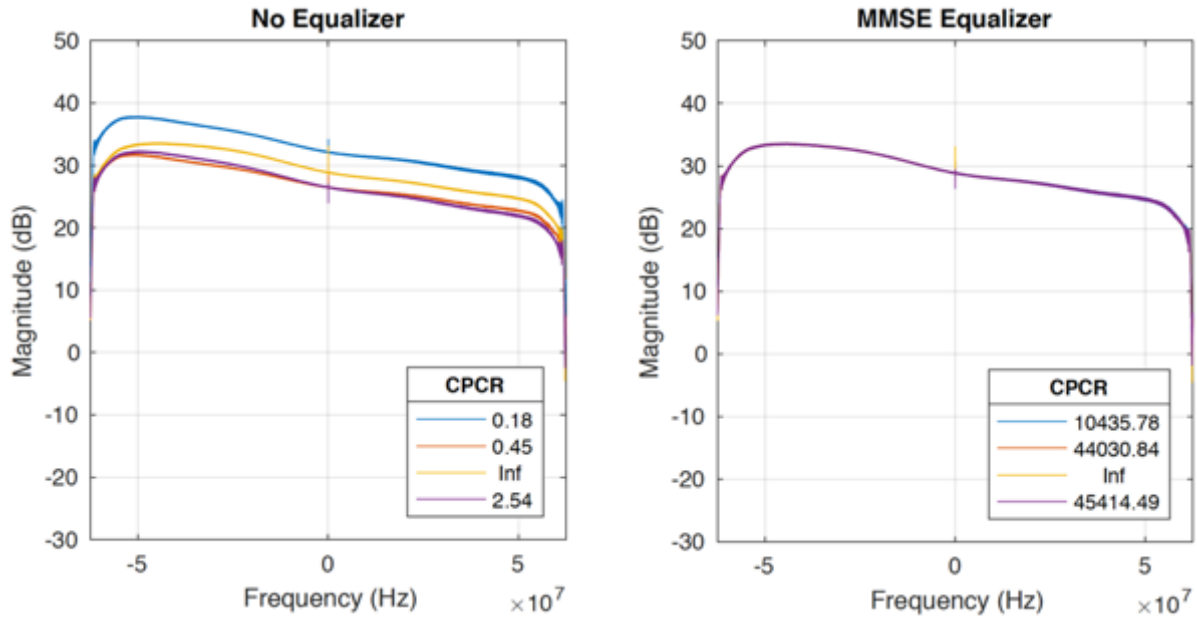


Figure 12: (LEFT) four-channel Horus data without equalization, and (RIGHT) with minimum mean square error (MMSE) equalization. The equalization algorithm was applied across the full band (i.e., not channelized).

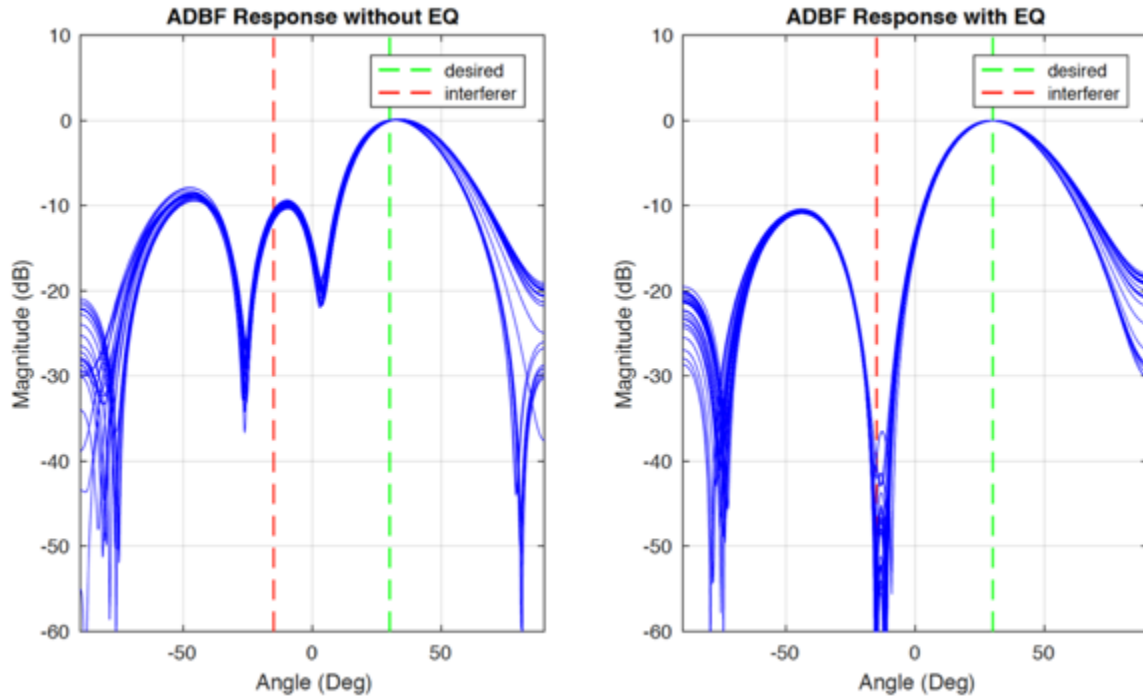


Figure 13: (LEFT) without equalization – a four-channel beamforming environment was created with an interferer and desired signal coming in at specific angles (-15 degrees and +30 degrees, respectively), and (RIGHT) beamforming environment with equalization. The overlaid blue lines are in 4.1 MHz steps over the entire 125 MHz.

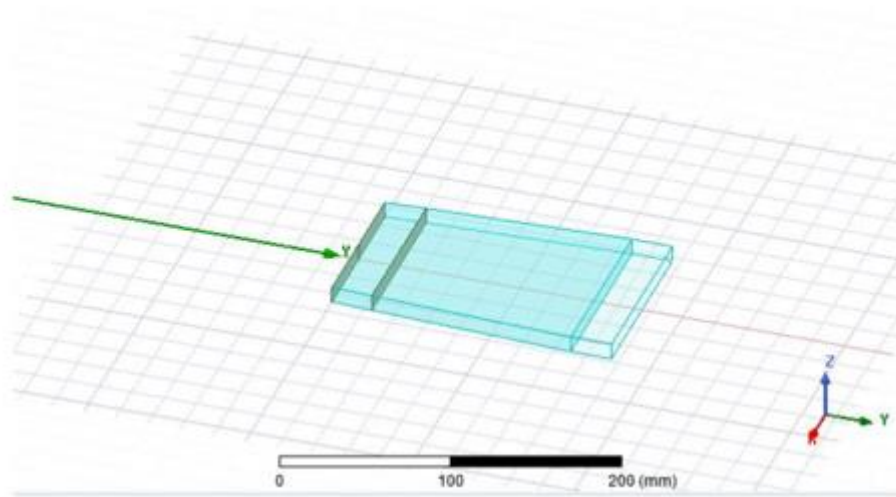


Figure 14: Simulation design of the base element.

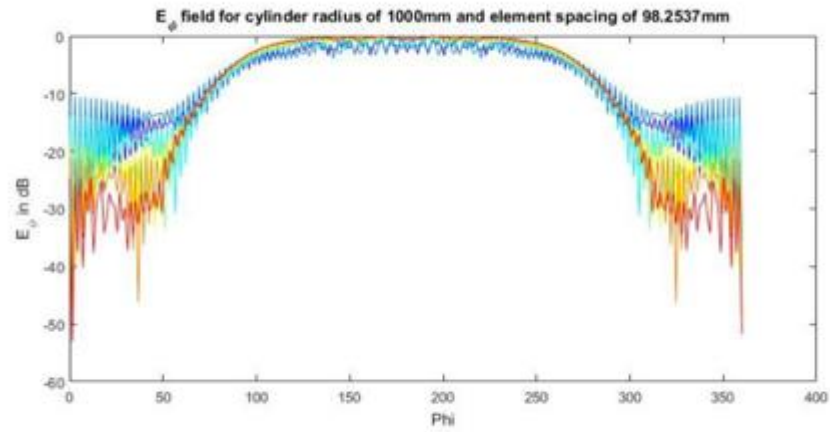


Figure 15: E_ϕ field for each PML position, see figure below for legend.

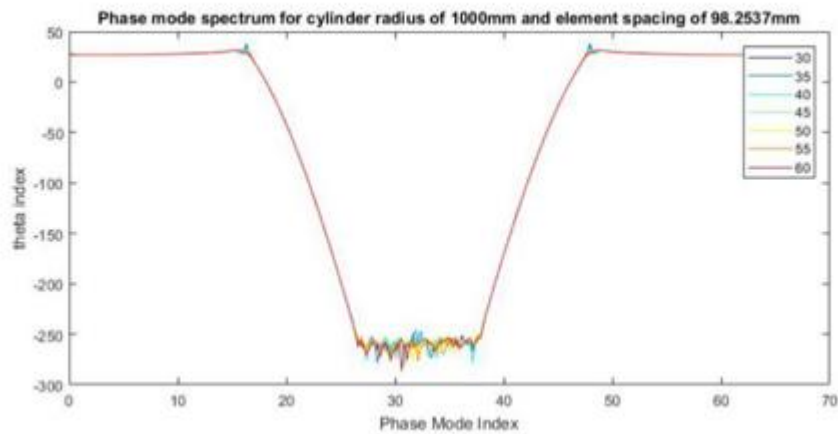


Figure 16: Phase mode spectrum pattern for each PML distance from the antenna in mm.

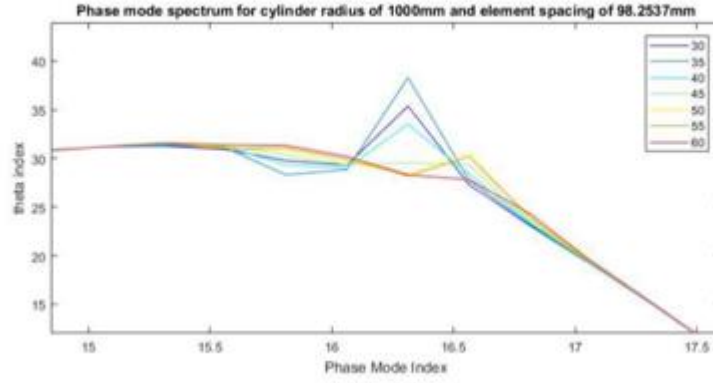


Figure 17: Detailed view of non-convergence areas in phase mode spectrum pattern for each PML Distance.

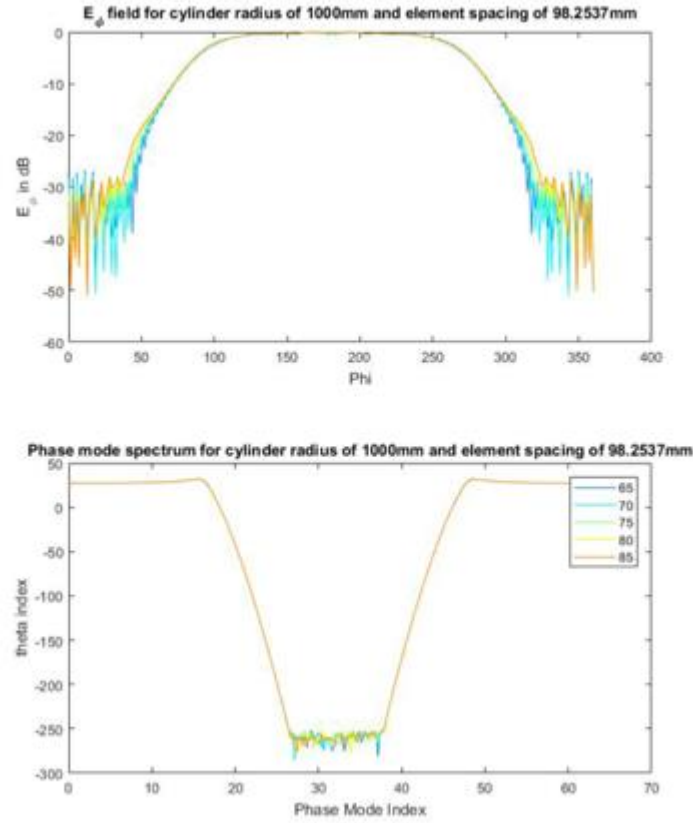


Figure 18: $E_\phi E_\phi$ field (top) Phase mode spectrum (bottom) patterns for each extended PML distance from the antenna in mm.

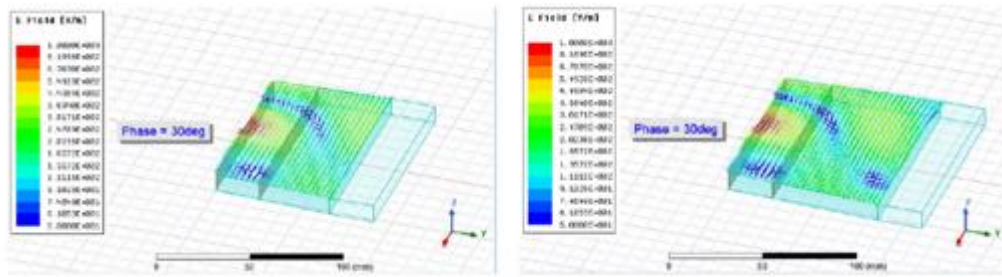


Figure 19: Electric field on wedge design for phase mode 17 with PML 65 mm (left) and 85 mm (right) away from the antenna.

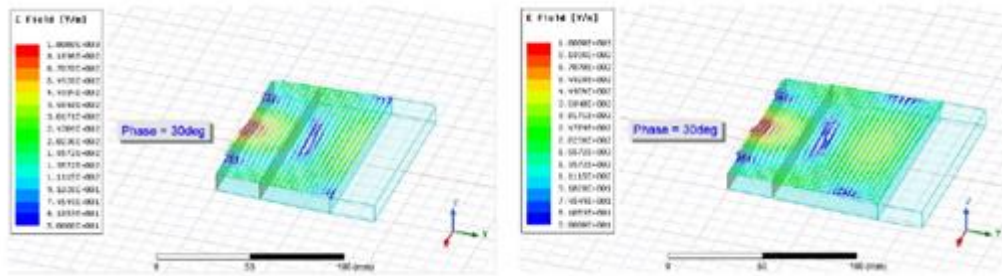


Figure 20: Electric field on wedge design for phase mode 32 with PML 65 mm (left) and 85 mm (right) away from the antenna.

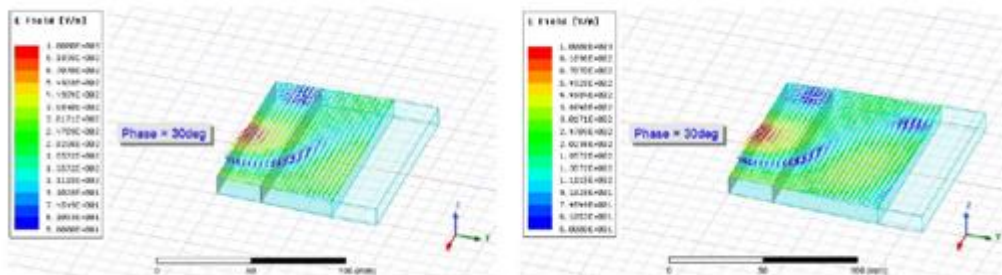


Figure 21: Electric field on wedge design for phase mode 47 with PML 65 mm (left) and 85 mm (right) away from the antenna.

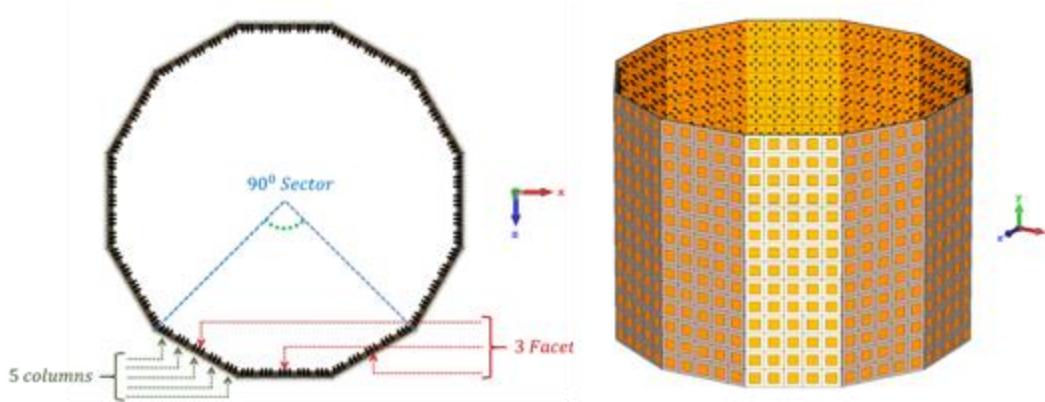


Figure 22: Cylindrical Multifaceted array antenna geometry.

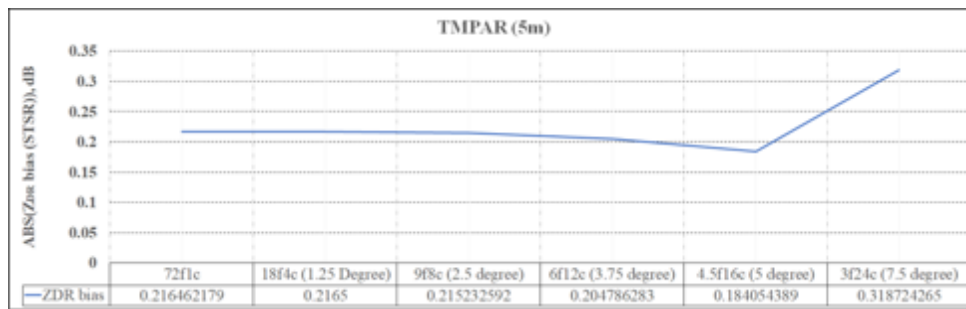


Figure 23: Bias of differential reflectivity of Multifaceted CPPAR.

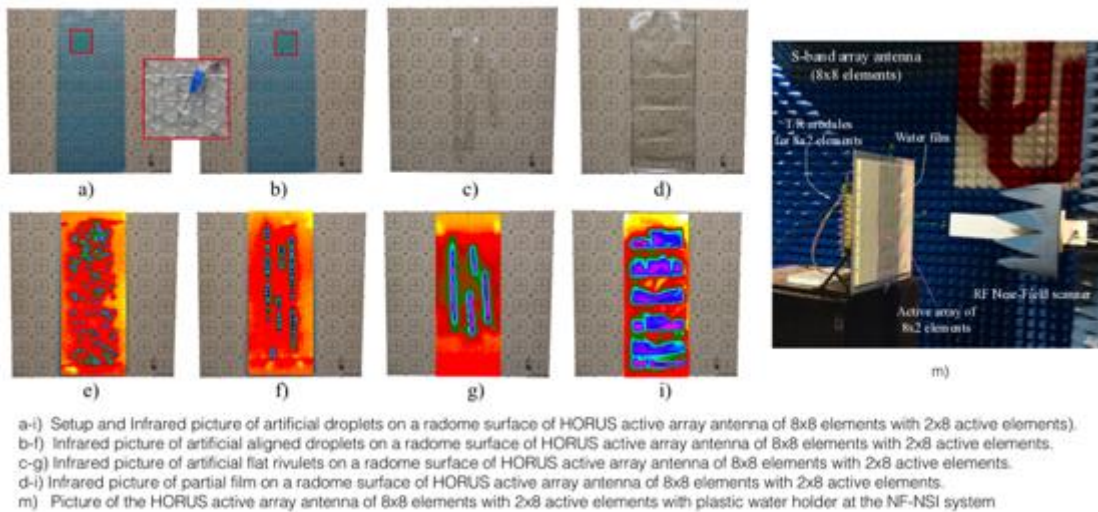


Figure 24: Measured results of HORUS active antenna array patterns with droplets and rivulets during the experiment conducted on April 04, 2018. In this experiment, 2x8 elements were excited with T/R modules for e-scanning beam and others were terminated. In this figure, a) to d) shows the setup of artificial droplets, rivulets and film water on the antenna surface. Since the antenna setup has to be vertical for NF test, a droplet holder (wrap-up plastic) was used to keep the droplets in place. Illustration from e) to i) shows the infrared images to illustrate the water formation (droplets, droplets aligned, rivulets and partial film water).

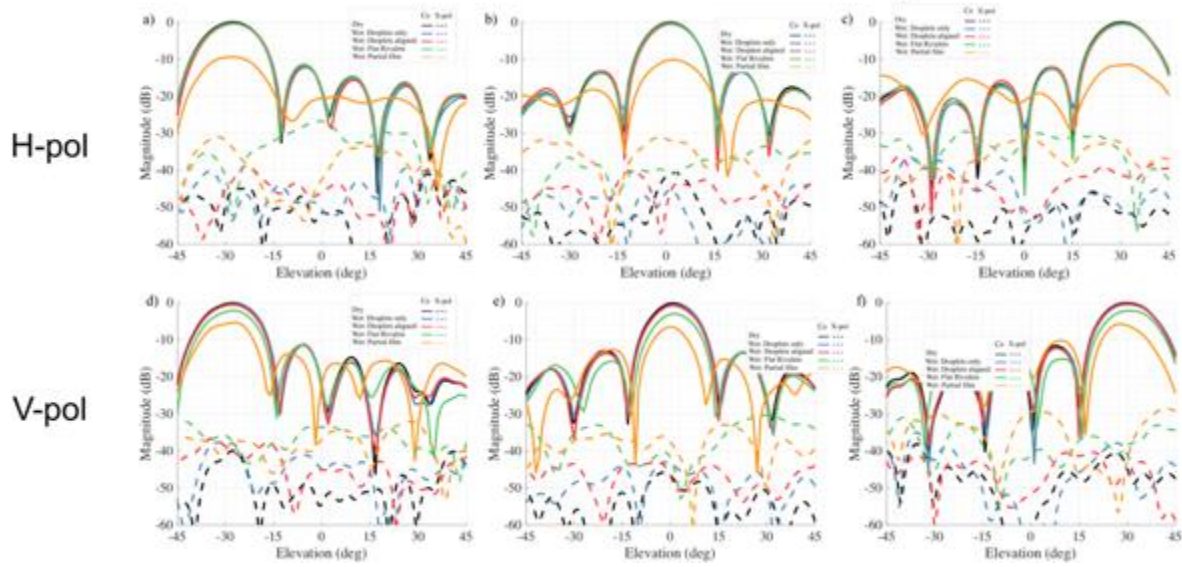


Figure 25: Measured e-scanned antenna patterns of 2x8 Horus active antenna array with the presence of droplets, droplets vertically aligned, rivulets and partial film water. The experiment was conducted on April 04, 2018. In the top, the scanned pattern for -30° , 0° and 30° for H-polarization and in the bottom for V-polarization (bottom). Rivulets and partial film water on a radome surface create a significant mismatch between H- and V-polarized radar signals.

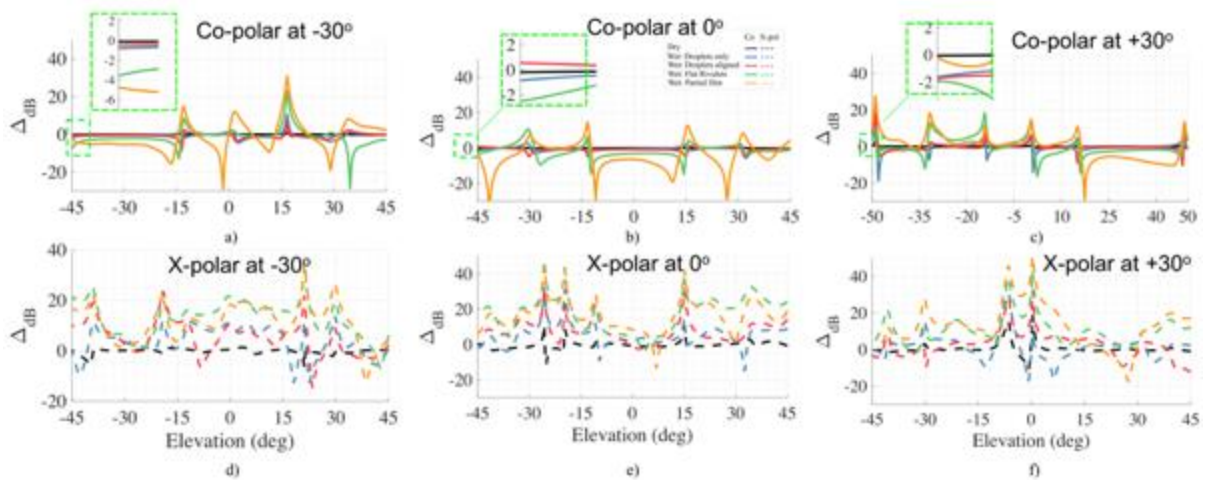


Figure 26: In the top mismatch for co-polar and in the bottom mismatch for cross-polar patterns. Rivulets and partial film water on a radome surface create a significant mismatch between H- and V-polarized radar signals.

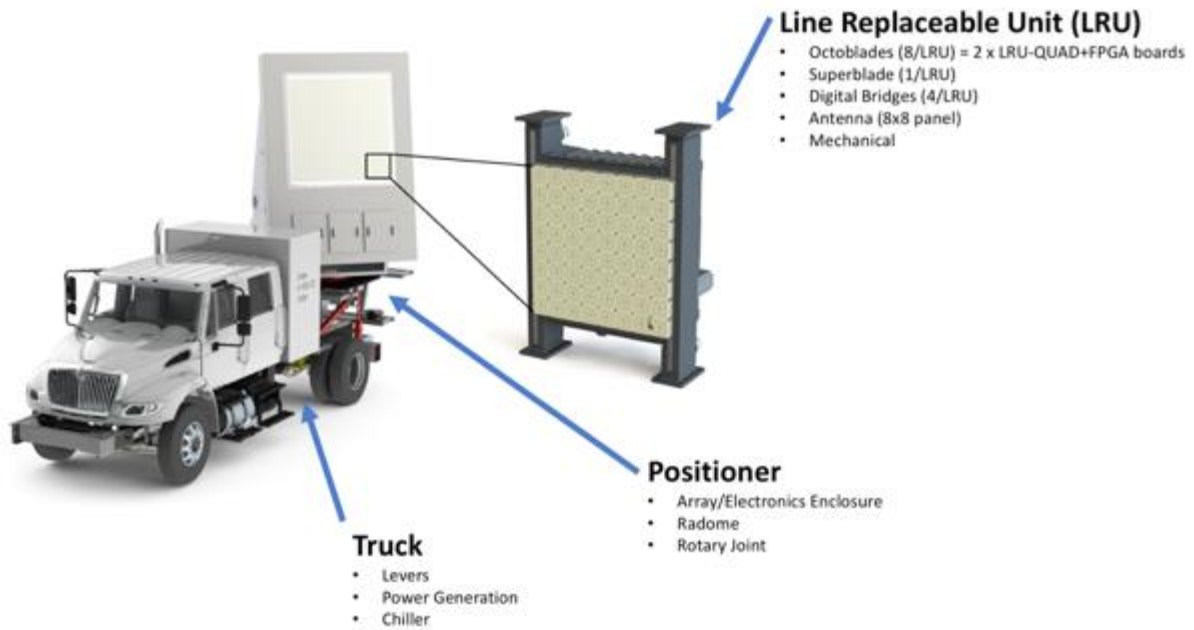


Figure 27: The all-digital Horus demonstrator along with major subsystems.

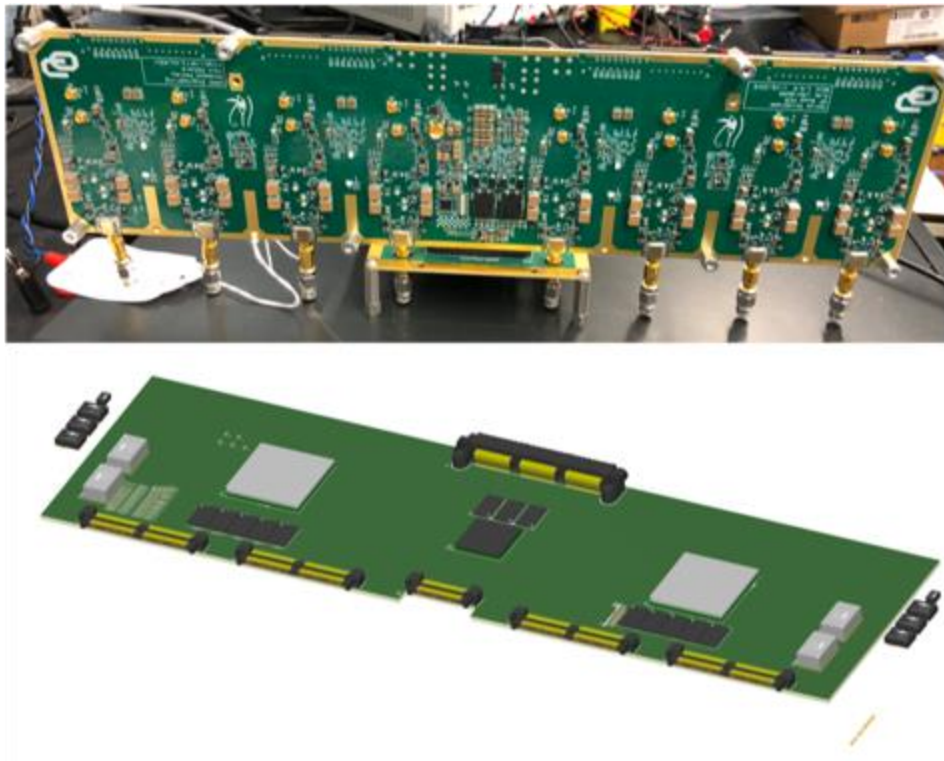


Figure 28: The Quadboard (top panel) along with a mockup of the FPGA board (bottom panel).

CIMMS Task III Project: Polarimetric Phased Array Radar Research in Support for MPAR Strategy – Continued

Guifu Zhang and Yan (Rockee) Zhang (OU School of Meteorology/ECE/ARRC), Lesya Borowska and Sudantha Perera, Mirhamed Mirmozafari, Zhe Li, and Mohammadhossein Golbonhaghighi (ARRC)

NOAA Technical Lead: Kurt Hondl (NSSL)

NOAA Strategic Goal 2 – *Weather Ready Nation: Society is Prepared for and Responds to Weather-Related Events*

Funding Type: CIMMS Task III

Objectives

Conduct theoretical analysis, numerical simulation, element/array design and fabrication, and system development of the Cylindrical Polarimetric Phased Array Radar (CPPAR), to better understand the scientific advantages, technical challenges & limitations and cost-performance tradeoffs, as well as to support SENSr strategy in decision making to sustain Norman's leadership in weather radar and to expand its radar expertise for broad research and multi-mission applications.

Accomplishments

Main accomplishments from this project include i) design and fabrication of high-performance dual-polarization dipole and patch antennas (Mirmozafari et al. 2018; Saeidi-Manesh et al. 2018), that are applicable to future CPPAR; ii) Optimization of CPPAR array configuration and weights for matched copolar beam patterns and low sidelobes/backlobes; and iii) rebuild of the OU/NSSL CPPAR demonstrator to have a stable system to demonstrate the polarization purity and high performance weather measurements. Fig. 1 shows pictures of the 6x6 dual-polarization crossed dipole array antenna. Using the pattern synthesis (Golbon-Haghighi et al. 2018), optimized CPPAR antenna patterns with matched copolar patterns and adjacent nulls are achieved, as shown in Fig. 2. Fig. 3 shows the pictures of the rebuilt CPPAR demonstrator.

Publications

- Mirmozafari, M., and G. Zhang, 2018: On sidelobe problem of configured array antennas. *IEEE Transactions on Antennas and Propagation*, **66**, 3475-3481.
- Mirmozafari, M., S. Saeedi, and G. Zhang, 2018: Highly isolated crossed dipole antenna with matched copolar beams, *Electronics Letters*, **54**, 470-471.
- Golbon-Haghighi, M.-H., H. Saeidi-Manesh, G. Zhang, and Y. Zhang, 2018: Pattern synthesis for the Cylindrical Polarimetric Phased Array Radar (CPPAR). *Progress in Electromagnetics Research M*, **66**, 87-98.
- Mirmozafari, M., S. Saeedi, H. Saeidi-Manesh, G. Zhang, and H. H. Sigmarsson, 2018: Direct 3-D printing of non-planar linear dipole phased array antennas, *IEEE Antennas and Wireless Propagation Letters*.
- Saeidi-Manesh, H., S. Saeedi, M. Mirmozafari, G. Zhang, and H. H. Sigmarsson, 2018: Design and fabrication of orthogonal mode transducer using 3D printing technology, *IEEE Antennas and Wireless Propagation Letters*.

Awards

Second place in the student paper award contest at the 2018 IEEE International Symposium on Antennas and Propagation and USNC-URSI Radio Science Meeting – **Mirhamed Mirmozafari**

William H. Barkow Scholarship for Electrical and Computer Engineering students for the 2018-19 academic year – **Mohammad Golbon**

Featured in the journal of *Electronics Letters* April 2018 issue about the paper "Highly Isolated Crossed Dipole Antenna with Matched Copolar Beams" – **Mirhamed Mirmozafari**

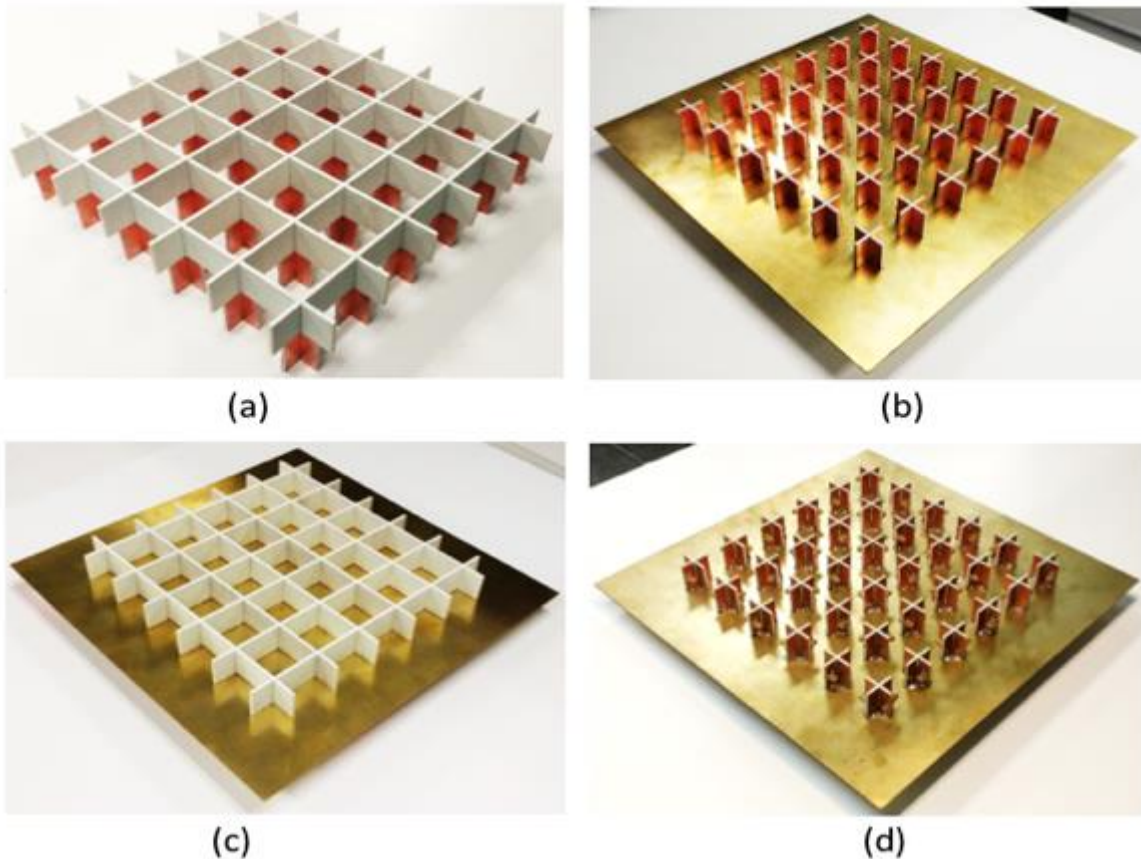


Figure 1. Dual-polarization crossed dipole array antenna. (a) After inserting 12 orthogonal boards into each other, (b) bottom view of the antenna after ground plane assembly, (c) top view of the antenna after ground plane assembly, (d) bottom view of the antenna after soldering the connectors.

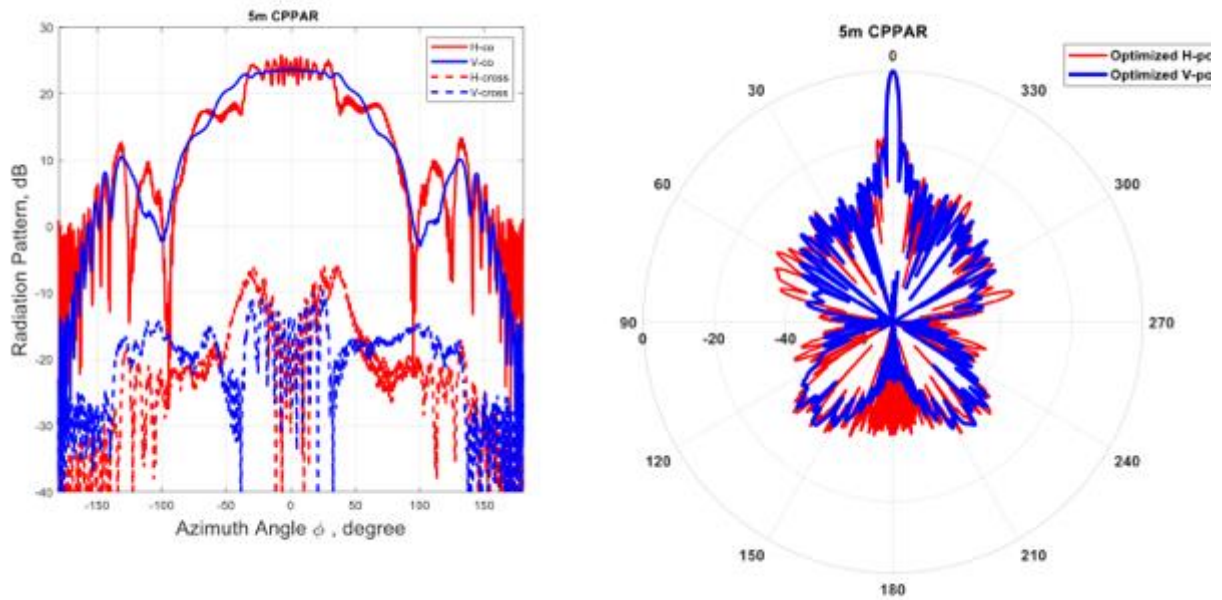


Figure 2: CPPAR antenna patterns: (a) embedded element patterns, and (b) synthesized CPPAR beam patterns with matched beams and low sidelobes.



Figure 3: Pictures of the rebuilt CPPAR demonstrator without (a) and with (b) radome.

Theme 2 – Stormscale and Mesoscale Modeling Research and Development

NSSL Project 3 – Numerical Modeling and Data Assimilation

NOAA Technical Leads: Pamela Heinselman, Michael Coniglio, and Adam Clark (NSSL)

NOAA Strategic Goal 2 – *Weather-Ready Nation – Society is Prepared for and Responds to Weather-Related Events*

Funding Type: CIMMS Task II

Overall Objectives

Develop and test numerical weather prediction models, data assimilation techniques, and diagnostic, visualization, and verification methods to improve severe weather forecasts.

Accomplishments

1. NEWS-e Forecast Viewer Restructuring and Redesign to Enhance User Experience and Resolve IT Issues

Jessica Choate, Emily Grimes, and Patrick Skinner (CIMMS at NSSL)

The visualization of Warn-on-Forecast output is provided via the NEWS-e Viewer. This viewer was used for the first time during the Spring Forecast Experiment in the Spring of 2017. After extensive use from a variety of meteorologists during that season, the WoF team received valuable feedback about possible improvements for the 2018 experiment which was a strong motivation for the recent redesign. More importantly, along with the cosmetic changes, was the complete restructuring of the website such that would not affect user interaction but greatly improve IT functionality and security.

It was found that the current viewer was open to several security threats such as SQL injection, data loss, malware threats, and server attacks where data could be accessed. Although these threats hadn't yet come to fruition it was important to secure the increasingly widely used site as soon as possible. Another IT issue was that the current viewer's code was sending 100 error messages per minute to the server error log which is owned by the NSSL Web Master. These error messages rendered the error logs unusable for any page with the "www.nssl.noaa.gov/" address. This rebuild became a necessity due to the security threat and error logs or IT would turn off the NEWS-e Viewer, an act that would have been detrimental to both R2O activities as well as research progress for the then upcoming 2018 season.

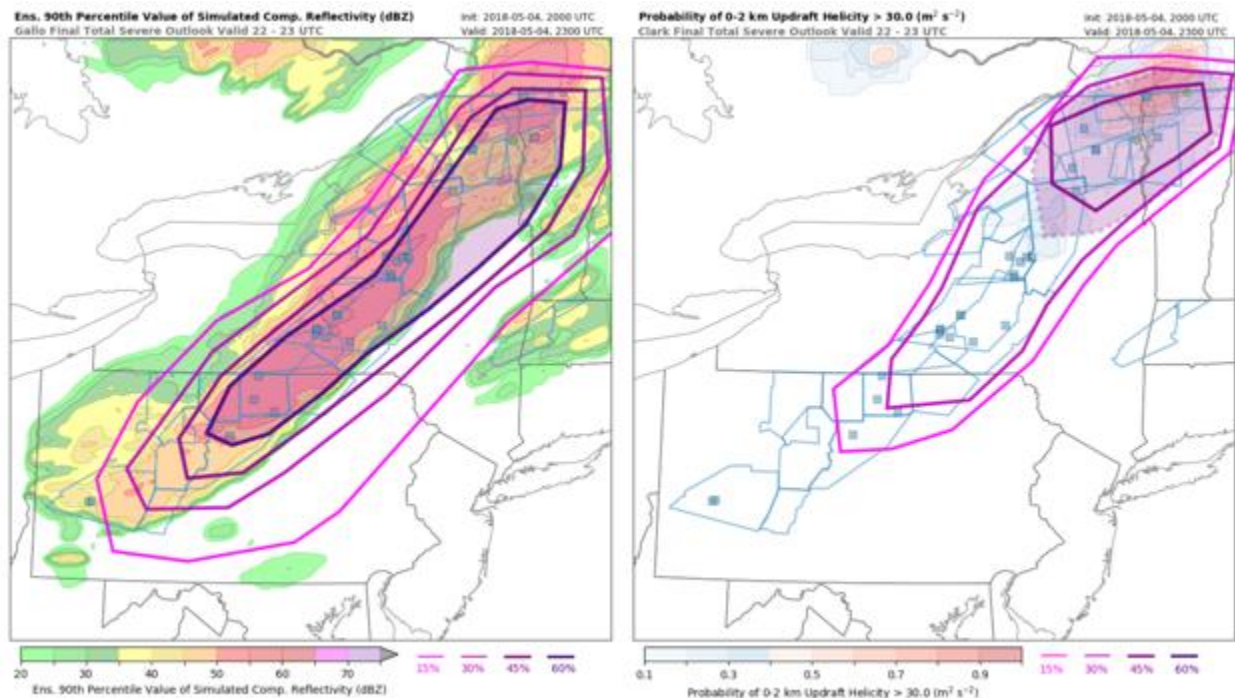
After the restructuring, the security threat was resolved by building the site from the front end of the server, meaning no outside source can access the server and data is retrieved safely. This also eliminated the many error messages, giving the Web Master

the ability to do her job efficiently and improving all NSSL websites. The new build is now extremely easy to duplicate and customize to meet the needs of the growing variety of users (including the Federal Aviation Administration, Weather Prediction Center, Storm Prediction Center, National Weather Service, and specific research initiatives). This new dynamic build also allowed for the implementation of many forecaster requests including new help links, an enhanced member viewer, and user surveys for continued improvement.

2. Examining the Use of the NSSL Experimental Warn-on-Forecast System for Ensembles for the Prediction of Severe Storms Through Short-Term Forecast Outlooks During the 2018 Spring Forecasting Experiment

Jessica Choate, Burkely Gallo, Emily Grimes, Patrick Skinner, and Katie Wilson (CIMMS at NSSL), and Adam Clark and Pamela Heinselman (NSSL)

NEWS-e guidance was used to create severe weather outlooks between the watch and warning time scales within NOAA's 2018 Hazardous Weather Testbed (HWT) Spring Forecasting Experiment. Participants were separated into two groups based on self-rated forecast experience, and a third group was comprised of a single forecaster with extensive operational experience. The primary goals of this experiment were to: 1) explore how the three groups used short-term ensemble forecast guidance from NEWS-e to produce a series of 1-hour severe weather outlooks, 2) evaluate participant perceptions of the NEWS-e forecasts, the submitted outlooks, and verification of the outlooks, and 3) gain insights into participants' product usage during the outlook activity. First, "practically perfect" outlooks generated from local storm reports were used to subjectively and objectively verify the 1-hour outlooks. Next, participant perceptions were analyzed through surveys issued after each set of outlook submissions during the activity as well as after discussion of the "practically perfect" verification the following morning. Lastly, information on each group's interactions with the NEWS-e web interface was collected and summarized to give a deeper understanding of participants' information consumption while producing short-term total severe outlooks, an example of product usage from May 4th, 2018 is below. Preliminary results from the analysis of these three areas of study will be presented through an oral presentation during the 2018 Severe Local Storms Conference and an abstract has been submitted for the 2019 AMS Annual Meeting.



The figures above show the final (produced based on 2000 UTC NEWS-e output) outlooks (magenta contours) for the 2200-2300 UTC period overlaid on the NEWS-e product their respective group requested most from the NSSL web server. Warnings issued and LSRs that occurred during that period are plotted as well.

3. Daily NSSL WRF, NMMB and SREF-Initialized Ensemble Members

Scott Dembek (CIMMS at NSSL), Adam Clark (NSSL), and Israel Jirak (SPC)

The twice-daily National Severe Storms Laboratory Weather Research and Forecasting model (NSSL WRF) has been generating real-time forecasts dating back to the fall of 2006. The forecast domain covers the Continental United States (CONUS) at a 4-km grid resolution, and utilizes convection-allowing dynamics. The NSSL WRF has been augmented with a variety of unique storm-scale diagnostic fields designed by NSSL researchers in collaboration with SPC forecasters, helping to identify the potential for convective-scale elements meant to improve forecast guidance. In addition to the NSSL WRF, the NOAA Environmental Modeling System (NEMS) Nonhydrostatic Multi-scale Model on the B grid (NMMB) has been modified with similar storm-scale diagnostic fields, and generates a single daily forecast offering a point of comparison to the daily NSSL WRF. Finally, an eight member ensemble of 4-km NSSL WRF forecasts initialized using NOAA's Short-Range Ensemble Forecast (SREF) runs daily and uses the same physical parameterizations as the deterministic NSSL WRF. The SREF-initialized NSSL WRF ensemble provides SPC forecasters with a view of the forecast spread associated with the differing initial conditions.

As the NSSL WRF has been adopted by and is now being run operationally at the NCEP Environmental Modeling Center, a decision was taken that the 4-km NSSL WRF, NSSL NMMB, and SREF-initialized NSSL WRF ensemble will be ending on August 31,

2018. Future experimental real-time modeling efforts at NSSL will concentrate on the use of the GFDL Finite Volume Cubed-Sphere Dynamical Core (FV3). Along with the FV3, a new 3-km NSSL WRF is being tested as a higher-resolution replacement for the 4-km NSSL WRF, and will be initialized at 0000 UTC daily over the CONUS. The 3-km NSSL WRF will make use of the same dynamical core as the 4-km version, with forecasts extending out to 60 hours rather than the previous 36 hours. This new experimental 3-km NSSL WRF will be post-processed using NCEP's latest Unified Post Processor, replacing the older WRF Post Processor currently being used with the 4-km NSSL WRF.

4. Develop and Evaluate at Least One Technique to Assimilate Total Lightning Data in the Variational Framework at the Convection Allowing to the Cloud Scales for High Impact Weather Events

Alexandre Fierro and Yunheng Wang (CIMMS at NSSL), and Gang Zhao (CAPS)

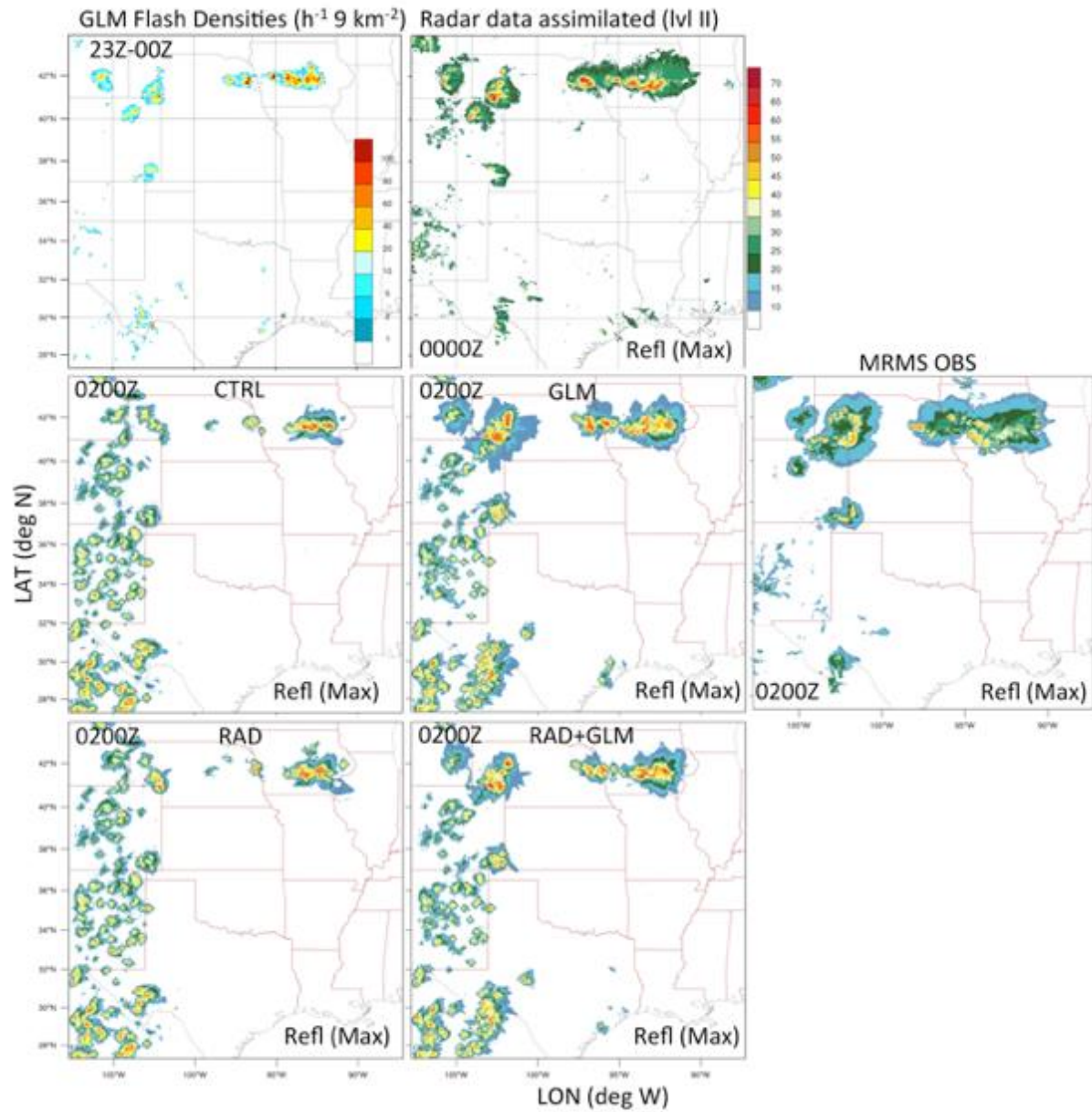
New LDA techniques were successfully implemented in GSI v3.5 and in the NSSL 3DVAR package (NEWS3DVAR) on NOAA's JET HPC Resources. Several quasi real-time forecasts at convection-allowing scales (3-4 km) over CONUS were performed during the Spring of 2017 and 2018 evaluating the impact of several key parameters such as the horizontal decorrelation scale of the adjusted pseudo-observations fields (water vapor mass) and the depth of adjustment layer. A summary of these results was elaborated and published in the JCSDA Quarterly Newsletter this Spring.

A 2-year NOAA Proposal funded (as PI) to continue working on the implementation and testing of novel cloud-scale LDA techniques within the NSSL 3DVAR framework.

We are continuing with the implementation and the development of a real time, multi-scale combined lightning and radar data assimilation system with automated graphics interface for verification (cf figures below). Present preliminary results to NCEP collaborators in September.

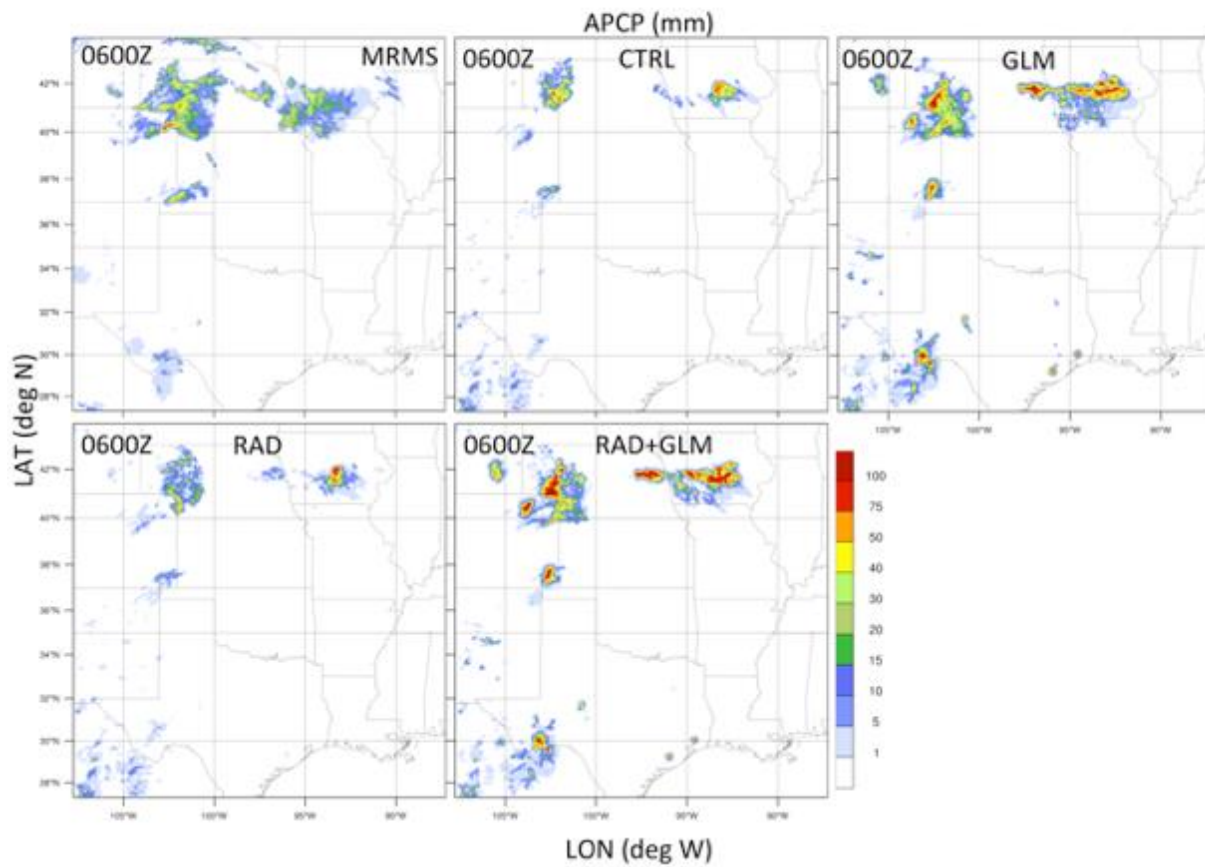
And we are collaborating with other institutions on lightning data assimilation work.

07 June 2018, 0000Z forecast (t=2h)

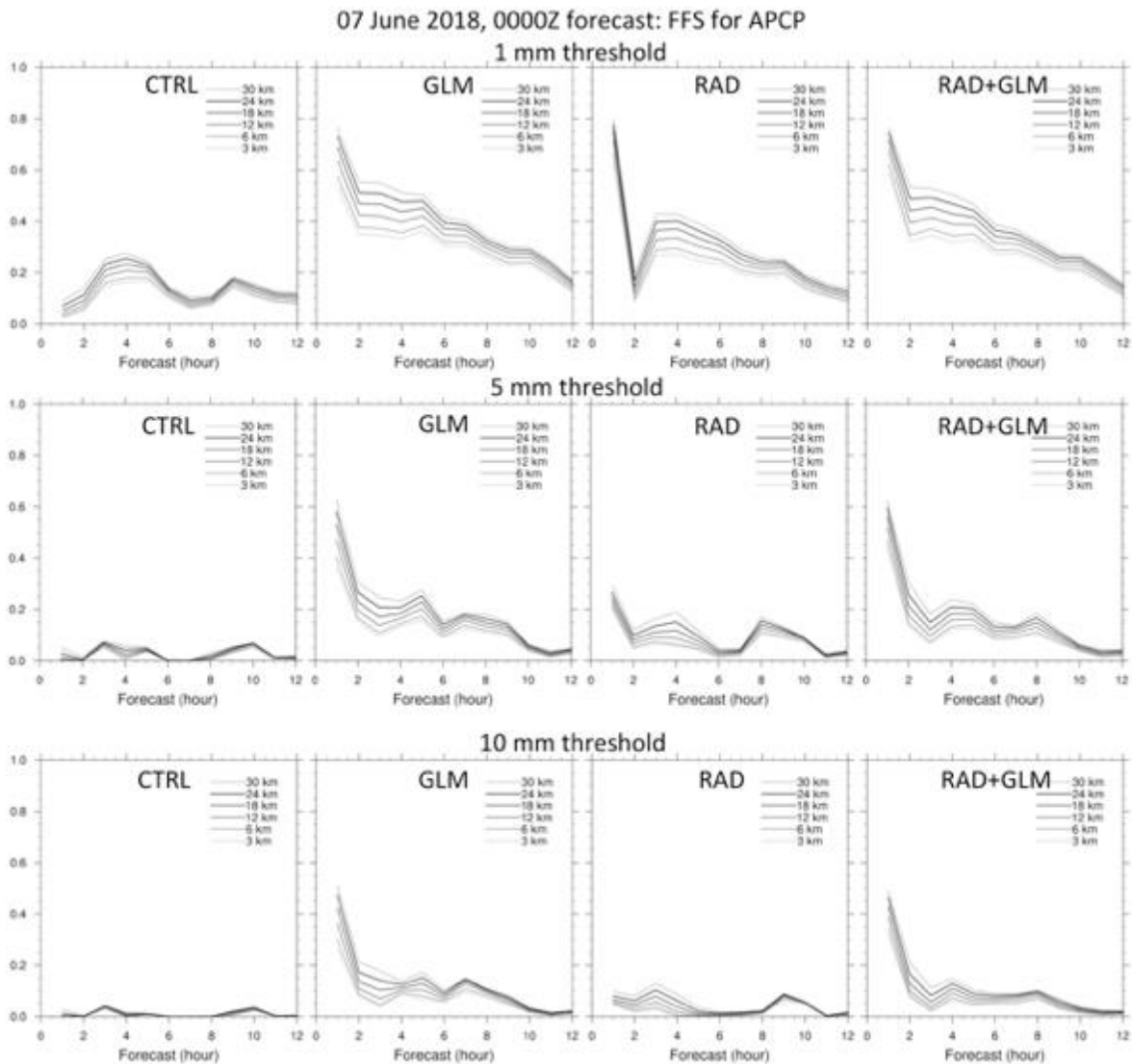


Observations (top left) and 2-h forecast of composite dBZ fields. The assimilated GLM lightning densities at 00Z are shown on the top left, for reference. Nomenclature for the experiments are: (i) CTRL: control experiment (no data assimilated); (ii) GLM: GLM densities assimilated; (iii) RAD: level II radar data (radial wind + reflectivity) assimilated and (iv) combination of (ii) and (iii).

7 June 2018, 0000Z forecast (t=6h)



Observed and forecast of accumulated precipitation at 12-h.



FFS of accumulated precipitation for various neighborhood radii and thresholds.

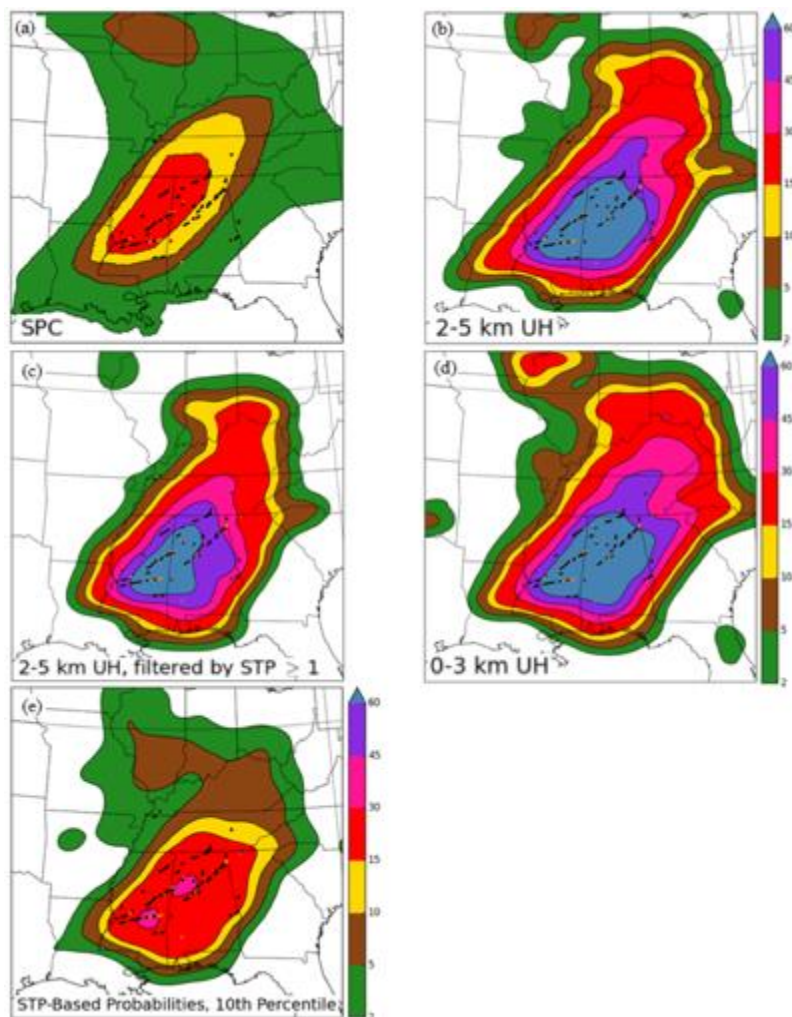
5. Generating Climatologically Calibrated Tornado Probabilities from High-Resolution Numerical Weather Prediction

Burkely Gallo and Scott Dembek (CIMMS at NSSL), Adam Clark (NSSL), and Israel Jirak, Bryan Smith, and Richard Thompson (SPC)

High-resolution convection-allowing ensembles can provide forecasters guidance regarding severe convective hazards such as tornadoes. However, tornadoes are typically forecasted too often when solely relying upon numerical output, necessitating calibration. This research calibrates ensemble tornado probabilities using the climatological frequency of a tornado given the existence of a right-moving supercell. The resulting probabilities are then compared to other methods of calculating tornado probabilities, and found to be both much more reliable than other numerical methods

and comparable to operational outlooks issued by the Storm Prediction Center (figure below). These probabilities are now implemented and available real-time in the High-Resolution Ensemble Forecast system (HREFv2) on the Storm Prediction Center's website, where they are used by some SPC forecasters.

An extension of this research includes the time of UH occurrence in generating the probabilities, to dampen a nocturnal false alarm signal seen by participants in the 2017 Spring Forecasting Experiment. Hourly tornado climatologies were generated and used to calibrate the numerical output; compared to using a time-independent climatology, these time-dependent climatologies had minimal effect on the probabilities. Rather, a larger effect was seen by also incorporating a climatology of the total number of hourly reports. Inclusion of the reports reduced nocturnal false alarm, but according to some statistics the inclusion degraded the forecasts.



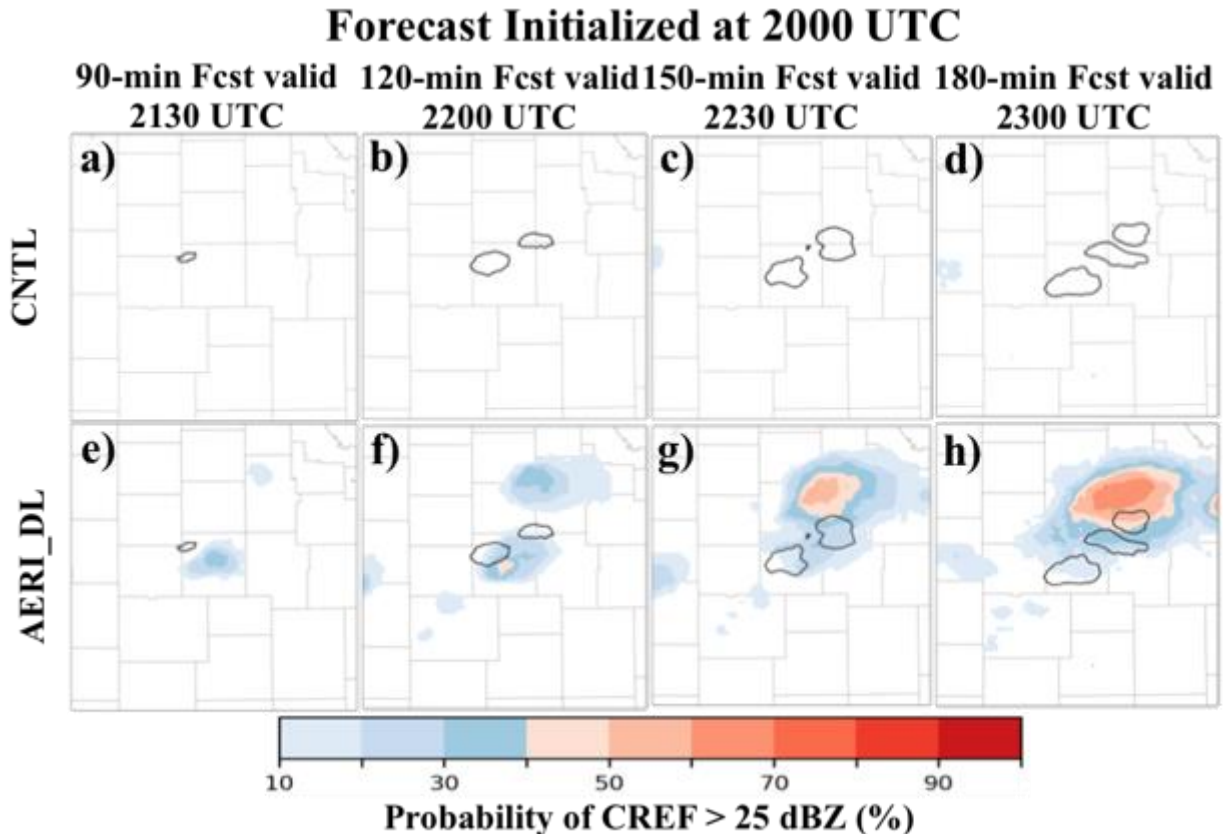
Forecast tornado probabilities for 28 April 2014 (a) issued at 0600 UTC by the SPC and generated with the NSSL-WRF ensemble, using (b) 2–5 km UH $\geq 75 \text{ m}^2\text{s}^{-2}$, (c) 2–5 km UH $\geq 75 \text{ m}^2\text{s}^{-2}$ moving into an environment with STP ≥ 1 , (d) 0–3 km UH $\geq 33 \text{ m}^2\text{s}^{-2}$, and (e) the 10th percentile of STP from the hour previous to 2–5 km UH $\geq 25 \text{ m}^2\text{s}^{-2}$. All (orange) and RM (black) tornado paths are overlaid. From Gallo et al. (2018).

6. Assimilation of Ground-Based Remote Sensing Boundary Layer Instruments into NSSL Experimental Warn-on-Forecast System for Ensembles (NEWS-e)

Junjun Hu, Nusrat Yussouf, and Thomas Jones (CIMMS at NSSL) and David Turner (ESRL GSD)

As part of NOAA Office of Weather and Air Quality FY2016 Joint Technology Transfer Initiative funded project, this research effort enhances NOAA's operational GSI-EnKF data assimilation (DA) system to incorporate the ability to assimilate retrievals from ground-based remote sensing boundary layer instruments into NEWS-e. The instruments include the Atmospheric Emitted Radiance Interferometer (AERI) and Doppler Lidar (DL). The hypothesis is that assimilating temperature, moisture and wind retrievals from those special instruments will provide better representation of near storm environment in NEWS-e and therefore, improve short-term forecasts of severe thunderstorms. Capabilities to assimilate dewpoint temperature as the moisture variable and adaptive inflation technique from Anderson (2009) also are incorporated into the GSI-EnKF system. The NEWS-e is tested using EF3 tornadic event near Nickerson, Kansas on July 13, 2015 from PECAN field campaign and the results are promising. As shown in the following figure, the experiment that assimilates AERI and DL (AERI_DL exp.) in addition to all other traditional observations predicts the initiation of the tornadic supercell much earlier than the CNTL experiment that only assimilates traditional observations. Further investigation reveals that this is largely due to the enhancement of the low-level convergence and humidity in near storm environment.

Real-time data feed of AERI and DL from the 5-station network in north-central Oklahoma by the Department of Energy's Atmospheric Radiation Measurement (ARM) program was setup to assimilate the retrievals from those instruments into the NEWS-e system during 2018 Hydrometeorology Testbed Flash Flood and Intense Rainfall (HMT-FFaIR) experiment. Work is in progress to evaluate the impact of AERI and DL retrievals in NEWS-e forecasts during the testbed experiment.



NEWS-e 1.5, 2, 2.5 and 3 hour forecast probability of composite reflectivity (color shadings) greater than 25 dBZ. The black contours overlaid is the MRMS 25 dBZ reflectivity contour. The top row (a-d) is from the CNTL experiment and the bottom row (e-h) is from the AERI_DL experiment.

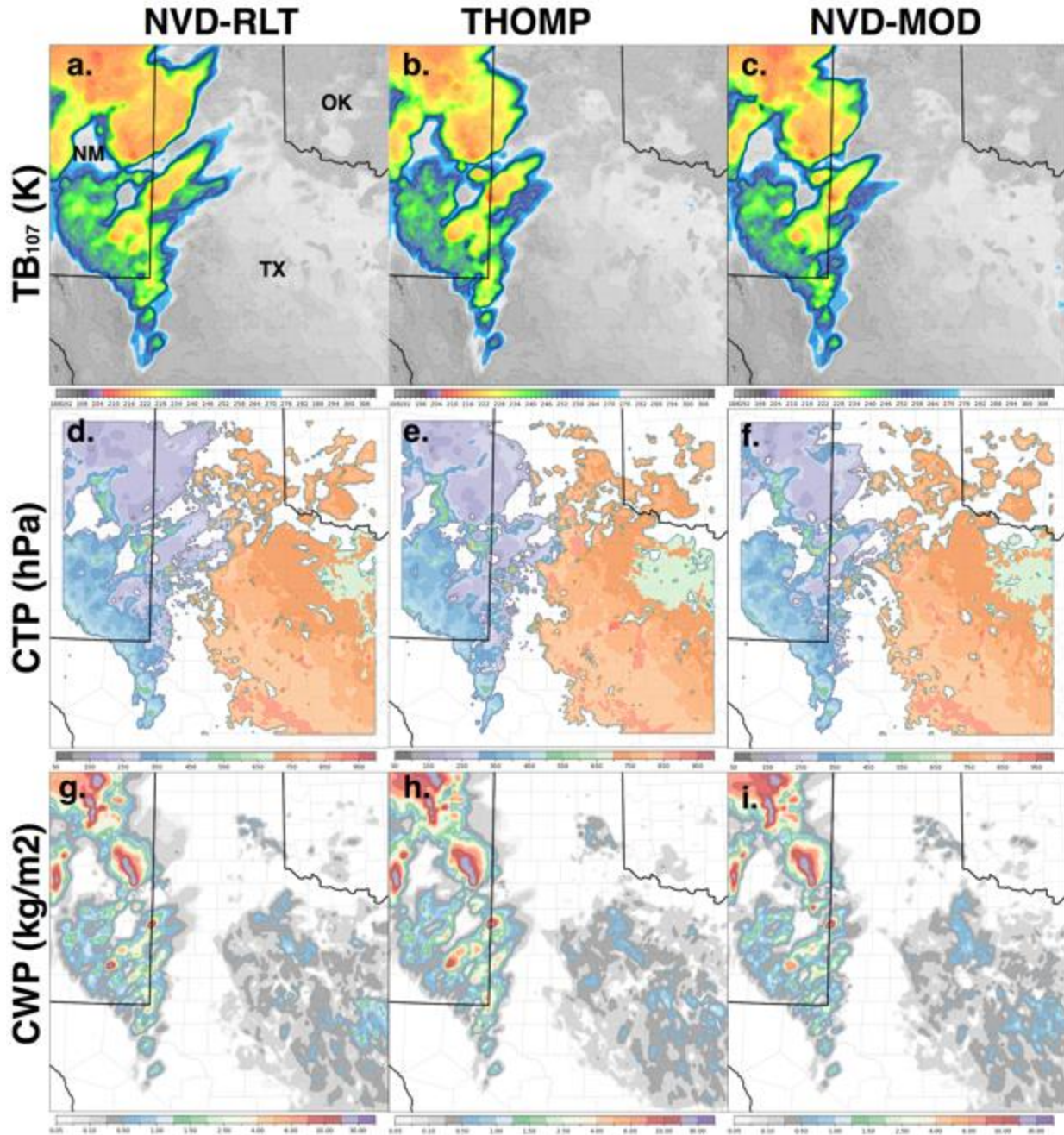
7. Storm-Scale Cloud Water Path Assimilation and Verification

Thomas Jones (CIMMS at NSSL), and Patrick Minnis and William Smith (NASA Langley)

Research is ongoing towards assessing the impacts of assimilating GOES-16 cloud water path (CWP) retrievals into the hi-resolution numerical weather prediction models. CWP was assimilated into the NSSL experimental WoF System for ensembles (NEWS-e) during real time testing for the 2018 HWT experiment. Assimilating these observations generally resulted in improved thermodynamic conditions over the storm-scale domain through better analysis of cloud coverage compared to radar-only experiments. These improvements often corresponded to an improved analysis of supercell storms leading to better forecasts of reflectivity and updraft helicity. This positive impact was most evident for events where convection was not ongoing at the beginning of the radar and satellite data assimilation period. Changes from 2017 include replacing GOES-13 with GOES-16 data, changes to observation errors, and a new objectively analyzed observation grid based on the MRMS data format.

Results from 2017 HWT experiment shows significant positive cloud biases in the upper-troposphere that assimilation was unable to correct. To address this concern, modifications were made to the NSSL 2-moment cloud microphysics scheme used in NEWS-e to correct this bias. Results of this modification proved successful with the modified scheme generation more realistic upper level clouds, while not substantially reducing skill for precipitation and rotation.

At 2300 UTC 9 May 2017, simulated ensemble mean 10.7 μm brightness temperature (TB107) indicates several existing and developing storms in eastern New Mexico and western Texas as shown in the figure below. Compared to the observed TB107 at this time, all experiments over-estimate the cirrus cloud coverage with the original NSSL scheme (RLT) generating the largest over-estimate. For example, this experiment generates a large area of $\text{TB107} < 225 \text{ K}$ in northwest TX associated with the supercell in north eastern NM, while the eastern extent of the cirrus generated by Thompson (THOMP) and the modified NSSL scheme (MOD) is significantly less (panel a-c).



Ensemble mean simulated TB_{107} , CTP, and CWP at 2300 UTC 9 May for NVD-RLT, THOMP, and NVD-MOD experiments. Note the greater coverage of $TB_{107} < 220$ K and $CTP < 225$ hPa in the NVD-RLT experiment compared to the others.

8. GOES Imager Water Vapor Channel Radiance Assimilation

Thomas Jones (CIMMS at NSSL)

GOES-13 imager clear-sky water vapor channel (6.5 μm) radiances have been assimilated into several case study experiments that occurred during springs 2016 and

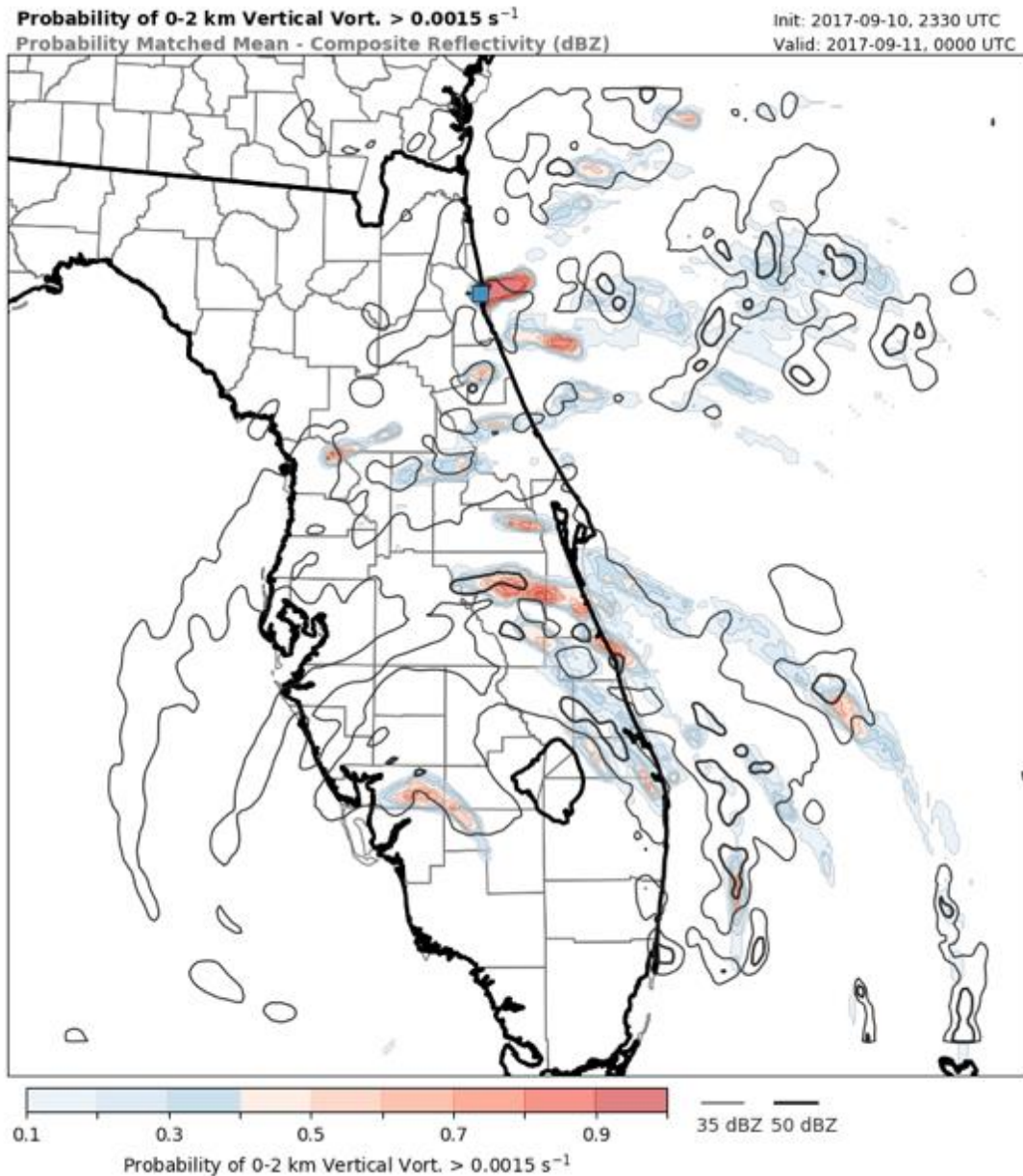
2017. Initial results showed that assimilating these data had the desired impact on the mid-tropospheric moisture analysis, and lowered moisture errors when compared against observations. With the launch and operational inauguration of GOES-16 data, three water vapor channels (6.2, 6.9, and 7.3 μm) are now available for assimilation. Each channel is sensitive to atmospheric moisture at various levels providing vertical information not available with the single channel GOES-13 water vapor channel data. The GSI-EnKF system was updated to assimilate these data, which required adding a GOES-16 observation operator and updates to the radiative transfer model to utilize the latest GOES-16 scattering coefficients. Initial testing has shown that GOES-16 water vapor assimilation is functional with full validation and optimization testing using spring and summer 2018 events is underway.

9. Application of Warn-on-Forecast System to Landfalling Tropical Cyclones

Thomas Jones and Patrick Skinner (CIMMS at NSSL)

During the 2017 Atlantic hurricane season, several strong tropical cyclones impacted the United States causing significant loss of life and billions of dollars in property damage. While medium to long range track and intensity forecasts have become increasingly skillful over the years, much less emphasis has been placed short-term (0-6 hour) forecasts of high-impact weather events such as tornadoes, localized severe winds, and flash flooding generated within landfalling tropical cyclones. Each of these phenomena occurred, often with multiple hazards impacting the same location, during the landfall of Hurricane Harvey in south TX on 25-26 August and Hurricane Irma in Florida on 10 September 2017.

The WoF system was extended to tropical cyclones by generating short-term, probabilistic forecasts of high impact weather during and after landfall of Hurricanes Harvey and Irma. Comparison with radar observations and storm reports indicates that the WoF system often identified the areas corresponding to locations specific high impact weather events up to 3 hours prior to their occurrence. A 30 minute forecast of the probability of low-level (0-2 km) vertical vorticity originating at 2330 UTC 10 September 2017 shows the potential of NEWS-e to predict rotation associated with a supercell embedded within a hurricane rainband (figure below). At this time, hurricane Irma was making landfall in southwest FL, with strong on-shore flow occurring along the entire eastern coast of the state. At 2330 UTC, areas of rotation convection were analyzed off the coast of northeast FL coast moving westward. They reached land just before 0000 UTC and generated several tornadoes. The 30 minute low-level vorticity forecast clearly identifies the area of rotation corresponding to the tornado reports (figure below). Note that no warning was issued for this particular tornado, strongly indicating that NEWS-e can provide important information to forecasters when available in a real-time setting.



Probability of 0-2 km vertical vorticity $> 0.0015 \text{ s}^{-1}$ for a 30 minute forecast originating at 2330 UTC on 10 September 2017. Blue square indicates the location of several tornado reports between 2350 and 0000 UTC.

10. Storm-Scale Data Assimilation and Ensemble Forecasting with the NEWS-e

Kent Knopfmeier, Nusrat Yussouf, Patrick Skinner, Thomas Jones, Jessica Choate, Katie Wilson, Junjun Hu, Swapan Mallick, Anthony Reinhart, and Gerald Creager (CIMMS at NSSL)

The NEWS-e was run in real-time during three periods (30 April – 1 June, 18 June – 29 June, and 9 July – 20 July) during spring/summer 2018 to support experimental activities during the 2018 NOAA HWT-SFE and HMT-FFaIR Experiment. Archived

NEWS-e cases from 2017 were provided to the HMT-Hydro Experiment for its experimental activities, with plans to provide real-time data in 2019. The 3-km, hourly cycled HRRR Ensemble (HRRRE), currently being developed at the ESRL/GSD, provided both the initial and boundary conditions for the 36-member, 3-km WRF-based NEWS-e in both the real-time and retrospective experiments.

During the 2018 HWT-SFE, the movable NEWS-e domain covered a 750 x 750 km wide region where severe weather was expected to occur and was chosen daily by experiment participants. The NEWS-e data assimilation cycling procedure was initialized at 1800 UTC and utilized the ensemble adjustment Kalman filter (EAKF) encoded within the Data Assimilation Research Testbed (DART) software to assimilate METAR, Oklahoma Mesonet (when available), MRMS reflectivity, WSR-88D Level II radial velocity and GOES-16 satellite (cloud/ice water path retrievals) data to generate a new ensemble analysis every 15-min through 0300 UTC the next day. 18-member forecasts were generated from the NEWS-e analyses every half hour, including a 6-hour forecast at 1900 UTC, a 5-hour forecast at 2000 UTC, and a 4-hour forecast at 2100 UTC. 3-hour forecasts were also produced at 1930 UTC, 2030 UTC, and from 2130 – 0300 UTC. To promote communication of the NEWS-e forecasts, a web-based forecast viewer (<https://www.nssl.noaa.gov/projects/wof/news-e/realtime/>) was created. A suite of forecast output fields was generated, ranging from basic environmental information (i.e CAPE) to probabilities of low-level (i.e. 0-2 km vorticity) and mid-level (i.e. 2-5 km updraft helicity) rotation.

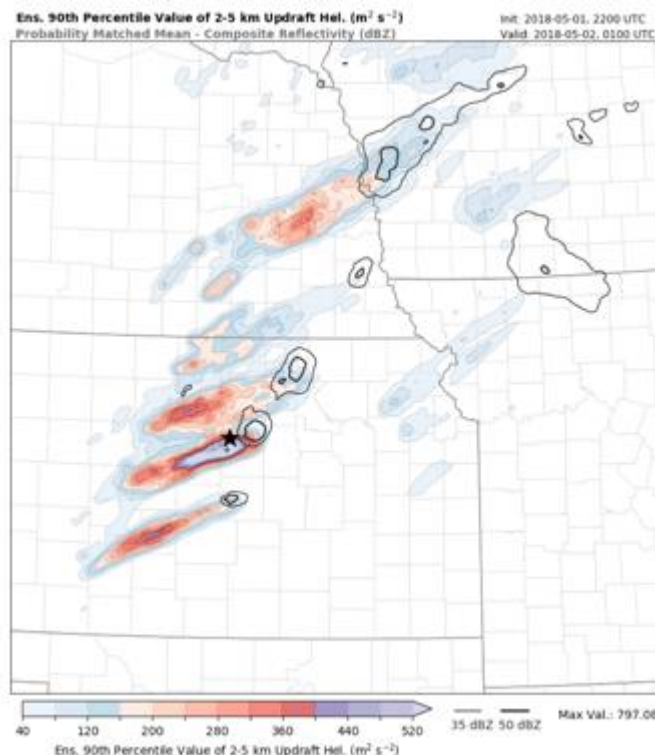
The NEWS-e output was used in two experimental forecasting activities during the HWT SFE, both emulating the creation of outlooks similar to those done operationally by the NOAA NWS Storm Prediction Center (SPC). One activity involved generating two 1-h outlooks, valid from 2100-2200 UTC and 2200-2300 UTC, with guidance provided by the 1900 UTC NEWS-e forecast output. The 2000 UTC NEWS-e forecast output was then utilized to update the outlooks. The second activity employed both of these NEWS-e forecast cycles to update probabilistic forecasts of hail, wind, and tornadoes valid from 2100-0100 UTC that were created earlier in the day.

During the 2018 HMT-FFaIR Experiment, the movable NEWS-e domain was increased in size to a 900 x 900 km wide region and centered on the area where the heaviest rainfall and flash flooding was expected to occur. The NEWS-e cycling procedure was similar to what was employed during the HWT-SFE, except that it was initialized at 1600 UTC, used the NOAA Community Gridpoint Statistical Interpolation – ensemble Kalman filter (GSI-EnKF) software to perform the data assimilation, and ended at 0400 UTC the next day. 18-member, 6-hour NEWS-e forecasts were produced at 1800 UTC, 1830 UTC, and 1900 – 0400 UTC. A web-based forecast viewer (<https://www.nssl.noaa.gov/projects/wof/news-e/wpc/>) similar to the one developed for the HWT-SFE was created, but focused on the display of rainfall accumulation products.

The NEWS-e output was used in two experimental activities during the HMT-FFaIR Experiment. The first activity involved utilizing the data to create an experimental probabilistic flash flood forecast valid for the period 2100 – 0000 UTC. This forecast

product was similar to the Excessive Rainfall Outlook issued by the NOAA NWS Weather Prediction Center (WPC). The second activity consisted of a subjective evaluation of NEWS-e accumulated rainfall forecasts from the 1900 UTC, 2000 UTC, and 2100 UTC forecasts ending at 0000 UTC the next day, which were compared to the operational Multi-Radar Multi-Sensor (MRMS) Quantitative Precipitation Estimate (QPE) product.

In addition to its use during the experimental activities mentioned above, the NEWS-e forecasts were utilized by operational forecasters at the WPC Met Watch Desk, the SPC, the NWSFOs in Norman, OK and Topeka, KS, and the FAA Air Traffic Control System Command Center during high-impact severe weather events. One such event occurred on 1 May 2018 near Tescott, KS where an EF-3 tornado produced a 15-mile long damage path. The 2200 UTC 3-hour NEWS-e forecast from that day provided useful guidance on individual severe thunderstorm tracks, including the supercell that produced the tornado near Tescott, as shown in the figure below. It depicts a consistent swath where the ensemble 90th percentile value of 2-5 km updraft helicity is greater than 500 m^2s^{-2} , with a maximum of near 800 m^2s^{-2} near the same time and location as the observed tornado. This forecast demonstrates the capability of the NEWS-e to predict the likelihood of strongly rotating severe thunderstorms as long as 3 hours in advance, which can provide operational forecasters increased lead time to alert public entities of the possibility of significant severe weather affecting their areas.



Ensemble 90th percentile values of 2-5 km AGL updraft helicity (m^2s^{-2} ; see label bar) from the 3-hour NEWS-e forecast initialized at 2200 UTC 1 May 2018. Light black line is the 35 dBZ probability matched mean composite reflectivity contour. Darker black line is the 50 dBZ probability matched mean composite reflectivity contour. The star icon is the location of the most significant (EF-3) tornado damage located just south of Tescott, KS.

11. Impact of Increased Resolution on Ensemble Forecasts of Thunderstorm Objects in the US Southeast

John Lawson and Corey Potvin (CIMMS at NSSL)

The VORTEX-SE program aims to reduce loss of life and property from tornado damage. Amongst the challenges of risk communication and warning systems, there is evidence that increased resolution of a limited-area numerical weather prediction model will better represent the updrafts associated with tornadogenesis in the southeastern US. These may occur in both cellular and linear convective modes. However, a threefold increase in grid resolution requires more than a nine-fold increase in computational demand; as such, given a finite computational resource, the number of ensemble members must be balanced with grid spacing. This project details results comparing 3-km to 1-km ensemble forecasts of severe thunderstorm outbreaks to assess resolution impact on skill and spread.

Evaluation is performed with a range of scoring techniques, including object-based and scale-aware methods, reflecting the multi-faceted challenge of storm-scale verification. We also address whether the majority of the ensemble envelope can be captured by a limited subset of ensemble members, which would free up computational power for use in resolution improvements. Preliminary results suggest a modest increase in probabilistic and deterministic skill; work is ongoing to determine the sensitivity of storm-object attributes — such as updraft speed, storm size, etc — to grid spacing, through use of newer, more appropriate metrics than traditional point-to-point evaluations.

12. Predictability of Thunderstorms in Buoyancy–Shear Space

John Lawson (CIMMS at NSSL)

Thunderstorms are difficult to predict due to their relatively small length scale and high rate of predictability destruction. The storm's predictability is constrained by properties of the flow in which it is embedded, such as buoyancy and vertical wind shear. To assess how inherent predictability of thunderstorms changes with the environment, two matrices of idealized simulations are performed over a range of buoyancy and shear values, using two microphysics schemes. The gradient in diagnostics (vertical motion, storm size, etc) across shear–buoyancy phase space represents sensitivity to small changes in initial conditions: a proxy for inherent predictability.

Results show little difference between the two microphysics schemes, indicating good generality, and suggest that initial-condition error may dominate model error in determining the predictability horizon. Storm structures can be split into two groups, separated by a U-shaped bifurcation in phase space, between (1) cells that split and continue strengthening after one hour versus (2) those that dissipate. Predictability loss takes two forms: (a) error growth from the largest and most powerful storms, churning air that is otherwise quiescent in the domain, and (b) tipping points at the U-shaped perimeter of the stronger storms. The former is associated with traditional forecast error

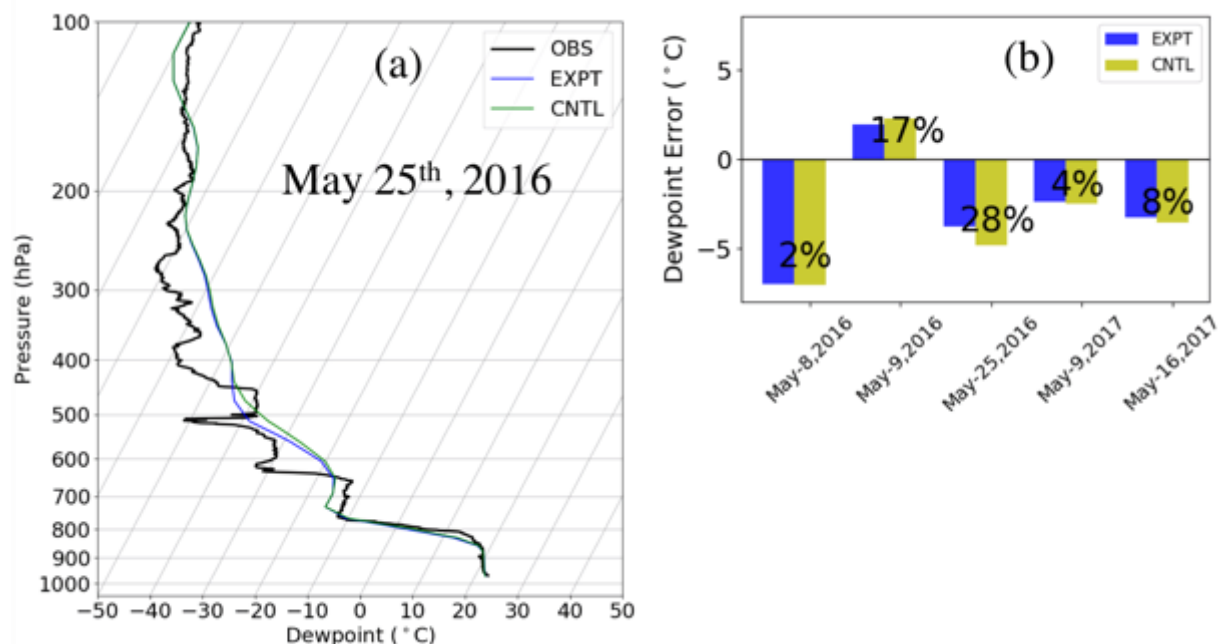
from continuous fields; the latter is associated with object-based or thunderstorm-mode error, a nature pertinent to human forecasters at the convective scale. A manuscript is currently in review.

13. Storm-Scale Assimilation of Hyperspectral Infrared Clear-Sky Radiances

Swapnan Mallick and Thomas Jones (CIMMS at NSSL)

The hyperspectral clear-sky radiances from Atmospheric Infrared Sounder (AIRS) and the Cross-track Infrared Sounder (CrIS) have been assimilated into convection allowing (~3 km) NWP models. Assimilation of satellite infrared radiances have the potential to improve the model analysis where conventional observations are sparse. Although the application of hyperspectral polar-orbiting satellite data in the high-resolution storm-scale model is limited due to the low temporal resolution, non-uniformity, and the lower model heights, there remains potential to improve the model environment in certain situations. This work aims to improve short-term (0-3 hour) forecasts of high impact weather. AIRS is a grating spectrometer with 2378 channels, a total of 120 channels are selected for assimilation according to the peak weighting function and meteorological importance. In addition, out of 1305 CrIS channels, a set of 134 channels are selected for assimilation into the WoF GSI-EnKF system. In addition to the satellite data, we assimilate the available conventional data from Oklahoma mesonet observations; WSR-88D reflectivity from the NSSL- Multi Radar Multi Sensor (MRMS) product and Level 2 Doppler radial velocity from all radars in the storm-scale domain. All the data sets were assimilated at 15-minute assimilation cycles into the WoF GSI-EnKF system. The initial and the boundary conditions are provided by an experimental High-Resolution Rapid Refresh ensemble (HRRR-e). The Community Radiative Transfer Model (CRTM) is used to calculate the simulated brightness temperature from the model state variables.

Five convective events are considered during the year 2016 and 2017 to assess the potential of assimilating satellite hyperspectral radiances into the WoF GSI-EnKF system to improving forecasts of high impact weather events. The impact to the overall model environment was verified using available upper-air observations from radiosondes. Results showed that assimilating these data had the positive impact on the mid-tropospheric moisture analysis.



Ensemble mean of all 36-member (a) vertical profiles and (b) level average errors from 700 to 400 hPa pressure layer between the simulated and observed (OBS) dewpoint for the five different case consider in this study. The two experiments, one is with clear-sky radiance (EXPT) from AIRS and CrIS satellite and the other is without clear-sky radiances (CNTL).

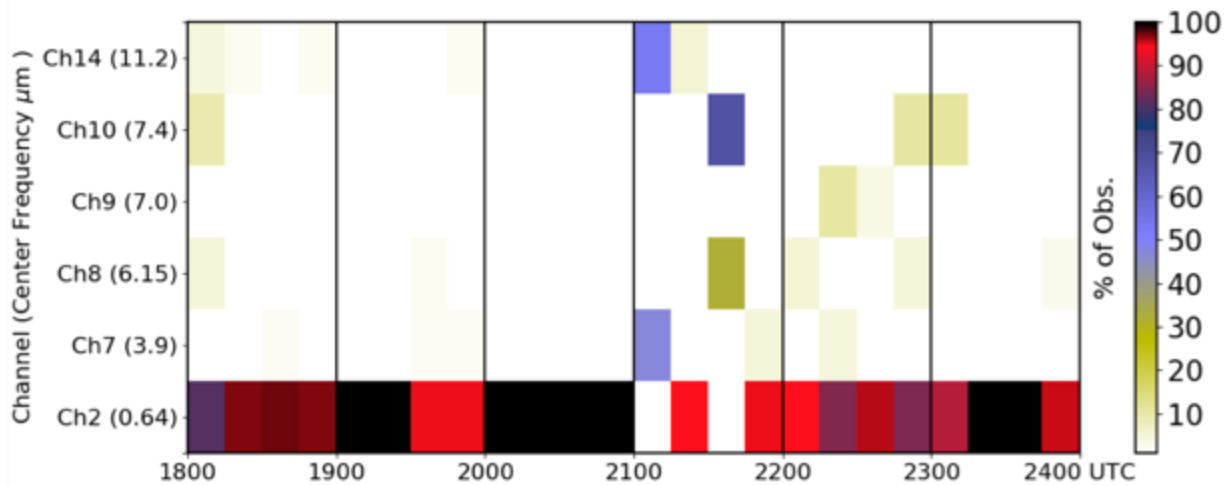
14. Assimilation of Satellite-Derived Winds from GOES-16 ABI into the High Resolution WoF GSI-EnKF system.

Swapnan Mallick and Thomas Jones (CIMMS at NSSL)

Beginning in 2018, research is ongoing towards assimilating and assessing the impacts of the satellite-derived wind or Atmospheric Motion Vectors (AMVs), with a planned 2019 operational implementation into the high-resolution WoF GSI-EnKF system. The wind speed and direction derived from cloud and moisture features of GOES-16 ABI are valuable with high temporal frequency data to create more accurate analysis fields. These data can supplement radial velocity observations in radar coverage gaps and add upper-level wind information where sounding and aircraft data are not assimilated. The AMV retrieval algorithm developed for the GOES-16 ABI is being used operationally at NOAA/NESDIS. A total of 6 ABI channels including one visible with 0.64 μm center frequency and 5 infrared (IR; 3.9 μm , 6.15 μm , 7.0 μm , 7.4 μm and 11.2 μm center frequency) are used to calculate AMVs.

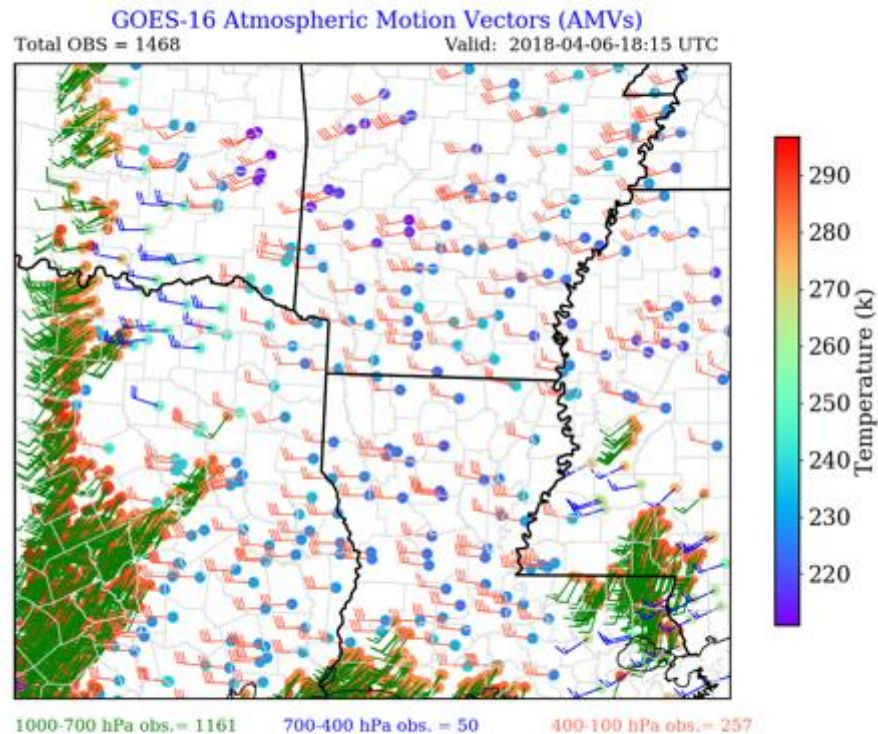
To ensure realistic use of AMVs into the high-resolution WoF GSI-EnKF system. Few studies have been made including data quality check, the number of observations over the domain use and the probability density of wind magnitude at different pressure levels from different channels. For AMVs, assigning a height to the tracked feature is one of the most significant error sources. The study shows that more than 70% of observations do not pass the quality control test due to an improper height assignment.

It has been noted that the median pressure used for height assignment from NCEP Global Forecast System (GFS) outside acceptable pressure range. In addition to that, the maximum number of observations (more than 80%, figure below) assimilated into the system are from the visible channel with the wavelength of 0.64 μm and ~ 0.5 km resolution.



Percentage of AMVs observation (% of Obs.) available from each GOES-16 ABI channels and at different assimilation cycle (1800 – 2400 UTC, 6th April 2018).

A spatial distribution of wind barbs from AMVs and the corresponding brightness temperature (in Kelvin) for the same location using all 6 channels at different pressure levels for a single assimilation cycle are shown in figure below.



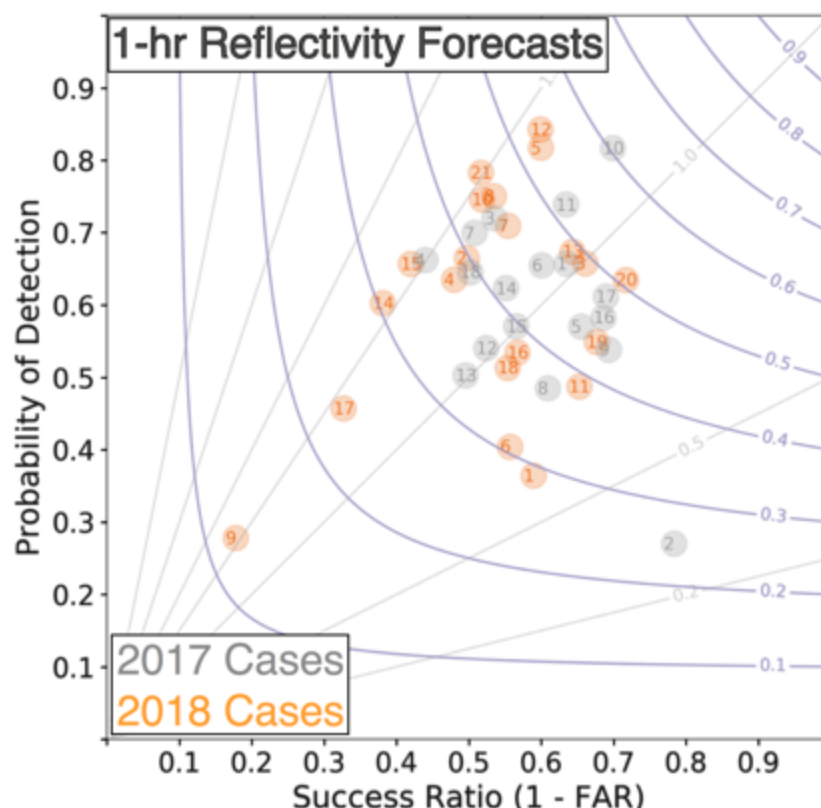
A spatial distribution of wind barbs computed from AMVs and the corresponding brightness temperature (in Kelvin) for the same location using all 6 channels at different pressure levels for a single assimilation cycle. The number on the top left represents the total number of observations over the considered domain.

15. Verification of a Prototype Warn-on-Forecast System

Patrick Skinner, Kent Knopfmeier, and Anthony Reinhart (CIMMS at NSSL), and David Dowell (ESRL GSD)

An object-based verification strategy has been developed for quantifying skill of short-term thunderstorm and mesocyclone forecasts from the NSSL Experimental Warn-on-Forecast System for ensembles (NEWS-e). Objects of composite reflectivity and updraft helicity in NEWS-e forecasts are matched to corresponding composite reflectivity and rotation track objects in Multi-Radar Multi-Sensor observations on space and time scales typical of a Severe Thunderstorm or Tornado Warning issued by the National Weather Service. Classification of forecast and observed objects as hits, misses, and false alarms allow contingency table-based verification metrics to be calculated across different forecast periods, initialization times, or individual cases. These verification metrics provide a means of quantifying NEWS-e forecast skill for

different forecast lengths, convective environments, and system configurations. Additionally, metrics were provided in real-time during the spring of 2018 allowing users to assess storm-to-storm variations in NEWS-e skill.



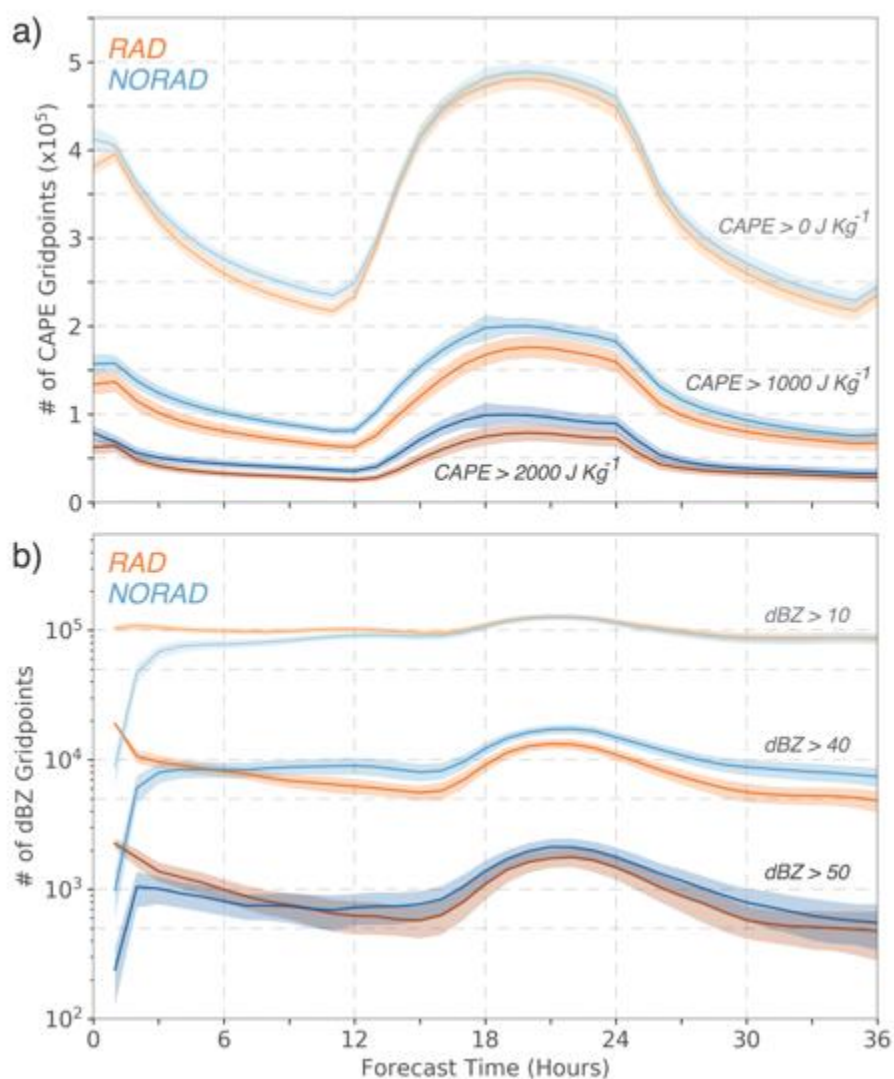
Performance diagram showing case-to-case object based verification scores for NEWS-e 1-hour composite reflectivity forecasts. Each circle represents the ensemble mean score for a single day of NEWS-e forecasts, with cases from 2017 shaded gray and cases from 2018 shaded orange.

16. Quantifying the Impact of Radar Assimilation in the 2016 Community Leveraged Unified Ensemble

Patrick Skinner (CIMMS at NSSL), Adam Clark (NSSL), Jamie Wolff, Tara Jensen, John Halley Gotway, and Randy Bullock (NCAR), and Ming Xue (CAPS)

The impact of radar assimilation in the 2016 Community Leveraged Unified Ensemble (CLUE) has been examined using neighborhood and object-based verification of composite reflectivity forecasts. Results show that radar assimilation typically improves the skill of thunderstorm forecasts for a 3–6 hour period following initialization; however, the skill of forecasts that do not assimilate radar data is higher for the remainder of the 36-hour forecast period. Variation in skill between the two sub-ensembles is attributable to contrasting biases in storm coverage, with forecasts initialized without radar assimilation overpredicting next-day thunderstorm coverage while those that include radar assimilation underpredict coverage. The contrasting biases are traced to differences in the convective environment, as forecasts initialized without radar

assimilation typically have larger convective available potential energy than those with radar assimilation. The results suggest that next-day thunderstorm forecasts can be improved through radar assimilation that improves short term forecasts while limiting biases introduced into the next-day thunderstorm environment.



Hourly ensemble mean counts of gridpoints exceeding thresholds of (a) 0, 1000, and 2000 J Kg⁻¹ of surface-based CAPE and (b) 10, 40, and 50 dBZ in composite reflectivity for forecasts that (orange) assimilate radar observations and (blue) do not assimilate radar observations. Shading indicates the region within one standard deviation of the mean and a logarithmic y-axis is used for composite reflectivity counts to improve clarity.

17. Real-Time Post Processing and Visualization of NEWS-e Forecasts

Patrick Skinner, Jessica Choate, and Anthony Reinhart (CIMMS at NSSL)

The NSSL Experimental Warn-on-Forecast System for ensembles is designed to provide short-term (0–6 hour), probabilistic guidance of severe thunderstorm hazards. NEWS-e forecasts consist of 18 members that produce 3–6 hour long forecasts at

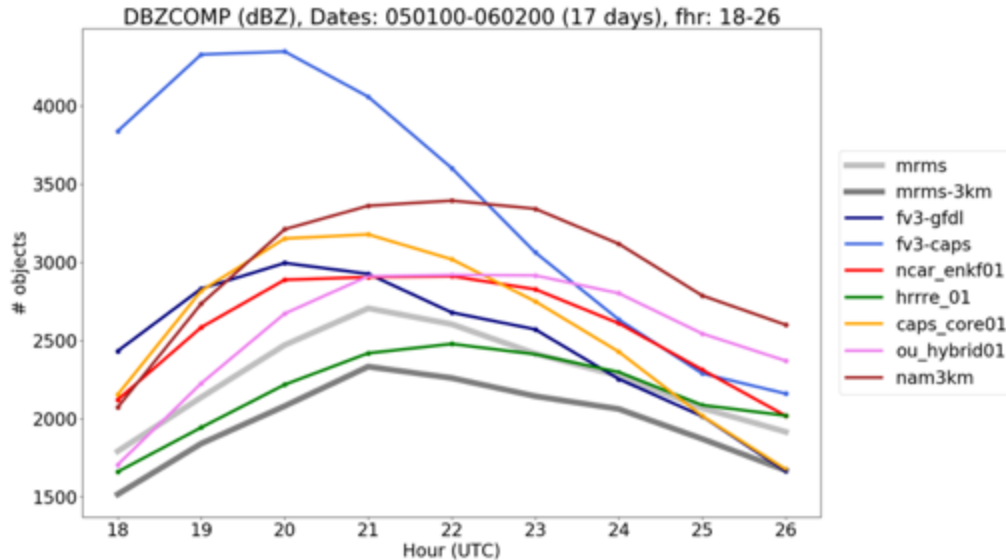
hourly, or sub-hourly, intervals with output available every 5 minutes. This configuration produces over 2 TB of data each day NEWS-e is run that needs to be post-processed and visualized in real time. In addition to the large amount of forecast data produced by NEWS-e, the short-term nature of the forecasts requires rapid post processing and visualization in order to be useful to forecasters. These requirements are addressed using customized, python-based post-processing and visualization software. The software is capable of post-processing raw NEWS-e output into over 100 probabilistic forecast products that are provided to operational meteorologists via web interface with minimal latency, with the full suite of NEWS-e products available for 3 (6) hour forecast 30 (45) minutes after initialization.

18. Inter-Model Comparisons of Storm-Scale Forecasts from the HWT Spring Forecasting Experiment

Corey Potvin, Anthony Reinhart, Patrick Skinner, and Burkely Gallo (CIMMS at NSSL), Adam Clark, Louis Wicker, and Jack Kain (NSSL), and Jacob Carley (NCEP EMC)

The 2016-2018 NOAA Hazardous Weather Testbed (HWT) Spring Forecasting Experiments (SFE) have featured the Community Leveraged Unified Ensemble (CLUE), a coordinated convection-allowing model (CAM) ensemble framework designed to provide empirical guidance for the development of operational CAM systems. The 2017 and 2018 CLUEs included 81 members that all used 3-km horizontal grid spacing, allowing direct comparison of forecasts generated using different dynamical cores, physics schemes, and initialization procedures. This study leverages the 2017 CLUE output to evaluate and compare the ability of various experimental and operational CAMs (initialized at 00 UTC) to realistically represent and predict thunderstorms at forecast hours 18-26. A major focus is identifying relative strengths and weaknesses of the ARW, NMM-B, and FV3 dynamical cores. The NSSL Multi-Radar/Multi-Sensor (MRMS) product suite is used to verify model forecasts and climatologies of observed variables. In the case of unobserved variables, the intermodel comparisons still prove useful for illuminating impacts of model design choices on storm prediction.

Results from a wide range of grid- and object-based metrics reveal operationally important model differences that correlate with dynamical core or can otherwise be attributed to differences in model design. For example, the storm diurnal cycle peaks too early in the FV3 models (blue curves in the following figure) and too late in the NMM-B models (pink, brown curves), and models initialized with direct radar data assimilation (green, pink curves) more accurately depict the diurnal cycle of storm frequency. The outcomes of this and similar comparisons will be crucial for improving existing CAMs and designing next-generation CAM systems.

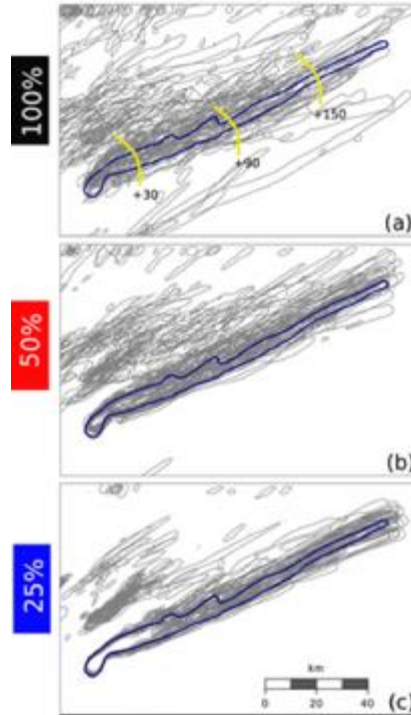


Time series of number of storms for NSSL MRMS data (gray) and various CLUE members (other colors). Storms are objectively identified using composite reflectivity.

19. Investigating Supercell Forecast Sensitivity to Initial Condition Spread

Montgomery Flora and Corey Potvin (CIMMS at NSSL), and Louis Wicker (NSSL)

As convection-allowing ensembles are routinely used to forecast the evolution of severe thunderstorms, developing an understanding of storm-scale predictability is critical. Using a full-physics numerical weather prediction (NWP) framework, the sensitivity of ensemble forecasts of supercells to initial condition (IC) uncertainty is investigated using a perfect model assumption. Three cases are used from the real-time NSSL Experimental Warn-on-Forecast System for Ensembles (NEWS-e) from the 2016 NOAA Hazardous Weather Testbed Spring Forecasting Experiment. The forecast sensitivity to IC uncertainty is assessed by repeating the simulations with the initial ensemble perturbations reduced to 50% and 25% of their original magnitudes. The object-oriented analysis focuses on significant supercell features, including the mid- and low-level mesocyclone, and rainfall. For a comprehensive analysis, supercell location and amplitude predictability of the aforementioned features are evaluated separately. For all examined features and cases, forecast spread is greatly reduced by halving the IC spread as shown in the following figure. By reducing the IC spread from 50% to 25% of the original magnitude, forecast spread is still substantially reduced in two of the three cases. The practical predictability limit (PPL), or the lead time beyond which the forecast spread exceeds some prechosen threshold, is case and feature dependent. Comparing to past studies reveals that practical predictability of supercells is substantially improved by initializing once storms are well established in the ensemble analysis.



The $300 \text{ m}^2 \text{ s}^{-2}$ UH isolines (gray) for 9 May 2016 supercell ensemble forecasts initialized with (a) 100%, (b) 50%, and (c) 25% of the spread in the original NEWS-e IC. The true $\text{UH} = 300 \text{ m}^2 \text{ s}^{-2}$ is overlaid in blue. Yellow lines show approximate timing of ensemble every 60 min after initial 30 min.

20. Using Machine Learning to Calibrate Storm-Scale Ensemble Forecasts

Montgomery Flora, Corey Potvin, and Patrick Skinner (CIMMS at NSSL), and Amy McGovern (OU School of Meteorology)

One focus of the NOAA Warn-on-Forecast (WoF) project is to provide rapid-update probabilistic guidance to human forecasters for short-term (e.g., 0-1 h) tornado forecasts. Tornadoes are unresolvable with current operational models, but convection-allowing ensembles (CAEs) such as the 3-km NSSL Experimental WoF System for Ensembles (NEWS-e) provide forecasts of low-level rotation that may potentially discriminate between tornadic and non-tornadic storms. However, CAE forecasts often contain large errors in storm intensity, timing, and location. Machine learning methods potentially mitigate these errors by leveraging ensemble uncertainty, incorporating multiple model variables, and accounting for forecast bias to produce calibrated probabilistic forecasts.

This study utilizes real-time NEWS-e forecasts generated during the 2016 -2018 NOAA Hazardous Weather Testbed Spring Forecasting Experiments and low-level azimuthal shear analyses from the NSSL Multi-Radar/Multi-Sensor (MRMS) product suite as input data for training various machine learning algorithms to produce calibrated 1-h probabilistic forecasts of low-level rotation. Given that strong low-level rotation occurs

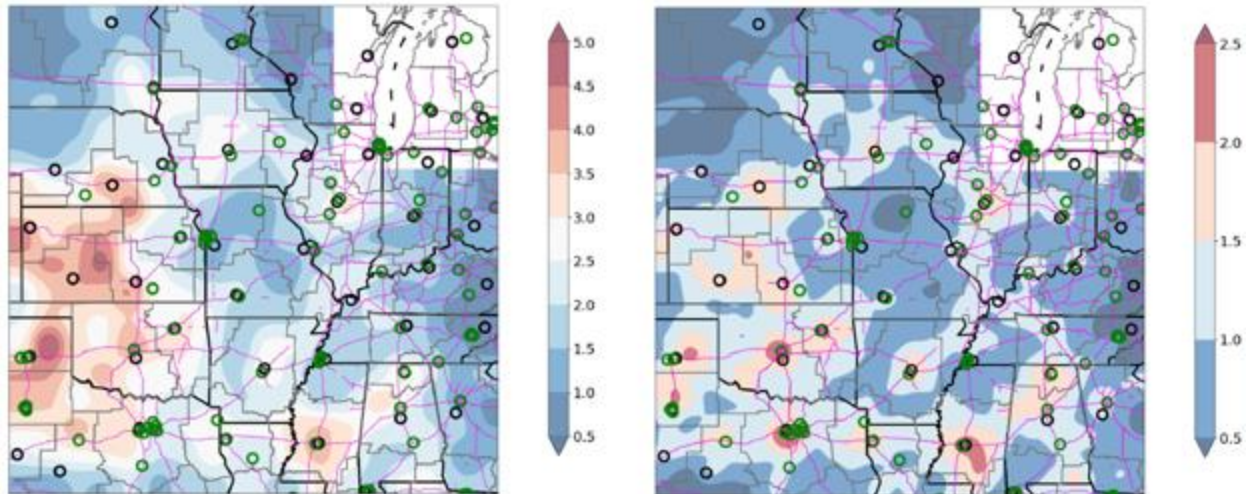
infrequently, we are oversampling the grid points within the MRMS azimuthal shear tracks to produce a more balanced dataset, which has been shown to improve machine-learning performance. Given that traditional, grid point verification statistics are limited in rare events, forecasts are evaluated using a novel verification strategy. Preliminary results indicate the calibrated probabilities substantially reduce an over-forecasting bias in the NEWS-e probabilities.

21. Identifying and Correcting Reporting Biases in SPC Tornado Database

Corey Potvin, Patrick Skinner, and Erik Rasmussen (CIMMS at NSSL), Harold Brooks (NSSL), and Chris Broyles (SPC)

The Storm Prediction Center (SPC) tornado database, generated from NCEI *Storm Data*, is indispensable for assessing United States tornado risk and investigating tornado-climate connections. Maximizing the value of this database, however, requires accounting for systemically lower reported tornado counts in rural areas owing to a lack of observers. This study uses Bayesian hierarchical modeling to estimate tornado reporting rates and expected tornado counts (cf figure below) over the central U.S. during 1975–2016. Our method addresses a serious solution non-uniqueness issue that may have affected previous studies. The adopted model explains 73% (> 90%) of the variance in reported counts at scales of 50 km (> 100 km).

Population density explains more of the variance in reported tornado counts than other examined geographical covariates, including distance from nearest city, terrain ruggedness index, and road density. The model estimates that approximately 45% of tornadoes within the analysis domain were reported. The estimated tornado reporting rate decreases sharply away from population centers; for example, while > 90% of tornadoes that occur within 5 km of a city with population >100,000 are reported, this rate decreases to < 70% at distances of 20–25 km. The method is directly extendable to other events subject to under-reporting (e.g., severe hail and wind), and could be used to improve climate studies, tornado and other hazard models for forecasters, planners, and insurance/reinsurance companies, and development and verification of storm-scale prediction systems.



Smoothed 1975-2016 tornado counts: (left) estimated by Bayesian model, and (right) recorded in SPC tornado database.

22. Advanced Dual-Doppler Wind Retrieval Techniques

Alan Shapiro, Nathan Dahl, and Joshua Gebauer (OU School of Meteorology), Corey Potvin (CIMMS at NSSL), and Adam Theisen (CIMMS at OU)

Vertical velocity (w) is generally the most difficult wind component to synthesize accurately from Doppler wind observations of intense convection, particularly when data are unavailable at low levels. The retrieval of w may be improved by including a vertical vorticity constraint in dual-Doppler analysis. This constraint requires an estimate of the local vertical vorticity tendency, which may be obtained through simple local time discretization of the horizontal wind field at adjacent observation times (the "brute force" method) or by applying advection correction.

To evaluate the performance of these methods when substantial data voids are present, we perform dual-Doppler analyses on synthetic radar observations of a high-resolution supercell simulation. Volume scan times from 10 to 150 s and radar ranges from ~10 to ~50 km are tested, and results with and without observations within the lowest 1 km AGL are compared. We find that including the vertical vorticity constraint consistently improves the w retrieval when a spatially-variable advection correction is applied, whereas the "brute force" method only has value for volume scan times on the order of 10 s.

A 3D version of the Shapiro et al. (2009) spatially variable advection correction technique is being developed and tested with mobile Doppler radar datasets. This method is expected to further improve dual-Doppler retrievals.

23. Evaluating the Relationship of Radar-Derived Rotation Signatures to Tornadogenesis in Supercells

Vincent Wood and Robert Davies-Jones (NSSL), and Corey Potvin (CIMMS at NSSL)

A large number of studies within the severe storms community have demonstrated that the upward tilting of intense low-level horizontal baroclinically-generated vorticity is a primary source of low-level vertical vorticity in supercell mesocyclones. To assess the potential utility of Doppler radar to exploring this process, we first develop equations for the three-dimensional velocity and vorticity components of radar targets defined in a right-handed radar coordinate system that accounts for earth curvature and beam refraction. Then, we generate radar pseudo-observations of a supercell simulated using the Advanced Research Weather Research and Forecasting (WRF-ARW) model with 111-m horizontal grid spacing and typical cloud model settings. A tornado develops ~110 min into the simulation and becomes very intense with surface winds briefly exceeding 110 m s^{-1} (EF5). Finally, we evaluate estimates of simulated low-level supercell azimuthal component of vorticity from the virtual Doppler radar data. Two salient findings are as follows: First, amplification of the Doppler azimuthal vorticity (horizontal rotation along the azimuthal direction) signatures at low levels were detected *prior* to the detection of Doppler normal vorticity (rotation perpendicular to the surface of constant elevation angle) signatures. Second, the Doppler azimuthal vorticity intensified as air advected spirally toward a region where upward tilting of low-level horizontal vorticity contributed to tornadogenesis. We hypothesize that these signatures may help forecasters issue earlier warnings of tornadogenesis.

24. Application of Machine Learning to Supercell and Tornado Prediction

Amy McGovern, Cameron Homeyer, Thea Sandmael, and Ryan Lagerquist (OU School of Meteorology), and Corey Potvin and Travis Smith (CIMMS at NSSL)

We use deep learning to predict whether or not a storm will be tornadic at any point within the next hour, in a framework suitable for real-time operations. Our predictors are composite (multi-radar) radar images and NWP-generated soundings; our labels (verification data) are tornado reports from the *Storm Events* archive. The two sources of radar images are the Multi-year Reanalysis of Remotely Sensed Storms (MYRORSS) (Ortega et al., 2012), which has 0.01° grid spacing (0.005° for azimuthal shear) and 5-minute time steps, covering 1998-2011; and GridRad (Homeyer and Bowman, 2017), which has 0.02° grid spacing and 5-minute time steps, covering selected days from 2011-present. The two sources of NWP soundings are the Rapid Update Cycle (RUC), for initialization times before 0000 UTC 1 May 2012, and the Rapid Refresh (RAP) for initialization times of 0000 UTC 1 May 2012.

Data are pre-processed (before machine learning) in four ways. First, storm cells are outlined and tracked through time, using an extension of the method introduced in Homeyer et al. (2017). Second, each tornado report is linked to the nearest storm cell, as long as the nearest storm cell passes within 10 km. Third, for each storm object (one

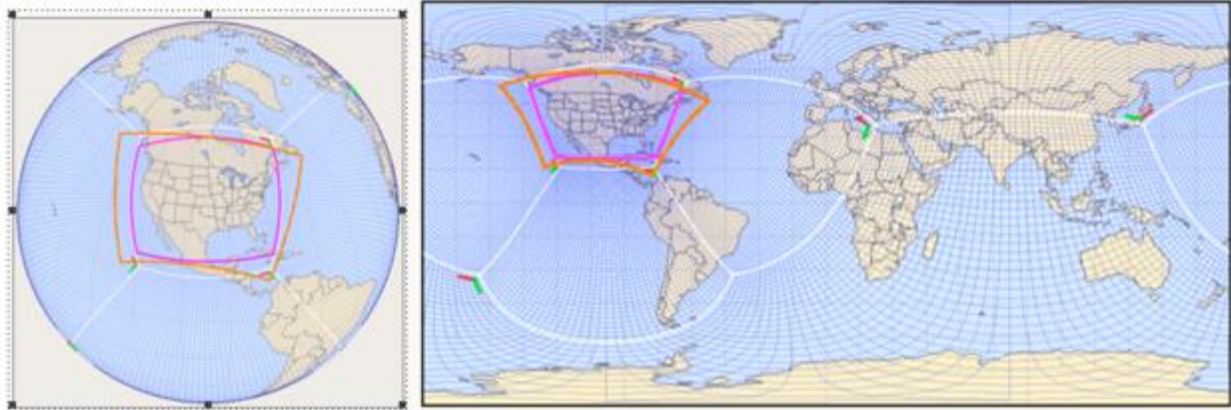
“storm object” is one storm cell at one time step), a storm-centered reflectivity image (with dimensions of $0.32^\circ \times 0.32^\circ$ at heights of 1, 2, 3, . . . , 12 km above sea level) is extracted. If MYRORSS data are available at the time, storm-centered images of low-level and mid-level azimuthal shear (with dimensions of $0.32^\circ \times 0.32^\circ$) are also extracted. Finally, the NWP sounding is interpolated in space and time to the center of the storm object. Interpolation is done via the nearest-neighbour method, so that the entire sounding is taken from one model grid point at one model time, which preserves physical consistency among the sounding variables.

We use NWP soundings, azimuthal-shear images (if available), and reflectivity images to train a convolutional neural network (CNN), which is the most common type of deep-learning model. The output is the probability that the storm will be tornadic at any point within the next hour. The main advantage of CNN’s is that they can learn from spatiotemporal images, without the need to precalculate features (e.g., CAPE, bulk shear, maximum reflectivity inside the storm, etc.). This saves time and prevents the user from imposing their preconceived notions on the model (e.g., only precalculating the features that they think are important, rather than letting the network determine the important features). Because soundings are 1-D (defined over a column), azimuthal-shear images are 2-D (defined over a horizontal plane), and reflectivity images are 3-D (defined over a volume), our CNN performs 1-D, 2-D, and 3-D convolution. To our knowledge, this approach is completely novel. Then the features detected by 1-D, 2-D, and 3-D convolution are combined, using trainable weights, to yield the output predictions.

25. Application and Evaluation of the FV3 at Convection-Allowing Scales for Severe Weather Forecasting

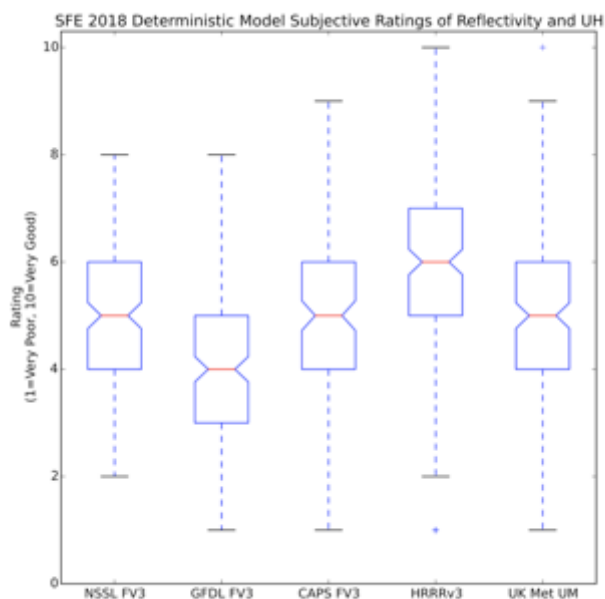
Adam Clark (NSSL), Yunheng Wang, Burkely Gallo, Brett Roberts, and Corey Potvin (CIMMS at NSSL), and Louis Wicker and Pamela Heinselman (NSSL)

In order to assess the performance and accelerate the development of the Finite-Volume Cubed Sphere Model (FV3) at convection-allowing scales, we developed a local NSSL configuration (called NSSL-FV3) of the global FV3 based on the NEMS FV3GFS developed at the Environmental Modeling Center (EMC) of NOAA. The NSSL-FV3 is initially a global configuration with grid-refinement to 3-km over the CONUS. Ultimately, it will be a stand-alone regional, convection-allowing version of FV3 suitable for operational implementation. The real-time NSSL-FV3 runs were made available starting in March 2018, and a schematic of the domain configuration is shown in the following figure.



NSSL-fv3 domain configuration within the FV3 C384 global grid (~25 km grid-spacing). The stretch factor is 2.0 for the tile over North America (grid-spacing ~ 13-km). The refine ratio for nesting is 4, which gives a model domain (purple) similar to the CONUS (orange) at ~ 3-km grid-spacing. Left: orthographic view; Right: Equidistant view.

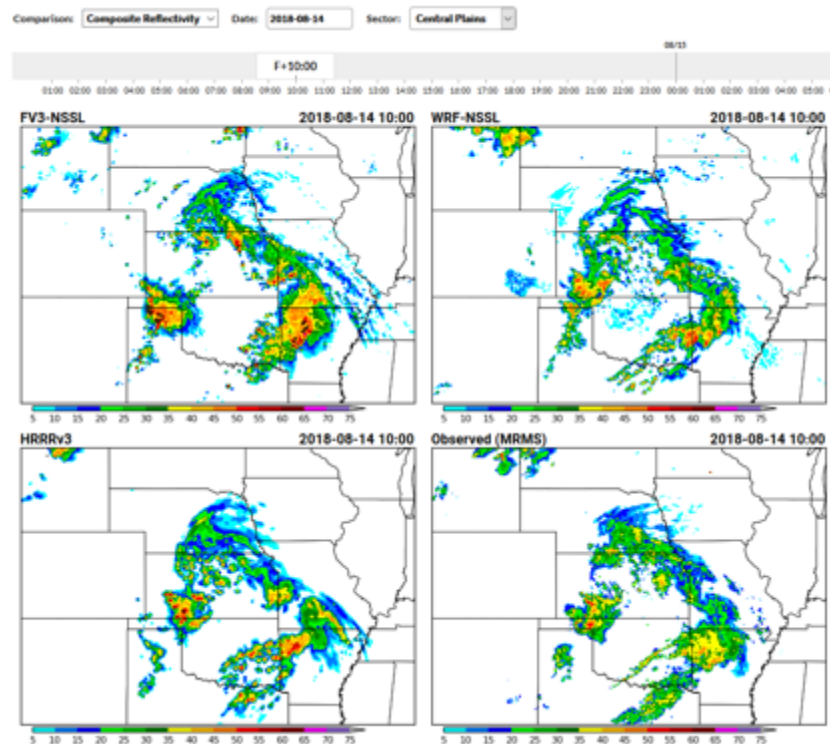
The real-time NSSL-FV3 was included in several different subjective evaluations conducted as part of the 2018 NOAA/Hazardous Weather Testbed (HWT) Spring Forecasting Experiment (SFE). These evaluations were also conducted for the operational High Resolution Rapid Refresh (HRRR) model, versions of FV3 being run at CAPS, a version of FV3 run at GFDL, and the regional convection-allowing configuration of the Unified Model (UM) run at the United Kingdom Met Office. Among all of the FV3 implementations evaluated in the SFE, the NSSL-FV3 was given the highest mean subjective rating as shown in the following figure.



Subjective ratings of the hourly simulated reflectivity and updraft helicity on a scale from 1-10 for a region of interest during the 2018 NOAA/Hazardous Weather Testbed (HWT) Spring Forecasting Experiment (SFE). Mean ratings (red line in the figure) are HRRR: 6.00, NSSL-FV3: 5.07, CAPS-FV3: 5.03 and GFDL FV3: 4.09.

In order to foster interest and solicit feedback from operational forecasters, a web framework for displaying NSSL-FV3 forecasts in real-time was developed and launched. Daily NSSL-FV3 forecasts are available on the web at <https://cams.nssl.noaa.gov>. The website provides a host of output fields relevant to convective, precipitation, winter, and other forecasting considerations. The web interface also includes data from two other CAMs (HRRR and NSSL-WRF) and observational plots for direct comparisons and evaluation of potential biases (one example is provided in the figure below).

Further research examines objective verification of three versions of the FV3 model run during the 2018 SFE and compares the FV3 versions to the HRRR, the current operational convection-allowing model run by NOAA. Attributes specific to severe weather forecasting are compared, specifically surrogate severe probabilities generated using updraft helicity (UH) and reflectivity. Preliminary results find that the climatology of UH (which indicates a simulated rotating updraft) is much different between the FV3 models and the HRRR. Therefore, post-processed severe weather metrics should take into account the differing climatologies. When the higher UH values of the FV3 are accounted for, surrogate severe probabilities perform comparably to the HRRR, although the HRRR scores higher across three statistical metrics than any tested FV3 configuration. These objective results support subjective evaluations conducted during the 2018 SFE.



Example of multipanel comparison on the NSSL FV3 real-time website. NSSL FV3 composite reflectivity forecast is at the upper left; two other CAM forecasts for the same valid time are at the upper right and lower left; and observational data (MRMS) for the corresponding time is at the lower right.

26. Optimal Temporal Frequency of the Next Generation Phased Array Radar Observations for Storm-Scale Data Assimilation

Derek Stratman and Nusrat Yussouf (CIMMS at NSSL), and Youngsun Jung, Bryan Putnam, and Tim Supinie (CAPS)

One goal of the cross-agency Spectrum Efficient National Surveillance Radar (SENSR) program is to evaluate the feasibility of the next generation multi-function surveillance radar network in order to replace the aging operational radar infrastructure currently in place. A potential replacement candidate to be employed is the phased array radar (PAR) system, which has the ability to provide full volumetric scanning of the atmosphere every ~1 min. The new PAR system will have to serve as a multi-function radar (i.e., MPAR), so full volumetric MPAR data may be temporally limited due to serving other purposes. How this temporal limitation might affect NSSL's Warn-on-Forecast (WoF) system is mostly unclear. Radar data assimilation is critical for the WoF system, which is a rapid update-cycle storm-scale ensemble data assimilation and forecast system for high-impact severe weather. As part of the SENSR and WoF programs, this project's goal is to determine the optimal temporal frequency of MPAR observations for storm-scale data assimilation.

Currently, National Weather Radar Testbed (NWRT) MPAR data from the 31 May 2013 deadly tornado and flash flood event, which occurred in parts of central and eastern Oklahoma, are being assimilated onto a 1-km grid. A multi-scale (15- and 3-km) GSI-EnKF data assimilation system (along with WRF-ARW) provides the initial and boundary conditions for the MPAR data assimilation experiments. Using CAPS's 4D-EnSRF data assimilation system, available MPAR data are assimilated from 2145 UTC to 2300 UTC every 5 and 15 min using every 1-, 2-, 5-, and 15-min volume of MPAR data. After data assimilation, short-term ensemble forecasts are produced. The ensemble analyses and forecasts are subjectively evaluated and objectively verified against MRMS-derived products, such as reflectivity and azimuthal shear.

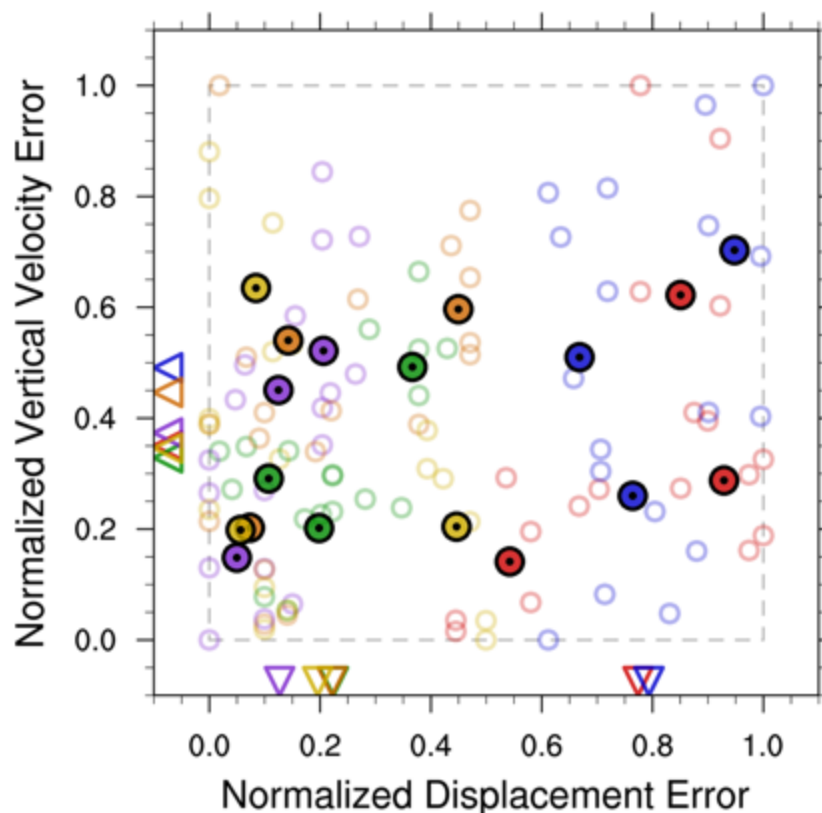
27. Correcting Storm Displacement Errors in Ensembles Using the Feature Alignment Technique (FAT)

Derek Stratman and Corey Potvin (CIMMS at NSSL), and Louis Wicker (NSSL)

Recent WoF-related studies have indicated the need to alleviate storm displacement errors in both storm-scale analyses and short-term forecasts. One promising method to reduce these errors is the feature alignment technique (FAT). The FAT mitigates displacement errors between observations and a model field while adhering to constraints to form a 2-D field of displacement vectors, which are used to adjust the prior model fields to more closely match the observations. This study merged the FAT with the CM1-LETKF (local ensemble transform Kalman filter) system to vet the FAT as a potential alleviator of errors associated with storm displacement errors using observation system simulation experiments (OSSEs).

An idealized nature run of a supercell on a 250-m grid is used to generate pseudo-radar observations (i.e., reflectivity and radial velocity). Analyses and forecasts of a supercell are produced on a 2-km grid using 50-member ensembles to test the capabilities and sensitivities of the FAT. The FAT uses the composite reflectivity field to generate a 2-D field of displacement vectors and applies the vectors to the model state variables at the start of each LETKF analysis cycle. The FAT-LETKF system is tested by displacing initial background fields and modifying the environmental vertical profile to produce various sources of error without substantially changing the structure of the storm. The results from these tests reveal the beneficial impact the FAT-LETKF system may have in cases of storm motion bias resulting from mesoscale analysis and/or model errors. The supercell OSSEs provide the foundation for future FAT-EnKF experiments with more complex scenarios and real data.

Displacement Error vs. Vertical Velocity Error

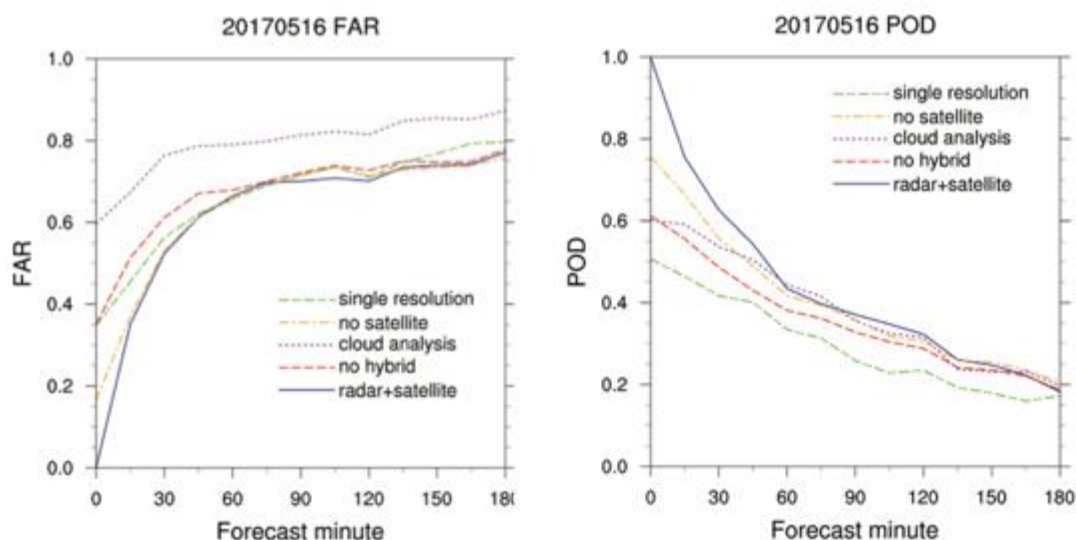


Summary plot comparing displacement errors and vertical velocity errors between the Truth run and ensembles during the free forecast. The errors are normalized using maximum and minimum values from all forecasts (i.e., six output times) for each experiment set, so a value of 0 (1) is the best (worst). Hollowed circles indicate ensembles with no data assimilation (red), LETKF only (blue), and variants of the FAT with LETKF (green, purple, orange, gold). Filled circles indicate the average of the ensemble forecast errors within each experiment set. The average errors across the three experiment sets are represented by the triangles on the bottom (displacement error) and left (vertical velocity error) sides of the plot. The grey dashed lines represent the upper and lower limits of the normalized errors.

28. Test of a Hybrid Data Analysis and Forecast System for the Warn-on-Forecast (WoF) Project

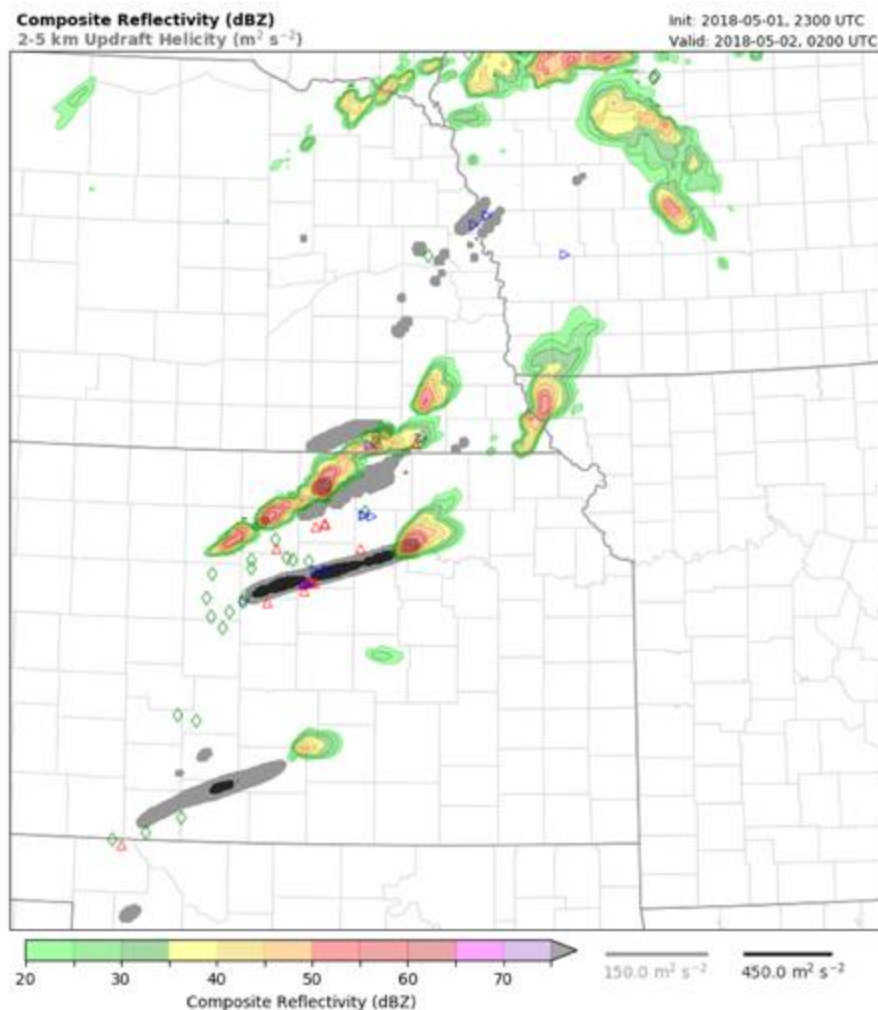
Yunheng Wang (CIMMS at NSSL) and Jidong Gao (NSSL)

This is a continuous development of the realtime weather-adaptive hybrid data analysis and forecast system for the Warn-on-Forecast (WoF) project. It is based on past experience with convective-scale rapid updated analysis experiments in 2016 and the hybrid data analysis and forecast experiments in 2017. The NSSL Experimental WoF System – variational component (NEWS-var) has been improved in several aspects, including the code structure for efficiency, the radar data pre-processing and the capabilities to assimilate new observations. The goal is to provide a deterministic physically-consistent gridded analysis to initialize convective-scale NWP for improved short-term (0-3 hour) forecasts of high impact weather. Based on results from sensitivity studies with significant cases in 2017 as shown in the following figure, several improvements have been implemented for the HWT spring experiments in 2018. First, the radar reflectivity is directly assimilated in the 3DVAR framework instead of using cloud analysis. Secondly, a dual-resolution technique is utilized while the ensemble forecasts are performed at 3 km resolution and the hybrid analysis is performed at 1.5 km resolution. The sensitivity studies have shown that the high-resolution analysis and deterministic forecast are important for maintaining the storm strength and location. Finally, both the radar radial velocity and the reflectivity data are replaced with better quality-controlled MRMS products and are processed in a timely manner.



Verification scores of the sensitivity studies in 2017 for one case (20170516). Left: Probability of detection (POD), right: False alarm ratio (FAR).

The following figure shows one 3-hour forecast example in 2018. It is shown that the forecast has captured the movement of several storms over Kansas pretty well on May 01, 2018, especially the middle one which passed through the central counties of Kansas. The north storm over northern Arkansas, however, is predicted with large phase error (far too north) and the prediction of the south storm is moving too fast. Active research and post-analysis of the real-time cases are in process which will try to address these issues effectively.



Forecasted middle-level (2-5 km) updraft helicity swath for a 3-hour period starting at 23 UTC on May 01, 2018 and the forecasted composite reflectivity valid at 02 UTC on May 02, 2018. The imposed markers are SPC storm reports during the 3-hour period, red triangles for tornadoes, green diamonds for hails and filled blue triangles for high winds.

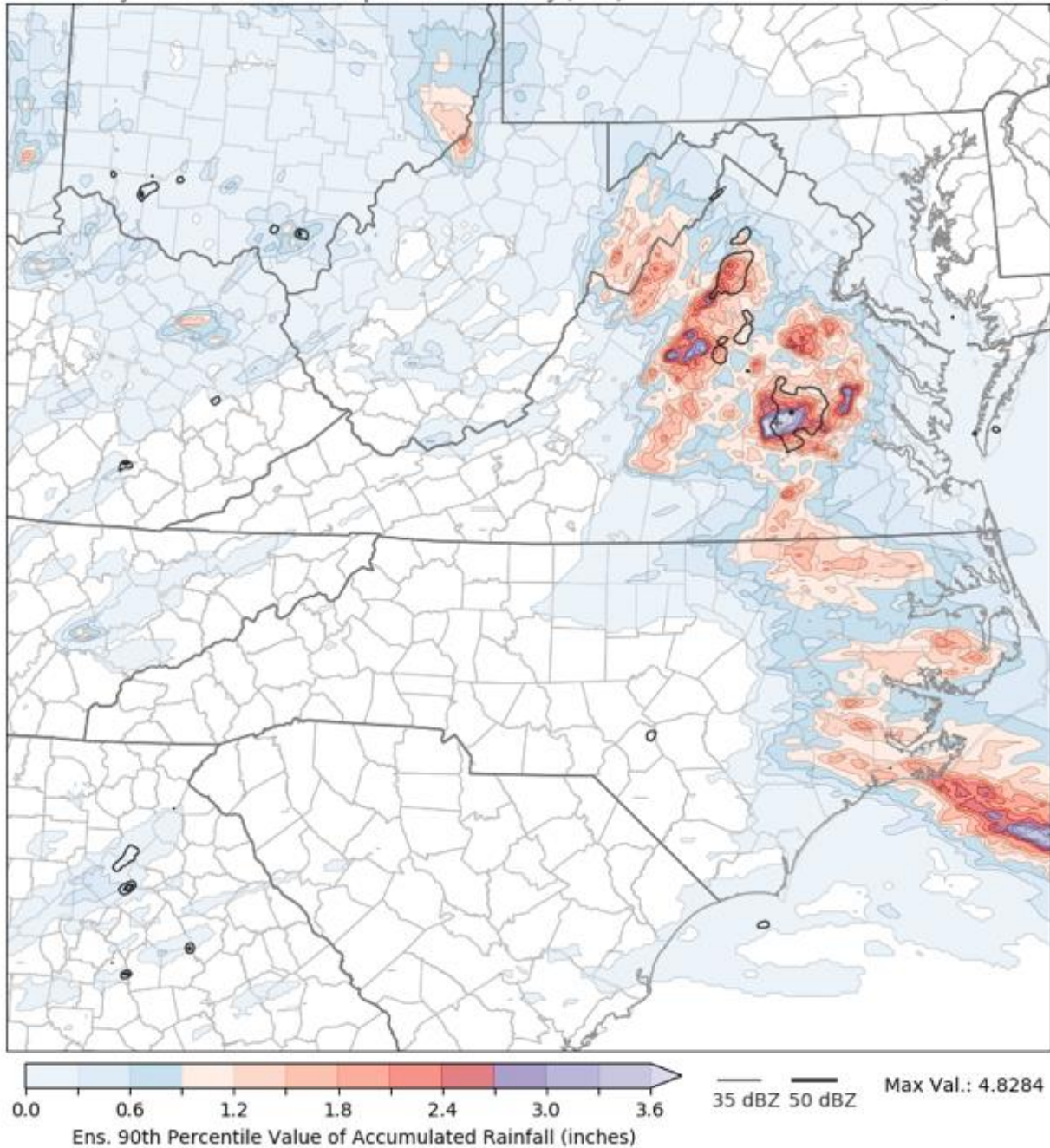
29. The NSSL Experimental Warn-on-Forecast System for Ensembles (NEWS-e) at 2018 NOAA Hydrometeorology Testbed

Nusrat Yussouf, Kent Knopfmeier, Patrick Skinner, Junjun Hu, Thomas Jones, Jessica Choate, Katie Wilson, Gerry Creager, and Anthony Reinhart (CIMMS at NSSL), Pamela Heinselman and Louis Wicker (NSSL), David Dowell, David Turner, Trevor Alcott, and Theresa Ladwig (ESRL GSD), and Xuguang Wang (OU School of Meteorology)

Excessive rainfall from severe thunderstorms can cause extensive flash flooding and threaten the lives of people living in the affected area. The Weather Prediction Center's (WPC) MetWatch desk is responsible for issuing Mesoscale Precipitation Discussions that are designed to enhance near-term 1–6 hr situational awareness for regions where heavy rainfall may lead to flash flooding. To aid WPC's MetWatch desk and Weather Forecast Office forecasters in predicting heavy rainfall and flash flood, the NEWS-e system is developed using the GSI-EnKF data assimilation (DA) system with the support from NOAA Office of Weather and Air Quality FY2016 Joint Technology Transfer Initiative funded grant. The DA system has the capability to assimilate ground-based remote sensing boundary layer observations (i.e. AERI and Doppler Lidar), GOES-R Advanced Base Imager clear sky radiance and cloud water path, MRMS reflectivity and WSR-88D radial velocity in addition to routinely available traditional observations. The 0–6 h probabilistic forecast products from the NEWS-e system is evaluated at the NOAA/NWS Weather Prediction Center Hydrometeorology Testbed Flash Flood and Intense Rainfall (HMT-FFaIR) experiment at WPC during June-July of 2018. A NEWS-e website is developed for WPC's MetWatch Desk forecasters with a focus on extreme rainfall events (<https://www.nssl.noaa.gov/projects/wof/news-e/wpc/>). The following figure shows the NEWS-e 90th percentile 6-h accumulated rainfall forecasts from 22nd June 2018. The heavy rainfall overnight on that day caused flash flooding and high water around Central Virginia.

Ens. 90th Percentile Value of Accumulated Rainfall (inches)
Probability Matched Mean - Composite Reflectivity (dBZ)

Init: 2018-06-22, 0400 UTC
Valid: 2018-06-22, 1000 UTC



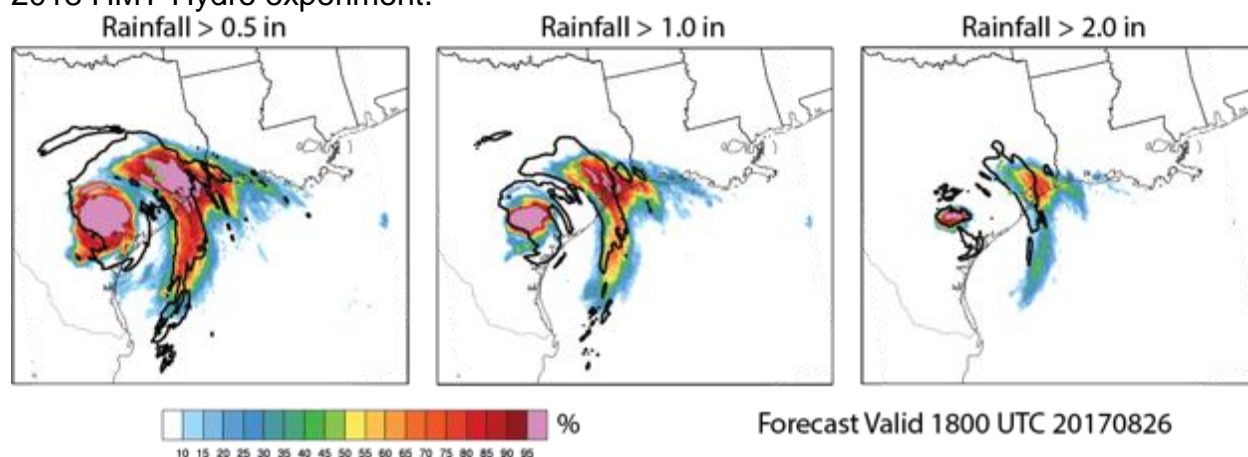
The NEWS-e 6-h 90th percentile accumulated rainfall forecast (color shading) initialized at 0400 UTC 22 June 2018. Heavy rainfall overnight caused flash flooding and high water around Central Virginia.

30. The NSSL Experimental Warn-on-Forecast System for Ensembles (NEWS-e) for Hazards Associated with Landfalling Tropical Cyclones

Nusrat Yussouf (CIMMS at NSSL)

Extreme rainfall, flash flood, high winds and tornadoes from landfalling tropical cyclones (LTCs) threaten human lives and property damage in the affected area. Year 2017 is an example of how LTCs like Harvey, Irma and Maria can create havoc to lives and properties. Hurricane Harvey alone caused more than \$125 billion in damages, killed 106 people and forced the displacement of 40,000 people. The National Hurricane Center, Storm Prediction Center, Weather Prediction Center, local Weather Forecast Offices and River Forecast Centers issue outlooks, watches and warnings for extreme rainfall, flash floods, tornadoes, high winds and other LTC related hazards. As such, short-term NEWS-e LTC forecasts will likely aid in the NWS watch-to-warning operations of TCs after they made landfall. The application of NEWS-e probabilistic model guidance for LTC is evaluated using Hurricane Harvey as a case study. Harvey made landfall on 25 August 2017 in the early evening hours. The excessive rainfall associated with Harvey and its remnants resulted in historic flooding along the Gulf Coast of Texas from 26 August through 1 September 2017. A NEWS-e experiment is conducted to assimilate WSR-88D radar reflectivity and radial velocity from Harvey as soon as radar echoes are visible in WSR-88Ds, in addition to all other traditional observations. Results indicate that the NEWS-e system predicts the heavy rainfall and low-level rotational characteristics associated with Harvey with good accuracy. The following figure is an example of NEWS-e 6-h probabilistic rainfall forecasts greater than 0.5, 1 and 2 inches. NEWS-e predicts the precipitation core approximately at the correct locations as observed (NCEP's Stage-IV rainfall contours shown in black) and verifies well with the NWS flash flood report (shown in green).

The NEWS-e PQPF from Hurricane Harvey is used to force NSSL's Flash hydrologic model and explicit probabilistic flash flood guidance from Flash system are evaluated in 2018 HMT-Hydro experiment.



The grid point based forecast ensemble probability (colors, 5% increment) of 0-6 h rainfall greater than 0.5 inches, 1.0 inches and 2.0 inches for Hurricane Harvey after it made landfall. The thick black contour overlaid is the Stage-IV rainfall for the threshold values. The green dots are the NWS flash flood reports during that forecast time period.

31. Hardware Management and Hardware/Software Support

Gerry Creager (CIMMS at NSSL)

Oversaw decommissioning of the “Loki” Cray computing resource. Managed (and participated in) installation of the new Cray computing resource (XC30, “Odin”) for NSSL and the Warn on Forecast operations from September through November 2017. Unanticipated issues with software installations caused significant delays in the installation process, based on problems configuring the software for NSSL’s and Warn on Forecast’s specific requirements.

Planned and managed acquisition of the upgrades to computational capabilities and mass storage of the NSSL Cray computing resource, Spring/Summer 2018.

Hardware/software support for Warn on Forecast and FFAIR operations on the Cray computing resource, Spring/Summer 2018.

Attended and completed Cray hardware and software administration training at Cray’s factory, Chippewa Falls, WI, in June 2018.

32. Outreach: Aviation Weather Symposium at the National Weather Center

Gerry Creager and Kim Elmore (CIMMS at NSSL)

Hosted an Aviation Weather Symposium, sponsored by the Aircraft Owners and Pilots Association, in concert with a major event held at Westheimer Airport, in September, 2017, at the National Weather Center. Over 200 pilots from across the U.S., representing a spectrum from student and private pilots to airline professionals attended. This symposium was recognized by the Federal Aviation Administration’s Safety Team for continuing education credits. It was sanctioned by NSSL. Personnel from CIMMS, as well as NSSL participated.

33. Outreach: American Meteorological Society High Performance Computing Symposium

Gerry Creager (CIMMS at NSSL)

Chair, Fourth Annual High Performance Computing Symposium at the 98th American Meteorological Society Annual Meeting. January, 2018, Austin, TX. Over 20 papers were presented on various aspects of High Performance Computing, ranging from operational issues to software techniques. The Symposium also partners with the Machine Learning/Artificial Intelligence, Python, and Coastal conferences to facilitate cross-cutting joint sessions.

In addition, participated as session chair for several Environmental Information Processing Technologies sessions, as a subject-matter expert, including Health (Wet-

Bulb Globe Temperature), and GIS (Geospatial Information Systems, and Coastal and Ocean Wave Model (ADCIRC) systems. Serving as Chair, Fifth Annual High Performance Computing Symposium, which will be held in conjunction with the 99th Annual AMS meeting, in Phoenix AZ in January 2019. Currently over 40 papers are to be presented.

34. Develop Advanced Adaptive Radar Data Quality Control Techniques for Operational Data Assimilation

Kang Nai (CIMMS at NSSL) and Qin Xu (NSSL)

Radar data quality control (QC) is very important for radar data assimilation. As an important part of radar data QC, aliased radial velocities in the raw radar data scanned from severe storm must be either corrected or removed (if not correctable). Toward this goal, the recently developed de-aliasing algorithms were combined adaptively and upgraded into a model-based velocity dealiasing technique. Using the wind fields predicted by the 3DEnVar system as references for dealiasing, the upgraded dealiasing technique was tested with radial-velocity data collected from 21 operational WSR-88D radars for the severe storm events on 26 May 2016 and 16 May 2017, and from 22 operational WSR-88D radars for the severe storm event on 19 May 2018. The test results were examined to identify difficult cases for detailed diagnoses and further improvements. The algorithm codes of the adaptively combined dealiasing technique were optimized for further real-time tests and applications with the 3DEnVar system. Tested with radial-velocity data collected from operational WSR-88D radars for the above severe storm events, the upgraded dealiasing technique was found to perform better (with improved dealiased-data coverage and no false dealiasing) than the previous non-model-based stand-alone dealiasing technique but still have some difficulties to cover isolated data areas far away from the radar site. The upgraded dealiasing technique was found capable to detect and correct aliased velocities in and around mesocyclones. An example is shown below.

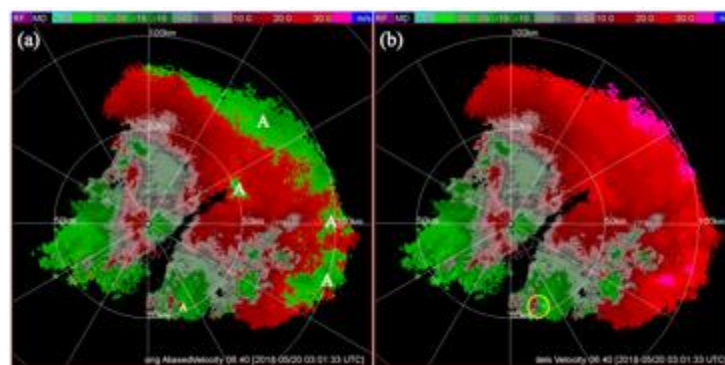


Image of raw radial velocities on 6.4° tilt at 03:01:33 UTC from the operational KLBB radar (in Lubbock, TX) for the severe storm on 19 May 2018; (b) As in (a) but for dealiased velocities produced by the upgraded dealiasing technique. In panel (a), the white letters “A” mark the aliased-velocity areas. In panel (b), the yellow circle marks the mesocyclone where aliased velocities were detected and corrected by the upgraded dealiasing technique.

Publications

- Clark, A. J., I. L. Jirak, S. R. Dembek, G. J. Creager, F. Kong, K. W. Thomas, K. H. Knopfmeier, B. T. Gallo, C. J. Melick, M. Xue, K. A. Brewster, Y. Jung, A. Kennedy, X. Dong, J. Markel, M. Gilmore, G. S. Gilmore, K. R. Fossell, R. A. Sobash, J. R. Carley, B. S. Ferrier, M. Pyle, C. R. Alexander, S. J. Weiss, J. S. Kain, L. J. Wicker, G. Thompson, R. D. Adams-Selin, and D. A. Imy, 2018: The Community Leveraged Unified Ensemble (CLUE) in the 2016 NOAA/Hazardous Weather Testbed Spring Forecasting Experiment. *Bulletin of the American Meteorological Society*, **99**, 1433–1448.
- Dafis S., A. O. Fierro, T. M. Giannaros, V. Kotroni, K. Lagouvardos, and E. Mansell, 2018: Evaluation of an explicit lightning forecast system. *Journal of Geophysical Research, Atmospheres*. **123**, 5130–5148.
- Dokken, D., P. Belik, C. K. Potvin, K. Scholz, and M. Shvartsman, 2017: Applications of vortex gas models to tornadogenesis and maintenance. *Open Journal of Fluid Dynamics*, **7**, 596-622.
- Fierro, A. O., G. Zhao S. Liu Y. Wang, J. Gao, K. Calhoun, C. L. Ziegler, E. R. Mansell, and D. R. MacGorman, 2018: Assimilation of total lightning with GSI and NEWS3DVAR to improve short-term forecasts of high impact weather events at cloud resolving scales. *JCSDA Quarterly Newsletter*, No. 58, Winter 2018, 5-12.
- Fierro, A. O., S. Stevenson, and R. Rabin, 2018: Evolution of GLM-observed total lightning in Hurricane Maria (2017) during the period of maximum intensity. *Monthly Weather Review*, **146**, 1641–1666.
- Fierro, A. O., and E. R. Mansell, 2018: Relationships between electrification and storm-scale properties based on idealized simulations of an intensifying hurricane-like vortex. *Journal of the Atmospheric Sciences*. **75**, 657-574.
- Fierro, A. O., and E. R. Mansell, 2017: Electrification and lightning in idealized simulations of a hurricane-like vortex subject to wind shear and sea surface temperature cooling. *Journal of the Atmospheric Sciences*, **74**, 2023–2041.
- Flora, M. L., C. K. Potvin, and L. J. Wicker, 2018: Practical predictability of supercells: Exploring ensemble forecast sensitivity to initial condition spread. *Monthly Weather Review*, **146**, 2361–2379.
- Gallo, B. T., A. J. Clark, B. T. Smith, R. L. Thompson, I. Jirak, and S. R. Dembek, 2018: Blended probabilistic tornado forecasts: Combining climatological frequencies with NSSL-WRF ensemble forecasts. *Weather and Forecasting*, **33**, 443–460.
- Jones, T. A., X. Wang, P. Skinner, A. Johnson, and Y. Wang, 2018: Assimilation of GOES-13 imager clear-sky water vapor (6.5 μ m) radiances into a Warn-on-Forecast system. *Monthly Weather Review*, **146**, 1077-1107.
- Lawson, J. R., J. S. Kain, N. Yussouf, D. C. Dowell, D. M. Wheatley, K. H. Knopfmeier, and T. A. Jones, 2018: Advancing from convection-allowing NWP to Warn-on-Forecast: Evidence of progress. *Weather Forecast.*, **33**, 599–607.
- McGovern, A., C. K. Potvin, and R. A. Brown, 2017: Using large-scale machine learning to improve our understanding of the formation of tornadoes. *Large-scale Machine Learning in the Earth Sciences*, A. N. Srivastava, R. Nemani, K. Steinhäuser, Eds., CRC Press, 95–112.
- Pan, S., J. Gao, D. J. Stensrud, X. Wang, and T. A. Jones, 2017: Assimilation of radar radial velocity and reflectivity, satellite cloud water path and total precipitable water for convective scale NWP in OSSEs. *Journal of Atmospheric and Oceanic Technology*, **34**, 67-89.
- Skinner, P. S., D. M. Wheatley, K. H. Knopfmeier, A. E. Reinhart, J. J. Choate, T. A. Jones, G. J. Creager, D. C. Dowell, C. R. Alexander, T. T. Ladwig, L. J. Wicker, P. L. Heinselman, P. Minnis, and R. Palikonda, 2018: Object-based verification of a prototype Warn-on-Forecast system. *Weather and Forecasting*, **33**, In Press.
- Stratman, D. R., C. K. Potvin, and L. J. Wicker, 2018: Correcting storm displacement errors in ensembles using the feature alignment technique (FAT). *Monthly Weather Review*, **146**, 2125–2145.
- Wang, H., Y. Liu, T. Zhao, M. Xu, Y. Liu, F. Guo, S. Shen, W. Y. Y. Cheng, E. R. Mansell, and A. O. Fierro, 2018: Incorporating geostationary lightning data into a radar reflectivity based hydrometeor retrieval method: An observing system simulation experiment. *Atmospheric Research*, **209**, 1-13.

Xu, Q., L. Wei, and K. Nai, 2017: A three-step method for estimating vortex center locations in four-dimensional space from radar observed tornadic mesocyclones. *Journal of Atmospheric and Oceanic Technology*, **34**, 2275–2281.

Awards

Best Student Poster Presentation, 29th Conference on Weather Analysis and Forecasting/25th Conference on Numerical Weather Prediction, "Enhancing Storm-Scale 1-h Probabilistic Low-Level Rotation Forecasts through Machine Learning", M. L. Flora, C. K. Potvin, A. McGovern, P. S. Skinner – **David Harrison**

NSSL Project 4 – Hydrologic Modeling Research

NOAA Technical Lead: Alan Gerard and Jonathan Gourley (NSSL)

NOAA Strategic Goal 2 – *Weather-Ready Nation – Society is Prepared for and Responds to Weather-Related Events*

Funding Type: CIMMS Task II

Objectives

The Hydrologic Modeling Research work for this reporting period focused on activities of four main sub-projects: 1) FACETs, 2) HMT-Hydro, 3) Nokia-Union Pacific Railroad, and 4) Stream Radar. The main objective of each sub-project is listed as follows:

- *FACETs*: To continue the development and implementation activities of flash flood probabilistic products.
- *HMT-Hydro*: To test recently developed flash flood probabilistic products using experimental real-time system settings.
- *Nokia-Union Pacific Railroad*: To deploy an upgraded system with improved forecasting capabilities.
- *Stream Radar*: To continue the installation the Stream Radars and to revisit them for maintenance as needed.

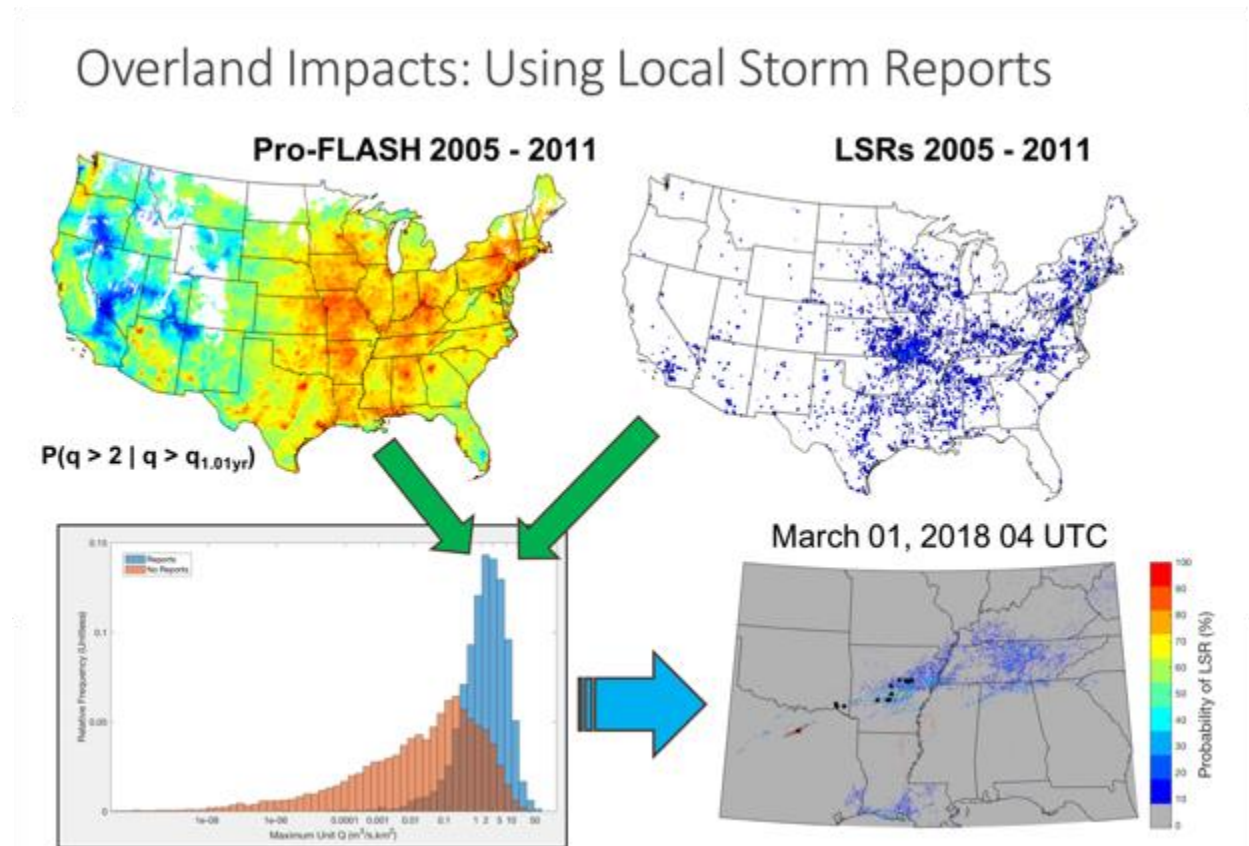
Accomplishments

1. *FACETs*

Humberto Vergara-Arrieta (CIMMS at NSSL) and Jonathan Gourley (NSSL)

The research work for the project Forecasting A Continuum of Environmental Threats (FACETs) continued focusing on the implementation of flash flood probabilistic products that were prototyped and developed in the FY17. The implementation was done on the systems featured in sub-projects 2 and 3 below. Figure 1 illustrates the building blocks and example application for one of the products that were implemented for the HMT-Hydro Experiment during Summer of 2018 (sub-project 2).

Some collaborative work with researchers from the Weather Prediction Center (WPC) - Cooperative Institute for Research in Environmental Sciences (CIRES) also continued. This work focused on testing the applicability of FLASH and Pro-FLASH products for WPC's Excessive Rainfall Forecasts.



Schematic of Probabilistic Model for forecasting the occurrence of a Flash Flood Local Storm Report using historical estimates of surface flow rates from FLASH and archived NWS Local Storm Reports.

2. HMT-Hydro

Steven Martinaitis, Humberto Vergara-Arrieta, Katie Wilson, Nusrat Yussouf, Andres Vergara-Arrieta, Tiffany Meyer, Alexander Zwink, and Kodi Berry (CIMMS at NSSL), and Jonathan Gourley and Pam Heinselman (NSSL)

The Hydrometeorology Testbed (HMT) Multi-Radar Multi-Sensor (MRMS) Hydro Experiment (hereinafter denoted as "HMT-Hydro Experiment") focuses on improving flash flood prediction and warnings. The 2018 edition of the HMT-Hydro Experiment focused on the transition from deterministic products to gridded probabilities for flash flood prediction. Moreover, the utilization of the short-term precipitation forecasts from the Warn-on-Forecast (WoF) system was also evaluated.

The HMT-Hydro Experiment was conducted for three weeks during the summer of 2008 in the Hazardous Weather Testbed. CIMMS and NSSL scientists worked closely with

the participating forecasters from the NWS to evaluate the new experimental tools in both real-time operations and archived cases. The real-time operations focused on the suite of probabilistic products and how it would impact flash flood warning decisions. Post-operational evaluations generated discussions on the coverage, range of values, and sensitivities of the probabilistic values when compared to reported flash flood events. Three archived cases were also presented to the forecasters. These cases included the use of WoF quantitative precipitation forecasts (QPFs) to examine how short-term QPFs can influence forecaster actions and potential warning decisions. The forecasters filled out data collection forms for each hour of data to analyze the progression from deterministic products to probabilistic products to probabilistic products with the WoF QPFs.



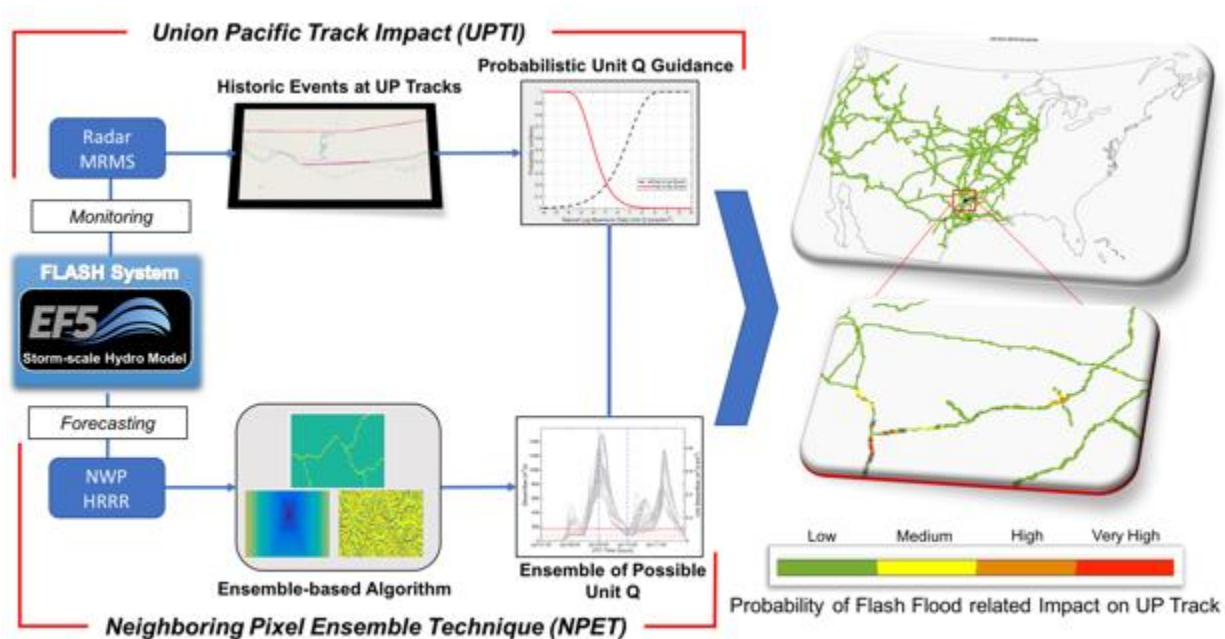
Participating forecasters discussing probabilistic and Warn-on-Forecast products and working through real-time warning operations during the HMT-Hydro Experiment.

3. Nokia-Union Pacific Railroad

Humberto Vergara-Arrieta, Ami Arthur, and Zac Flamig (CIMMS at NSSL), and Jonathan Gourley (NSSL)

The team has been working with Nokia (formerly Space Time Insight, Inc.) since January of 2017 for the development of a forecasting system for railroad track impacts caused by flash floods. The railroad track network is operated by Union Pacific (UP) Corporation. The forecasting system consists of FLASH's modeling framework with inputs from the MRMS system for real-time monitoring and from the High-Resolution Rapid Refresh (HRRR) operational Numerical Weather Prediction (NWP) modeling system for forecasting up to 18 hours into the future. Figure 3 shows the overall workflow that was developed for the UP track impact forecasting system. The aforementioned system was optimized to forecast impacts on railroad tracks with historical reports of water-related incidents. Furthermore, an ensemble technique was developed, tested and calibrated to account for the uncertainty in the determination of impact location due to uncertainty in the NWP rainfall forecasts. These forecast products are provided to collaborators at Nokia who generate the final probabilistic products and visualizations for the partners at Union Pacific.

During this reporting period, the work focused on upgrading the system to increase the spatial resolution of the hydrologic modeling component from 1-km to 250-m for the railroad network wide system. Likewise, precipitation inputs from the Global Forecasting System (GFS) were added to increase forecasting capabilities up to 72 hours into the future. Work was also completed to develop nested modeling systems at a very high-resolution of 10-m for selected segments of the track. The performance of the system has been rated positively by both Nokia and Union Pacific.



Overall workflow for the flash flood forecast system developed for track impacts.

4. Stream Radar

Humberto Vergara-Arrieta and Jorge Duarte (CIMMS at NSSL), and Jonathan Gourley and Daniel Wasielewski (NSSL)

This project entails the siting and installation of 14 Stream Radars and the transfer of their real-time data for inclusion in the operational National Water Model. In previous reporting periods, the team was able to install 7 Stream Radars. Work to install the remaining 7 Stream Radars has been done during this reporting period. The work involves the acquisition and assembly of the equipment as well as obtaining permission for installation at candidate sites, surveying the location and ultimately installing the Stream Radar systems. Figure 4 illustrates some of the Stream Radar system installations.

During this reporting period, the project team continued to engage landowners, researchers, and both private and commercial operational entities for collaboration at local sites. Current and potential collaborators include the Colorado Department of

Transportation, United States Geological Survey, Chickasaw Nation (Wayne Kellogg), National Park Service (Noel Obsborn), Falls Creek Baptist Conference Center and Campground (Chad Fielding), University of Oklahoma (Dan Allen), Texas State University (Thom Hardy), Edwards Aquifer Authority (Chad Furl), the United States Department of Agriculture, and Union Pacific Railroad.

The project team's field work and Stream Radar installations have been featured in the December 2017 edition of the Civil Engineering Magazine - Volume 87 (11), p. 40-41.



Examples of Stream Radar systems installation sites.

NSSL Project 7 – Synoptic, Mesoscale and Stormscale Processes Associated with Hazardous Weather

NOAA Technical Lead: Alan Gerard, Pamela Heinselman, and Donald MacGorman (NSSL)

NOAA Strategic Goal 2 – Weather-Ready Nation – Society is Prepared for and Responds to Weather-Related Events

Funding Type: CIMMS Task II

1. VORTEX-SE Planning and Grant Guidance

Erik Rasmussen (CIMMS at NSSL)

Dr. Erik Rasmussen of CIMMS is the Project Manager for VORTEX-SE, a Congressionally-mandated research program to investigate the aspects of tornadoes in the Southeast U.S. that are associated with unusually high mortality. As Project Manager, Dr. Rasmussen leads the work of a 24-member Scientific Steering Committee, monitors and facilitates research through approximately fifty research grants, and incorporates the guidance of a four-agency (NOAA, NSF, NASA, NIST) leadership team.

The fourth consecutive grant competition was conducted via a Federal Funding Opportunity. This competition resulted in awards of around \$2.5M. In addition, a collaborative research proposal was solicited from several OAR laboratories, with funding beginning in the summer of 2018. Funding emphases continue to be the reduction of forecast uncertainties at all time/space scales relevant to the Southeast U.S. tornado problem, as well as to understand a variety of issues related to hazard communication and vulnerability in that region.

VORTEX-SE conducted its first multi-domain observing campaign in northern Alabama and the Mississippi Delta region of northeast Louisiana, involving fixed-site research radars, mobile C-band dual-polarization Doppler radars, and the NOAA P-3 research aircraft. Planning is underway for our first "pan-season" observing campaign, "Meso18-19", involving observations across the entire Southeast from November 2018-April 2019, as well as a campaign to improve understanding of "non-classic tornadic storms" in 2019-2020.

2. Rivers of Vorticity in Supercells (RiVorS) Data Analysis

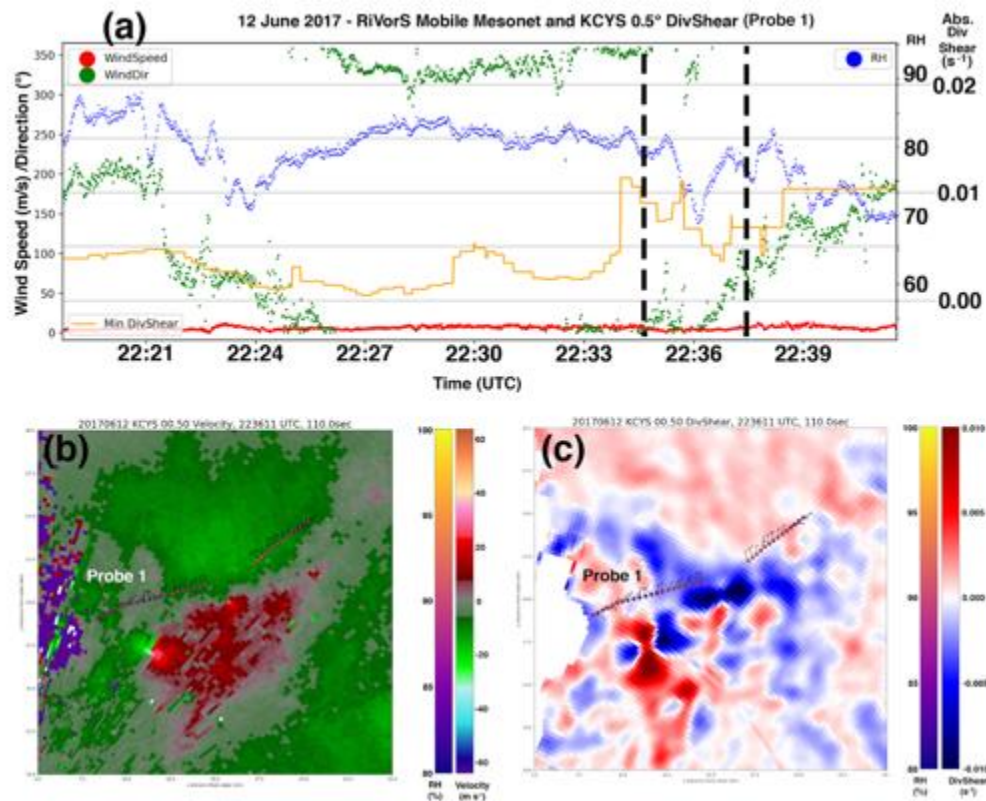
Matt Mahalik and Erik Rasmussen (CIMMS at NSSL), and Sean Waugh (NSSL)

The Rivers of Vorticity in Supercells (RiVorS) field project of 2017 was among the first attempts to directly observe theoretical "rivers" of locally-enhanced vorticity commonly found between the main precipitation region and the low-level updraft of numerically simulated supercells. During the data collection phase of the project, a diverse dataset of mobile mesonet (MM) and mobile Doppler radar measurements from both tornadic and non-tornadic storms was collected.

One focus of the analysis of kinematic fields observed in the RiVorS dataset is the detection and interrogation of convergent boundaries that may relate to vorticity rivers or the processes that produce them. This analysis was conducted by calculating azimuthal (AzShear) and divergent (DivShear) shear fields for WSR-88D and mobile radar data to examine the structure in low and near-ground levels of storms that produced notable surface kinematic features. The radial velocity-derived fields were spatiotemporally matched to quality-controlled mobile mesonet data to explore the evolution of these

features and their parent storms. This analysis represented one of the first direct comparisons between AzShear, DivShear, and surface observations.

Preliminary analysis of observed kinematic fields from RiVorS provided proof-of-concept that DivShear and AzShear behave as expected in theory: AzShear maxima are observed with rotating features, and DivShear maxima are present along easily identifiable convergent boundaries such as gust fronts. In several supercells, significant DivShear fluctuations were also often collocated with cyclonic wind shifts observed by MMs near the storm core, many of which also appeared near areas of enhanced rotation. Transient, very small-scale but significant fluctuations observed in MM thermodynamic traces were also noted in the vicinity of convergence regions. While a larger sample size is necessary to draw conclusions, the results of this study will be used to help steer observational strategies in future supercell and tornado field campaigns.



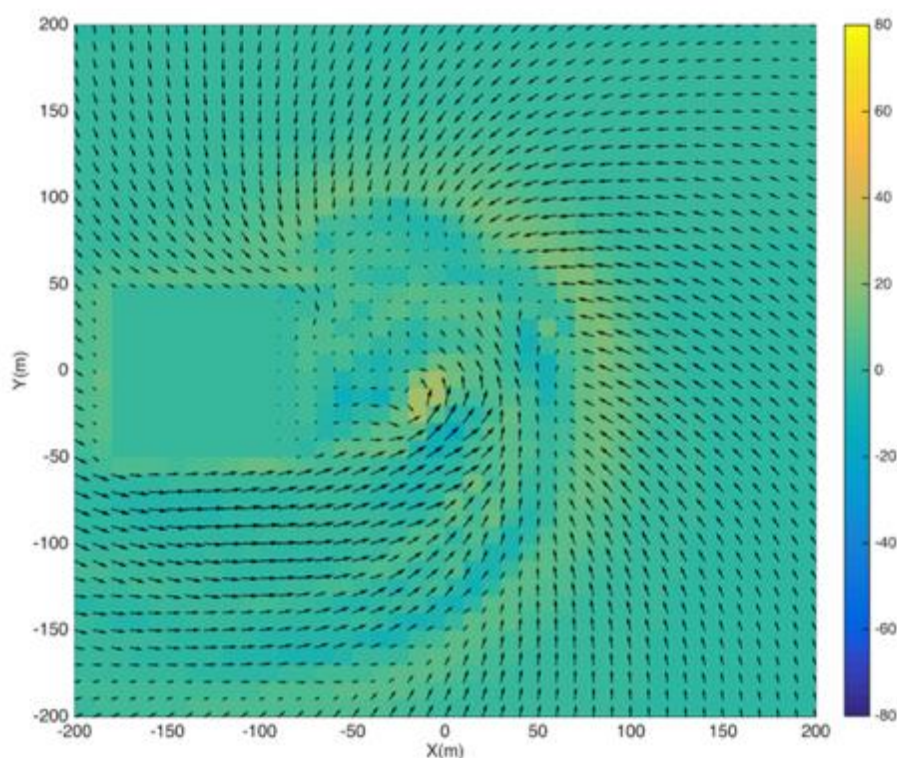
(a) Time series showing one-second-interval wind speed (red) and direction (green) and relative humidity (blue) observed by a mobile mesonet, and minimum absolute DivShear within 1 km of the mesonet location as derived from KCYS radar (yellow) for a 22-minute period of RiVorS operations in and around a tornadic supercell near Cheyenne, Wyoming, on 12 June 2017. (b) KCYS 0.5° velocity and (c) DivShear from the 2236 UTC scan, with mobile mesonet locations and wind barbs plotted for the 3.5-minute period indicated by the vertical dashed lines in (a).

3. Exploration of Terrain Effects on Tornado and Supercell Dynamics in the Southeast United States

Anthony Reinhart (CIMMS at NSSL), David Bodine (ARRC), and Frank Lombardo (University of Illinois at Urbana-Champaign)

This NOAA funded VORTEX-SE project is beginning to develop new understanding of how terrain impacts supercell and tornado processes and how these terrain-induced changes impact the public to these tornado hazards. These efforts are being explored using numerical modeling with tornado LES simulations and WRF/CM1 idealized simulations. This year's efforts saw the implementation of a new immersion boundary method in the LES. This allows for different types of terrain and terrain heights as well as buildings to be included in the LES simulation (figure below). CM1 simulations with different types of terrain (hills and valleys) showing how supercell propagation differs depending upon terrain were also conducted and are still being analyzed and expanded.

We are working with the NWS office in Morristown, Tennessee to help us focus the study on being able to improve their warning decision ability. We currently have monthly meetings to make sure the project will help the NWS offices in warning decision process. Events from their region are being used as a template for some of the terrain features used in this ongoing study.



10-m horizontal wind speeds (black arrows) and vertical velocities (shaded colors) for the 100-m wide building simulation. The building is centered around $X=-130$ m, $Y=0$ m.

4. Numerical Simulations of Electrification Processes and Lightning

Alexander Fierro (CIMMS at NSSL), and Don MacGorman, Ted Mansell, and Conrad Ziegler (NSSL)

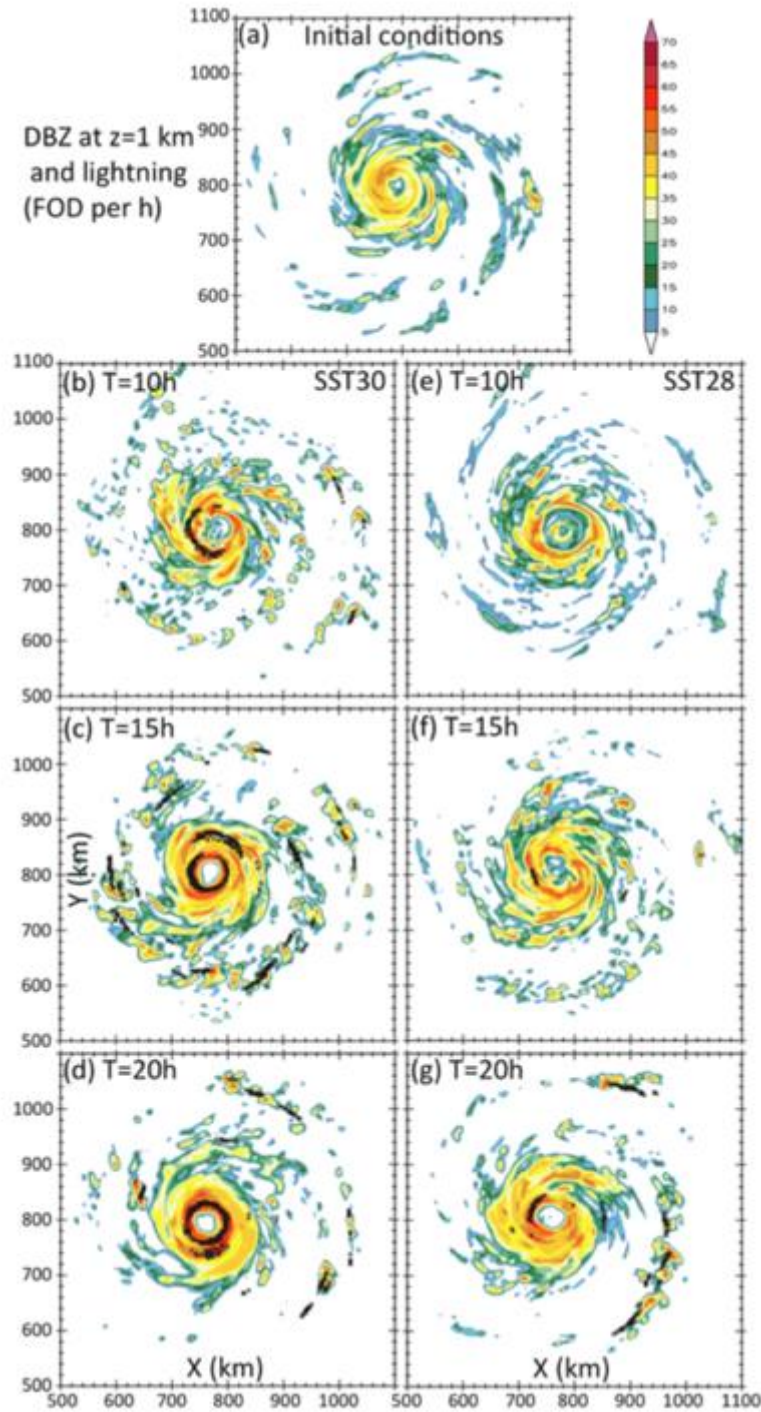
We conduct cloud-scale (≤ 2.5 km) real or idealized numerical simulations of the small-scale electrification processes within high impact weather systems such as tropical cyclones (TCs) to augment our understanding on these processes and, potentially, to derive functional relationships between various lightning metrics and storm microphysics/kinematics. Analyse total lightning observations within high impact weather systems to better understand their relationships with storm intensity and evolution. One chief deliverable of this research is help develop forward operators to assimilate lightning in NWP models (NSSL Project 3).

With the assistance of Dr. Mansell, we continue to implement new physics and initialization procedures into the NSSL COMMAS model to simulated idealized hurricanes. Finalized and performed in depth analyses of the model output from cloud-scale, idealized, intensifying electrified TCs simulations. Submitted a new manuscript to JAS 2018 and attended ICAE conference in Nara, Japan to present/disseminate the work.

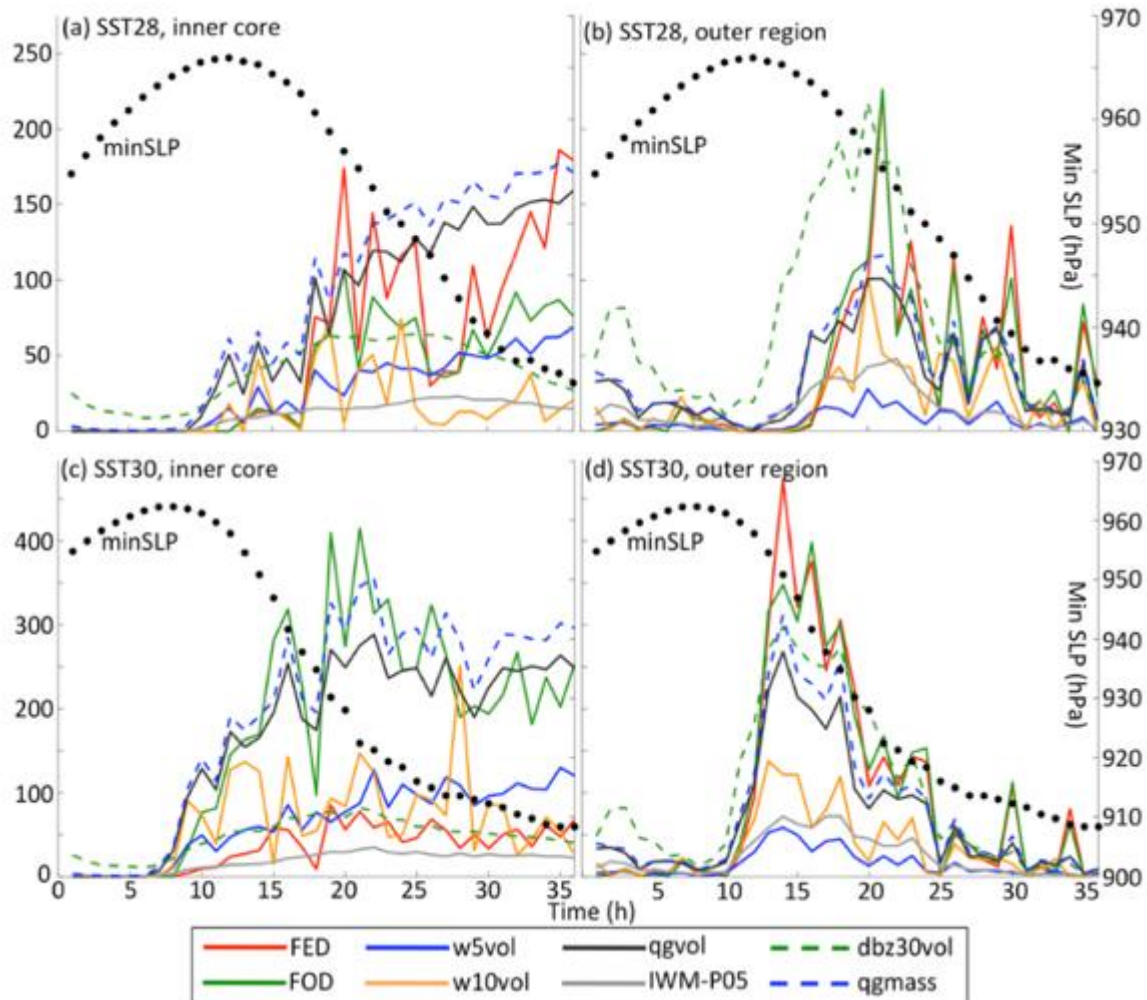
Continued to oversee (including troubleshooting and helping students) the archival, processing and transfer of the real time OKLMA data onto NSSL's local machines. Also handle and prepare data requests from collaborators.

Collaborated with lightning research group in Greece to explicitly forecast lightning over the Mediterranean using the official release of the lightning forecast model implemented into WRF in 2013 (E-WRF, Fierro et al. 2013). Published a manuscript in JGR summarizing these results.

Updated and maintained E-WRF and provide support to interested research groups/teams). Collaborated with other institutions wishing to use E-WRF for research or real time lightning forecasting.



Horizontal cross sections of radar reflectivity fields at 1 km MSL overlaid with the hourly lightning initiation locations (black cross) for (b)-(d) SST30 and (e)-(g) SST28 during intensification at 10, 15, and 20h, respectively. (a) The initial conditions, which are identical for both simulations, shown for reference.



Time series of hourly minSLP (hPa, right y-axes, black dots) overlaid with times series (left y-axes) of the following scaled quantities: FED (red), FOD (green), w5vol (blue), w10vol (orange), qgvol (black), IWM-P05 (dark gray), dbz30vol (dashed green) and qgmass (dashed blue) from both SST28 and SST30 inner cores and outer regions.

5. Geostationary Lightning Mapper Observations within Tropical Cyclones

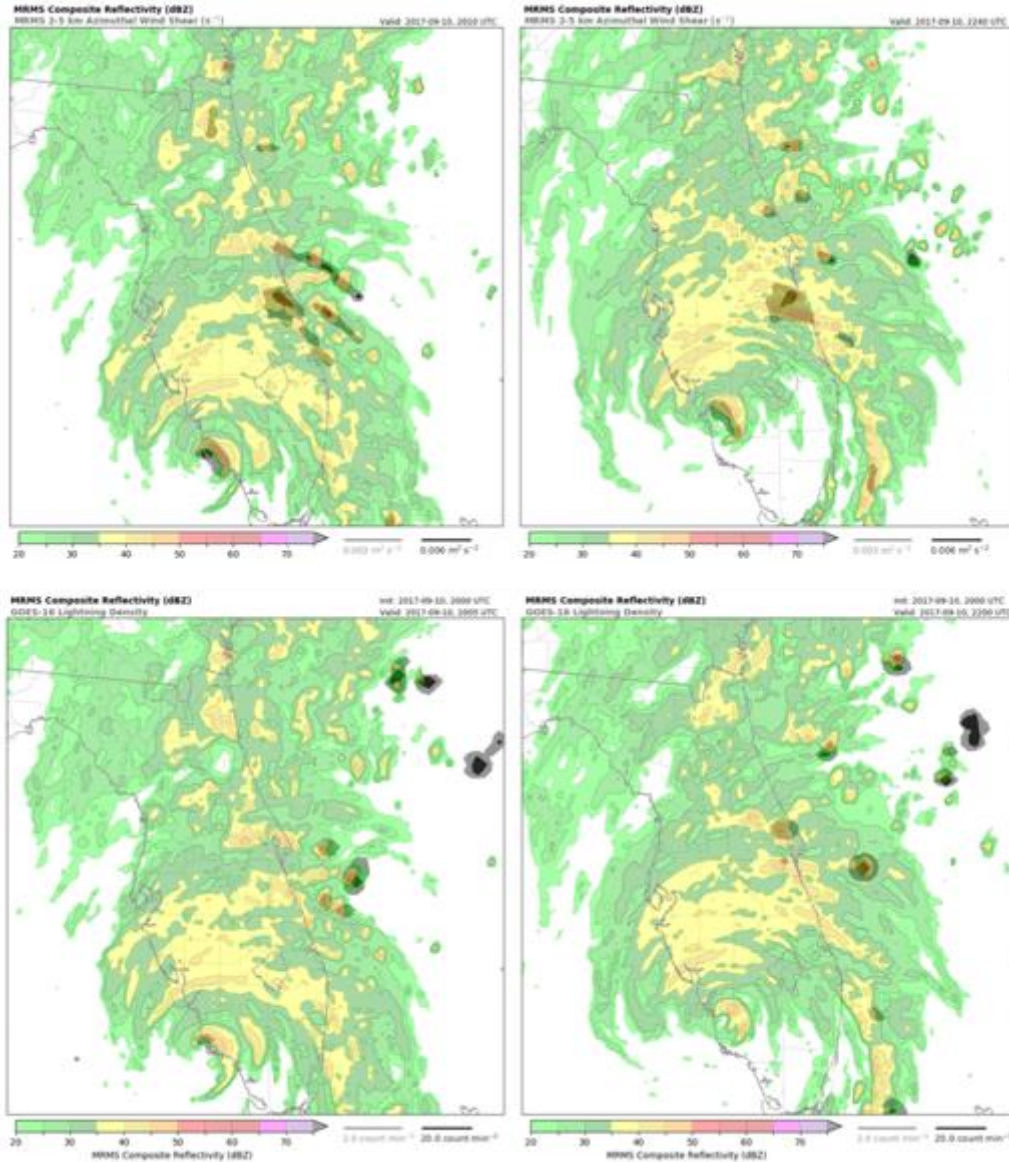
Kristin Calhoun, Alex Fierro, Darrel Kingfield, Anthony Reinhart, and Matthew Mahalik (CIMMS at NSSL), and Bob Rabin (NSSL)

The launch of the Geostationary Operational Environmental Satellite-16 (GOES-16) satellite provides a new opportunity to investigate and better understand lightning trends of Atlantic Hurricanes during development, intensification, and landfall. The Geostationary Lightning Mapper (GLM) and the Advanced Baseline Imager (ABI) from GOES-16 provides coverage of tropical cyclones both spatially and temporally that has not been previously available for study. Additionally, the 2017 Atlantic Hurricane season provided a wide variety of tropical cyclone intensity and coverage for this comparison.

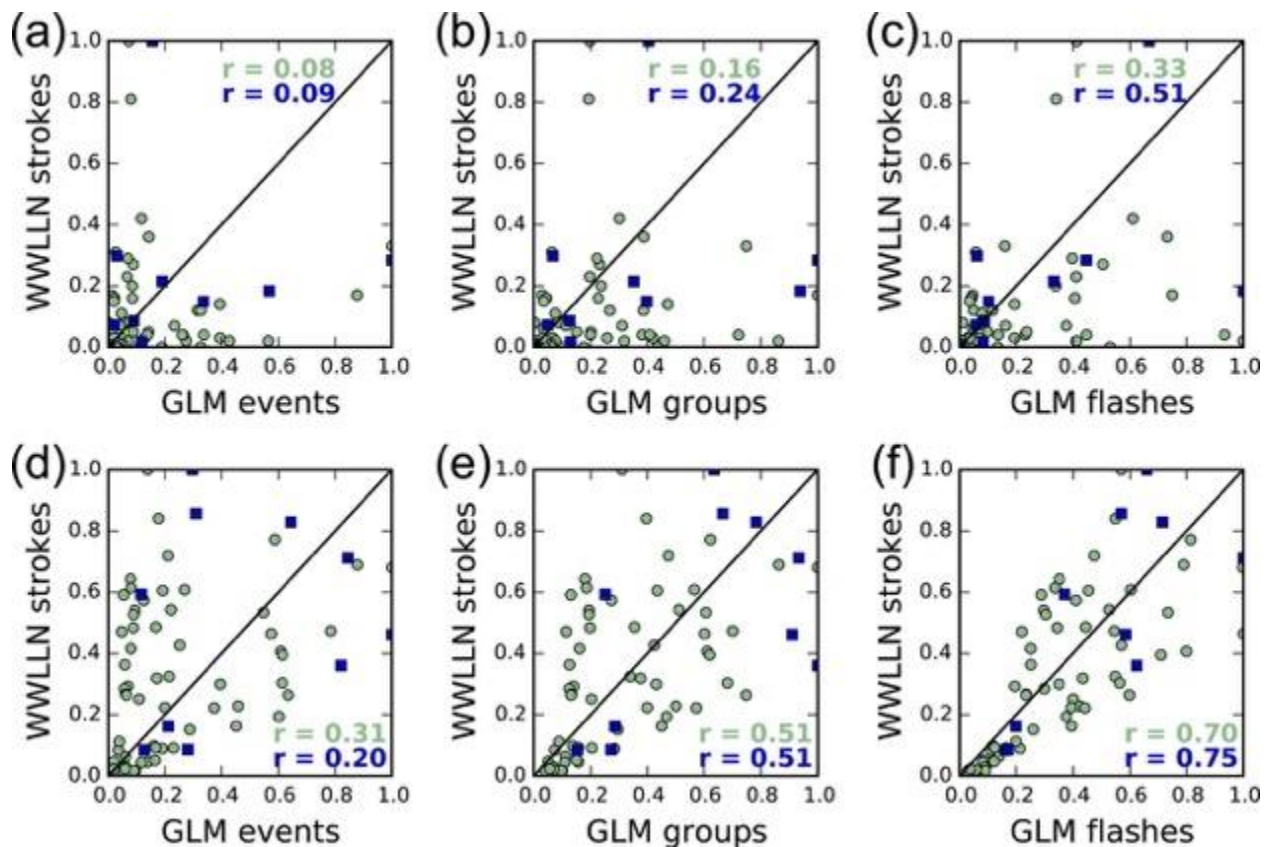
Lightning data from GLM was compared with the blended Multi-Radar Multi-Sensor (MRMS) quantifications of reflectivity and azimuthal shear for individual storm cells at the time of landfall of hurricanes Harvey and Irma on the southeast coast of the United States. This combination of lightning data throughout the tropical cyclone lifetime, including landfall when available, should allow for the increased use of lightning data in support of tropical cyclone forecasting and within local severe and hazardous warnings in the future. Regardless of whether this study demonstrates a clear-cut concept of operational utility, we articulate a plausible path forward of the GOES-16 data based on the results of this study of the initial data.

There are many challenges in using operational severe weather algorithms to detect Tropical Cyclone (TC) rotation due to the quite subtle rotational signatures within these relatively shallow storms. Though we have seen advancements in recent years in terms of scanning strategies and radar upgrades, many of these challenges are still applicable. Fundamentally, there are systematic differences in the degree of shear, lift, and instability needed for the production of TC tornadoes compared with the conceptual model of tornado production in the central plains. Supercellular TC tornadoes in the outer rainbands are accompanied by somewhat greater vertical shear than those occurring from other modes elsewhere in tropical cyclones, yet still minimal compared to tornadic supercells of the central plains of the United States. Tornadoes in TCs accompanying non-supercellular radar echoes tend to occur closer to the TC center, where CAPE and shear tend to weaken relative to the outer TC envelope, though there is considerable overlap of their respective radial distributions and environmental parameter spaces. In Harvey and Irma, there was evidence of both supercellular and non-supercellular tornadoes at and following the time of landfall. We see clear evidence both the small scale and larger scale relationships noted above in both Irma and Harvey at the time of landfall. MRMS diagnosis of azimuthal shear in both Harvey and Irma also depict variable track lengths and enhancements in vorticity in both the inner core and eyewall region at the time of landfall. For example, during Hurricane Irma (first figure, top), the MRMS rotation tracks product depicts this enhanced likelihood along the east coast of Florida in the right front quadrant of the storm throughout landfall as the storm eye moved northward along the west coast. Simultaneously, this was also the region that had enhanced levels of lightning activity as detected by the GLM (first figure, bottom).

Prior to rapidly intensifying from a category 1 to 5 storm, Maria produced few inner-core flashes. Increases in total lightning in the inner core ($r \leq 100$ km) occurred during both the beginning and end of an intensification cycle, while lightning increases in the outer region ($100 < r \leq 500$ km) occurred earlier in the intensification cycle and during weakening. Throughout the analysis period, the largest lightning rates in the outer region were consistently located in the southeastern quadrant, a pattern consistent with modeling studies of electrification within hurricanes. A brief comparison between flash rates from GLM and a very low-frequency ground-based network for Hurricane Maria revealed that not all lightning peaks are seen equally, with hourly flash-rate ratios between both systems sometimes exceeding two orders of magnitude (second figure).



Top panels: MRMS Composite Reflectivity (dBZ) and mid-level (2-5 km) Azimuthal Shear (overlaid at 0.003, light gray and 0.006 m² s⁻², dark gray) for Hurricane Irma at 2010 and 2240 UTC. 30 min accumulation of azimuthal shear provides guidance for embedded storm cells and locations with higher potential for tornadoes. Bottom panels: MRMS Composite Reflectivity (dBZ) and 5-min GLM lightning event density (overlaid at 2 counts, light gray and 20 counts, dark gray per 5 min) for Hurricane Irma at 2005 and 2200 UTC. GLM event density highlights stronger updrafts with potentially a higher likelihood for tornadoes in the northeast quadrant of the storm.



Normalized scatterplots of the (top) inner core and (bottom) outer region hourly (green) and 6-hourly (blue) lightning rates recorded by GLM (xaxis) and WWLLN (y axis) during the 60-h period of interest beginning at 1200 UTC 18 Sep. WWLLN comparisons were made with GLM (a),(d) events, (b),(e) groups, and (c),(f) flashes. The black line shows a 1:1 relationship (i.e., exactly similar), and the respective Pearson correlation coefficients are displayed for both the hourly and 6-hourly data.

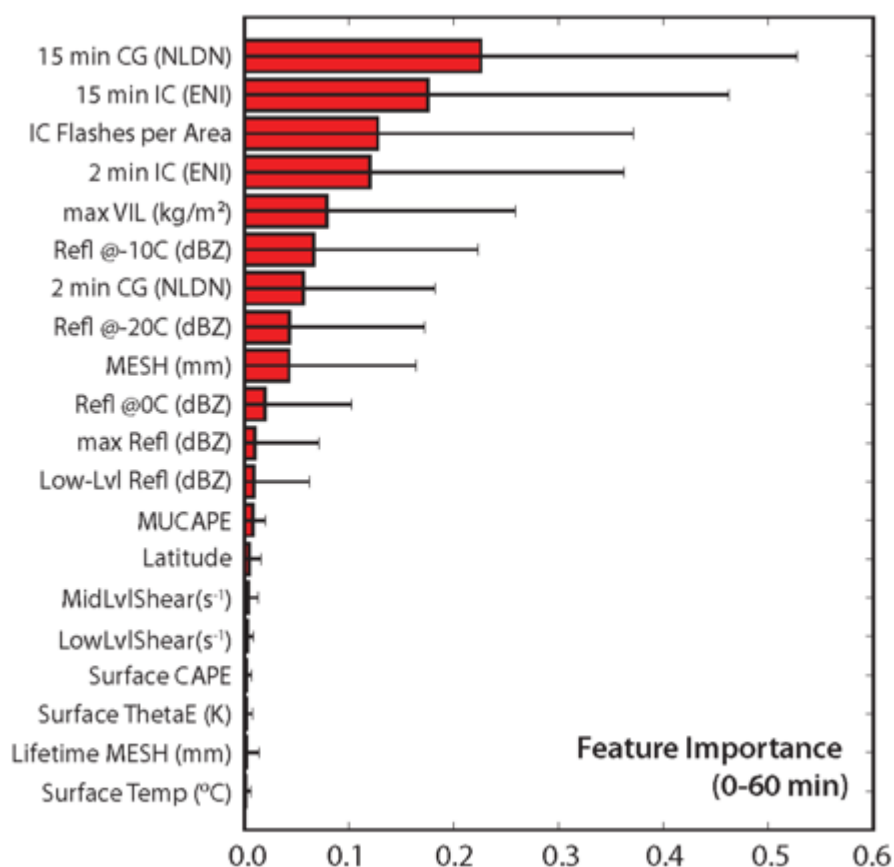
6. Development of Cloud-to-Ground Lightning Probabilistic Guidance

Kristin Calhoun and Tiffany Meyer (CIMMS at NSSL)

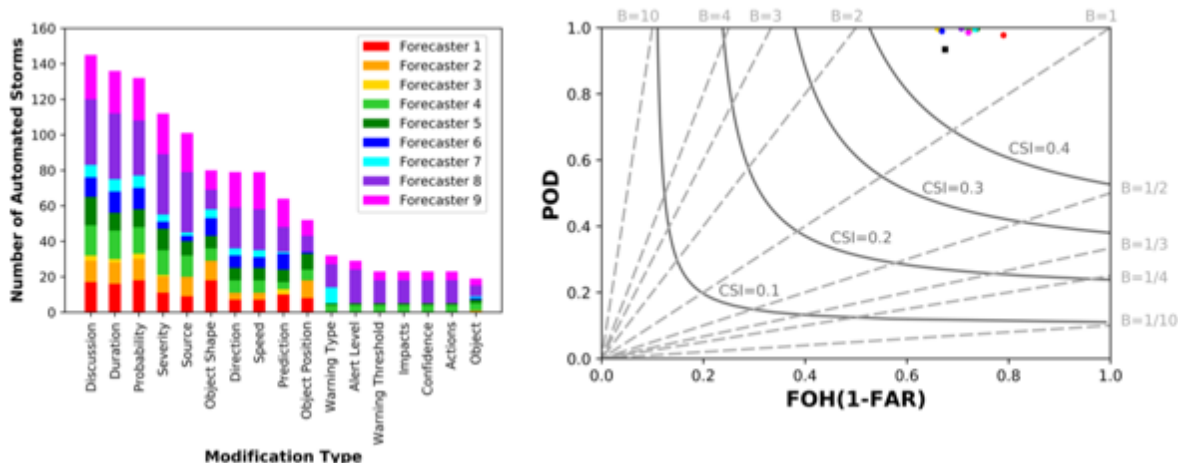
A new cloud-to-ground (CG) lightning probability algorithm has been developed using machine-learning methods. With storm-based inputs of Earth Networks' in-cloud lightning, Vaisala's CG lightning, multi-radar/multi-sensor (MRMS) radar derived products including the Maximum Expected Size of Hail (MESH) and Vertically Integrated Liquid (VIL), and near storm environmental data including lapse rate and CAPE, a random forest algorithm was trained to produce probabilities of CG lightning up to one-hour in advance. The random forest methodology provides details on feature importance through a combination of tree rankings (how high the decision point is using that feature) and inter-tree variability (how often that included and at what decision point on the tree). For the CG lightning algorithm, knowledge if a storm is or has recently produced lightning had the greatest importance (National Lightning Detection Network – NLDN and Earth Networks (ENI) 15 min lightning ranked the highest, first figure below).

However, the system was found to be nearly as reliable with slightly decreased Briar Skill Scores even when lightning data was not available.

As part of the Prototype Probabilistic Hazard Information experiment, National Weather Service forecasters were asked to use this CG lightning probability guidance to create rapidly updating probability grids and warnings for the threat of CG lightning for 0-60 minutes. The output from forecasters was shared with end-users, including emergency managers and broadcast meteorologists, as part of an integrated warning team. These forecaster and automated objects were verified and aspects of their performance, such as the probability of detection, were compared to see if the forecasters added value to the automated system. Forecasters added value to the system by adding discussion to the objects and through modifying the size, severity, duration, and probability of the lightning storms (second figure below). However, forecasters found the task particularly tedious to complete. The areas where the forecasters are adding the most value could be used to improve the automated system's performance at predicting CG lightning, further reducing forecaster workload.



Feature importance from random forest-based algorithm of the one hour storm-based prediction of cloud-to-ground lightning. Red bars provide the overall feature importance and the black line the inter-tree variability.



Left: Types and frequency of modifications to automated objects by NWS forecasters for the probability of CG lightning. Forecasters most commonly modified the automation by adding discussion, changing the duration (decreasing), and modifying the probabilities. Right: Reliability diagram of automation (black square) and forecasters (colored circles, same as left plot) for the 1 Sept 2016 event over the Melbourne, FL forecast area. Forecasters were able to improve the probability of detection and reduce the false alarm rate over the algorithm alone.

7. Rivers of Vorticity in Supercells (RiVorS) Basic Research

Erik Rasmussen (CIMMS at NSSL)

Most high-resolution simulations of supercell thunderstorms show the existence of a kinematic feature in the left-flank that is usually called a "vorticity river" or a "streamwise vorticity current" (SVC). It is thought that this feature is an important source of rotation to the low-level updraft and perhaps required for tornado formation. The objective of this research, led by Dr. Erik Rasmussen, is to assess the existence and character of the SVC in all available observational data sets, and begin to understand its dynamics, association with tornadoes, and association with the supercell environment. This multi-scale multi-tool analysis is aimed at improving tornado warning reliability and lead time based on modeled and analyzed near-storm environments.

A Hollings Scholar student recipient, Shawn Murdzek, assembled ~20 useful data sets, containing mobile mesonet data and close-range radar data, from past observing campaigns from VORTEX94-95 through the Rivers of Vorticity in Supercells (RiVorS) campaign of 2017. Mr. Murdzek will be working with Erik Rasmussen to analyze these data sets with the goal of 1-2 formal publications in early 2019. The focus is on 1) identifying wind shifts from mobile mesonet data in the supercell left flank that may be associated with SVCs; 2) identifying associated close-range radar features; 3) identifying spatial patterns and contrasts in surface parcel potential buoyancy and inhibition from mobile mesonet data.

Dr. Rasmussen has commenced a study of five close-range (< 20 km) mobile Doppler data sets to identify patterns in the vertical shear of Doppler velocity that would be

associated with SVCs, if they exist. Close-range data is required because two sweeps of data are needed within ~300 m of the ground, which is the approximate location of the SVC in numerical simulations. The results will be reported in a formal publication in early 2019. Once this preliminary work is done, related analyses will be conducted to determine if there are signatures of the SVC in conventional WSR-88D observations.

Publications

- Dafis S., A. O. Fierro, T. M. Giannaros, V. Kotroni, K. Lagouvardos and E. Mansell, 2018: Performance evaluation of an explicit lightning forecast system. *Journal of Geophysical Research, Atmospheres*, **123**, 5130–5148.
- Fierro, A. O., and E. R. Mansell, 2017: Electrification and lightning in idealized simulations of a hurricane-like vortex subject to wind shear and sea surface temperature cooling. *Journal of the Atmospheric Sciences*, **74**, 2023–2041.
- Fierro, A. O., and E. R. Mansell, 2018: Relationships between electrification and storm-scale properties based on idealized simulations of an intensifying hurricane-like vortex. *Journal of the Atmospheric Sciences*, **75**, 657-574.
- Fierro, A. O., S. Stevenson, and R. Rabin, 2018: Evolution of GLM-observed total lightning in Hurricane Maria (2017) during the period of maximum intensity. *Monthly Weather Review*. **146**, 1641–1666.
- Fierro, A. O., G. Zhao, S. Liu, Y. Wang, J. Gao, K. Calhoun, C. L. Ziegler, E. R. Mansell and D. R. MacGorman, 2018: Assimilation of total lightning with GSI and NEWS3DVAR to improve short-term forecasts of high impact weather events at cloud resolving scales. *JCSDA Quarterly Newsletter*, No. 58, Winter 2018, 5 -12.
- Wang, H., Y. Liu, W. Y. Y. Cheng, T. Zhao, M. Xu, S. Shen, K. M. Calhoun, and A. O. Fierro, 2017: Improving lightning and precipitation prediction of severe convection using lightning data assimilation with NCAR WRF-RTFDDA. *Journal of Geophysical Research: Atmospheres*, **122**, 12296–12136.
- Wang, H., Y. Liu, T. Zhao, M., Xu, F. Guo, S. Shen. W. Y. Y. Cheng, E. R. Mansell, and A. O. Fierro, 2018: Incorporating geostationary lightning data into a radar reflectivity based hydrometeor retrieval method: An Observing System Simulation Experiment. *Atmospheric Research*, **209**, 1-13.

CIMMS Task III Project – Probabilistic Precipitation Rate Estimates from GOES-R for Hydrologic Applications

Pierre Kirstetter (ARRC), Jonathan Gourley (NSSL), Robert Kuligowski (NESDIS STAR), and Jian Zhang (NSSL)

NOAA Technical Leads: Dan Lindsey and Andy Heidinger (NESDIS)

NOAA Strategic Goal 2 – Weather Ready Nation: Society is Prepared for and Responds to Weather-Related Events

Funding Type: CIMMS Task III

Objectives

The high-resolution and low-latency of GOES-R observations is essential for the monitoring and prediction of floods and flash floods, specifically in the Western United States where the vantage point of space can complement the degraded weather radar coverage of the NEXRAD network. The GOES-R rainfall rate algorithm will yield deterministic quantitative precipitation estimates (QPE). Accounting for inherent

uncertainties will further advance the GOES-R QPEs that will be improved through the new bands, higher resolution, and basic algorithmic improvements. With quantifiable error bars, the rainfall estimates can be more readily fused with ground radar products and incorporated into ensemble hydrologic forecast applications. On the ground, the high-resolution NEXRAD-based precipitation products from the Multi-Radar/Multi-Sensor (MRMS) system, which is now operational in the National Weather Service (NWS), provides QPEs suited for flash flood monitoring and forecasting. However, NWS operations are challenged across the intermountain West due to a lack of suitable coverage of operational weather radars over complex terrain. An opportunity exists to combine the observations from GOES-R and MRMS to provide seamless, high-resolution and low-latency precipitation estimates across the CONUS. The goal of this research project is to derive consistent, accurate and fine-resolution precipitation rates with uncertainties over the CONUS. An already created MRMS-based precipitation database will provide an independent and consistent reference to document, analyze and design GOES-R QPE over a broad sample of precipitation situations. GOES-R precipitation estimates will be matched to the MRMS-based rainfall database in order to derive and analyze distributions of QPE uncertainties associated with the GOES-R deterministic retrievals. The probabilistic model mitigates biases compared to the deterministic GOES-R QPE and quantifies the associated uncertainty. It provides the basis for the generation of GOES-R precipitation ensembles suitable to 1) merge with MRMS-based probabilistic QPEs from ground radar-based algorithms already developed to advance multisensor QPE integration (Kirstetter et al. 2015a) and 2) serve as input to a framework being developed in an already funded project for probabilistic flash flood prediction across the U.S. (Gourley et al., 2013, 2016). The product will be further tested in an operational environment in order to improve its use for weather and water forecasting.

Accomplishments

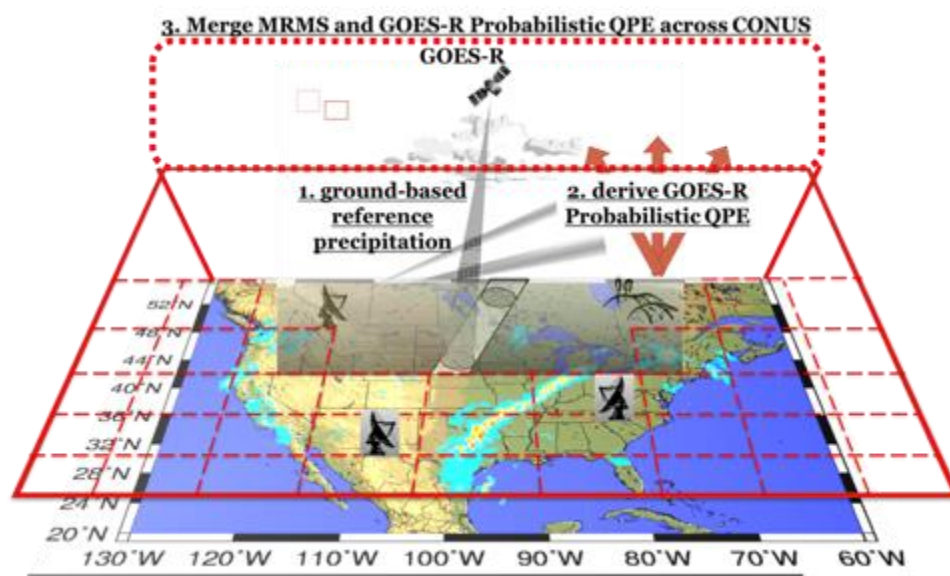
The first year of the project has been devoted to developing a database of matched GOES-16 and MRMS data in preparation of the GOES-16 probabilistic precipitation estimates. The completed milestones are on-track with the project schedule.

Ground-based MRMS products to match with GOES-16 have been identified: instantaneous rain rate, radar quality index, surface precipitation type. These products are stored in real-time and processed to derive a ground reference at the retrieval scale of GOES-16 precipitation. Over areas with good radar coverage identified through a radar quality index, precipitation qualitative (e.g. typology) and quantitative (e.g. rate) products are post-processed using correction/filtering procedures relevant for space-borne sensors precipitation retrievals (<http://wallops-prf.gsfc.nasa.gov/NMQ/Docs/DailyProducts.pdf>). It provides an independent and consistent ground-based reference matching the retrieval scale of GOES-16 precipitation estimates.

Interactions with the MRMS team and collaborator R. Kuligowski enabled to optimize the GOES-16 and MRMS data flows. Since February 2, 2018 precipitation estimates output from the SCaMPR science code have been transferred and stored to populate

the archive, in anticipation of the second year of the project. Data have been collected through Spring 2018. The matching procedure between MRMS and GOES-16 precipitation estimates is currently being refined.

The project has been advertised in telecons with the Hydrology Initiative working group lead by R. Ferraro (NOAA/NESDIS), at conferences (AMS 2018 annual meeting, EGU2018, ERAD2018) and seminars (National Weather Center, University of Oklahoma, Norman, OK, US; Laboratoire de Meteorologie Physique, Clermont-Ferrand, France; Laboratoire Atmospheres, Milieux, Observations Spatiales, Paris, France; Laboratoire des Sciences du Climat et de l'Environnement, Paris, France). The PI has been invited to NCAR to discuss the broader perspectives of the project with Andrew Newman's group (NCAR/RAL/HAP).



Research framework and overview flowchart of the project.

Publications

Kirstetter, P.E., N. Karbalaee, K. Hsu, and Y. Hong, 2018: Probabilistic precipitation rate estimates with space-based infrared sensors. *Quarterly Journal of the Royal Meteorological Society*, **144**, 1–15.

CIMMS Task III Project – Post-Processing of Solid-State Polarimetric Weather Radar Data for Hydrology

Pierre Kirstetter (ARRC), and Boon-Leng Cheong and Tian-You Yu (ARRC)

NOAA Technical Lead: Kenneth Howard (NSSL)

NOAA Strategic Goal 2 – Weather Ready Nation: Society is Prepared for and Responds to Weather-Related Events

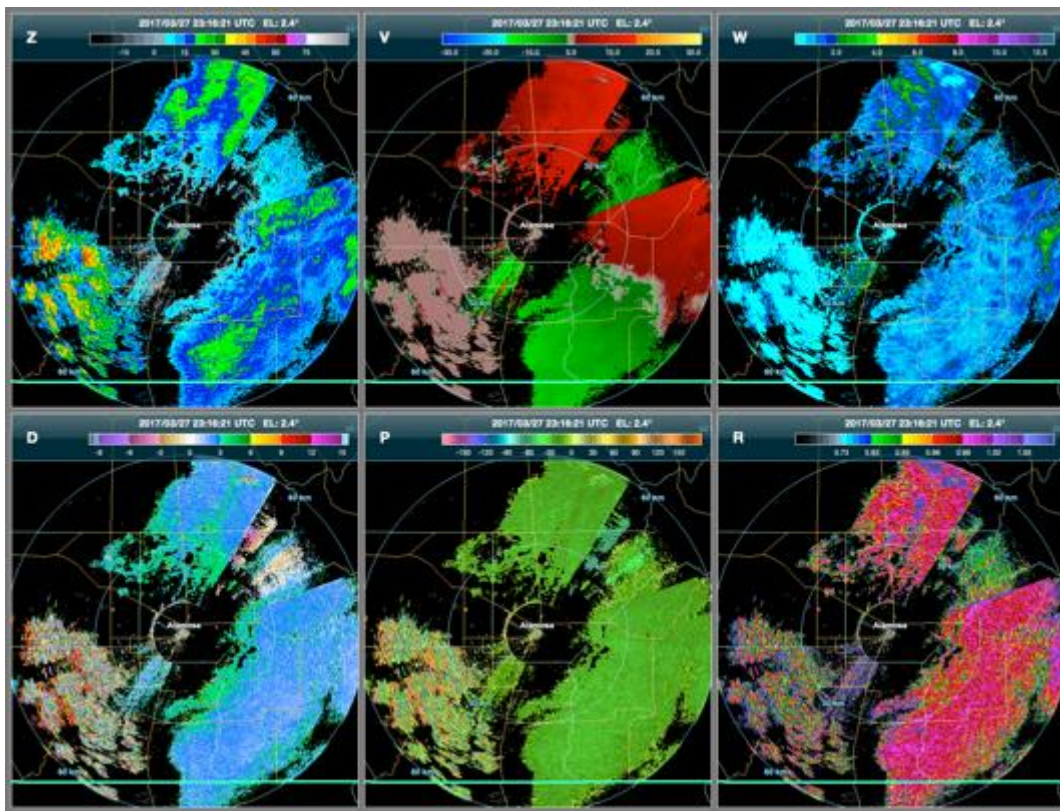
Funding Type: CIMMS Task III

Objectives

The PX-1000 radar was operated to monitor winter storms in Colorado during the Winter 2016-2017. It will be post-calibrated to interpret the observations gathered during the field campaign. The expected outcome of this proposal is to generate datasets for studies of snowflakes scattering properties, identification of the melting level and quantitative precipitation estimation.

Accomplishments

The PX-1000 radar was post-calibrated and the data post-processed to interpret the observations gathered during the field campaign. Data archives were generated.



PX-1000 radar moments observed on 27 March 2017 in Alamosa, CO.

CIMMS Task III Project – Using Total Lightning Data from GLM/GOES-R to Improve Real-Time Tropical Cyclone Genesis and Intensity Forecasts

Alexandre Fierro (CIMMS at NSSL), Ted Mansell, Conrad Ziegler, Don MacGorman, and Bob Rabin (NSSL), Mark DeMaria (NOAA NCEP NHC), Andrea Schumacher and Renate Brummer (CIRA-Colorado State University), and Stephanie Stevenson (CSU and NOAA NCEP NHC)

NOAA Technical Lead: Dan Lindsey (NESDIS) and Mark DeMaria (NCEP NHC)

NOAA Strategic Goal 2 – *Weather Ready Nation: Society is Prepared for and Responds to Weather-Related Events*

Funding Type: CIMMS Task III

Objectives

Conduct and subsequently utilize the output from cloud scale (250-m – 2-km) numerical simulations of the small-scale electrification processes within tropical cyclones (TCs) to augment our understanding on these processes and, ultimately, derive functional relationships between various lightning metrics and the microphysics/kinematics of TCs. Whenever possible, these relationships will be verified against (and complemented with) observations to ultimately develop total lightning predictors that could be used to assimilate total lightning observations directly into NHC's statistical prediction model (SHIPS). Total lightning is emphasized because it is much better correlated to convective strength than cloud-to-ground lightning is. Lightning information is particularly critical in regions where radar data are scarce, such as over oceans where all TCs develop and eventually intensify. When available, the simulations should be complemented with preliminary GLM observations within TCs.

Accomplishments

The PI's visits to collaborators at CIRA and NHC and subsequent meeting of the PIs during the AMS Tropical/Hurricane meeting in April 2016 lead to the elaboration of a work plan for the remainder of the funding period. Namely, the results obtained in Fierro et al. (2015) during Year 1 needed be complemented with at least one TC lightning study in the idealized framework to help generalize/improve the functional relationships obtained in that study. With the help of the main developer of the NSSL fractal-like, stochastic 3D cloud electrification model (COMMAS) (Mansell), an idealized hurricane initialization/model based on Alex Fierro PhD work (Fierro et al. 2007) was successfully incorporated into this model over the course of Winter 2015. Over Spring 2016, several initial test simulations of idealized electrified TCs (on JET HPC resources) were conducted. The results motivated the inclusion of new physics along with improved vortex initializations [based on WRF-ARW]. Wind shear, relative humidity and sea surface temperature were varied using a base state substitution technique, which also was included into COMMAS (Mansell). With these model enhancements, realistic TC lightning behaviour and morphologies were obtained. The PI completed a manuscript draft during the course of Summer 2016 summarizing the results of three main simulations: Control (steady state major TC), a shear increase case and an SST cooling run. This study was accepted to JAS this Spring (Fierro and Mansell, 2017a). During the course of Spring 2017 a new, companion JAS manuscript (Fierro and Mansell, 2017b) was elaborated in which additional simulations/experiments focusing on intensifying TCs were analysed. As indicated in the conclusions of Fierro and Mansell (2017a), the focus on intensifying TCs was a logical follow-on because the three cases analysed in Fierro and Mansell (2017a) either were steady state or weakening TCs. This new study provides statistical analyses (correlations, linear regression, etc.) between different lightning metrics (flash extent density, flash origin density and source density) and various bulk microphysical and dynamic quantities within two key regions of the TC;

namely the inner core and the rainband. Such analyses are of particular interest to NHC in the context of their statistical model called SHIPS (via the “RII” index). Results for the inner core are consistent with recent observational studies. Outer band convection, on the other hand, revealed being a far more difficult problem to tackle owing to its dependence on mesoscale/synoptic inhomogeneities that cannot be represented in idealized simulations or because of physics relevant to TC dynamics that are not included in COMMAS [such as PBL schemes, full radiation schemes, coupled ocean model]. Some preliminary tests were conducted with WRF-ARW [which features all of the above] but appeared to reveal similar biases [i.e., weaker-than-observed rainband convection]. Interestingly, no studies have addressed even partially this obvious bias because TC intensification is chiefly tied to inner core dynamics. In the light of this, it is very likely that ongoing work on this topic will continue beyond the funding period of this grant.

We organized a conference call with NHC in spring 2017 to synthesize the above results and, concomitantly, to discuss potential future collaboration on the subject. Emphasis was especially directed onto potential collaboration with NHC/CIRA regarding to the analysis of GLM/GEOS-R total lightning data within observed TCs – which shall begin once the GLM instrument is fully calibrated and these data become available. In subsequent months, a detailed study documenting - for the first time - the evolution of GLM-observed total lightning within a major hurricane was published in an influential AMS journal. This work was conducted in collaboration with NHC in which WWLLN stroke data were evaluated against the GLM. This is particularly relevant to NHC as WWLLN data have been used for more than a decade by forecasters (e.g., within SHIPS at NHC) and researchers alike for monitoring the evolution of deep moist convection within these systems far at sea, out of reach from ground-based systems.

Publications

- Dafis S., A. O. Fierro, T. M. Giannaros, V. Kotroni, K. Lagouvardos, and E. R. Mansell, 2018: Evaluation of an explicit lightning forecast system. *Journal of Geophysical Research*, **123**, 5130–5148.
- Fierro, A. O. and E. R. Mansell, 2018: Relationships between electrification and storm-scale properties based on idealized simulations of an intensifying hurricane-like vortex. *Journal of the Atmospheric Sciences*, **75**, 657-674.
- Fierro, A. O., S. Stevenson, and R. Rabin, 2018: Evolution of GLM-observed total lightning in Hurricane Maria (2017) during the period of maximum intensity. *Monthly Weather Review*, **146**, 1641–1666.
- Fierro, A. O., and E. R. Mansell, 2017: Electrification and lightning in idealized simulations of a hurricane-like vortex subject to wind shear and sea surface temperature cooling. *Journal of the Atmospheric Sciences*, **74**, 2023-2041.
- Wang, H., Y. Liu, T. Zhao, M. Xu, F. Guo, S. Shen, W. Y. Y. Cheng, E. R. Mansell, and A. O. Fierro, 2018: Incorporating geostationary lightning data into a radar reflectivity based hydrometeor retrieval method: An observing system simulation experiment. *Atmospheric Research*, **209**, 1-13.
- Wang, H., Y. Liu, W. Y. Y. Cheng, T. Zhao, M. Xu, S. Shen, K. M. Calhoun, and A. O. Fierro, 2017: Improving lightning and precipitation prediction of severe convection using lightning data assimilation with NCAR WRF-RTFDDA. *Journal of Geophysical Research: Atmospheres*, **122**, 12296–12136.

CIMMS Task III Project – Lightning Mapper Array Operation in Oklahoma and South Texas to Aid Verification and Application Research for the GOES-R and GOES-S GLMs

Alexandre Fierro (CIMMS at NSSL); Don MacGorman (NSSL), Crystal Nassir and Justin Kleiber (CIMMS Undergraduate Research Assistants), Doug Kennedy (NSSL), and Dennis Nealson (CIMMS at NSSL)

NOAA Technical Lead: Steve Goodman (NESDIS)

NOAA Strategic Goal 2 – *Weather Ready Nation: Society is Prepared for and Responds to Weather-Related Events*

Funding Type: CIMMS Task III

Objectives

The primary objective of this grant is to maintain and operate the Oklahoma Lightning Mapping Array (OKLMA), which provides data for continuing basic storm research, for testing possible applications of total lightning mapping data in National Weather Service operations, and for providing ground truth data to validate performance of the new Geosynchronous Lightning Mapper (GLM) on GOES-16 and GOES-17. This grant also included a subcontract to Texas A&M University to operate the Houston area Lightning Mapping Array (HLMA) for the same purposes.

Accomplishments

OKLMA data sets collected during the GOES-16 Geostationary Lightning Mapper (GLM) field campaign in spring 2017 were uploaded to the campaign's website in Huntsville, AL later in 2017. Data continue to be collected this fiscal year and have been used for additional comparisons with the GLM on GOES-16 and more recently with the GLM on GOES-17. Furthermore, in a collaborative project New Mexico Tech brought their wide-bandwidth interferometer to central Oklahoma and operated it in conjunction with the OKLMA to provide lightning mapping with much higher time resolution and with better detection of positive leaders in lightning flashes. These data are expected to expand understanding of the lightning characteristics affecting lightning detection by the GLM. We also have been comparing OKLMA detections with GLM detections in the Hazardous Weather Testbed at the National Severe Storms Laboratory and have analyzed lightning data from both the OKLMA and GLM in storm studies, including the hurricanes that occurred during fall 2017. OKLMA data also have been provided to other scientists investigating topics of interest to the GLM program.

Of particular interest, are studies of total lightning throughout the intensification and weakening cycles of hurricanes, made possible for the first time by the GLM. Fierro et al (2018) published the first such study, an analysis of GLM data during Hurricane Maria in fall 2017. The study found increases in total lightning rates in the inner core during both the beginning and end of an intensification cycle. Lightning increases in the outer rainbands occurred earlier in the intensification cycle and as the hurricane weakened.

In a correlation analysis, the most robust and systematic relationship with storm intensity was found with inner-core lightning and maximum surface wind speed.

We have published a journal paper describing the methodology we developed in previous years of this project to construct a decade-long climatology of the total lightning detected by the OKLMA. This initially required that we determine how to correct the lightning detections for the rapid decrease with range in the fraction of flashes detected. We tried two techniques: (1) determining the weakest signals from lightning detected reliably at the farthest range of our analysis and then using that as a threshold to eliminate weaker signals from the detections at all ranges; (2) evaluating whether the range effect could be obviated by using flash detections, instead of using every detected signal. Our conclusion was that using flashes eliminated the range dependence as well as the thresholding of signals did, because the signals radiated by a flash have a range of amplitudes and typically included enough signals with stronger amplitudes to be detected by the OKLMA. Because we were computing flashes for some aspects of our climatology, we decided simply to use flashes for all aspects of our climatology to avoid range effects. Now that we have completed the paper detailing our evaluation of the two techniques for correcting range effects, we will prepare a paper describing the climatology derived from the OKLMA.

A draft of another paper based on OKLMA data is expected to be submitted to a journal this fall, this one documenting the kinematic and microphysical processes leading to the formation of secondary thunderstorms within the anvil of a supercell. This research has been presented to the Annual Fall Meeting of the American Geophysical Union and to the annual meeting of the American Meteorological Society. OKLMA data also were the subject of papers at the International Conference on Atmospheric Electricity in Osaka, Japan, in June 2018.

In addition to these efforts using OKLMA data, we also began using GLM data in data assimilation experiments using 3DVAR and ensemble techniques developed previously using OKLMA data and total lightning data from the ENTLN network. Simulation forecasts have been run successfully using historical GLM data, and we began assimilating real-time GLM data for a few select test cases this year. Thus far, forecast results compare favorably with results from assimilating WSR-88D radar data.

The subcontract to this grant for Texas A&M to operate the Houston area Lightning Mapping Array (HLMA) provided data this past year to GOES-16 GLM verification efforts at the University of Alabama at Huntsville and elsewhere. The data collected by the network this year are also being provided for GOES-17 GLM verification efforts. HLMA data were the subject of two papers presented by Dr. Logan and his Texas A&M students at the AMS Annual Meeting in January 2018. Of particular interest were the data collected during the sustained heavy rainfall and flooding in the Houston area from Hurricane Harvey in fall 2017. They found a strong relationship between WSR-88D radar reflectivity and lightning rates from the HLMA, especially during episodes of deep convection in the hurricane.

Publications

- Fierro, A. O., G. Zhao, S. Liu, Y. Wang, J. Gao, K. M. Calhoun, C. L. Ziegler, E. R. Mansell, D. R. MacGorman, 2018: Assimilation of total lightning into GSI and NEWS3DVAR to improve short-term forecasts of high impact weather events at cloud resolving scales. *JCSDA Quarterly Newsletter*, Winter 2018, 5-12.
- Fierro, A. O., 2018: Evolution of GLM-observed total lightning in Hurricane Maria (2017) during the period of maximum intensity. *Monthly Weather Review*, **146**, 1641-1666.
- Weiss, S. A., D. R. MacGorman, and E. C. Bruning, 2018: Comparison of two methods for correcting for bias in detection efficiency with range of the Oklahoma Lightning Mapping Array. *Journal of Atmospheric and Oceanic Technology*, **123**, 1273-1282.

CIMMS Task III Project – Ensemble Kalman Filter and Hybrid Data Assimilation for Convective-Scale “Warn-on Forecast”

Xuguang Wang and Yongming Wang (OU School of Meteorology)

NOAA Technical Lead: Pamela Heinselman (NSSL)

NOAA Strategic Goal 2 – Weather Ready Nation: *Society is Prepared for and Responds to Weather-Related Events*

Funding Type: CIMMS Task III

Objectives

Given the size of tornado-like vortex (TLV) is usually less than 1 km, its explicit forecast needs a sub-kilometer resolution. Most previous studies simulate TLV starting from the interpolated initial conditions (ICs) at a coarser resolution rather than a firsthand sub-kilometer ICs. In the last report period, we found significant differences between two ICs and between their subsequent TLV predictions. The 8 May 2003 Oklahoma City tornadic supercell storm is used. Stronger cold pool, more intense kinetic fields with finer scale features, and large hydrometeors distributing in higher levels are found in the firsthand ICs than downscaled ICs. Simulated TLV starting from the firsthand sub-kilometer ICs matches better with the observed tornado damage track in both timing of TLV's phase transitions and longevity. In this report, detailed diagnostics are conducted to understand 1) the causes of these differences between the two ICs during the DA period and 2) the impacts of each category of differences on the subsequent TLV predictions.

Accomplishments

1. Introduction

The ability to accurately predict a tornado's evolution can conduce to social timely response well ahead of its occurrence and allow to deeply understand related dynamics and thermodynamics governing its evolution. Recently, accumulated studies (e.g., Dowell et al. 2004; Jung et al. 2012; Tanamachi et al. 2013; Johnson et al. 2015; Yussouf et al. 2013; Wang and Wang 2017) have employed ensemble-based data assimilation (DA) methods to initialize the parent storms that spawn tornadoes by

assimilating radar observations and conducted ensemble forecast at 1-3 km grid. These studies did not directly predict tornado itself, but a proxy forecast of tornado existence is applied by successfully predicting a tornadic storm with strong mid- and low-level rotations. However, some studies (e.g., Trapp 1999; Markowski et al. 2011; Marquis et al. 2012; Thompson et al. 2015) have documented the strength and existence of mid- and low-level mesocyclone may not agree well with tornado occurrence. In other words, the presence of mid- and low-level rotations is not reliable to indicate tornado potential. Therefore, more certainty of tornado potential can be obtained by explicitly forecasting the tornadoes or tornado-like vortices (TLV). Given most of tornado vortices has a spatial scale less than 1 km (Wurman and Kosiba 2013), a sub-kilometer resolution is essential to resolve the fine-scale properties of tornadoes or TLV.

A few studies (Mashiko et al. 2009; Schenkman et al. 2012; Xue et al. 2014; Schenkman et al. 2014; Dawson et al. 2015; Hanley et al. 2016) have attempted to predict real tornadoes or TLV with a sub-kilometer grid spacing. Despite TLV can be produced with a sub-kilometer grid resolution in these studies, they initialized a high-resolution forecast starting from the analyzed ICs at a coarser resolution, mostly greater than 1 km. Given the small size of TLV, the spatial resolution used during initialization of the parent storms may not be able to resolve the TLV. In other word, ICs downscaling from a coarser resolution may lose the finer scale characteristics associated with TLV during the DA period. In addition, a common concern existing in all above TLV predictions is whether interpolated ICs at a coarser resolution can favor to correctly predict the TLV within a finer grid.

The purpose of this study is to investigate the aforementioned issues associated with high-resolution TLV predictions initialized from a coarse grid. To accomplish this goal, both coarse and fine resolution ICs need to be directly generated from radar DA systems and a comparison between their subsequent high resolution TLV forecasts will be conducted for the 8 May 2003 Oklahoma City tornadic supercell storm. The evolution of this storm was successfully predicted by Wang and Wang (2017) using a model grid with a 2-km grid spacing. Their study proposed a new method for radar reflectivity assimilation within GSI-based EnVar system. Given the promising results on analyzing this thunderstorm achieved in Wang and Wang (2017) and other ensemble-based radar DA studies (e.g., Dowell et al. 2011; Yussouf et al. 2013; Johnson et al. 2015), we will initialize ICs at a sub-kilometer resolution using an ensemble-based DA system in the present study. However, as mentioned in Marquis et al. (2014), it is challenging for ensemble-based DA to run ensemble members at a sub-kilometer grid spacing due to the expense of computational costs, especially from an operational perspective

An effective dual-resolution (DR) approach for ensemble-based DA was applied to produce a high-resolution analysis by combining a finer resolution first-guess with a coarser resolution ensemble in several recent studies (Gao and Xue 2008; Rainwater and Hunt 2013; Schwartz et al. 2015; Schwartz 2016; Lu et al. 2017). Gao and Xue (2008) and Rainwater and Hunt (2013) employed the variations of DR ensemble Kalman Filter (EnKF) DA systems within idealized frameworks and found the DR methods can produce similar accurate analyses with significant reduced computational

costs relative to single high-resolution DA. The same merits of DR methods are also studied in DR EnVar DA systems (Schwartz et al. 2015; Schwartz 2016; Lu et al. 2017). In the present study, we extend the capability of GSI-based EnVar system to include DR method for the Advanced Research Weather Research and Forecasting Model (WRF ARW). The newly proposed radar DA method in Wang and Wang (2017) is also adopted to better utilize radar observations, especially for reflectivity. In the present study, the extended system is employed to directly produce the high-resolution ICs with first-guess and analysis control at a 500-m grid spacing ingesting a coarse ensemble at a 2-km resolution. To distinguish from DR method, coarse resolution ICs are generated from the single resolution (SR) method. The analysis using Thompson microphysics scheme (Thompson et al. 2008) produced in Wang and Wang (2017) is adopted as the coarse resolution ICs at a 2-km grid spacing and further interpolated for predicting TLV at a 500-m grid spacing to be consistent with the previous TLV prediction studies. Comparisons between the ICs of DR and SR and their subsequent TLV predictions are used to address the following questions. 1) Are there significant differences between the interpolating kilometric resolution ICs and the firsthand sub-kilometer ICs? This is correct and has been confirmed in last report period. 2) If so, how are these differences generated in the DA period and what are their impacts on TLV's predictions? We primarily focus on this question in this report.

2. Event Overview and Experiment Design

a. Overview of the 8 May 2003 Oklahoma City Tornadoic Supercell and Embedded Tornadoes

A series of studies have introduced and conducted experiments based on the 8 May 2003 Oklahoma City tornadoic thunderstorm, e.g., Romine et al. (2008), Hu and Xue (2007), Yussouf et al. (2013), Xue et al. (2014), and Wang and Wang (2017). An isolated supercell developed along a dryline located in west-central Oklahoma and is found at around 2200 UTC with a pronounced hook appendage. The supercell storm propagated east-northeastward, and began to weaken after 2300 UTC, and dissipated by 0020 UTC 9 May. According to the official National Weather Service (NWS) survey results¹, this supercell produced three tornadoes that passed through Moore, southern Oklahoma City, Midwest City, and Choctaw. The first reported tornado existed for 1-minute from 2200 to 2201 UTC with a damage path for about 0.3-km but was not available in any WSR-88D radar products (Romine et al. 2008). The segmented paths produced by the second and third tornadoes listed in the National Climate Data Center Storm Data publication (NCDC 2003, 340-342) are shown in Fig. 1. A F0 tornado persisted from 2204 to 2208 UTC in southwest of Moore tracked on the ground for about 3-km. Within same storm, another widespread F2-F4 damage tornado formed at 2210 and dissipated at 2238 UTC with a ~30-km east-northeast track path. The previous studies (Schenkman et al. 2012; Xue et al. 2014; Schenkman et al. 2014) associated with tornado predictions for this thunderstorm case focused on the third

¹ The NWS report for the 8 May 2003 Oklahoma City is summarized in <https://www.weather.gov/oun/events-20030508>

tornado only. Different from these studies, experiments in this present study will be conducted related to both the second and third tornadoes.

b. Configuration of Data Assimilation and Forecast Experiments

The numerical model and EnVar system configurations are similar to Wang and Wang (2017). Descriptions for the configurations are briefly introduced. A one-way nested domain (Fig. 2) is adopted to run all experiments in this study. The grid spacing is 2-km in the outer domain with 226×181 horizontal grid points and 500-m in the inner domain with 361×281 horizontal grid points. All grids are configured with 51 vertical levels. Version 3.6.1 of WRF-ARW is employed to produce the weather predictions. The same physics schemes are applied for two domains. Specifically, the employed model configuration includes the Thompson microphysics scheme (Thompson et al. 2008), the Mellor–Yamada–Janjić planetary boundary layer scheme (Mellor and Yamada 1982; Janjić 1990, 1994, 2002), the Noah land surface model (Chen and Dudhia 2001), and the Rapid Radiative Transfer Model for general circulation models scheme (RRTMG; Iacono et al. 2008) as the longwave and shortwave radiation scheme.

Two experiments are designed to compare the performances of ICs initialized at different resolutions (2-km vs. 500-m) on TLV predictions at a 500-m grid spacing. Two-way coupled GSI-based single resolution and dual resolution EnVar systems are respectively applied to directly produce ICs at 2-km and 500-m grid spacings by assimilating radial velocity and radar reflectivity and corresponding experiments are denominated as Exp-SCR and Exp-DR. Two systems are conducted with similar procedures except the control analysis at 500-m for Exp-DR and 2-km for Exp-SCR ingesting a 45-member ensemble at 2-km resolution. The flowchart of radar data assimilation and the subsequent forecast for two experiments is shown in Fig. 3. As Wang and Wang (2017), the radar observations are assimilated every 5-min from 2100 UTC to 2200 UTC 8 May 2003. For Exp-SCR, the 2-km control analysis from the final radar data assimilation cycle initialized at 2200 UTC is downscaled to 500-m horizontal resolution. Two 1-h high-resolution TLV deterministic forecasts are launched from the control analyses initialized at 2200 UTC at a 500-m grid spacing for Exp-SCR and Exp-DR.

Besides Exp-SCR and Exp-DR that are used to investigate the differences of two ICs and their impacts on the subsequent TLV predictions, four additional experiments are designed to understand the mechanisms for different performances produced by Exp-SCR and Exp-DR and detailed descriptions for the four experiments can be found in section 3c.

3. Results

a. Comparison of the Evolutions of Predicted Tornado-Like Vortices (TLV)

The predicted TLVs from Exp-SCR and Exp-DR have been compared in last report period. The comparison is briefly summarized here. As shown in Fig. 4, Exp-DR

produces two near surface significant vortices (vertical vorticity greater than 0.03 s^{-1})² generally following the observed tornado damage track during the 40-min forecast period, the first around 2205-2210 UTC and the second re-intensifying after 2212 UTC and persisting 2212-2232 UTC. While only one significant vortex is found from 2205-2218 UTC in Exp-SCR, in which the predicted TLVs paths almost coincide in the first 20-min forecast period and increasingly displace southeastward after 2220 UTC with the observed tracks. The comparison for 10-m wind speed suggests the similar better performance of Exp-DR than Exp-SCR in Fig. 5. These comparisons of low-level rotations and 10-m wind speeds between both experiments reveal that the predicted TLVs in Exp-DR performs better over that in Exp-SCR in the timing of the TLVs evolutions and the longevity of the significant vortices.

Diagnostics of vertical vorticity equation for near surface vertical vorticity in Fig. 5 suggest that the stretching term is much greater than the tilting and advection terms at almost all forecast period and therefore is more favorable to enhance the near surface TLV. This result is consistent with the diagnostics for the low-level vorticity intensification in Kelm and Rotunno (1983). Further studies indicate the importance of convergence to stretching terms in Fig. 6. In the low levels, Exp-DR produces two periods of persisting average updraft enhancement, 2203-2209 UTC and 2213-2226 UTC; while only one period from 2202 UTC to 2216 UTC with the enhanced convergence can be found in Exp-SCR.

During the significant vortex period in both experiments, vertical columns of strong vertical vorticity that spans upward to 5 km AGL at most are found. Such column, consistent with the finding of Markowski et al. (2012), may be associated with tornadoes. As the positive stretching peak occurs near surface and mostly distributes below 1 km AGL (Figs. 6c, d), the existence of midlevel mesocyclone is implied as another critical part to maintain the vertical column of strong rotations (Figs. 6a, b). Therefore, the differences in the upper level between Exp-SCR and Exp-DR may result in significant impacts on the evolutions of predicted TLV.

The comparisons between Exp-DR and Exp-SCR are briefly summarized in the following. Relative to Exp-SCR, Exp-DR performs closer to the observations in timing and longevity of the predicted TLVs evolution. The different performances may be associated with the significant differences between both simulations in both near surface and upper levels.

b. Comparison of Analyses from Single- and Dual-Resolution EnVar

The differences between both TLV simulations result from the different ICs. To understand the causes of differences in ICs, their first-guess and analysis during the DA period are respectively compared in Figs. 7 and 8. During the first 20-min DA cycling, similar distributions and magnitudes for cool pool, vertical motions and reflectivity are

² The two vortices are identified based on the existence of the vorticity intensifications. In this paper, as the vorticity before intensifying or after weakening is found to be lower than 0.03 s^{-1} , the threshold value of 0.03 is used artificially to determine the significant vortex.

produced in Exp-SCR and Exp-DR. In the following DA cycling, cold pool in the rear flank region and its surroundings is rapidly enhanced in both experiments. However, such enhancement is more significant in Exp-DR than in Exp-SCR (Figs. 7c-f vs. 7o-r; Figs. 7i-l vs. 7u-x), which may be caused by the greater downdraft in the bottom of the storms carrying more precipitation loading (Figs. 8c-f vs. 8o-r; Figs. 8i-l vs. 8u-x). Further diagnostics suggest the differences between experiments arise from both model integrations between DA cycles and DA process, but the model integration appears to have more contributions.

Along with the DA cycling, the impacts of integrating and analyzing high-resolution fields in Exp-DR relative to Exp-SCR are accumulated and compared in Figs. 8f, l, r, x and 9. A strong downdraft in Exp-DR inserts into the updraft core in the upper levels over the rear-flank region, where a much weaker updraft is present with a weaker downdraft in the west of the updraft core in Exp-SCR (Figs. 9a, b). Much colder air distributes in an area extending from the rear-flank region northwestward into the forward flank in Exp-DR than in Exp-SCR (Figs. 9c, d). We also notice the $2\text{--}4\text{ m s}^{-1}$ stronger updraft in Exp-DR than Exp-SCR at 2 km AGL and therefore, relatively large reflectivity can distribute in higher levels (Figs. 8l, x). Their specific impacts on the subsequent TLV predictions will be introduced in the following section 3c.

c. Impact of Differences in the Initial Conditions Produced Between SCR and DR EnVar

Based on the comparisons in section 3b, significant differences between the final analyses respectively from SCR and DR EnVar are mainly embodied in three categories, the distributions of hydrometeor mixing ratios, the magnitude of cold pool, and the kinetic structures. Consistent with the previous report, to isolate impact of each category, we conduct 4 additional sensitivity tests (Table 1) by replacing the analyzed fields associated with each category in Exp-SCR with those in Exp-DR. The performances of sensitivity experiments are examined through comparing the timing and magnitude of low-level vertical vorticity, as shown in Fig. 10. The comparison indicates that the strength and longevity of the second TLVs are determined by the magnitude of the analyzed potential temperature, more specifically, the cold pool in ICs. Such impact of the analyzed cold pool is consistent with the comparison between Exp-SCR and Exp-T. In a word, the analyzed kinetic fields determine the timing of first TLV's phase transitions, including its dissipation and re-intensification; the longevity of the second TLVs is associated with the potential temperature in ICs; the impacts of the analyzed hydrometeor mixing ratios are limited but unneglected relative to other analyzed fields.

d. Impact of Analyzed Kinetic Fields

Stronger occlusion downdraft in ICs of Exp-DR (Fig. 9) subsequently results in more hydrometeor mixing ratios downward into the ground of the rear-flank region relative to Exp-SCR. Therefore the cold pool in rear-flank region from Exp-DR, Exp-UVW, and Exp-UVWT are found to be stronger than that from Exp-SCR during the forecast period, and their RFGF then travels more eastward (not shown).

As Exp-DR and Exp-UVW/Exp-UVWT have similar storm structures during the first TLV stage, the comparisons between Exp-SCR and Exp-DR as examples are shown in Figs. 11-12. The updraft cores along the southern and northern RFGFs in the upper levels are gradually divided from 2206 UTC to 2215 UTC (Figs. 11a-c) in Exp-DR. Along with the changes in updraft cores, the vertical column of strong rotation indicated by the green dots in Figs. 12a-c also varies. The vertical column of significant vorticity is increasingly tilted in a southeast-northwest orientation and weakening as the southern RFGF travels eastward from 2206 to 2211 UTC (Fig. 11b). After 4-min, the TLV reintensifies with the low-level rotation vertically collocated with the upper-level rotation associated with the updraft core along the southern RFGF (Fig. 11c). On the contrary, the motion of the southern RFGF is almost consistent with, but slightly rapider than that of the northern RFGF in Exp-SCR during 2206-2215 UTC (Figs. 11d-f). The vertical column of strong rotations that span from near ground upward into the updraft core along the northern RFGF is vertically erect persisting from 2206 to 2215 UTC (green dots in Figs. 12a-c) and longer leading time. With such structure, strong stretching therefore can be maintained (Fig. 6d) and the TLV with a great vertical vorticity unrealistically persists a longer time (Fig. 6c) than the first TLV in Exp-DR.

e. Impact of Analyzed Potential Temperature

The comparisons between Exp-SCR (Exp-UVW) and Exp-T (Exp-UVWT) suggest that the longevity and strengthen of the second TLVs period depend on the analyzed potential temperature, e.g., cold pool, in the later forecast. Relative to Exp-SCR (Exp-UVW), more negative buoyance at low levels associated with a stronger cold pool in Exp-T (Exp-UVWT) at the analysis time is speculated to induce a greater downward directed pressure gradient based on the momentum equation in the vertical direction (Klemp and Rotunno 1983). In this manner, more precipitation loading and evaporation cooling occur and in turn produce a stronger cold pool in the following forecast. With such feedback, the stronger cold pool can persist in the entire forecast period for Exp-T (Exp-UVWT) than Exp-SCR (Exp-UVW), for example, the $\theta_e\theta_e$ in rear-flank cold pool in Exp-T (Exp-UVWT) is generally ~ 2 K colder than that in Exp-SCR (Exp-UVW) at 2222 UTC (Figs. 13, 14).

With colder air in the cold pool, a rapider RFGF motion is produced (Markowski et al. 2008) in Exp-T (Exp-UVWT) relative to Exp-SCR (Exp-UVW). In addition, the relatively colder air in the rear-flank cold pool can provide more sufficient baroclinity horizontal vorticity (Markowski et al. 2008) as the source of vertical vorticity (Klemp and Rotunno 1983) in the vicinity of the RFGF, consistent with the TLV developing in the apex of the primary RFGF in Figs. 13a, c, 14a, and c. So longer-lived TLVs are produced in Exp-UVWT and Exp-T. On the contrary, insufficient baroclinic vorticity due to the warmer RF cold pool may be unable to maintain the strong vertical vorticity. In addition, the dominated downdraft under 2 km AGL between 2225 and 2230 UTC may be associated with the typical broadening large-scale downdraft (e.g., Lemon and Doswell 1979; Wicker and Wilhelmson 1995; Marquis et al. 2016) and further reduce the stretching (Fig. 7b). The low-level TLVs along the southeastward extending downdraft therefore

travels southeastward in later forecast as shown in Fig. 4b. Therefore, the second TLVs in Exp-SCR and Exp-UVW persist shortly.

f. Impact of Analyzed Hydrometeor Mixing Ratios

Notice a short-lived but slightly stronger TLV in Exp-Hydro than in Exp-SCR is reintensified during 2222-2230 UTC. This reintensification of the vertical vorticity in Exp-Hydro results from the farther distance between the TLV and low-level downdraft region relative to Exp-SCR at around 2225 UTC (Fig. 15) and may be explained in the following hypothesis. At the analysis time, the vertical cross sections in Fig. 10 shows the larger reflectivity distribute in the upper level in Exp-DR and in the low level in Exp-SCR. Such that the descant in the bottom of the storm carries less precipitation in Exp-Hydro than in Exp-SCR and thus slightly warmer cold pool is produced in the following forecast period, especially over the forward flank region. For example, ~ 2 K warmer θ_e over the rear- and forward-flank regions in Exp-Hydro (Fig. 15b) relative to in Exp-SCR (Fig. 15a) at 2225 UTC provides an evidence. The more positive buoyance in turn promotes less precipitation loading and evaporation cooling. Therefore, compared with Exp-SCR, the second TLVs in Exp-Hydro can be slightly more enhanced by the convergence along the primary RFGF before being inhibited by the delayed trailing large-scale downdraft.

Publications

Wang Y., and X. Wang, 2018: Impact of the analysis resolution on the prediction of tornado like vorticity and surface wind using the dual resolution GSI-based EnVar data assimilation system: methodology and experiment with the May 8th, 2003 Oklahoma City tornado case. To be Submitted to *Monthly Weather Review*.

Table 1. List of the replaced analyzed fields in sensitivity experiments.

Experiments	Fields to be replaced in the ICs
Exp-Hydro	Hydrometeor mixing ratios, including QRAIN, QSNOW, QGRAUP, and QICE
Exp-T	Potential temperature (T)
Exp-UVW	Kinetic fields (U, V, and W)
Exp-UVWT	Potential temperature (T) and kinetic fields (U, V, and W)

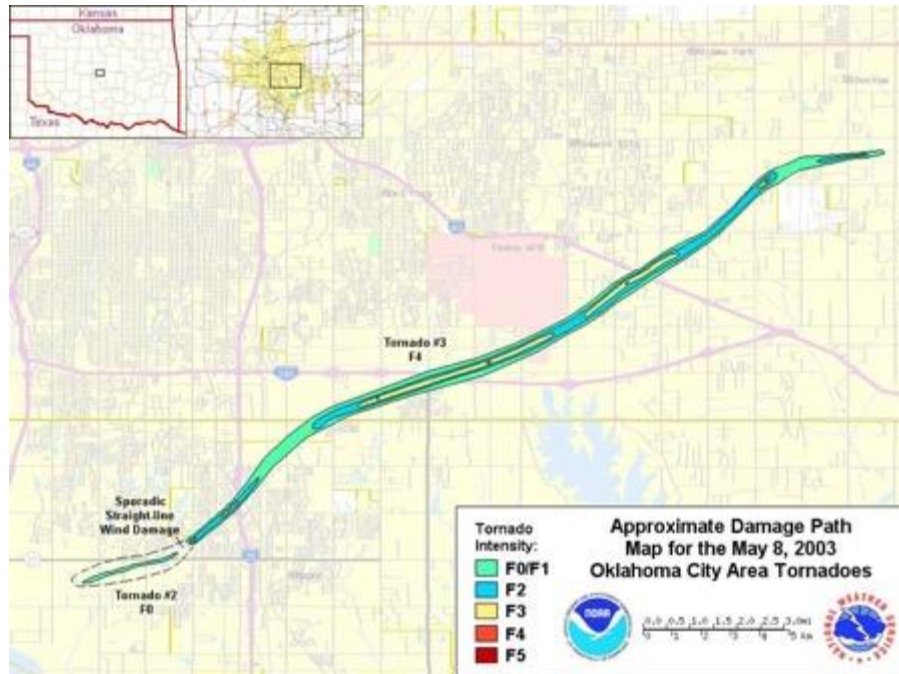


Figure 1. The observed damage path of the 8 May 2003 Oklahoma City (OKC) tornado overlaid on the map of the Moore-south OKC area. Image is obtained from the National Weather Service website, <https://www.weather.gov/oun/events-20030508>.

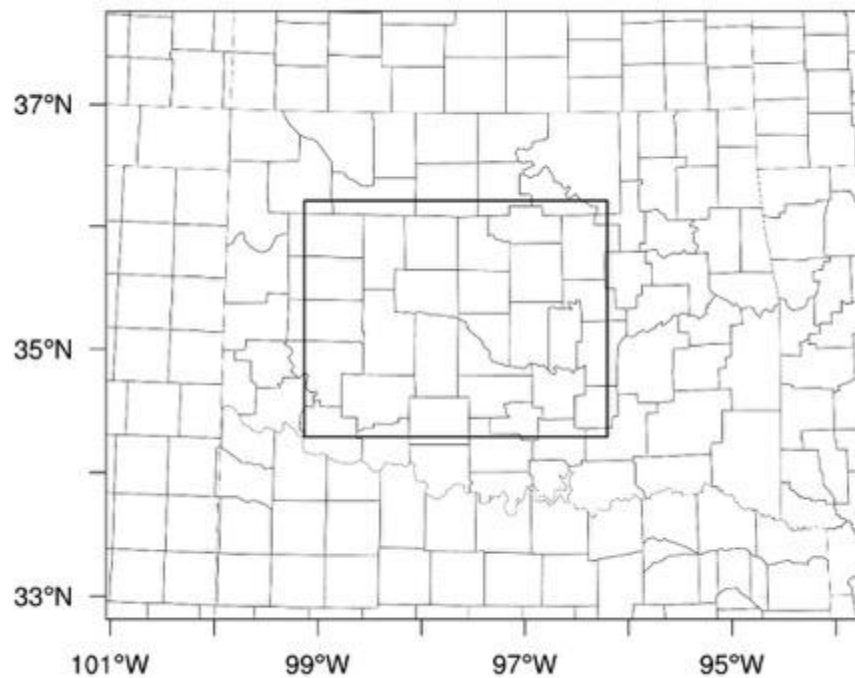


Figure 2. The outer and inner domains with 2-km and 500-m horizontal grid spacing, respectively.

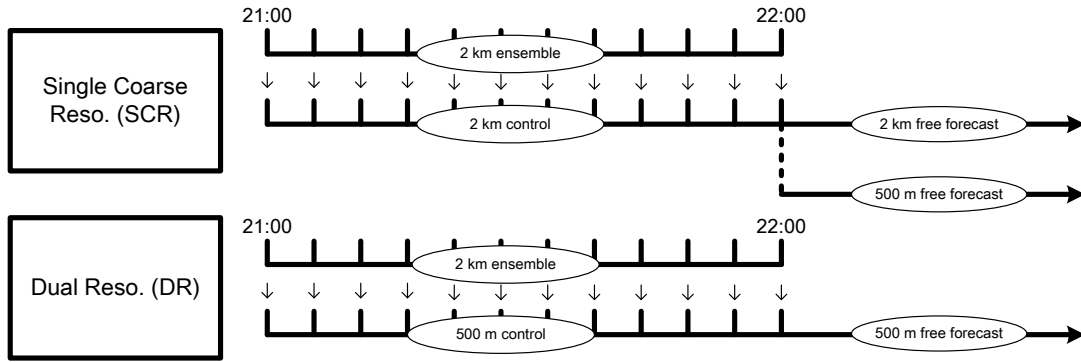


Figure 3. Schematics of the analyses and forecasts for Exp-SCR and Exp-DR. Both experiments assimilate the radar data every 5-minute from 2100 to 2200 UTC. The analyses at 2-km and 500-m resolutions are respectively generated in Exp-SCR and Exp-DR by ingesting an ensemble at 2-km grid spacing. To be comparable with Exp-DR, the analysis from Exp-SCR is downscaled to 500-m grid. One-hour 500-m forecasts are then initialized by both analyses at 2200 UTC after 1-hour assimilation.

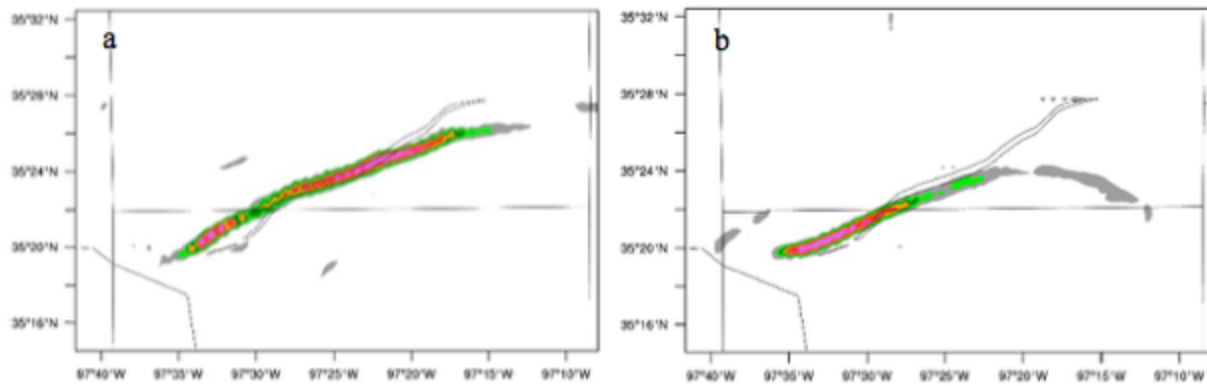


Figure 4. Evolution of the near-surface vertical vorticity associated with the simulated TLVs from Exp-DR (a) and Exp-SCR (b).

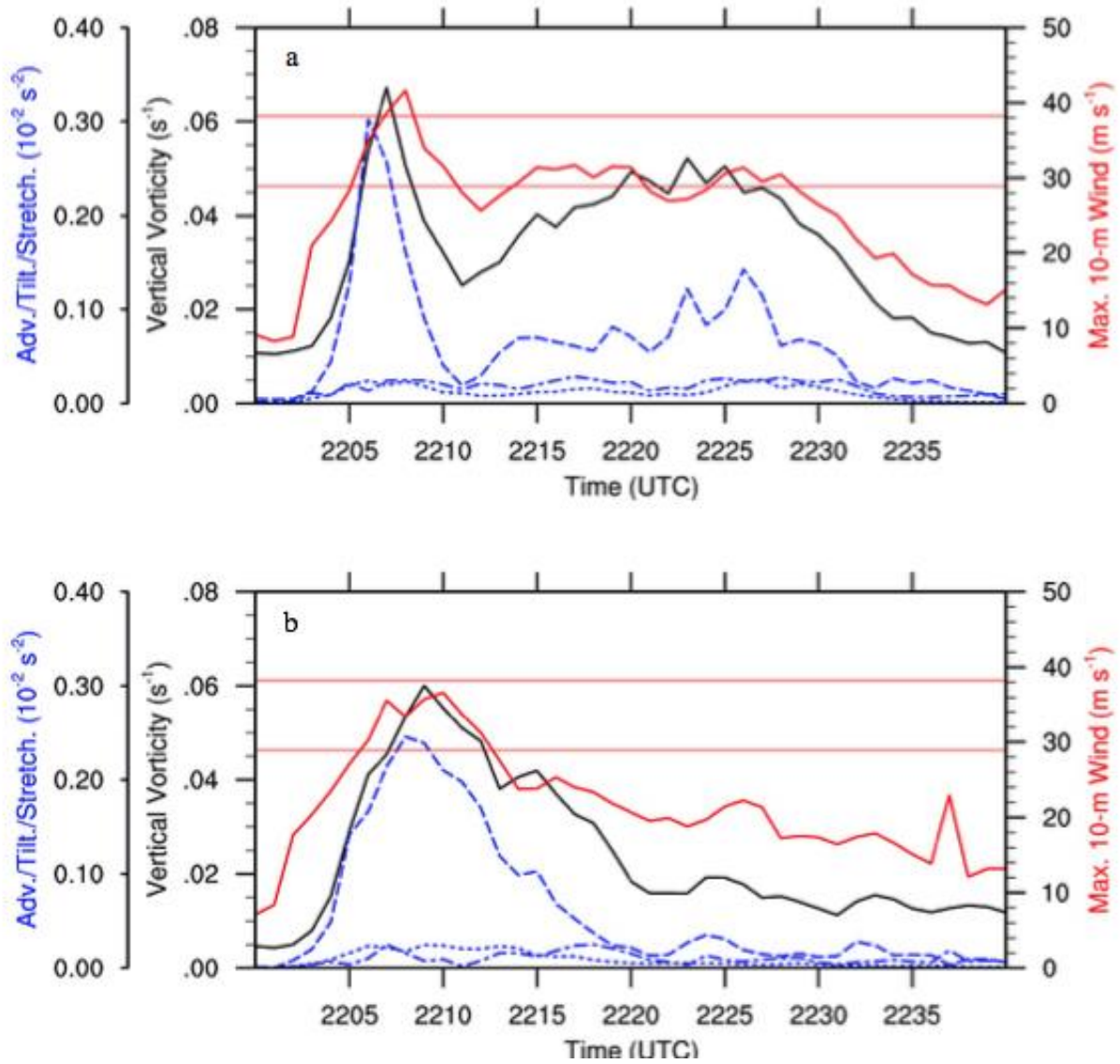


Figure 5. The time-series of maximum 10-m wind speed (red), vertical surface vorticity (black), and maxima of the horizontal advection (dot-dash), tilting (dot) and stretching (dash) terms in the vertical vorticity equation within a 1-km horizontal distance of the peak surface vorticity from Exp-DR (a) and Exp-SCR (b).

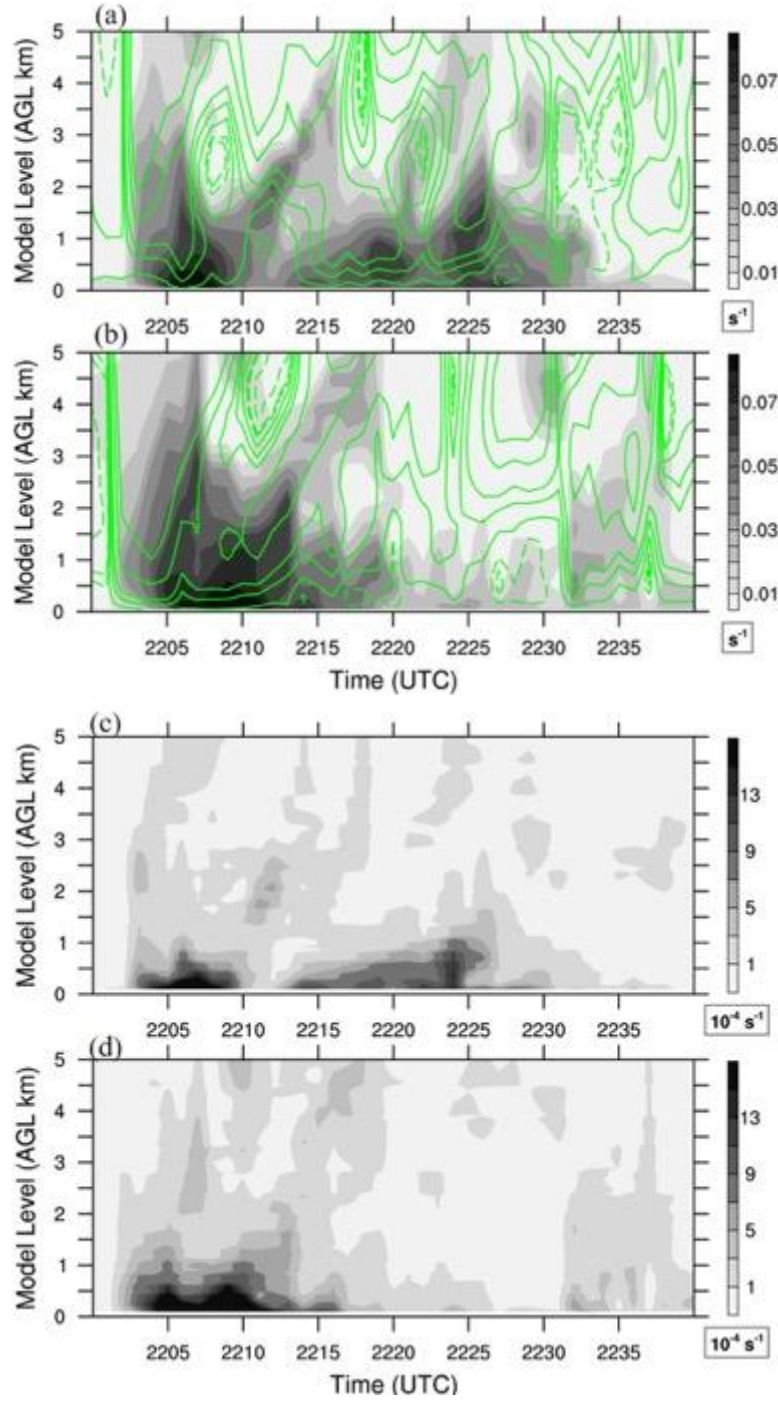


Figure 6. Peak vertical vorticity (shaded) and mean vertical motion (contours from $-10 m s^{-1}$ to $10 m s^{-1}$ at $3 m s^{-1}$ interval; $m s^{-1}$) within the surface maxima vertical vorticity as a function of height and time for (a) Exp-DR and (b) Exp-SCR during 2200–2240 UTC. Stretching of vertical vorticity at the surface vorticity maximum for (c) Exp-DR and (d) Exp-SCR during 2200–2240 UTC.

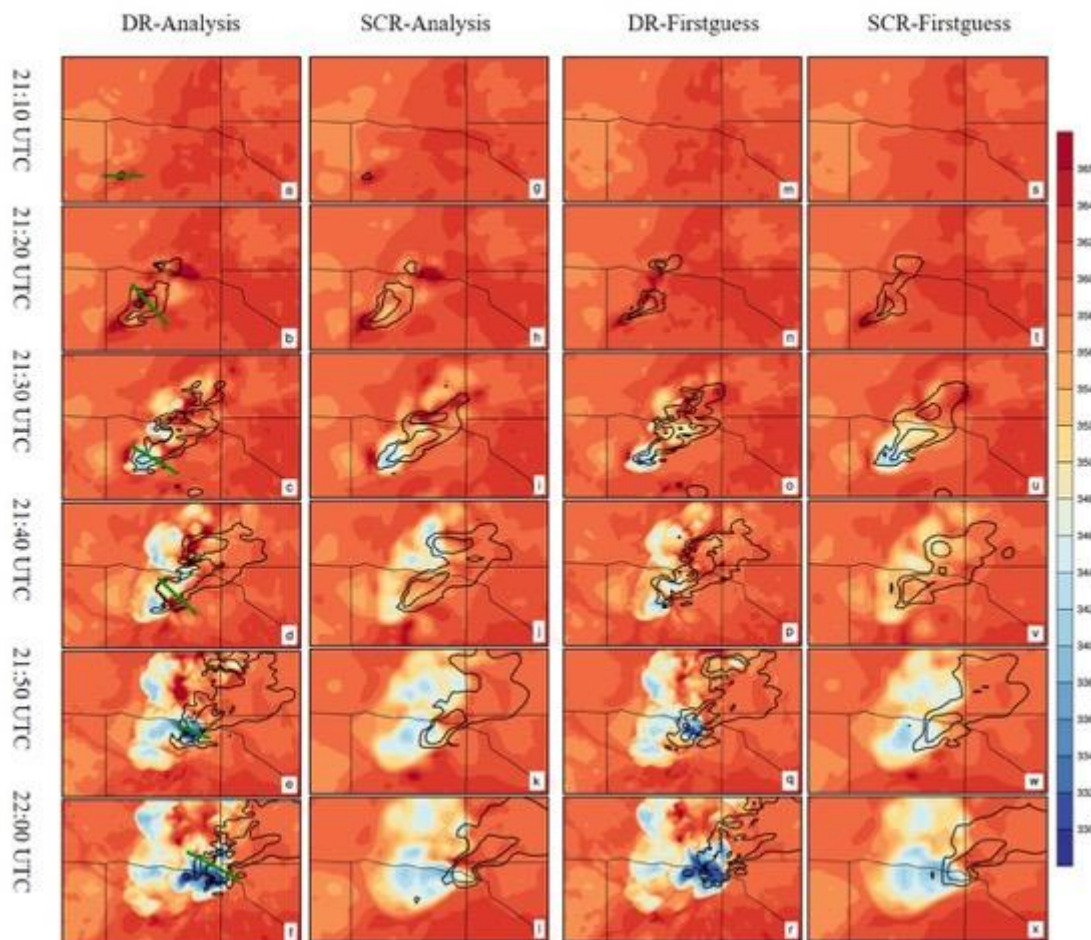


Figure 7. The reflectivity (contours from 20 dBZ to 60 dBZ at 20 dBZ intervals; dBZ) at 1 km AGL and surface equivalent potential temperature (colors; K) analysis (a-l) and first-guess (m-x) for Exp-DR (a-f and m-r) and Exp-SCR (g-l and s-x) from data assimilation cycles valid at 2110, 2120, 2130, 2140, 2150, and 2200 UTC. Green lines in the 1st column represent the position of 0-12 km vertical cross sections in Fig. 6.

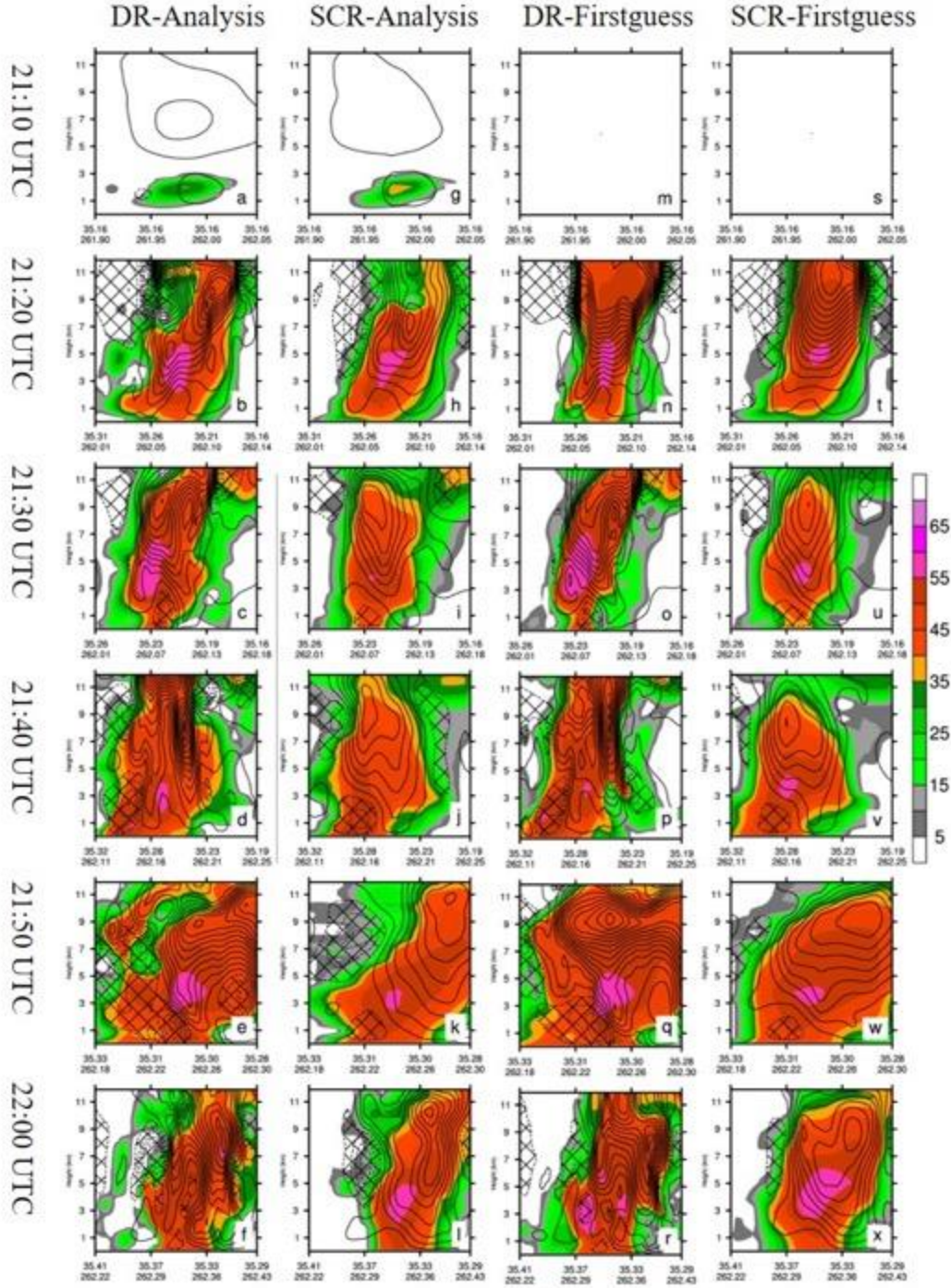


Figure 8. Vertical cross sections of reflectivity (colors; dBZ) and vertical motions (contours from - 38 m s^{-1} to 50 m s^{-1} at 4 intervals; m s^{-1}) analysis (a-l) and first-guess (m-x) for Exp-DR (a-f and m-r) and Exp-SCR (g-l and s-x) from data assimilation cycles valid at 2110, 2120, 2130, 2140, 2150, and 2200 UTC. Solid contours (pattern shading) represent upward (downward) motion.

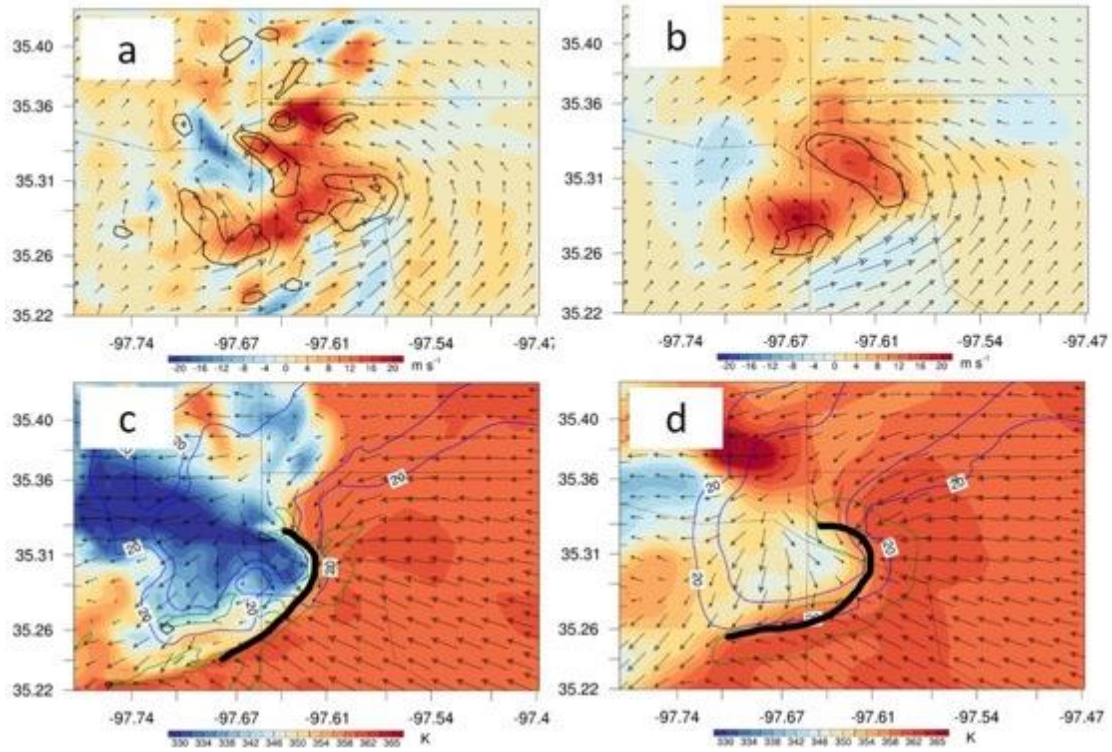


Figure 9. The vertical velocity (colors; m s^{-1}) and cyclonic vorticity (contours from 0.01 s^{-1} to 0.04 s^{-1} at 0.01 s^{-1} intervals; s^{-1}) at 2-km AGL at the analysis time for Exp-DR (a) and Exp-SCR (b). The equivalent potential temperature (colors; K), upward motions (green contours from 1 m s^{-1} to 3 m s^{-1} at 1 m s^{-1} interval; m s^{-1}), and reflectivity (blue contours at 20 and 40 dBZ) near the ground valid at 2200 UTC for Exp-DR (c) and Exp-SCR (d). The position of rear-flank gust front (RFGF; thick black line) are subjectively determined based on the convergence and wind speed fields.

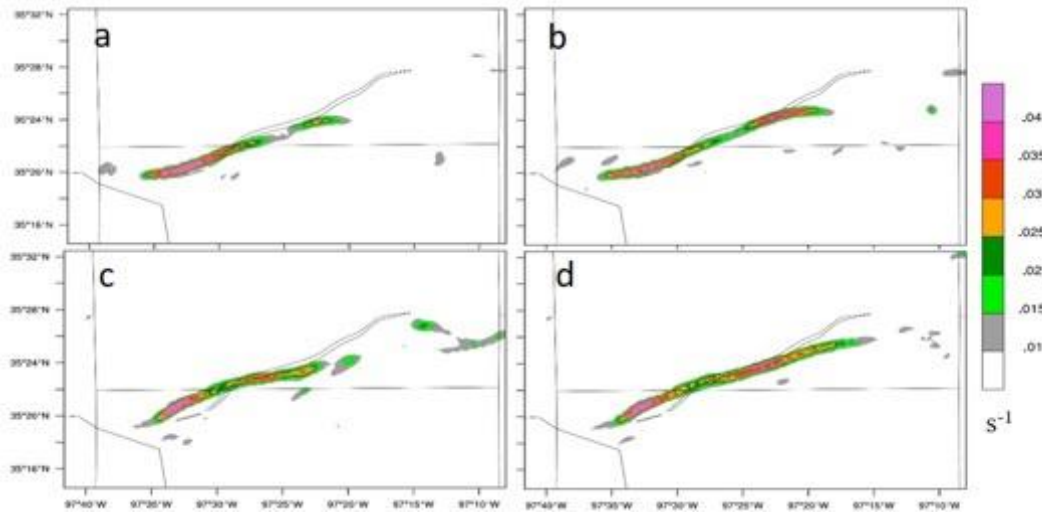


Figure 10. As in Fig. 4, but for (a) Exp-Hydro, (b) Exp-T, (c) Exp-UVW, and (d) Exp-UVWT in Table 1.

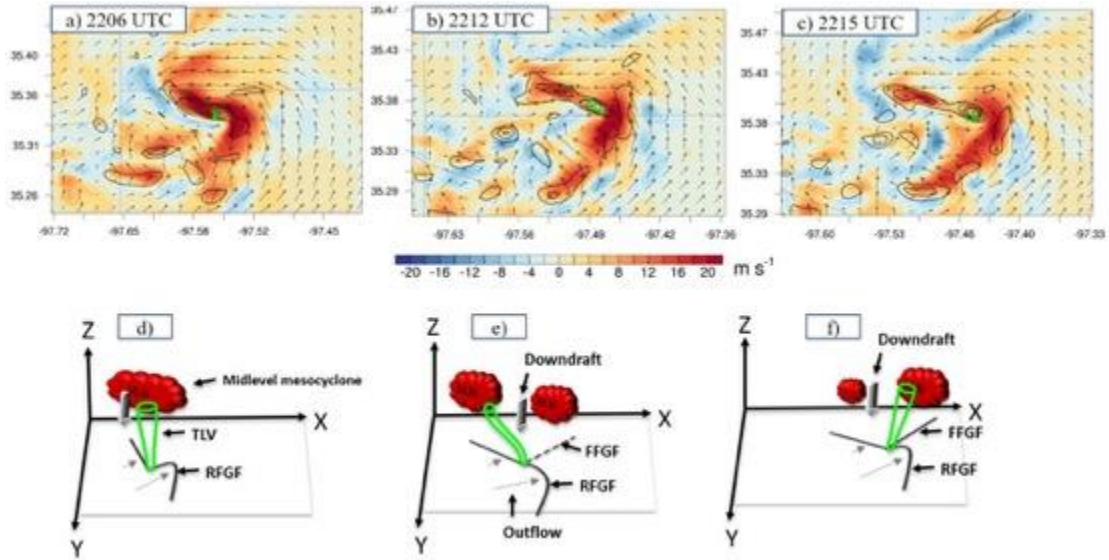


Figure 11. The vertical velocity (colors; m s^{-1}) and cyclonic vorticity (contours from 0.01 s^{-1} to 0.04 s^{-1} at 0.01 s^{-1} intervals; s^{-1}) at 2-km AGL in the forecasts valid at (a) 2206 UTC, (b) 2212 UTC, and (c) 2215 UTC for Exp-DR. The darkening green dots in (a-c) represent the maximum cyclonic vorticity at 0.1, 1, 2.5, 4 km AGL. Schematic diagram of the TLV evolution process from 2206 to 2215 UTC is illustrated in d-f. Green columns refer to the structure of TLV, gray thick vectors indicate the downdraft trailing the gust fronts, and MLM represents the midlevel mesocyclone. The intensity of TLV is indicated schematically with the thickness of green column. In the x-y horizontal sections, the gray thin vectors indicate the cold pool outflow and its strength is indicated schematically with the length of vectors; near-surface gust fronts are traced with bold black lines.

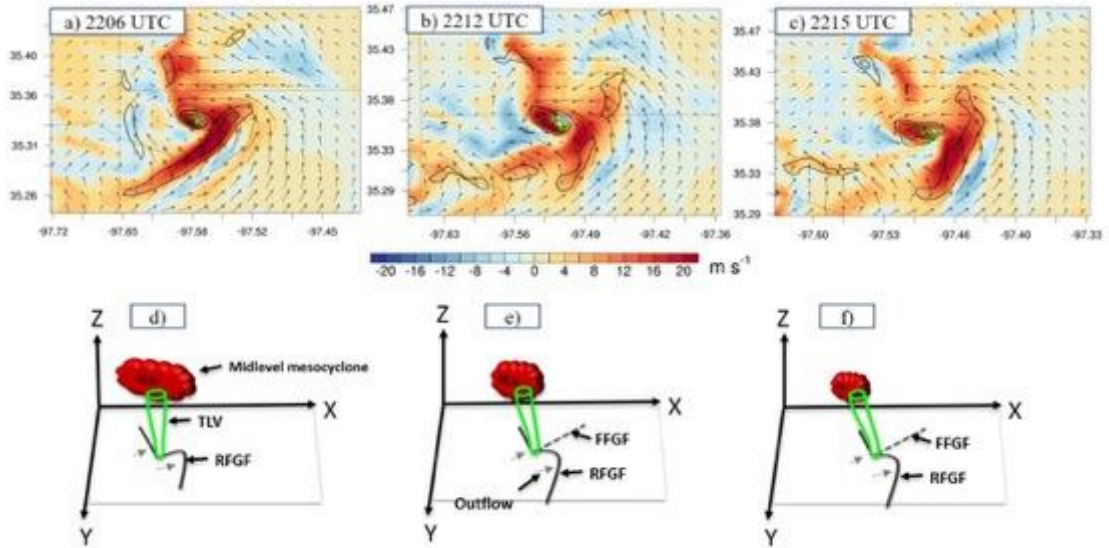


Figure 12. As in Fig. 11, but for Exp-SCR.

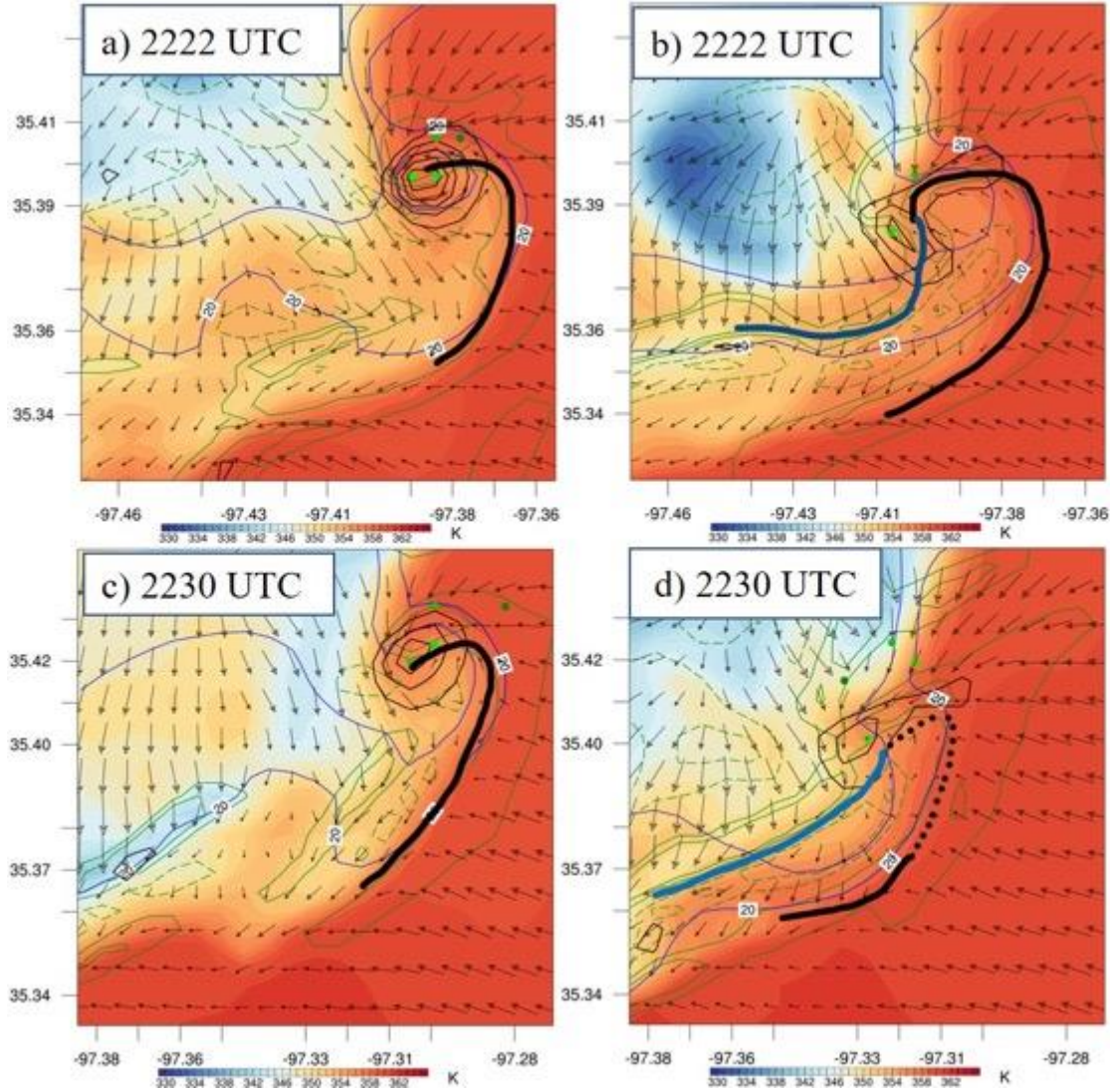


Figure 13. The equivalent potential temperature (colors; K), vertical vorticity (thin black contours from 0.01 s^{-1} to 0.08 s^{-1} at intervals 0.01 s^{-1} ; s^{-1}), vertical motions (green solid contours from 0.75 m s^{-1} to 1.5 m s^{-1} at 0.75 m s^{-1} interval; green dash contours from -1.5 m s^{-1} to -0.75 m s^{-1} at 0.75 m s^{-1} interval; m s^{-1}), and reflectivity (blue contours at 20 and 40 dBZ) near the ground valid at 2222 (a, b) and 2230 (c, d) UTC for Exp-UVWT (a, c) and Exp-UVW (b, d). Thick black lines represent the schematically determined primary rear-flank gust fronts (RFGF); thick blue lines indicate the positions of secondary RFGF. Green dots from light to dark indicate vertical vorticity maxima at 0.1, 1, 2.5, and 4 km AGL.

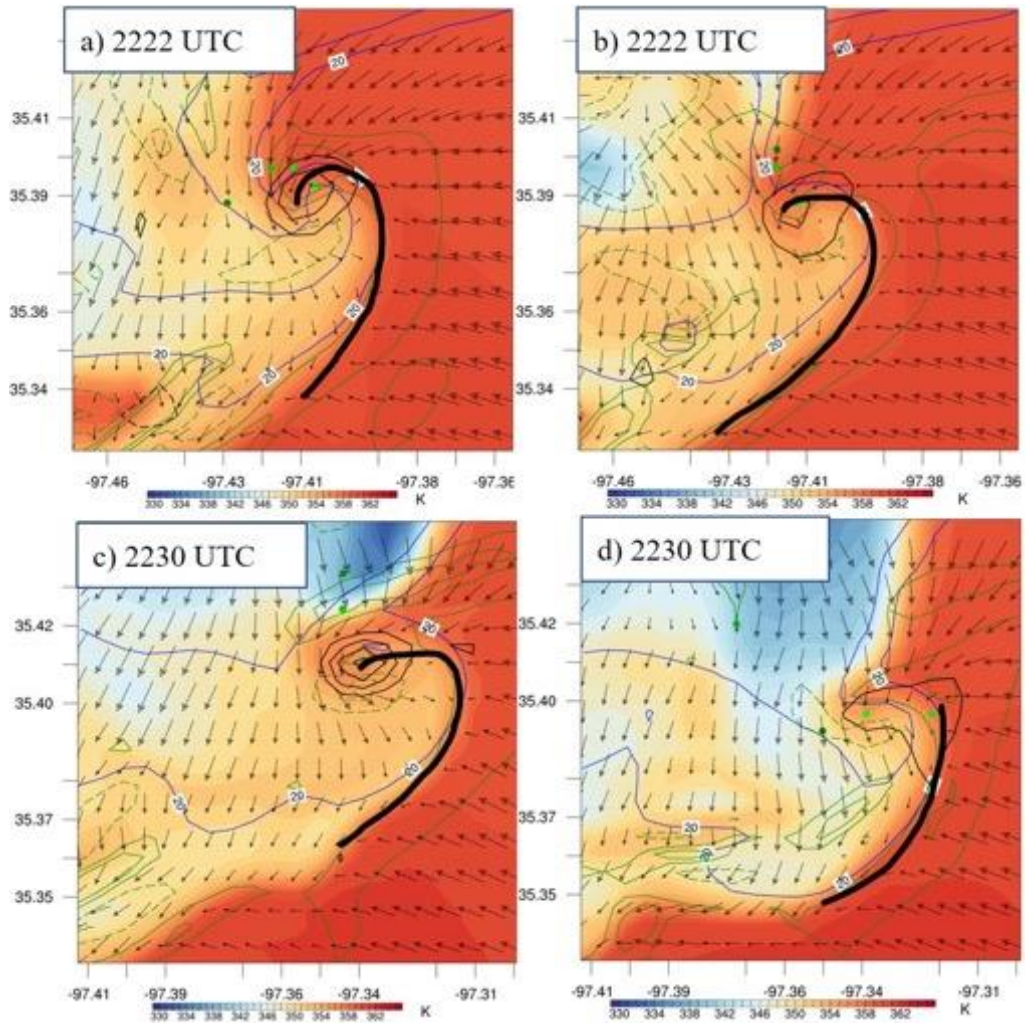


Figure 14. Same in Fig. 13, but for Exp-T (a, c) and Exp-SCR (b, d).

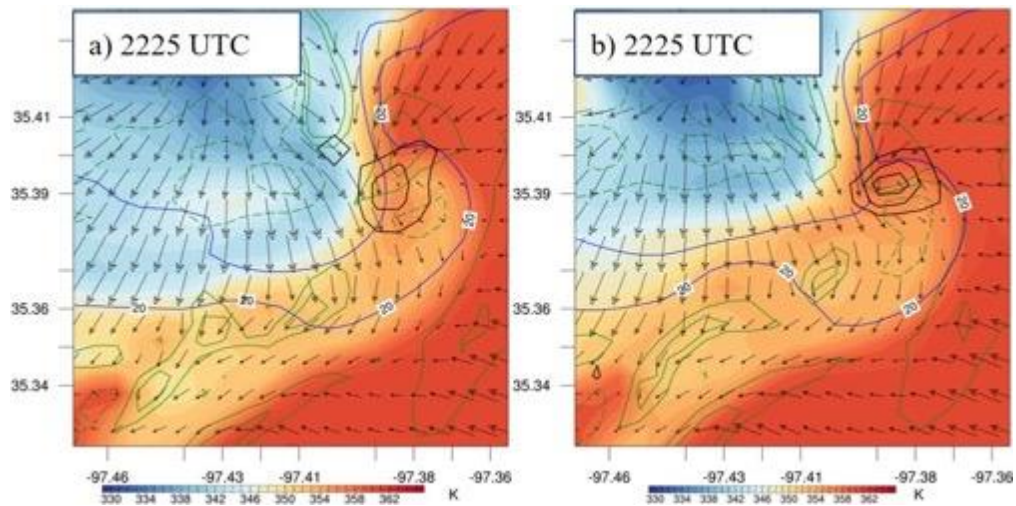


Figure 15. Same in Fig. 13, but valid at 2225 UTC for Exp-SCR (a) and Exp-Hydro (b).

CIMMS Task III Project – MPAR Targeting Observation Research for WoF

Xuguang Wang and Chris Kerr (OU School of Meteorology)

NOAA Technical Lead: Pamela Heinselman and Mark Weber (NSSL)

NOAA Strategic Goal 2 – *Weather Ready Nation: Society is Prepared for and Responds to Weather-Related Events*

Funding Type: CIMMS Task III

Objectives

The adaptive nature of MPAR will allow rapid sampling of convective storm sectors as well as clear-air environments. An ensemble-based targeted observation method is used to estimate the impact of radial velocity observation assimilation *before* the observation are collected. Knowing assimilation impact estimates beforehand will permit optimal use of MPAR resources (either weather or aviation related). This study also verifies the estimates through assimilation. Since clear-air radial velocity observations are typically not assimilated given low SNR, the second portion of this study assesses the impact of near-storm inflow clear-air radial velocity observations on low-level rotation forecasts since one function of MPAR, adaptive dwell time, can provide clear-air radial velocity observations with higher SNR.

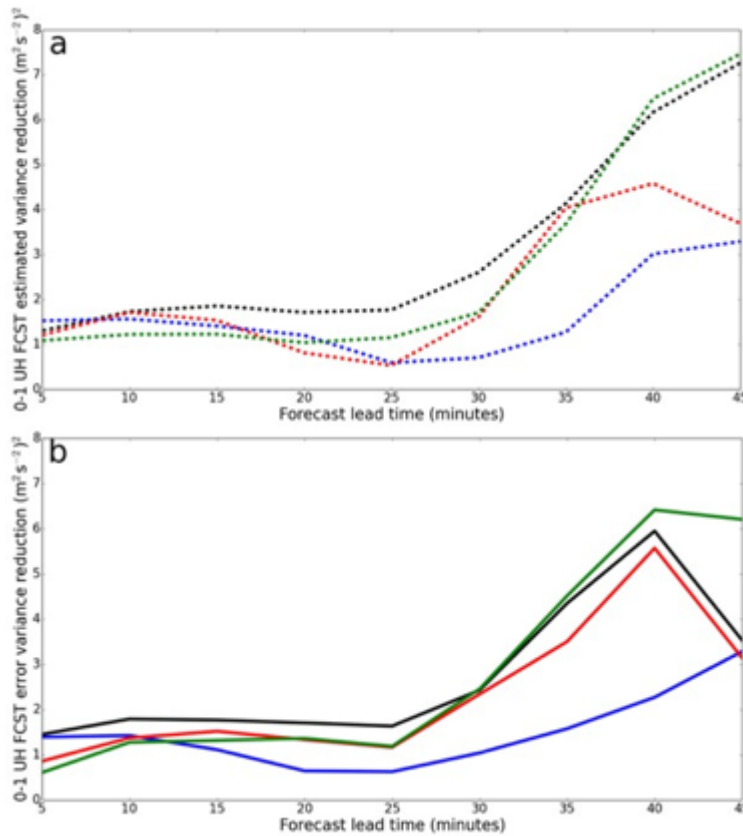
Accomplishments

1. Targeted Supercell Radial Velocity Observations

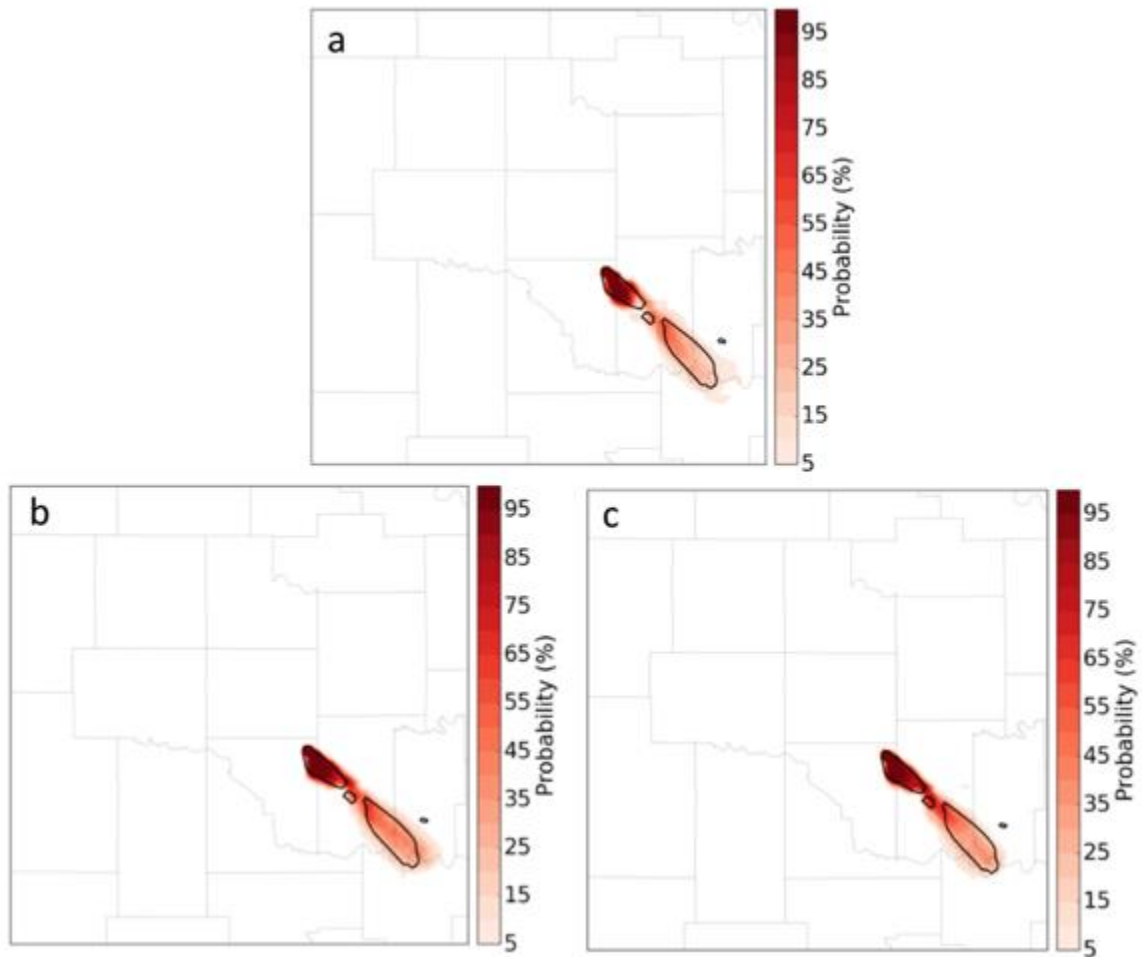
The potential future installation of a multi-function phased-array radar (MPAR) network will provide more frequent updates compared to the current WSR-88D network with capabilities of case-specific adaptive scanning. Many factors will affect adaptive scanning strategies including very short-term convective-scale model forecasts. An ensemble-based targeted observation algorithm is applied to an Observing System Simulation Experiment (OSSE) where the impacts of synthetic idealized supercell radial velocity observations are estimated before the observations are “collected” and assimilated. This method is able to sufficiently predict how MPAR observation sets will impact the accuracy of a low-level rotation forecast metric (0-1 km updraft helicity), a surrogate for tornado prediction (first figure below). In some scenarios, a subset of a full-volume scan assimilation produces better forecasts than all observations within the full volume. Assimilating the full-volume scan increases the number of potential spurious correlations arising between the forecast metric and radial velocity observation induced state perturbations which may degrade the forecast metric accuracy. The targeted observation algorithm is able to reasonably predict this advantage before the observation time. Knowing the impacts adaptive scanning may have on short-term forecasts will influence scanning strategy decision-making in hopes to produce the most optimal ensemble forecast while also benefiting human severe weather warning decision-making.

2. Supercell Clear-Air Inflow Environment Sampling and Assimilation

Several OSSEs are performed to analyze the impacts of clear-air radial velocity observation within the storm inflow region on low-level rotation forecasts. The first experiment assimilates “storm” radial velocity observations every minute for five minutes before initializing a 90-minute ensemble forecast. Two additional experiments include the addition of clear-air radial velocity observations along with the storm observations in the previously described experiment. One of these experiments only assimilates the clear-air observations at the first and last assimilation times (5-min interval). The other assimilates the clear-air observations every minute. The results suggest the addition of clear-air inflow observations improves forecasts, especially lead times of 45-90 minutes, by reducing ensemble spread and increasing spatial ensemble probabilities of 0-1 km UH (second figure below). These increased probabilities are co-located with the truth simulation 0-1 km UH swath. The frequency of clear-air radial velocity assimilation (1-min versus 5-min) does not significantly affect the results. Therefore, a 5-min frequency would free MPAR resources while also permitting increased radar dwell times when observing the clear-air region, reducing observation error and increasing SNR.



Averaged over three observation times (a) estimated 0-1 km UH variance reduction and (b) actual error variance reduction of an ensemble forecast initialized prior to the observation collection and assimilation time for full-volume scans (black), low-sector (blue), mid-sector (red), and high-sector (green).



Probability swathes of 0-1 km UH for 90-minute forecasts initialized after assimilating radial velocity (a) storm only observations every minute for 5-min (b) storm observations every minute and clear-air observations the first and last minute (5-min period) (c) storm and clear-air observations every minute for 5-min.

CIMMS Task III Project – GSI-based Dual Resolution EnVar Data Assimilation for Convective-Scale “Warn-on Forecast”

Xuguang Wang and Yongming Wang (OU School of Meteorology)

NOAA Technical Lead: Pamela Heinselman (NSSL)

NOAA Strategic Goal 2 – Weather Ready Nation: Society is Prepared for and Responds to Weather-Related Events

Funding Type: CIMMS Task III

Objectives

To explicitly resolve convection, there is a continuous increase in horizontal grid resolution to model inner structures and evolution of various mesoscale convection

systems (MCSs). However, increasing horizontal resolution alone does not always guarantee a better solution. Much less attention has been given to evaluate the impacts of vertical grid resolution on resolving convection. Thus, one of objectives of this project is to examine the sensitivity of the explicit simulation of the 8 May 2003 Oklahoma City tornadic supercell storm to varying vertical resolutions in terms of its embedded tornado-like vortex (TLV)'s intensity and structure. In addition, we have explored and demonstrated the necessity of high horizontal resolution during data assimilation (DA) to TLV predictions. Similarly, the refined vertical grid resolution will be applied and explored in the DA processes. Another objective of this project is to produce an analysis at refined grid resolutions. Considering the expense of ensembles with higher resolutions, an efficient dual resolution EnVar approach is developed with ensemble at coarser horizontal and vertical grid resolutions and control member at higher ones.

Accomplishments

1. Introduction

Rapid growth in computing power recently has allowed us to explicitly model inner structures and evolutions of various mesoscale convection systems (MCSs) with small horizontal grid spacing, even down to sub-kilometer. Lindzen and Fox-Rabinovitz (1989) and Pecnick and Keyser (1989) respectively derived consistency criterions between horizontal resolution and vertical resolution. In addition, Zhang and Wang (2003) and Kimball and Dougherty (2006) demonstrated the hurricane intensity and structures are significantly improved with refined vertical grids. However, much less attention has been given to evaluate the impacts of vertical grid configurations on modeling tornadic thunderstorms and embedded tornadoes.

Our previous study (Wang and Wang 2018) has compared impacts of interpolated high resolution initial conditions (ICs) with firsthand high resolution ICs on predictions of tornado-like vortex (TLV). Significant improvements are produced by predictions with the firsthand ICs relative to the interpolated ICs. Similarly, we will further evaluate the refined vertical grid configurations on initializing high resolution TLV predictions. Given the expense of high resolution ensemble within ensemble-based data assimilation (DA) method, an efficient dual resolution EnVar approach is developed and implemented with ensemble at a coarser horizontal resolution and control member at a higher one (Schwartz et al. 2015; Schwartz 2016; Lu et al. 2017; Wang and Wang 2018). However, all of them used same vertical grid resolution between ensemble and control members. Rather limited studies investigated the consistency criterion between horizontal and vertical grid resolutions and the impacts of the refined vertical grid configurations on both DA and prediction of convection.

Considering the above objective, the following will be conducted. The present report firstly tests various vertical grid configurations for TLV predictions with Exp-DR in Wang and Wang (2018) as a reference. The dual resolution EnVar system in Wang and Wang (2018) is further extended in vertical grid resolution and initial diagnostics are also performed.

2. Event Overview and Experiment Design

a. Overview of the 8 May 2003 Oklahoma City Tornadic Supercell and Embedded Tornadoes

A series of studies have introduced and conducted experiments based on this 8 May 2003 Oklahoma City tornadic thunderstorm, e.g., Romine et al. (2008), Hu and Xue (2007), Yussouf et al. (2013), Xue et al. (2014), and Wang and Wang (2017). An isolated supercell developed along a dryline located in west-central Oklahoma and is found at around 2200 UTC with a pronounced hook appendage. The supercell storm propagated east-northeastward, and began to weaken after 2300 UTC, and dissipated by 0020 UTC 9 May. According to the official National Weather Service (NWS) survey results³, this supercell produced three tornadoes that passed through Moore, southern Oklahoma City, Midwest City, and Choctaw. The first reported tornado existed for 1-minute from 2200 to 2201 UTC with a damage path for about 0.3-km but was not available in any WSR-88D radar products (Romine et al. 2008). The segmented paths produced by the second and third tornadoes listed in the National Climate Data Center Storm Data publication (NCDC 2003, 340-342) are shown in Fig. 1. A F0 tornado persisted from 2204 to 2208 UTC in southwest of Moore tracked on the ground for about 3-km. Within same storm, another widespread F2-F4 damage tornado formed at 2210 and dissipated at 2238 UTC with a ~30-km east-northeast track path. The previous studies (Schenkman et al. 2012; Xue et al. 2014; Schenkman et al. 2014) associated with tornado predictions for this thunderstorm case focused on the third tornado only. Different from these studies, experiments in this present study will be conducted related to both the second and third tornadoes.

b. Experimental Design and Extension of Vertical Dual Resolution EnVar DA System

Control simulation with the ICs at 500-m grid spacing generated through dual resolution EnVar in Wang and Wang (2018) is used as a reference to simulations using various increased and reduced vertical grid resolutions. Control simulation has 51 vertical levels and is denoted as L51. To evaluate the sensitivity of TLV prediction to vertical grid resolution, simulations with various vertical grid configurations are conducted, in addition to that of L51. As shown in Fig. 2, the experiment reduces the vertical levels near surface and is denoted as L49; L65L is conducted with increasing bottom levels; the L65H simulation is run with middle levels increased; simulation with lower levels increased is L54. These simulations will be compared to determine the best refined vertical grid configuration for TLV predictions.

Given the strong impacts of vertical grid configurations on inner-core cloud structure of hurricane (Zhang et al. 2003), the following microphysical schemes are used to evaluate the sensitivity of these schemes to vertical grid configurations on thunderstorms, Kessler scheme (Kessler, 1969), Lin et al. scheme (Lin et al. 1983), WRF Single-

³ The NWS report for the 8 May 2003 Oklahoma City is summarized in <https://www.weather.gov/oun/events-20030508>

Moment 6-class scheme (Hong and Lim 2006), Thompson scheme (Rasmussen and Hall 2008; 2009), Morrison double-moment scheme (Tatarskii 2009), WRF Double-Moment 6-class scheme (Lim and Hong 2010), NSSL 2-moment scheme (Mansell et al. 2010).

To extend the dual resolution EnVar system in Wang and Wang (2018) with the ability to produce an analysis ingesting ensemble at a different refined vertical grid, an interpolation operation adopted from *v_interp* is implemented to refine the vertical grid of ensemble within GSI. Figure 3 shows the flowchart of newly extended GSI-based dual resolution DA system for WRF-ARW. Prior ensemble and control firstguess at a coarser resolution (2-km) are respectively updated through GSI-based EnKF and single resolution (SR) EnVar; control firstguess at refined horizontal and vertical resolutions is initialized by GSI-based dual resolution (DR) EnVar. Same prior ensemble is used to calculate flow-dependent error covariance for both EnVar. To force the EnKF perturbations to evolve with the trajectory of the hybrid forecast (Wang et al. 2013), 500-m & refined vertical resolution (VG) analysis control is upscaled and merged with 2-km analysis control; 2-km ensemble analyses are then recentered with the merged 2-km analysis control. Ensemble and 2 control analyses are advanced to next DA cycle.

3. Results

a. Sensitivity of TLV Predictions to Various Refined Vertical Grids

The predicted TLV is represented using the near-surface vertical vorticity maxima, as shown in Fig. 4. With the near surface levels are reduced, the surface vertical vorticity peak is much stronger in L49 than in L51. However, the timing of TLV evolution in L49 departs more away from observations with the unrealistically delayed first TLV evolution. When we increase the bottom levels, the magnitude and longevity of TLV in L65L are significantly weakened and shortened relative to L51, especially for the second TLV period. Increasing mid-levels in L65H almost resembles L51 and indicates impact of this refined vertical grid configuration is limited. Reintensification of the second TLV in L51 costs ~10-min to reach the vorticity greater than 0.04 s^{-1} . The reintensification time can be reduced to ~5-min in L54 with a stronger 10-m wind speed during the second TLV period as shown in Fig. 5.

Taking advantage of diagnostics on TLV evolutions in Wang and Wang (2018), the differences in the above TLV predictions are explained in the following Figs. 6-8. In L51, as the southern rear-flank (RF) gust front travels more rapidly than upper level mesocyclone along the northern RF gust front, the first TLV persists shortly. Reducing near-surface vertical levels in L49 produces warmer RF cold pool (Fig. 6) and then the motion of southern RF gust front is slower and more consistent with the northern RF gust front. Therefore, the vertical column of strong rotations spanning from surface to upper levels persists much longer. Generally, thicker bottom levels may not well resolve the surface turbulence momentum and thermal fluxes and have larger heat capability. The cold pool is much stronger in L49 than in L51 and can be demonstrated in the cold pool over forward flank area. On the other hand, the updraft along the RF gust front is

much weaker with thicker bottom levels, so the weaker downdraft as a compensation trailing the updraft and warmer cold pool trailing the RF gust front can be found in Fig. 6. Simulation L65L has the first model level much closer to the ground and a warmer cold pool relative to L51 in Fig. 7. With less baroclinic vorticity, the vertical vorticity in L65L is less likely to be enhanced. Comparisons among L51, L49, and L65L suggest the vertical grid configurations for the low-levels in L51 may be most appropriate. Given tornadoes are associated with the vertical column of strong rotations, the upper levels may need to be refined to further improve TLV predictions. Simulation L65H indicates increasing 16-30 levels may have limited impacts on TLV. When the 11-15 levels in L51 is further refined in L54, the second TLV can be reintensified within a shorter time than L51. Figure 8 shows similar vertical motions and cold pool between L54 and L51 are found near surface at 2215 UTC. Further diagnostics suggest L54 with better resolving upper level mesocyclone reintensify much faster than L51.

b. Sensitivity of Microphysical Schemes to a Refined Vertical Grid Configuration

The predicted TLVs are used in this section to evaluate the sensitivity of microphysical schemes to a refined vertical grid configuration. Figures 9 and 10 provides the simulated TLV with various microphysical schemes using vertical grid configuration of L51 and L54, respectively. Among the 7 schemes, Lin et al., WDM6, NSSL2, and Thompson seem to be more sensitive to the refined vertical configuration. The second TLV is improved with most of these schemes in L54 than in L51. Notice that most of more sensitive schemes are double-moment schemes; while the less sensitive schemes are single-moment ones. These results may indicate the resolved cloud structure using double-moment schemes can be further improved with a refined vertical grid.

c. Initial Test for Dual Resolution EnVar Extended for the Vertical Direction

A single observation test is performed to test the initial implementation of GSI-based vertical dual resolution EnVar system. An observation is placed at 35.30N, -97.78W with 1 km AGL, and the reflectivity observation is set to be 30-dBZ larger than the corresponding background value and has an observation error standard deviation of 5-dBZ. Two experiments are conducted applying same ensemble with the vertical grid configuration of L51. Exp-VDR and Exp-CTL respectively employs the vertical grid of L65L and L51 for control member. To validate the newly extended vertical dual resolution EnVar, the control member of Exp-VDR is directly interpolated from that of Exp-CTL. Therefore, the analyses from both experiments should be almost same for the successfully developed system. The increments for rainwater mixing ratio at 1 km AGL for Exp-VDR and Exp-CTL are respectively shown in Figs. 11a, b. Both experiments exhibit rain water increments that centered on the observation point. Similar increment distributions are produced but a slightly stronger magnitude in Exp-VDR than in Exp-CTL is found. Such increments are also found in vertical increment distributions, which are along zonal direction crossing the observation for both experiments (Figs. 11c, d).

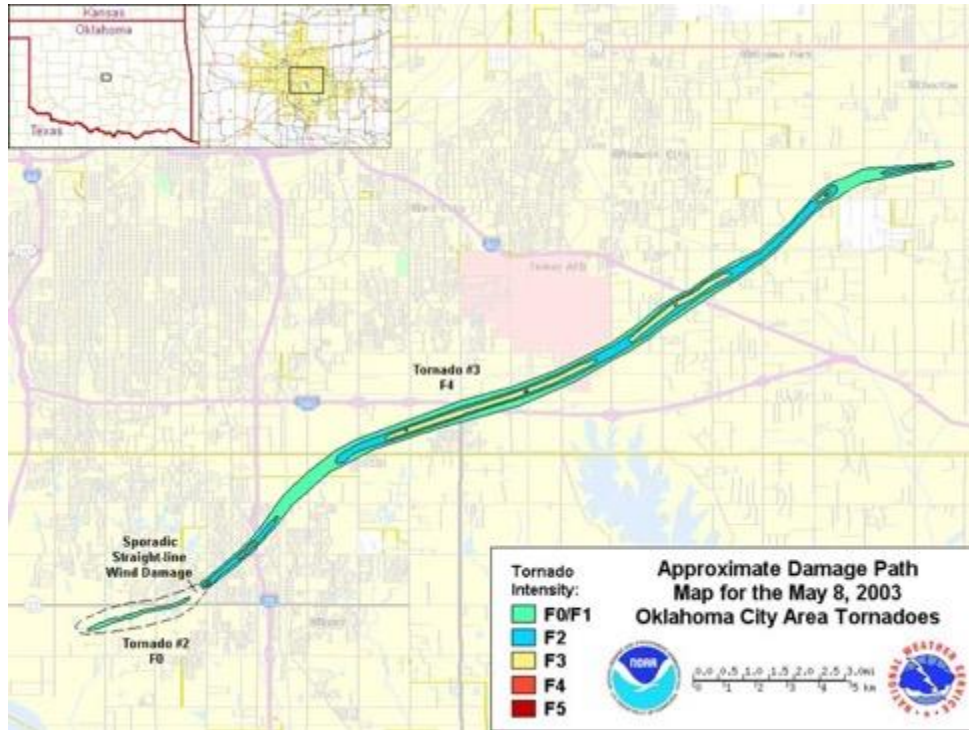


Figure 1. The observed damage path of the 8 May 2003 Oklahoma City (OKC) tornado overlaid on the map of the Moore-south OKC area. Image is obtained from the National Weather Service website, <https://www.weather.gov/oun/events-20030508>

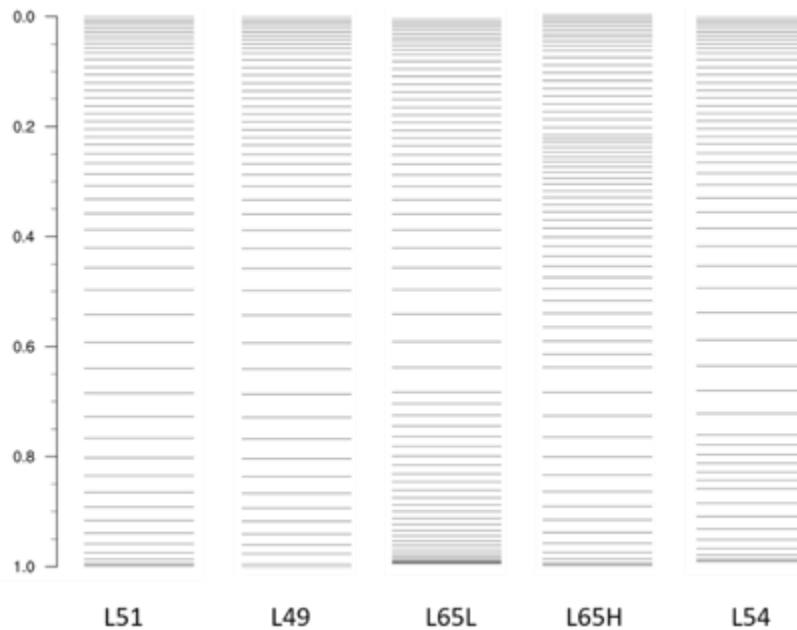


Figure 2. Vertical distributions of eta levels for each sensitivity experiments.

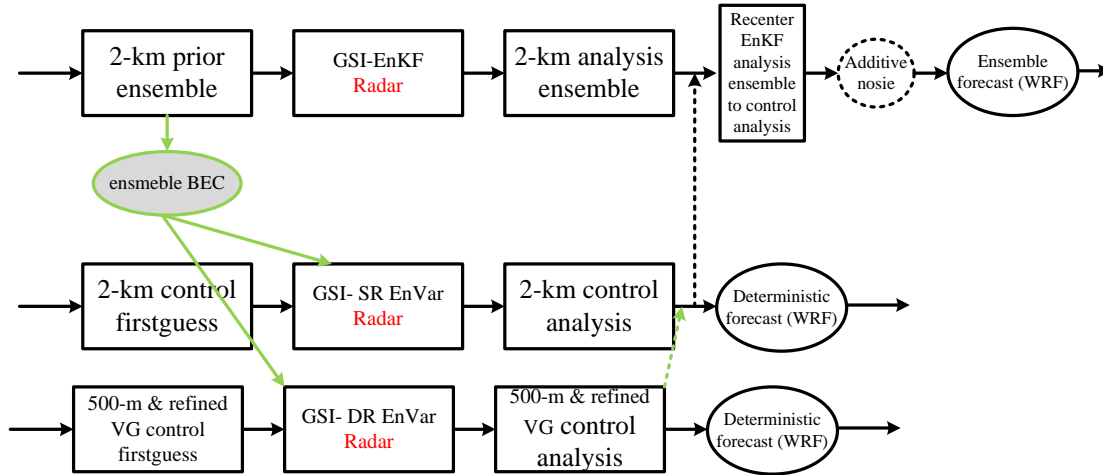


Figure 3. Flowchart of extended dual resolution EnVar system.

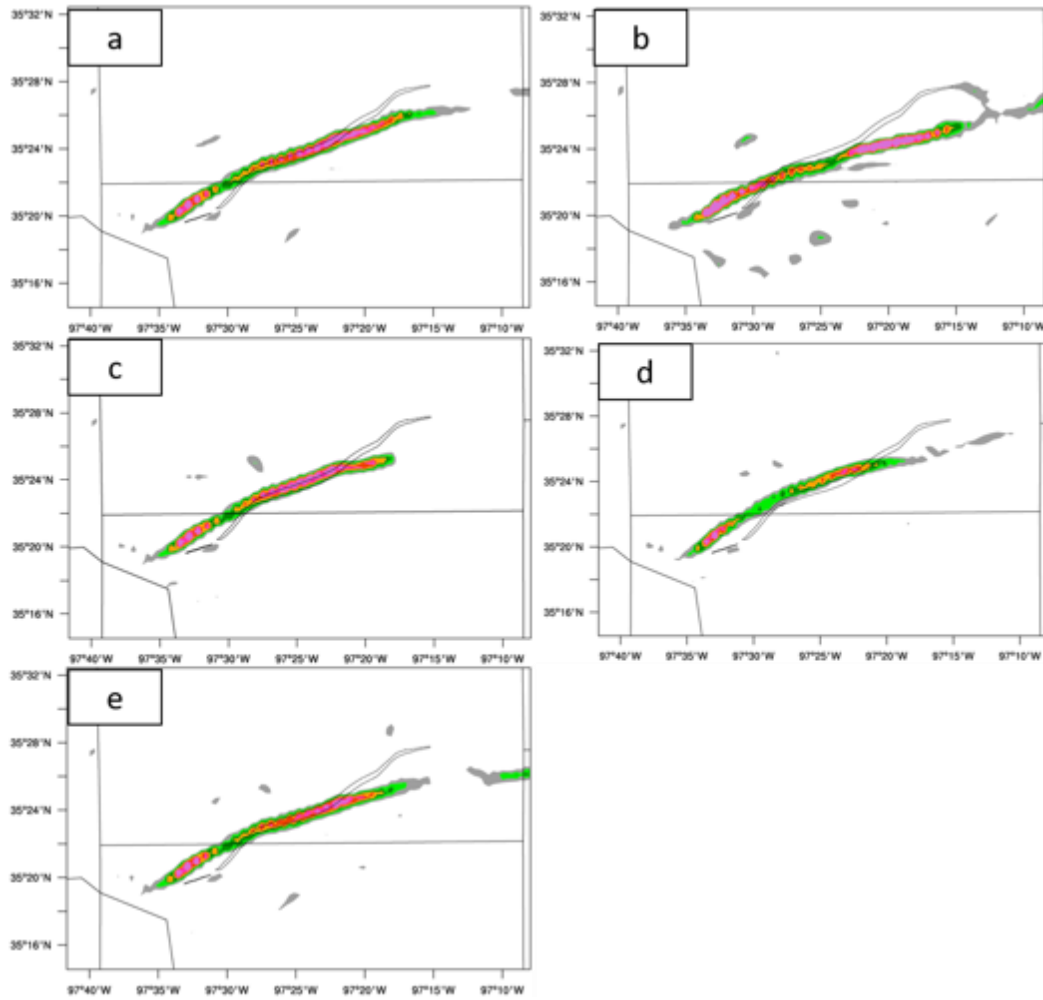


Figure 4. Evolution of the near-surface vertical vorticity associated with the simulated TLVs using vertical grid configuration of L51 (a), L49 (b), L54 (c), L65L (d), and L65H (e) in Fig. 2.

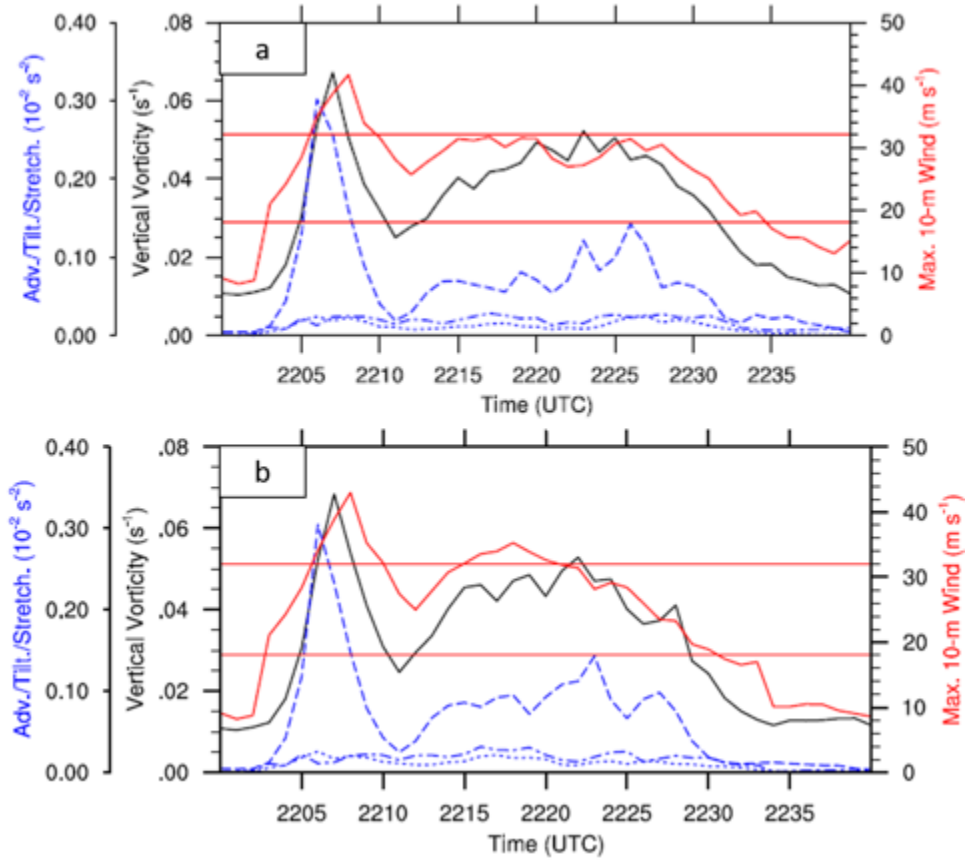


Figure 5. The time-series of maximum 10-m wind speed (red), vertical surface vorticity (black), and maxima of the horizontal advection (dot-dash), tilting (dot) and stretching (dash) terms in the vertical vorticity equation within a 1-km horizontal distance of the peak surface vorticity using vertical grid configuration of L51 (a) and L49 (b) in Fig. 2.

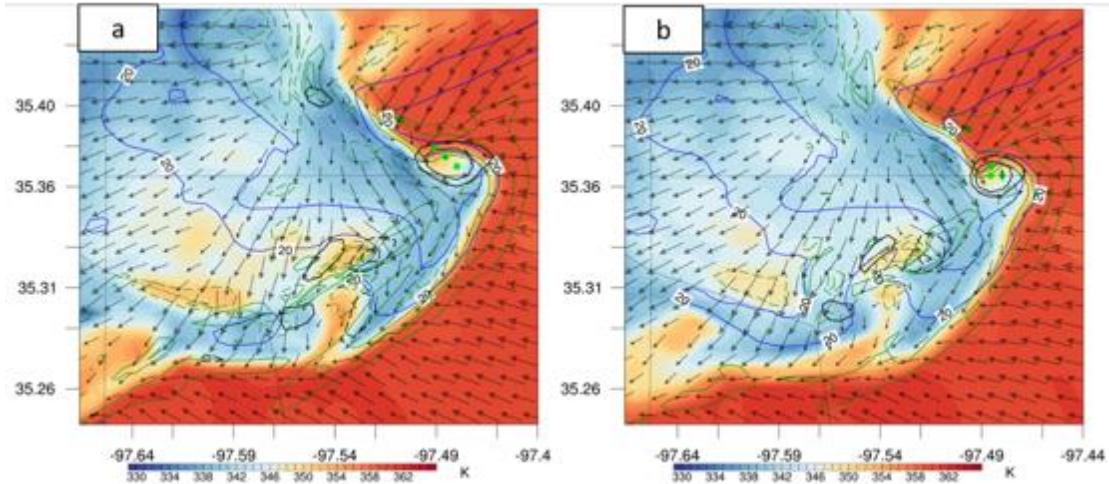


Figure 6. The equivalent potential temperature (colors; K), upward motions (green contours from 1 m s^{-1} to 3 m s^{-1} at 1 m s^{-1} interval; m s^{-1}), and reflectivity (blue contours at 20 and 40 dBZ) near the ground valid at 2212 UTC for simulations using vertical grid configurations of L51 (a) and L49 (b) in Fig. 2.

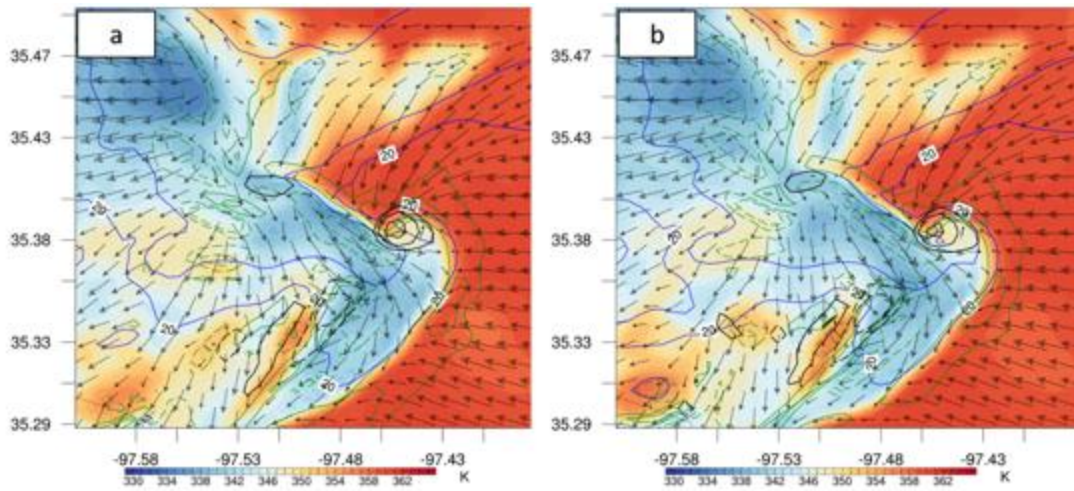


Figure 7. Same as Fig. 6, but valid at 2215 UTC for L51 and L54.

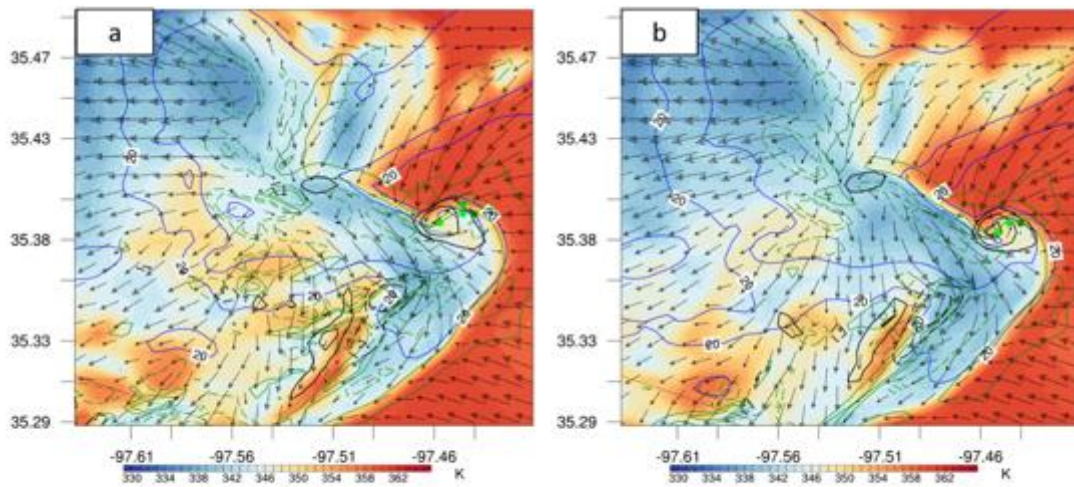


Figure 8. Same as Fig. 6, but valid at 2215 UTC for L51 and L65H.

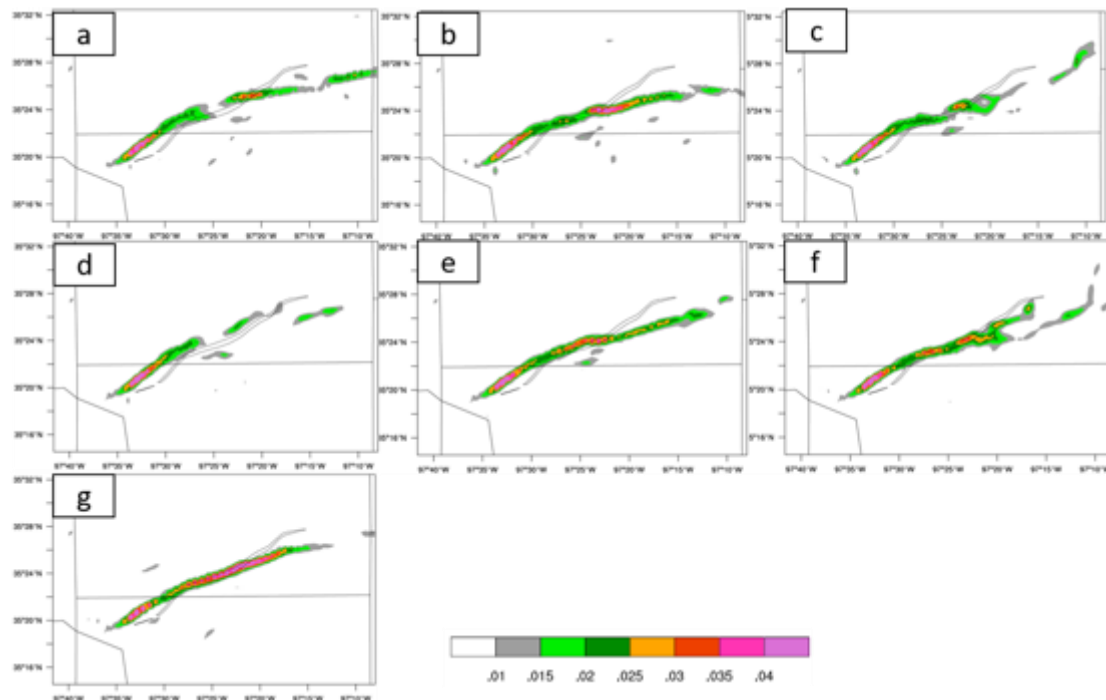


Figure 9. Same as Fig. 4, but for simulations using L51 vertical grid with Kessler (a), Lin et al. (b), WSM6 (c), Morrison (d), WDM6 (e), NSSL2 (f), and Thompson (g) microphysical schemes.

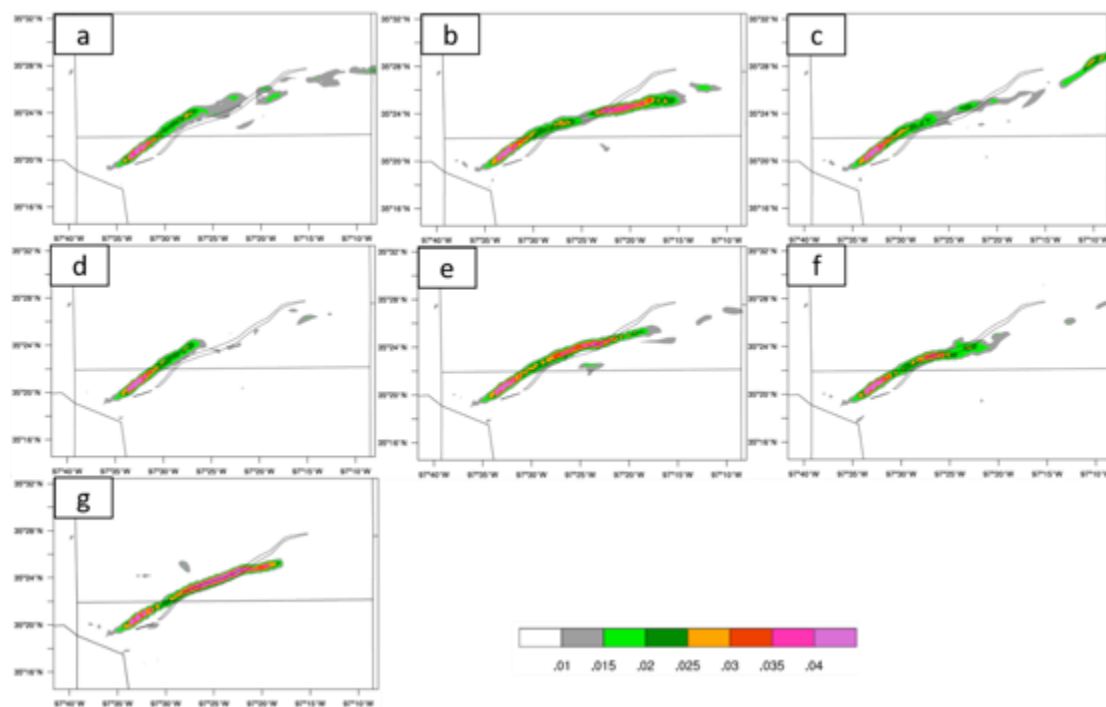


Figure 10. Same as Fig.9 but using L54 vertical grid.

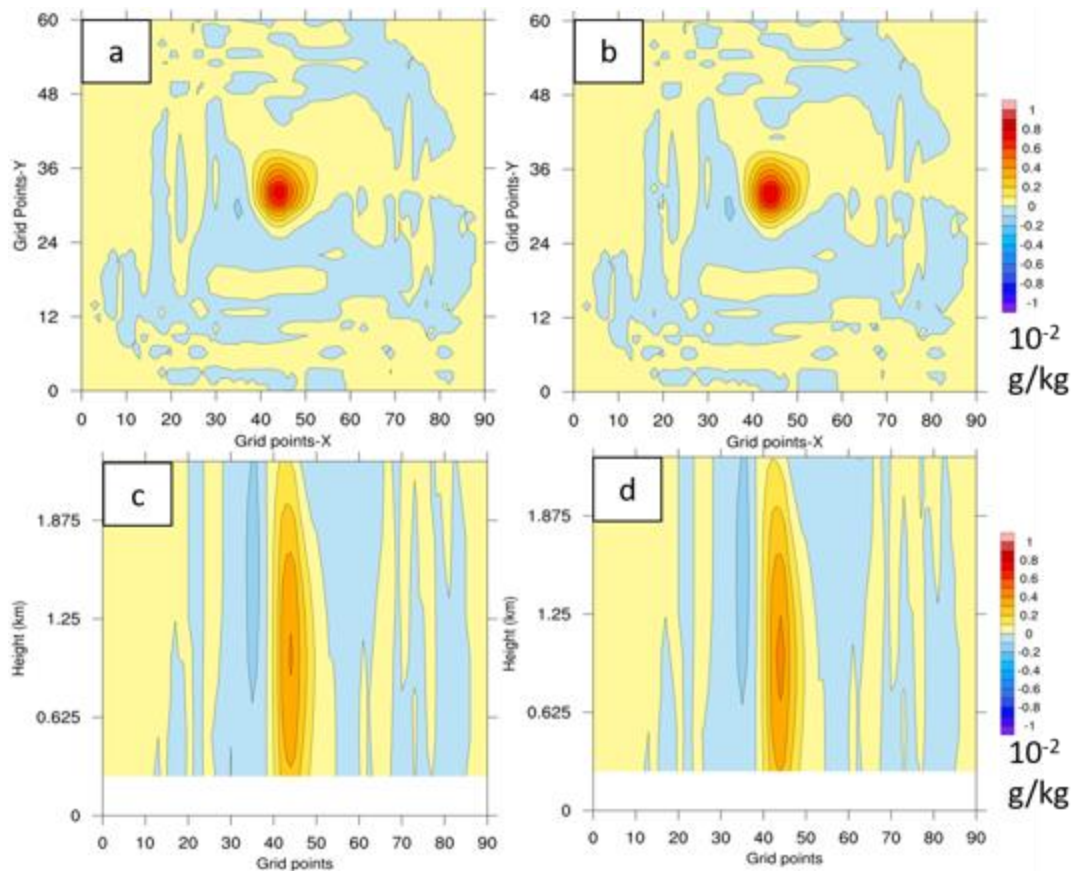


Figure 11. Rain water mixing ratio (10^{-5} kg/kg) resulting from the assimilation of a single reflectivity observation at 1 km AGL (30 dBZ innovation, 5 dBZ observation error) in two experiments with control member and ensemble members at same vertical resolution (a, c) and different vertical grid resolutions (b, d). The horizontal sections at 1 km AGL are shown in a, c. The vertical sections crossing the observation are shown in b, d.

CIMMS Task III Project – Assimilation of High Resolution GOES-R ABI Infrared Water Vapor and Cloud Sensitive Radiances Using the GSI-based Hybrid Ensemble-Variational Data Assimilation System to Improve Convection Initiation Forecast

Xuguang Wang (OU School of Meteorology), Aaron Johnson and Thomas Jones (CIMMS at NSSL), Jason Otkin (University of Wisconsin), and Yanqiu Zhu (NOAA EMC)

NOAA Technical Lead: Pamela Heinselman (NSSL)

NOAA Strategic Goal 2 – Weather Ready Nation: Society is Prepared for and Responds to Weather-Related Events

Funding Type: CIMMS Task III

Objectives

The primary objectives of the project include (a) further extend the GSI EnKF/EnVar DA system for assimilating high resolution GOES-R ABI infrared water vapor and cloud sensitive radiance observations by ingesting convection resolving model's own high-resolution EnKF ensemble rather than the GFS ensemble and by directly updating cloud hydrometeor variables; (b) improve the usage of GOES-R ABI water vapor and cloud sensitive radiances for rapidly updated DA by refining data quality control, using high-resolution infrared land surface emissivity databases and exploring all-sky bias correction and observation error methods, and (c) test different DA configurations and evaluate the impact of assimilating GOES-R water vapor and cloud sensitive radiance observations for the prediction of diverse CI events when combined with ground based observation networks.

Accomplishments

1. Case Selection

A case study from 18 May 2017 is selected for an initial evaluation of the impacts of assimilating GOES ABI data into a convective scale model. The SPC severe reports from this case (Fig. 1) show that this was a high impact event with numerous tornado reports and severe weather occurring over much of the Southern Plains. Of particular interest for this study is the cluster of supercells in northern Texas and southwestern Oklahoma (Figure 2). At 1800 UTC the first weak radar reflectivity echoes are starting to appear in northern Texas (Fig. 2a). Once convective initiation (CI) occurs, the storms develop very rapidly. By 1900 UTC (Fig. 2b) there are several well-established supercells where there were not any high reflectivity values an hour earlier. Between 1900 and 2000 UTC the coverage of storms continues to increase (Fig. 2c) and a few of the stronger cells first become tornadic during this time. By 2330 UTC, the first wave of storms has weakened and moved east into central OK, while a new wave of strong convection occurs along the Red River in southwest OK and north TX (Fig. 2d).

The forecast initialization time for the experiments is selected as 1800 UTC, just before CI. At later initialization times, radar reflectivity observations can help initialize the developing storms into the model. We hypothesize that the high time and space resolution GOES ABI radiances will provide the model with previously unavailable information about not only the mesoscale environment around the incipient storms, but also the convective scale details of the incipient storms even before a clear radar signature appears. Due to the explosive convective development in cases like this, and the rapid organization into tornadic supercells, even small improvements to the CI forecast lead time and the early storm evolution forecast could provide large societal benefits by directly improving NWS warnings and watches.

2. Code Development

Significant code development and testing was undertaken during this reporting period to:

- (a) ingest pre-processed netCDF format GOES ABI observations into GSI
- (b) treat the ABI observations as a new observation type, distinct from previous satellite observations
- (c) properly link to the latest CRTM version 2.3.0.
- (d) further pre-process the ABI radiances
- (e) improve bias correction and QC

3. Development of Pre-Processing Codes

Since the magnitude of the systematic bias of the L1b radiances is more than 6 K less than the previous dataset (in the water vapor channels) for our case study, we developed our own pre-processing software to convert the radiance to brightness temperature for all ten channels, perform thinning of the data to three times the model resolution, and apply parallax correction of the cloudy pixels. Cloud variables from the L2 radiance data set, including Cloud Optical Depth, Cloud Top Height, Cloud Top Pressure, Cloud Fraction and Cloud Probability were also added to the data set and GSI routines were updated accordingly to monitor these additional variables.

4. Development of GSI/EnKF for Improved Bias Correction and QC

The addition of the five additional cloud-related variables in the GSI data structures will allow for more refined cloud-aware bias correction procedures. Quality control routines are also relaxed to properly assimilate all-sky radiances. Based on our previous experiences with radar reflectivity data assimilation, where very large observation minus first guess values can occur with small displacements in/near convective storms, we no longer assume that all observations with significant differences from the first guess should be omitted from data assimilation. The gross error check is therefore increased from 2 K to 20 K. This allows for larger departures of the first guess from good observations that should be kept, while still checking for extreme differences that the data assimilation step would have trouble properly correcting during the present cycle even if the observation is good. This large ob-ges tolerance is especially important for our purpose of improving the prediction of initiating convection because it allows for rapid spin-up of convective storms while the model catches up to the observations. The distribution of observed brightness temperatures at 1710 UTC 18 May 2017 is shown in Figure 3a, while the ensemble mean first guess of all observations without bias correction is shown in Fig. 3b. Figure 4 shows the corresponding innovations only of observations passing the updated quality control checks. The larger ob-ges values that are passing QC show areas where the model is able to be brought closer to the all-sky radiances where large differences between the observation and model first guess are related to deep convection or high clouds, rather than unreliable observations. Although this would of course provide some limited improvement to the CI forecast, additional work to improve the bias correction procedure using non-linear cloud-sensitive methods is also ongoing in order to demonstrate the full potential for ABI infrared radiance assimilation to improve convective scale CI forecasts.

5. Data Assimilation Baseline Experiment

For these experiments, the ensemble is initialized from GEFS and SREF member analyses and 3-h forecasts, respectively at 0000 UTC 18 May 2017. Conventional surface and upper air observations from the NDAS data stream are assimilated hourly from 0100 UTC to 1700 UTC. Convective scale assimilation is then cycled every 10 minutes from 1710 to 1800 UTC. For the “RADAR” experiment, only NEXRAD radar reflectivity (as well as the conventional observations) are assimilated during this one-hour period. As a first test of the new development, an experiment assimilating ABI clear air radiance is designed and performed. For the “GOES_CLEAR_ch9” experiment, the configuration from RADAR is kept the same, except for adding clear air radiances from GOES ABI channel 9 (6.93 micron).

The forecast (initialized at 1800 UTC) from the RADAR experiment is summarized by the 6-hourly ensemble maximum updraft helicity in Figure 5. This figure shows that the baseline experiment without ABI data assimilated does have a reasonable depiction of the regional and mesoscale areas where rotating updrafts, and correspondingly severe weather, were likely. However, as anticipated there are still some notable errors in both the mesoscale organization (e.g., lack of strong helicity in far western Oklahoma due to time it takes model to spin up CI) and the convective scale details (e.g., individual storm tracks and times) that may be improved by assimilating the ABI radiances.

The GOES_CLEAR_ch9 (Figure 6) experiment shows a general increase in helicity values and an extension of the higher helicities southwestward into north Texas. This indicates that even just assimilating the clear air data can improve the mesoscale environment enough to increase the intensity of the forecasted event, which is more consistent with the very intense observed storms. However, further improvement to this forecast is clearly possible. This experiment emphasizes the importance of the cloudy radiances that were omitted, because without the cloud observations included there is no way to initialize the incipient clouds/storms into the model forecast to improve the convective scale details of the individual storm cells.

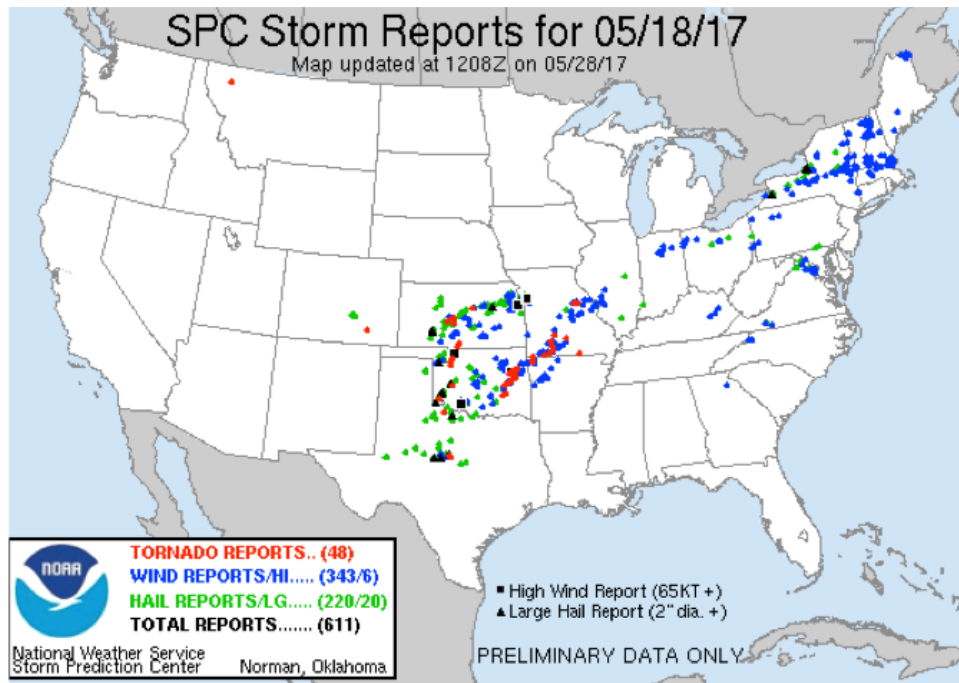


Figure 1: Severe Storm Reports from the Storm Prediction Center (SPC) for 18 May 2017.

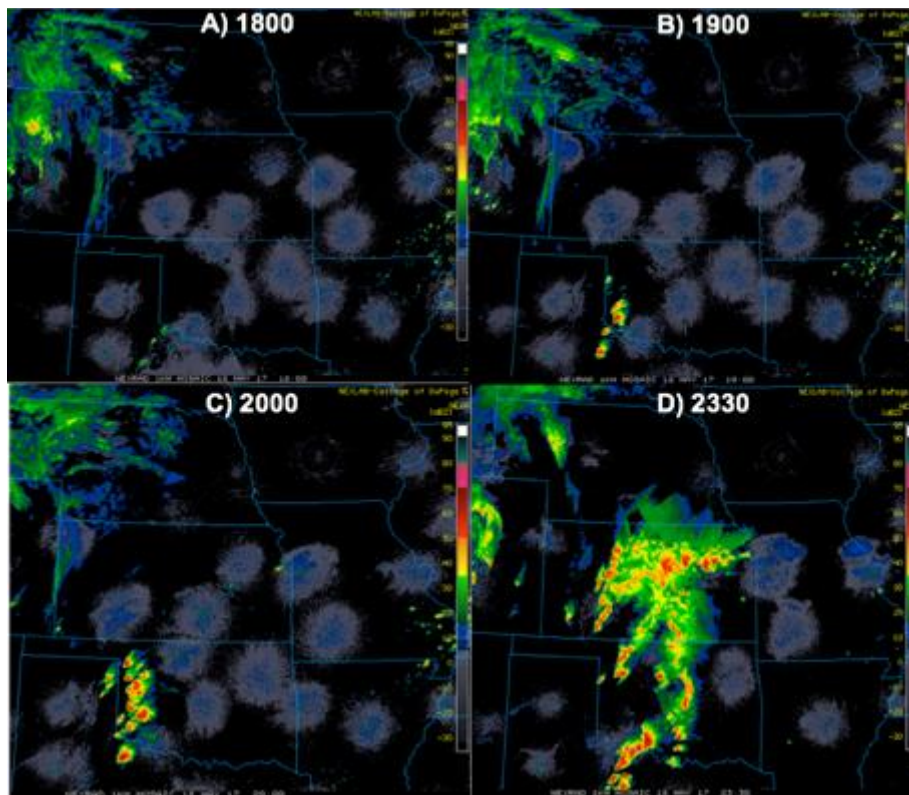


Figure 2: NEXRAD composite reflectivity mosaic on 18 May 2017 at (a) 1800 UTC, (b) 1900 UTC, (c) 2000 UTC and (d) 2330 UTC.

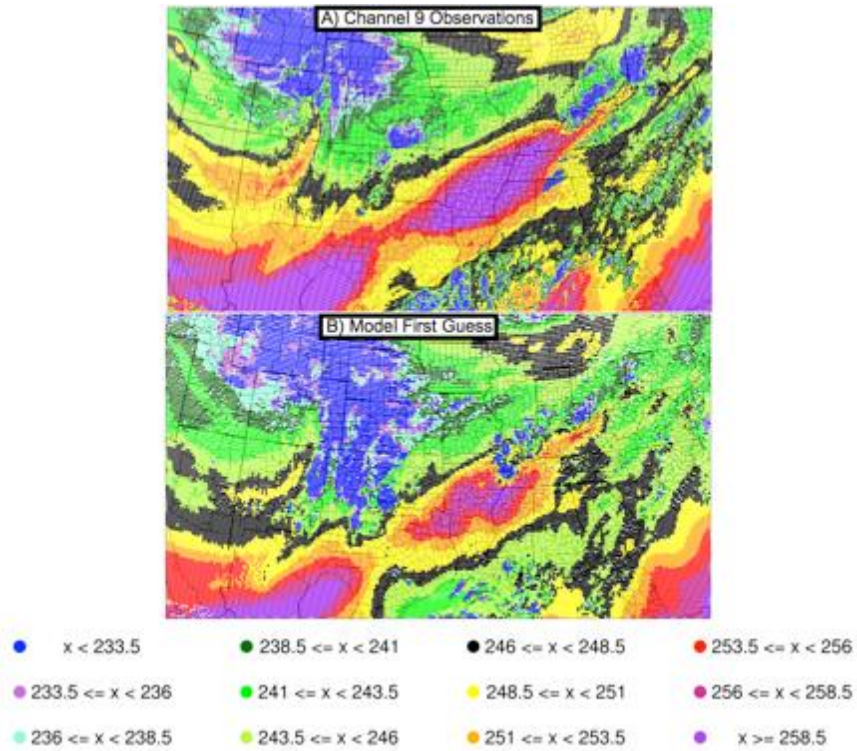


Figure 3. Observation space plot of 6.93 micron ABI channel brightness temperatures (degrees Kelvin) at 1710 UTC 18 May 2017 (a) for the observations and (b) for the ensemble mean model first guess.

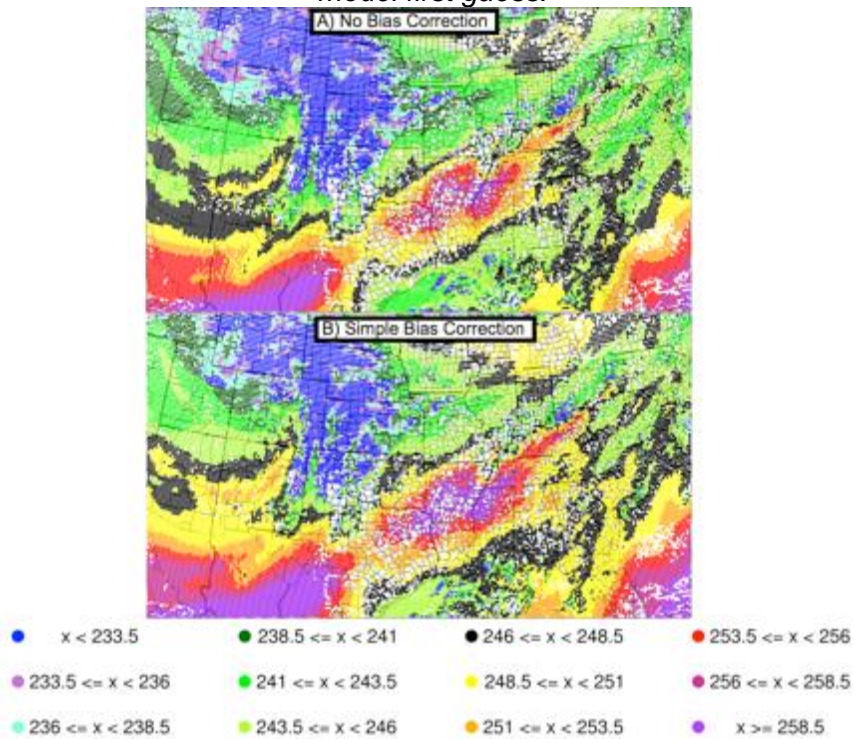


Figure 4. Model first guess of observations assimilated (i.e., passing QC check for large innovations and partial cloudy pixels) (a) before and (b) after applying a standard average bias correction.

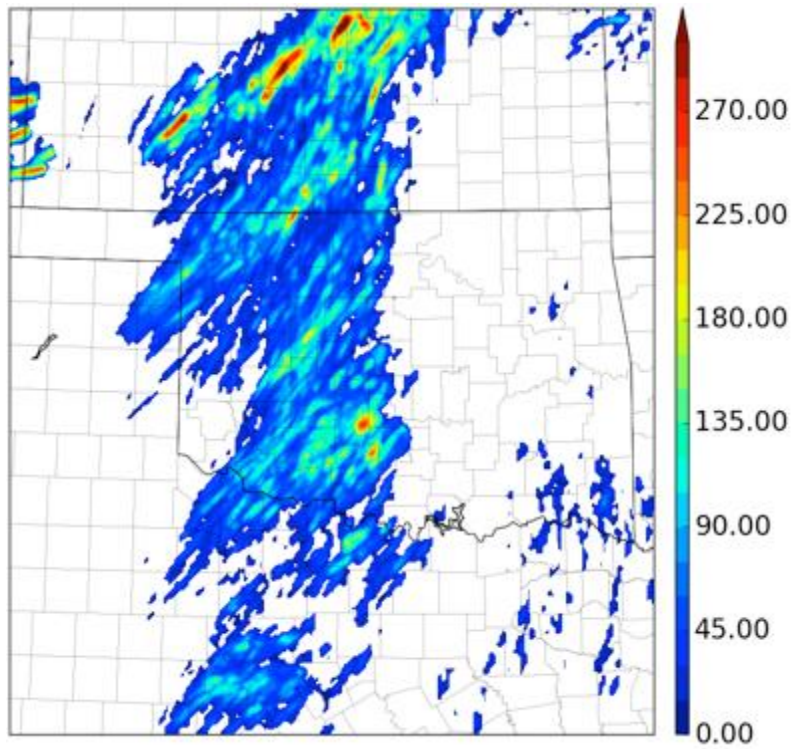


Figure 5. 6-hourly (1800-0000 UTC) ensemble (10 forecast members) maximum of updraft helicity from the baseline forecast without ABI data assimilated.

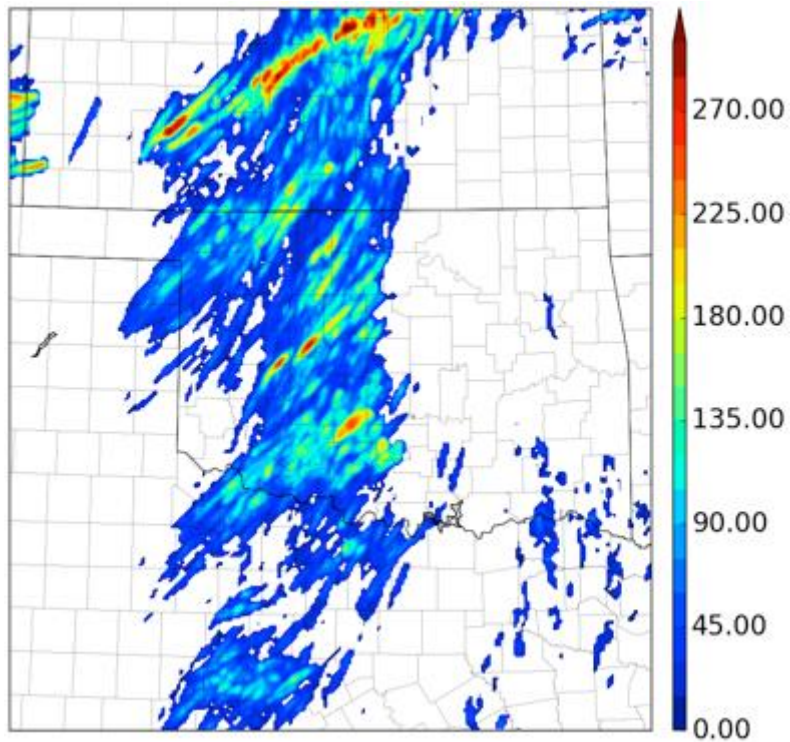


Figure 6. As in Fig. 6, except for the GOES_CLEAR_ch9 experiment with ABI clear air radiances assimilated.

Theme 3 – Forecast and Warning Improvements Research and Development

NSSL Project 5 – Hazardous Weather Testbed

NOAA Technical Leads: Alan Gerard and Pamela Heinselman (NSSL)

NOAA Strategic Goal 2 – *Weather-Ready Nation – Society is Prepared for and Responds to Weather-Related Events*

Funding Type: CIMMS Task II

Objectives

Experimental Forecast Program (EFP) objectives include:

- Evaluate the utility of high-resolution ensemble forecast systems for severe storm guidance at both 3 and 24 hourly time scales;
- Continue improving information extraction from the ensembles and verify high-resolution forecasts.

Experimental Warning Program (EWP) objectives include:

- Evaluate the accuracy and the operational utility of new science, technology, and products in a testbed setting to gain feedback for improvements prior to their potential transition into NWS severe convective weather warning operations;
- Foster collaboration between NSSL and GOES-R scientists and operational meteorologists.

Accomplishments

1. 2018 Spring Forecasting Experiment

Brett Roberts (CIMMS at NSSL/SPC), and Burkely Gallo and Kent Knopfmeier (CIMMS at NSSL)

The 2018 Hazardous Weather Testbed Spring Forecasting Experiment (HWT-SFE) was conducted 30 April - 1 June with nearly 100 participants from the operational and research meteorological community. The primary emphasis of the 2018 HWT-SFE focused on the generation of probabilistic hazard forecasts on short (0-4 h) time periods. The primary goal of the experimental forecasts created by HWT-SFE participants is to add temporal and spatial specificity to the longer-term outlooks currently issued by the Storm Prediction Center (SPC). For the third year, a suite of 3-km convection-allowing modeling systems (CAMs) called the Community Leveraged Unified Ensemble (CLUE) was utilized to create these forecasts. In addition, the coordinated framework of the CLUE permitted the design of carefully controlled experiments to aid in the identification of optimal configuration strategies for operational CAM-based ensembles.

In addition to a 1600 to 1200 UTC outlook created during the morning to mimic the operational SPC Day 1 Convective Outlook, new timing products called potential severe timing areas (PSTs) were created. PSTs highlighted the 4-h periods when severe weather was expected to occur. Groups of participants generated PSTs using different subsets of the CLUE, allowing participants to explore the experimental model data more thoroughly than in previous experiments. The PSTs were then updated during the afternoon using newly available CLUE guidance, newly available operational model guidance, and/or observational data.

Two types of formal evaluations were completed during the 2018 HWT-SFE, looking at either experimental forecast products or model output fields. The experimental product evaluations had participants compare their forecasts to observed radar reflectivity, local storm reports, NWS warnings, and Multi-Radar Multi-Sensor (MRMS) radar-estimated hail sizes over the same valid time periods and subjectively evaluate the strengths and weaknesses of their forecasts. Some experimental outlooks were also objectively verified and participants could compare their subjective impressions to quantitative metrics such as the fractions skill score (FSS). The goal of the experimental product evaluation was to determine the relative skill of the human-generated forecasts, and therefore evaluate the viability of issuing high-temporal resolution severe weather outlooks. The second formal evaluation type examined different ensemble diagnostics and CLUE subsets. Subjective comparisons were made between CLUE subsets with differing physics configurations and microphysical schemes, between different configurations of the High-Resolution Ensemble Forecast system (HREF), and between the global and high-resolution versions of the Unified Model provided by the UK Meteorological Office. Another evaluation of particular interest documented the forecast sensitivity of the Finite Volume Cubed-Sphere (FV3) model to physics parameterization choices using eleven different members (provided by the Center for the Analysis and Prediction of Storms) by examining thermodynamic fields, reflectivity, updraft helicity, and atmospheric soundings. Finally, an ensemble object-based verification evaluation, which analyzed storm mode and morphology, was led by the OU-Multi-scale Data Assimilation and Predictability (MAP) group.

HWT-SFE activities have been conducted primarily through a series of web-based applications for several years. For 2018, these applications were overhauled and consolidated into a more unified package than the versions used in previous years. One major new feature was the integration of the forecast-issuing interface into the main data-viewing interface, allowing participants to draw forecast products on top of any HWT-SFE dataset (Fig. 1). Participants' exploration of the data was greatly aided by the this interface. Another major feature addition was the display of real-time verification statistics for several NWP datasets. These statistics were computed in collaboration with the Developmental Testbed Center using their Model Evaluation Tools (MET) software package (Fig. 2).

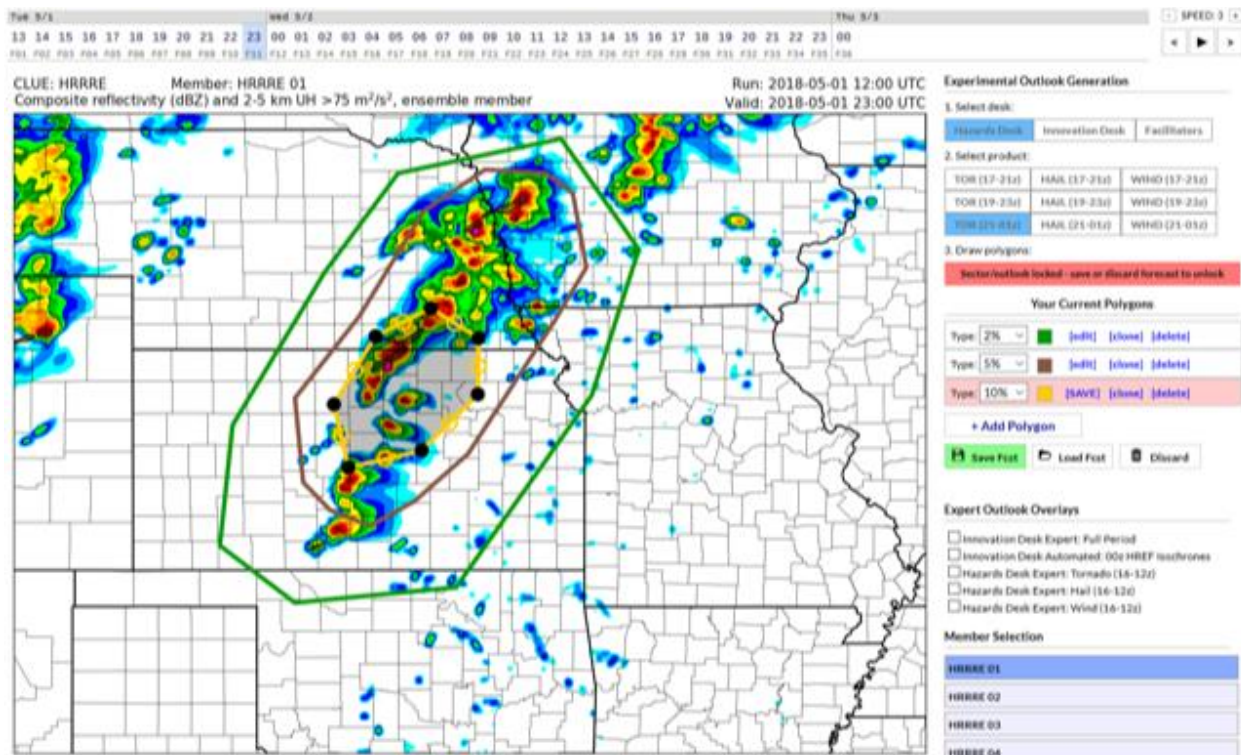


Fig. 1. SFE 2018 web interface for participants to view data and create experimental forecast products.

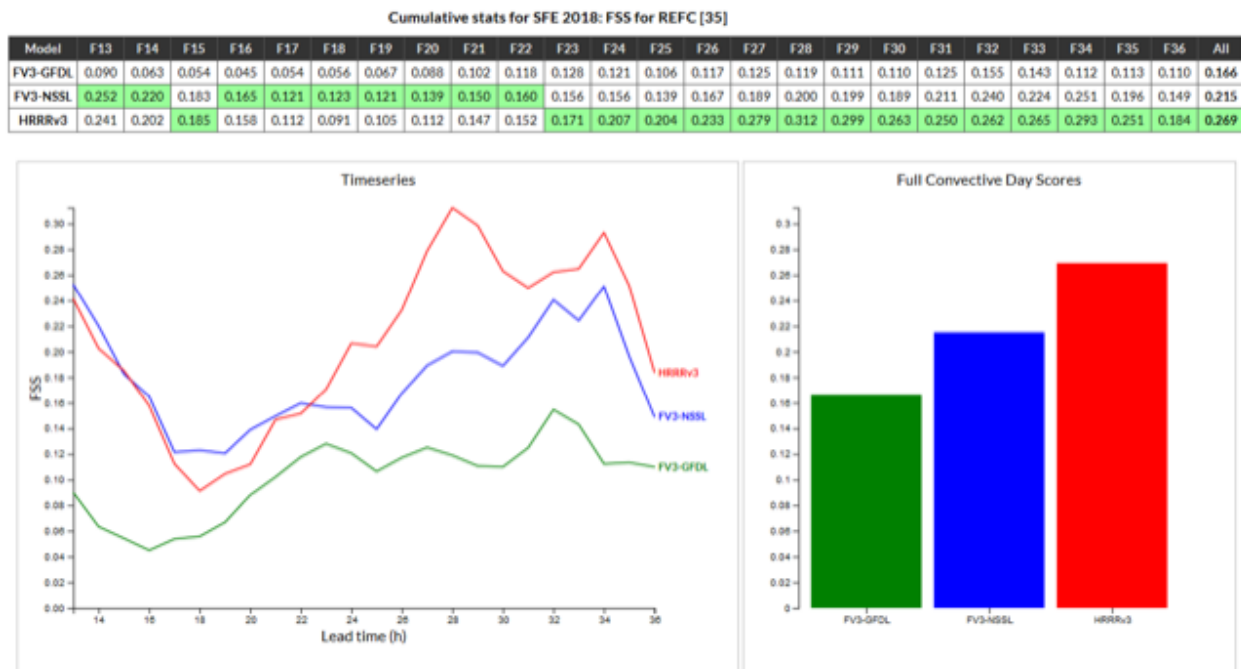


Fig. 2. Example of real-time verification statistics for NWP datasets displayed on the SFE website.

2. Spring Forecast Experiment NEWS-e Activity

Katie Wilson (CIMMS at NSSL), Pamela Heinselman (NSSL), Patrick Skinner, Jessica Choate, and Burkely Gallo (CIMMS at NSSL), Adam Clark (NSSL), and Kim Klockow McClain and Kent Knopfmeier (CIMMS at NSSL)

The Spring Forecast Experiment provides opportunity for testing of NEWS-e forecast guidance in real time during the severe weather season. During FY18, the Warn-on-Forecast team at NSSL/CIMMS has (1) analyzed responses from a 2017 SFE survey to investigate meteorologists' interpretations of storm-scale ensemble-based forecast guidance, and (2) collaborated with the 2018 SFE Innovation Desk to test and evaluate NEWS-e forecasts during the issuance of severe weather outlooks. The first accomplishment is based on the analysis of 20 questions designed to test 62 meteorologists' understanding of probabilistic and percentile representations of forecast uncertainty. Presented with a mix of multiple-choice and open-ended questions, respondents were required to make sense of, extract information from, and explain graphics depicting meteorological variables. Respondents were also required to combine probability and percentile representations of meteorological variables to decipher the nature of the weather event (e.g., high/low probability with a high/low consequence; Fig. 1). Using frequency counts for multiple-choice questions and thematic coding methods for open-ended questions, 60%–95% of participants' responses aligned with the researchers' intended responses. The most challenging questions proved to be those requiring qualitative explanation (e.g., what does the 70th percentile value of accumulated represent in an ensemble-based probabilistic forecast?). Additionally, participants providing answers not aligning with the intended response oftentimes appeared to consider the given information with a deterministic rather than probabilistic mindset. A manuscript describing the methods and findings of this survey is currently in preparation for submission to an AMS journal.

In the most recent 2018 SFE, data collection efforts were focused on the NEWS-e activity that was conducted 3–4pm during each day of the five-week experiment. Beginning with a training session each Monday 3–4pm, participants were provided with an overview of Warn-on-Forecast and the related NEWS-e website and forecast products. To become familiar with the NEWS-e activity, participants then worked in small groups with a researcher to practice navigating the NEWS-e website and issue outlooks. During the actual activity on Tue–Fri, participants worked in small groups with one of the two Innovation Desk facilitators (Burkely or Adam) to issue two 1-hour total severe outlooks (2100–2200 UTC and 2200–2300 UTC) using the 1900 UTC NEWS-e forecast, which were then updated using the 2000 UTC NEWS-e forecast. Group assignment was based on participants' subjective assessment of their own forecasting experience. To balance operational expertise, we aimed to include professional forecasters in both groups. In addition to the outlooks generated, both survey data and product usage data were collected. The survey data captured forecasters' perceptions of the NEWS-forecast performance both during the preliminary outlook issuance, final (updated) outlook issuance, and verification of the outlooks the following morning. The product usage data will give insight into the type of NEWS-e products participants

attend to most frequently. Our next steps will be to analyze these three date sets, and to explore differences in participants' perceptions and use of NEWS-e forecast guidance for the range of weather events sampled during the 2018 SFE. Finally, one researcher worked solely with a retired SPC forecaster, Jack Hales, to collect outlook, survey, and product usage data throughout each day of the experiment. These data will also be analyzed to assess trends in NEWS-e usage behavior from the perspective of an experienced forecaster.

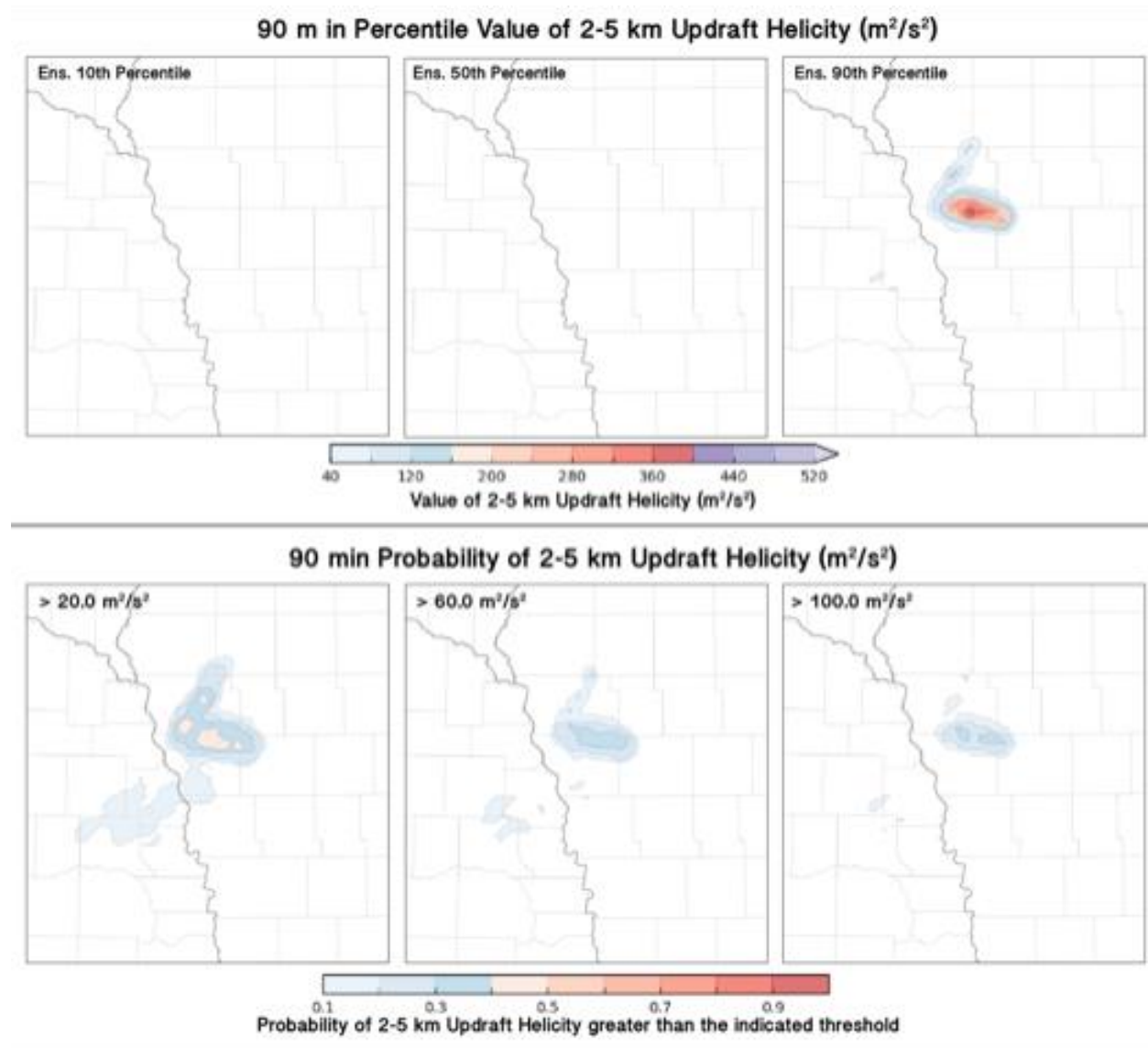


Figure 1. (top row) Percentile and (bottom row) probability swaths of 2–5 km updraft helicity (m^2/s^2) for storms A and B.

3. Initial Development and Testing of a Convection-Allowing Numerical Weather Prediction Scorecard

Burkely Gallo (CIMMS at NSSL), Adam Clark (NSSL), Israel Jirak (SPC), Brett Roberts (CIMMS at NSSL/SPC), and Tara Jensen and Christina Kalb (NOAA DTC)

Evaluation of numerical weather prediction (NWP) is critical for determining strengths and weaknesses of the NWP, as well as highlighting aspects that need improvement. However, standardized evaluation metrics for convection-allowing models (CAMs) do not yet exist, hindering the effort to broadly compare high-resolution NWP and advance the field as a whole. A CAM-based scorecard composed of metrics relevant to severe convective weather forecasting was developed and implemented for the 2018 Spring Forecasting Experiment (SFE). This scorecard was developed using the Model Evaluation Toolkit (MET). Model output fields that were evaluated using MET include the composite reflectivity and surrogate severe fields generated using updraft helicity. Output from three deterministic CAMs (the Finite Volume Cubed [FV3] from NSSL and GFDL and the high-resolution rapid refresh [HRRR] model) and two CAM ensembles were analyzed during the five-week experiment. Preliminary results show that the GFDL-FV3 had a significantly lower Fractions Skill Score than the HRRR and the NSSL-FV3 at all reflectivity thresholds during most forecast hours (Fig. 1). Composite reflectivity guidance at most forecast times from the NSSL-FV3 and the HRRR did not perform significantly differently (Fig. 2). Further work is being done to determine the most relevant analyses to include on the scorecard and apply the scorecard framework to more NWP.

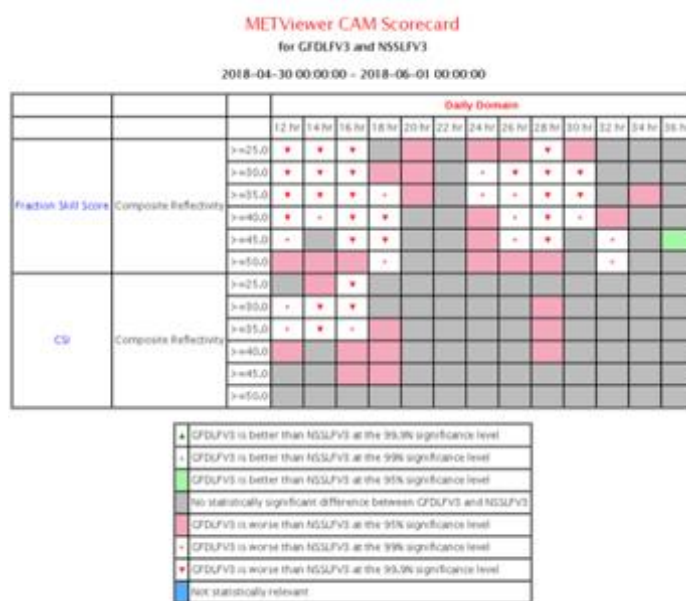


Figure 1. Scorecard summarizing composite reflectivity scores every two hours for the GFDL-FV3 and the NSSL-FV3 for 12–36 h forecasts.

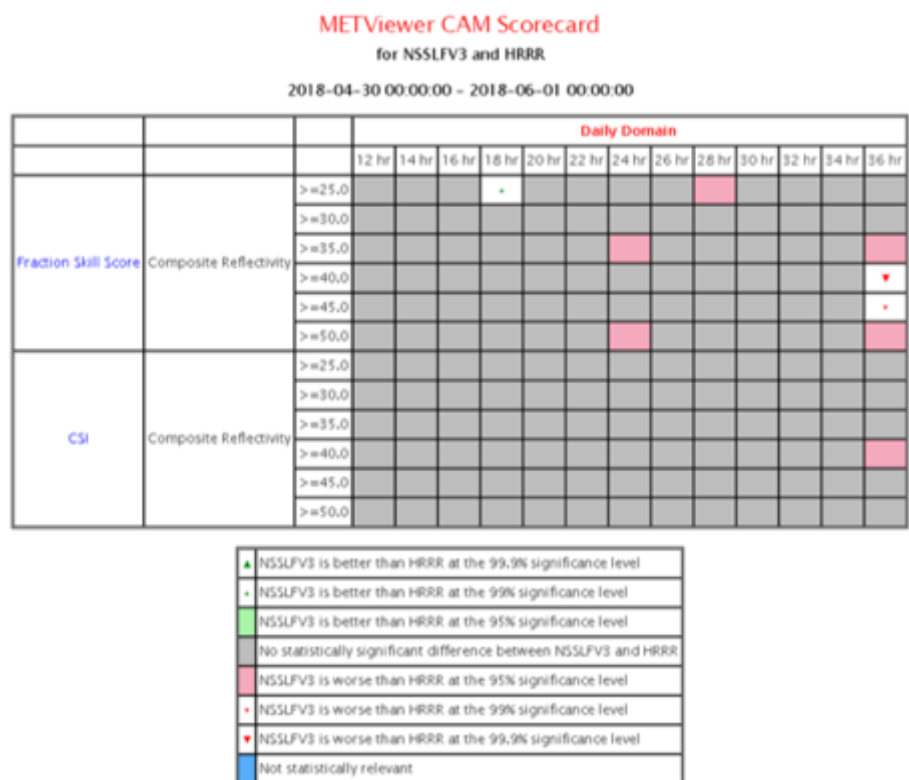


Figure 2. Scorecard summarizing composite reflectivity scores every two hours for the NSSL-FV3 and the HRRR for 12–36 h forecasts.

4. Geostationary Lightning Mapper Product Development and Evaluation

Kristin Calhoun, Tiffany Meyer, and Adrian Campbell (CIMMS at NSSL)

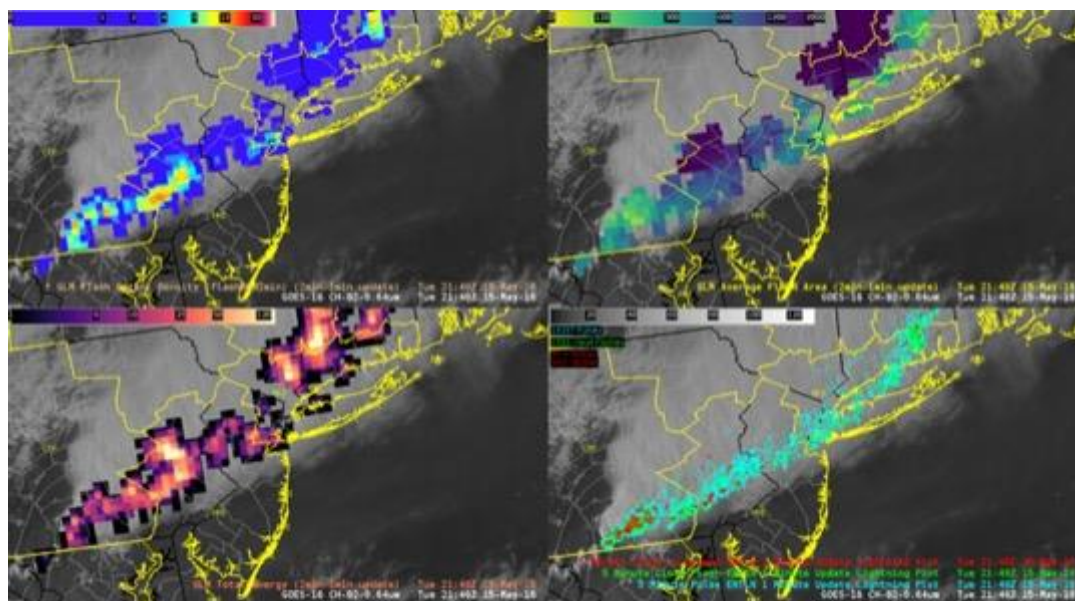
The Geostationary Lightning Mapper (GLM) was introduced to National Weather Service (NWS) forecasters and broadcast meteorologists as part of the 2018 Hazardous Weather Testbed (HWT) and GOES/JPSS Proving Ground Spring Experiment. Throughout the month of May, forecasters evaluated the GLM products in the context of live severe and hazardous weather issuing regional discussions, special weather statements, and warnings; forecasters provided feedback through surveys, live blogs, and lightning scientists. The 2018 GLM products were developed based upon forecaster feedback from the 2017 HWT and Operations Proving Ground evaluations and through previous research focused on visualizing the spatial and temporal applications of total lightning data.

Initial products in 2018 included (all at 1-min with 1-min updates): Flash Extent Density, Event Density, Group Extent Density, Average Flash Size, Average Group Size, Total Optical Energy, Flash Centroid Density and Group Centroid Density. Immediate feedback early in the experiment resulted in the creation of 5-min and 2-min summary products (with 1-min updates) to provide forecasters a better visualization of lightning trends over time. Forecasters highly utilized the 5-min Flash Extent Density (with one-

min updates) as the primary GLM product. For deeper storm interrogation, storm-electrification understanding, and spatial coverage prediction forecasters also gravitated to the Average Flash Size and Total Optical Energy products at 5 min totals (with one-minute updates). Other products such as the Flash Centroid Density were not highly utilized by forecasters in an operational environment but will likely see use in data fusion applications that incorporate flash rates and for data assimilation efforts into convective allowing models such as the High-Resolution Rapid Refresh (HRRR).

Based on feedback and survey results from 2018, we have three recommendations regarding operational implementation of the GLM data:

1. Flash Extent Density, Average Flash Size, and Total Optical Energy products (5 min and 1 min products both with 1 min update) are a minimal baseline for operational display of the GLM data within NWS. The products mutually reinforce one another, promoting forecaster confidence and clear thinking about storm processes.
2. Due to the inherent use of the data within rapidly changing environments, the latency of the product needs to be consistently no more than 1-2 min maximum.
3. Increased training opportunities need to be provided to forecasters at the time of the operational implementation beyond previous required training modules and quick guides. These training modules should be developed with a regional and applied focus, allowing forecasters to participate in *active* and practical training options in context of other data and within local, real weather events. In addition to storm-growth and severe-storm-interrogation, training should address likely GLM uses such as Decision-Support Services and lightning safety, fire weather, aviation warnings and use over radar-sparse regions.



Flash Event Density (top left), Flash Size (Top right) and Total Energy (lower left) from GLM and ground-based lightning detections from Earth Networks Total Lightning Network (ENTLN) at 2140 on 15 May 2018.

5. Warn-on-Forecast in the NOAA HWT Hydrometeorology Testbed

Katie Wilson, Nusrat Yussouf, and Steve Martinaitis (CIMMS at NSSL), Jonathon Gourley (NSSL), Humberto Vergara-Arrieta, Andres Vergara-Arrieta, and Tiffany Meyer (CIMMS at NSSL), and Alex Zwink (CIMMS at WDTD)

The 2018 Hydrometeorology Testbed – Hydro (HMT-Hydro) took place over three weeks during June and July 2018. Split into real time operations and archived case playback, each week provided forecasters with an opportunity to test and evaluate new products for flash flood prediction. In particular, the archived case playback activities were designed to investigate the strengths and limitations of flash flood prediction tools from a hydrologic model that is forced by either only quantitative precipitation estimates (QPE) or a combination of QPE and ensemble quantitative precipitation forecasts (QPFs). These ensemble QPFs were obtained using the Warn-on-Forecast prototype system, NEWS-e (NSSL Experimental Warn-on-Forecast System for ensembles). Over two days per week for three weeks, participants evaluated either two or three weather events (N=10 participants for two cases and N=7 participants for one case) (Fig. 1). Evaluations focused on obtaining feedback about the usefulness and potential application of deterministic forecast guidance (condition 1), QPE-forced probabilistic forecast guidance (condition 2), and combined QPE-QPF-forced probabilistic forecast guidance (condition 3). The first two conditions provided guidance only valid at the top of the hour, while the third condition provided guidance valid out to 3 hours. At the top of each forecast hour, participants independently cycled through viewing guidance for the three conditions and answered a set of questions designed to elicit what information they found useful, how they perceived the current and future flash flooding threat, and whether they felt actionable decisions were justified. Analysis of these qualitative data will provide insight into what utility probabilistic forecast guidance has over the traditional deterministic forecast guidance for flash flooding. Finally, transcriptions from group discussions held at the end of each week will be analyzed to identify and summarize participants' initial impressions and suggestions for use of probabilistic forecast guidance for flash flood prediction.

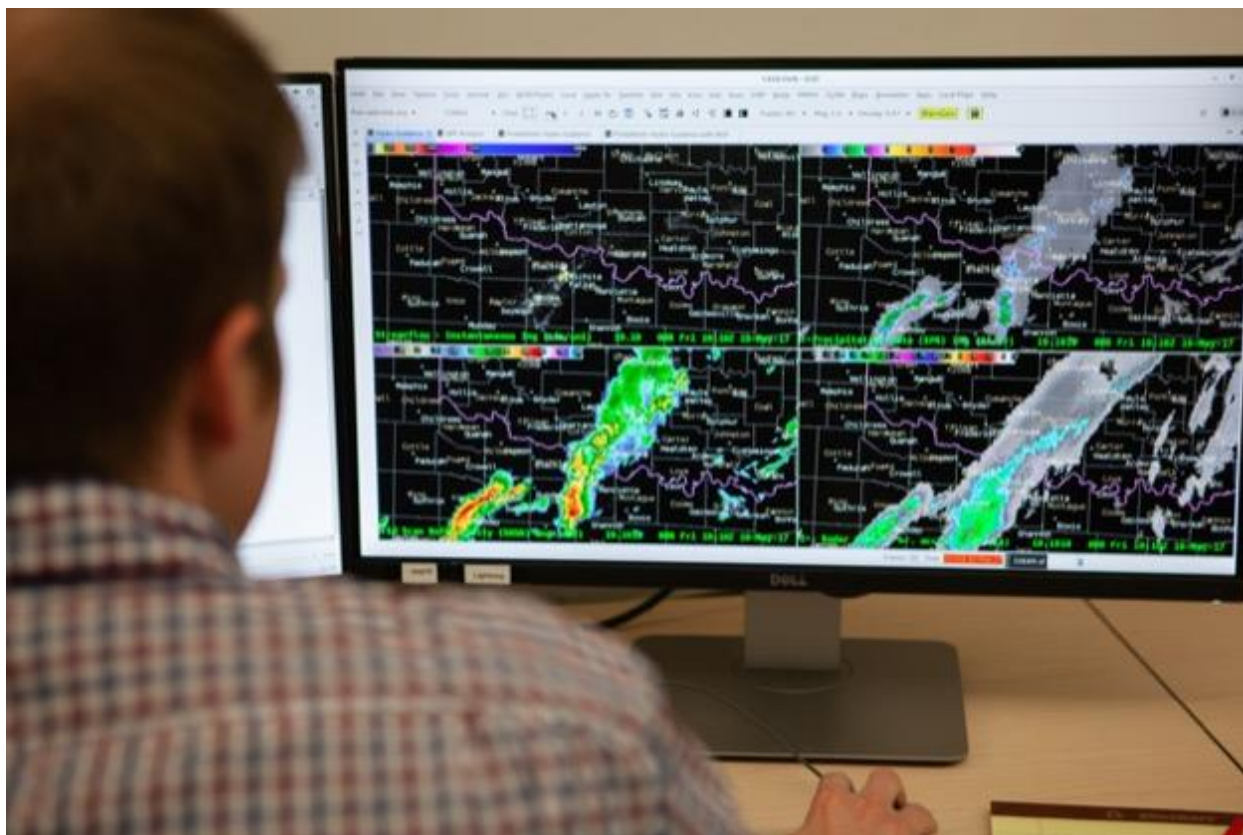


Figure 1. Participant evaluating flash flood prediction products in archived case study mode during the 2018 HMT-Hydro.

6. Phased Array Radar Innovative Sensing Experiment (PARISE)

Katie Wilson (CIMMS at NSSL), Pamela Heinselman (NSSL), Charles Kuster (CIMMS at NSSL), and Ziho Kang (OU ISE)

Data collected from the 2015 Phased Array Radar Innovative Sensing Experiment (PARISE) was analyzed during FY2018. First, a qualitative analysis of six focus groups was completed. This analysis was based on feedback from thirty forecasters and explored a number of considerations related to 1) forecasters' use of rapidly-updating radar data during experimental simulated warning operations, and 2) how forecasters envision these data being successfully integrated into warning operations in the future. Second, data from an eye-tracking experiment conducted during the 2015 PARISE were analyzed. These data were collected while forecasters worked a weather scenario (Fig. 1) and were used as an objective supplement to forecasters' retrospective recall data. Using both AOI bulk fixation measures and MultiMatch scanpath similarity scoring methods, forecasters' eye movements were compared to one another. Treating radar data temporal resolution as the independent variable, this eye-tracking experiment aimed to investigate whether statistically significant differences exist between two groups using either 1-min or 5-min radar updates. While such differences were not observed, analysis of these data demonstrated how forecasters' eye movements can be

used to reveal differences in how they interact with the radar display and warning interface, identify instances in which technological challenges emerged, and provide evidence of forecasters' varying approaches to similar tasks. Analyzed in conjunction with video and retrospective recall data, this eye-tracking study provides support for mixed-methods approaches for detecting and understanding individual differences in forecasters' eye movements and subsequent distributions of attention. We believe that such an approach would be particularly useful in usability studies that aim to improve the human-computer interaction experience of weather forecasters.

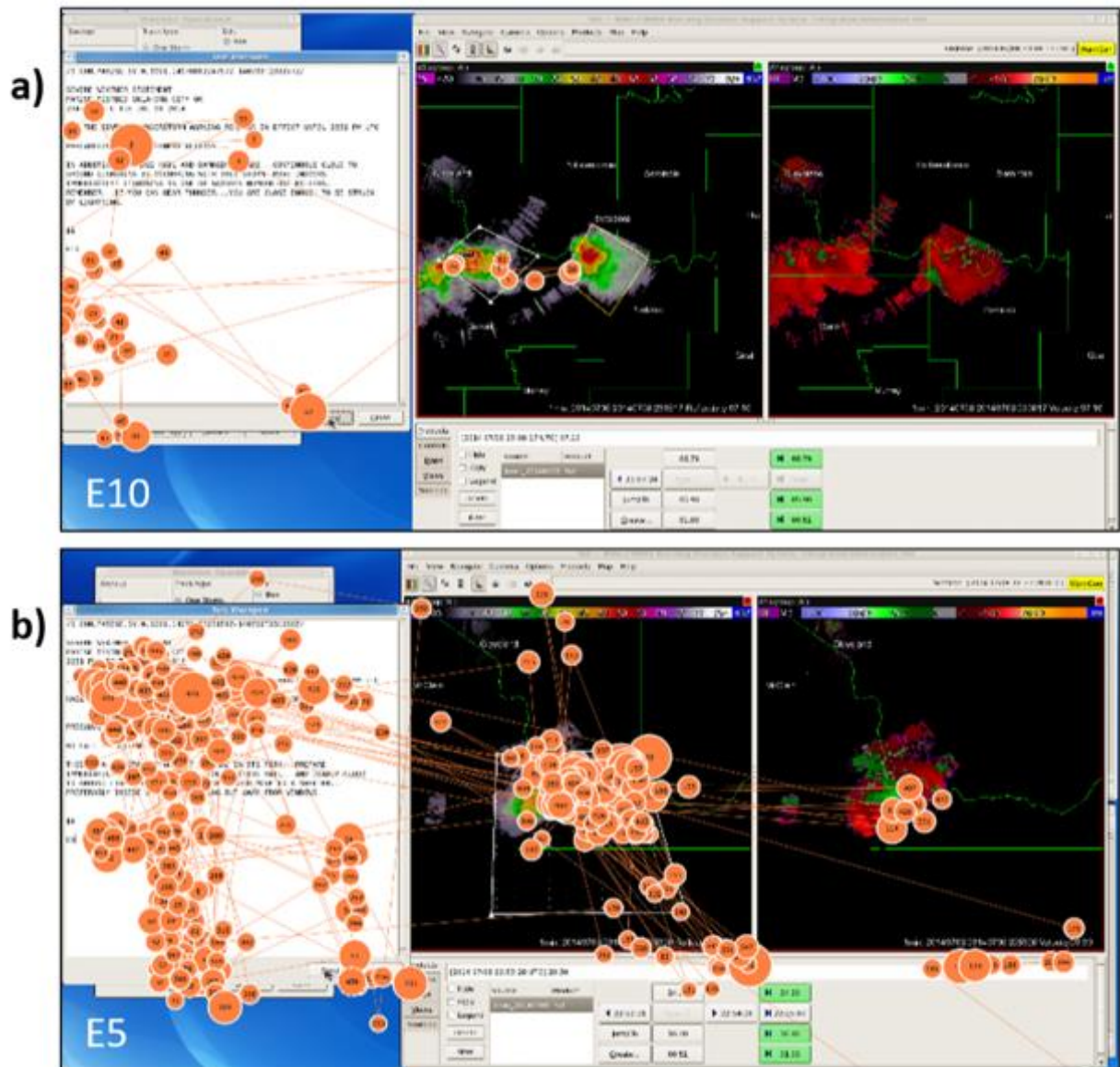


Figure 1. Gaze plots depicting the scanpaths of participants (a) E10 and (b) E5 during the issuance of a severe thunderstorm warning.

7. Executive Officer of the Hazardous Weather Testbed

Kodi Berry (CIMMS at NSSL)

The Executive Officer of the Hazardous Weather Testbed (HWT) served as a coordinator across all experiments conducted in the HWT, including: Hazard Services-Probabilistic Hazard Information, Spring Forecasting Experiment, JPSS/GOES Convective Applications, Probabilistic Hazard Information Prototype, and Hydrometeorology Testbed (HMT) - Hydro. More than 140 forecasters, broadcasters, emergency managers, and researchers participated over 13 weeks during the spring and summer of 2018. The HWT Executive Officer's coordination activities included experiment planning, facility management, participant recruitment, participant selection, and logistics planning. Key accomplishments include:

- Participated in NOAA's Testbed and Proving Ground Coordination Committee workshop and meetings
- Attended planning meetings with lead project scientists
- Managed experiment schedules
- Coordinated test plans for NOAA-funded projects
- Approved progress reports and test plans for NOAA-funded projects
- Developed and distributed participant recruitment letters
- Collaborated with NOAA managers to recruit participants
- Oversaw participant application process
- Coordinated across participant selection committees
- Coordinated travel logistics for participants
- Coordinated participant facility access with NOAA and University security
- Provided pre-experiment information to participants
- Observed experiment operations
- Coordinated and provided interviews for NSSL Bite-Sized Science videos
- Coordinated with the A/V Specialist to capture videos and photographs of each experiment
- Updated the HWT website

8. Technical Advisor to the Hazardous Weather Testbed Experimental Warning Program

Tiffany Meyer (CIMMS at NSSL)

Each experiment conducted in the HWT has different objectives, operating times, and software requirements. The Technical Advisor for the Hazardous Weather Testbed (HWT) Experimental Warning Program (EWP) coordinated with the HWT Executive Officer, project principal investigators, and NSSL IT Support to ensure each project has the correct number of machines, correct software, and adequate time to upgrade machines before each project start date. The Hazard Services - Probabilistic Hazard Information (HS-PHI) experiment required an older standalone build of AWIPS-2, version 16.2.1 with an experimental version of Hazard Services (from ESRL/GSD) for

forecasters to run through simulations and issue PHI. Once the HS-PHI experiment was complete, 14 standalone machines and 8 realtime servers were updated and configured to AWIPS-2, version 17.2.1, and the operating system was upgraded from Red Hat Enterprise Linux 6 to Community Enterprise Operating System 7 (which was coordinated with NSSL IT).

The Hydrometeorological Testbed (HMT) - Hydro experiment required a new build of Hazard Services to be installed and configured for realtime use, as well as modifications to the Hazard Information Dialog (HID). These updated modifications to the HID allowed forecasters to record information during the issuance of flash flood warnings and save it for further evaluation. Further, the HMT-Hydro experiment conducted simulations using the WES-2-Bridge software, from Warning Decision Training Division and is compatible with AWIPS-2, to review archived cases in a "playback" mode.

The GOES-R experiment required a specific AWIPS-2 installation and configuration for NUCAPS, GLM, and GOES-R products. For all experiments, many configurations were made within AWIPS-2 to visualize the data including modifying/creating menus, grid rules, stylerules, colormaps, and procedures. Not only were machines configured in preparation of each experiment, but technical support was provided during operations of all experiments in the event of technical difficulties or questions. During the GOES-R experiment, the Technical advisor received feedback from the forecasters and coordinated with developers to make changes on-the-fly and improve the experimental products (see Subproject #4 for more details). Because of the increase in number of experiments in the HWT throughout the year and demand for operating during the spring tornado season, the Technical Advisor led coordination with NSSL IT to purchase of 10 new standalone machines and monitors to have a secondary "HWT" in the Devlab, also located on the 2nd floor of the National Weather Center.

9. Facilitation of Probabilistic Hazard Information (PHI) Experiments

Adrian Campbell and Tiffany Meyer (CIMMS at NSSL), and Jonathan Wolfe (NWS Duluth, MN WFO)

In support of the 2018 HWT spring experiments, the PHI Prototype Tool was developed to play back stored data for several historical cases. These cases were successfully displayed, via the Enhanced Data Display (EDD) and GR2Analyst tools, during two weeks of emergency manager experiments and three weeks of broadcast meteorologist experiments.

As the Prototype PHI tool was not operational at the start of 2018, the first development activity was a detailed study of the tool's code and identification of the architecture that needed to be restored for the experiments. This analysis resulted in a diagram (Fig. 1) showing all data flow components between the Prototype PHI Tool, the EDD, and the GR2Analyst Tool.

In previous years, the data flow to the EDD and GR2Analyst was run from the system clock of the machine running the PHI Prototype Tool, with historical cases being played back by resetting that machine's system clock. For the 2018 experiments, the data flow was redeveloped to run from the PHI Tool display clock instead. This greatly simplified the running of the cases and enabled the creation of a standalone virtual machine that could encompass the entire data flow. This virtual machine proved useful as a development environment and was also used to present demonstrations of PHI at the Integrated Warning Team Workshop in Grand Junction, Colorado. To further assist in running cases, the code was also modified to remove all temporary case files when the PHI Prototype tool is reloaded.

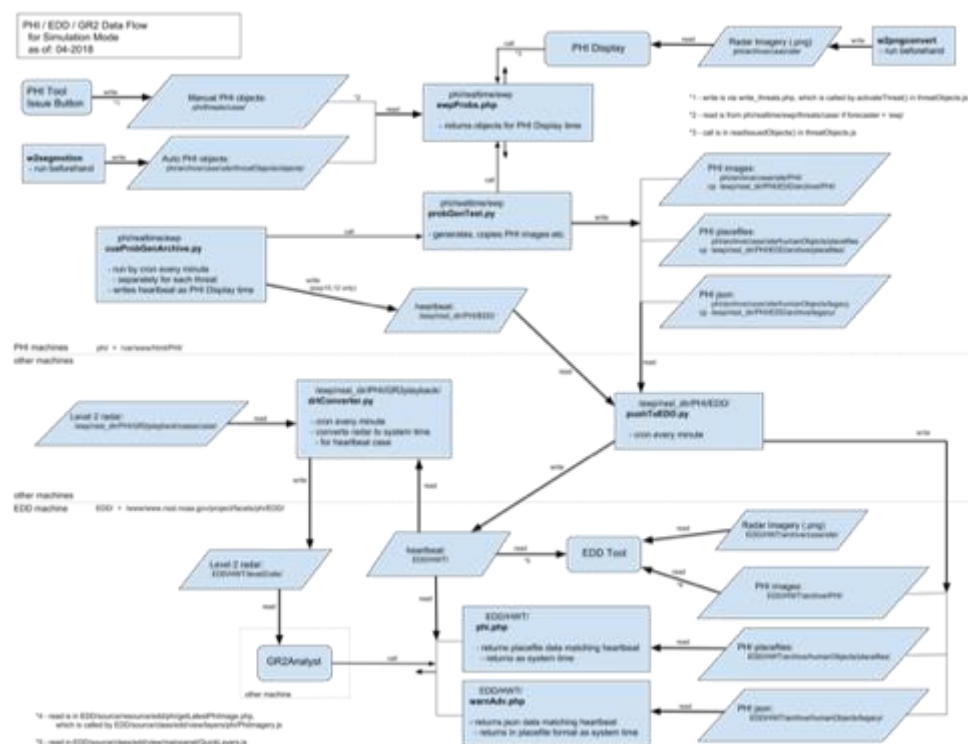


Figure 1. Data flow between the Prototype PHI Tool, the EDD, and the GR2 Analyst Tool.

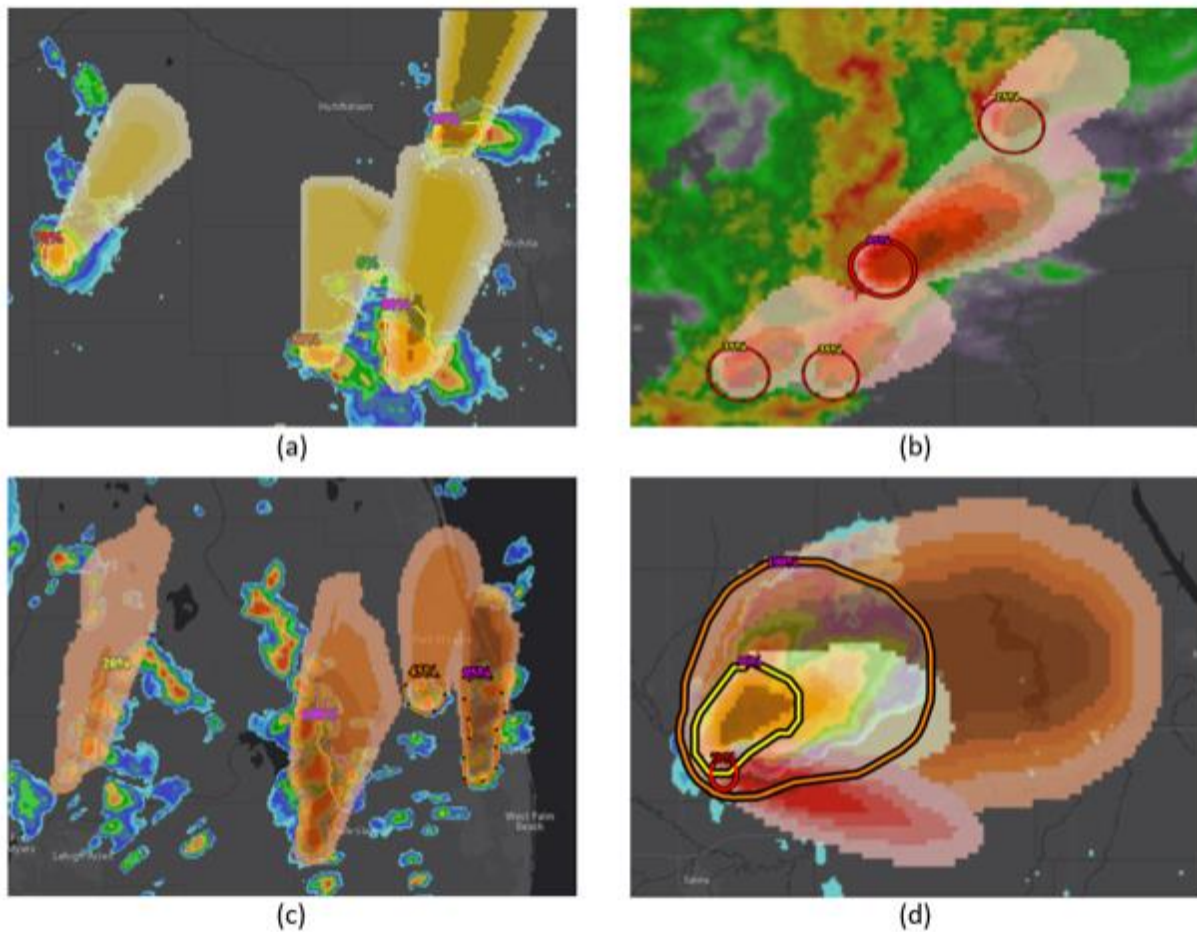


Figure 2. Monochromatic PHI plumes for severe storm (a), tornado (b), and lightning (c) hazards as displayed in the EDD tool. A combined hazard display is shown in (d).

Publications

- Clark, A. J., I. L. Jirak, S. R. Dembek, G. J. Creager, F. Kong, K. W. Thomas, K. H. Knopfmeier, B. T. Gallo, C. J. Melick, M. Xue, K. A. Brewster, Y. Jung, A. Kennedy, X. Dong, J. Markel, M. Gilmore, G. S. Romine, K. R. Fossell, R. A. Sobash, J. R. Carley, B. S. Ferrier, M. Pyle, C. R. Alexander, S. J. Weiss, J. S. Kain, L. J. Wicker, G. Thompson, R. D. Adams-Selin, and D. A. Imy, 2018: The Community Leveraged Unified Ensemble (CLUE) in the 2016 NOAA/Hazardous Weather Testbed Spring Forecasting Experiment. *Bulletin of the American Meteorological Society* **99**, 1433-1448.
- Wilson, K. A., P. L. Heinselman, and C. M. Kuster, 2017: Considerations for phased-array radar data use within the National Weather Service. *Weather and Forecasting*, **32**, 1959–1965.
- Wilson, K. A., P. L. Heinselman, and Z. Kang, 2018: Comparing forecaster eye movements during the warning decision process. *Weather and Forecasting*, **33**, 501–521.

NSSL Project 6 – Development of Technologies and Techniques in Support of Warnings

NOAA Technical Lead: Alan Gerard (NSSL)

NOAA Strategic Goal 2 – *Weather-Ready Nation – Society is Prepared for and Responds to Weather-Related Events*

Funding Type: CIMMS Task II

Objectives

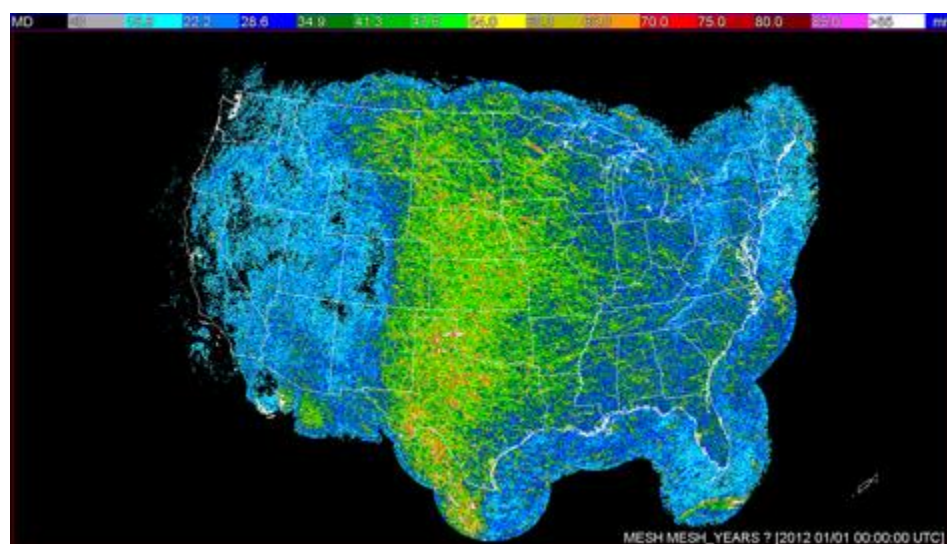
The primary goals for this reporting period were to develop algorithms to detect storm scale features in radar and satellite data, and to use these features to issue probabilistic short-term predictions of severe weather events.

Accomplishments

1. Multi-Year Reanalysis of Remotely Sensed Storms (MYRORSS)

Kiel Ortega, Skylar Williams, Anthony Reinhart, and Travis Smith (CIMMS at NSSL)

This project builds upon previous years work with the continuation of processing and quality control of the data. Currently, a MESH climatology is being compiled for the years 1998 - 2011 while a rotation track climatology is still needed with the updated LLSD algorithm. The AzShear reprocessing has been completed for 2003 - 2011 while reprocessing for 1998 - 2002 is ongoing as well as the quality control for all years. Progress has been made in the development for processing on OU's supercomputer Schooner. This additional resource will be used for the processing of the dual-pol era of radar data (2012-present).

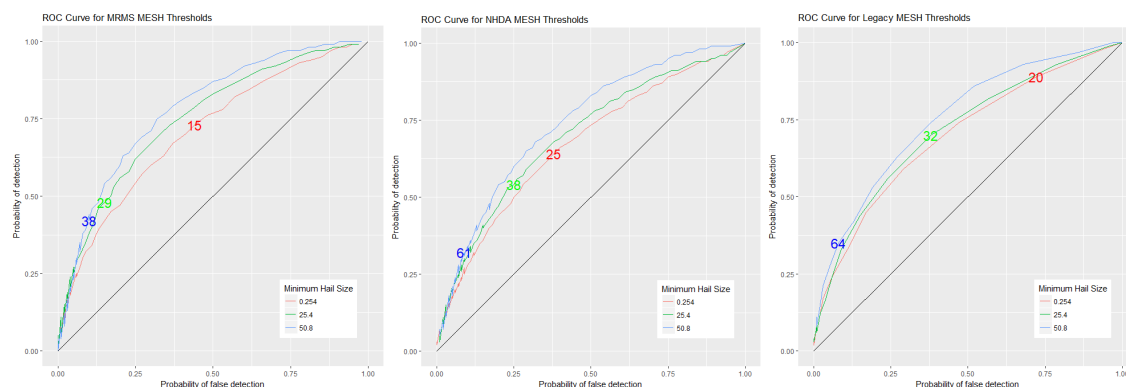


MESH accumulated for 1998 - 2011.

2. New Hail Detection Algorithm (NHDA)

Kiel Ortega (CIMMS at NSSL)

Worked continued to develop a new Hail Detection Algorithm (NHDA) to enhance both the Enhanced Hail Detection Algorithm (HDA; Witt et al. 1998) and the Hail Size Discrimination Algorithm (HSDA; Ortega et al. 2016). The NHDA work explored the validity of the probability of hail (POH) and probability of severe hail (POSH) that were implemented within the HDA. The POH methodology was found to be invalid, but the POSH product showed some skill and needs further calibration for reliable probabilities. The Maximum Expected Size of Hail (MESH) product was explored in three different contexts: the original, cell-based method; a single radar gridded method for the NHDA; and the Multi-Radar, Multi-Sensor (MRMS) version. Performance of discriminating hail size categories was similar between all three versions. Further, it was found that the original design of MESH, where at least 75% of reports would be less than the MESH value, was fairly accurate among all three methods.



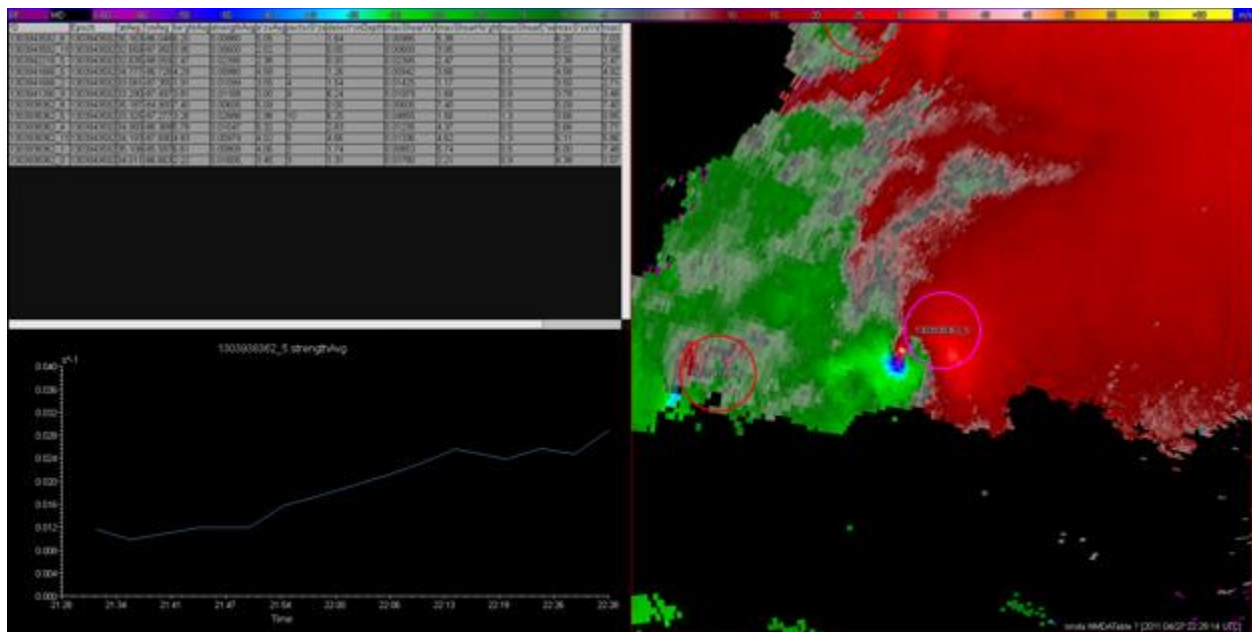
Receiver operating characteristic (ROC) curves for MESH in the three version: MRMS (left), gridded single-radar (center), and cell-based (right).

3. New Mesocyclone Detection Algorithm (NMDA)

Brandon Smith and Matthew Mahalik (CIMMS at NSSL)

A prototype of the single-radar New Mesocyclone Detection Algorithm (NMDA) for the WSR-88D radar network was developed from late 2017 through June 2018. The NMDA is an effort to replace the internal “engine” of the current Mesocyclone Detection Algorithm (MDA) with newer operational products and techniques that were not available during the creation of the MDA. Using velocity-derived azimuthal shear (AzShear) as the main catalyst for detection, along with the velocity-derived products of shear diameter and velocity difference (both smoothed with a median filter), the NMDA identifies and tracks 3D mesocyclone objects over time and space. To perform this, the NMDA begins by identifying areas of interest where gates meet or exceed a set threshold of AzShear, shear diameter, and velocity difference. From these areas of interest, gates are pared down through various checking methods to obtain the final 2D

detection. After this process is repeated for each tilt of a given volume, then the 2D mesocyclone detections are linked in the vertical to create 3D mesocyclone detections. This is performed through a series of methods that use the 2D detection's various attributes, including mesocyclone type (cyclonic, anticyclonic), strength, and height, to create the 3D detections. These 3D detections can be tracked with time once the NMDA algorithm has two successive volume scans. For each 3D detection available in the older volume, a possible downstream location is found by using a combination of the 0-6 km storm relative motion calculated from a RAP derived sounding table and the time difference between the radar volume scans being compared. If a 3D detection is found in the newer volume scan, the detections are then linked.



Output from the prototype NMDA algorithm shown within the display of the WDSS-II development environment. Shown is the visual output of the 3D mesocyclone detections overlaid with dealiased velocity data (right), a tabular view of all the 3D mesocyclone detections available on this scan along with their attributes (top left), and a trend graph of the 3D mesocyclone's maximum AzShear value over time.

4. New Tornado Detection Algorithm (NTDA)

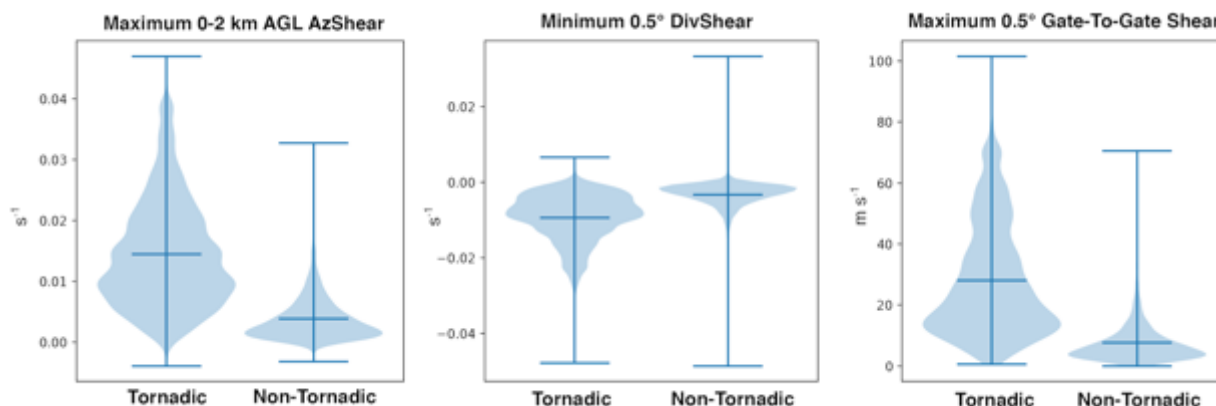
Kim Elmore, Matthew Mahalik, Brandon Smith, and Don Burgess (CIMMS at NSSL)

Work continues toward the development of a New Tornado Detection Algorithm (NTDA) prototype proposed to replace the existing WSR-88D Tornado Detection Algorithm. It is designed to utilize a random forest machine learning technique and radar-derived statistics of storm attributes to distinguish tornadic velocity signatures from non-tornadic features. The algorithm consists of two primary components: (1) a preliminary detection that identifies potentially tornadic (“candidate”) circulations and calculates their relevant attributes, and (2) a random forest that classifies these candidate circulations as either tornadic or non-tornadic by using a combination of their past and present statistical attributes as predictors.

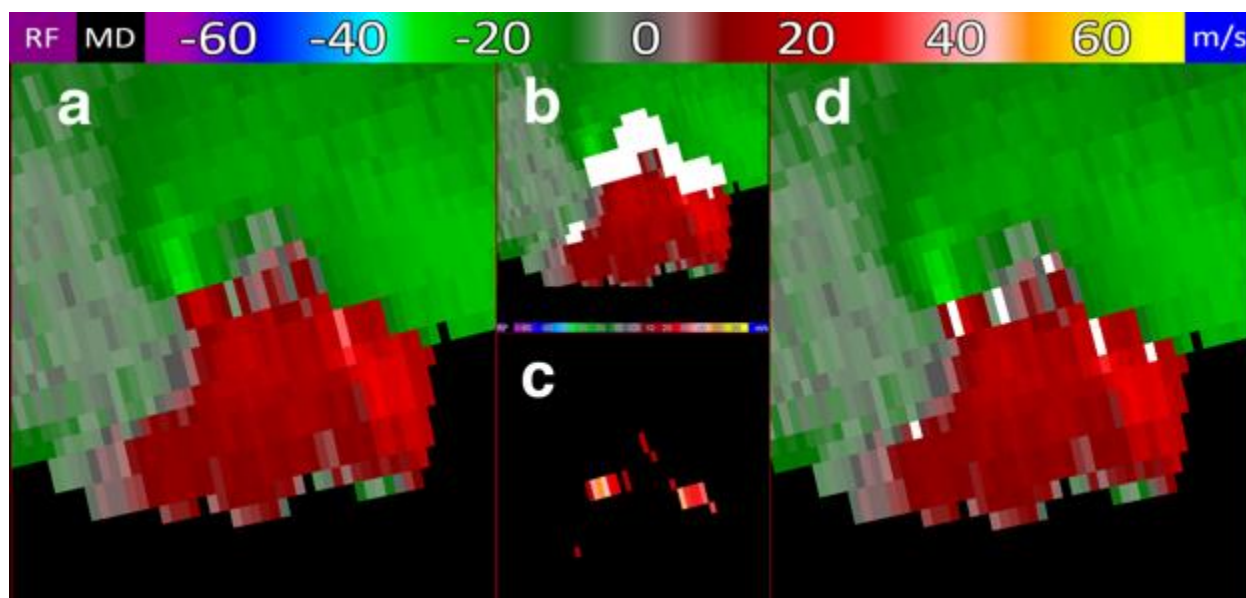
The NTDA random forest training dataset consists of radar-derived storm attributes calculated for a severe storm database provided by the Storm Prediction Center (SPC). The database includes over 20,000 individual data points from storms that produced severe wind, hail, or tornado reports during a two-year period from 2014-2015. Each event was labeled as tornadic or non-tornadic, and the non-tornadic events were used as null cases. The list of tornadic cases was developed using the time and location of individual damage indicators listed in the NWS Damage Assessment Toolkit (DAT) dataset, also supplied by SPC. The DAT dataset also serves as a truth dataset during algorithm testing and verification. For each event, radar data were matched in time and space to the severe weather report. Then, minimum, maximum, median, and mean values within a fixed 2 km radius of the event location were calculated for all available reflectivity, velocity, and velocity-derived radar variables.

An analysis was completed to select the most skilled tornado predictors, which include single-radar fields of reflectivity, dealiased velocity, shear diameter, peak-to-peak velocity difference, gate-to-gate (GTG) shear, AzShear, and DivShear. Initial candidate circulations are identified using AzShear, GTG shear, and rotational velocity (V_{rot}), and their attributes are then passed to the random forest. Following 500 random forest iterations, each object is classified as a tornado or non-tornado. For each tornado detection in the volume, its location and attributes are then stored and displayed.

NTDA is scheduled for evaluation in the Spring 2019 Hazardous Weather Testbed, and work to improve algorithm performance and refine its detection logic is ongoing. Additional NTDA capabilities under development include implementation of multiple elevation scans and feature tracking and trending.



Example violin plots showing the distributions of three of the many NTDA predictors for tornadic and non-tornadic events. These include (left to right) layer-maximum low-level AzShear, minimum 0.5° DivShear, and maximum 0.5° gate-to-gate shear.



An example showing several intermediate steps of NTDA initial tornado identification process, including (a) input radial velocity field, intermediate paring down of rotation objects using AzShear (white; in b) and gate-to-gate shear (colored by shear magnitude; in c), and center gates of the circulations that are passed to the NTDA random forest for final classification (white; in d). This example uses 0.5° KCYS velocity data of a supercell that produced several tornadoes near Harrisburg, Nebraska, on 12 June 2017.

5. Conditional Probability of Tornado Intensity (CPTI)

Matthew Mahalik, Brandon Smith, and Travis Smith (CIMMS at NSSL)

Development of a real-time, gridded, Conditional Probability of Tornado Intensity (CPTI) product is in progress. CPTI is designed to utilize radar-derived products such as Multi-Radar Multi-Sensor (MRMS) azimuthal shear (AzShear) and environmental data to

produce real-time, gridded probabilities of tornado intensity. Previous work conducted by the Storm Prediction Center (SPC) derived empirical relationships between tornado intensity, near-storm environment parameters, and manually-calculated low-level rotational velocity (V_{rot}), resulting in an hourly-updated, 40-km resolution, tornado intensity probability conditional on the presence of a tornado in a right-moving supercell. This work builds upon these experimental projects by statistically bridging AzShear to V_{rot} and allowing for a real-time, stormscales, automated tornado intensity probability gridded product.

Using a two-year tornado dataset provided by SPC, maximum AzShear was found and compared to the V_{rot} manually calculated for each report. A moderate correlation between AzShear and V_{rot} provided a proof-of-concept for implementing AzShear in a capacity similar to that of V_{rot} . From there, a linear regression model was derived to statistically relate Rapid Refresh (RAP) environmental attributes, radar-derived rotation attributes (including AzShear and shear diameter), and tornado damage rating. The regression model was integrated into an experimental WDSS-II algorithm, which is currently undergoing initial testing and evaluation. The experimental CPTI algorithm will be integrated into the local VM RMS system for testing and will be evaluated by NWS forecasters as part of the Hazardous Weather Testbed in Spring 2019.

6. Evaluating the Utility of Radar-Derived Divergence in Tracking Tornadoic Features

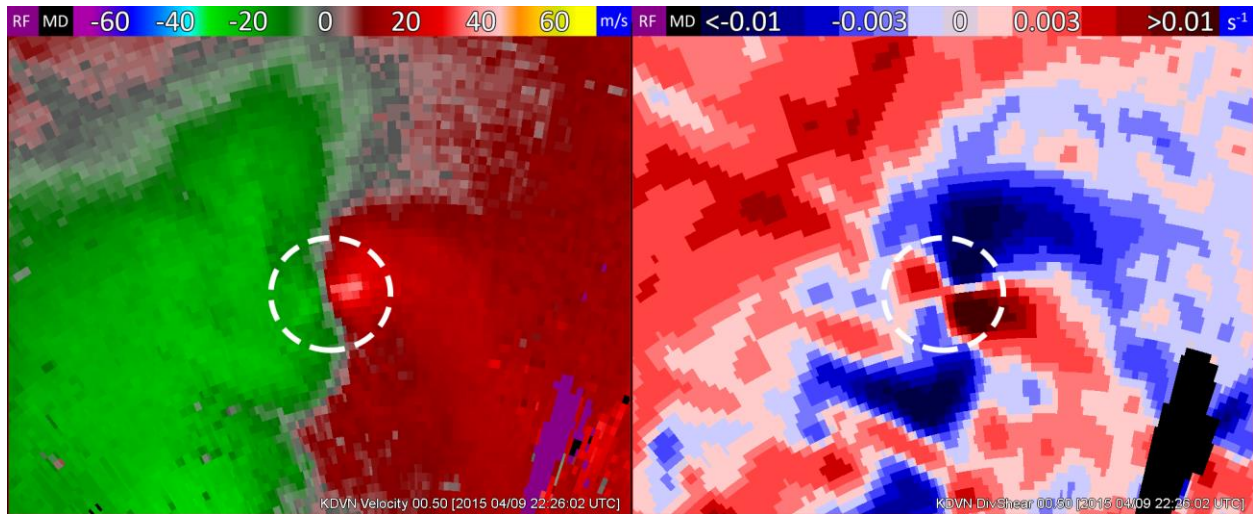
Matthew Mahalik and Kim Elmore (CIMMS at NSSL)

Divergent shear (DivShear) is the along-azimuth gradient of a radial velocity field, which physically represents two-dimensional half-divergence, in the linear, least-squares derivative (LLSD) technique. To better understand DivShear characteristics in and around potentially tornadoic circulations, maximum and minimum DivShear were calculated for and attributed to 1,047 unique velocity representations of in-progress tornadoes within 75 km of a NWS WSR-88D in 2014-15, as recorded in a two-year NWS Damage Assessment Toolkit storm survey dataset provided by SPC.

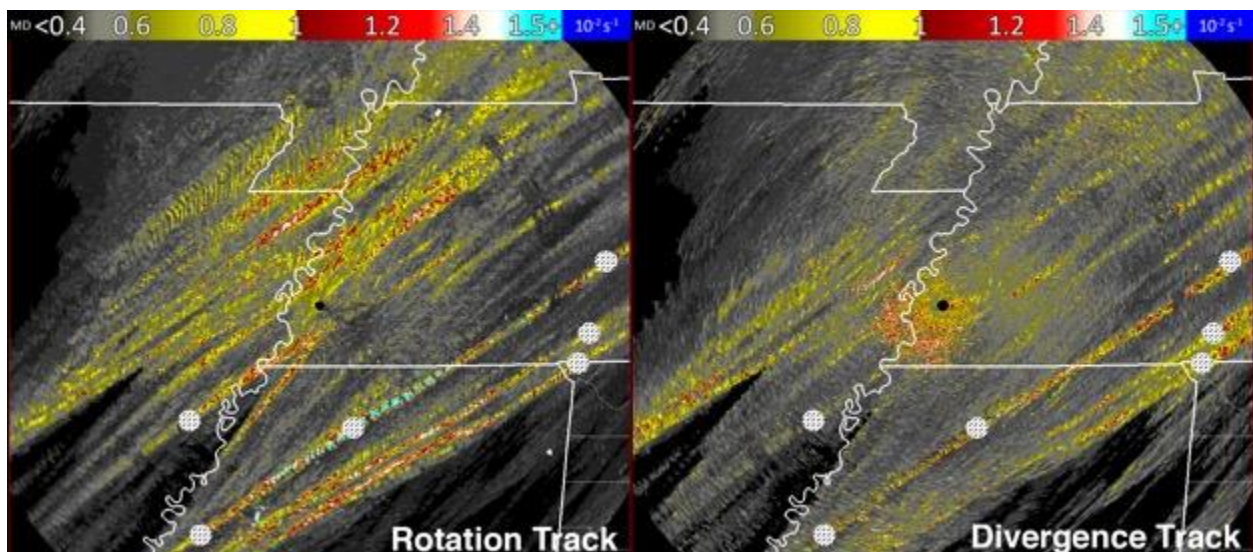
Qualitatively, a prevalent signature found in intense, low-level vortices was a DivShear quadrupole: a pattern of four alternating, nearly symmetric regions of strongly positive and negative DivShear usually collocated with a maximum in rotational shear (AzShear). A majority of tornadoes was associated with local extrema of both convergence (DivShear < 0) and divergence (DivShear > 0). Across all cases, although the sample size of violent tornado (EF-3+) cases was low, the magnitude of both the average maximum and minimum DivShear values increased for increasing tornado rating, suggesting that the magnitude of DivShear extrema may provide skill as a tornado strength indicator, particularly when considered alongside other data.

A preliminary investigation of several events yielded mixed results in the ability of time-accumulated maximum or minimum DivShear to track tornadoes and mesocyclones. DivShear tracks often successfully highlighted significant tornado paths but not weaker

ones. In many of these cases, rotation tracks were partially contaminated by high-AzShear areas along convergent boundaries such as gust fronts, but these features were not present in maximum DivShear (i.e., divergence) tracks. However, DivShear tracks tended to be more susceptible to ground clutter at close range to the radar. While more interrogation is necessary, these preliminary findings suggest that DivShear could be leveraged to help distinguish pure rotation from linear features.



Single-radar, 0.5° radial velocity (left) and corresponding DivShear (right) for a supercell producing an EF-1 tornado near Clinton, Iowa, on 9 April 2015. A DivShear quadrupole signature is evident near the mesocyclone center (circled).



12-hour low-level (0-2 km AGL) rotation tracks (accumulated maximum AzShear; left) and divergence tracks (accumulated maximum DivShear; right) from KNQA radar of a tornado outbreak on 23 December 2015. Actual tornado touchdown locations are marked by white circles.

7. Time Stamp Mosaic

Heather Reeves, Robert Toomey, Karen Cooper, Jeff Brogden, and Brian Kaney (CIMMS at NSSL)

This project addresses latency in the MRMS mosaics by mosaicking the time stamp along each radial into a three-dimensional mosaic. This year's efforts focused on the engineering of the mosaic, including the development of the throughput code for the time stamp information to pass the information into MRMS, through the quality-control algorithm, the initial merger, and then the final merger. An initial roll-out of the product was tested at 3-km ASL starting in December 2017. In July 2018, the full three-dimensional mosaic was initialized producing output every 10 minutes on all vertical levels. Data is archived on the vMRMS system operated at NSSL. Visualization is provided on the internal MRMS webpages at the following url:

https://mrms-dev.nssl.noaa.gov/qvs/simple_product_maps.php

Select "3D Mosaic Age" from the menu on the left, then choose the desired layer from the pop-up menu. The included figure shows a screenshot of the time stamp mosaic valid at 0642 UTC 20 Aug 2018.

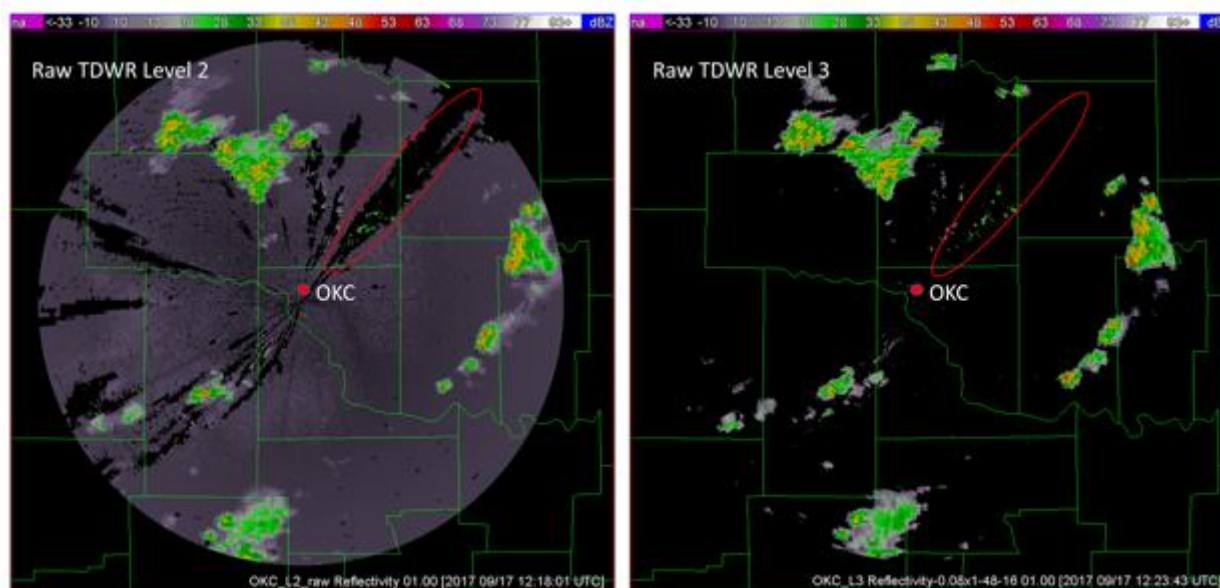


The pixel time stamp at 5 km ASL valid at 0642 UTC 20 Aug 2018. Only those areas with reflectivity greater than -35 dBZ are assigned a time stamp.

8. Radar Quality Control of Non-WSR88D Radars

Shawn Handler and Heather Reeves (CIMMS at NSSL)

This project focused on the feasibility of incorporating non-WSR-88D radars into the MRMS mosaic with particular emphasis on Terminal Doppler Weather Radars (TDWRs). For this work, the quality-control protocols from the Canadian radar network were adapted to work with the TDWR scanning strategies. Clutter maps for each of the TDWRs were also produced. Additional steps were taken to generate a universal quality control algorithm that is adaptable for any single-polarized radar. Other radars from the Caribbean area were also included in this effort, including two dual-polarized radars at Cayman Islands and Campeche, Mexico and a single-polarized radar at Belize. While the efforts to develop a quality control algorithm that is effective were largely successful, two issues presented themselves. First, some radially-oriented artifacts appear in some scans of the TDWRs that could not be removed using artificial intelligence (see figure below). Second, the attenuation of the TDWR leads to differences in the reflectivity along convective lines in excess of 10 dBZ. This may have significant repercussions on the eventual incorporation of these radars into the national mosaic.



The (left) non-QC'd and (right) QC'd TDWR returns from 1223 UTC 17 September 2017. The ellipse denotes a region of false echo that could not be removed using traditional artificial intelligence.

Publications

- Hwang, Y., T-Y Yu, V. Lakshmanan, D. M. Kingfield, D-I Lee, and C-H You, 2017: Neuro-fuzzy gust front detection algorithm with S-band polarimetric radar. *IEEE Transactions on Geoscience and Remote Sensing*, **55**, 1618-1628.
- Kingfield, D. M., and K. M. de Beurs, 2017: Landsat identification of tornado damage by land cover and an evaluation of damage recovery in forests. *Journal of Applied Meteorology and Climatology*, **56**, 965-987.

McGovern, A., K. L. Elmore, D. J. Gagne, II, S. E. Haupt, C. D. Karstens, R. Lagerquist, T. M. Smith, and J. K. Williams, 2017: Using artificial intelligence to improve real-time decision making for high-impact weather. *Bulletin of the American Meteorological Society*, **98**, 2073-2090.

ROC Project 10 – Analysis of Dual Polarized Weather Radar Observations of Severe Convective Storms to Understand Severe Storm Processes and Improve Warning Decision Support

NOAA Technical Leads: Terry Clark, Christina Horvat, Chris Gilbert, and Jessica Schultz (ROC)

NOAA Strategic Goal 2 – *Weather-Ready Nation – Society is Prepared for and Responds to Weather-Related Events*

Funding Type: CIMMS Task II

1. Analysis of Radar Lighting Strikes, Improvement of Processes, Monitoring of Communication Outages and Improve Warning Decision Support

Jon Ballard and Christa Martin (CIMMS Students at ROC)

Objectives

The NWS Radar Operations Center (ROC) Engineering Branch has the responsibility for designing, integrating, and deploying WSR-88D hardware, software, and communications improvements. To do this we need engineering project management tools for planning, track and reporting on modifications and upgrades. We need tools to quickly determine the progress of proposed system modifications and to generate various statistics and graphs for engineering management. We also need tools to improve the WSR-88D fleet for better operational availability or to rapidly prototype small parts.

Accomplishments

Mr. Jon Ballard and Ms. Christa Martin, university students, made significant contributions to the following critical projects for ROC Engineering. 1) Mr. Ballard and Ms. Martin developed documentation and made presentations detailing NEXRAD motor failures, flexible motor coupler failures, and radar lighting strikes, including frequency, cost, and trend analysis. These reports help identify problematic sites and regions. Their follow up work resulted in improved field support response time. 2) Mr. Ballard and Ms. Martin worked on auto generated backup communications failover statistics that aid in the creation of a monthly report. The report provides communications statistics on 4G or VSAT backup communication utilization during severe weather. Backup communications statistics are critical for reporting and ensuring continued reliability forecasts and warnings. These statistics are used identify the need for improvement. They also assisted with VSAT equipment testing. 3) Mr. Ballard and Ms. Martin assisted in improvements to the Engineering Lab. They developed drawings for prototyping radar components and models with a Fused Deposition Modeling Style 3D printer. They learned about subtractive and additive manufacturing and applied their

knowledge to develop 3D printed prototypes, and production level parts. Currently, they are working on experimenting with different materials, and post printing processes that can both strengthen their designs, and allow them to handle higher temperature environments. This gives the Engineering Branch the ability to rapidly prototype in house designs and refining this ability to reduce the amount of time it takes us to test, procure and provide critical parts that are needed to keep radars running.

They have both been exemplary students that take the personal initiative to learn new things every day at the ROC.

2. Giant Hail in Association with the El Reno Tornadoic Storm of 31 May 2013

Don Burgess (CIMMS at ROC)

Objectives

Determine Dual-Polarization parameter values for supercell storms that produce giant hail (>7 cm diameter).

Accomplishments

The 31 May 2013 El Reno tornado was very wide and very violent, producing severe damage and loss of 8 lives. Less well known is that the El Reno supercell storm produced giant hail in and near El Reno. After an extensive search, 17 reports of giant hail were found, some as large 16 cm diameter. After analysis of rapid-scan KOUN radar dual-polarization data (update time of ~100 sec), it was found that the hail fell in two preferred areas; the southwest and northeast edges of the supercell updraft (Fig 1). The exception was one stone (#6) that was caught up in the circulation of the large tornado and carried to within the tornado damage path. The southwest/northeast hail locations were away from the main hail area of the storm, which was northwest of the updraft; the traditional location for supercell hailfall. The giant hailfall location was confirmed for part of the hailfall time by Dual-Polarization observations from the RaXPol mobile radar (not shown).

Plots of Dual-Polarization parameters for the giant hail to the northeast of the updraft show values often associated with large hail; low differential reflectivity (Z_{dr}), low correlation coefficient (R_{hv}), and very low specific differential phase (K_{dp}) (see Fig 2). The one radar parameter with values different from those normally seen with large hail was reflectivity (Z). During the fall of giant hail, reflectivity values were between 41 and 49 dBZ. Values less than the 55-75 dBZ usually found with large hail. The lower reflectivities are thought to have resulted from the sparse fall of the giant hail. Reported giant hail densities on the ground were on the order of one stone per 4 m². The hailstones were also reported to be monodispersed, meaning that no smaller hail fell with the giant hail. This probably came about from the hail falling at the very edge of the strong updraft where intermediate values of vertical velocity kept smaller hail aloft while the giant hail was heavy enough to fall to the ground. Distributions of Dual-Polarization and reflectivity parameters and observations of the hailfall southwest of the updraft (not shown) were similar to those for northeast of the updraft.

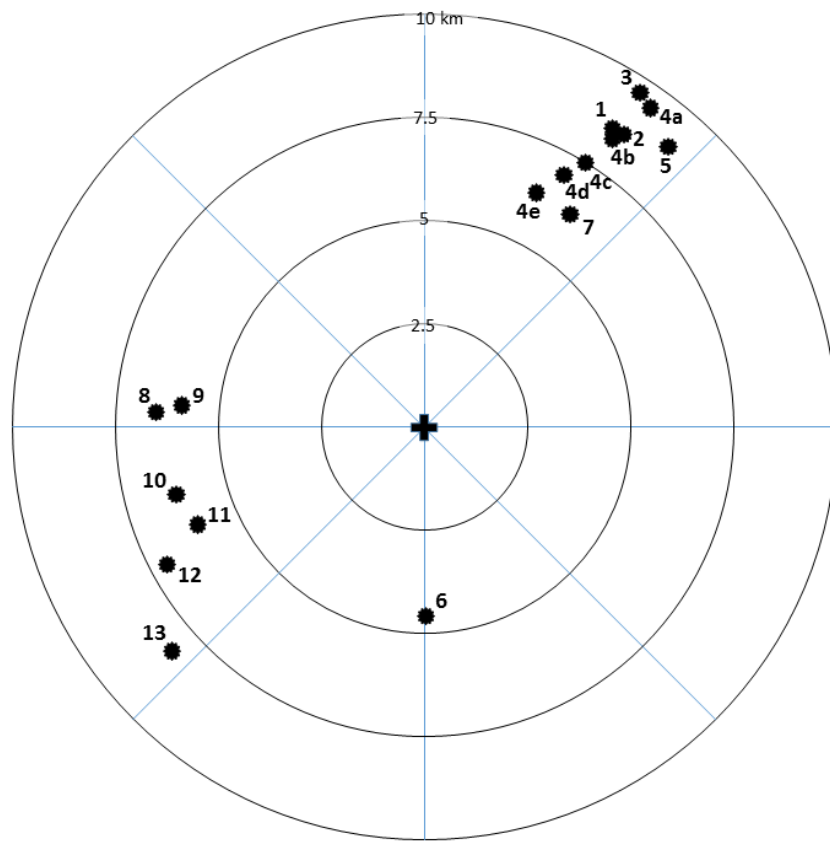
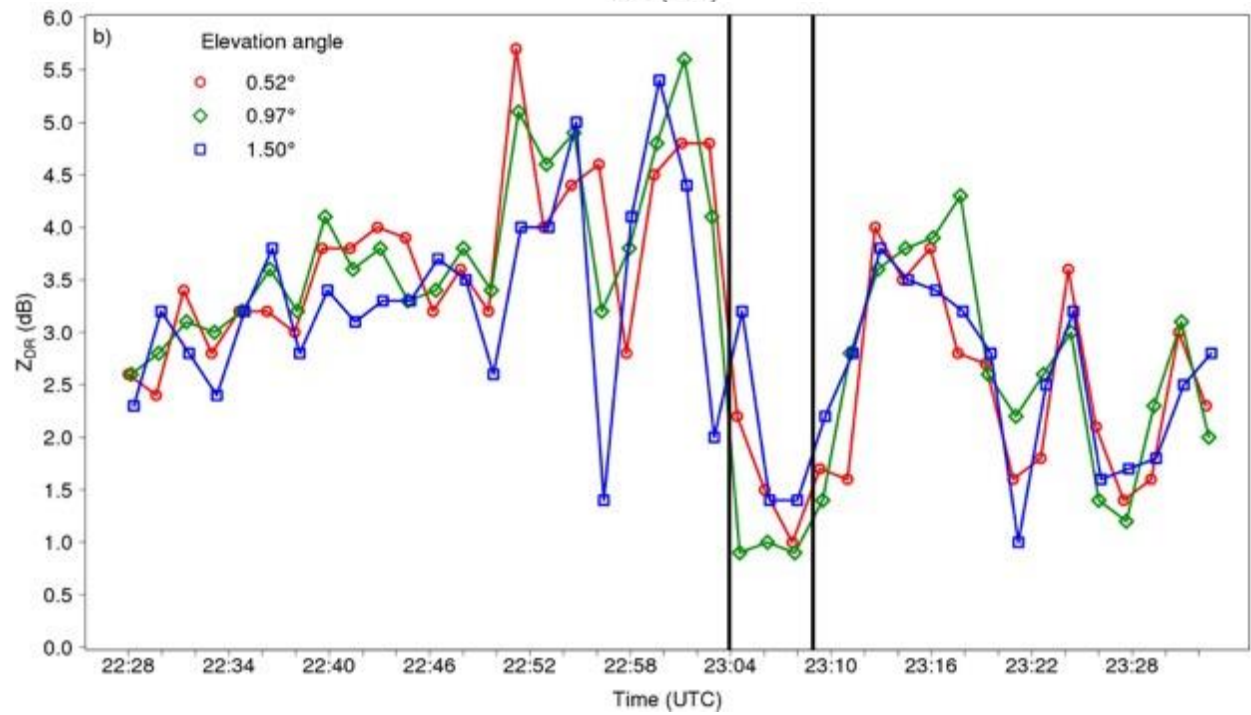
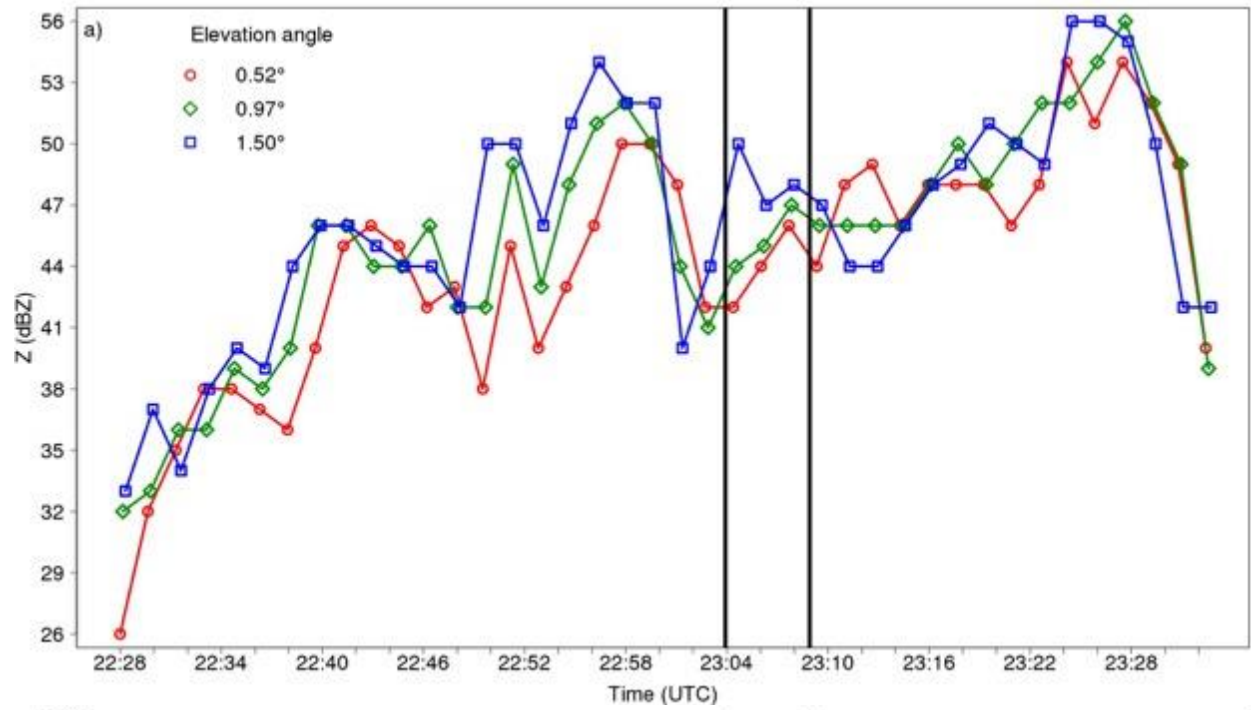


Figure 1. Locations of the giant hailstone observations relative to the center of the main storm updraft.



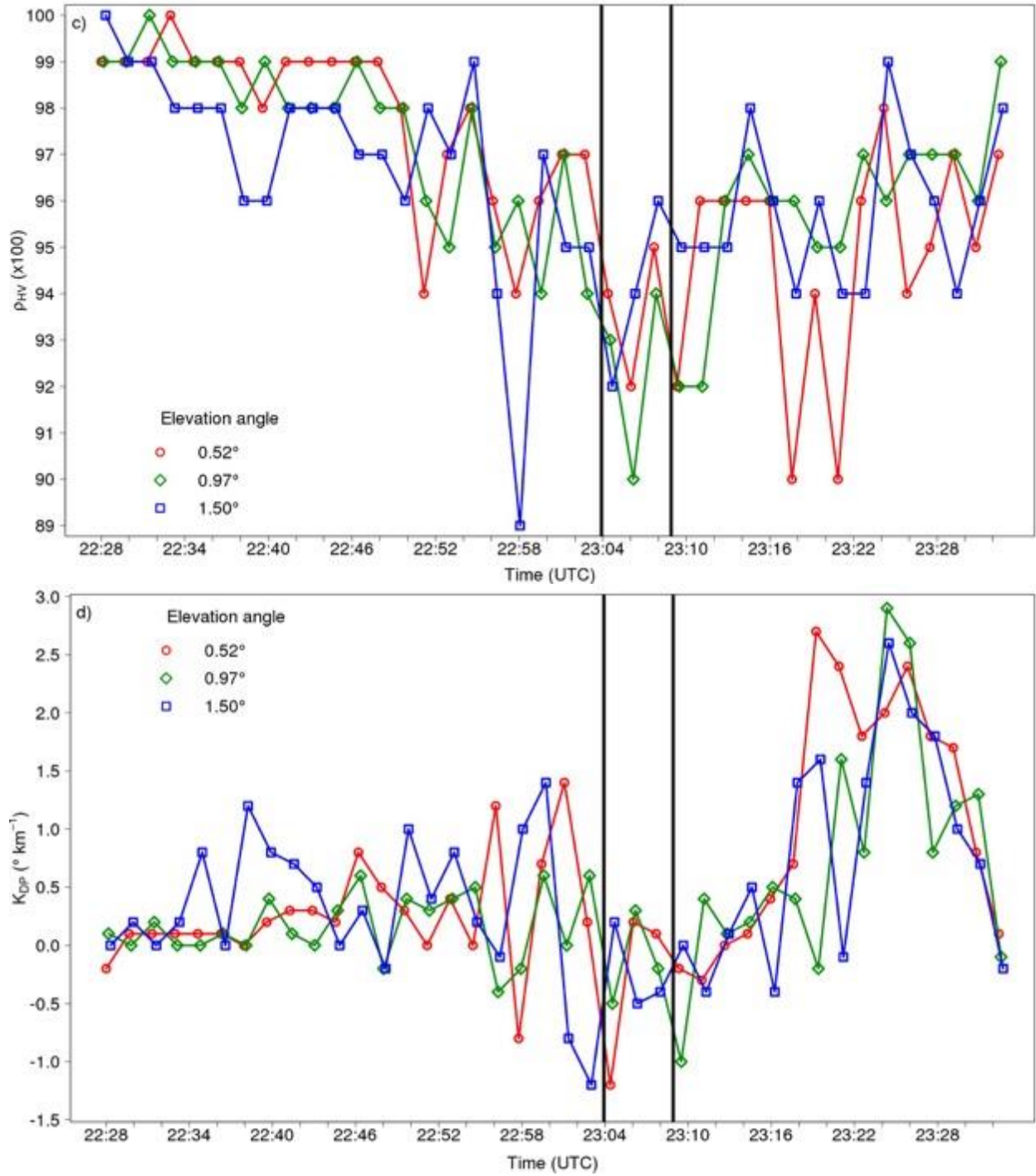


Figure 2. Time series of low-altitude KOUN observations of (a) Reflectivity (Z), (b) Differential Reflectivity (Z_{dr}), (c) Co-polar Correlation Coefficient (R_{hv}), and (d) Specific Differential Phase (K_{dp}) for the giant hailfall northeast of the updraft. The vertical black lines indicate the time period of the giant hailfall (2304-2309 UTC). The altitudes of the three elevation angles at the giant hailfall location are 0.7, 1.1, and 1.7 km ARL.

3. Instructional Manual for Data Case Playback

Stephen Castleberry (CIMMS at ROC)

One of the common tasks performed within the ROC Applications Branch is the playback of radar data in a controlled environment. A need for standardized procedures combined into an instructional manual become a necessity during a large test case study centered on the performance of the Dual Polarization QPE algorithm compared to rain gauges. The standardized procedures ensured repeatable playback of radar data.

4. Data Case Playback and Analysis/Evaluation of Data Quality

Sam Emmerson (CIMMS Student at ROC)

The Applications Branch continues to investigate techniques to improve the Dual Polarization Quantitative Precipitation Estimator (QPE) algorithm. As part of this effort, test cases must be identified and support ground truth data collected in order to conduct the necessary tests of these new techniques. Sam's participation consisted of conducting data playback of radar data, documenting net changes in the algorithm performance, and assembling presentations of the results.

The Applications Branch was tasked to verify the impact of a new MIT Lincoln Laboratory algorithm called Aviation Classification Algorithm (ACA) that somewhat duplicated the structure and data ingest of the existing WSR-88D Hydrometeor Classification Algorithm. Sam's task was to assist in the collection of data sets, conduct radar playback of these data to compare products created with and without the ACA active. Algorithm products were compared both textually and graphically along with running CPU usage tests to determine impact on baseline WSR-88D performance.

Sam also assisted in development of a new volume-based statistical method for the purpose of automatically detecting data quality issues stemming from hardware problems related to a defective azimuth joint. The method relies on comparing the variances of the horizontal and the vertical noise to detect large changes.

5. Data Quality Investigation and Analyses

Nicholas Goldacker (CIMMS Student at ROC)

a. Validation of KLWX Yielding "Good" Radar Data during the Ellicott City & Catonsville, Maryland Heavy Rainfall and Flash Flooding Event 27 May 2018

Nicholas worked with Heather Grams (ROC) to provide an analysis of the quality of the KLWX radar data for the case study on the Ellicott City flooding event. He performed a validation of the radar for being cleared of hardware problems or atmospheric temperature influence during the event so that the radar data could be deemed reliable. The radar was performing exceptionally well during this event.

b. Mid-volume Rescan of Low-level Elevations (MRLE)

With the implementation of MRLE into Build 18 beta test sites, Nicholas created a methodology for identifying mesoscale meteorological case studies that can be used to playback Level II radar data and test the compatibility of various base moment and dual polarization algorithms such as velocity, spectrum width, quantitative precipitation estimation (QPE), and gate-to-gate shear/azimuthal shear for radar sites running MRLE. The methodology created involved storm reports, mesoscale analyses, and hydrological observations. He also created a spreadsheet shared with various ROC personnel that he personally updated with cases that have been scrutinized using the methodology. After he trained the three new employees and several existing employees on how to conduct this methodology and update the spreadsheet, he turned over the spreadsheet to a student employee to manage with my remote guidance.

c. Validation of “Good” Radar Sites

With the introduction of numerous hardware failures across the WSR-88D system including azimuth rotary joint deteriorations, bull gear failures, gear box deformations, radio frequency generator signal interference, transmitter sensitivities to outside ambient temperature, economizers failing in air conditioners, thermoelectric degradations in transmitter oil bath due to moisture contamination, Nicholas created a methodology that serves as a checklist to ensure that radar sites involved in algorithm testing and modified playbacks are of good quality. This will minimize the dilemma that bad data being inserted into an algorithm will inherently yield bad results irrespective of algorithm performance, quality, and reliability. The methodology created is used by ROC personnel to ensure that the radar sites and times chosen for data analyses are/were performing appropriately.

d. Investigation of Signal Noise on WSR-88D Data Quality with National Severe Storms Laboratory

Nicholas worked with Research Scientist Michael Simpson from NSSL and Richard Murnan from ROC on a 2018 MOU Tech Transfer project identifying signal noise problems and their subsequent effects on radar performance and data quality. His role was contributing to the research paper identifying the origin of signal noise within the WSR-88D system and partially instructing Michael on how to identify azimuth rotary joint problems and temperature biases on transmitter performance/data quality of ZDR level II product fields. He presented numerous real-time and historic cases outlining both types of problems and worked with him on ways to identify calibration points where adding additional calibration procedures specifically for ZDR and BR quality control could be necessary.

e. Understanding and Improving the Effects of Temperature on Z_{DR} Offset and Its Impact on Z_{DR} Level II Data

After performing numerous case studies on ZDR liquid rain, ZDR dry snow, ZDR Bragg, ZDR offset, and ZDR weighted mean correlations, chemical analyses on the oil used in the transmitter oil bath, correlations between calibration scans and the behaviors between ZDR liquid rain and ZDR dry snow, multi-variable graphical correlations using ROCSTAR, and numerous discussions with Engineering Branch, NEXRAD Hotline, and WSR-88D electronic technicians, a correlation was observed between Outside Ambient Temperature and Transmit Imbalance, XMTR Peak Power, and ZDR Offset variables in the Level II metadata when temperature outside of the RDA shelter is influencing the performance of the transmitter and power output as a result. This observation was notable with cases at KFFC, KPUX, and KICT. For KFFC and KPUX, the identified source of influence was improperly opened transmitter exhaust louvers that enabled outside air to flow through the ductwork into the transmitter inside the transmitter cabinet within the RDA shelter. This concept was turned into a research project which analyzed all 159 radar sites with the “Validation of ‘Good’ Radar Sites” methodology and identified a statistical threshold of when the transmitter exhaust louvers should be checked for being mechanically frozen in the open position to minimize the impact of outside temperature on transmitter performance and life expectancy. Nicholas’ role in this project was identifying the problem, creating/conducting a project to analyze the effects of the problem, and provide a solution to mitigate this problem.

f. Multi-year Analysis of Correlations between Outside Ambient Temperature and XMTR Peak Power

Temperature influence on XMTR Peak Power not only has the potential to alter ZDR Offset data, but can shorten the life of the transmitter. KICT has been exhibiting strong fluctuations in peak power corresponding with diurnal patterns and boundary/front passages associated with temperature changes which is a concern since this site is participating in the MRLE test. Transmitter exhaust louvers, air conditioner economizers, and pressure-weighted air condition duct louvers are not suspected to be the cause of this problem, and software calibration parameters currently are suspected to be the cause of the problem.

Publications

Witt, A., D. Burgess, A. Seimon, J. Allen, J. Snyder, and H. Bluestein, 2018: Rapid-scan radar observations of an Oklahoma tornadic hailstorm producing giant hail. *Weather and Forecasting*, in press.

SPC Project 11 – Advancing Science to Improve Knowledge of Mesoscale Hazardous Weather

NOAA Technical Leads: Russell Schneider and Israel Jirak (SPC)

NOAA Strategic Goal 2 – *Weather-Ready Nation – Society is Prepared for and Responds to Weather-Related Events*

Funding Type: CIMMS Task II

Overall Objectives

Lightning Prediction: The main objective for this project is to develop probabilistic calibrated forecasts of cloud-to-ground (CG) lightning density through Day 8 based on input from operational numerical weather prediction (NWP) models including convective allowing and ensemble models. Collaborating with National Weather Service (NWS) partners and the wildfire community is imperative to develop a broader unified probabilistic guidance suite that includes lightning occurrence and dry lightning. The probabilistic CG lightning density guidance will be distributed to NWS offices and external customers in a gridded format. The guidance will enhance the ability of fire agencies to prepare for lightning ignited wildfires by prepositioning and allocating appropriate wildfire suppression resources.

GOES-R and JPSS Proving Ground: The Storm Prediction Center (SPC) and Hazardous Weather Testbed (HWT) provide the GOES-R and JPSS Proving Ground with an opportunity to conduct demonstrations of Baseline, Future Capabilities and experimental products associated with the next generation GOES-R geostationary and JPSS polar satellite systems. Many of these products have the potential to improve hazardous weather nowcasting and short-range forecasting. Feedback from forecasters in the SPC and HWT has led to the continued modification and development of GOES-R and JPSS algorithms.

HWT Liaison: The HWT liaison works between the social science community, the HWT, and Warn-on-Forecast programs on behalf of the SPC. This includes studying the capability of convection-allowing models (CAMs) and ensembles, relating the output to forecasters through social science methods, and bringing this knowledge to, and testing it in, the HWT.

Project IMPACTS: Project IMPACTS (Integrated Machine-based Predictive Analytics for Convective Threats to Society) involves the development of a statistical model that estimates the plausible impacts to life and property due to tornadoes and other convective hazards.

Accomplishments

1. Lightning Density Prediction

Nicholas Nauslar and David Harrison (CIMMS at SPC), Steven Weiss, Israel Jirak, Patrick Marsh, Andy Dean, and Matt Elliott (SPC)

The new calibrated probabilistic CG lightning guidance based on the Short Range Ensemble Forecast (SREF) (new SREF calibrated thunder) was made available to view in operations during Summer/Fall 2017. Forecasters were able to view the new 1+ and 25+ CG guidance and compare it to other thunderstorm guidance including the current SREF calibrated thunder probabilities. Additionally, an internal webpage was created to view enhanced thunderstorm outlooks based on the current SREF calibrated thunder, the new SREF calibrated thunder, and outlooks created by forecasters. Verification

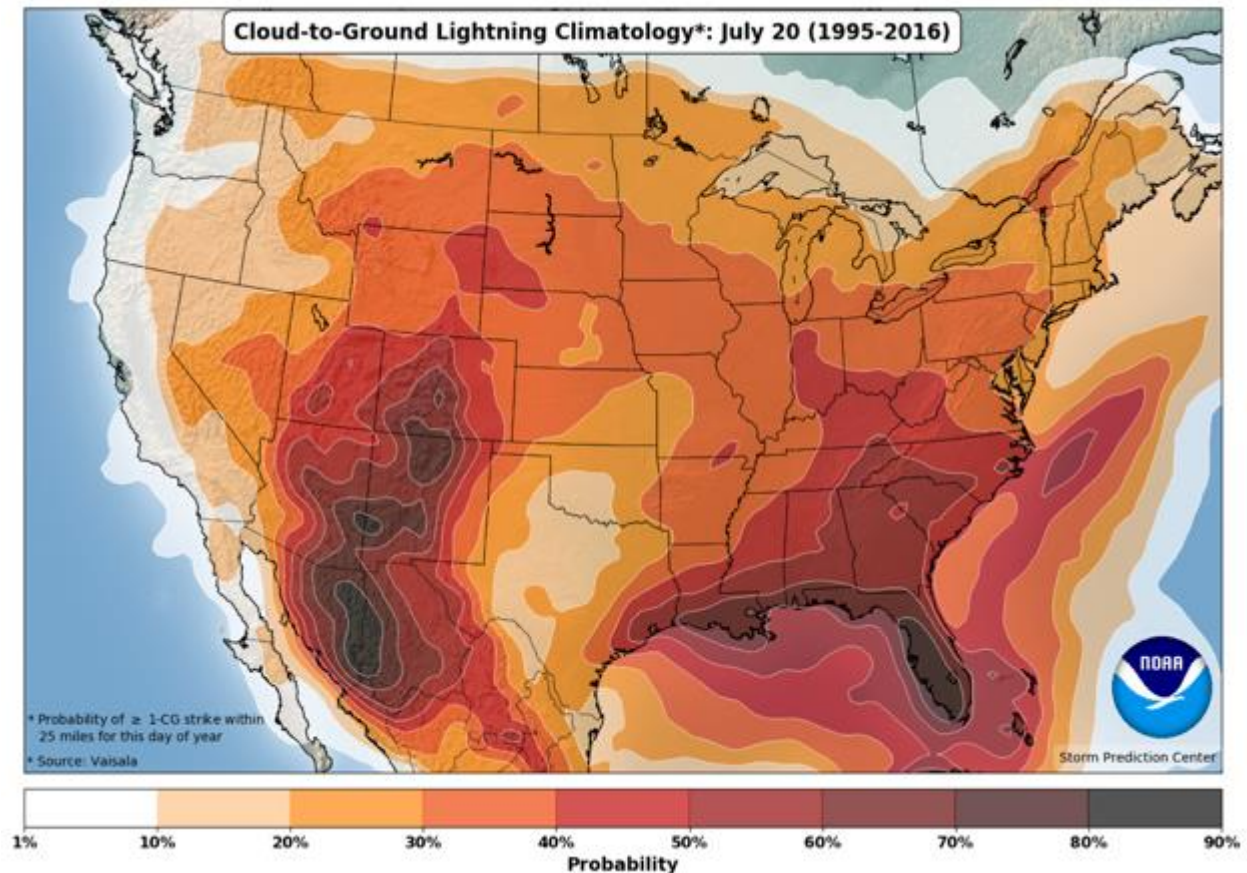
statistics were also generated to help compare the different forecasts. This process continued for several months and based on forecaster feedback and verification, adjustments were made to the new SREF calibrated thunder guidance. While bulk verification statistics show a slight improvement over the current SREF calibrated guidance, day-to-day verification and forecaster feedback deemed the new SREF calibrated guidance in need of improvement. Research and refinements continue for the new SREF calibrated thunder.

The convection allowing eight-member High-Resolution Ensemble Forecast (HREF) was also utilized to create probabilistic CG lightning forecasts while the other experiment continued. HREF model data dating back to April 2017 was examined to identify possible important predictors and create a probabilistic model of CG lightning. Exploratory data analysis (e.g., box plots, correlation, etc.) helped identify potential predictors and threshold values for predictors. Some of the most important predictors included most unstable convective available potential energy (MUCAPE), lifted index, and updraft velocity. Other variables such as composite reflectivity and hourly maximum 1-km reflectivity also showed predictive potential.

Random Forests were also implemented to confirm potential important predictors and to create a machine-learning based probabilistic model for CG lightning. Another reason for choosing Random Forests was the inconsistency among variable available and how variables were calculated among the different HREF members. For example, MUCAPE was treated as a separate variable for each HREF member to examine if it was a good predictor and if one member's MUCAPE showed better predictive potential than another. Additionally, it limited the issues associated with MUCAPE being calculated slightly differently among the members. More than 60 variables were utilized in the Random Forest approach.

The HREF data utilized by the Random Forest was modified. The hourly HREF data is on a roughly 3-km grid, but our current working definition of CG lightning is on a 40-km grid over 3-24 hours. Therefore, a neighborhood maximum approach was implemented to re-grid the data to a 40-km grid and consider the hour preceding and following the valid hour. This helped train the process and improve the model's results. Additionally, the raw Random Forest generated probabilities were calibrated using a variety of techniques to improve their accuracy and reliability. Verification statistics showed mixed results and research continues to create HREF-based probabilistic CG lightning forecast guidance.

CG lightning climatology maps were generated on a CONUS 40-km grid based on several temporal periods (e.g., hourly, 4-hourly, daily, daily 4-hourly, daily hourly, etc.) using NLDN data from 1995-2016. These maps are currently being refined and will be made publicly available on the SPC website in the near future.



Daily 40-km cloud-to-ground lightning climatology map valid July 20.

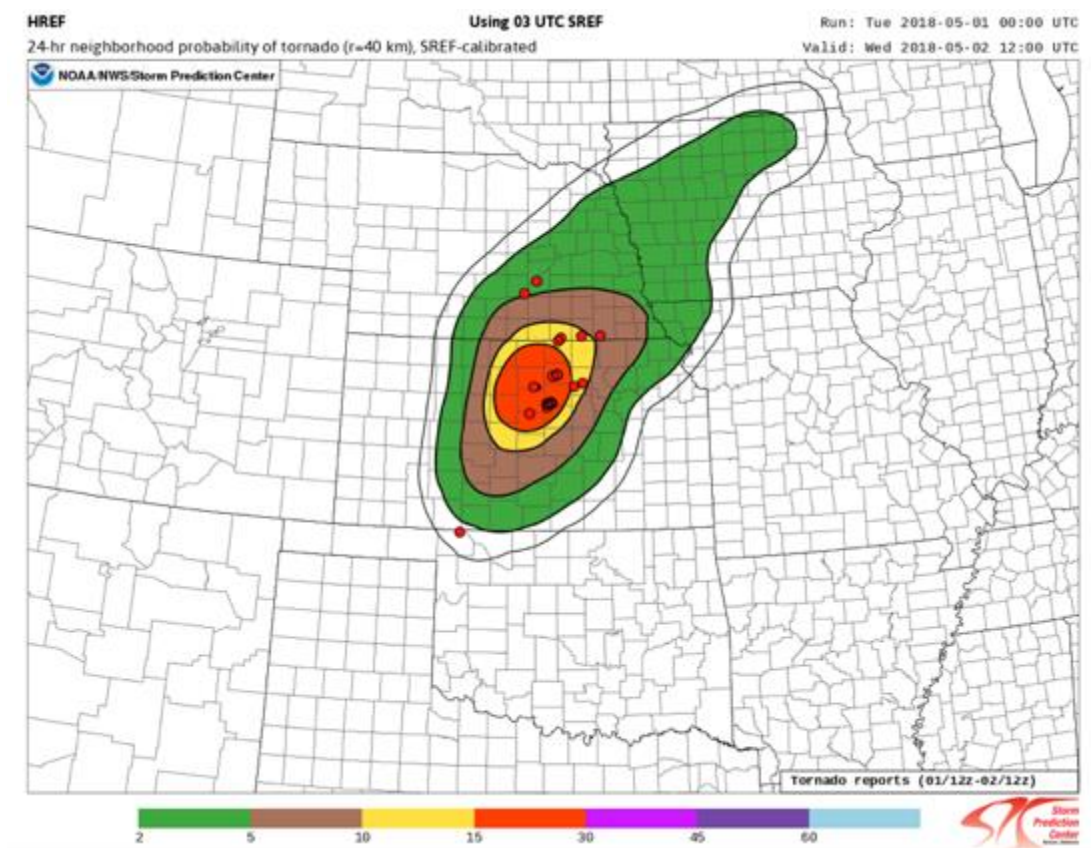
2. HREF/SREF Calibrated Guidance

Caleb Grunzke (CIMMS at SPC) and Israel Jirak (SPC)

This subproject updates the previous Storm-Scale Ensemble of Opportunity (SSEO)/Short-Range Ensemble Forecast (SREF) system Calibrated Guidance to use the newly operational High-Resolution Ensemble Forecast (HREF) system. 4 and 24-hr forecasts are produced for all 3 hazards (i.e., tornado, hail, and wind) and are valid until 1200 UTC the next day. The HREF/SREF Calibrated Guidance uses the nearly the same methodology as the SSEO/SREF Calibrated Guidance. A few differences to note are: 1. The 4-hour neighborhood probabilistic updraft helicity (UH) threshold was increased to $75 \text{ m}^2\text{s}^{-2}$. The HREF's higher resolution of 3-km allows more intense convection to be simulated. 2. The HREF/SREF Calibrated Guidance now runs 4 times per day [2100 (prior day; based on 0000 UTC HREF and 2100 UTC {prior day} SREF), 0300 (based on 0000 UTC HREF and 0300 UTC SREF), 0900 (based on 1200 UTC HREF and 0900 UTC SREF), and 1500 UTC (based on 1200 UTC HREF and 1500 UTC SREF)]. The HREF webpage and HREF/SREF Calibrated Guidance became operational on SPC's website (www.spc.noaa.gov/exper/href) November 1, 2017. The

SSEO webpage and SSEO/SREF Calibrated Guidance were thus discontinued immediately.

The HREF/SREF Calibrated Guidance was tested and evaluated within the 2018 Hazardous Weather Testbed (HWT) Spring Forecasting Experiment (SFE). Each day, participants in the experiment considered the guidance during the daily real-time forecasting activities. The next day, as part of the assessment of experimental forecasts and guidance for the previous day, participants evaluated the utility of the guidance and gave a subjective rating for the placement and magnitude of the forecast probabilities for each severe hazard. Daily and cumulative Fractions Skill Scores (FSS) were also computed for the 2018 HWT SFE 5-week period.



0300 UTC HREF/SREF Calibrated Guidance for tornadoes valid on May 2, 2018 at 1200 UTC over the previous 24 hours for the Central Plains. Tornado reports from May 1, 2018 1200 UTC to May 2, 2018 1200 UTC are shown by the red dots.

3. Calibrated STP Tornado Intensity Guidance

Caleb Grunzke (CIMMS at SPC), and Israel Jirak, Bryan Smith, and Richard Thompson (SPC)

This subproject continued to build off work on the Calibrated STP Tornado Intensity Guidance from the previous year. A couple of accomplishments are as follows: 1.

Increasing the guidance output interval to every hour instead of every 2-hours, and 2. Migrating the guidance creation code to SPC's operational server.

The calibrated tornado intensity guidance was tested and evaluated within the 2018 HWT SFE. Each day, participants in the experiment considered the guidance during the daily real-time forecasting activities. The next day, as part of the assessment of experimental forecasts and guidance for the previous day, participants evaluated the utility of the tornado intensity guidance and gave a subjective rating for the placement and magnitude of the forecast probabilities for the tornado intensity. Daily and cumulative FSSs were also computed for the 2018 HWT SFE 5-week period.

4. GOES-R and JPSS Proving Ground Activities

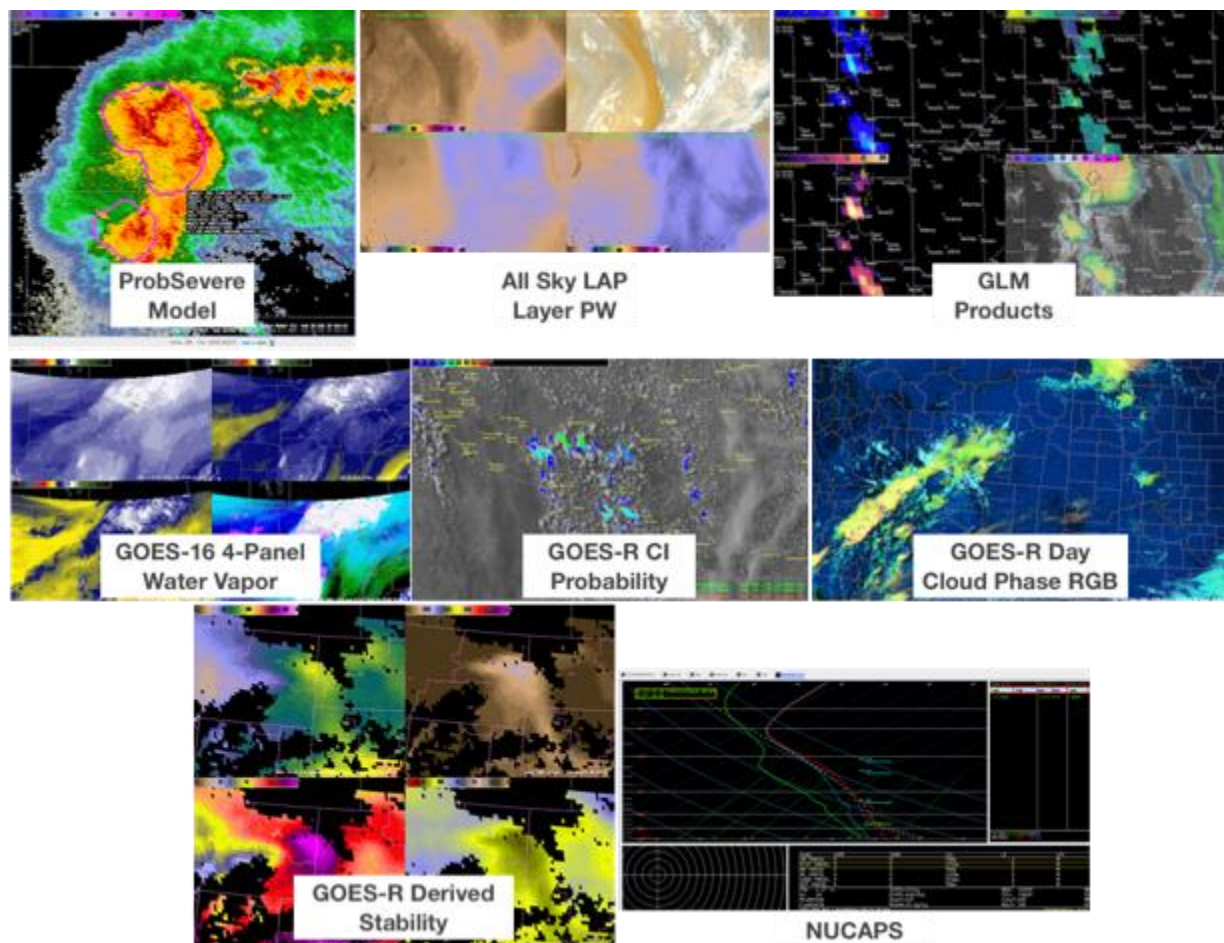
Michael Bowlan (CIMMS at SPC)

During the HWT 2018 GOES-R/JPSS Spring Experiment, GOES-R and JPSS products were demonstrated within the real-time, simulated warning operations environment of the Experimental Warning Program (EWP) using AWIPS-II (see figure below). This experiment was conducted Monday-Friday during the weeks of April 30, May 7, May 14, and May 21, and participants included a new group of three visiting NWS forecasters and one broadcast meteorologist each week 2 -4, with five NWS forecasters testing the products during the first week. Product developers from various collaborating institutions were also in attendance to observe the activities and interact with the forecasters. Monday-Thursday included eight hour forecast/warning shifts, while Friday was a half-day dedicated to final feedback collection. During the simulated forecast shifts, the four forecasters utilized the baseline GOES-16 data along with other experimental satellite products, in conjunction with operationally available meteorological data, to issue non-operational short-term mesoscale forecast updates and severe thunderstorm and tornado warnings. Forecaster feedback was collected through the completion of daily and weekly surveys, daily and weekly debriefs, and blog posts.

GOES-R algorithms demonstrated during the HWT 2018 GOES-R/JPSS Summer Experiment included: GOES-16 baseline ABI cloud and moisture imagery, GOES-16 baseline derived products such as GOES derived stability indices, TPW, and derived motion winds, GOES-16 multi-spectral RGB composites, GOES-16 channel differences, UW/CIMSS ProbSevere Model and ProbTor Model, the GOES-16 Geostationary Lightning Mapper (GLM), the All-Sky LAP Layer Precipitable Water, Total Precipitable Water, and stability indices, and the University of Alabama in Huntsville Convective Initiation Probabilities. Many of the products for GLM were new this year and needed extensive testing and evaluation of their effectiveness before releasing to the field. The experiment proved invaluable in testing this data and on the fly modifications were made per forecaster request to give them the products that they want. Ultimately the GLM products viewed most positively in the 2018 experiment were released to the field in the summer.

From the JPSS program, the NOAA Unique Combined Atmospheric Processing System (NUCAPS) temperature and moisture profiles were demonstrated in the AWIPS-II NSHARP sounding analysis program. An experimental version of the NUCAPS profiles, which applies a boundary layer correction, was also demonstrated again this year with further updates from the previous year. Also, this year the NUCAPS soundings were available via a direct broadcast method which reduced the latency of the soundings from the Suomi-NPP satellite to typically less than an hour. This method was well received by forecasters and was a welcomed addition to the experiment based on feedback from the previous three years of testing in the HWT. The NUCAPS profiles derived parameters were also able to be looked at in a gridded plan view and cross section format.

The SPC has been involved in additional activities related to the launch and data flow of GOES-R series satellites. SPC has been receiving and using GOES-16 data operationally since late 2017 via the local GRB satellite antennas. GOES-16 has been used extensively in operations this severe weather season by SPC forecasters and the satellite liaison has been training staff on the new technologies and products of the satellite. SPC is still awaiting the receipt of GLM data once it is released and preparing ways to best view the data in the forecasters' operational environment. SPC was also still awaiting the arrival of GOES-17 data into operations for testing and evaluation of the new satellite which will become the operational west satellite by the end of the year. Results from the 2017 GOES-R and JPSS product demonstrations in the SPC and HWT were documented by the satellite liaison in final reports and presented at various science meetings. Finally, the satellite liaison continues to contribute to the GOES-R training plan and development.



GOES-R and JPSS products and capabilities demonstrated during the HWT 2018 Spring Experiment.

5. Hazardous Weather Testbed

James Correia, Jr. (CIMMS at SPC)

Supported activities within the Experimental Forecast Program activities of 2018 including:

- A. Grant project (*Test and Evaluation of Rapid Post-processing and Information Extraction from large Convection-Allowing Ensembles applied to 0-3hr Tornado Outlooks*) implementation of object based, rapid post-processing techniques in warning operations for probabilistic hazard information.
- B. The above grant work was implemented in partial form (full gridded fields as opposed to sparse grids) so that NEWS-e data could be ingested into N-AWIPS for 6 and 5 hr forecasts rapidly.

6. Tornado Warning Verification

James Correia, Jr. (CIMMS at SPC)

While investigating convection allowing model uptake in the NWS, Harold Brooks and I noticed through quick verification of warnings that performance had suddenly changed. We have been updating tornado warning verification and its implications for performance as it relates to philosophy and informal policy of perceived problem areas. This work has cross collaboration with previous PHI work and is relevant to SPC's mission given the recent work on tornado report environments in an effort to improve performance resulting from continued improvements in discrimination between environments that produce tornadoes and those that do not. This work further has implications on formal product changes and informal policy changes that may be detectable as the SPC product suite evolves.

7. Mentoring

James Correia, Jr. (CIMMS at SPC)

Emily Tinney and Ronald Kennedy Jr. were mentored as part of the Research Experience for Undergraduates program run by Dr. Daphne LaDue. Emily investigated low level jets from the NSSL Experimental Warn on forecast System for ensembles (NEWS-e). Ronald researched regional NWS tornado warning performance.

8. Public-Facing Outlook Graphics

James Correia, Jr. (CIMMS at SPC)

Explored the use of combined graphical representations of both SPC convective and WPC excessive rainfall outlook graphics when both severe weather and excessive rain overlap posing a double threat to areas of the United States.

9. Project IMPACTS – SPC Predictive Analytics System

Robert Clark (CIMMS at SPC), Patrick Marsh and Russell Schneider (SPC), and Somer Erickson (DHS FEMA)

This year, we continued to extend and improve the IMPACTS system. We began to extend our weather generator concept from tornadoes to encompass other severe convective hazards, like damaging winds and large hail. We substantially improved the tornado portions of the weather generator, by identifying additional conditional tornado intensity probability density functions (PDFs) based on the characteristics of certain types of SPC Tornado Outlooks. These PDFs are defined as follows:

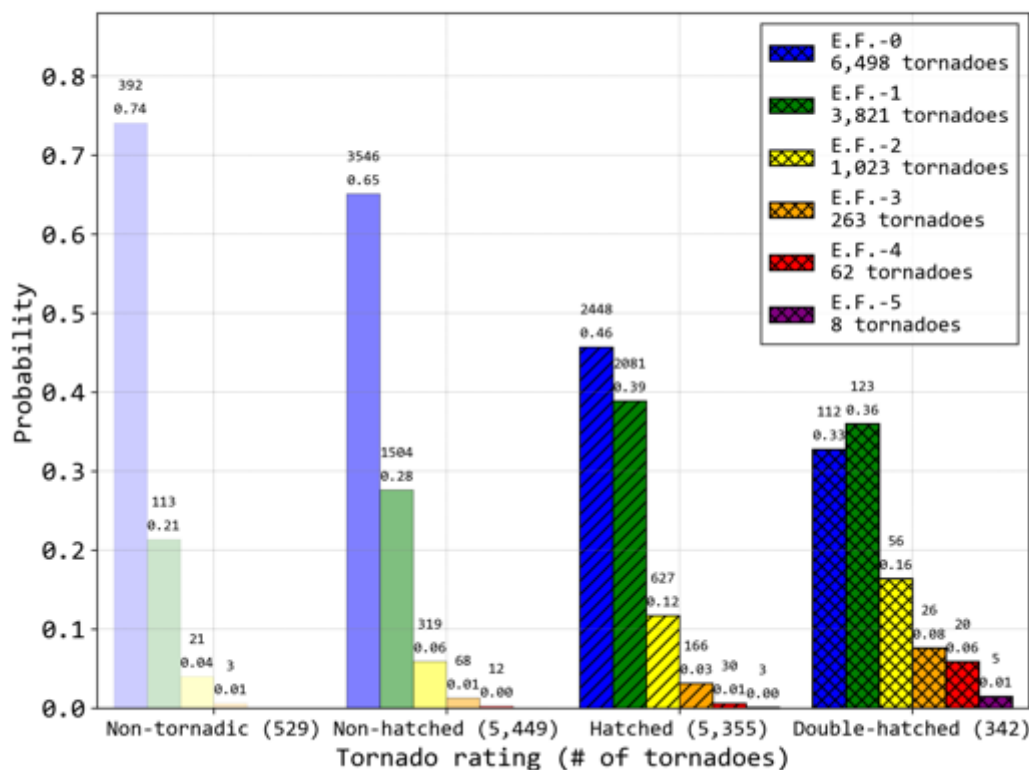
- a.) Non-tornadic: no tornado forecast in effect anywhere in the U.S.

- b.) Non-hatched: in the warm season (May-October), a tornado forecast is in effect but no forecast of significant (\geq EF-2) tornadoes is in effect
- c.) Hatched: in the cool season (November-April), a tornado forecast is in effect somewhere in the U.S., or, in the warm season, a significant tornado forecast is in effect
- d.) Double-hatched: the tornado occurred inside a significant tornado forecast AND a inside a 30% or greater tornado coverage forecast area.

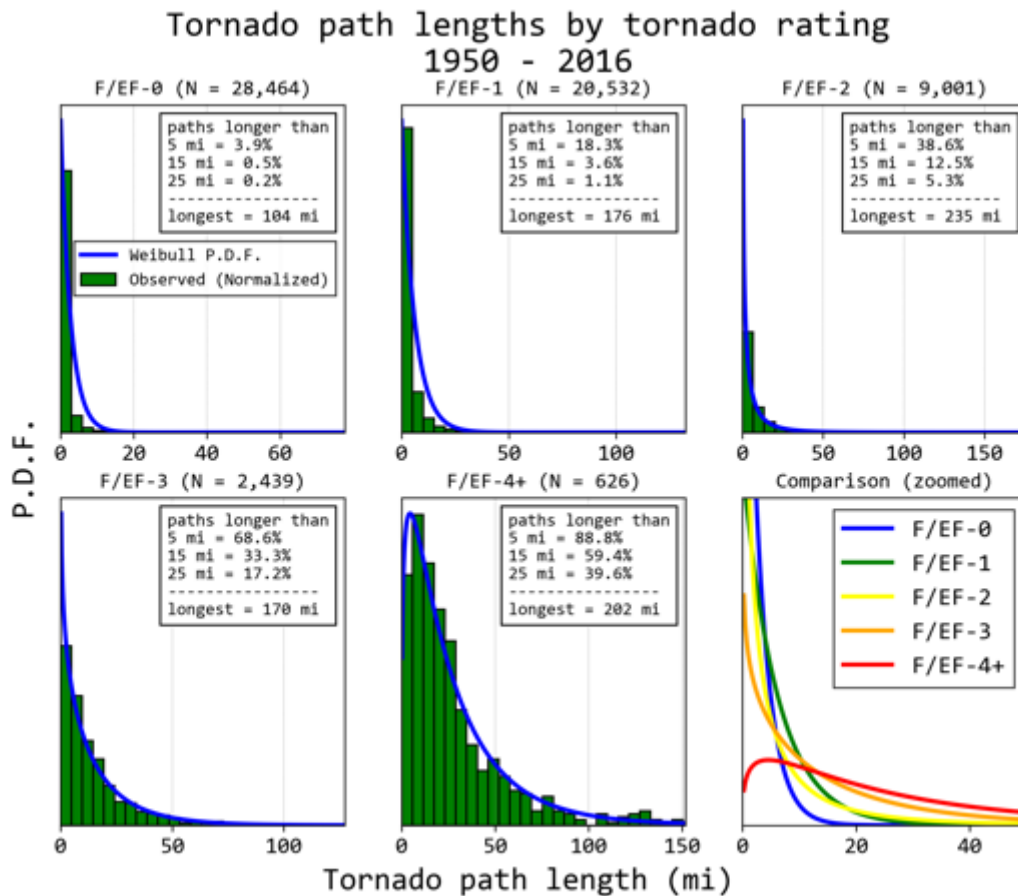
This exercise demonstrates that the conditional probability of a strong (\geq EF-3) tornado increases *exponentially* as the conditional tornado intensity PDF moves from a.) to d.). The final additions we made to the tornado generator are relationships yielding tornado length and width as a function of tornado intensity.

We refactored the code underlying IMPACTS to yield major improvements in simulation speed. Last year, it took approximately 45 minutes to run 10,000 IMPACTS simulations. We've managed to reduce this to approximately 5 minutes for 10,000 simulations today. We've also made major changes to how output from the system is stored, which makes for much speedier post-processing of model results. Finally, we also extended the output from the IMPACTS system, from population exposed to hospitals, mobile home units, powerlines, and power substations exposed.

Tornadoes by rating P.D.F. (0600z S.P.C. Tornado Outlooks)
April 2008 - December 2017



Tornadoes grouped by tornado rating PDF, based on initial Day 1 SPC Tornado Outlooks issued between April 2008 and December 2017.



Distributions of tornado lengths by tornado rating, based on the SPC tornado database from 1950-2017.

Publications

- Blumberg, W. G., T. J. Wagner, D. D. Turner, and J. Correia, Jr., 2017: Quantifying the accuracy and uncertainty of diurnal thermodynamic profiles and convection indices derived from the atmospheric emitted radiance interferometer. *Journal of Applied Meteorology and Climatology*, **56**, 2747-2766.
- Gallo, B. T., and Coauthors, 2017: Breaking new ground in severe weather prediction: The 2015 NOAA/Hazardous Weather Testbed Spring Forecasting Experiment. *Weather and Forecasting*, **32**, 1541-1568.
- Karstens, C. D., and Coauthors, 2018: Development of a human-machine mix for severe convective events. *Weather and Forecasting*, **33**, 715-737.

WDTD Project 12 – Warning Decision-Making Research and Training

NOAA Technical Lead: Ed Mahoney (WDTD)

NOAA Strategic Goal 2 – Weather-Ready Nation – Society is Prepared for and Responds to Weather-Related Events

Funding Type: CIMMS Task II

Objectives

Increase expertise among NOAA/NWS personnel and their core partners on the integrated elements of the warning process. CIMMS scientists conduct applied research, develop and deliver training, and build applications to support the mission of meeting this goal. In doing so, we help NOAA/NWS warning forecasters and their core partners better serve the general public during warning operations and other hazardous weather events that require weather decision support services.

Accomplishments

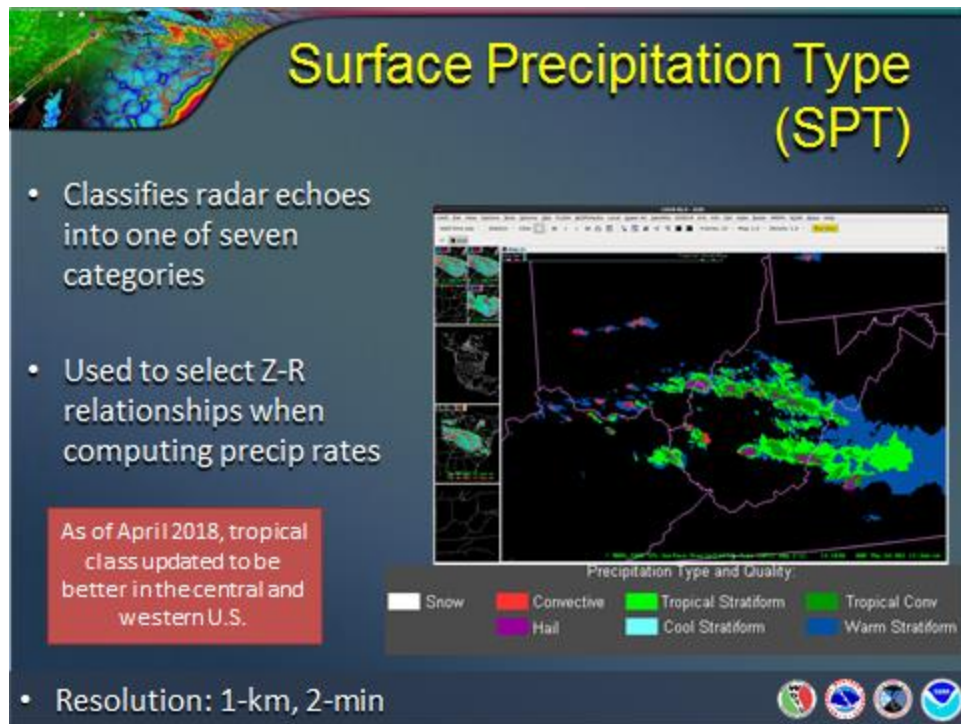
1. Multi-Radar/Multi-Sensor (MRMS) Training

Alyssa Bates, Jill Hardy, Eric Jacobsen, Andrew Wood, and Brad Workman (CIMMS at WDTD), and Steven Martinaitis (CIMMS at NSSL)

The NSSL developed MRMS products over the past decade to overcome limitations inherent in single-sensor products. Many of the MRMS products have been fielded for operational use across the NWS for almost 2 years. CIMMS scientists have been heavily involved in the testing and training for this operational deployment of the MRMS system across the NWS.

WDTD created the initial training for MRMS products as part of the original release in 2014, and continue to maintain and update the available training. In November 2017, CIMMS staff released several updated MRMS product lessons as part of the Version 11.5 product upgrade. These lessons included revised content on hydrometeorological and reflectivity-derived products. CIMMS staff attended weekly MRMS development meetings to stay abreast of product and/or algorithm changes that could affect training. Additionally, CIMMS staff frequently interacted with both NWS forecasters and NSSL developers about MRMS applications in warning decision-making. Future work by CIMMS staff will focus on product updates for the forthcoming MRMS Version 12.

In addition to training modules, CIMMS scientists maintain an in-depth reference guide of MRMS product descriptions in the NOAA/NWS Virtual Laboratory (VLab). NWS forecasters can access this reference guidance on their operational Advanced Weather Interactive Processing System – II (AWIPS-2) workstations, as needed, using the AWIPS Interactive Reference tool when viewing MRMS data during an event. This work is ongoing.



This is a slide from the MRMS Hydro Products Overview lesson that was updated for Version 11.5.

2. Radar & Applications Course

Alyssa Bates, Jill Hardy, Austin Harris, Eric Jacobsen, Dale Morris, Stephen Mullens, Kaitlin Rutt, Chris Spannagle, Matt Sienkiewicz, Stanislav Speransky, Phillip Ware, Brad Workman, Andrew Wood, and Alex Zwink (CIMMS at WDTD)

The Radar & Applications Course (RAC) remains a critical way to prepare forecasters for using the WSR-88D during NWS warning operations. The NWS requires all new forecasters who may be responsible for issuing warnings in the future to complete the course. Recently, more experienced forecasters who needed refresher training have also been able to participate in the course, also. The RAC is taught through a blended approach that combines teletraining, web-based instruction, on-station training, and in-residence training. The course includes a variety of topics regarding the WSR-88D and NWS warning operations, such as weather radar theory and key principles, radar data interpretation, severe storm interrogation techniques, and flash flood threat assessment and forecasting.

Because of this course's size (over 150 individual learning objects that take over 75 hours to complete), CIMMS staff members are heavily involved in all aspects of the RAC. Collaborative work occurs between CIMMS, WDTD federal instructors, Radar Operations Center engineers and software developers, and numerous other forecasters and scientists in order to provide RAC participants with the best training experience possible. This collaborative work ensures recent radar and other meteorological

improvements (including how changes impact a forecasters' abilities to assess severe weather and flash flooding threats) are incorporated into the course. CIMMS participation includes developing numerous on-line training lessons, in-residence exercises, instructor-led training sessions, and simulations. Their work also involves delivering presentations, facilitating simulations, and providing expertise and feedback on warning-decision making issues to the class participants.

CIMMS staff members play a particularly important role during the RAC in-residence training. During this five day workshop, CIMMS instructors maintain and update the Weather Event Simulator – II (WES-2) Bridge lab software, which allows for previous weather events to be replayed on a lab of Advanced Weather Interactive Processing System – II (AWIPS-2) displays. Similar to the flight simulators that pilots use, the WES-2 Bridge lab allows forecasters to collaborate in small groups that act as a single weather forecast office (WFO) that shares warning responsibilities for a specific area. CIMMS staff members work with WDTD federal instructors and contractors to maintain the lab software and hardware and develop training experiences (such as warning simulations, mini-scenarios, and case exercises) that makes this lab a world-class training facility. This work is on-going



National Weather Service forecasters participate in one of four week-long severe weather warning workshops during the Radar & Applications Course held in Norman, OK.

3. Warning Operations Course (WOC)/Seasonal Readiness Training – Core Track

Austin Harris, Dale Morris, Stephen Mullens, Chris Spannagle, Phillip Ware, and Andrew Wood (CIMMS at WDTD)

The Warning Operations Course remains a key component in the WDTD's training delivered each year to NWS forecasters on warning decision making. Instructors use a blended learning curriculum that builds upon knowledge learned during the Radar & Applications Course (RAC) and other foundational training. The WOC training material covers a variety of content in four content areas: Core decision making, flash flooding, severe weather, and winter weather. The most foundational of those content areas is contained in the WOC Core Track (WOC Core). This course contains training on warning decision-making concepts that apply to all weather threats. The WOC Core content can be accessed by students in two ways. Traditionally, forecasters access all of the WOC Core content sequentially to complete the entire track, usually in the year or two after completing the RAC. Recently, the WDTD has created a new learning initiative known as Seasonal Readiness Training (SRT). With SRT, WOC instructors provide forecasters and local training officers with a needs assessment tool with questions related to the WOC content. For any questions the forecaster misses, specific WOC training can be suggested to help the forecaster gain knowledge in these gap areas. By using the SRT needs assessment tool, all forecasters can choose to take a subset of training in a WOC topic area to become more knowledgeable in that topic.

CIMMS staff have worked collaboratively with WDTD instructors over the years developing WOC Core. That collaboration on the course content and SRT assessment tool continued for the FY18 WOC Core. Four lessons in this track were authored by CIMMS scientists with updates for the FY18 release. In addition to their work on the lesson content, they also provided the questions and feedback for the SRT tool on those modules. CIMMS scientists also worked with a team of NWS forecasters as they developed a series of videos delivered via YouTube on finding weather reports using social media applications. These videos were included as optional content in WOC Core. CIMMS personnel also provided a variety of logistical support, including responding to questions from NWS forecasters, reviewing and providing exercise feedback, assisting local training facilitators, creating statistical progress reports for monitoring completions, and providing certificates of completions to students. This work is ongoing as the FY19 course will be released in January 2019.



This image shows a screen shot from a YouTube developed by a NWS forecaster on using Facebook to search for weather reports. CIMMS personnel collaborated with the team that developed a series of 21 videos on using social media, curated the videos as an optional component to WOC Core, and integrated some of their suggestions into existing WOC Core lessons.

4. Warning Operations Course (WOC)/Seasonal Readiness Training – Flash Flood Track

Jill Hardy, Andrew Wood, Chris Spannagle, Dale Morris, Alex Zwink, Brad Workman (CIMMS at WDTD)

The Warning Operations Course – Flash Flood Track (hereby, WOC Flash Flood) provides training on advanced warning decision-making techniques to every NWS forecaster with flash flood warning responsibility. Throughout the years, CIMMS scientists (in collaboration with WDTD instructors) have been heavily integrated into the development, delivery, and support of WDTD's WOC Flash Flood. Additionally, WOC Flash Flood content is repackaged to deliver annual Seasonal Readiness Training (SRT). The SRT framework allows interested training officers and/or forecasters a method to determine which training they may need prior to the local flash flood season. CIMMS scientists developed tools to assess these training needs, as well as cataloging

the available training that can help address any gaps in knowledge. SRT has been very successful in promoting an individualized training plan approach for the WOC Flash Flood that pinpoints the needs of each forecaster.

Numerous updates were made to the WOC Flash Flood by CIMMS scientists this year that brought the latest in flash flood research, tools, and best practices to NWS forecasters. CIMMS staff developed five new online lessons covering topics such as forecasting flash floods in the west, using various AWIPS tools to improve flash flood responsibilities, and best practices for using the Flooded Locations And Simulated Hydrographs (FLASH) suite of products for enhanced warning operations. These upgrades resulted in nearly 30% of the FY18 WOC Flash Flood online content being new or significantly updated from previous years. CIMMS scientists managed the delivery of the course. In addition to performing the course needs analysis and designing the curriculum, CIMMS staff provided logistical support such as responding to questions from NWS forecasters, assisting local facilitators, providing certificates of completion to students, and producing statistical progress reports of students using the Commerce Learning Center (CLC) learning management system.

The work on WOC Flash Flood is ongoing as an important part of training NWS forecasters. Besides managing the formal WOC Flash Flood course, CIMMS scientists represented the WDTD in several collaborations with high-level NWS hydrometeorological experts. During one such situation, a CIMMS scientist at WDTD represented the Office of the Chief Learning Officer (OCLO) on the national Rapid Onset Flood Services team. NWS management tasked this team to create a report on the future of flash flood services in the NWS. Additionally, CIMMS staff facilitated webinars with Weather Prediction Center forecasters about their flash flood products and services. CIMMS scientists will continue to participate in such collaborations that aid the NWS mission.

For the FY18 release of WOC Severe, CIMMS scientists performed several important roles with the course. CIMMS staff updated lessons to improve content on total lightning and added a series of lessons on convection allowing models (CAMs). CIMMS researchers worked collaboratively with WDTD instructors to create a new WES-2 Bridge simulation for the course that better supports the current course objectives. Additionally, CIMMS staff created scripts, updated webpages, and managed two separate ten-week iterations of the Severe Forecast Challenge, an applied learning exercise where forecasters apply concepts learned from the WOC Severe track in a forecasting environment. This past year, the forecast challenge included 345 NWS forecasters who issued over 13,800 individual forecasts. CIMMS scientists also contribute logistical support for the WOC Severe course and its management. This support includes responding to questions from NWS forecasters, assisting local facilitators, providing certificates of completions to students, and producing statistical progress reports of students and forecast offices using NOAA's Learning Management System. This work is on-going.

What are CAMs?

Section Roadmap

- No convective parameterization
- Convection "allowing" not resolving

- CAMs are **high resolution** models
- Horizontal grid spacing (Δx) $\leq 4-5$ km
- Convective parameterization turned off

HOME **Next >**

This figure shows an example slide from one of the new convective allowing model (CAM) lessons developed for the FY18 version of WOC Severe. These lessons cover both deterministic and ensemble CAM fundamentals, as well as other key details that aid forecasters in interpreting their output during severe weather warning operations.

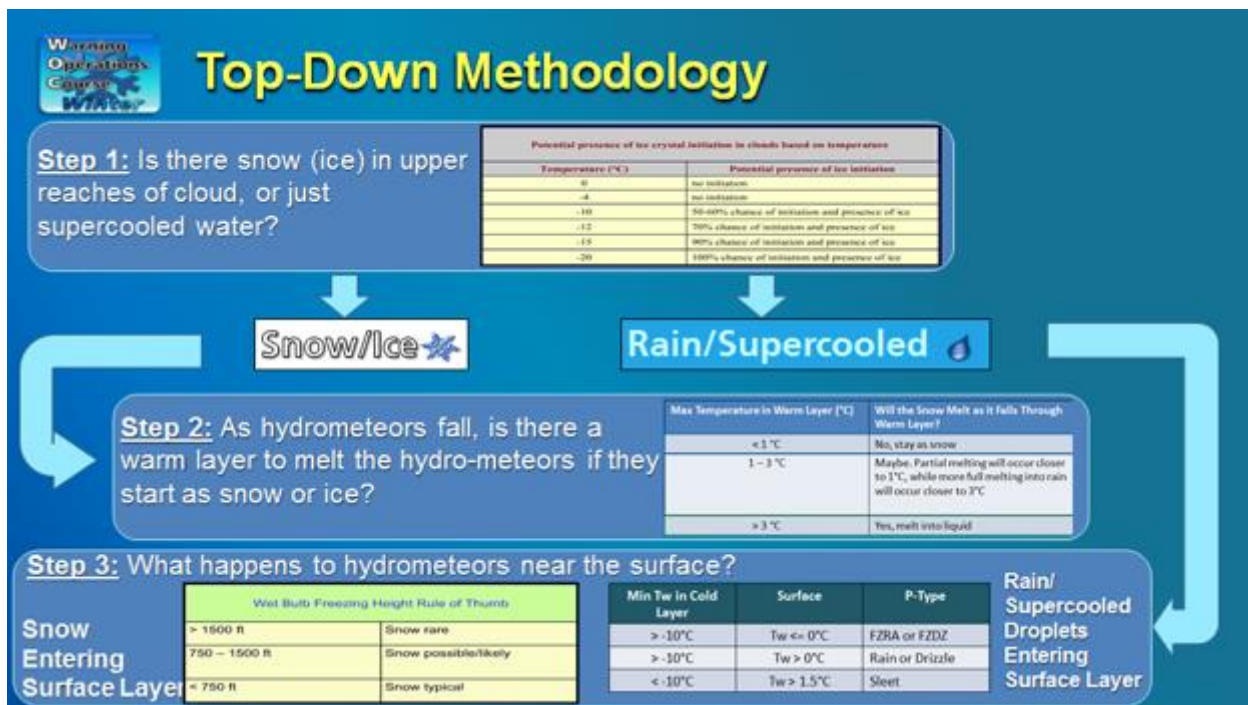
6. *Warning Operations Course (WOC)/Seasonal Readiness Training – Winter Track*

Alyssa Bates, Stephen Mullens, Matt Sienkiewicz, Chris Spannagle, and Andrew Wood (CIMMS at WDTD)

The Warning Operations Course – Winter Track (hereby, WOC Winter) provides training on advanced warning decision-making techniques to every NWS forecaster with winter weather warning responsibility. This course released an updated version (with completely new content) after a hiatus of several years in September 2017. CIMMS staff worked with WDTD instructors and subject matter experts from universities, the National Weather Service (NWS), and the National Center for Environmental Prediction (NCEP) Weather Prediction Center (WPC) to develop and deliver the FY17 WOC Winter. The modules covered various topics, including conceptual models, forecasting hazards, physiogeographic systems, remote sensing of winter hazards, the forecast warning process, and winter weather impacts. The WOC Winter course also included a Seasonal Readiness Training (SRT) needs assessment tool. With SRT, the WDTD provides forecasters and local training officers with questions related to the WOC content. For whatever questions the forecaster misses, forecasters can take suggested WOC training to gain knowledge and overcome any gaps they have. By using the SRT needs assessment tool, forecasters can choose to take an entire section of training in a WOC topic area to become more knowledgeable in that topic.

CIMMS staff contributed to the course in numerous ways. They coordinated the course development effort with many of the subject matter experts and reviewers, provided feedback to the developers, and created the SRT assessment and other evaluation materials. CIMMS staff also coordinated training webinars with the WPC Winter Weather Desk team. Their tasks included reviewing presentation material, hosting the webinars, and recording and post-processing a version for release online. CIMMS scientists contributed to the course in a third way: The Winter Forecast Challenge. The Winter Forecast Challenge is an applied learning exercise loosely based on the NWS Probabilistic Snowfall Experiment where forecasters used concepts learned from the WOC Winter training content to issue pseudo-probabilistic snowfall forecasts for a user-defined location. CIMMS staff developed and implemented the challenge for the 48 NWS forecasters and WOC Winter enrollees who participated. The participants collectively issued more than 700 unique forecasts over the eight-week duration of the challenge.

This work is ongoing. CIMMS staff started work on an interactive simulation to help reinforce WOC Winter concepts and practice applications for the FY19 version of the course. The forecast challenge will be hosted by WDTD again next year as part of the WOC Winter, too.



This figure is from the WOC Winter lesson entitled "Precipitation Type: Forecasting Methodology." The information was compiled by an NWS Weather Forecast Office supervisor and designed by CIMMS staff.

7. Weather Surveillance Radar – 1988 Doppler (WSR-88D) Build Improvement Training

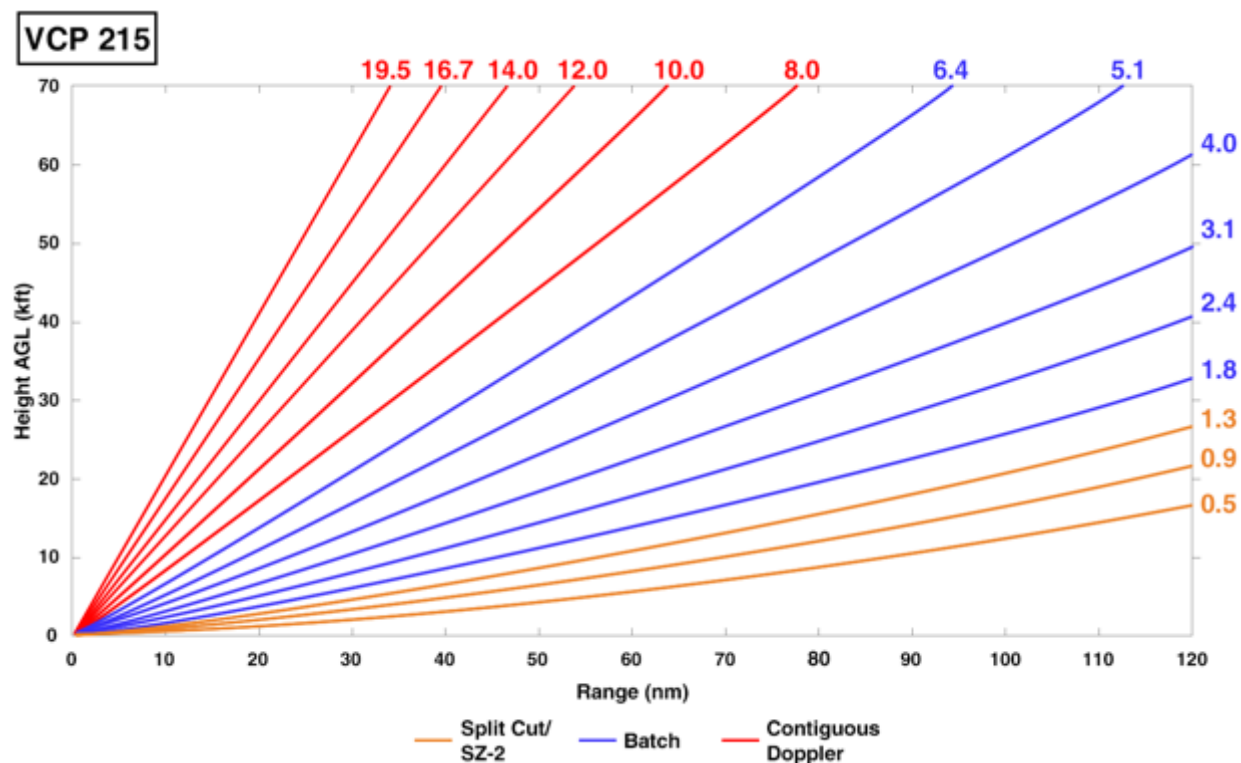
Brad Workman and Andrew Wood (CIMMS at WDTD)

The WSR-88D radar upgrades occur routinely, approximately once a year during its life cycle to maintain the system and integrate new science and technology. As these build updates to the system occur, CIMMS personnel work closely with WDTD instructors and partners at the Radar Operations Center (ROC) during training development and delivery for NWS staff. Additionally, the WSR-88D training can be accessed by NWS partners who work with the radar. CIMMS work on this project includes supporting training development and delivery for the build release, ensuring new functionality details gets integrated into other WDTD radar courses, making various radar training courses easily available for NWS partners (including dual-polarization radar technology training), answering questions from NWS forecasters about WSR-88D build details, and collaborating with experts to help optimize the list of radar products accessed by NWS weather forecast offices (WFOs) nationwide.

During the past year, CIMMS staff supported the development of training for the most recent radar build release (Build 18.0). The Beta test for RDA/RPG Build 18 occurred in early 2018 with deployment starting in May 2018. Several significant changes occurred with this update, including removal of several previously existing Volume Coverage Patterns (VCPs), the implementation of two new VCPs (one for clear air and one for

general weather surveillance), and significant operating system and Human Control Interface upgrades.

This work is ongoing as the WSR-88D continues to receive periodic software and hardware upgrades.



This schematic shows the elevation angles in one of the new Volume Coverage Patterns (VCP 215) that was introduced in Radar Data Acquisition Unit (RDA)/Radar Product Generator (RPG) Build 18.0. VCP 215 was developed for general weather surveillance. CIMMS personnel developed graphics like this one for use in Build 18 related radar training for NWS staff. This image is just one of many ways that CIMMS scientists aid WDTD instructors with training development.

8. AWIPS (Advanced Weather Information Processing System) Training

Eric Jacobsen, Stanislav Speransky, Dale Morris, Alex Zwink, Thao Pham, and Phillip Ware (CIMMS at WDTD)

During the past fiscal year, CIMMS meteorologists and federal WDTD instructors continued to work together to train NWS meteorologists in support of the AWIPS (Advanced Weather Interactive Processing System) build update release schedule. This work included updating the AWIPS Fundamentals course, which provides new NWS employees with a baseline understanding of the AWIPS system. Subsequent AWIPS training builds upon this fundamental course. The course uses a series of training videos, exercises, and job aids that incorporate the Weather Event Simulator (WES-2) Bridge to meet these training goals. In addition to this course, CIMMS staff developed

new AWIPS Informational Overview training modules that coincide with software release schedules. These short, stand-alone modules focus on the new enhancements and tools packaged in each software update. The builds released during this past training year include AWIPS 17.2.1, and 17.3.1. Besides these online training materials, CIMMS staff also contributed significantly to the technological configurations of AWIPS used in residence workshops at the WDTD (such as the Radar and Applications Course) and instructed the laboratory sections of these courses.

Also especially noteworthy, CIMMS staff continued to develop expertise for the approaching rollout of Hazard Services, which is a framework developed by the Global Systems Division (GSD) laboratory that will eventually unify and replace existing critical warning and product generation software (WarnGen, RiverPro, and certain components of the Graphical Forecast Editor) used by NWS field offices. The CIMMS team leveraged proficiency with AWIPS installations and dataset management to enable rapid configuration and testing of dozens of versions of the Hazard Services software, allowing critical feedback and contributions to performance improvements. Simultaneously, CIMMS employees also explored the establishment of a training platform for Hazard Services through WES-2 Bridge development and other innovations including computer virtualization. Furthermore, they collaborated with GSD, the AWIPS prime contractor Raytheon, and NWS staff in weekly planning calls, and attended on-site workshops to gather information and share best practices on the configuration and use of Hazard Services. As this software begins to roll out in the upcoming year, CIMMS will continue to play a central role in training NWS staff and supporting its adoption.

Finally, CIMMS staff at WDTD continue to expand their detailed AWIPS expertise while serving as technical focal points for supporting the training mission of the WDTD. This expertise includes development of comprehensive datasets to be used in case analysis and simulations for all WDTD training projects. Additionally, CIMMS created new utility programs for more efficiently sharing data and configuration resources among WDTD and NWS offices. The testing of new software and products, which has resulted in bug identification and software improvements impacting NWS products, continues to involve collaboration with the Radar Operations Center (ROC), National Severe Storms Laboratory (NSSL), the Hazardous Weather Testbed (HWT), GSD, other NOAA partners, and Raytheon.

As the rapid pace of evolution of AWIPS persists, CIMMS will continue providing a vital contribution to the testing, familiarization, and training delivery of this critical software to both the entire NWS organization.

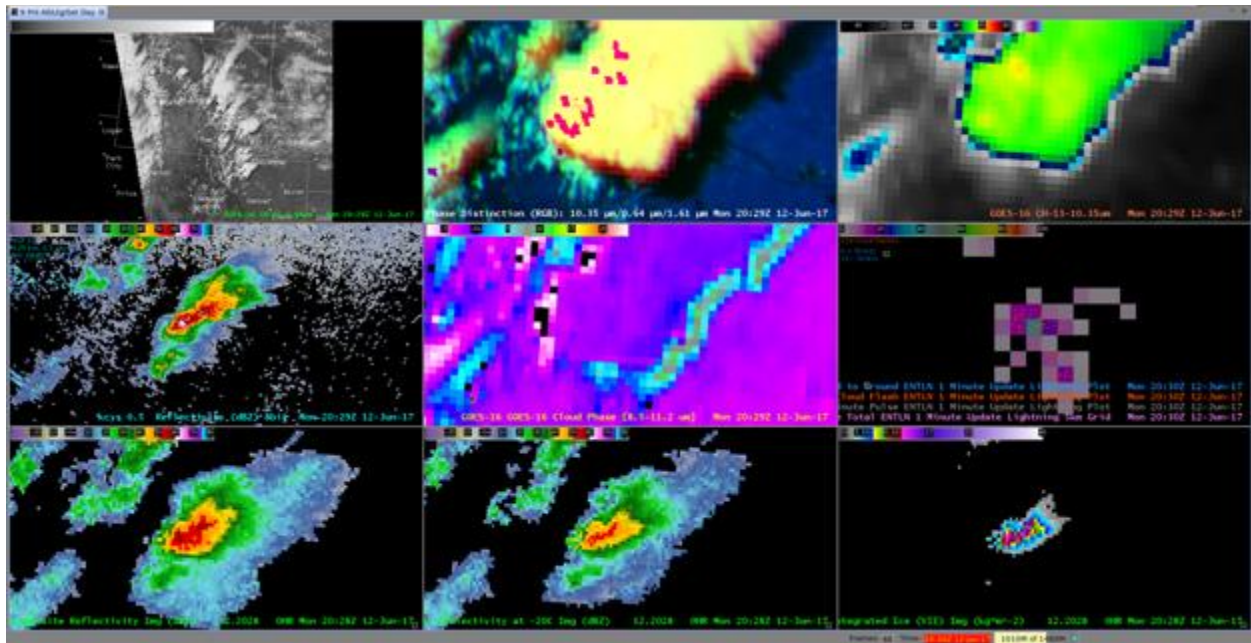
9. GOES-R (Geostationary Operational Environmental Satellite - R) Infusion into WDTD Training

Kaitlin Rutt, Dale Morris, and Alex Zwink (CIMMS at WDTD)

The main goal of GOES-R training development by CIMMS researchers at WDTD was to develop exercises for fusing GOES-R series satellite data with other data sources with the aim of instructing forecasters in best practices in solving short-term forecast and warning problems. The first such problem involved anticipating initial cloud-to-ground lightning strikes with up to a one-hour lead time – a common challenge for forecasters when providing decision support to other government agencies tasked with public safety for large outdoor venues. With this focus on detecting signals for convective initiation and first lightning, CIMMS staff examined several archived cases and developed visualization techniques using the Advanced Weather Information Processing System (AWIPS) and the Weather Event Simulator so the techniques would be directly applicable and transferable into NWS operations. The data fusion aspect of this project considered the NLDN (National Lightning Detection Network), Total Lightning, GOES-16 mesoscale and CONUS (continental United States) sectors, the WSR-88D, and the MRMS (Multi-Radar Multi-Sensor) product suite. Additional considerations centered on the timings and latencies involved with the minute-by-minute availability of each source.

Factors examined in these case studies included which data sources were most valuable in situations based on day versus night, the availability of GOES-16 mesoscale sector, and the proximity of convection to WSR-88D units. The cases also spanned the southeast US to the western US. Depending on the presence or absence of cirrus, sometimes GOES-R provided lead time in detecting new cells compared to the radar or MRMS.

One other aspect of developing training using GOES-16 case studies involves challenges of archival of this data at NWS forecast offices due to the voluminous nature of this data. WDTD staff also developed a data processing technique to utilize archived GOES-16 data from the Comprehensive Large Array-data Stewardship System (CLASS) system at the National Centers for Environmental Information (NCEI) in conjunction with the Weather Event Simulator. The GOES-16 data from CLASS is in a slightly different format from what NWS forecast offices receive but the resulting AWIPS displays are equivalent as what forecasters normally view. This work is ongoing.



Sample nine-panel visualization in AWIPS of products considered for diagnosing the convective initiation problem: top-left: Visible imagery from GOES-R (Channel 2); top-middle: GOES-16 false-color, multi-spectral, composite (RGB) imagery designed for cloud phase distinction using channels 13, 2, and 5 for Red, Green, and Blue, respectively; top-right: GOES-16 imagery for Channel 13; left-middle: base reflectivity at 0.5 degree elevation from the KCYS WSR-88D; center, GOES-16 Cloud Phase product (difference between Channels 11 and 14); right-middle: Total Lightning from Earth Networks; bottom-left: MRMS composite reflectivity; bottom-middle: MRMS reflectivity at -20°C; bottom-right: MRMS Vertically Integrated Ice. Note that all these products rapidly update and are valid to within two minutes of the analysis time at 2030 UTC on Monday, 12 July 2017.

10. SOO (Science and Operations Officer) Development Course Support

Alex Zwink and Dale Morris (CIMMS at WDTD)

The Science and Operations Officer (SOO) at a National Weather Service (NWS) Weather Forecast Office (WFO) serves as the training officer for that particular office. In this role, they oversee and facilitate the professional development of the staff at that office, as well as infuse new science into the operational workflow at the office. Prior to 2015, SOOs attended two separate courses to train them on both of these aspects of their position. The first course, called the COMET Mesoscale Analysis and Prediction (COMAP) course, focused on mesoscale science topics. The second course, taught by WDTD, taught adult learning facilitation skills to SOOs and their counterparts at River Forecast Center offices (i.e., Developmental and Operational Hydrologists, or DOHs).

In 2015, the NWS Office of the Chief Learning Officer (OCLO) decided to create a new course for SOOs that combined elements from both COMAP and the WDTD facilitation training. The 2017 version of this course was held at the NWS Training Center (NWSTC) in Kansas City, and OCLO plans to conduct this course on a bi-annual cycle.

For the 2017 version, CIMMS worked with the NWSTC to establish a seven-workstation mini-laboratory with WES (Weather Event Simulator) workstations and helped to assemble archived cases for laboratory sessions on severe weather and FLASH (Flood Locations And Simulated Hydrographs). Finally a session on data archiving and using the WES for building exercises and simulations was presented to the attendees.

This work is ongoing, but CIMMS involvement is dependent on the exact agenda that is developed for each course which varies for each offering.



Laboratory session of the 2017 SOO Development Course at the NWS Training Center in Kansas City, MO. Participants are using the Weather Event Simulator to study a severe weather event that took place in the Jackson, MS, county warning area that features new high-resolution datasets like convection-allowing models, MRMS, and GOES-16 imagery. CIMMS staff were instrumental in configuring this mini-lab with the latest WES software, assisting the Jackson WFO in archiving the case data, and retrieving the AWIPS configuration files from the Jackson office for this exercise.

11. VLAB (Virtual Lab) Training

Steve Corfidi, Eric Jacobsen, and Stanislav Speransky (CIMMS at WDTD)

The primary purpose of WDTD's Virtual Laboratory (VLab) initiative is to develop training to effectively integrate the VLab into NWS training and operations. CIMMS staff initially focused on gaining familiarity with VLab, and on developing an introductory training package for VLab users. This training, "VLab Fundamentals Training – Module 1: Introduction for Community Users", provided an overview of the techniques needed for using VLab's most fundamental collaborative tools (e.g., blogs, forums, and wikis).

Because the NWS's Meteorological Development Laboratory (MDL) updated the VLab's underlying software from *Liferay 6.2* to *Liferay DXP* ("Digital Experience"), significant changes resulted in VLab's "look and feel" along with file access and management changes for both VLab administrators and regular users. As a result, the above fundamentals module was updated to bring it into compliance with *Liferay DXP*. The module's accompanying jobsheet also was updated.

A CIMMS scientist also is designing a follow-up module addressing VLab community management. "Communities" are groups of VLab users assembled to collaborate on a common mission or topic. Default VLab communities have been set up for each local National Weather Service Forecast Office and River Forecast Center to facilitate project collaboration at the local level. Additional communities exist for NWS-wide projects, such as AWIPS and GOES-R and many others. For the default local office communities, management is a responsibility of the office SOO (Science and Operations Officer), DOH (Development Operations Hydrologist), or ITO (Information Technology Officer). This new module provides community managers and content contributors with an introduction to management tasks. The module and an accompanying job sheet are planned for release in September 2018.

Previous VLab development included an integrative component into AWIPS called the AWIPS Interactive Reference (AIR) tool. CIMMS staff at WDTD continued to upload and maintain a growing set of reference materials for many of WDTD's core deliverables available both inside and outside of the AWIPS system. CIMMS staff also continued to contribute to VLab redesigns and best practices, and provide support to many users throughout the NWS as the VLab's reach and capabilities continue to evolve. This work is ongoing.

Permissions for Portlets

...require check of the Edit Control icon:



Sample training slide from the VLAB focal point module on configuring permissions for collaborative blogs.

12. WES (Weather Event Simulator) Development

Dale Morris, Alex Zwink, Thao Pham, Phillip Ware, Ali Virani, and Eric Jacobsen (CIMMS at WDTD)

The Weather Event Simulator (WES) located in each NWS Weather Forecast Office (WFO) allows forecasters to meet the NWS Directive 20-101 requirement for every forecaster to complete two simulations prior to each significant weather season – the only such training requirement in the NWS Directive system. The NWS recently conducted an internal survey (presented by Frank Alsheimer, the Science and Operations Officer from the Columbia, SC, Weather Forecast Office) of over 400 forecasters and managers focused on human factors and office culture issues involved in warning decision making for tornadoes. Most of the respondents (78%) agreed or strongly agreed that the training they receive is effective. In responses to open-ended questions, WES cases were the most-often noted beneficial training activity.

To meet the need for NWS forecasters to apply training concepts in particular weather scenarios, CIMMS staff at WDTD developed the first generation WES over a decade

ago. As the NWS routinely upgrades their Advanced Weather Interactive Processing System (AWIPS-2), CIMMS staff continues to develop the simulator to maintain this important capability. WES allows forecasters to both simulate past weather events for training purposes, as well as view and analyze archived weather for local research projects, while preserving a critically-important operational representativeness (i.e., forecasters interact with the data and create forecasts and warnings in exactly the same ways as they do during regular operational shifts). This system is also called WES-2 Bridge, and sometimes abbreviated to WES-2, because this system serves as a prototype for eventual inclusion of simulation and training capability in AWIPS itself.

The simulator represents significant engineering development because WES, as a training tool, has requirements above and beyond the normal AWIPS-2 system it emulates. The simulator features a tool (the WES Scripting Language or WESSL) for streamlined presentation of non-AWIPS information (such as spotter reports, video, briefings, web-based presentations, and engaging forecasters with feedback) during a simulation. Also, forecasters use the WES in two primary modes: (1) simulations with time-sequenced revelation of data (called displaced real-time or DRT) and (2) case reviews where they can choose the time to view from a local WFO archive.

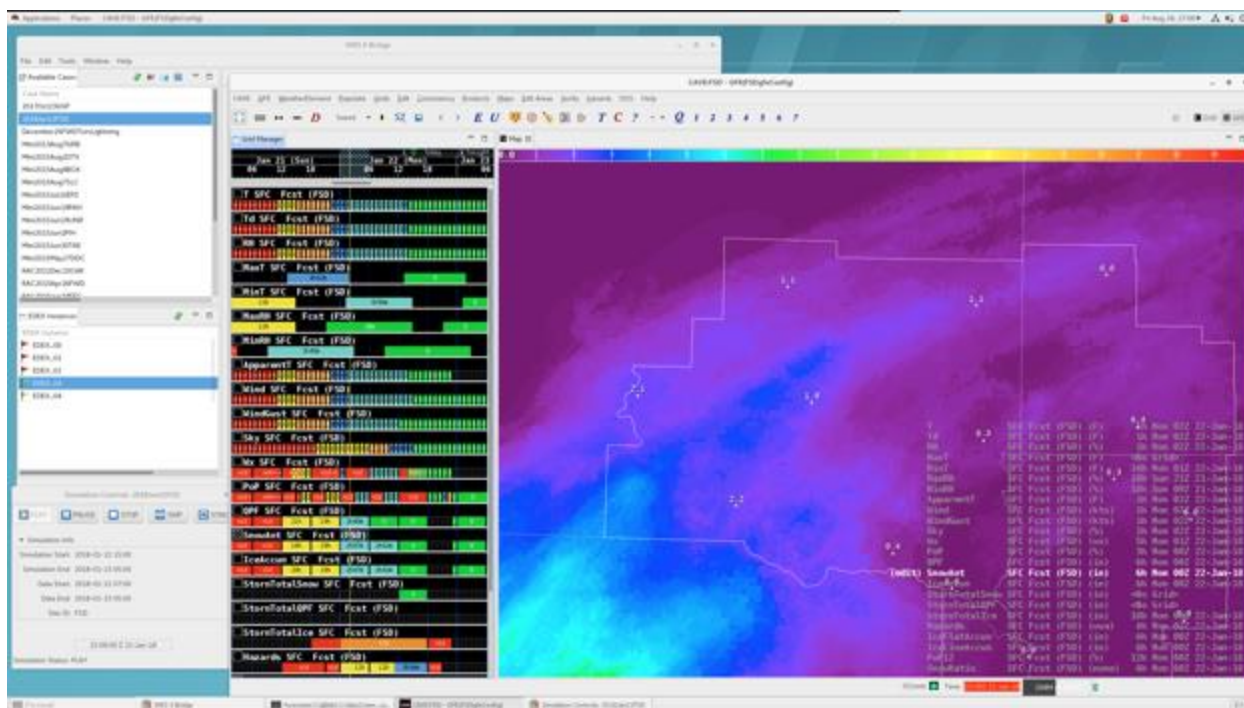
Significant work was conducted by CIMMS staff over the past year on upgrades to the WES. First, the system was upgraded to be compatible with AWIPS build 17.1.1. Additional development tasks included work towards a capability for converting AWIPS-1 data archives to AWIPS-2 accessible formats. This version of the simulator also included capabilities to support the AWIPS Graphical Forecast Editor (GFE). GFE is the primary tool that forecasters use to prepare and issue forecasts, the majority of routine text forecast products, and long-fuse watch, warning, and advisory products. With the addition of GFE capability, forecasters will use WES as part of an updated Warning Operations Course (Winter Weather) for a more operationally relevant training experience. Additional substantial effort was required for the next planned upgrade (version 17.3.1) due to operating system changes and security benchmarks mandated by the NWS.

Simulator equipment provided by the NWS exists at each WFO, but certain challenges, mostly related to the time and space required for data archiving and constraints within the operational AWIPS system, sometimes require more effort to prepare simulations at local offices than is desired. Consequently, a SOO (Science and Operations Officer) WES Advisory Team (SWAT) convened to develop requirements to inform future directions not only for CIMMS staff at WDTD but also for NWS management. Accordingly, the NWS AWIPS program plans to add this simulator capability in the “baseline” system in the future, and CIMMS personnel at WDTD serve a critical role as subject matter experts for these future enhancements and for details related to data archival.

The SWAT team also documented that physical and operational constraints currently result in additional problems such as multiple NWS offices independently and redundantly archiving the same datasets as well as conducting simulations in an

isolated fashion. This second concern means there is a lack of practicing critical communication and collaboration team skills inherent in a distributed forecast and warning system that presently operates within the NWS field office structure. Both concerns result in a lack of sharing of simulation resources within the NWS. Consequently, CIMMS staff have started to investigate the feasibility of deploying the simulator and an accompanying archival system in virtualized cloud-based computing systems. Initial results are promising as the WES has been successfully deployed in two different cloud platforms, though other challenges and development needs exist. The NWS is also beginning to test cloud-based platforms for their own internal development needs and the WES is part of their current planning efforts.

CIMMS also continued to develop and maintain an AWIPS/WES laboratory at WDTD. This unique 28-workstation environment incorporates centralized command and control of simulator functions. It also features flexible configurability from single-user simulations to multi-user, collaborative simulations where groups of trainee forecasters act as a single WFO and share warning responsibilities. In this mode, one forecaster issues a simulated warning and his/her partner can modify the warning with updated information, exactly as in real-world NWS operations. This laboratory plays a significant role in the Radar and Applications Course (RAC) workshops. Additionally, CIMMS staff used this lab in several outreach activities. Work on the WES, as well as WDTD's lab, is ongoing.



Screen capture of a WES simulation featuring the AWIPS Graphical Forecast Editor (GFE). The image shows the gridded snowfall forecast from the Sioux Falls, SD, NWS Weather Forecast Office valid at 0000 UTC on 22 January 2018.

13. WES (*Weather Event Simulator*) Support

Alex Zwink, Dale Morris, Thao Pham, and Phillip Ware (CIMMS at WDTD)

CIMMS staff at WDTD have provided WES support to NWS Weather Forecast Offices (WFOs) since the simulator's inception. As development of the current generation WES moves forward, technical and logistical WES support for the NWS continues in earnest; support takes several forms. Forecasters can contact CIMMS staff through a variety of tools, such as Google chat, phone calls, direct e-mail, and e-mail lists. They ask various questions that relate to either general technical issues, data archiving, or help implementing specific WDTD training on these workstations. When necessary, CIMMS staff can access a local office's WES workstation through a remote connection over the NWS Advanced Weather Interactive Processing System (AWIPS) network. This direct access provides CIMMS staff the ability to directly troubleshoot both hardware and software issues. The complexity of the simulator (and especially the underlying and routinely changing AWIPS system) makes this level of access crucial to providing quality customer support. CIMMS staff exploited this direct access to remotely update some of the software components when needed. Finally, CIMMS staff maintain a WES-2 webpage with technical documentation and other support information for forecasters to access when CIMMS personnel are not immediately available or for solutions to routine problems.

CIMMS staff also provide guidance and support to other CIMMS and NWS instructors at WDTD as well as colleagues at NSSL and the Cooperative Institute for Research in the Atmosphere (CIRA) who also use the system. In these situations, they provide guidance in AWIPS data collection, simulation development, and case deployment for training. Their aid in these areas, as well as distributing material for training simulations to NWS WFOs, provides a critical area of support for a variety of WDTD training projects. CIMMS expertise has helped NSSL utilize the WES as a simulation platform for some of their Hazardous Weather Testbed experiments. This gives NSSL more flexibility in using archived weather events while also using less system resources. Finally CIMMS staff have collaborated with the NWS National Reconditioning Center when WFOs experienced a WES-related hardware issue.

Publications

Department of Commerce, 2017: Commerce Learning Center (CLC). Available at: <http://doc.csod.com/>
Warning Decision Training Division, 2017: Radar & Applications Course (RAC). Available at: <http://training.weather.gov/wdtd/courses/rac/>
Warning Decision Training Division, 2017: Multi-Radar/Multi-Sensor (MRMS) Training. Available at: <http://training.weather.gov/wdtd/courses/MRMS/>
Warning Decision Training Division, 2018: Severe Weather Forecast Challenge. Available at: <https://secure.training.weather.gov/wdtd/secure/AWOC/NWS/Online/>
Warning Decision Training Division, 2017: Winter Weather Forecast Challenge. Available at: <https://secure.training.weather.gov/wdtd/secure/woc/winter/forecast-challenge/>
Warning Decision Training Division, 2017: Warning Operations Course (WOC). Available at: <http://training.weather.gov/wdtd/courses/woc/>
Warning Decision Training Division, 2017: WSR-88D Build Training. Available at: <http://training.weather.gov/wdtd/buildTraining/RPG-RDA.php>
Warning Decision Training Division, 2017: Weather Event Simulator II (WES-II) Bridge. Available at: <http://training.weather.gov/wdtd/tools/wes2/>
Corfidi, S., 2017: Forecasting Severe Convective Storms. In *Oxford Research Encyclopedia of Climate Science*, Oxford University Press.

Awards

NOAA Team Member of the Month for August 2017 – **Dale Morris**
National Weather Association Special Lifetime Achievement Award, September 2017 – **Stephen Corfidi**

OST Project 13 – Research on Integration and Use of Multi-Sensor Information for Severe Weather Warning Operations – MRMS

NOAA Technical Lead: Stephan Smith (NOAA OST)

NOAA Strategic Goal 2 – *Weather-Ready Nation – Society is Prepared for and Responds to Weather-Related Events*

Funding Type: CIMMS Task II

Objectives

Work with CIMMS/NSSL scientists in developing multiple-radar/multiple-sensor (MRMS) severe weather warning applications and advanced display systems and transferring that technology to NWS operational systems; collaborate with the NOAA Hazardous Weather Testbed - Experimental Warning Program at the National Weather Center in Norman.

Accomplishments

1. General Overview

Greg Stumpf (CIMMS at OST/MDL/DAB)

The 14th full year of the CIMMS/NWS-Meteorological Development Laboratory (MDL) scientist position was completed during this review period. This project (OST13) has been supported by the CIMMS/MDL scientist throughout this period.

The CIMMS/MDL scientist remained the liaison between the NOAA Hazardous Weather Testbed's (HWT) Experimental Warning Program (EWP) and NWS-MDL. The EWP is a proving ground for evaluating new applications, technology, and services designed to improve NWS short-fused (0-2 hour) hazardous convective weather warning decisions. He continues to collaborate with National Severe Storms Laboratory (NSSL) scientists who are involved in the EWP, including attending scientific and technical meetings.

The CIMMS/MDL scientist continues to be involved with the severe weather warning R&D activities at CIMMS and NSSL and served as a co-principal investigator and subject matter expert for the multiple-radar / multiple-sensor (MRMS) severe weather warning products. The process to transfer MRMS technology to operations at the National Center for Environmental Prediction was completed in FY15, and the CIMMS/MDL scientist has been involved in the following activities related to the MRMS tech transfer, 1) MRMS point-of-contact for NWS Office of Science and Technology Infusion, 2) development manager for creating the capability to display operational MRMS products in the National Weather Service AWIPS2 system, and, 3) supporting the collaborative MRMS "community" on the NOAA Virtual Laboratory (VLab).

Activity during FY18 has been much less than previous years, as the CIMMS/MDL scientist's job responsibilities have shifted to OST Project 15 – Research on Integration and Use of Probabilistic Hazard Information for Severe Weather Warning Operations. Nevertheless, there is a small amount of information to be reported here, much of which is the same work and roles carried over from last year.

2. MRMS Product Display for AWIPS2

Greg Stumpf (CIMMS at OST/MDL/DAB), Darrel Kingfield (CIMMS at NSSL – now CIRES, Boulder CO), and Tiffany Meyer (CIMMS at NSSL)

The operational MRMS system at NCEP went online and began disseminating data to the weather enterprise, including the National Weather Service, on 1 October 2014. The CIMMS/MDL scientist is the development manager overseeing an NSSL employee doing the software coding. Toward the end of FY18 (and continuing into FY19), some work was done to display the new v12 products from MRMS in AWIPS2 19.1.1. These include changes for lightning probability, multi-sensor Quantitative Precipitation Estimation (QPE), and Outside of Continental United States (OCONUS) products.

3. MRMS in the NOAA Virtual Laboratory (VLab)

Greg Stumpf (CIMMS at OST/MDL/DAB)

The CIMMS/MDL scientist is the site owner of the MRMS community in the NOAA Virtual Laboratory (VLab). In addition, the CIMMS/MDL scientist serves on the VLab Support Team, to help design, develop, and implement the NWS VLab as a whole. The CIMMS/MDL scientist leads the bi-monthly NOAA VLab Community and Project Owners' Meetings.

OST Project 15 – Research on Integration and Use of Probabilistic Hazard Information for Severe Weather Warning Operations – PHI and FACETs

NOAA Technical Lead(s): Stephan Smith (NOAA OST)

NOAA Strategic Goal 2 – *Weather-Ready Nation – Society is Prepared for and Responds to Weather-Related Events*

Funding Type: CIMMS Task II

Objectives

Work with CIMMS/NSSL and NOAA/ESRL/GSD scientists in research and development of Probabilistic Hazard Information (PHI) in support of the Forecasting a Continuum of Environmental Threats (FACETs) initiative to improve the nation's severe convective weather warning and forecast services; collaborate with the NOAA Hazardous Weather Testbed - Experimental Warning Program at the National Weather Center in Norman.

Accomplishments

1. General Overview

Greg Stumpf (CIMMS at OST/MDL/DAB)

The 14th full year of the CIMMS/NWS-Meteorological Development Laboratory (MDL) scientist position was completed during this review period. The work described in this project (OST15) has been supported by the CIMMS/MDL scientist for several years prior to FY17, but the project now has its own identifier. In previous years, work on this task was reported in OST13. This is the 2nd year of reporting this work under the OST15 project identifier. The bulk of the CIMMS/MDL scientists efforts were concentrated in the OST15 project, and mostly in the HS-PHI project described within.

The CIMMS/MDL scientist remained the liaison between the NOAA Hazardous Weather Testbed's (HWT) Experimental Warning Program (EWP) and NWS-MDL. The EWP is a proving ground for evaluating new applications, technology, and services designed to improve NWS short-fused (0-2 hour) hazardous convective weather warning decisions. He continues to collaborate with National Severe Storms Laboratory (NSSL) scientists who are involved in the EWP, including attending scientific and technical meetings.

The CIMMS/MDL scientist was a co-principal investigator and subject matter expert on two subprojects funded by the USWRP R2O grant "Probability of What?" that was awarded to several agencies to fund initial research and development activities for the Forecasting A Continuum of Environmental Threats (FACETs) initiative to change the severe weather forecast and warning paradigm for the NWS. The USWRP grant period ended on 31 May 2018. The first subproject, Hazard Services – Probabilistic Hazard Information (HS-PHI), has a continuity of funding via a new Joint Technology Transfer

Initiative (JTTI) grant for the three-year period starting 1 November 2017. The second subproject, Probabilistic Hazard Information (PHI) Verification, has received a no-cost extension – and the project has will continue into FY19. Both of these projects are reported below.

In addition, the CIMMS/MDL scientist authored and submitted two proposals for a project entitled “Inter-Office Collaboration Affecting Severe Weather Warning Services” to the: a) Round 3 of Research to Operations Initiative: NOAA Testbeds Funding Opportunity Number: NOAA-NWS-NWSPO-2018-2005317, and the b) FY 2018 Joint Technology Transfer Initiative - NOAA-OAR-OWAQ-2018-2005496. The project was awarded a grant from the JTTI, and work will begin during FY19.

2. Hazard Services – Probabilistic Hazard Information (HS-PHI)

Greg Stumpf (CIMMS at OST/MDL/DAB), Tiffany Meyer (CIMMS at NSSL), and Alyssa Bates (CIMMS at WDTD)

The CIMMS/MDL scientist is co-team leader, along with a NOAA/ESRL/Global Systems Division (GSD) software engineer, to transfer the technology of the NSSL-developed Probabilistic Hazard Information (PHI) Prototype tool. The PHI-Prototype has been under development since 2013 and has been tested in the NOAA HWT during the springs of 2014-2017. Beginning after the 2015 experiment, GSD software developers and meteorologists began implementing the NSSL PHI Prototype concepts into AWIPS2 Hazard Services, a new application platform from which all NWS watches, warnings, and advisories will be issued in the new future.

The CIMMS/MDL scientist is the “product owner” – the HS-PHI project’s key stakeholder in “agile” programming parlance. He is responsible for defining the requirements, developing extensive test procedures, conducting weekly software tests, and working with the ESRL/GSD development team in implementing and prioritizing the development work. He organizes and conducts bi-weekly development team meetings, provides demos of the software to visiting groups (including the OAR FACETs Working Group and the NWS Analyze Forecast and Support (AFS) Office’s Severe Weather Service Program Team), and gives presentations at various scientific conferences.

The CIMMS/MDL scientist was also the operations coordinator for a 3-week NOAA HWT experiment (Fig. 1) for the third year in a row, conducted in March and April 2018, using visiting NWS forecasters to test this new Hazard Services – PHI (HS-PHI) application. This included helping guide the GSD software development, selection of archive case scenarios designed to train forecasters on the HS-PHI software and PHI concepts, and test various operational decision making situations including inter-office collaboration. Warning Decision Training Division scientists also collaborated on the experiment, in order to start the process of developing best operational practices. Forecasters used HS-PHI in 8 archived weather events in displaced real-time scenarios, which included severe pulse storms, hail storms, tornadic supercells, squall lines, bow echoes, and QLCS tornadoes. The evaluation included a human factors component

collecting forecaster workload data. Figure 1 shows a screen capture of the HS-PHI application, as well as forecasters and researchers working together in the 2018 HWT experiment.

Over the past three years of development, we have brought the software to over 95% compliance with the 2015 baseline version of the NSSL PHI Prototype. New functionality added for 2018 include:

- The “Convective Recommender” which processes CIMSS ProbSevere detections into Hazard Services – PHI objects.
- Levels of Automation:
 - Forecasters can create manual objects.
 - Forecasters can assume partial or full control of automated objects, and relinquish control back to automation one attribute at a time.
- New object drawing tools: ellipses, rotation, resizing
- Ownership of hazard objects and locking
- Redraw polygon feature
- Better drawing colors to enhance visibility of objects on radar data

The 2018 HWT experiment exhibited the most stable-version of the software since development began. Since the 2018 HWT experiment concluded, work has been underway to identify the remaining 2015 baseline functionality and develop a plan to complete that work.

With the USWRP grant ending in May 2018, the focus of the development is shifting to items that have been defined for the first year of the JTTI grant, to be delivered by 1 November, 2018. The CIMMS/MDL scientist has been involved in planning and design meetings for these new features:

- Intermediate “Threats-In-Motion” (TIM) warnings (without PHI) – see more below
- Warning product generation
- Lightning PHI (both guidance and forecast grid creation)

“Threats-In-Motion” (TIM) is an intermediate solution to smoothly phase the warning paradigm from the current NWS warnings and fully-implemented PHI. The TIM concept comprises deterministic storm-following warning polygons that update at one-minute intervals. TIM has been shown to double location-specific lead times by giving all locations downstream of storms more equitable lead times. TIM also automatically clears out warnings after the events of passed, effectively reducing “departure time” to near zero.

Finally, the CIMMS/MDL scientist was involved in the PHI End User experiments this year, helping define and create PHI objects for 3 of their 6 scenarios, and acting in the warning forecaster role during operational exercises with emergency managers and broadcasters.



Figure 1. Images from the Hazard Services – Probabilistic Hazard Information (HS-PHI) 2018 spring experiment in the NOAA Hazardous Weather Testbed, including various forecaster and researcher interactions with the software and during group discussions. Also shown is screen capture of the HS-PHI application, showing probabilistic severe thunderstorm and tornado “plumes” (outlined in yellow and red respectively) for a system of severe storms in central Texas.

3. Probabilistic Hazard Information (PHI) Verification

Greg Stumpf (CIMMS at OST/MDL/DAB) and Adrian Campbell (CIMMS at NSSL)

The CIMMS/MDL scientist is co-investigator, along with scientists at NOAA/ESRL/GSD, to develop a real-time verification system for the PHI Tool, which will use 1) a new way to blend, in real-time, remotely-sensed data from the MRMS system with live storm reports, and 2) innovative warning verification techniques that have been under development for several years, which include new measures such as False Alarm Area and False Alarm Time in verified warnings as well as location-specific lead- and departure-time.

A gridded verification system for severe thunderstorm reports (hail ≥ 1 " diameter and/or wind ≥ 25 ms⁻¹) was completed. The system scores both severe thunderstorm warnings and tornado warnings against ground observations of severe hail and wind on a 1 km² x

1 min grid (Fig. 2a), and calculates grid-based Probability of Detection, False Alarm Ratio, Lead Time, and new metrics False Alarm Area, False Alarm Time, and Departure Time. Since last year, data from 2017 have been added to the overall dataset, and the system has been re-run on the entire storm-based Severe Thunderstorm Warning and Tornado Warning and Local Storm Report database from October 2007 – December 2017. This includes sub-dividing the database by year, month, and time of day (60-minute segments).

The portion of the work conducted by GSD was completed by the conclusion of the USWRP grant period (31 May 2018). GSD completed the development of a model which blends Multiple-Radar / Multiple-Sensor (MRMS) Maximum Estimated Size of Hail (MESH) fields, RAP model data, and local storm reports to create a probabilistic hail observation grid. The work included modifying the model to account for report locations that fall outside the location of storms in the model – these reports are now ignored. The model can now run on the geospatial verification system on archived data sets.

The portion of the work conducted by the CIMMS/MDL remains incomplete. Because the CIMMS/MDL scientist was the principal scientist and receives no funding from the grant, the remainder of the work will be conducted through FY19 as a no-cost extension of the USWRP grant. The work that remains includes refining the verification code to score probabilistic forecasts (PHI) against probabilistic observations so that it can be tested against the complete 2011 probabilistic hail data set – computing resource issues were discovered that will require a significant refactor of the code. Work to convert the system to a real-time application had also been put on hold pending the decision to integrate the system in the NSSL PHI Prototype Tool - instead of HS-PHI - during FY19, now that a new PHI Prototype developer has been hired by CIMMS (Campbell).

In the meantime, analysis of the code used to create THunderstorm Environmental Strike Probability Algorithm (THESPA; Dance et al. 2010) revealed a minor error in one of the equations in their journal paper. With that correction, we've recomputed probabilistic threshold and reliability statistics for the 27 April 2011 southeast U.S. tornado outbreak data set (Fig. 2). As expected, as one decreases the probability threshold such that locations farther downstream from an event get greater lead time for an event, there is the trade-off of higher false alarms (Figs. 2a, 2b). And reliability appears to improve with the THESPA plume model error corrected (Figs. 2c, 2d). The THESPA 27 April 2011 dataset is being used as a proof-of-concept for the probabilistic verification code mentioned above, after which the probability plumes will be human-generated within the PHI Prototype Tool.

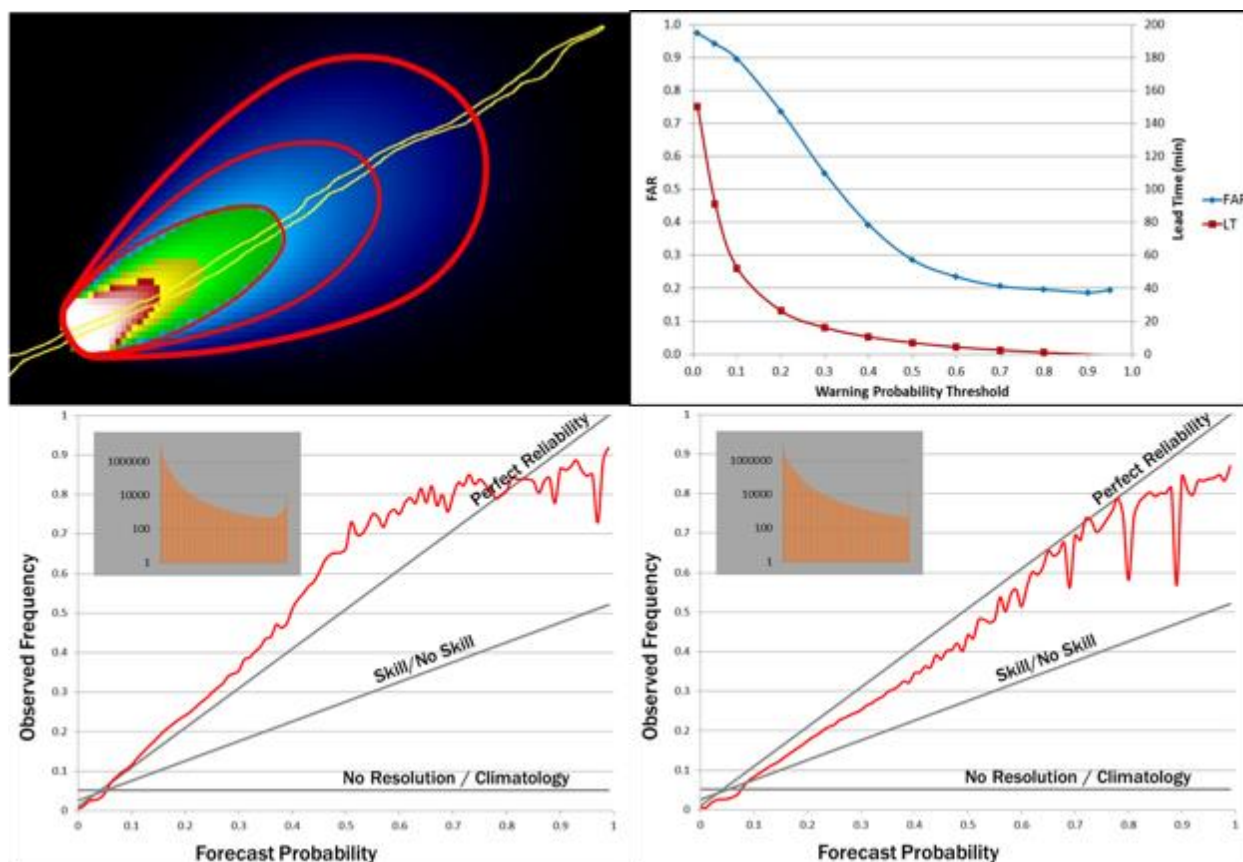


Figure 2: a) upper left: A THESPA-derived probabilistic grid at one time during the Tuscaloosa storm. The thin yellow contour is the outline of the Tuscaloosa AL tornado damage survey. The red contours are three arbitrary warning “polygons”, thick, normal, and thin, corresponding to low, middle, and high probability values, respectively., b) upper right: Variation of lead time (red) and false alarm ratio (blue) for different warning probability thresholds., c) lower left: Reliability diagram for all THESPA probabilities for the mesocyclones/TVSs with the storms in the afternoon-overnight period of the 27 April 2011 outbreak using THESPA with the plume model error, and d) lower right: same as (c) but with the THESPA plume model error corrected. The probability distribution is shown in the insets of (c) and (d).

Publications

Rothfus, L. P., R. Schneider, D. Novak. K. Klockow, A. E. Gerard, C. Karstens, G. J. Stumpf, and T. M. Smith, 2018: FACETs: A proposed next-generation paradigm for high-impact weather forecasting. *Bulletin of the American Meteorological Society*, **99**, in press.

NWSTC Project 14 – Forecast Systems Optimization and Decision Support Services Research Simulation and Training

NOAA Technical Leads: Jeff Zeltwanger (OCLO) and Kim Runk (OPG)

NOAA Strategic Goal 2 – Weather-Ready Nation – Society is Prepared for and Responds to Weather-Related Events

Funding Type: CIMMS Task II

A. OCLO

Objectives

1. Impact-Based Decision Support Services Research and Development

Sub-Objective 1: Prepare all operational NWS employees for providing decision support services from their offices. To accomplish this goal, operational employees need online training. This is the main goal behind the Impact-Based Decision Support Services Professional Development Series.

Sub-Objective 2: Prepare NWS employees for deployment in the field, and train them to communicate weather information to the public and partners effectively. Accomplishing this is the main goal of the Impact-Based Decision Support (IDSS) Deployment Boot Camp residence course.

Sub-Objective 3: Conduct or assist with training sessions outside of IDSS Deployment Boot Camp that continues learning in communication best practices. This may include guest speaking in other residence courses in Kansas City, or consulting with offices or individuals as requested.

Sub-Objective 4: To support Weather-Ready Nation goals, conduct training on impact-based decision support services as applicable specifically to hurricane messaging. This is the primary function of the Effective Hurricane Messaging Course hosted in Miami, Florida.

2. Advanced Training Development

Sub-Objective 1: Develop expertise in useful technology, best practices, and methodologies in effort to produce better training and share information. This might include attending professional development training and conferences, and pushing the boundaries of instructional design, training, and technology.

Sub-Objective 2: Help OCLO and OPG employees grow and learn new tools for training and collaboration.

Sub-Objective 3: Reach out to others in the agency through various methods, and spread information about available training, professional development, and the roles NWS staff play in a Weather-Ready Nation.

Sub-Objective 4: Use expertise to join and help OCLO and OPG focal point teams.

Sub-Objective 5: Prepare new NWS employees for work in the federal government. Accomplishing this is the main goal of the New-Hire Orientation Training course.

Accomplishments

1. Impact-Based Decision Support Services Research and Development

As part of the Weather-Ready Nation initiative, the NWS is undergoing a change in culture. Part of this change includes providing more impact-based decision support services to NWS core partners and improving communication to partners and the public. During this reporting period, numerous training initiatives occurred in effort to support this need. These include:

Sub-Project 1: Impact-Based Decision Support Services (IDSS) Professional Development Series (PDS)

Megan Taylor (CIMMS)
Denise Balukas (CIMMS)
Brent Pesel (CIMMS)
John Ogren (OCLO)
Jeff Zeltwanger (OCLO)
Jim Keeney (OCLO)
Marco Bohorquez (OCLO)
Doug Streu (OCLO)
Jerry Griffin (OCLO)
Hattie Wiley (OCLO)
Cathy Burgdorf (OCLO)
Brooke Bingaman (OCLO)
Christina Crowe (OCLO)

Kim Runk (OPG)
Katie Edwards (NWSH)
Derek Deroche (CRH)
Aimee Fish (AR)
Chris McKinney (SRH)
Charlie Woodrum (NWS)
Seth Binau (NWS)
Al Pietrycha (NWS)
John Quagliarello (NWS)
Bill Rasch (NWS)
Marc Singer (NWS)
Numerous reviewers, subject-matter experts, etc. (too many to list).

During this reporting period, development of the IDSS PDS PCUs 1-7 was completed. The training was released in the Fall of 2017 and has been well received throughout the NWS. Development continues on PCUs 8 and 9. The curriculum is as follows:

Completed:

Professional Competency Unit 1 - Intro to IDSS Basics and Incident Command Structure (FEMA)
Professional Competency Unit 2 – Partner-Focused Support
Professional Competency Unit 3 – Effective Communication
Professional Competency Unit 4 – Preparing for Deployment
Professional Competency Unit 5 – Communicating During Deployment
Professional Competency Unit 6 – Risk Assessment and Deployment Tools
Professional Competency Unit 7 – Exercises and Evaluation

In Development:

Professional Competency Unit 8 – Advanced Topics
Professional Competency Unit 9 – Endorsements

PCUs 1-3 are required for all operational NWS employees regardless of location or office type. PCUs 4-7 are for those operational employees wishing to be “Deployment-Ready.” PCUs 8-9 involve advanced studies into specific types of incidents.

Beginning in 2015, the IDSS PDS is the result of numerous years of analysis, planning, research, and development. Megan Taylor, Denise Balukas, and Brent Pesel with assistance from Jeff Zeltwanger, Doug Streu, and Hattie Wiley, researched and performed analysis related to IDSS concepts, analyzed audience type, need, gaps, etc. for the training series. Recurring collaboration within the NWS and with external partners was utilized to focus the content and maximize the effectiveness of the training.

Megan Taylor, Denise Balukas, and Brent Pesel built numerous online courses within the IDSS PDS. Brent Pesel developed the final wrap up activity for PCU 3 with input from the entire PDS staff. Brent Pesel also created the splash page for the IDSS PDS on the Commerce Learning Center. Megan Taylor was largely responsible for the research, design, and development of PCUs 4-7. The IDSS PDS was released on-schedule in the Fall of 2017. Megan Taylor, Denise Balukas, and Brent Pesel were an integral part of this milestone accomplishment.

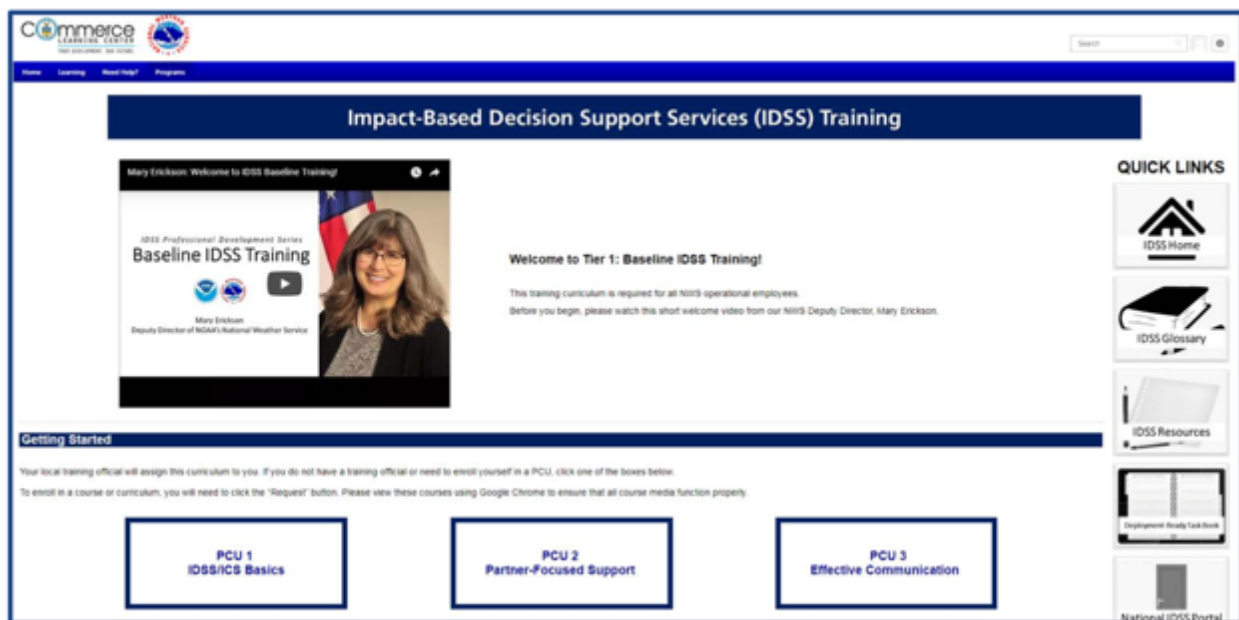


Figure 1: Screenshot of the “Splash Page” for the IDSS PDS PCUs 1-3 which were released in September 2017.

Sub-Project 2: Conduct IDSS Deployment Boot Camp

Megan Taylor (CIMMS)
Denise Balukas (CIMMS)
Brent Pesel (CIMMS)
Katie Vigil (CIMMS)
Jim Keeney (OCLO)

Jeff Zeltwanger (OCLO)
Marco Bohorquez (OCLO)
Doug Streu (OCLO)
Brooke Bingaman (OCLO)
Dave Cokely (OCLO)

Jerry Griffin (OCLO)
Christina Crowe (OCLO)
Kim Runk (OPG)
Derek Deroche (CRH)

Chris Foltz (CRH)
Bill Rasch (NWS)
Numerous contributors, reviewers, and
guest instructors (too many to list)

The popular Impact-Based Decision Support Services Deployment Boot Camp was held twice during the reporting period. The goal behind these courses is to prepare NWS employees for deployment in the field and train them to communicate weather information to partners and the public. These were the last offerings of the course before the release of the new Boot Camp curriculum in the Summer of 2018. It has been completely redeveloped during this reporting period (Sub-Project 3) to reflect a more realistic, hands-on approach to deployment training. This course is now built into the IDSS Professional Development Series (Sub-Project 1).

Megan Taylor's responsibilities and contributions: 1. Directly support the course lead by communicating with students, guests, program leaders, and other instructors. 2. Create and/or review course exercises and drills, including all primary and supporting content. 3. Run exercises and drills in class including media exercises, and a full-day simulation. 4. Provide coaching and feedback to participants.

Denise Balukas' responsibilities and contributions: 1. Directly support the course lead by communicating with students, guests, program leaders, and other instructors. 2. Provide logistical and administrative support in all aspects of the course. 3. Develop and distribute supporting material to participants. 4. Facilitate and coach participants during the simulation. 5. Provide coaching and feedback to participants. 6. Analyze feedback from guest instructors and participants.

Brent Pesel's responsibilities and contributions: 1. Provide logistical support in all aspects of the course. 2. Participate as an actor in the simulation. 3. Provide feedback to participants on effective media communication after the simulation.



Figure 2: Jim Keeney and Jerry Griffin acting in the full-day simulation for IDSS Boot Camp (left). Denise Balukas, Brooke Bingaman, and Dave Cokely prepare for a presentation for the class (right).

Sub-Project 3: Re-develop IDSS Deployment Boot Camp Curriculum

Megan Taylor (CIMMS)
Denise Balukas (CIMMS)
Katie Vigil (CIMMS)
Jim Keeney (OCLO)
Jeff Zeltwanger (OCLO)

Doug Streu (OCLO)
Brooke Bingaman (OCLO)
Dave Cokely (OCLO)
Jerry Griffin (OCLO)
Christina Crowe (OCLO)

During this reporting period, the IDSS Boot Camp was re-developed into a “Flipped Classroom” training experience. The course now consists entirely of exercises, simulations, and drills designed to mimic the experiences and challenges that NWS personnel may face in a variety of deployment scenarios. This “Flipped Classroom” training has been the ultimate goal of the IDSS Deployment Boot Camp since its inception in 2011. The release of the prerequisite training within the IDSS PDS PCUs 1-7 has enabled this to become a reality. The new IDSS Deployment Boot Camp will be held numerous times in the 2018/2019 reporting period.

Megan Taylor and Denise Balukas are part of the core team of developers on this project. They have been integral in the analysis, research, and development of all

aspects of the course curriculum, assessment strategies, documentation, and logistics, and supporting material.



Figure 3: Megan Taylor films Brooke Bingaman, Christina Crowe, and Brent Pesel for the course expectations video for the revised Boot Camp (left). Emergency management vests will add to the realism in the new full-day simulation (right).

Sub-Project 4: Conduct Additional IDSS-related Training Sessions

Because IDSS training is needed in many avenues of operational life in the NWS, additional training opportunities were pursued and continued during this reporting period. These additional sessions included:

IDSS Virtual Conference Webinars

Megan Taylor (CIMMS)
Denise Balukas (CIMMS)
Brent Pesel (CIMMS)
Jeff Zeltwanger (OCLO)
Marco Bohorquez (OCLO)
Charlie Woodrum (NWS)
Numerous Guest Speakers (too many to list)

NWS Headquarters and OCLO hosted numerous IDSS Virtual Conference webinars over the reporting period. These webinars focused on a different topic each time, and gave numerous guest speakers a chance to share some IDSS best practices with the agency.

Megan Taylor's responsibilities and contributions: 1. Attend webinars to inform research and development for ongoing IDSS training development. 2. Contact presenters to serve as subject matter experts for IDSS training.

Denise Balukas' responsibilities and contributions: 1. Attend webinars to inform research and development for ongoing IDSS training development. 2. Contact presenters to serve as subject matter experts for IDSS training.

Brent Pesel's responsibilities and contributions: 1. Attend webinars to inform research and development for ongoing IDSS training development.

Tropical Operations Webinar Series

Denise Balukas (OU CIMMS)

Brooke Bingaman (OCLO)

Shannon White (OCLO)

Jeff Zeltwanger (OCLO)

Jessica Schauer (NWS)

Joel Cline (NWS)

Dave Sharp (NWS)

Mike Brennan (NHC)

Dan Brown (NHC)

Numerous Contributors and Speakers (too many to list)

Representatives from Eastern and Southern Region field offices and the National Hurricane Center have put together a Tropical Operations Webinar Series to discuss best practices for tropical cyclone events. The following topics have been covered in these webinars: Guidance Limitations for Tropical Forecasts, Operational Workflow During Tropical Events, Lessons Learned from the 2017 Hurricane Season, Tropical Watch/Warning Decision Process.

Denise Balukas' responsibilities and contributions: 1. Participate in meetings to identify and develop content for the webinar series. 2. Design the presentation template to be used by presenters in the webinar series. 3. Review content and provide feedback. 4. Attend webinars to inform research and development for ongoing IDSS training development.

Warning Coordination Meteorologist (WCM) Development Course

Megan Taylor (CIMMS)
Doug Streu (OCLO)
Dave Cokely (OCLO)
Jerry Griffin (OCLO)
Jeff Zeltwanger (OCLO)
Numerous Guest Speakers (too many to list)

IDSS concepts such as communication and customer service are essential to the role of Warning Coordination Meteorologist (WCM).

Megan Taylor's responsibilities and contributions: 1. Conduct media training reviews and interview strategies session. 2. Participant in mock-interviews as requested. 3. Act as a reporter in the class simulation. 4. Consult on communication-based topics as course developers prepare presentations and activities.

NWS Public Speaking Video Series & Coaching

Megan Taylor (CIMMS)
Cathy Burgdorf (OCLO)
Jeff Zeltwanger (OCLO)
Brooke Bingaman (OCLO)
Renee Wise (WFO Aberdeen)
Dave Snider (NOAA Alaska TV)

Megan Taylor's responsibilities and contributions: 1. Assist Brooke Bingaman in management of the program and website (as needed). 2. Act a speech and performance coach for NWS employees as needed, including 2 people at the end of the reporting period.

Cooperative Network Operations Course

Megan Taylor (CIMMS)
Brent Pesel (CIMMS)
Marco Bohorquez (OCLO)

IDSS concepts such as communication are vital to the success of the Cooperative Observer Program.

Megan Taylor's responsibilities and contributions: Prepare materials and teach communications in the residence course.

Brent Pesel's responsibilities and contributions: Provide logistical support before, during, and after the course.

Local Office Media Training

Megan Taylor (CIMMS)
John Koch (NWS Eastern Region)
David Manning (NWS Eastern Region)
Judy Levan (NWS Buffalo)
John Quagliarello (NWS Columbia)

NWS Eastern Region Headquarters requested that Megan Taylor train employees participating in their regional DSS Road Shows. During this reporting period, Megan trained the following offices: WFO Wilmington, NC; WFO Buffalo, NY; WFO Boston, MA. During these sessions, Megan conducts a 1-hour training session on media and interview techniques. She then conducts mock interviews with each participant and provides both verbal and follow-up written feedback.

Sub-Project 5: Conduct Effective Hurricane Messaging (EHM) Course

Denise Balukas (CIMMS)
Marco Bohorquez (OCLO)
Brooke Bingaman (OCLO)
Shannon White (OCLO)
Jeff Zeltwanger (OCLO)
Jim Keeney (OCLO)
Jen McNatt (SRH)
John Koch (ERH)
Robbie Berg (NHC)
Mike Brennan (NHC)
Dan Brown (NHC)
John Cangialosi (NHC)
Cody Fritz (NHC)
Jamie Rhome (NHC)

Matt Moreland (NWS)
David Sharp (NWS)
Pablo Santos (NWS)
Lance Wood (NWS) Numerous Contributors and Speakers (too many to list)

The EHM course supports the goal of Weather Ready Nation. Like the Deployment Boot Camp, one of the primary objectives of the EHM is that students gain the ability to effectively communicate weather and water threats, impacts, forecasts, and other technical information to both the public (primarily through media interviews and social media) and to core NWS partners such as emergency management and Coast Guard (through various means including remote and on-site briefings). Another primary goal of both Boot Camp and EHM is to instill the importance of developing the trust of core partners and of fostering deep and lasting relationships with these partners. Because of the unique nature of the hurricane threat, the EHM has hazard-specific components related to the appropriate use and messaging of the National Hurricane Center tropical cyclone products which are addressed during the course.

Denise Balukas' responsibilities and contributions: 1. Directly support the course lead by communicating with students, guests, program leaders, and other instructors. 2. Work with the team to refine course content, develop exercise strategies and create simulation materials. 3. Provide logistical and administrative support in all aspects of the course. 4. Design and construct the student course guide. 5. Develop the resource tool-kit which provides quick access to hurricane related support and informational products. 6. Facilitate during the simulation. 7. Record feedback. 8. Redevelop the online student feedback assessment (with Katie Vigil).



Figure 4: Students and facilitators learn about the tropical cyclone forecast process from the hurricane specialists at NHC during the Effective Hurricane Messaging Course.

2. Advanced Training Development

The OU CIMMS stationed in the OCLO and OPG building must maintain a level of expertise in many areas in order to fully support the local NWS staff. This may mean developing new or more advanced skills, training others in the office, participating in outreach, or joining one of the building teams. The activities relevant to this objective is as follows:

Sub-Project 1: Develop expertise in technology, best practices, & methodologies to better fulfill roles and help others

Office Visits:

NWS Topeka, KS - Denise Balukas, Brent Pesel
National Hurricane Center Miami, FL - Denise Balukas
NWS Miami, FL - Denise Balukas
National Reconditioning Center/National Logistics Support Center Grandview, MO – Brent Pesel
NWS Buffalo, NY - Megan Taylor
NWS Boise, ID - Megan Taylor

NWS/NOAA Training:

HFO Tropical Curriculum - Denise Balukas
EHM Tropical Prerequisite Training - Denise Balukas
IDSS PDS PCU 1-3 - Denise Balukas, Megan Taylor, Brent Pesel
Incident Meteorologist Workshop - Megan Taylor

Internal Training:

Effective Survey Development and Design (by Katie Vigil) - Katie vigil, Denise Balukas, Megan Taylor, Brent Pesel
Instructional Design Training (by Hattie Wiley) – Denise Balukas, Megan Taylor, Brent Pesel, Katie Vigil
Intro to Dreamweaver - Brent Pesel
Writing Basics (bi-weekly) - Denise Balukas, Megan Taylor, Brent Pesel, Katie Vigil
Designing visuals (monthly) - Denise Balukas, Megan Taylor, Brent Pesel, Katie Vigil
Annual Instructional Design Refresher – Denise Balukas, Megan Taylor, Brent Pesel

Additional Training:

FEMA ICS 300: Intermediate ICS for Expanding Incidents – Denise Balukas, Brent Pesel
Mid-America Regional Council (MARC): Personal Strengths and Leadership Styles - Denise Balukas
SkillPath: Communicating With Tact, Diplomacy, and Professionalism - Denise Balukas

KC Federal Executive Board: Instructor Development Training - Denise Balukas

Community Support and Outreach:

FEMA: Community Emergency Response Team (CERT) Training - Denise Balukas completed the CERT program and additional CERT training as a moulage artist. Moulage is the art of makeup application and costume design to simulate wounds and injuries. After completing this training, Denise Balukas participated in a CERT exercise as a moulage artist. She performed moulage on 15 FEMA volunteers during this exercise. Marco Bohorquez from the NWSTC was one of these volunteers.



Figure 5: Incident Meteorologist (IMET) workshop participants giving the morning weather briefings (left). Megan Taylor and the IMET participants tour the National Interagency Fire Center, including the Smoke Jumper building (right).



Figure 6: Marco Bohorquez volunteering as a victim during a FEMA CERT exercise in Kansas City. Denise Balukas applied moulage makeup techniques simulating severe injuries to the all of the volunteer "victims".

Sub-Project 2: Develop the Introduction to NOAA Weather Radio (NWR) Distance-learning Course

Denise Balukas (CIMMS)
Jim Poole (OCLO)
Jeff Zeltwanger (OCLO)
Russ Munson (OCLO)
Shane Shadwick (OCLO)
Michael Ready (OCLO)

The Introduction to NWR distance learning module will prepare NWS employees with background knowledge of NOAA Weather Radio (NWR) components, hardware, structure, functions that are universal to all NWR systems so that the residence course can transition more quickly to the unique characteristics of specific NWR systems on which the participants will be working. Design and development for this course is ongoing. Projected release date is Winter 2019.

Denise Balukas' responsibilities and contributions: 1. Create and maintain the project plan, timeline, and schedule. 2. Research of applicable portions of the current NWR residence course for adaptation to distance learning specifications. 3. Edit written content to adhere to adult learner specifications and best practices. 4. Content design and development with the technical support from OCLO team.

Sub-Project 3: Assist with the New-Hire Orientation Training course

Megan Taylor (CIMMS)
Denise Balukas (CIMMS)
Brent Pesel (CIMMS)
Katie Vigil (CIMMS)
Hattie Wiley (OCLO)
Jeff Zeltwanger (OCLO)
Marco Bohorquez (OCLO)
Christina Crowe (OCLO)
Brooke Bingaman (OCLO)
Doug Streu (OCLO)

The course is designed to prepare newly hired NWS employees for federal employment. During the course, they receive information on the organization, federal benefits, the employee union, travel, and time reporting. They also receive training on effective teamwork, leadership, communication, and learning.

Brent Pesel's responsibilities and contributions: 1. Provide logistical and administrative support before, during, and after the course. 2. Develop and maintain tracking system for course materials and inventory. 3. Organize and execute the New Hire Benefits Fair. 4. Lead the final session of the course, the Course Wrap-Up.

Megan Taylor's responsibilities and contributions: 1. Teach Communications Basics section. 2. Participate in the New Hire Benefits Fair.

Denise Balukas' responsibilities and contributions: Teach Written Communications section.

Katie Vigil's responsibilities and contributions: Introduce the Operations Proving Ground to new employees during the benefits fair.



Figure 7: Brent Pesel (left) and Megan Taylor (right) during the NWS 101 New Hire Course.

Sub-Project 4: Assist OCLO teams with course development

Social Science Distance Learning Module - Denise Balukas recorded the audio for this online module. Megan Taylor consulted with the course writer/designer and provided advice for content.

Digital Aviation Services - Brent Pesel assisted with the development of quizzes for the Digital Aviation Services online module. He also helped during the testing and evaluation phases of the project.

Sub-Project 5: Help NWSTC employees learn new tools and methodologies for training and collaboration

NWSTC Intranet - Brent Pesel assumed responsibilities for updating and maintaining the NWS intranet page. Through his work the intranet went through a major revision to update information and facilitate easier access to frequently used items by the NWSTC staff.

Internet/Training Portal - Brent Pesel was tasked with assisting in updating the NWS Training Center homepage and all sub pages to PHP format as requested by the IT office of the OCLO. This required both formal and informal training in HTML and PHP scripting through Adobe Dreamweaver software. Brent also went through the portal and updated/deleted obsolete content and materials.

Sub-Project 6: Use expertise to join and help OCLO and OPG focal point teams

Recycling Focal Point – Denise Balukas is in charge of recycling toner, contacting recycling company, and ensuring the building has opportunities to recycle various items.

Social Media Team – Megan Taylor (team lead) posts all social media activity via Facebook and YouTube. She is also working on expanding platforms and combining efforts with other OCLO divisions. Katie Vigil (team member) assists with reviewing posts and submitting ideas.

Apple Device Team – Megan Taylor leads a team of two others, who monitor, administer, and check out Apple Devices. This team also helps teach others how to use Apple Devices.

Google Applications Trainer/Troubleshooter – Megan Taylor (team lead) and Jeff Zeltwanger ensure staff can use Google Applications (Gmail, Calendar, Drive, etc.), and understand any updates. They also help troubleshoot and answer questions when needed.

Internet/Training Portal – Brent Pesel assists Hattie Wiley in maintaining and updating the NWSTC webpage and the OCLO training portal.



Figure 8: Logos from a few of the internal teams in which Katie Vigil, Brent Pesel, Denise Balukas, and Megan Taylor participate.

Awards & Recognition

NOAA Team Member of the Month award, April 2018 – **Megan Taylor**

B. OPG

1. NWS Operations Proving Ground Research-to-Operations Activities

Sub-Objective 1: Collaborate with the Aviation Weather Testbed to assess Digital Aviation Services (August 2017)

Sub-Objective 2: NWS GOES-16 Applications Workshop (November 2017)

Sub-Objective 3: Collaborate with the Aviation Weather Testbed to assess Digital Aviation Services for Winter Weather (March 2018)

Sub-Objective 4: Think Tank with NWS Science and Operations Officers to Evaluate the Role of the Weather Forecast Office Mesoanalyst (February 2018)

Sub-Objective 5: Validate, Disseminate, and Evaluate GOES-16 Geostationary Lightning Mapper (GLM) Data for the NWS (March through June 2018)

Accomplishments

1. NWS Operations Proving Ground Research-to-Operations Activities

Sub-Project 1: Collaborate with the Aviation Weather Testbed to assess Digital Aviation Services

Katie Vigil (CIMMS) Chad Gravelle (CIMMS) Kim Runk (NWS OPG) Matthew Foster (NWS OPG) Jack Richardson (IT Contractor)	Steve Lack (AWC) Austin Cross (AWC) Stephanie Avey (CSU CIRA) Joshua Scheck (AWC) Cammye Sims (NWS ASB) ESRL's Global Systems Division
---	---

For two weeks In August 2017, the third Aviation Weather Testbed (AWT) Digital Aviation Services (DAS) evaluation took place at the OPG. The six participating forecasters were from NWS Weather Forecast Offices (WFOs) in Western, Central, Eastern, and Southern Regions. The forecasters evaluated tools, methods, and the collaborative process between AWC and WFOs in the OPG to produce a single set of ceiling and visibility grids that serve both national and local needs for aviation products and services.

The goals of this evaluation were:

- 1) Obtain forecaster feedback on the effectiveness, viability, and workload associated with generating enhanced short-term aviation grids and products necessary to support NWS aviation partners.
- 2) Qualitatively (OPG) and statistically (AWC) assess how forecaster modifications impacted the AWT First Guess Cloud and Visibility Grids.
- 3) Obtain feedback on the AWC-WFO collaboration process, the tools available to accomplish it, and the potential impacts on workload.
- 4) Evaluate whether national ceiling and visibility grids can be efficiently transferred from AWC to WFOS and back, via the LDM. Forecasters only edited grids with live weather data.

Katie Vigil's Responsibilities – To organize, plan, run, and assess the evaluation as the project lead in conjunction with the Aviation Weather Testbed.

Chad Gravelle's Responsibilities – To help plan and execute the evaluation.



OPG and Aviation Weather Testbed visiting forecasters collaborating on Digital Aviation Services (DAS) grids.

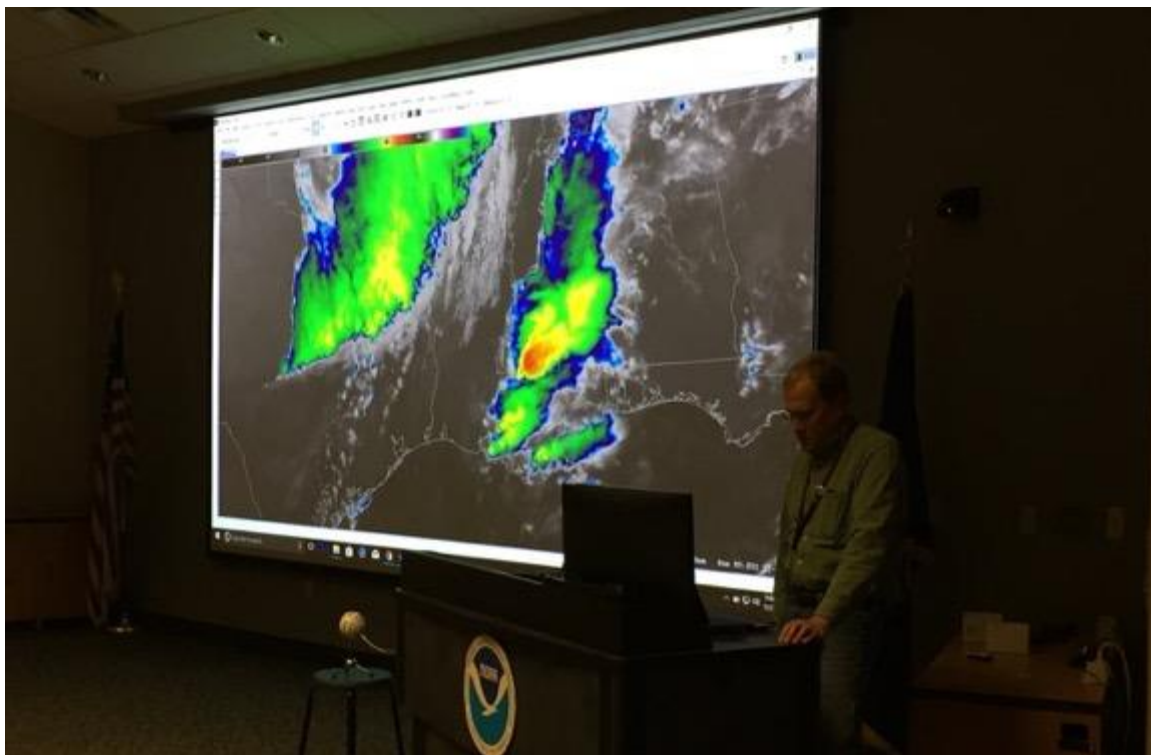
Sub-Project 2: NWS GOES-16 Applications Workshop

Chad Gravelle (CIMMS)
Katie Vigil (CIMMS)
Kim Runk (NWS OPG)
Matthew Foster (NWS OPG)
Jack Richardson (IT Contract)
OCLO
COMET

The OPG hosted a GOES-16 Applications Workshop for NWS forecasters, which drew praise from a variety of sources for its practicality and innovation. The primary goal of the workshop was to share success stories, best practices, and ongoing challenges associated with integrating GOES-16 imagery and products into operations. Content was harvested, developed and presented by NWS forecasters directly from a Thin Client connection to the OPG AWIPS. In addition to allowing presenters use of their operational system to tell their stories, this method promoted a more interactive and engaging format that is not possible with static PowerPoint slides. For remote participants, the sessions were streamed in high-definition on YouTube Live. At one time, there were 91 connections to the live stream, including dozens of NWS offices and at least four international weather services.

Chad Gravelle's Responsibilities – To plan, execute, and run the GOES-16 Satellite Imagery Workshop as the project lead.

Katie Vigil's Responsibilities – To assist in executing the workshop.



OPG SOO Matt Foster preparing presentation for the GOES-16 satellite imagery workshop.

Sub-Project 3: Collaborate with the Aviation Weather Testbed to assess Digital Aviation Services for Winter Weather

<p>Katie Vigil (CIMMS) Chad Gravelle (CIMMS) Kim Runk (NWS OPG) Matthew Foster (NWS OPG) Jack Richardson (IT Contract)</p>	<p>Steve Lack (AWC) Austin Cross (AWC) Stephanie Avey (AWC) Joshua Scheck (AWC) Cammye Sims (NWS ASB) ESRL's Global Systems Division</p>
--	--

In March of 2018, the fourth and final AWT DAS evaluation took place at the OPG. This evaluation specifically targeted DAS for winter weather scenarios. The evaluation was one week long with three NWS forecasters from Central and Eastern Regions. The goal of this evaluation was to obtain forecaster feedback on the effectiveness, viability, and workload associated with generating enhanced short-term aviation grids and products

necessary to support NWS aviation partners from a common starting point and creating TAFs derived from those grids. Forecasters only edited grids with live weather data.

Katie Vigil's Responsibilities – To organize, plan, run, and assess the evaluation as the project lead in conjunction with the Aviation Weather Testbed.

Chad Gravelle's Responsibilities – To help plan and execute the evaluation.



CIMMS Research Scientist Katie Vigil introducing DAS participants to the OPG.

Sub-Project 4: Think Tank with NWS Science and Operations Officers to Evaluate the Role of the Weather Forecast Office Mesoanalyst

Chad Gravelle (CIMMS) Katie Vigil (CIMMS) Kim Runk (NWS OPG) Matthew Foster (NWS OPG) Jack Richardson (IT Contract) Jenni Laflin (NWS EAX)	Chauncy Schultz (NWS BIS) Ariel Cohen (NWS TOP) Seth Binau (NWS ILN) Brian Carcione (NWS HUN) Dan Hawblitzel (NWS OHX) Corey Mead (NWS OAX)
---	--

The OPG is leading an initiative to emphasize the importance and value of expert mesoanalysis in crafting Impact-based Decision Support Services (IDSS) messaging for high-impact events. Arguably the most significant opportunity for the NWS to improve its

services for convective weather events lies in the temporal gap between watches and warnings – i.e., the time frame from about six hours prior to onset down to the time when severe weather is considered imminent and a warning is issued, typically around 15-20 minutes in advance. By effectively leveraging data such as GOES-16/17 imagery, MRMS, WSR-88D Dual Pol data, convection-allowing models, and probabilistic decision aids, forecasters can now provide targeted, tactical decision-making information with a precision and timeliness that was not possible prior to the real-time availability of these data. By investing in the combined skills of expert mesoanalysis and effective risk communication, a practical step can be taken toward delivering a continuous flow of critical information to core partners that leads directly to saving lives and mitigating property loss.

Chad Gravelle's Responsibilities – To plan and run the mesoanalyst think tank as the project lead.

Katie Vigil's Responsibilities – To assist with planning and executing the think tank.



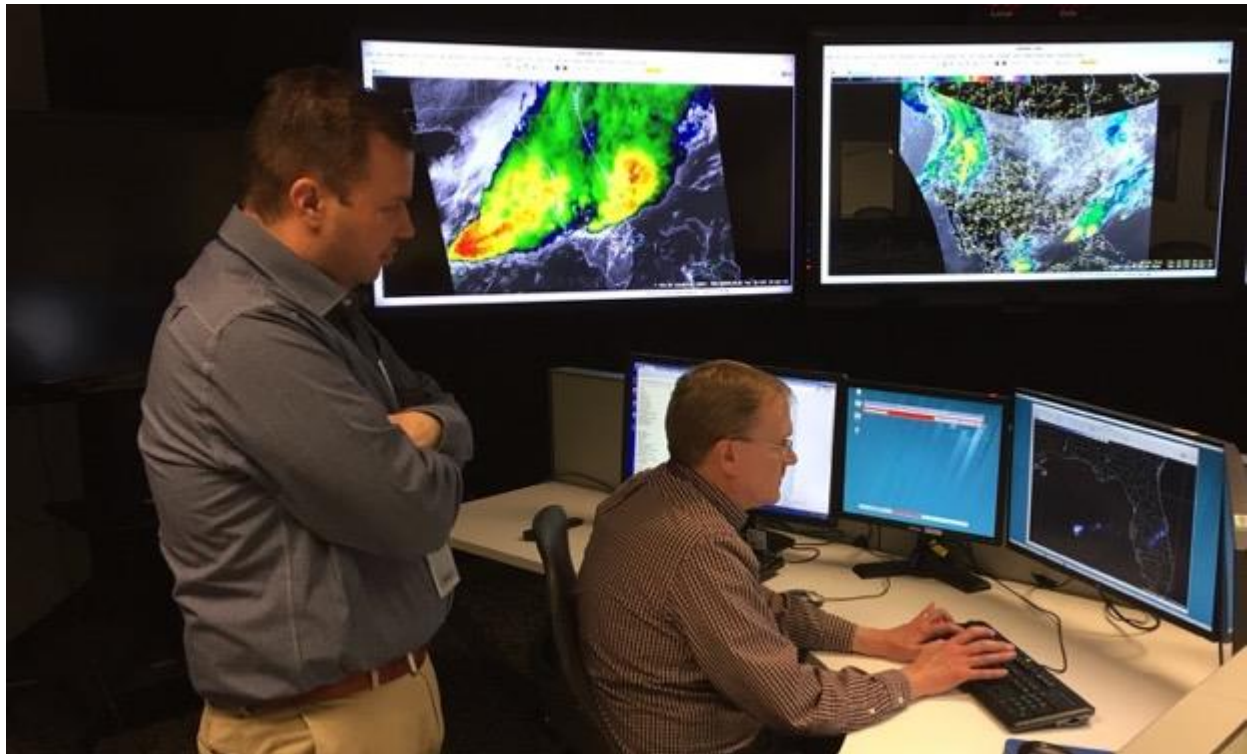
NWS SOO's and OPG staff discuss the development of an evaluation that will look at the role of the mesoanalyst in collaborative severe weather IDSS.

Sub-Project 5: Validate, Disseminate, and Evaluate GOES-16 Geostationary Lightning Mapper (GLM) Data for the NWS

Chad Gravelle (CIMMS)
Matthew Foster (NWS OPG)
Office of Observations
NESDIS
NASA SPoRT

The OPG played a key role in validation of GOES-16 Geostationary Lightning Mapper (GLM) data to ensure readiness for operational use. A collaborative effort between the OPG, the Office of Observations, NESDIS, and NASA SPoRT led to the distribution of the first gridded GLM products over non-operational channels in July. The GLM captures 500 images per second to report lighting occurrence and characteristics through the GOES field of view. This new optical instrument differs from the ground-based lightning detection networks most familiar to forecasters by detecting light energy vs. radio signals. The strength of the radio lightning networks is their capacity to report point locations of the most energetic portions of lightning flashes. However, via GLM it is now possible to visualize the full spatial extent of lightning flashes. Combining both these capabilities will enhance forecasters' ability to accurately diagnose and communicate lightning threats to core partners.

Chad Gravelle's Responsibilities – As OPG's satellite expert, Chad worked with OPG staff, the Office of Observations, NESDIS, and NASA SPoRT to ensure operational readiness for the GLM. He also led applied GLM research with the NWS WFO in Jacksonville, FL.



Research Scientists Chad Gravelle and OPG SOO Matt Foster work on GLM data validation.

Awards and Accomplishments:

Larry R. Johnson Special Award from the National Weather Association – **OPG Team Award**
NOAA Bronze Medal (officially presented to OPG's two federal employees) – **OPG Team Award**
Became a Certified Project Management Professional – **Katie Vigil**

ARL Project 15 – Weather and Climate Change Monitoring and Research Support of the Atmospheric Turbulence and Diffusion Division of NOAA’s Air Resources Laboratory

NOAA Technical Leads: Bruce Baker and Sarah Roberts (ARL/ATDD)

NOAA Strategic Goal 2 – *Weather-Ready Nation – Society is Prepared for and Responds to Weather-Related Events*

Funding Type: CIMMS Task II

Objectives

Conduct atmospheric research related to severe storm development, boundary layer structure, and analysis of climate.

Accomplishments

1. *Boundary Layer Research*

Michael Buban and Temple Lee (CIMMS at ARL/ATDD)

This research involves studying the impacts of differences in land characteristics on the lower boundary layer (BL), particularly how surface heterogeneities influence BL structures, convection initiation (CI), and local development of severe weather. Datasets from surface micrometeorological towers, rawinsondes, small Unmanned Aircraft Systems (sUAS), and more have been collected and analyzed from the Verification of the Origins of Rotation in Tornadoes Experiment in the Southeast US (VORTEX-SE) and the Land Atmosphere Feedback Experiment (LAFE). These data sets are being used to initialize and evaluate Large Eddy Simulations (LES) to study the BL (Figures 1-2). The VORTEX-SE data sets are helping to evaluate high resolution weather forecast models such as the High-Resolution Rapid Refresh (HRRR), as shown in Figure 3. The LAFE datasets are currently being used to develop and improve flux gradient relationships, as shown in Figure 4, that are used in numerical models.

In addition to our involvement with VORTEX-SE and LAFE, we are continuing to develop our small sUAS program and have been using sUASs to obtain very high-resolution observations of the boundary layer, as is shown in the example of vertical profiles of potential temperature and specific humidity from LAFE (Figure 5). In addition to using them in LAFE and VORTEX-SE we have also used sUASs to study the 2017 Great American Eclipse, and to study the thermodynamic structure and evolution of 2017’s Hurricane Maria.

As a component of this work, we have also performed calibration and validation work on new sensors used for BL sampling, including U.P.S.I. fast response relative humidity sensors and iMet-XQ temperature/relative humidity/pressure sensors, as well as eMote

temperature humidity sensors that can act as Lagrangian drifters when deployed from manned or unmanned aircraft.

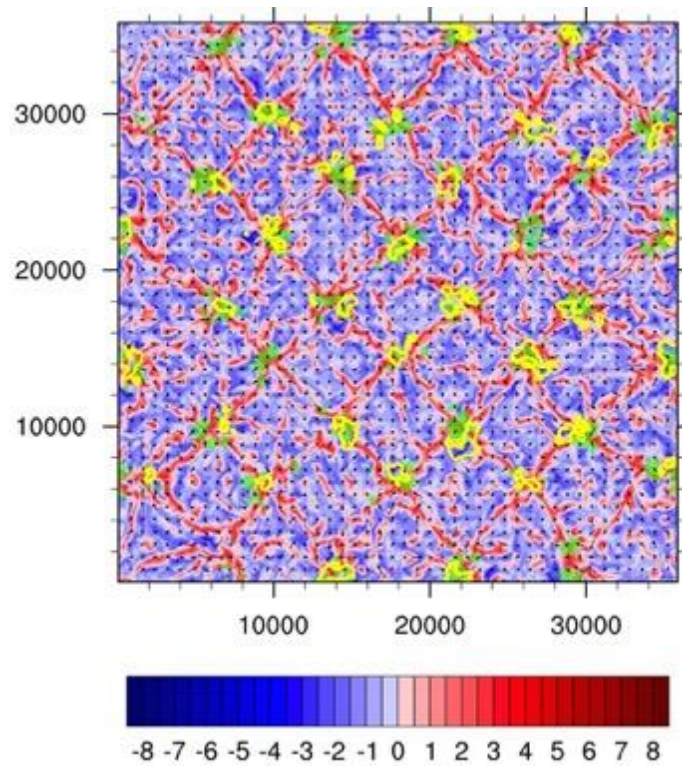


Fig. 1 LES of BL vertical motion at 500 m AGL (color filled), cloud water (shaded green) and rain water (contoured yellow) illustrating the effects of differences in surface heat flux on BL structure and CI.

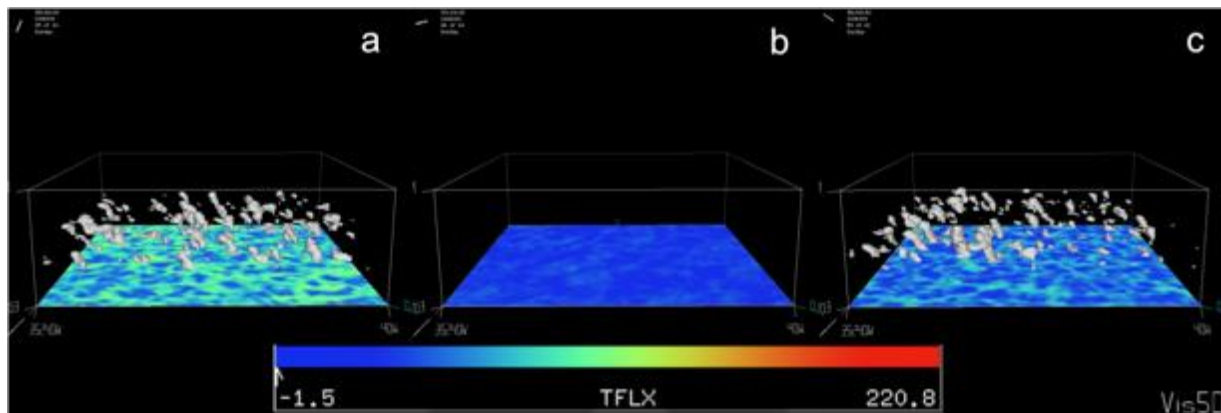


Fig. 2 LES of the Great American Eclipse on 21 Aug 2017. Sensible heat flux (W m^{-2}) color filled at the surface and cloud water (white surfaces) showing BL cumuli development prior to the eclipse (panel a), diminishment during the eclipse (panel b), and redevelopment after the eclipse (panel c).

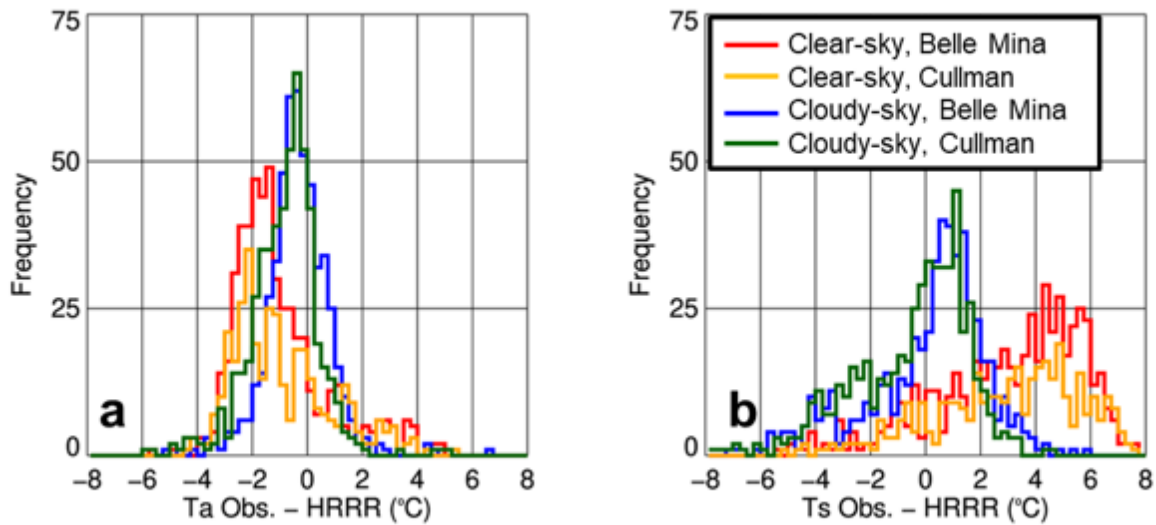


Fig. 3: Example showing results from evaluating the HRRR model using micrometeorological tower observations installed at Belle Mina, AL and Cullman, AL to support VORTEX-SE. The histograms show the difference between observations of air (a) and surface (b) temperature and the HRRR model over the period 1 August 2016 through 30 April 2017 under select meteorological conditions.

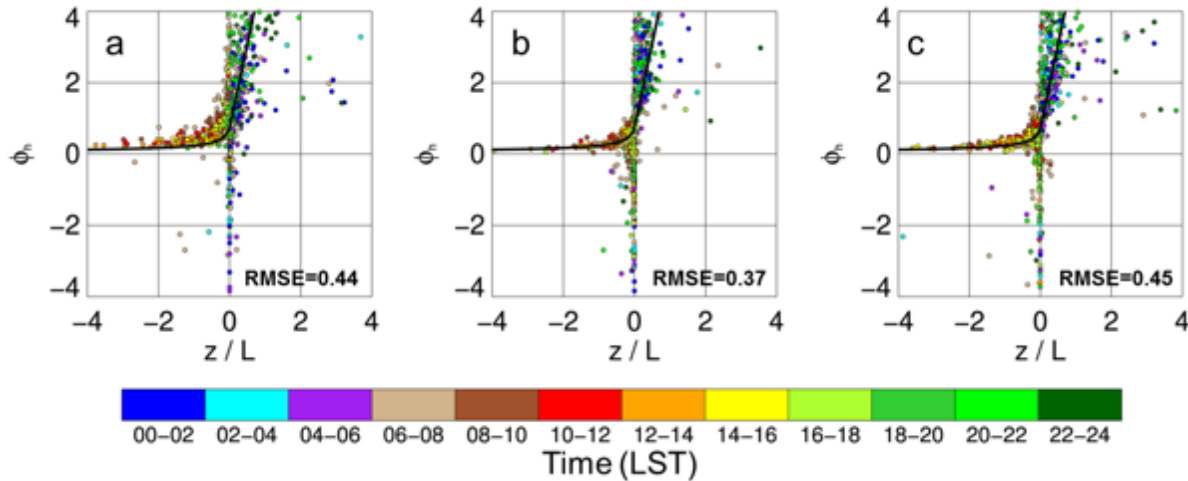


Fig. 4: Example of using observations from the three 10 m micrometeorological towers that NOAA/ARL/ATDD installed during LAFE (1-31 August 2017) to evaluate flux-gradient relationships in the surface layer. The above plots show ϕ_h as a function of $\frac{z}{L}$ at Tower 1, which was installed in an early growth soybean field (panel a); Tower 2, which was installed in a native grassland (panel b); and Tower 3 which was in a soybean field (c). The black line shows the expected relationship between ϕ_h and $\frac{z}{L}$ developed from previous studies. The points are colored by time of day in local standard time, and the root mean square error (RMSE) is shown at bottom right of each panel.

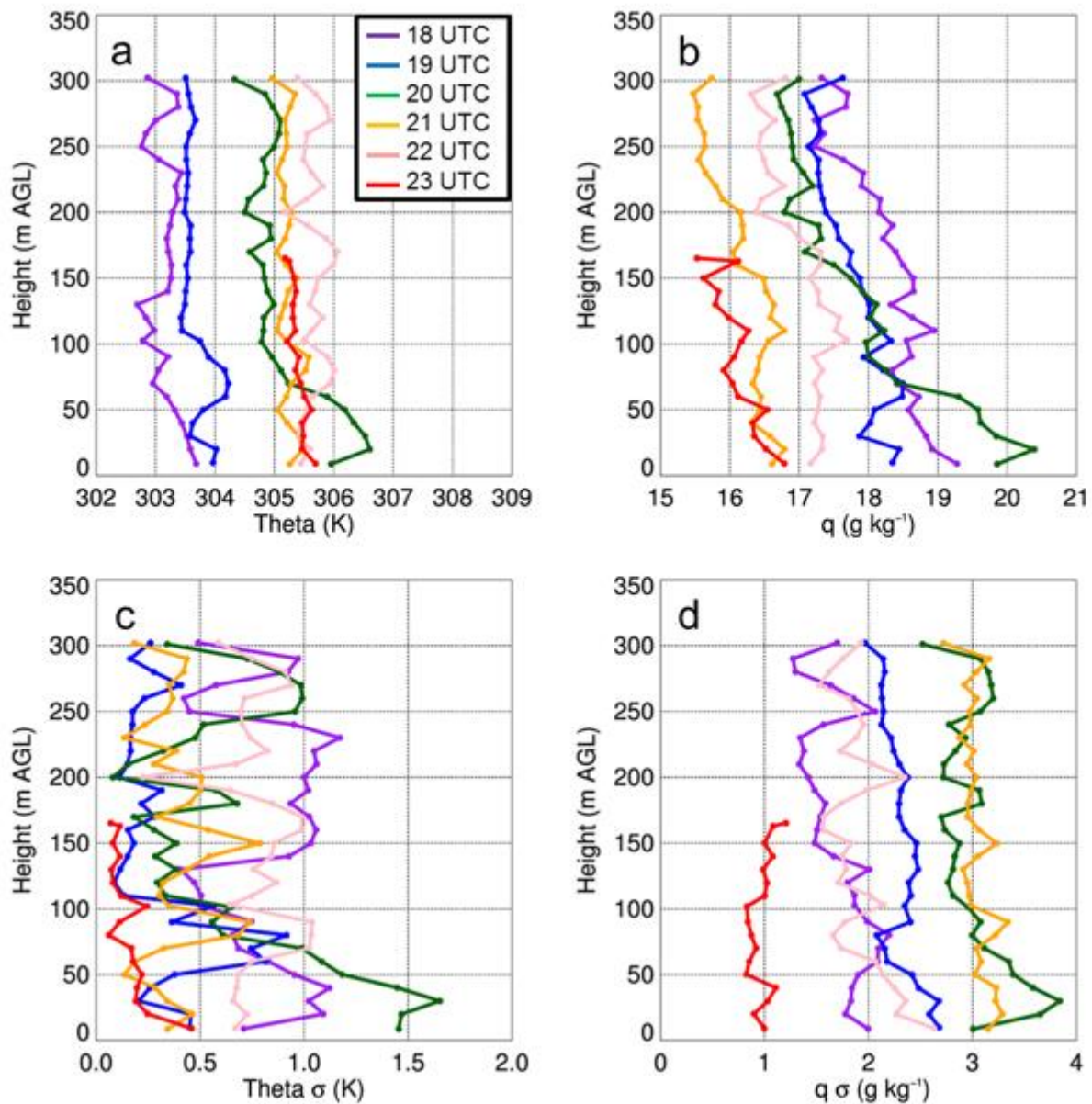


Fig. 5: Examples of vertical profiles of potential temperature (a) and specific humidity (b) as a function of height for select sUAS flights with the DJI S-1000 sUAS during LAFE on 17 August 2017. Panels (c) and (d) show the standard deviation (σ) in potential temperature and specific humidity, respectively.

2. Climate Monitoring

Michael Buban, Temple Lee, and Grant Goodge (CIMMS at ARL/ATDD)

We are involved in analyzing data from the United States Climate Reference Network (USCRN). In particular, we are creating gridded data analyses for public consumption

(Fig. 6) and developing a method for using other high-resolution datasets, including for example precipitation from the Parameter Elevation Regressions on Independent Slopes Model (PRISM) and evapotranspiration estimates from the Atmosphere-Land Exchange Inverse (ALEXI) model, with our USCRN datasets to produce a detailed observationally-based soil moisture product (Fig. 7).

We also used the USCRN data to study rapid near-surface meteorological changes that occurred over the US during the Great American eclipse on 21 August 2017. These changes were documented in an Eos article (Lee et al. 2018) and are summarized in Fig. 8.

We also participated in a science workshop with the University of Tennessee (UT) on 12 September 2017 to discuss potential collaborations. We also performed outreach activities during this reporting period that included a weather balloon launch for UT students on 27 September 2017, as well as weather balloon launch and demonstration of meteorological instruments for students from Rockwood Middle School in Rockwood, TN on 28 March 2018. Finally, as a component of this work, we also mentored one graduate student, Alex Lacey from the University of Tennessee, who assisted with analyses of the USCRN and PRISM datasets.

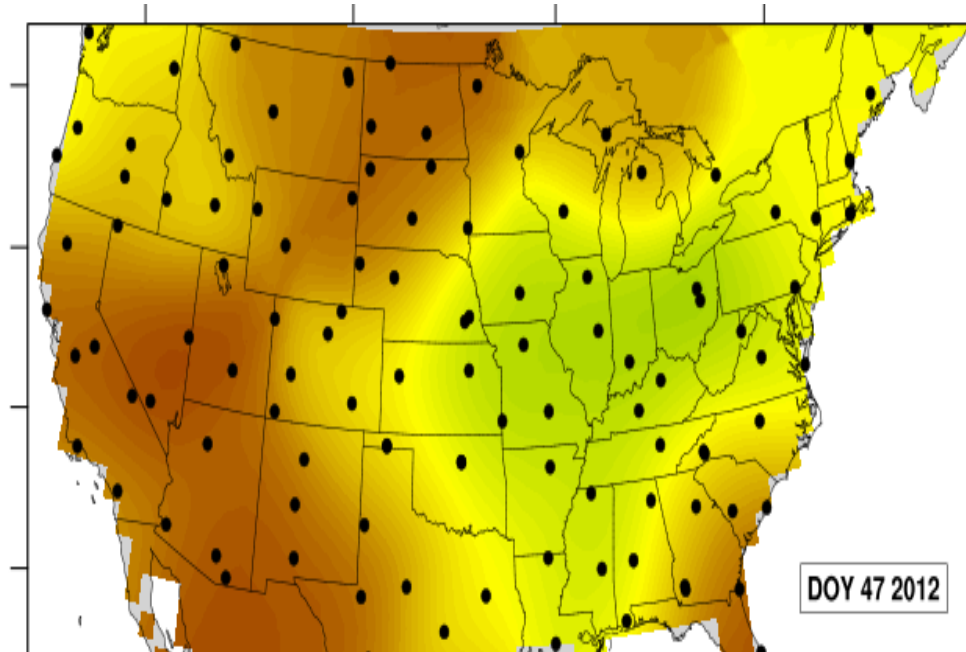


Fig. 6 Fractional soil moisture on 16 Feb. 2012, objectively analyzed from the USCRN stations (locations represented by black dots).

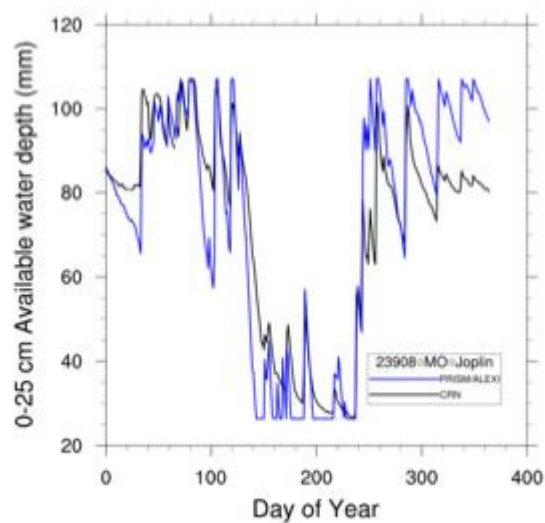


Fig. 7: Comparison of 0-25 cm soil moisture depth (mm) between the USCRN measurements (black) and a model based on a source precipitation from the PRISM dataset and sink evapotranspiration from the ALEXI dataset.

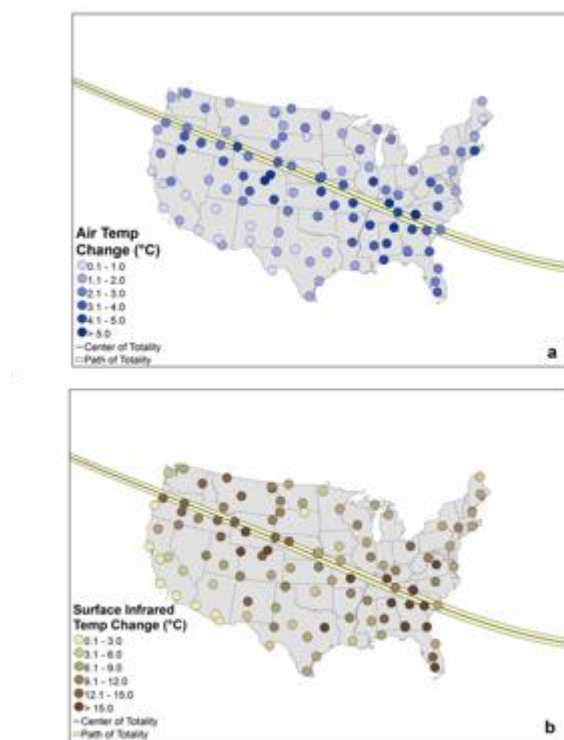


Fig. 8: Decreases in air temperature (a) and surface infrared temperature (b), between the maximum temperature within the 2 hours prior to the closest approach to totality and the minimum temperature during the eclipse event at the USCRN stations in the conterminous United States.

As another component to the climate monitoring work, we are also monitoring the incoming data stream from the USCRN. As the QC Focal Point for the USCRN Program, Grant W. Goodge's primary responsibilities are to monitor the hourly data input and flag messages from 140 specialized climate monitoring stations in the US, Canada, and Russia. This monitoring is done on a daily basis regardless of weekend or holidays. This also involves the close inspection of station data output after the completion of annual maintenance visits (AMVs) by NOAA/ARL/ATDD engineers to confirm all sensors and support equipment including the transmitter are operating normally prior to the departure of the engineers from the site.

Radar, satellite, and surface observation data from other networks are also used as ancillary cross checks of the USCRN data, particularly in the case of significant extreme events as with Hurricane Harvey in late August of 2017. The eye of the hurricane moved directly over one of our stations near Port Aransas (Fig. 9), TX with no damage done to the station. Unlike some other automated stations the USCRN station is equipped with battery back-up and solar panels therefore allowing it to continue operation throughout the event despite the loss of AC power, as shown in the example in Fig. 10.

In the longer term, files are maintained for each station for temperature and precipitation that allow comparison of recent events and preexisting records. For precipitation, the files include values for the following periods: 5 minutes, hourly, daily, monthly, and annual. In the case of significant precipitation events like that of Hurricane Harvey we compare the storm values to the tables given in NOAA Atlas -- 14 which present the Point Precipitation Frequency Estimates for intervals from 1 to 1,000 years. Also by the use of extreme value analysis of the 5 minute values we have been able to flag false values that were created either by an electronically induced error, or one resulting from a "slip-through" of frozen precipitation from the collection chute of the precipitation gauge. This is important in preserving an un-skewed precipitation data file.



Fig. 9: On August 25 2017, the center of the eye of Hurricane Harvey made landfall on the southeast Texas coast just south of the USCRN site (green arrow above). This placed the USCRN station at Port Aransas, TX near the north side of the eye wall as Harvey slowly moved inland.

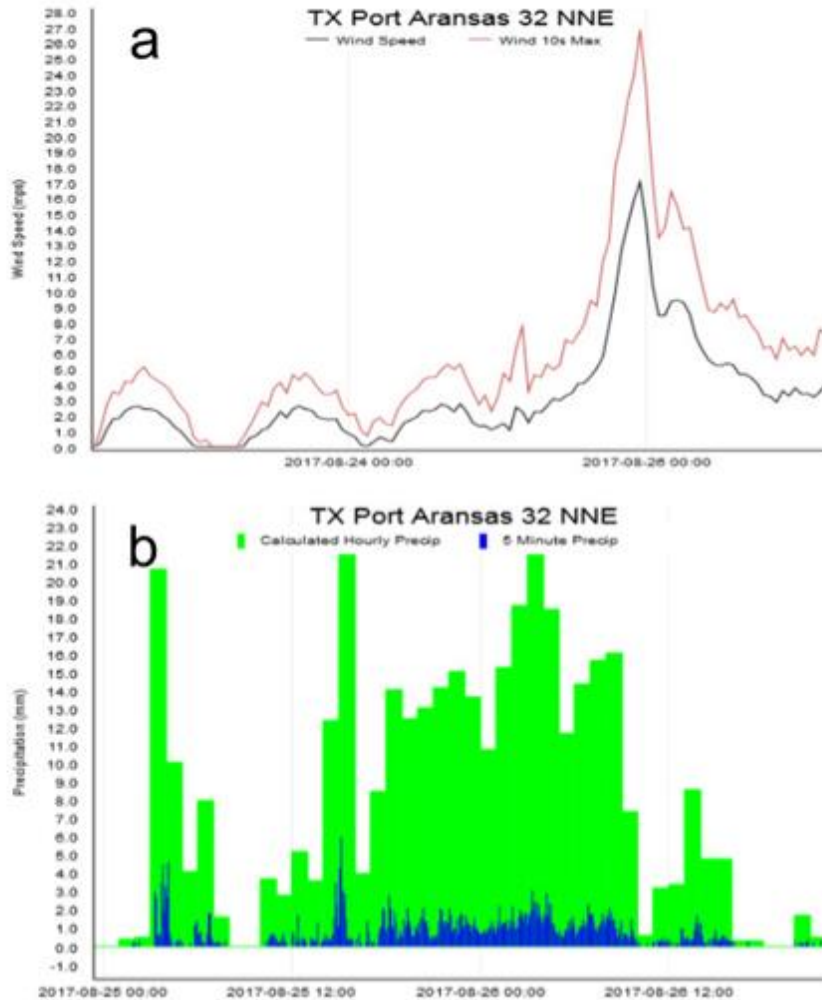


Fig. 10: The Port Aransas, TX station measured a maximum 10-second wind speed of 60 mph (26.9 m s^{-1}) (panel a). For climate purposes, the wind speed sensors on the USCRN stations are located 1.5 m above the ground, while the wind sensors at airports are at about 10 m above the ground. The gust duration of the aviation sites are also for a shorter period (3 seconds). Applying an adjustment to the USCRN value to account of the increased height and decreased time of the aviation measurements, the 60 mph value would have been measured at a standard height in the 75-80 mph ($33.5\text{-}35.7 \text{ m s}^{-1}$) range. Fortunately, there was no wind damage to the site, and it continued to operate throughout the storm. The 60 mph peak 10-second wind value was a new station record; the previous record was 31 mph (14.0 m s^{-1}) set in December 2009. The storm also brought new station record rainfall amounts for various periods (panel b). The maximum 24 hour total was 11.69" (296.0 mm), easily eclipsing the previous record of 6.04" (153.4 mm) on September 18-19 2010. The storm total of 15.05" (382.3 mm) brought the August monthly total to 19.10" (485.1 mm) which was not only a new record for August, but also for any month. The previous station record for any month was 17.44" (443.0 mm) set September 2010.

Publications

- Biederman, J. A., R. L. Scott, T. W. Bell, D. R. Bowling, S. Dore, J. Garatuza-Payan, T. Kolb, P. Krishnan, D. J. Krofcheck, M. E. Litvak, G. E. Maurer, T. P. Meyers, W. C. Oechel, S. A. Papuga, G. E. Ponce-Campos, J. C. Rodriguez, W. K. Smith, R. Vargas, C. J. Watts, E. A. Yepez, and M. L. Goulden, 2017: CO₂ exchange and evapotranspiration across dryland ecosystems of southwestern North America. Wiley Online in *Global Change Biology*, 1-8.
- Buban M. S., T. R. Lee, E. J. Dumas, C. B. Baker, and M. Heuer, 2018: Observations and numerical simulation of the effects of the 21 August 2017 North American total solar eclipse on surface and atmospheric boundary layer evolution. *Boundary-Layer Meteorology* (Accepted).
- Dobosy, R., D. Sayres, C. Healy, E. Dumas, M. Heuer, J. Kochendorfer, B. Baker, and J. Anderson, 2017: Estimating random uncertainty in airborne flux measurements over Alaskan tundra: Update on the Flux Fragment Method. *Journal of Atmospheric and Oceanic Technology*, Early Online Release, doi.org/10.1175/JTECH-D-16-0187.1.
- Kochendorfer, J., R. Rasmussen, M. Wolff, B. Baker, M. E. Hall, T. Meyers, S. Landolt, A. Jachcik, K. Isaksen, R. Brækkan, and R. Leeper, 2017: The quantification and correction of wind-induced precipitation measurement errors. *Hydrology and Earth System Sciences*, **21**, 1973-1989.
- Lee, T. R., M. Buban, E. Dumas, and C. B. Baker, 2017: A new technique to estimate sensible heat fluxes around micrometeorological towers using small unmanned aircraft systems. *Journal of Atmospheric and Oceanic Technology*, **34**, 2103-2112.
- Lee, T. R., M. Buban, M. A. Palecki, R. D. Leeper, H. J. Diamond, E. Dumas, T. P. Meyers, and C. B. Baker, 2018: Great American Eclipse data may fine-tune weather forecasts. *Eos*, **99**.
- Nelson, A. J., S. Koloutsou-Vakakis, M. J. Rood, L. Myles, C. Lehmann, C. Bernacchi, S. Balasubramanian, E. Joo, M. Heuer, M. Vieira-Filho, and J. Lin, 2017. Season-long ammonia flux measurements above fertilized corn in central Illinois, USA, using relaxed eddy accumulation. *Agricultural and Forest Meteorology*, **239**, 202-212.
- Sayres, D. S., R. Dobosy, C. Healy, E. Dumas, J. Kochendorfer, J. Munster, J. Wilkerson, B. Baker, and J. Anderson, 2017: Arctic regional methane fluxes by ecotope as derived using eddy covariance from a low-flying aircraft. *Atmospheric Chemistry and Physics*, in press.
- Wulfmeyer V., D. D. Turner, B. Baker, R. Banta, A. Behrendt, T. Bonin, W. A. Brewer, M. Buban, A. Choukulkar, E. Dumas, R. M. Hardesty, T. Heus, D. Lange, T. R. Lee, S. Metzendorf, T. Meyers, R. Newsom, M. Osman, S. Raasch, J. Santanello, C. Senff, F. Späth, T. Wagner, and T. Weckwerth, 2018: A new research approach for observing and characterizing land-atmosphere feedback. *Bulletin of the American Meteorological Society*, in press.

CIMMS Task III Project – Utilizing Sub-Flash Properties of GLM to Monitor Convective Intensity with Probabilistic Guidance

Kristin Calhoun (CIMMS at NSSL), Christopher Schultz (NASA Marshall Space Flight Center), and Phillip Bitzer and Larry Carey (University of Alabama-Huntsville)

NOAA Technical Lead: Don MacGorman (NSSL)

NOAA Strategic Goal 2 – Weather Ready Nation: Society is Prepared for and Responds to Weather-Related Events

Funding Type: CIMMS Task III

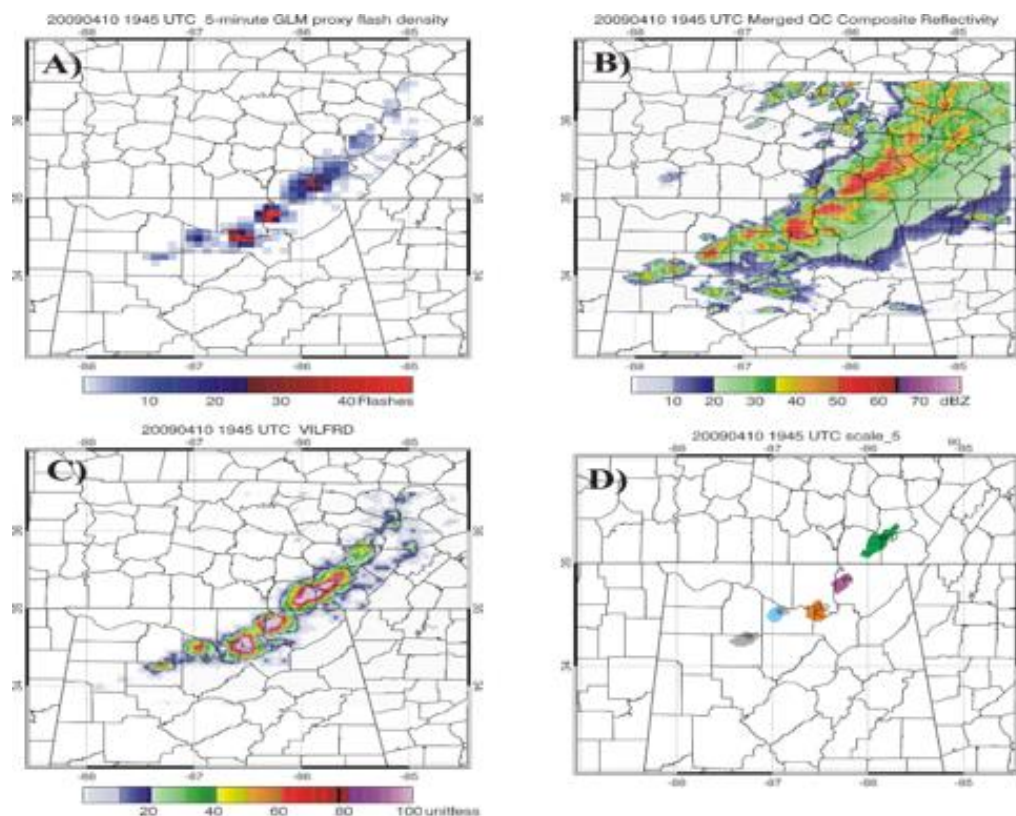
Objectives

Rapid increases in total lightning (lightning jumps) are the result of increases in mixed-phase updraft speed and size. Recent work has developed a lightning jump algorithm to objectively identify when a storm has produced a lightning jump using lightning flash data. With the successful launch into orbit of GOES-16, the Geostationary Lightning

Mapper brings a opportunity to measure lightning from space, providing both spatial and density information even in remote and oceanic regions. The GLM instrument provides sub-flash properties of lightning that directly relate to physical processes within the lighting channel and thunderstorm. Therefore, the goal of this research is to understand the impact of and integrate the sub-flash components from the GLM into the operational lighting jump algorithm to improve assessment of thunderstorm strength. In addition to GLM flashes, a total of 3 GLM derived sub-flash lightning properties are examined in this study: optical radiance from lightning, GLM groups and GLM events.

Accomplishments

Tracking of the thunderstorms are on blended sub-field that incorporates both GLM data and radar data. The current algorithm being tested for real-time implementation blends 5-min accumulation of GLM flash extent density with vertically-integrated liquid (VIL) from the Multi-Radar Multi-Sensor (MRMS) product suite. The advantage this algorithm has is the potential to operate on GLM alone where radar data are sparse or not available (e.g., over oceans, in mountainous terrain). The fused tracking approach means any thunderstorm within the field of view of GOES-16 (and GOES-17, future) can be tracked for assessment of convective intensity. Evaluation of the lightning jump algorithm as attached to this new tracking methodology will be the goal of both case studies and real-time experiment in year 2 of the grant (2019).



Example of combined GLM and VIL tracking methodology. (A) 5-min gridded GLM proxy flash density. (B) Merged Composite Radar Reflectiity (C) VIL-FlashRate Density merged product. (D) tracked clusters.

CIMMS Task III Project – Integration of the Geostationary Lightning Mapper with Ground-based Lightning Detection Systems for National Weather Service Operations

Kristin Calhoun, Darrel Kingfield, and Tiffany Meyer (CIMMS at NSSL)

NOAA Technical Lead: Don MacGorman (NSSL)

NOAA Strategic Goal 2 – *Weather Ready Nation: Society is Prepared for and Responds to Weather-Related Events*

Funding Type: CIMMS Task III

Objectives

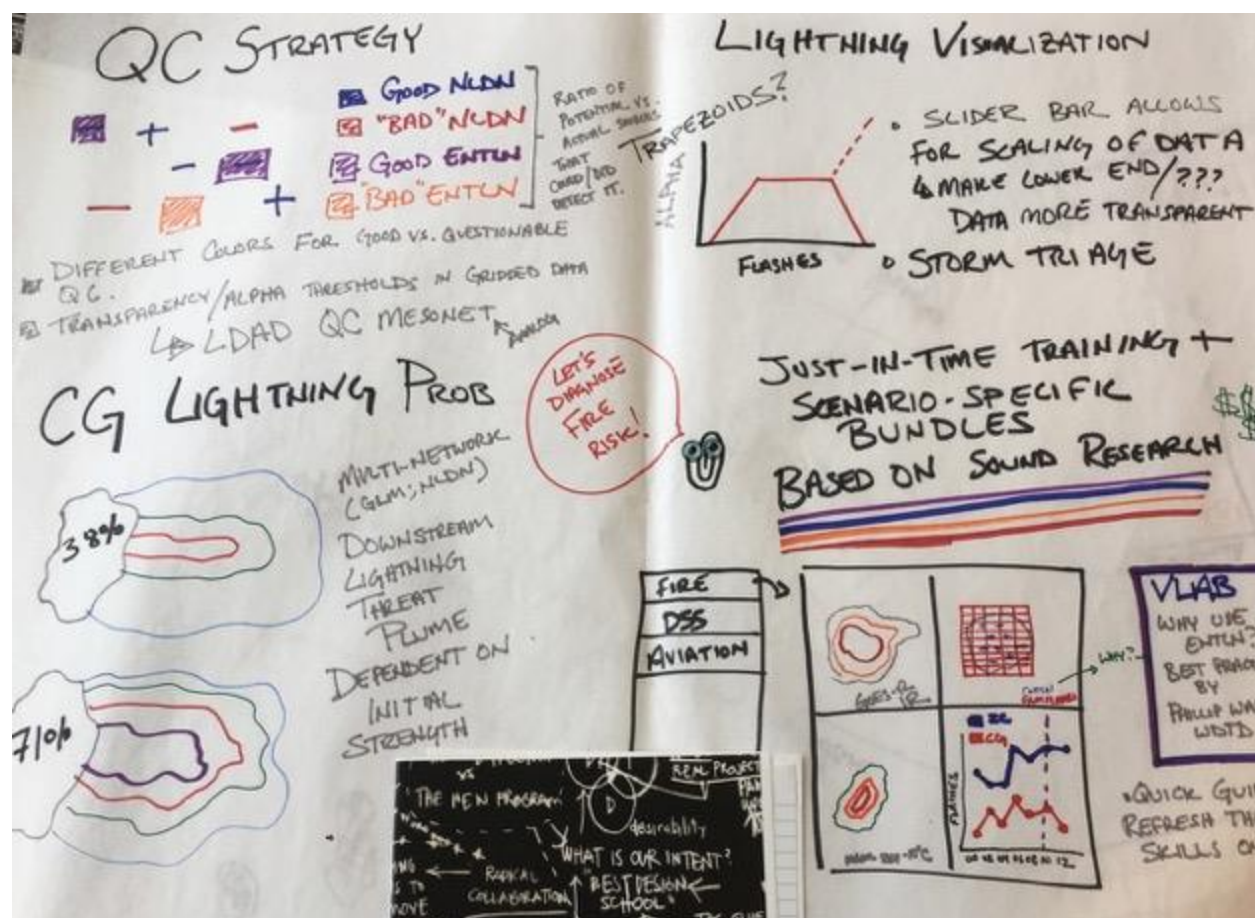
With the continued increase of data, forecasters under the time constraints of warning decisions and decision-support services (DSS) can greatly benefit from the availability of single lightning product or bundle within operations. Since the methodology for the detection of lightning from each network is different (i.e., high frequency radiation, low frequency radiation, or optical detection), different segments of lightning flashes will be detected by each system. A combined detection algorithm may be able to better contribute to the overall understanding storm development and lightning safety. This project utilizes the operational Multi-Radar/ Multi-Sensor (MRMS) system and capabilities to blend the satellite-based lightning detection data from the new GOES satellites with that from ground-based systems (e.g., Vaisala National Lightning Detection Network or Earth Networks Total Lightning Data). The primary goal is to create a blended product for forecasters every 2 min with little-to-no delay into operations. We will test different aspects of lightning detection from the systems against severe storm and hazardous weather properties and work with NWS forecasters to determine the optimal lightning properties and resolution requirements for NWS operational use. These gridded products will be developed with current forecaster needs, sequencing, and data interrogation methods in mind.

Accomplishments

In order to adequately and properly address the NWS forecaster needs, we invited our NWS co-investigators as well as forecasters from each NWS region (working with the regional SSD Chiefs) to a workshop in August of 2017 in Norman, OK. This workshop utilized the ideas of “design thinking” from the Institute of Design at Stanford to better define the forecaster need then provide ideas and prototypes for a merged product (see figure below).

The results of the workshop were surprising and greatly enhanced our development process. The number one need forecasters stressed in all situations was a level of confidence in the system or specifically a knowledge in how each network is performing relative to each other and a “truth”. This combination “Quality Control” product is now a key focus in our initial development. We also learned from NWS forecasters that a jointly visualized product should be fundamentally designed to address a specific use

goal in mind (e.g., decision-support services, fire weather, severe weather forecasting). The design-elements of each product thus each have different qualities and inherently different combinations from the multiple operational systems.



Example of Design Process from Group 2 participating in the August 2017 HWT workshop. Similar graphics and design elements were provided by all groups. Workshop completed by developing prototypes based on individual groups designs. Feedback and ideas from the NWS forecasters will ultimately prioritize the MRMS design and implementation.

CIMMS Task III Project – Development of an Archival System for the Integration of High Resolution GOES-R, Radar and Lightning Data for Improving Severe Weather Forecasting and Warning Capabilities

Kristin Calhoun, Darrel Kingfield, Anthony Reinhart, and Thomas Jones (CIMMS at NSSL), and Shane Hubbard and Wayne Feltz (CIMSS at University of Wisconsin-Madison)

NOAA Technical Lead: Alan Gerard, Don MacGorman, and Bob Rabin (NSSL)

NOAA Strategic Goal 2 – Weather Ready Nation: Society is Prepared for and Responds to Weather-Related Events

Funding Type: CIMMS Task III

Objectives

The Geostationary Operational Environmental Satellite (R-Series; GOES-R) will provide coverage (spatially and temporally) that, particularly when integrated with ground-based systems such as WSR-88D radars, can actively support severe weather forecasting and warnings. With the launch of GOES-R, space-based and ground-based observations will be in cadence with each other, providing the ability to create a top to bottom, linked profile of a severe thunderstorm through direct observation. It is vitally important that stakeholders such as scientists at the National Severe Storms Laboratory (NSSL), developers integrated with the Storm Prediction Center, forecasters at various National Weather Service (NWS) offices, and training entities such as the Warning Decision Training Division (WDTD) have access to the GOES-R data to integrate the data into their current research, algorithm development, and training.

Accomplishments

We have established and maintain an archive of all of relevant GOES-R data related to severe and hazardous weather. Hardware was purchased (200TB storage initially, purchased and installed Dec 2017) and a daily data pull (via FTP) was established coordinated with the Cooperative Institute for Meteorological Satellite Studies (CIMSS) at the University of Wisconsin-Madison (Feb 2018). The data in this archive is available through open access (goes16.metr.ou.edu) and may be used by all interested parties with the goal of integration and development of severe weather applications and algorithms. Data from this archive is being integrated into a number of projects led by CIMMS/NSSL scientists including a comparison of GLM flash and sub-flash products to tropical cyclone strength and development of data assimilation processes for both the High Resolution Rapid Refresh (HRRR) and Warn-on-Forecast applications. Additionally, a graduate student (Kevin Thiel) was selected to begin Aug 2018 to focus on the spatiotemporal intercomparisons between Multi-Radar Multi-Sensor (MRMS) isothermal and vertically integrated products to Advanced Baseline Imager (ABI) and Geostationary Lightning Mapper (GLM) products on GOES-R in the development of severe weather guidance using data available from this archive.

CIMMS Task III Project – National Sea Grant Weather & Climate Extension Specialist Activities

Kodi Berry (CIMMS at NSSL) and Alan Gerard (NSSL)

NOAA Technical Lead: Elizabeth Rohring (NOAA Sea Grant)

NOAA Strategic Goal 2 – *Weather-Ready Nation – Society is Prepared for and Responds to Weather-Related Events; and*

NOAA Strategic Goal 1 – *Climate Adaptation and Mitigation: An Informed Society Anticipating and Responding to Climate and its Impacts, and Weather-Ready Nation – Society is Prepared for and Responds to Weather-Related Events*

Funding Type: CIMMS Task III

Objectives

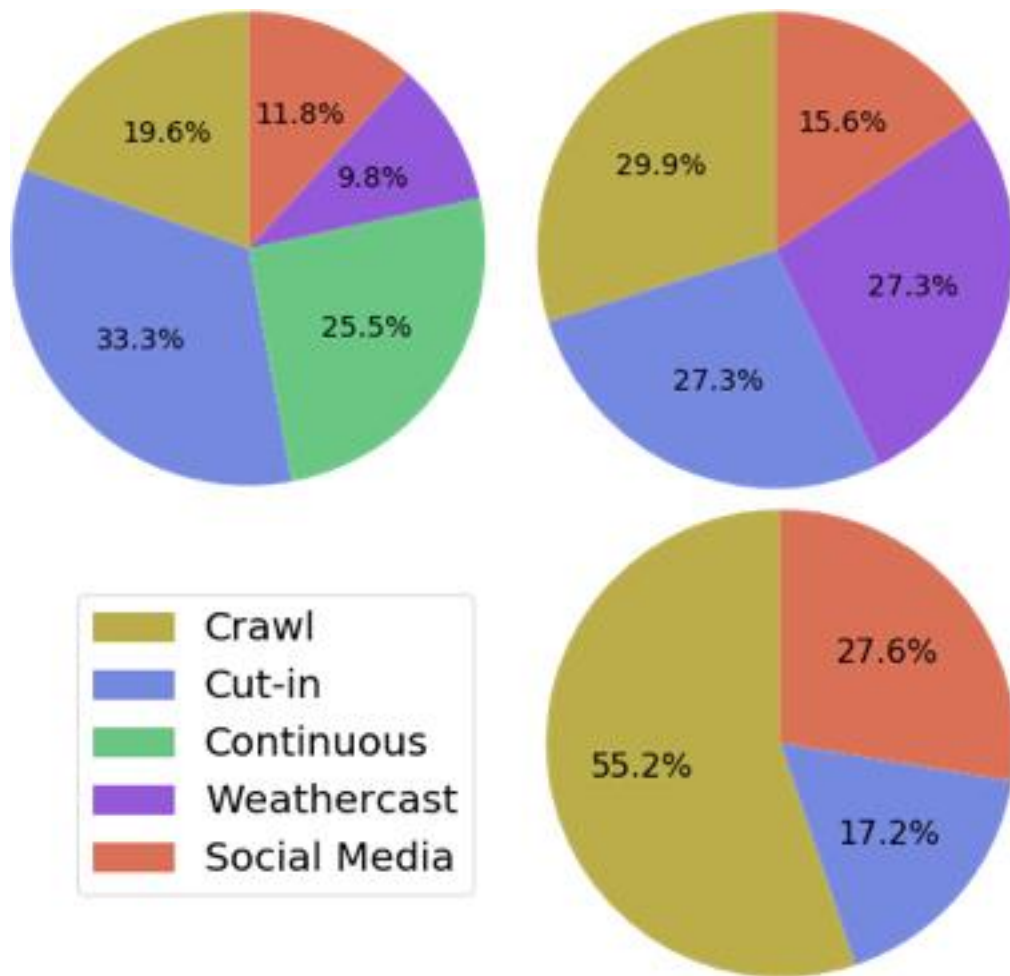
Connect NSSL research with the Sea Grant Extension Network, and develop a capacity to forecast high-impact threats for coastal communities using the FACETs framework and methodologies.

Accomplishments

The Sea Grant Weather & Climate Extension Specialist at CIMMS/NSSL and Holly Obermeier (CIMMS at NSSL, now CIRES at the University of Colorado) conducted an analysis of results from the broadcast meteorologist project of the 2017 Hazardous Weather Testbed (HWT) Probabilistic Hazard Information (PHI) experiment. One broadcast participant per week performed typical job functions under a simulated television studio environment as they received experimental probabilistic advisories and warnings from NWS forecasters during three realtime and three displaced realtime events. Research protocols were used to investigate how broadcast meteorologists interpreted, used, and communicated both probabilistic information and experimental warning messaging. In the 2017 project, warning update frequencies were varied daily to better understand the optimal flow of information for the specific needs of broadcast meteorologists and their television stations. In addition, probability thresholds for coverage decisions were tracked. Results reveal that participants preferred the gradual increase in update frequency throughout the week. The default, two-minute updates were deemed too fast for crawl systems and potentially station bandwidth constraints. Participants stated that 5 to 10 minutes was a more optimal update frequency for on-air presentation and viewer consumption. However, the frequent updates coupled with multiple warnings led participants to believe that additional personnel would be needed to handle the workload. Participants also found that they generally preferred to view and communicate the warning polygon outlines with radar, while viewing the probabilistic plumes on a separate screen.

Building off these findings, the Sea Grant Weather & Climate Extension Specialist and Holly Obermeier planned and conducted the 2018 broadcaster project with two broadcast participants per week working in a team environment. Participants received actual NWS warnings and experimental PHI during six displaced realtime events. The weather studio was upgraded with a chroma key, wireless microphones, camera, lighting, and protected Facebook and Twitter accounts. The additional broadcaster led to more realistic handling of severe weather coverage. Researchers concentrated on communication challenges and decision points of interest, but also investigated the interplay between the probabilistic plume and the traditional warning polygon. Researchers explored and tested whether the PHI plume and warning polygon should be intrinsically connected.

The Sea Grant Weather & Climate Extension Specialist actively participates in the Experimental Hazard Services Collaborators team and FACETs (Forecasting A Continuum of Environmental Threats) Science and Technology Integration (STI) Team. The Sea Grant Extension Specialist is leading the development of videos to 1) educate NWS forecasters on how the FACETs warning paradigm will impact their role as a forecaster and 2) educate the general public on research with broadcast meteorologists.



Breakdown of television coverage decisions by hazard type over the three-week project. Participants had five different options for coverage, including cut-ins and continuous (wall-to-wall) coverage over commercials and/or programming.

CIMMS Task III Project – Enhancement and Evaluation of NGGPS Model FV3 at Convection-Allowing Resolutions through Hazardous Weather Testbed Spring Experiment towards Accelerated Operational Implementation of FV3 for Mesoscale Applications

Ming Xue, Chunxi Zhang, Tim Supinie, Fanyou Kong, Nate Snook, Kevin Thomas, Keith Brewster, and Youngsun Jung (CAPS)

NOAA Technical Leads: Shian-Jiann Lin and Lucas Harris (GFDL)

NOAA Strategic Goal 2 – *Weather Ready Nation: Society is Prepared for and Responds to Weather-Related Events*

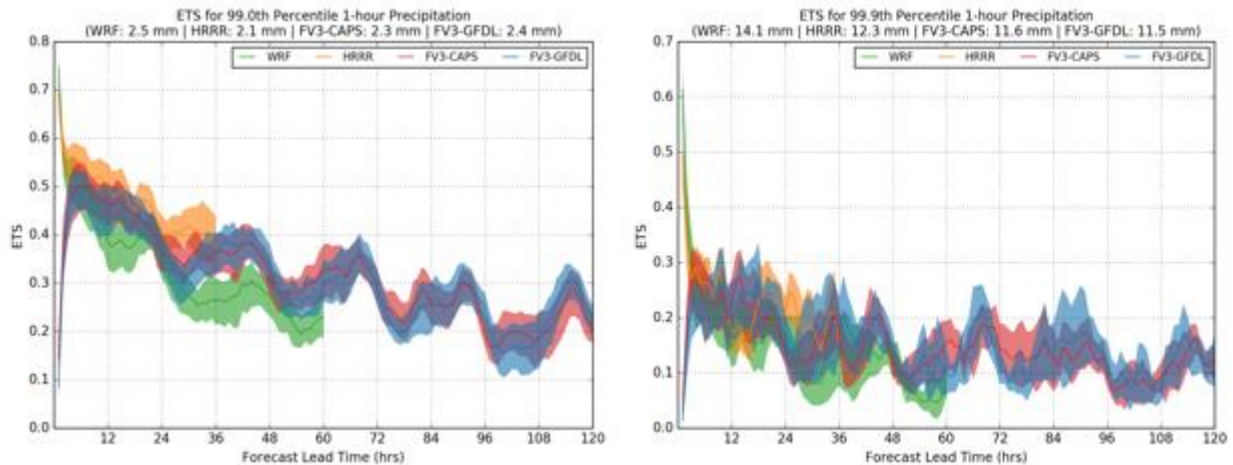
Funding Type: CIMMS Task III

Objectives

In this project, CAPS was to work on the physics enhancement and realtime prediction using FV3 at a convection-allowing ~3 km grid spacing over the CONUS domain, and to produce realtime forecasts for evaluation during the 2017 HWT Spring Forecast Experiment.

Accomplishments

- 1) CAPS configured FV3 with the current operational GFS physics package, but with the GFS microphysics replaced by the GFDL version of Lin single-moment ice microphysics, to have ~ 3km grid spacing over CONUS for convection-permitting resolution predictions of up to 3 days. A ~3km grid over the CONUS is nested in a stretched global ~ 13km grid. This configuration was tested in a retrospective mode with the cases from spring 2016.
- 2) CAPS implemented a few physics schemes into FV3, including partially double-moment Thompson microphysics scheme, fully double-moment Milbrant-Yau, NSSL and Morrison microphysics schemes; the first order non-local YSU PBL scheme and the scale-aware version of YSU PBL schemes; the higher-order Mellor-Yamada scheme, e.g., MYNN and scale-aware version of MYNN scheme; the new Tiedtke cumulus scheme. Those schemes were tested with five selected cases from spring and summer in 2017.
- 3) CAPS ran the FV3 with nested 3-km CONUS grid and the Thompson microphysics during the 2017 HWT Spring Experiment for evaluations at HWT, and compared the forecasting results with ensemble forecasts of other regional models and the FV3 runs by GFDL. GFDL ran a parallel set of forecasts with the same grid configurations but with the GFDL Lin microphysics (See figure below).
- 4) CAPS developed software for diagnostic analysis and forecast evaluations with Python and NCL, and conducted evaluations of the 2017 HWT forecasting results.
- 5) Going beyond originally proposed, CAPS ran 11 FV3 forecasts each day, using different combinations of microphysics and PBL schemes, and two cumulus parameterization schemes on the global grid during 2018 HWT Spring Forecast Experiment. Initial results are reported in a paper submitted to Geophysical Research Letter recently.



Neighborhood ETS of 1-hr precipitation accumulation as a function of forecast lead time for FV3-CAPS (red), FV3-GFDL (blue), the CAPS SSEF control member (green), and the experimental HRRR version 3 (orange) for 19 cases during the 2017 HWT SFE. The neighborhood radius is 45 km, and the threshold for the ETS calculation is the (a) 99th and (b) 99.9th percentiles of hourly precipitation. The shaded region contains the 5th-95th percentiles of the mean of 10000 bootstrap-sampled forecasts.

CIMMS Task III Project – Assimilation of High-Frequency GOES-R Geostationary Lightning Mapper (GLM) Flash Extent Density Data in GSI-Based EnKF and Hybrid for Improving Convective Scale Weather Predictions

Ming Xue and Rong Kong (OU/CAPS), and Alexandre Fierro (CIMMS at NSSL)

NOAA Technical Leads: Edward Mansell and Donald MacGorman (NSSL), and Shun Liu (EMC)

NOAA Strategic Goal 2 – Weather Ready Nation: Society is Prepared for and Responds to Weather-Related Events

Funding Type: CIMMS Task III

Objectives

In this project, direct assimilation capabilities for GOES-R GLM data will be developed within the operational GSI framework, using ensemble Kalman filter (EnKF) and hybrid ensemble-variational (EnVar) methods. The capabilities developed will be first tested using selected, representative cases, then evaluated extensively in real time during the Hazard Weather Testbed (HWT) Spring Experiment. The major goal of this project is to accelerate the use of GOES-R GLM data in operational numerical weather prediction (NWP) models at NCEP, and thereby help meet the Weather Ready Nation objectives and realize the Warn-on-Forecast goals.

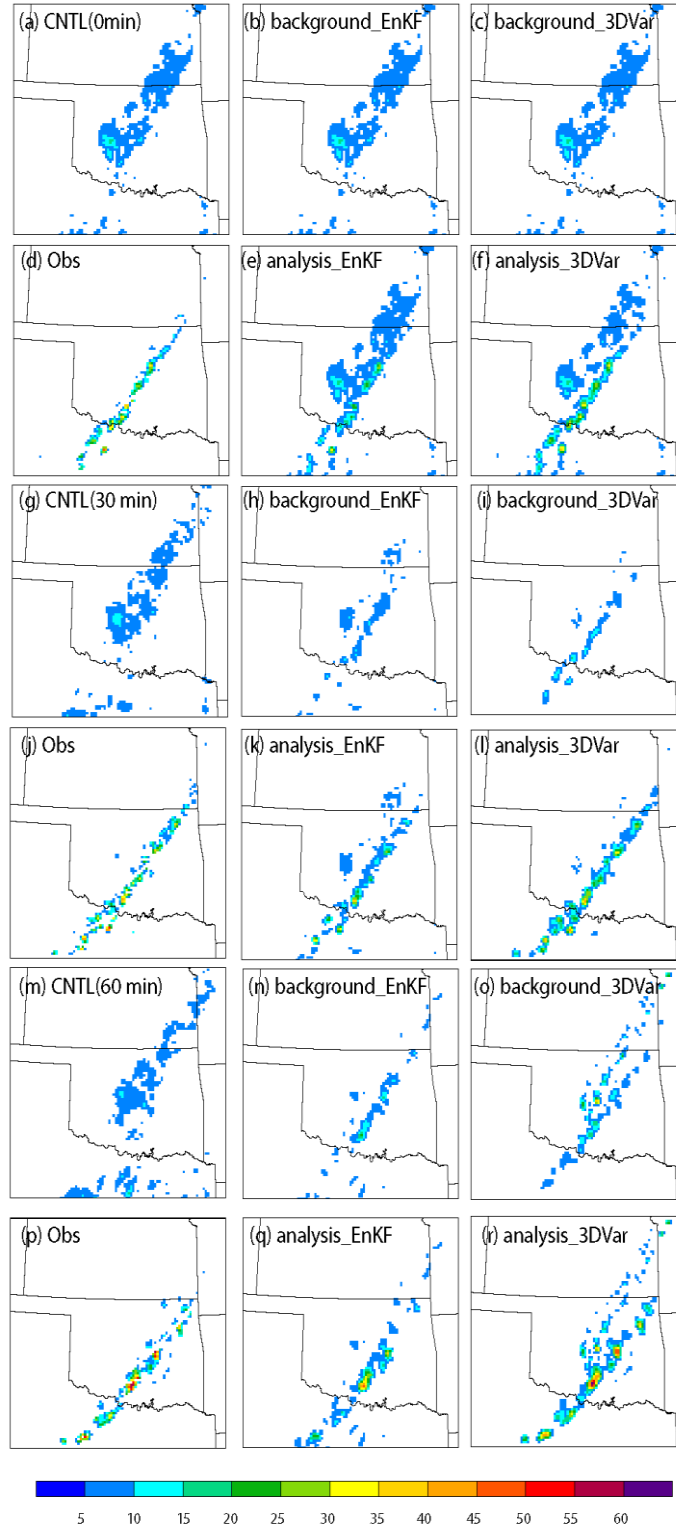
Accomplishments

During this reporting period, adjoint code of GLM FED observation operator was developed and implemented within the GSI variational framework. The lightning DA

capability was incorporated into the GSI-3DVar and hybrid En3DVar. The GLM data are preprocessed to produce accurate estimates of flash extent densities (FED). Further, the FED observations are converted to the BUFR format, which is the format used by GSI.

Two high-impact cases of October 22, 2017 and July 13, 2018 were used to test FED DA using GSI-3DVar and EnKF. The initial perturbations for the EnKF are derived from the operational Short-Range Ensemble Forecast (SREF) system. Additional smaller-scale smoothed Gaussian random perturbations are added to further increase the spread of the initial ensembles at small scales. The initial ensembles are advanced two or three hours using the WRF ARW model to spin up the model states. Mixed physics options are used in the WRF ensemble forecasts. FED observations are assimilated every 15-min for 1 hour using GSI EnKF or 3DVar.

Preliminary results for the October 2017 case are shown in the figure below. Relative to observations, the intensity of the simulated FED from forecast of the control run (ensemble mean forecast without assimilating FED observations) is much weaker. The forecast squall line is behind (westward of) the observed location. After the FED DA, both EnKF and 3DVar are able to significantly alleviate and correct this location error of the squall line. The locations and rates of the simulated FED centers for EnKF and 3DVar are in better agreement with the observations in both the analyses and forecasts relative to the control run. There are, however, some spurious FED forecasts in the 3DVar cycles (especially in the last two cycles), which are well suppressed in EnKF cycles due to the use of the ensemble covariance.



Comparisons of simulated FED for control forecast (ensemble mean without FED DA, a, g, m), observations (d, j, p), background forecasts (b, h, n) and analyses (e, k, q) for EnKF, background forecasts (c, i, o) and analyses (f, l, r) for 3DVar for October 22, 2017 case. Figures are shown for cycles at 0 min (a ~f), 30 min (g~l), and 60 min (m~r) respectively (unit: $\text{pixel}^{-1}\text{min}^{-1}$).

CIMMS Task III Project – Advanced Data Assimilation and Prediction Research for Convective-Scale “Warn-on-Forecast”

Ming Xue, Youngsun Jung, Tim Supinie, Chengshi Liu, Rong Kong, Marcus Johnson, and Chunxi Zhang (CAPS)

NOAA Technical Lead: Pamela Heinselman (NSSL)

NOAA Strategic Goal 2 – *Weather-Ready Nation: Society is Prepared for and Responds to Weather-Related Events*

Funding Type: CIMMS Task III

Objectives

A key component towards achieving the ‘Warn-on-Forecast (WoF)’ vision (Stensrud et al. 2009; Stensrud 2010) for severe weather is to obtain sufficiently accurate initial conditions of convective-scale numerical weather prediction (NWP) models. Advanced data assimilation (DA) is the essential procedure for obtaining such initial conditions. To realize probabilistic forecasting, which is also a key part of the WoF vision, an ensemble of initial conditions is needed to initialize the ensemble forecasts. As a partner of the WoF project, most of its efforts on developing, refining and applying ensemble-based data assimilation systems to storm-scale deterministic and probabilistic predictions. Efforts will also be made to develop a hybrid ensemble-variational data assimilation system that seeks to combine the strengths of both variational and ensemble methods. Specific objectives for CAPS over the past year include: 1. The development and intercomparison of ensemble-based DA methods for selected cases; 2. A study on the impact of assimilating fast-scan MPAR data on convective storm analysis and prediction; 3. The development and application of a dual-pol radar simulator and the evaluation of microphysics schemes using dual-pol data; 4. Implementation of better PBL schemes into the FV3 model and evaluate the performance of FV3 for convection-permitting forecasts.

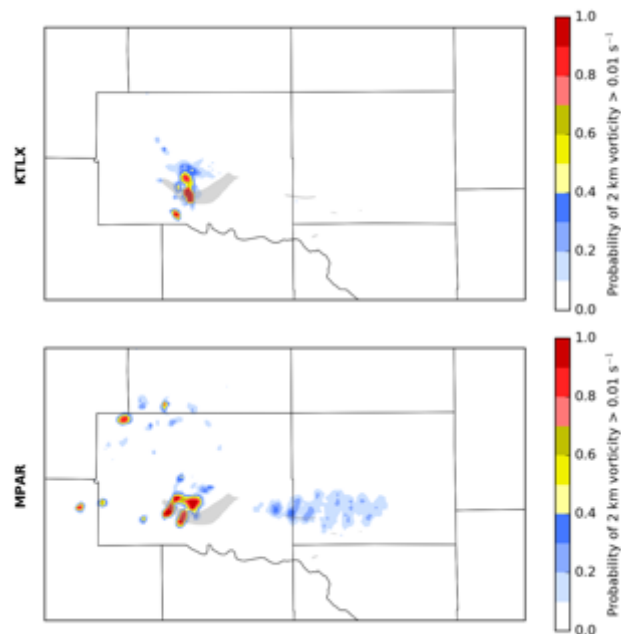
Accomplishments

1. Development and Intercomparison of Ensemble-Based Data Assimilation Methods for Select Cases

The capabilities to directly assimilate radar radial velocity and reflectivity data in the ARPS hybrid ensemble-3DVar (HEn3DVar) DA system was developed by coupling the En3DVar system with the EnKF system. The performance of HEn3DVar was compared with those of 3DVar, EnKF, and a deterministic forecast EnKF (DfEnKF) for a supercell storm in OSSE and the results were published in the Monthly Weather Review (Kong et al., 2018). Here, DfEnKF uses a single deterministic forecast as the background but perturbations from the EnKF system, making it algorithm-wise parallel to the pure (one-way-coupling) En3DVar algorithm. The updated CAPS’s EnKF and EnVar DA systems have been delivered to NSSL.

The Hen3DVar system was further evaluated using the 10 May 2010 Oklahoma tornadic supercell storm case. The model has a 1 km grid spacing, covering central Oklahoma. Four WSR-88D radars (KTLX, KFDR, KINX, and KVNXX) and the Oklahoma mesonet observations are assimilated every 5 minutes for an hour. Then one-hour forecasts are initialized from the final analyses using the HEn3DVar, EnKF, DfEnKF, or 3DVar. After 45 ~ 60 minutes of forecasts, all experiments are able to capture the storm that produced the EF3 tornado through the north part of Seminole County (figure below). Hybrid En3DVar with 75% weight given to the static background error covariance outperforms the other algorithms in better capturing the hook echo structure as well as the intensity of the mesocyclone. The above results are in preparation for peer reviewed publication.

The nonlinear reflectivity forward operator causes many problems using mixing ratios as a control variable (CVq) or a logarithmic mixing ratio as a control variable (CVlogq) in the variational framework. To mitigate the adverse effects of the nonlinear forward operator, some treatments were developed, including: (a) a lower limit on hydrometeor mixing ratios or equivalent reflectivity imposed on the reflectivity observation operator for CVq; (b) a separate analysis pass to assimilate reflectivity and radial velocity for CVq; and (c) a lower limit added to the background when converting the $\log(q)$ increment to q increment for CVlogq. Through observing system simulation experiments with a simulated supercell storm, these treatments directly help improve reflectivity assimilation (Liu et al., 2018a). These treatments and the temperature-dependent background error profiles were implemented in a GSI hybrid DA system.



Probability of vertical vorticity greater than 0.01 s^{-1} at 2 km AGL over the 50-minute forecast for the (a) KTLX and (b) MPAR experiments. The observed tornado tracks are given in the gray shaded regions.

2. Study on the Impact of Assimilating Fast-Scan MPAR Data on Convective-Storm Analysis and Prediction

The impact of PAR data on hazardous weather forecasting was further examined using the ARPS 4D ensemble square root filter (4DEnSRF) for the 31 May 2013 supercell case. The ensemble uses 36 members at 1 km grid spacing. The experiment that assimilates only MPAR data is compared with the experiment that assimilates only KTLX data. Data from the respective radar are assimilated over a 45-minute period beginning at 2225 UTC and ending at 2310 UTC. Analyses are produced every 5 minutes during the assimilation period using a 5-minute DA window centered on the analysis time.

A 50-minute ensemble forecast was run from the final analysis, and the reflectivity and vorticity probabilities were examined during that forecast. The reflectivity probabilities showed the supercell moving too fast in both experiments, which is a common feature of supercells in 1-km simulations. Additionally, both experiments were unable to capture convections developed behind the initial supercell, which were responsible for a major flash flood in the Oklahoma City metro area after the initial supercell moved through.

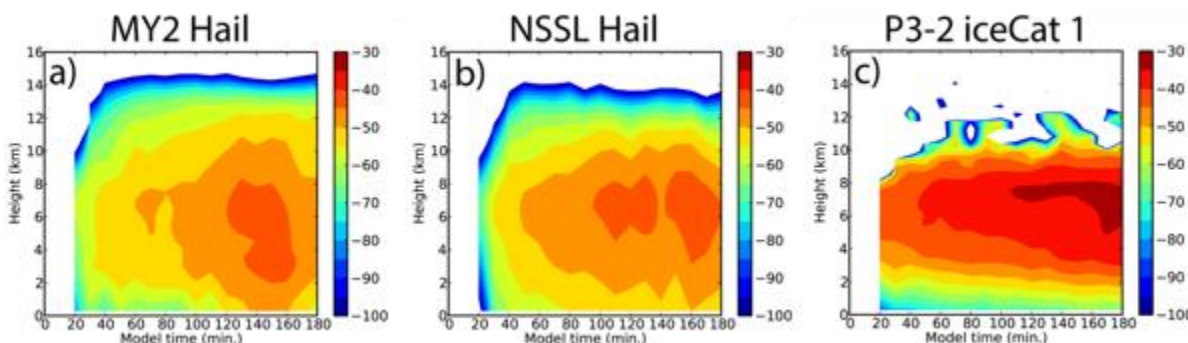
In the vorticity probability forecast (Fig. 1), the initial mesocyclone dissipates too early in both experiments, but the MPAR experiment better captures the mesocyclone associated with the second smaller tornado east of the initial large tornado. Work is underway to determine why the initial mesocyclone is too weak in both experiments.

An intermediate covariance inflation method has also been implemented in the 4DEnSRF. This method runs relaxation to prior spread (RTPS) inflation multiple times during DA. For example, the RTPS inflation subroutine is called after assimilation of every volume scan when several radar volume scans are assimilated with the 4DEnSRF. This method should help maintain the spread during the assimilation of large amounts of observations and increase impact of observations assimilated later during one DA cycle. The effects of the new method on the analysis and forecasts are currently under investigation.

3. Development and Application of Dual-Pol Radar Simulator and Evaluation of Microphysics Schemes Using Dual-Pol Data

The latest version of the predicted particle properties (P3) scheme permits multiple ice categories where each ice category can span a continuous ice spectrum and changes distribution shape. The CAPS polarimetric radar data simulator (CAPS-PRS) is applied to an idealized supercell storm simulated with the Milbrandt-Yau (MY2), NSSL, and the P3 (P3-2) scheme that contains two categories of rimed ice (e.g., graupel and hail). Both the MY2 and NSSL schemes replicate a Z_{DR} arc, while the P3-2 scheme is unable to replicate this signature despite properly simulating ice size sorting. Only the NSSL scheme simulates the correct location of the hail signature in the forward flank downdraft. The figure below shows frequencies of rimed ice diameter D exceeding 15 mm (the demarcation between graupel and hail) normalized by the number of grid

points. The P3-2 scheme, indeed, can produce more “hail-like” rimed ice compared to the other BMPs. However, between 3 and 4 km, these frequencies begin to rapidly diminish toward the surface. The largest frequencies reaching the surface over the model run is at least three orders of magnitude lower than large rimed ice above the melting layer. This comparatively stronger frequency gradient implies that, due to excessive melting, large rimed ice is diminishing more rapidly than MY2 and NSSL hail. This explains why the scheme is unable to simulate the hail signature in the forward flank, as large rimed ice in the scheme cannot reach the surface. The results have been summarized for publication and the manuscript is in internal review.

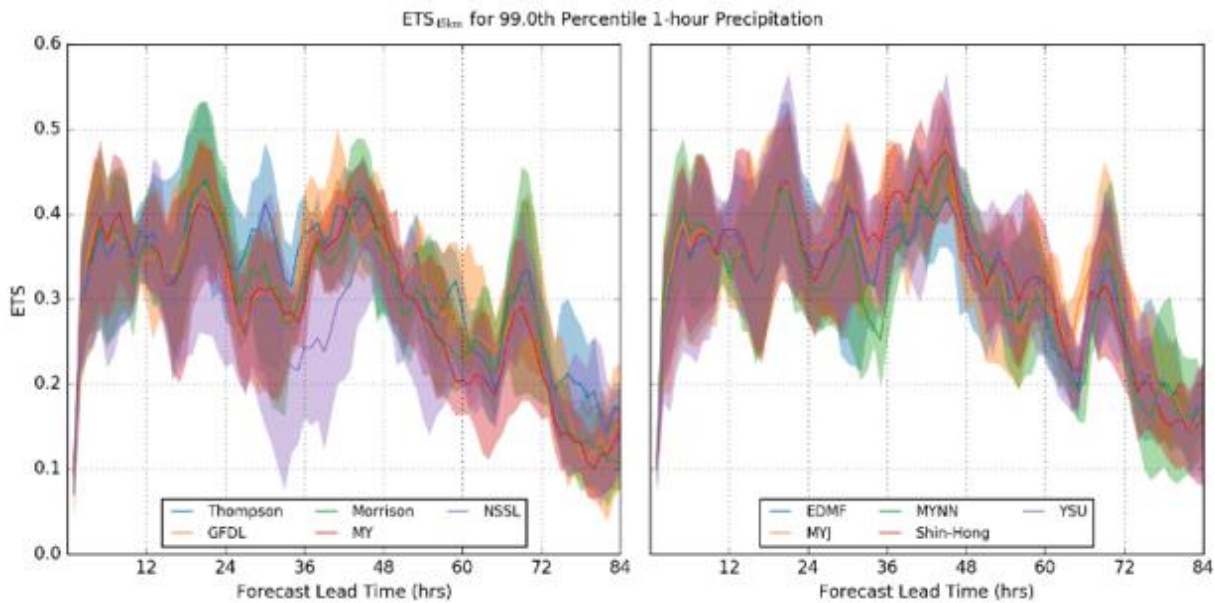


Large rimed ice frequencies with diameter larger than 15 mm for (a) MY2 hail, (b) NSSL hail, and (c) P3-2 ice category 1.

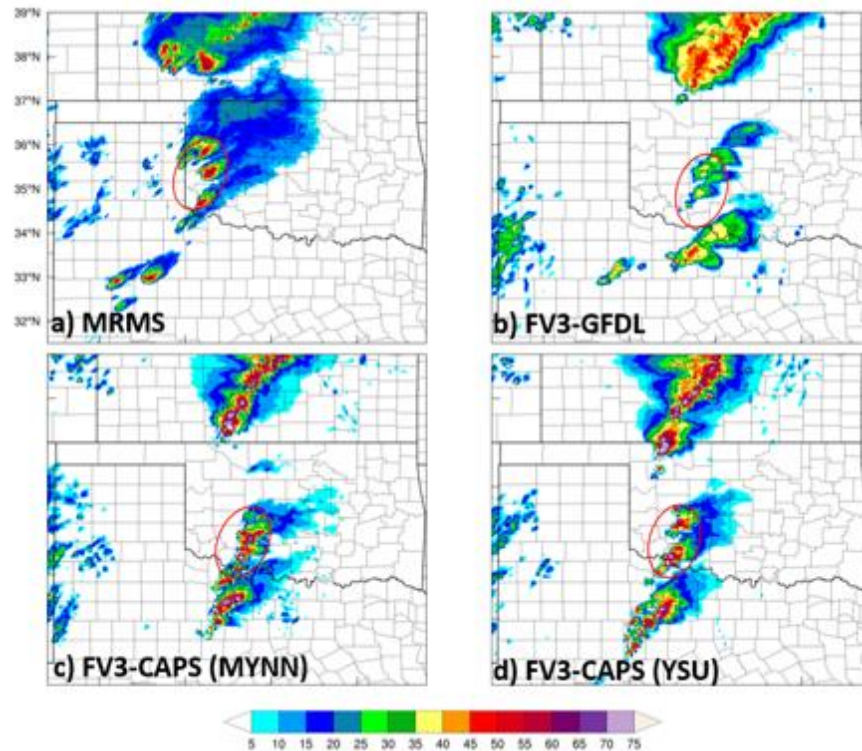
4. Implement a Better PBL Parameterization Scheme into the Next-Generation FV3 Model and Evaluate the Performance of FV3 Model for Convection-Permitting Forecasts related to an Existing Scheme in FV3

The Finite Volume Cubed-Sphere (FV3) dynamical core aims for a unified model for forecasting across all scales and is planned to be operational for global forecasts in 2019. Regional application is planned for future dates at NCEP. The operational Global Forecasting System (GFS) physics suite includes the hybrid eddy diffusivity/mass flux (EDMF) planetary boundary layer (PBL) scheme and GFDL’s single-moment microphysics scheme and has already been coupled with FV3 for global forecasts. However, they are not necessarily suitable for convective-scale prediction. CAPS implemented a number of advanced PBL and microphysics (MP) schemes into FV3, which are more widely used in convective-scale forecasting. The implemented PBL schemes include YSU, Shin and Hong scale-aware YSU, MYJ and MYNN. The MP schemes include the Thompson, NSSL, Milbrandt and Yau (MY), and Morrison schemes. To evaluate the performance of various PBL and MP schemes, two groups of experiments have been carried out for five severe weather cases selected during the 2017 HWT and HMT periods. In the first group, EDMF, YSU, Shin and Hong SA-YSU, MYJ and MYNN PBL schemes are combined with the Thompson MP scheme. In the second group, GFDL, Thompson, NSSL, MY and Morrison MP schemes are coupled with the EDMF PBL scheme. The simulations were conducted with a convection-permitting 3-km grid covering the continental US (CONUS) nested within a global FV3 grid with 13-km grid spacing. The first figure below shows the neighborhood equitable

threat scores (ETS) of hourly precipitation from these experiments. The forecast skill of each scheme varies significantly case to case. The results show that no single PBL or MP scheme clearly outperforms the others in precipitation skill. However, the results are still inconclusive due to the small number of cases. For the 16 May 2017 dryline test case, the second figure below shows that FV3 using YSU and MYNN PBL coupled with Thompson MP produced much better supercell forecasts in terms of structure and intensity than FV3-GFDL using the GFS PBL scheme coupled with GFDL MP. The YSU scheme predicted the best dryline position. During the 2018 HWT SFE, CAPS ran 10 FV3 members with combinations of five PBL (scale-aware MYNN, MYNN, scale-aware YSU, YSU, and EDMF) and two MP (NSSL and Thompson) schemes, which will provide platforms for more systematic evaluation of these schemes.



Time-series of neighborhood ETS (using a 45 km neighborhood radius) for members using different microphysics scheme (left panel) and different PBL scheme (right panel) in FV3 for hourly precipitation exceeding the 99th percentile. The lines are mean values from five selected cases, while the shaded region indicates the ranges of variation. Stage IV precipitation is used as observation.



Composite reflectivity (Z_H ; dBZ) for a) MRMS observations, b) GFDL FV3, and CAPS FV3 using c) YSU and d) MYNN PBL schemes for the 24-hour forecast valid at 0000 UTC 17 May 2017.

Publications

- Kong, R., M. Xue, and C. Liu, 2018: Development of a hybrid en3DVar data assimilation system and comparisons with 3DVar and EnKF for radar data assimilation with observing system simulation experiments. *Monthly Weather Review*, **146**, 175–198.
- Johnson, M., Y. Jung, D. Dawson, T. Supinie, M. Xue, J. Park, and Y.-H. Lee, 2018: Evaluation of unified model microphysics in high-resolution NWP simulations using polarimetric radar observations. *Advances in Atmospheric Science*, **35**, 771–784.
- Supinie, T. A., N. Yussouf, J. Cheng, Y. Jung, M. Xue, and S. Wang, 2017: Comparison of the analyses and forecasts of a tornadic supercell storm from assimilating phased array radar and WSR-88D observations. *Weather and Forecasting*, **32**, 1379–1401.
- Liu, C., M. Xue, and R. Kong, 2018: Direct assimilation of radar reflectivity data using 3DVAR: Treatment of hydrometeor background errors and OSSE tests. *Monthly Weather Review*, conditionally accepted.

CIMMS Task III Project – Impact of Assimilating Polarimetric Phased Array Radar Observations on Convective-scale Numerical Weather Prediction Model for Severe Weather Forecasts

Youngsun Jung, Ming Xue, Bryan Putnam, and Tim Supinie (CAPS), and Nusrat Yussouf and Derek Stratman (CIMMS at NSSL)

NOAA Technical Leads: Kurt Hondl and Mark Weber (NSSL)

NOAA Strategic Goal 2 – Weather Ready Nation: Society is Prepared for and Responds to Weather-Related Events

Funding Type: CIMMS Task III

Objectives

Accurate prediction of rapidly evolving convective weather hazards is critical from both meteorological and public service/societal impact perspectives, but remains a major challenge. Assimilation of radar reflectivity data is a common practice for convection-allowing numerical weather prediction (NWP) model in these days but the model state variables are still significantly under-constrained. Aligned with ongoing efforts to develop a dual polarization phased array radar, this project aims to evaluate the impact of high-temporal polarimetric data on the analysis and short-term probabilistic forecasts of convective hazardous weather.

The main goal of the proposed research is to develop the capability to assimilate polarimetric PAR observations into the operational data assimilation (DA) system and evaluation its impact on the analysis and short-term ensemble forecasts. More specifically, proposed work will consist of three main components: 1) implementation, testing, and optimization of a complex polarimetric radar data forward operator within the Weather Research and Forecasting (WRF) model, 2) development of capabilities to assimilate polarimetric radar observations in the gridpoint statistical interpolation (GSI) based ensemble Kalman filter (EnKF) system, and 3) development and testing of a four-dimensional ensemble data assimilation (4DEnKF) capability within the GSI-EnKF system.

Accomplishments

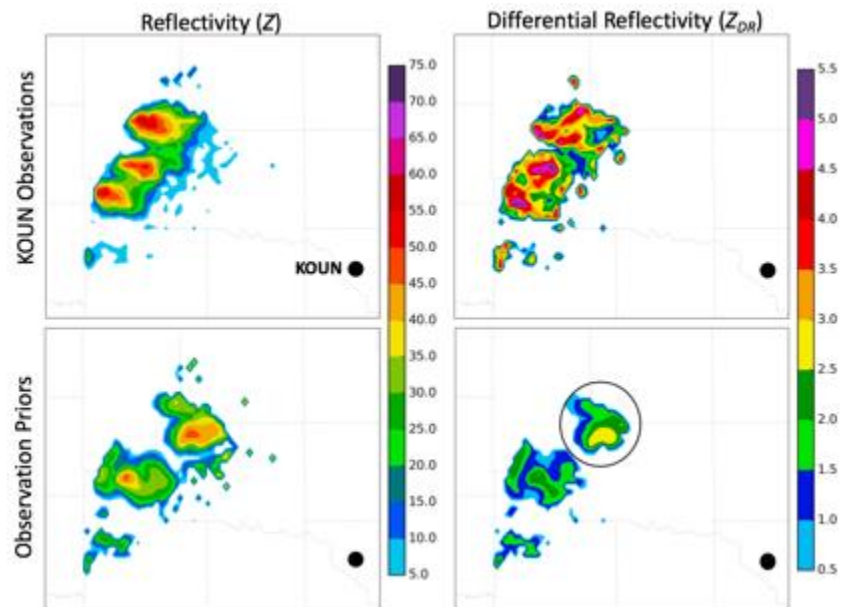
This is collaborative research with “Impact of Assimilating Phased Arrays Radar Observations on Convective-Scale Numerical Weather Prediction Models for Severe Weather Forecasts” lead by Nusrat Yussouf, Pamela Heinzelman, and Louis Wicker at CIMMS and NSSL. The capability to assimilate rapid-scan polarimetric radar observations has been developed in the GSI-based EnKF DA system for future use as the NSSL’s Warn-on-Forecast system. Experimental sector scan observations have been taken for multiple convective storm events at a faster rate than the current national WSR-88D S-band radar network (~ 2 min/volume) using NSSL’s KOUN radar. These observations serve as a proxy for a future rapid-update polarimetric phased array radar (PPAR) observation network. Completed work on this project to date includes case selection (including a background model forecast for initialization), additional quality control on NOUN polarimetric observations, and implementation of the dual-pol forward operator within the GSI-EnKF system.

The 31 May 2013 El Reno tornado and Oklahoma City flash flooding event has been selected for initial testing of the system, and the initial ensemble has been set up. An outer grid with 15-km grid spacing initialized using the National Center for Environmental Information’s Global Ensemble Forecast System (GEFS) serves to provide the initial and boundary conditions for an outer-domain 3-km grid spacing ensemble where conventional non-radar observations (temperature, pressure, etc.) are assimilated. This ensemble is interpolated down to a 401 x 401 km grid with 1-km grid

spacing centered over central Oklahoma. KOUN reflectivity (Z) and differential reflectivity (Z_{DR}) observations are assimilated in experiments following a 45-minute spin-up forecast on this grid. The Warning Decision Support System–Integrated Information algorithms (WDSS-I; Lakshmanan et al. 2007) is used to interpolate the KOUN observations onto a generic Multi-Radar Multi-Sensor (MRMS) system grid (Smith et al. 2016), and to remove non-meteorological echoes (eg., biological returns and ground clutter) and smooth the observations.

The advanced polarimetric observation operators were successfully implemented within the GSI system and observation priors have been produced. These operators include a size dependent water fraction estimation for large rimed ice and the interface to complex multi-moment microphysics schemes, including the NSSL double-moment microphysics scheme. The figure below shows an example of observation priors produced by GSI for Z and Z_{DR} at 2145 UTC 31 May 2013. The top two panels are the Z and Z_{DR} observations on the MRMS grid and the bottom two panels are the observation priors. The updated operators produce reasonable values within the ranges of the Z and Z_{DR} observations. In addition, the Z_{DR} pattern in the northernmost storm in the forecast (identified by the black circle) exhibits larger values of Z_{DR} along the southern portion of the storm, which indicates the size-sorting of raindrops (Kumjian and Ryzhkov 2008).

Fast spread reduction is a major issue with the EnKF system when assimilating dense observations. To mitigate this issue for 4DEnKF, an inter-volume covariance inflation (IVCI) technique has been developed and implemented in the CAPS 4DEnKF system. This procedure runs relaxation to prior spread (RTPS) covariance inflation between the assimilation of each radar volume scan from a high-temporal resolution radar, such as the PAR. Initial tests show that the spread reduction is slower when IVCI is employed.



Reflectivity and differential reflectivity observations (top panels) and calculated observation priors from a 45-minute forecast (bottom panels) valid at 2145 UTC 31 May 2013. The location of KOUN is noted by the black dot.

CIMMS Task III Project – Mobile Radar Operations to Support VORTEX-SE

Michael Biggerstaff, Gordon Carrie, and Addison Alford (OU School of Meteorology), and David Bodine (ARRC)

NOAA Technical Lead: Steven Koch (NSSL)

NOAA Strategic Goal 2 – *Weather-Ready Nation – Society is Prepared for and Responds to Weather-Related Events; and*

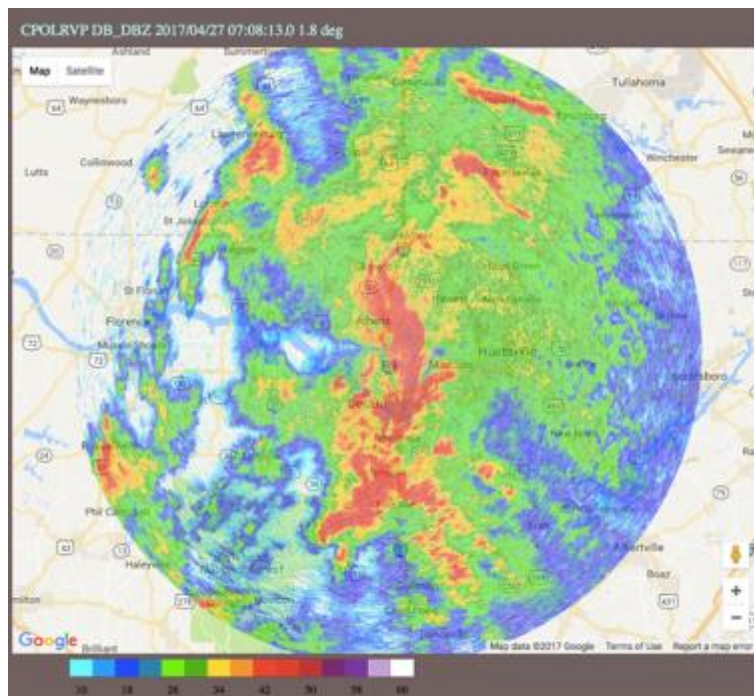
Funding Type: CIMMS Task III

Objectives

Conduct data collection and quality assurance of the Shared Mobile Atmospheric Research and Teaching (SMART) radar and the rapid scanning X-band dual-polarimetric (RaXPOL) radar in support of the VORTEX-SE project. The data were sent to an archive so other VORTEX-SE scientists could conduct analysis.

Accomplishments

The SMART radar (SR) deployed eight times and the RaXPOL deployed four times. More than 50 hours of data were collected with the SR. The data were quality assured to correct time and geolocation of the data. After quality assurance, the data were delivered to the National Center for Atmospheric Research (NCAR) Earth Observing Laboratory (EOL) for archive.



Radar reflectivity from SR2 at 0708 UTC on 27 April 2017 showing hybrid supercell thunderstorms embedded within a mesoscale convective system over northern Alabama.

CIMMS Task III Project – VORTEX-SE Operations Risk Reduction Exercise (ORRE 2018) for Non-Classic Tornadoic Storms and Environmental Heterogeneity

Michael Biggerstaff, Gordon Carrie, Addison Alford, and Kyle Pennington (OU School of Meteorology)

NOAA Technical Lead(s): Steve Koch (NSSL)

NOAA Strategic Goal 2 – *Weather Ready Nation: Society is Prepared for and Responds to Weather-Related Events*

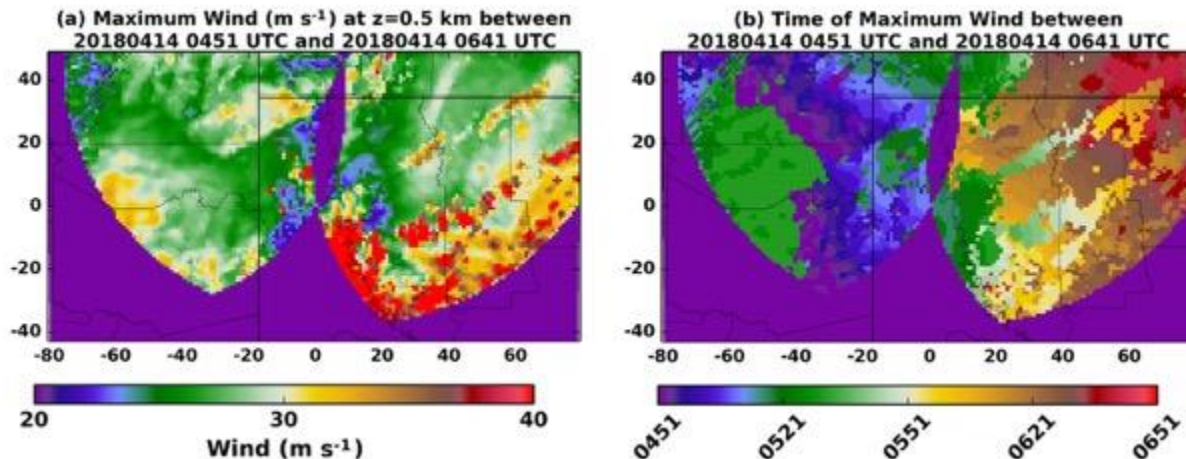
Funding Type: CIMMS Task III (NOAA/NSSL; NOAA Congressional Line Item)

Objectives

The ORRE 2018 objectives fall into three categories: (i) scientific hypothesis refinement, (ii) integrated analysis evaluation, and (iii) platform coordination logistics. In this project, we deployed the two Shared Mobile Atmospheric Research and Teaching (SMART) radars in coordination with the NOAA P-3 aircraft and the University of Louisiana-Monroe S-band dual-polarimetric radar and the observing facilities at the University of Alabama-Huntsville to study non-classic tornadoic storms, particularly quasi-linear convective systems (QLCS) and hybrid supercells embedded within multicell thunderstorm systems in the southeastern USA. The project included data collection, quality assurance, analysis, and archive.

Accomplishments

The two SMART radars (SRs) deployed six times. Five of those deployments resulted in tornado warnings within the observing network, including a QLCS in northern Alabama that produced at least 30 tornadoes and another QLCS near Shreveport that produced more than 20 tornadoes. The SRs and NOAA-P3 collected integrated data on two occasions to evaluate airborne and ground-based platform data integration methods. Analysis for the two high-priority QLCS cases is underway.



(a) Maximum winds at 500 m altitude for the tornadic QLCS observed during 13-14 April 2018 over northern Louisiana derived from dual-Doppler analyses conducted every 2.5 minutes between 0451 and 0641 UTC on 14 April 2018. (b) Time of occurrence of the maximum winds shown in panel (a). Note the vortex tracks are well defined in the max wind plot while the time of occurrence shows that a rear-inflow jet descended later in the period.

CIMMS Task III Project – Three-Dimensional Profiling of the Severe Weather Environment

Phillip Chilson (OU School of Meteorology), Robert Huck (OU College of Engineering), Andrea L’Afflitto (OU Aerospace and Mechanical Engineering), and Jorge Salazar (OU Electrical and Computer Engineering)

NOAA Technical Lead: Steve Koch (NSSL)

NOAA Strategic Goal 2 – Weather Ready Nation: Society is Prepared for and Responds to Weather-Related Events

Funding Type: CIMMS Task III

Objectives

The RFP objective proposed for evaluation was to “evaluate options for UAS profiling of the lower atmosphere with applications for severe weather”. In recent reports from the National Research Council and instrumentation workshops (Dabberdt et al., 2005; NRC, 2009; Hoff, et al. 2012), strong recommendations have been made to develop and evaluate observing systems capable of providing detailed profiles of temperature, moisture, and winds within the atmospheric boundary layer (ABL) to help determine the potential for severe weather development. Unfortunately, these measurements are not very easy to acquire. Satellite observations of the storm environment lack the needed vertical resolution in the ABL and are primarily limited to cloud-free conditions, whereas ground-based remote sensing instruments provide profiles at essentially one location. In this study we have shown that unmanned aircraft systems offer a promising approach to capture the non-homogeneity of the ABL with superb vertical resolution. We have: 1)

developed small UAS (sUAS) capable of acquiring needed wind and thermodynamic profiles and transects of the ABL; 2) adapted and tested miniaturized, high-precision, and fast-response atmospheric sensors for obtaining such measurements; 3) gained experience in collecting atmospheric measurements from a proven fixed-wing aircraft and two alternatives for VTOL (Vertically Take Off and Landing) UAS with sophisticated autopilot systems; and 4) conducted targeted short-duration experiments at the Atmospheric Radiation Measurement (ARM) Southern Great Plains (SGP) site in northern Oklahoma and a second site to be chosen in “real-time” from the Oklahoma Mesonet in coordination with the National Weather Service (NWS)-Norman Forecast Office.

Accomplishments

1. Further Developments of the OU CopterSonde

Since completing the formal portion of the experiment, we have continued to improve upon the OU CopterSonde, which was developed for EPIC. Here we report on a Field Campaign conducted in Finland and some measurements collected at the OU Kessler and Ecological Field Station (KAEFS).

Measurement in Finland

Here we describe the University of Oklahoma’s participation in the ISOBAR (Innovative Strategies for Observations in the Arctic Atmospheric Boundary Layer) program. This is a multi-year research project supported by the Norwegian Research Council aimed at investigating stable arctic boundary layers using unmanned aircraft systems (UAS) in addition to other surface-based instruments. The University of Oklahoma participated in the project the entire month of February by operating weather UAS on the island of Hailuoto, Finland, located at 69 degrees North latitude just off the coast of Oulu. We did not have time to include this information during the February update. The University of Oklahoma was selected to join the experiment based (in part) on account of technical development and operational experience gained during EPIC.

Teams from the University of Bergen (Norway), Finnish Meteorological Institute (Finland), University of Tübingen (Germany), University of Applied Science Ostwestfalen-Lippe (Germany), and the University of Oklahoma combined efforts for a 4-week long campaign. Deployed on the ice was a 10 m tower with sonic anemometers and thermodynamic sensors at multiple levels, as well as an eddy covariance flux station. There were two sodars, one vertically scanning and the other capturing horizontal winds. A Doppler wind lidar was also deployed halfway through the campaign. Participants were allowed to fly to 6500 feet AGL with no restrictions beyond line of sight or based on daylight hours. This allowed for continuous nighttime operations during intensive operations periods, which OU participated in. For more details about the project as a whole, see the ISOBAR blog at <https://isobar2018campaign.w.uib.no/campaign-plan/>.

The University of Oklahoma employed four total UAVs, two fixed-wing and two rotary-wing. For thermodynamic profiling, a new generation of CopterSonde was deployed. These aircraft had a few design differences from one another, notably that one version made use of a ducted fan for sensor aspiration. Further testing is to be done to determine the true benefits of this setup, but preliminary results are very encouraging. On a whole, the University of Oklahoma CopterSondes flew close to 100 total missions, and broke several CASS records: highest altitudes flown (6000 ft), nighttime flights, beyond visual line of sight, coldest temperatures, strongest inversions, just to name a few. See the next section for corresponding data and figures. While one of the CopterSondes did suffer a hard landing, it is still salvageable. The CopterSonde with the ducted fan performed without incident the entire campaign.

In addition to thermodynamic profiling, the University of Oklahoma brought along two Tuffwing fixed-wing models. One was equipped with a specialized camera for photogrammetry missions, and the other equipped with a carbon dioxide gas analyzer. These both flew several missions successfully, however the photogrammetry Tuffwing suffered motor failure mid-flight due to water shorting out one of the magnetic coils. The rest of the aircraft and sensors are in okay condition; it has been determined that the fault was of the manufacturer.

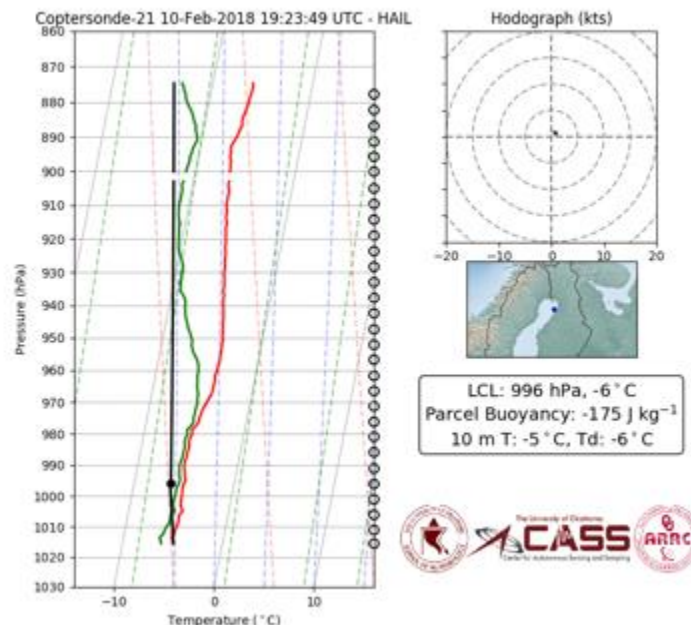


Figure 1: CopterSonde 2.1 sounding from CASS record highest altitude flight to 6000 ft (1800 m) during IOP 2 on 10 February 2018. Note: wind speeds are yet to be calibrated, so wind barbs on this and all figures are not representative.

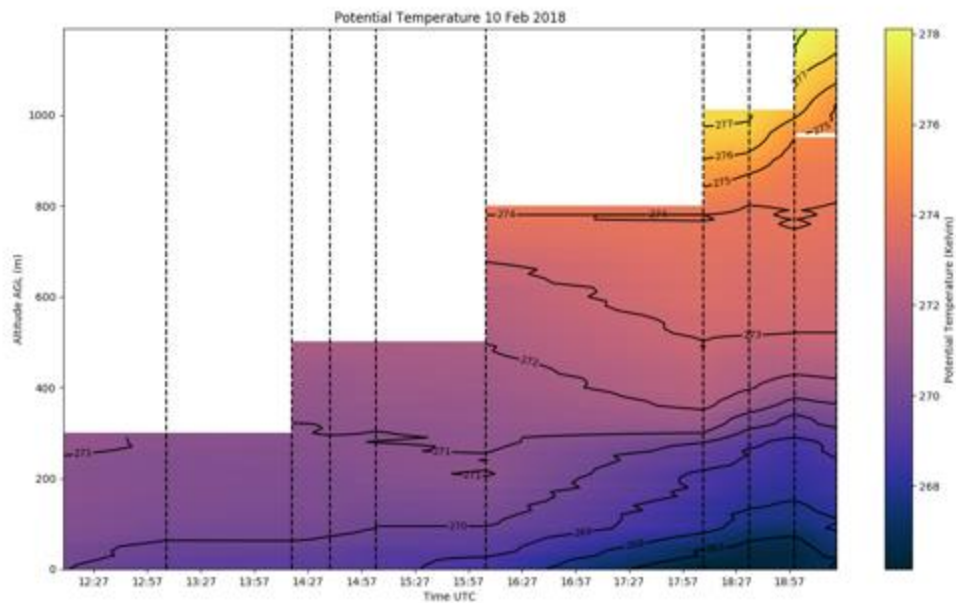


Figure 2: Time-height of potential temperature from IOP2. Hailuoto is situated at UTC+2. Stable boundary layer clearly present after sunset in early afternoon.

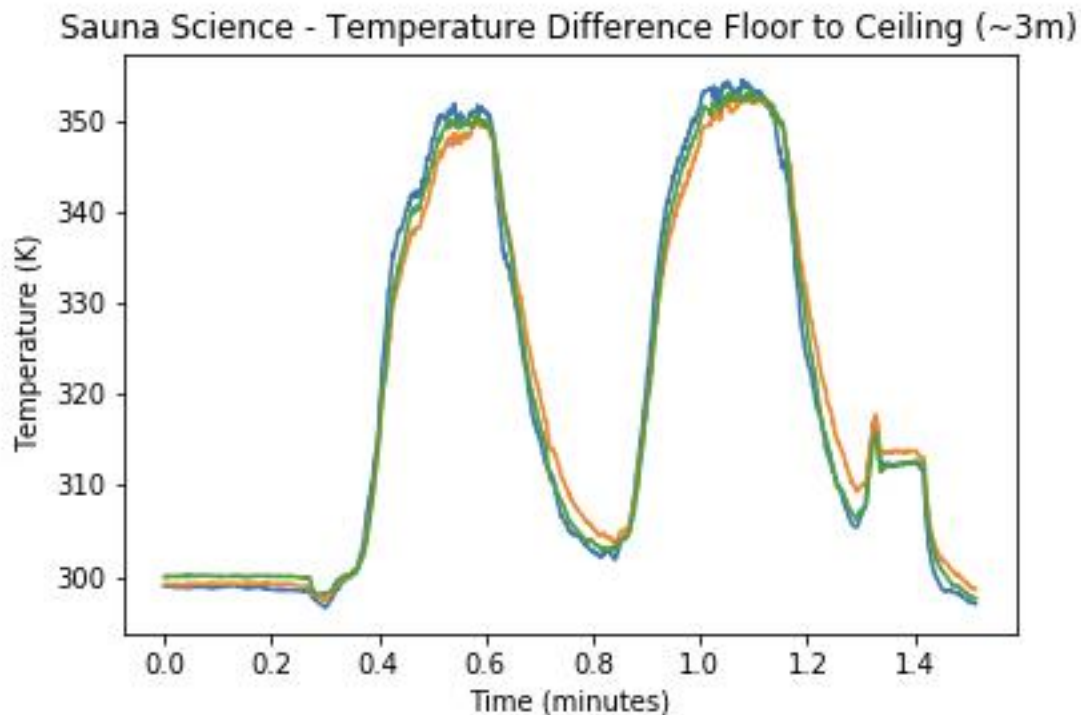


Figure 3: On one of the overlap days for the two OU teams, winds were too strong for safe operations. To make the most of this time, the OU team decided to test sensor response inside of the sauna at our host location. Depicted here is the difference in temperature from the floor to ceiling of the sauna, a height of roughly 3 meters.

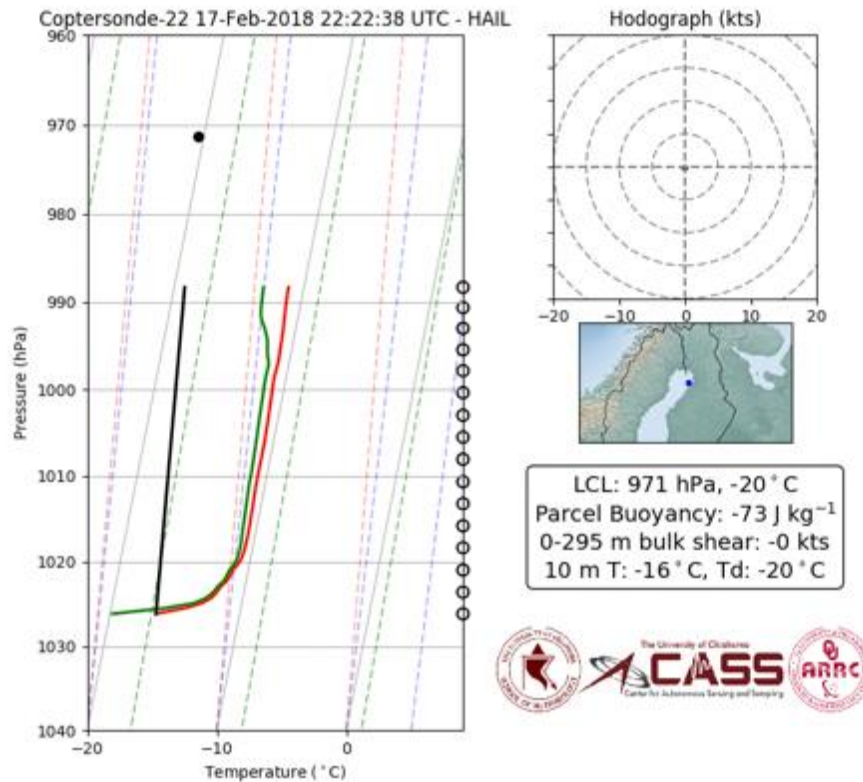


Figure 4: Sounding from IOP3 using CopterSonde 2.2 with the ducted fan. Impressive inversion close to 8 K in just 100 feet.

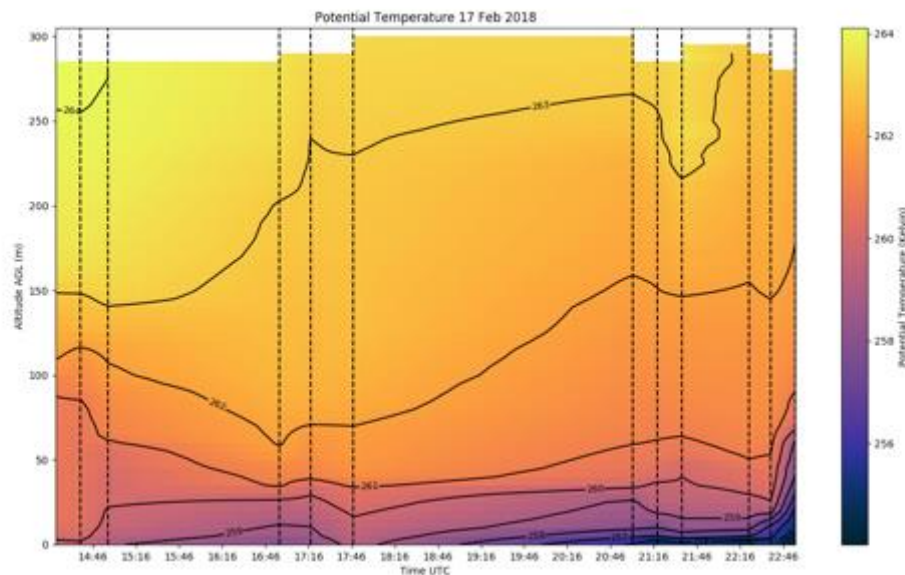


Figure 5: Time-height of potential temperature from IOP3.

2. Measurements at KAEFS

During April 2018, two primary missions were carried out using the OU CopterSonde, both taking place at Kessler Atmospheric and Ecological Field Station in Washington, Oklahoma. On April 5 and 24, sunrise profile flights were conducted to 2500 feet AGL in accordance with a COA, with the primary intention of sampling the morning planetary boundary layer transition. These flights were also in support of a new research objective to determine the feasibility of estimating vertical sensible and latent heat flux profiles using the method outlined in Bonin et al. (2012)

On April 5, a total of seven profiles were flown until an error with the Pixhawk 1 GPS unit made conditions unsafe to continue. While the data collected were of good quality, the environment was mostly cloudy and windy, which violates most of the assumptions used by the algorithm. Time-height cross sections of potential temperature and mixing ratio are included in Figures 1a, b

On April 24, a total of 12 profiles were flown in sunny, warm, calm conditions ideal for flux estimations. The CopterSonde's autopilot had been upgraded to a PixHawk 2.0. These profiles exemplified a textbook boundary layer transition, with a stable layer extending a few hundred meters high and a residual mixed layer atop. By 11 am local time, a well-mixed layer extended the depth of the measurable region (Figures 2a, b). According to previous studies on surface flux measurement observations (e.g., Angevine et al., 2001; Lapworth, 2006), and LES output (e.g., Fedorovich et al., 2004), surface heat fluxes take 2-3 hours after sunrise to increase from negative to positive. Therefore, temperature increases in this time period is largely due to turbulent mixing downwards from the stable layer aloft. Figure 3a, b demonstrate the estimated sensible (latent) heat fluxes shaded over potential temperature (specific humidity). These results are in great agreement with observations in the literature, with negative values of sensible heat fluxes in the early morning and negative values at increasing altitudes in conjunction with the top of the surface inversion layer. Furthermore, sensible heat fluxes at the surface increase in magnitude as the solar radiation increased throughout the morning. Results from latent heat fluxes are subject to an appreciable amount of error since the RH sensors collecting data were several months old with diminished sensitivity

Finally, a paper regarding temperature sensor placement on the OU CopterSonde and submitted to the EGU journal *Atmospheric Measurement Techniques* was accepted for public discussion and is available online at: <https://www.atmos-meas-tech-discuss.net/amt-2018-65/>.

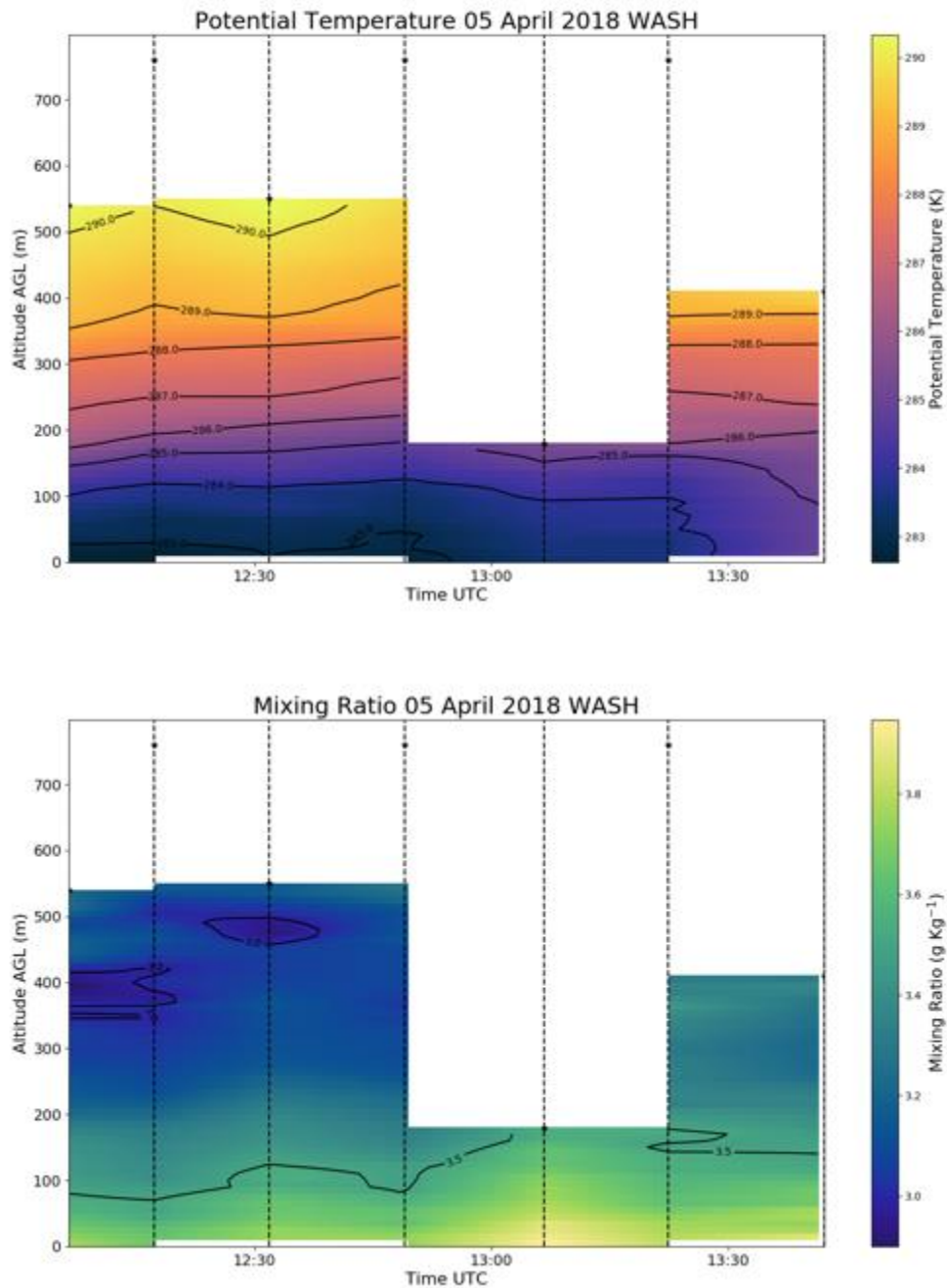


Figure 1: 5 April 2018 flights at KAEFS a) Time-height cross section of potential temperature and b) mixing ratio. Flights were halted early due to GPS errors, but classic features of a PBL transition are still apparent.

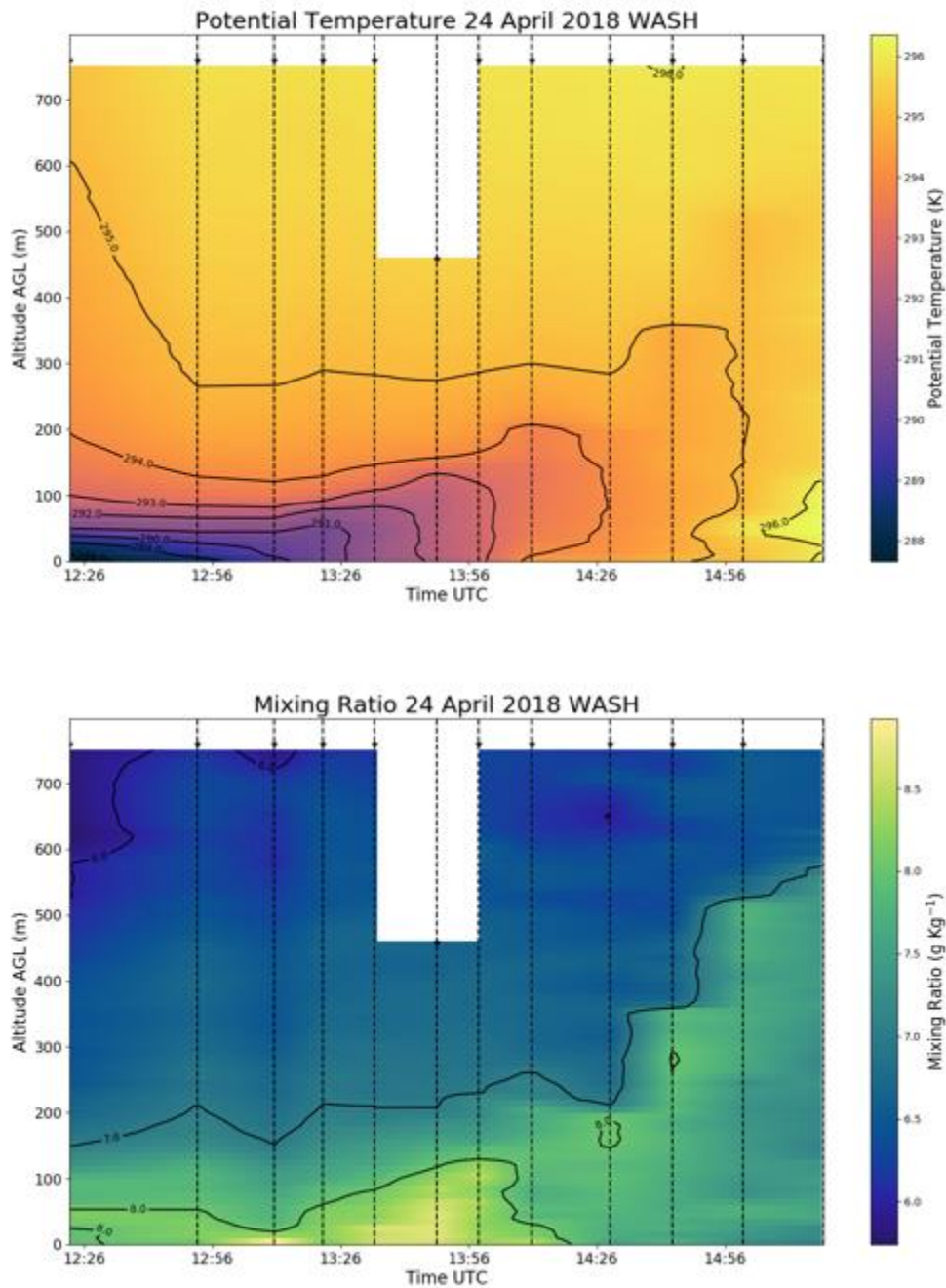


Figure 2: 24 April 2018 flights at KAEFS a) potential temperature and b) mixing ratio. Classic depiction of stable layer in the early morning with residual layer aloft increasing exponentially in time. Well mixed layer extending majority of the profile after 15 UTC.

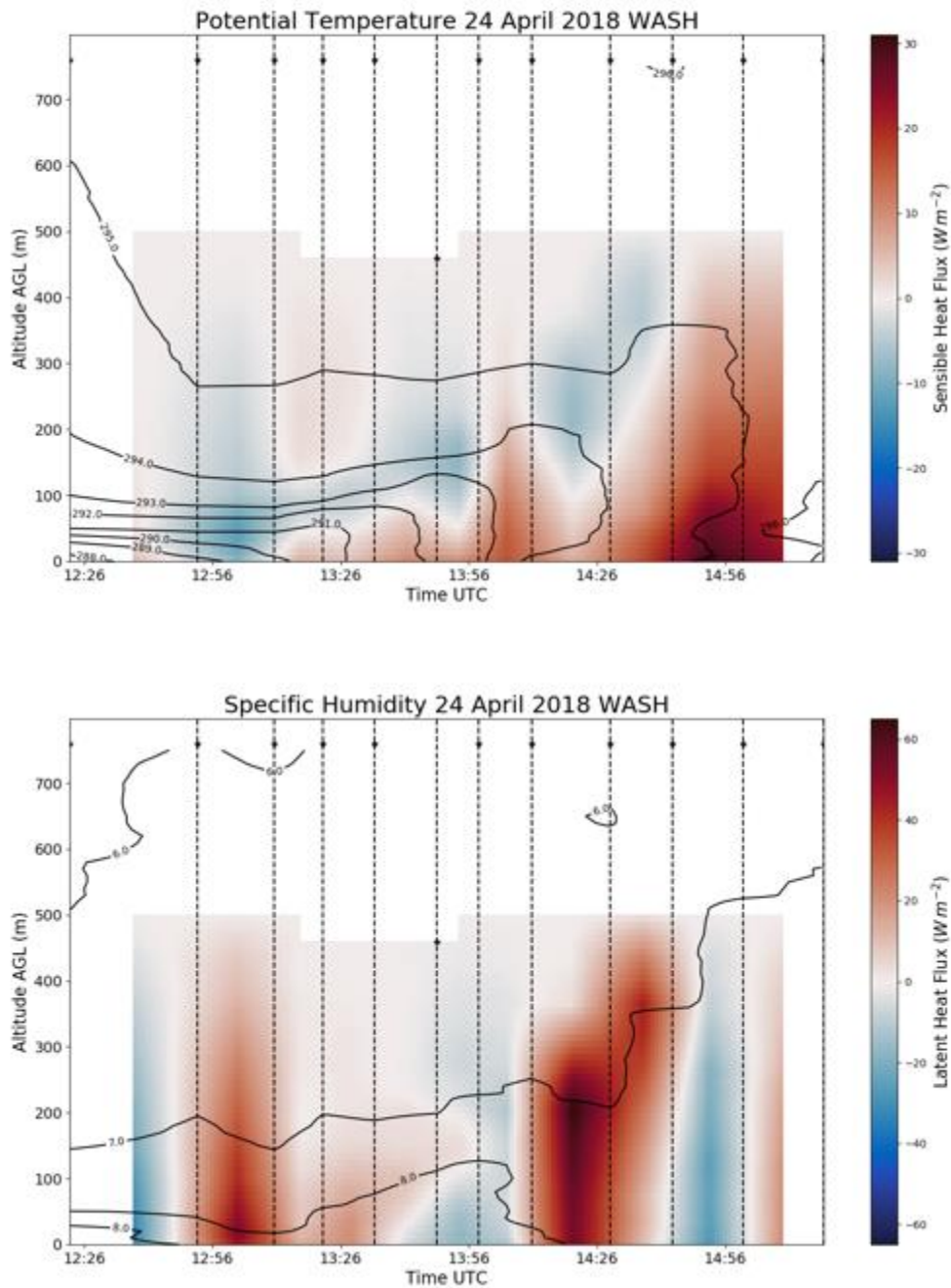


Figure 3: 24 April 2018 a) sensible heat fluxes colored, potential temperature contoured and b) latent heat fluxes colored, specific humidity contoured. Negative values of sensible heat flux indicating entrainment near the inversion height throughout the morning match well with predicted theory. Sensible heat fluxes align decently well with fog and dew evaporation, but are subject to error due to aged RH sensors.

3. Differential GPS Evaluation and Results for NOAA UAS Project

The post-processing kinematics (PPK) performance of the Emlid Reach DGPS unit has been tested in stationary operation (i.e., UAV on the ground), at four different locations behind the RIL, installed on the OU CopterSonde. These four locations were separated approximately 20 m apart and with 900 sample points per set, to determine the precision of the DGPS unit. The following table summarizes the measured standard deviations for the position in the x, y, and z axes, for the Reach DGPS.

Parameter	Single GPS					Reach DGPS (PPK)				
	Set 1	Set 2	Set 3	Set 4	Average	Set 1	Set 2	Set 3	Set 4	Average
σ_x (cm)	64.4	117.8	110.2	90.9	95.83	0.90	2.10	3.20	5.20	2.85
σ_y (cm)	130.4	94.5	118.4	115.6	114.73	2.40	2.70	3.60	7.10	3.95
σ_z (cm)	295.8	244.5	319.0	265.7	281.25	0.70	1.00	0.80	1.50	1.00

An approximate improvement of two orders of magnitude has been achieved when compared to the single GPS position measurements. However, with the Reach module, it was very difficult to obtain the RTK (real-time kinematics) Fixed in flight, for which another DGPS unit was suggested.

With the SwiftNav Piksi DGPS, RTK Fixed mode is more easily and consistently achieved, both on the ground and in flight. Similar ground tests have been conducted at 4 different locations to determine the precision of the Piksi DGPS unit installed on the DJI S900 for the SENSR UAV calibration project. The table below summarizes the measured standard deviations for the position in the x, y, and z axes for the Piksi.

Parameter	Single GPS					Piksi DGPS (RTK)				
	Set 1	Set 2	Set 3	Set 4	Average	Set 1	Set 2	Set 3	Set 4	Average
σ_x (cm)	69.62	59.57	41.37	51.38	55.49	0.72	0.73	0.73	1.24	0.86
σ_y (cm)	81.31	52.03	53.16	47.20	58.43	0.96	0.63	0.76	0.92	0.82
σ_z (cm)	111.93	121.74	118.34	166.57	129.65	1.49	2.11	2.48	3.89	2.49

Again, in stationary mode, the improvements of the DGPS over the single GPS are remarkable. The Piksi DGPS unit even shows an improvement in RTK Fixed over the Reach DGPS in PPK, with the precisions in the x-, and y-axes under 1 cm. The precision in the z-axis is under 3 cm for the second set of tests, whereas for the first set of tests is close to 1 cm. This is presumably due to the lidar being used to aid in altimeter readings in the first set of tests, while the second set of tests might have not been using said device.

Publications

Greene, B. R., A. R. Segales, S. Waugh, S. Duthoit, and P. B. Chilson, 2018: Considerations for temperature sensor placement on rotary-wing unmanned aircraft systems. *Atmospheric Measurement Technology*, Early Online Release, <https://doi.org/10.5194/amt-2018-65>

Koch, S. E., M. Fengler, P. B. Chilson, K. L. Elmore, B. Argrow, D. L. Andra, Jr., and T. Lindley, 2018: Unmanned aircraft sampling of the pre-convective boundary layer. *Journal of Atmospheric and Oceanic Technology*, accepted.

Theme 4 – Impacts of Climate Change Related to Extreme Weather Events

CIMMS Task III Project – The Assimilation, Analysis, and Dissemination of Pacific Rain Gauge Data (PACRAIN)

Scott Greene (OU Department of Geography and Environmental Sustainability), Mark Morrissey (OU Department of Geography and Environmental Sustainability Emeritus), Susan Postawko (OU School of Meteorology Emeritus), and Ethan Cook and Emily Wong (OU Department of Geography and Environmental Sustainability)

NOAA Technical Lead: Howard Diamond (CPO)

NOAA Strategic Goal 1 – *Climate Adaptation and Mitigation: An Informed Society Anticipating and Responding to Climate and its Impacts*

Funding Type: CIMMS Task III

Objectives

Our overall objective is to support the NOAA effort to “build and sustain the global climate observing system that is needed to satisfy the long-term observational requirements of the operational forecast centers, international research programs, and major scientific assessments”. Our current and future efforts include expanding our mission to collect, analyze, verify, and disseminate global rainfall data sets and products deemed useful for Operational Forecast Centers, International Research Programs and individual researchers in their scientific endeavors. The Comprehensive Pacific rainfall Database (PACRAIN) and the Schools of the Pacific Rainfall Climate Experiment (SPaRCE) have built upon work from past NOAA-supported projects to become a database for scientists to obtain scarce rain gauge data and to conduct research into verification and other research activities. These data are continually analyzed to produce error-assessed rainfall products and are easily assessable via our web page (<http://pacrain.ou.edu>). We are also actively involved using PACRAIN data in providing new value added products, investigating the spatial and temporal trends in tropical pacific precipitation, and in assessing the quality of other NOAA OCO supported projects.

Accomplishments

Our major accomplishments this past year have been focused on three main areas. Each of them are discussed below:

1. Gridded Precipitation Project

Our biggest accomplishment for the past year is that we have formally finished and produced a gridded product. To provide an analysis tool for areal rainfall estimates, gridded monthly sea level rainfall estimates have been derived from historical atoll rainfall observations contained in the Pacific Rainfall (PACRAIN) database. The purpose of this product is to produce monthly gridded rainfall estimates for the Tropical

Pacific Ocean with validated standard error estimates, derived solely from in situ low elevation and atoll rainfall measurements, and all of that information is available on our website going back in time until 1930, and updated monthly with the most recent observations. These grids are important in the sense that they are ‘uncontaminated’ by remotely sensed rainfall estimates which are ‘calibrated’ via surface observations. The relatively fine resolution of the PACRAIN grids allows for aggregation and valid comparison to model output and to remotely sensed estimates, both of which are inherently areal-averaged in terms of their statistical properties. These gridded rainfall estimates were generated using statistical and spatial analysis using Kriging, and employ only rainfall observations taken at locations where orographic effects can safely be taken as non-existent (e.g., atoll stations as mentioned above). The results of this work has recently been submitted to the *Journal of Atmospheric and Oceanic Technology*.

2. Analysis of Precipitation Trends in the Equatorial Pacific

As part of the increasing interest of climate change’s effects on rainfall distribution and amounts, this work considers observed changes in tropical Pacific sea level rainfall amounts and their potential response to climate change. Observations were taken from the Comprehensive Pacific Rainfall Database (PACRAIN), using a very strict data selection criteria of >99% data completeness and low-elevation sites only (in order to reflect open ocean rainfall condition) to select observations from 8 stations for the period 1971 to 2017. This study used these data to analyze temporal and spatial rainfall patterns based on several variables – annual rainfall amount and frequency, 95th percentile extreme rainfall events, and length of drought/flooding events. The overall annual trends show a tendency towards reduction in rainfall amounts and frequency across the tropical Pacific Ocean, as well as increases in the length of drought events. This result is consistent with those of previous work. The impact of changes in the Interdecadal Pacific Oscillation’s (IPO’s) phase shift to a negative phase in the late 1990s is also examined. There is some evidence of the impact of the IPO, as well as of the El-Niño Southern Oscillation (ENSO), especially when monthly patterns are analyzed. However, they are less important than the overall large-scale pattern. This is in line with previous research, and provides some evidence that the driving cause of much of the recent observed change in tropical Pacific Ocean are not shifts in the IPO or ENSO, but rather overall climate change, though further work shall be necessary to verify the potential causality. The results of this work has recently been submitted to *Climate Research*.

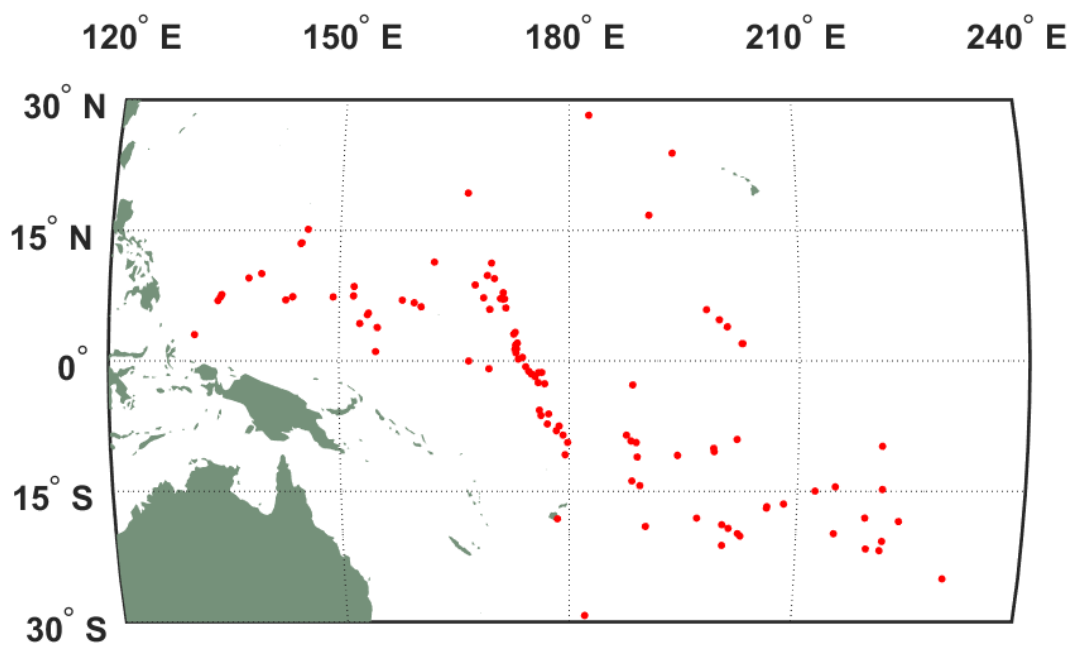
3. Educational Outreach and Capacity Building

Our Pacific educational program, the Schools of the Pacific Rainfall Climate Experiment (SPaRCE; <http://sparce.ou.edu/>) directly enhances the PACRAIN database through the contribution of Pacific schools taking manual read daily rain gauge measurements while learning about the importance of weather and climate. Although the data from SPaRCE schools has not been as strong as it has been in the past, two of our PACRAIN researchers have recently permanently moved out to the Pacific islands, and have been

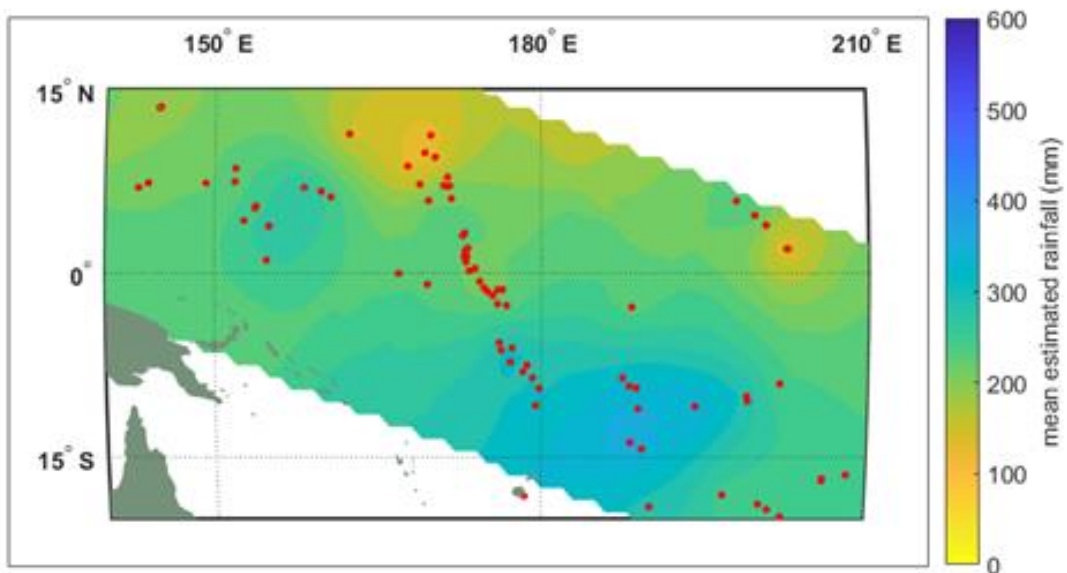
reaching out to expand our SPaRCE collaborations and data. Underlying these projects is the long-term effort to help build the stakeholder outreach capacity of the all the Pacific Islands Meteorological Services (PIMS). We continue to contribute to this effort by providing what we can in terms of needed supplies, education and communication infrastructure and collaboration with PIMS. One recent example of this is that we have developed a partnership with the Cook Islands meteorological service to expand their observing network, and within the last month we have sent to them 30 direct read rain gauges. We will be working with them to collect this data and incorporate into PACRAIN, and to assist them in expanding their observing systems. We are also working with them to involve more of Cook Island schools in the SPaRCE program.

Cook, W. E., and J. S. Greene, 2018: Gridded monthly rainfall estimates derived from historical atoll observations. Submitted to *Journal of Atmospheric and Oceanic Technology*.

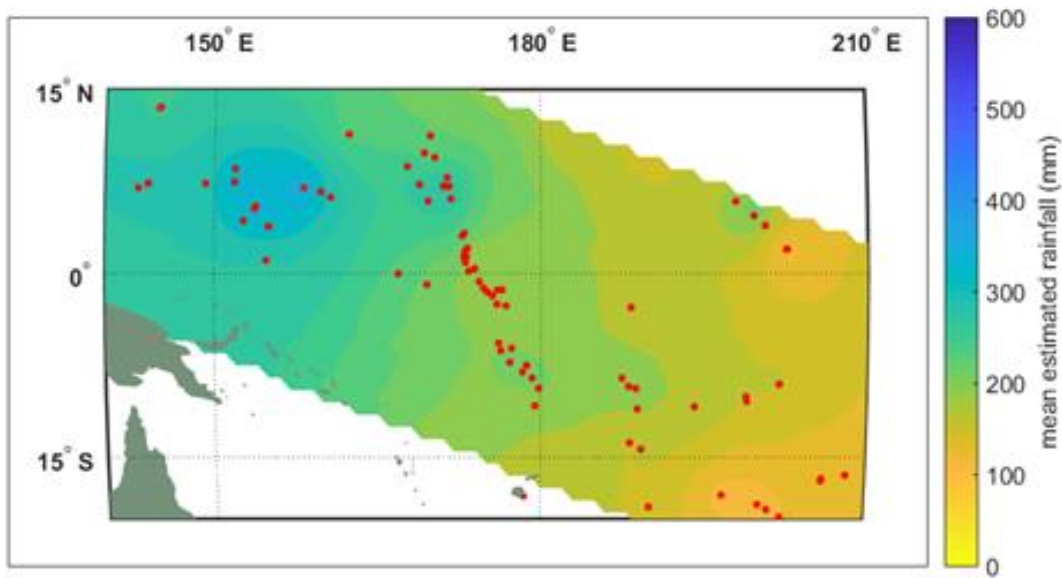
Wimhurst, J. J., and J. S. Greene, 2018: Updated analysis of gauge-based sea level precipitation patterns over the equatorial Pacific Ocean. Submitted to *Climate Research*.



Pacific atoll station locations.

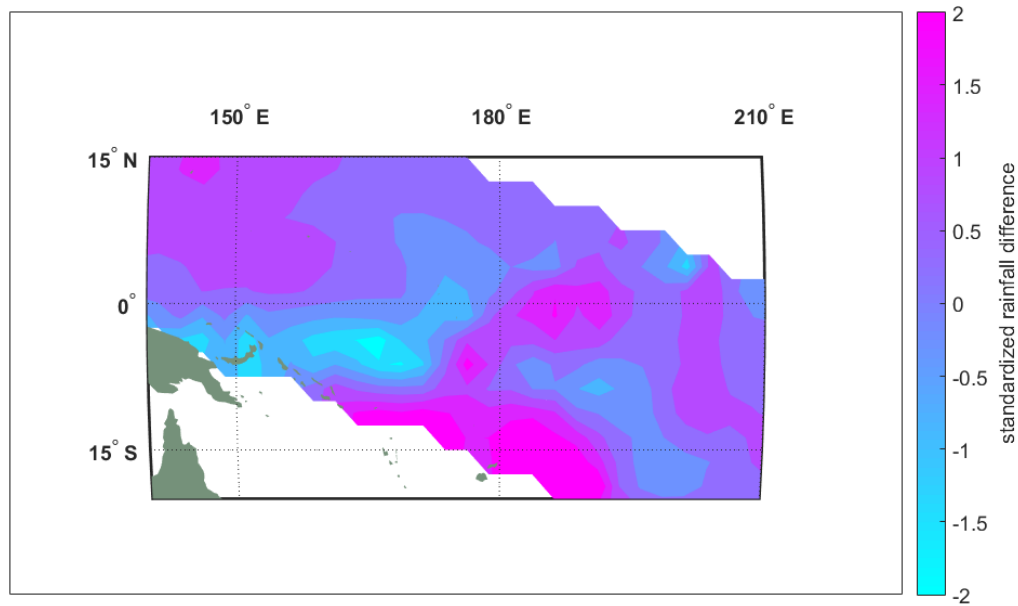


January

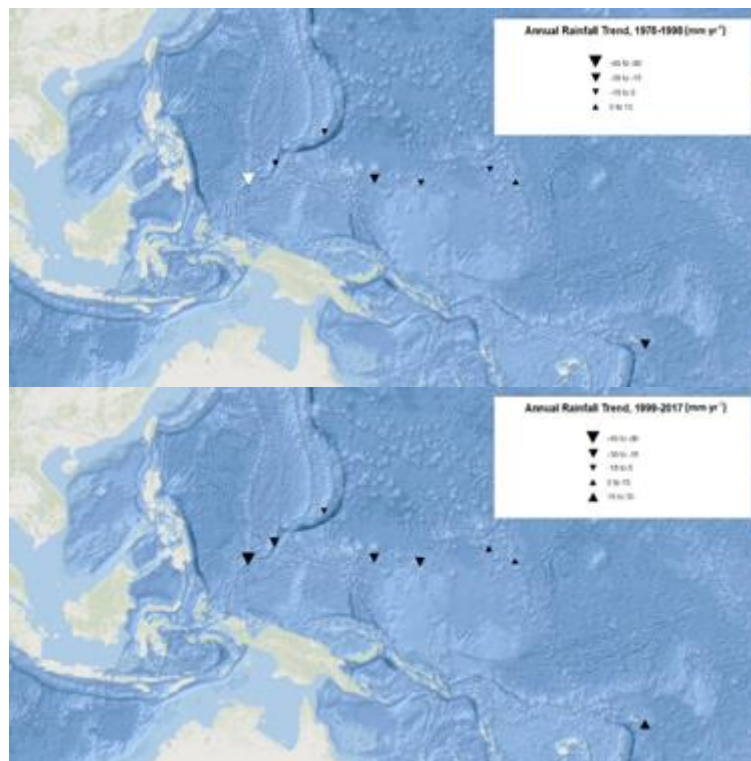


July

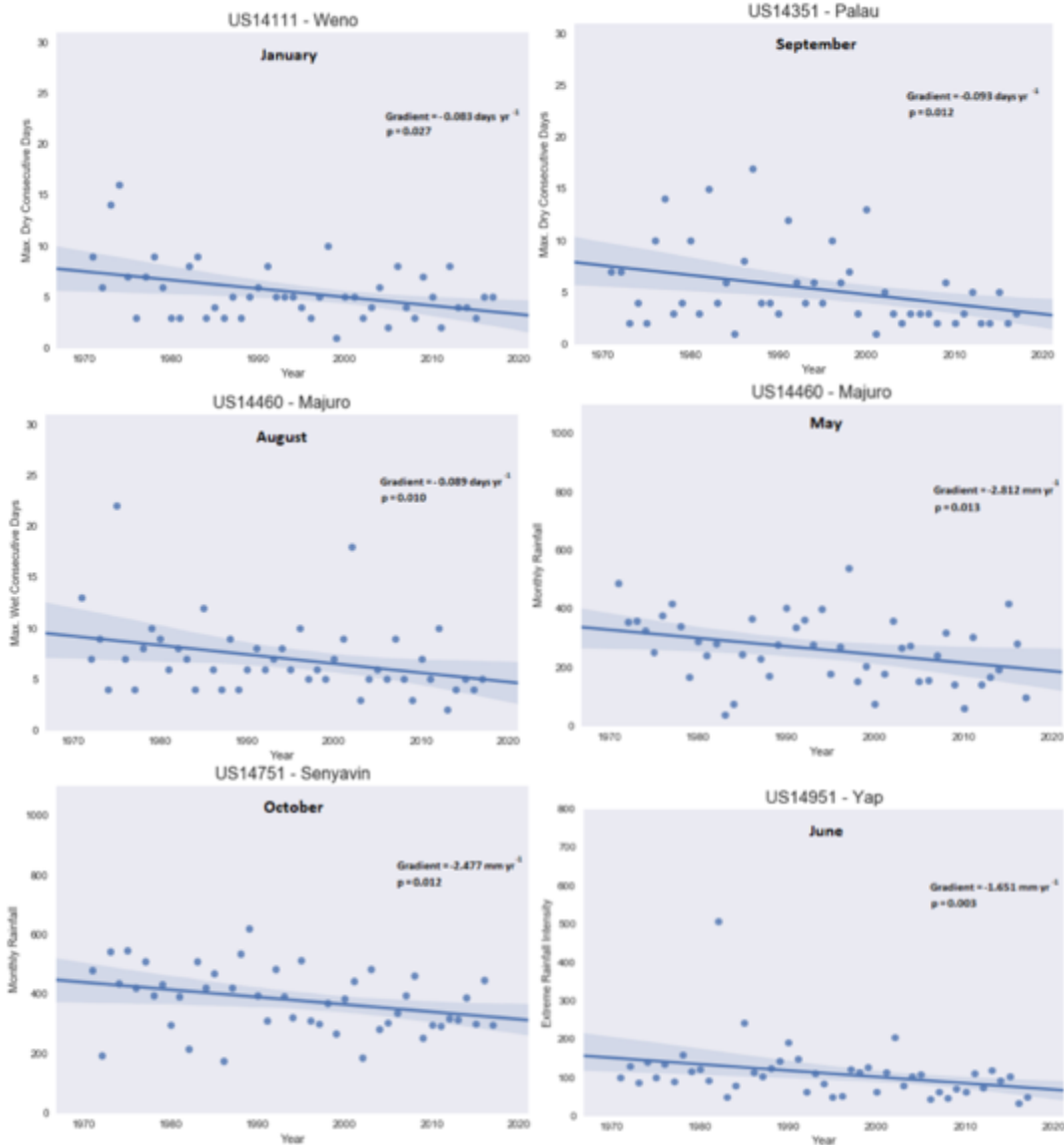
Example Gridded product output: Mean Estimated Rainfall for January and July.



Standardized Rainfall Difference January 1983 [(Atoll – GPCP)/Kriging Std. Err].



Maps showing trends in Annual Rainfall (in mm yr⁻¹) at all stations from 1978-1998 (top) and 1999-2017 (bottom). White triangles indicate trends that are statistically significant at the 90% confidence level ($p < 0.1$).



Scatterplots of statistically significant changes of measurements of tropical Pacific Ocean rainfall trends against the study period 1971-2017 for several select combinations of month, variable, and station. From top left to bottom right, the scatterplots are as follows: Maximum Dry Consecutive Days on Weno in January, Maximum Dry Consecutive Days on Palau in September, Maximum Wet Consecutive Days on Majuro in August, Monthly Rainfall on Majuro in May, Monthly Rainfall on Senyavin in October, Extreme Rainfall Intensity on Yap in June, and Extreme Rainfall Proportion on Yap in June.

Theme 5 – Societal and Socioeconomic Impacts of High Impact Weather Systems

NSSL Project 8 – Warning Process Evolution and Effective Communication to the Public

and

NSSL Project 9 – Evaluating the Impact of New Technologies, Data, and Information in the Operational Forecasting Environment

NOAA Technical Lead: Alan Gerard and Pamela Heinselman (NSSL)

NOAA Strategic Goal 2 – *Weather-Ready Nation: Society is Prepared for and Responds to Weather-Related Events*

Funding Type: CIMMS Task II

Overall Objectives

Studies that are both developing and exploring the integration and use of new information – such as probabilistic hazard information and warn-on-forecast guidance – that are expected to enhance the duties of operational partners.

Accomplishments

1. Probabilistic Hazard Information for the Aviation Sector

Heather Reeves (CIMMS at NSSL)

This project is to create probabilistic hazard information for convective sigmets. This is a new project that will eventually use the NEWS-e forecasts to provide 0–8 hr guidance on the probability of convective sigmet criteria being reached. As a start, the MRMS Vertically-Integrated Liquid (VIL) is used to generate automated convective sigmets. Convective sigmets have certain criteria ($VIL \geq 6.4 \text{ kg m}^2$ covering at least 40% of an area that is 3000 mi^2) that can be detected using artificial intelligence (AI). However, our early attempts at using AI indicate that true sigmet conditions are almost never met. This is demonstrated in Fig. 1. The polygon indicates a region where the minimum VIL has been met and that is 3000 mi^2 . As is obvious, the minimum VIL threshold does not occupy 40% or more of the polygon. However, the NOAA Aviation Weather Center (AWC) did have a sigmet issued for this convective line. Moreover, the cell at the southern end of the line produced large hail that resulted in significant damage to an American Airlines A320 Airbus, necessitating an emergency landing at El Paso. The CIMMS PI is currently collaborating with AWC personnel to calibrate MRMS VIL to better fit the human-generated sigmets. These will then be applied to NEWS-e and HRRR-e forecasts to assess the usability of probabilistic sigmet forecasts.

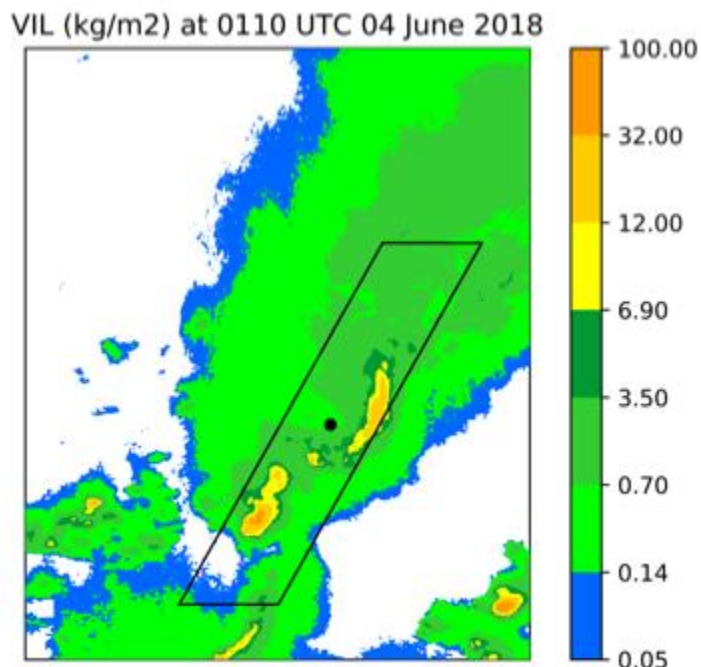


Figure 1: The MRMS Vertically-Integrated Liquid Water valid at 0110 UTC 4 June 2018 and a hypothetical sigmet that is 3000 m² in area.

2. Experimental Use of NEWS-e in Operations

Katie Wilson and Patrick Skinner (CIMMS at NSSL), Pam Heinselman (NSSL), Nusrat Yussouf, Kent Knopfmeier, and Jessica Choate (CIMMS at NSSL), Todd Lindley (NWS Norman), Kristopher Sanders and Ariel Cohen (NWS Topeka), Andrew Orrison (MetWatch WPC), and Michael Eckert (FAA ATCSCC)

Members of the Warn-on-Forecast team have collaborated with two local NWS forecast offices (Norman and Topeka) and the MetWatch Desk at the Weather Prediction Center (WPC) to explore experimental use of the NSSL Experimental Warn-on-Forecast System for ensembles (NEWS-e) forecast guidance during operations. The purpose of this work was to obtain early feedback on the strengths, limitations, and applications of 0–6 hour storm-scale probabilistic forecast guidance. This feedback will be used to guide the development of this prototype system so that it is most useful to operational meteorologists. Our interactions with each of these three entities varied, including the type of feedback obtained. Informal feedback (via telephone and email) was gathered from the Topeka WFO following their use of NEWS-e during several severe weather days. Our co-location with the Norman WFO allowed for in-person debriefs, emails, and occasional observation. In particular, Norman WFO's use of NEWS-e on 2 May 2018 has led to an interesting case study, in which NEWS-e output was directly used to create products with greater timing and location specificity that was shared with the public (Fig. 2). This guidance also proved especially useful in the issuance of a flash flood advisory and subsequent flash flood warning. Findings from the feedback and observations gathered on this day will be shared at the 2018 annual NWA meeting. In

addition to working with local forecast offices, our interactions with WPC for FY18 began in the early spring. Since MetWatch forecasters were planning to use NEWS-e experimentally during May–July, Katie and Pam visited WPC to learn about their workflow, understand the potential applications of NEWS-e within their operational objectives, and provide MetWatch forecasters with an educational overview of Warn-on-Forecast and the NEWS-e website. These in-person interactions also resulted in the creation of an online survey tool that enabled MetWatch forecasters to provide routine and structured feedback following their use of NEWS-e. This survey was completed on 25 occasions, and the feedback will be analyzed in the coming months. Finally, impromptu experimental use of NEWS-e to support decision support services at the FAA Command Center (Warrenton, VA) on 10 May 2018 was reported. This user group identified the usefulness of the frequent 30-min NEWS-e updates for adjusting the timing of thunderstorm impacts for major airports, as well as particular aspects of the forecast guidance that could be improved. Real time running of NEWS-e will begin again in spring 2019, and we are planning to grow and expand our collaboration with the Norman and Topeka WFOs, WPC, and other operational end-users, such as the FAA, who may also benefit from this forecast guidance.



Figure 2. Research observations and scientific support for experimental use of NEWS-e at Norman WFO on 2 May 2018.

3. Correcting, Improving, and Verifying Automated ProbSevere Guidance

David Harrison (CIMMS at NSSL and OU School of Meteorology), Amy McGovern (OU Department of Computer Science), and Chris Karstens (SPC)

The NOAA/CIMSS ProbSevere model's storm identification and tracking algorithms have been implemented as first-guess guidance in the prototype Probabilistic Hazards Information (PHI) warning software to help forecasters better issue and maintain continuously updating severe weather information. During the 2015 and 2016 PHI prototype experiments performed at the NOAA Hazardous Weather Testbed (HWT), participating forecasters noted a number of potential improvements that could be made to the automated guidance in order to better achieve forecaster goals. Three primary areas of improvement were addressed during the evaluation period.

First, forecasters and researchers observed that the automated system frequently lost tracking on identified storms. After further investigation, it was discovered that ProbSevere would often change the unique tracking identification numbers of storm objects when the associated storm underwent a meteorological evolution such as a split or merger. In addition, ProbSevere would occasionally change the identification number of an object with no notable changes in the associated storm. To correct these breakages, a new algorithm, known as Best Track: Real Time, was developed to identify and repair instances when an object's identification number improperly changes. This algorithm was added to the PHI prototype software, and forecasters have noted improved results in subsequent experiments.

The second point of improvement was to perform a detailed analysis of the conditional performance characteristics of the ProbSevere storm identification and tracking algorithms in order to improve forecaster trust of the guidance. A combination of traditional and new verification techniques were utilized to produce these performance characteristics for both automated PHI products and operational storm-based warnings issued during the same time period. Results from this study indicate that forecasters would be able to achieve similar performance metrics using the automated ProbSevere guidance and PHI products as they do with storm-based warnings today. These results were shown to forecasters in subsequent experiments, and increased use of the automated guidance was noted.

Finally, forecasters had noted the need for guidance to help them predict how a storm's probability of producing severe weather would change over time. A machine learning algorithm was developed to predict storm-scale severe weather trends, and the resulting model was implemented in the PHI prototype system (Fig. 1). Results from subsequent experiments indicate that forecasters frequently utilized the new guidance and were able to add value to the automated forecasts.

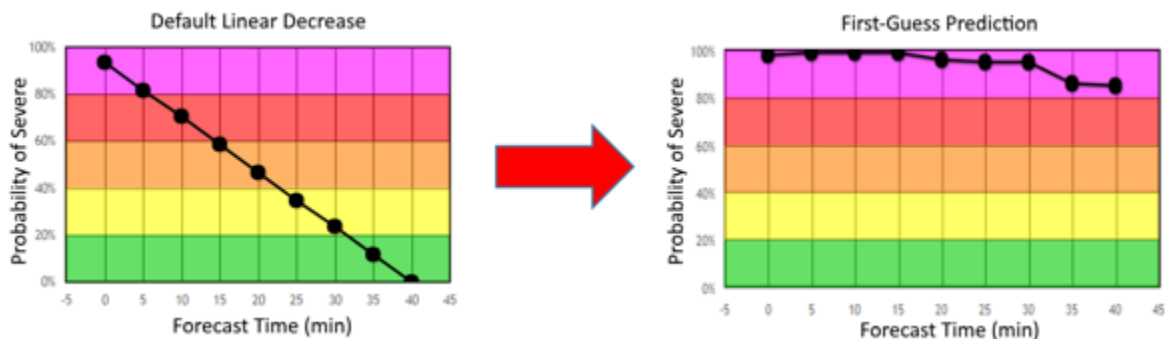


Figure 3. Example showing the difference between the default linear decrease probability trend provided to forecasters in 2016 (left), and the machine learning probability trend predictions provided in 2017 and 2018 (right).

4. Probabilistic Hazard Information Experiments with End Users

Kodi Berry and Kim Klockow McClain (CIMMS at NSSL), Holly Obermeier (CIMMS at NSSL and CIRES – Boulder, CO), and Tiffany Meyer, Adrian Campbell, and Makenzie Krocak (CIMMS at NSSL)

The 2018 Probabilistic Hazard Information (PHI) Emergency Manager and Broadcaster experiments took place over five weeks in May and June 2018. CIMMS research scientists designed and executed both of the end-user experiments. The PHI experiments allow these researchers to test how a continuous flow of probabilistic information may impact end users and their decision making. During the 2018 PHI experiments, emergency managers and broadcast meteorologists performed typical job functions under a simulated work environment as they received National Weather Service warnings and experimental PHI (tornado, wind/hail and lightning) during displaced realtime events. The displaced realtime events were designed to test the strengths and limitations of the PHI system for communicating multiple-hazard threats from a variety of storm types and geographies. CIMMS researchers recruited and selected participants through a nationwide search based on jurisdiction (e.g., hospital, city, county, state), designated market area, years of experience, and geographic location (e.g., southeast, northeast, plains). An emphasis was placed on broader representation this year as compared to previous years to better capture the full array of end-user environments and experiences.

During the 2018 PHI Emergency Manager experiment, four emergency managers per week worked together under a simulated emergency operations center environment with an experimental version of the Enhanced Data Display, GR2Analyst, NWSChat, and location and activity assignments. Increasing the variety of EM perspectives and geographies revealed that PHI was particularly useful for EMs on more marginal severe weather days. Emergency managers appreciated having guidance of any kind for airmass thunderstorm-type convection and for areas where radar coverage is traditionally poor. Generally, participants reported that the presence of PHI increased their confidence in responding to warnings and improved their calibration to the threats

facing their jurisdictions. Many EM decisions happen ahead of the warning scale, and PHI add a significant benefit where little information currently exists. While they wanted PHI to update as frequently as possible (2 min in the experiment), they noted that during real-world operations, they would not be able to monitor PHI evolution as closely as they did during the experiment.

During the 2018 PHI Broadcaster experiment, two broadcast meteorologists per week functioned under a simulated television studio environment with a chroma key wall, camera, lighting and lapel microphones. Participants used an experimental version of the Enhanced Data Display, GR2Analyst, NWSChat, television programming schedule, and protected Facebook and Twitter accounts to create and communicate coverage of hazardous weather. Decision points of interest for broadcast meteorologists included when to run crawls, post to social media, interrupt commercials, and interrupt programming. CIMMS researchers designed the experiment to concentrate on communication challenges and decision points of interest, but also investigate the interplay between the PHI plume and the traditional warning polygon. This investigation allowed researchers to better understand whether the PHI plume and warning polygon should be intrinsically connected. Preliminary results indicate the continued need for a warning threshold or trigger, however, participants strongly desired the inclusion of probabilistic information in tandem with the warning polygon. In addition, participants expressed more confidence in their television coverage decisions with the use of PHI because it contained additional forecast information not available from traditional warnings.

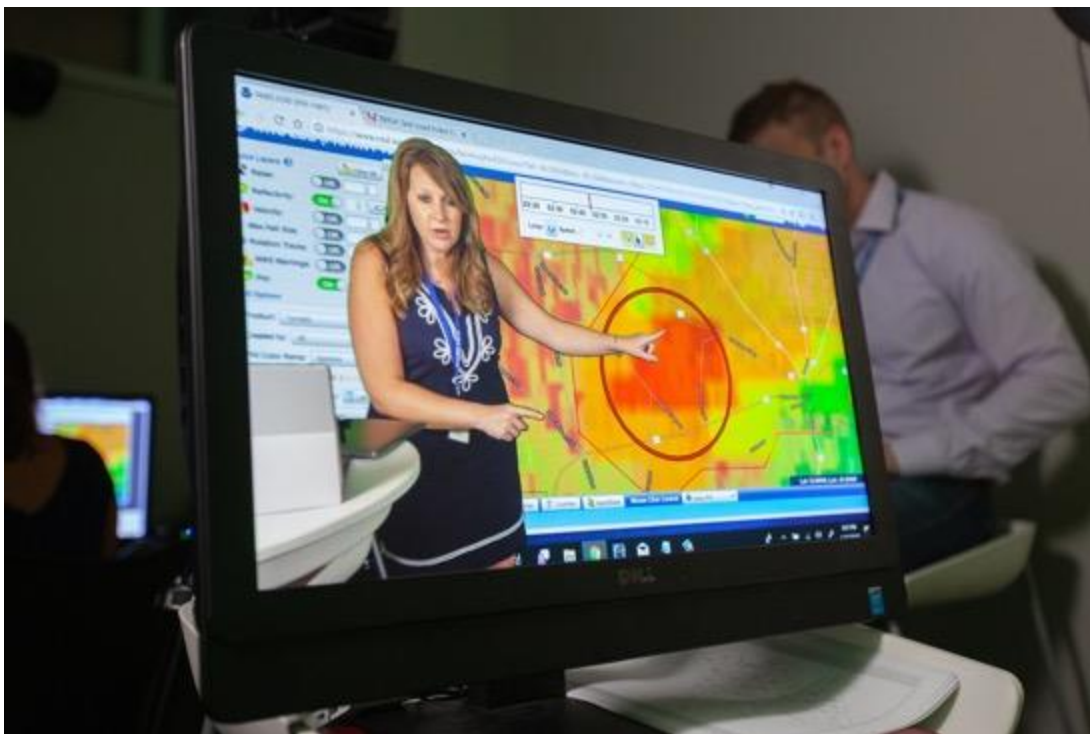


Figure 4. Participant utilizing probabilistic products in a simulated broadcast during a displaced real time case of the 2018 PHI experiment.

5. Visualization and Communication of Probabilistic Lightning Hazard Information for a Broad Spectrum of End Users

Tiffany Meyer, Kim Klockow McClain, Kodi Berry, Kristin Calhoun, and Holly Obermeier (CIMMS at NSSL), Nick Nausler (SPC), and the Grand Junction, CO NWS Forecast Office

Currently, the National Weather Service (NWS) does not provide a product specifically for lightning threats. Because a lightning specific product does not currently exist, it can be difficult for end users such as emergency managers, park rangers, fire personnel, and others to obtain cloud-to-ground (CG) lightning data. NWS forecasters are often asked by these end users to provide decision support services for lightning, indicating a need for specific guidance. At CIMMS/NSSL, a new multi-radar multi-sensor cloud to ground (CG) lightning probability guidance was created and trained using a random forest machine learning algorithm in 2016. As part of the Probabilistic Hazard Information (PHI) Prototype experiment in Hazardous Weather Testbed(HWT), an integrated warning team simulated a real-world environment in which forecasters issued PHI and end-users received the output. Forecasters were given automated lightning PHI guidance, which they had the option to modify and/or add a discussion. Upon issuance, emergency managers and broadcast meteorologists received lightning PHI using a web based program called the Enhanced Data Display (EDD). End-users utilized lightning PHI to perform their typical job duties. It is critical that a lightning product can be communicated in an effective manner. The feedback received over the past several years from forecasters and end users in the HWT showed a strong desire for CG lightning hazard information, however the current lightning objects, plumes, and probabilities were often confusing in meaning and appearance. Based on this feedback a proposal was submitted and funded by NSSL DRRF to explore formal focus groups and surveys aimed at end-users.

Three focus groups occurred at NWA in 2017 between CIMMS researchers and broadcast meteorologists. The broadcasters were asked a few questions about how they use lightning in their current job, ie. where they typically received their lightning information, how do they communicate lightning. They usually got their current lightning information from the private sector (Weatherbug, WSI, Baron) and it was highly dependent on geography, time of year, events, outdoor venues, etc. on how they communicated lightning to the public. Generally, they would never cut into TV programming for the threat of lightning, but they would post about it on social media. Next they were shown some examples of plumes with different color schemes, shading, and labeling (see attached figures 1 and 2). Their general preference was for a monotonic color scheme so the plume stood out from the radar reflectivity, but they had reservations on showing the plumes on air to the public. If they did, they chose to show a qualitative (Med-Low) threat vs a numeric (20%) threat.

After a few months of planning with the National Weather Service - Grand Junction Office, a 1-day Lightning Integrated Warning Team Workshop was held in April of 2018. Attendance included 18 coordinating personnel (CIMMS and NWS) and 34 end users

(Ski Patrol, Fire Protection/Department, County/City/State Emergency Management, National/State Parks, City Parks and Rec, Bureau of Land Management, US Forest Service). The morning was focused on giving the end users different uses/examples of lightning data, current NOAA/CIMMS related lightning research projects and both a public safety/outdoor and fire management panel. In the afternoon, the end users were broken out into focus groups and asked the same set of questions the broadcasters were asked at NWA. Unlike the broadcasters, the end users typically didn't have a way to get lightning data currently, so they would rely on their eyes/ears. Their main concerns were relying on information via cell phones because of the spotty coverage out west and the limitations of money for private phone apps or web services. Originally when viewing the plumes, they liked the rainbow color scheme because it highlighted the threats better (ex. red is bad). However, once they saw that overlaid with radar or other threats, they preferred a monotonic color scheme.

By sharing this feedback with Adrian Campbell and Jonathan Wolfe prior to the 2018 PHI Experiment, they were then able to make modifications to the PHI Tool and EDD. (see more on how this was incorporated in NSSL Project 5, accomplishment #9).

Publications

Karstens, C. D., J. Correia, D. S. LaDue, J. Wolfe, T. C. Meyer, D. R. Harrison, J. L. Cintineo, K. M. Calhoun, T. M. Smith, A. E. Gerard, and L. P. Rothfusz, 2018: Development of a human-machine mix for forecasting severe convective events. *Weather and Forecasting*, 33, 715–737.

Awards

13th *Symposium on Societal Applications: Policy, Research, and Practice* 1st Place Overall Presentation awarded for the following presentation: Harrison, D., C. D. Karstens, and A. McGovern 2018: Using Machine Learning Techniques to Predict Near-Term Severe Weather Trends. 98th *Annual Meeting*, Austin, TX, Amer. Meteor. Soc., 11.6. – **David Harrison**

CIMMS Task III Project – Development of a Digital Collaboration Environment for The Alliance for Integrative Approaches to Extreme Environmental Events, Phase I: Scoping and Functional Requirements Development

Kelvin K. Droegemeier (OU School of Meteorology) and Kim Klockow McClain (CIMMS at NSSL)

NOAA Strategic Goal 2 – *Weather Ready Nation: Society is Prepared for and Responds to Weather-Related Events*

Funding Type: CIMMS Task III

Objectives

The *Alliance for Integrative Approaches to Extreme Environmental Events* (or more simply, the Alliance), is an informal public-private partnership comprising researchers from social, behavioral and economic science (SBES) disciplines, engineers, mathematicians and technologists, research and operational meteorologists, emergency managers, and other strategic partners including Federal agencies, non-profit organizations, philanthropists, entrepreneurs, and the private sector. Funded initially by

a \$3 million private gift, which is a seed planted with the intent of catalyzing long-term funding from many other sources in a true multi-sector partnership, *the goal of the Alliance is twofold: first, to help members of the broad community overcome obstacles to meaningful interaction so that progress can be made on challenges holistically, and collaboratively, in their full complexity utilizing all resources available; and second, to facilitate interdisciplinary research, and the associated transition of research outcomes to practice – including rapid technology prototyping and insertion – in ways that advance the Nation’s agenda to substantially reduce societal harm from extreme environmental events.*

In support of these goals, the current project represents the first phase of developing the Alliance (Digital) Collaboration Environment (ACE). As noted above, and in light of the Alliance’s key goal of building, and facilitating dynamic, sustained interaction among, a broad community of scholars, ACE plays a foundational role in all aspects of the Alliance’s mission. This includes but is not limited to:

- a) Identifying and connecting people working in traditionally distinct disciplines and sectors in risk communication, physical science, technology, social and behavioral science, and disaster science as a means for creating and growing interdisciplinary collaborative teams;
- b) Serving as a portal for the exchange of research insights, research questions, funding opportunities, and relevant collaboration material; and
- c) Serving as a foundation to be used in furthering Alliance collaborations among individuals having shared interests or synergistic capabilities.

ACE is being crafted as a state-of-the-art framework that is both extensible and makes maximum use of existing and planned resources within the community. Additionally, it is being constructed in phases to maximize effectiveness in design and promote community engagement in its development. Finally, the Alliance will work with experts in library and information sciences, data science, and the corporate sector to develop an innovative approach to ACE that spans all relevant Alliance disciplines and sectors.

The specific phases of ACE are as follows:

- **Phase I: Scoping and Functional Requirements Development (12 months)** – which is the CURRENT PROJECT.
- **Phase II: Framework Creation (18 months, beginning in month 6 of Phase I).**
- **Phase III: Prototype Testing (12 months, beginning in month 6 of Phase II).**
- **Phase IV: Deployment (beginning at month 24).**

Accomplishments

Goal 1 - Establishing Functional Design Requirements for ACE: For the Alliance Phase 1, the goal was to establish design requirements and user preferences for the online digital platform ACE. Web-based surveys were conducted with the potential

Alliance user community and two subsequent, in-person focus group sessions were held based on the list of participants that was finalized after meetings with co-PI.

Three Key Obstacles: Focus group discussions revealed three main categories of obstacles and common barriers that inhibit Interdisciplinary Research (IR). Across both focus group sessions, participants specifically expressed strong and similar concerns regarding (1) communication issues (e.g., lack of common language, technical jargon, miscommunication), (2) disagreements and lack of familiarity about methodology and common disciplinary standards/goals, and (3) lack of sufficient time to address or evaluate communication and methodology issues.

Essential Leadership & Communication Needs: Almost all participants agreed that (a) strong leadership and strong team culture seemed essential for overcoming many of the hurdles people face in conducting IR (e.g., essential for motivation, persistence, recognition, advocacy). With regard to the Alliance website, participants also noted (b) a strong preference for supporting and enhancing essential in-person conversations that could be facilitated via online platforms.

Website Content Preferences: Participants widely-agreed that the online platform (ACE) would ideally provide information about (i) funding options, (ii) calls for proposals, (iii) calls for collaborations, (iv) student/scientists membership information (e.g., list of researchers with their expertise and areas of interest, and how their expertise can align with Alliance needs/goals), (v) a bibliography searchable by keywords that can include discipline, topic, hazard, and methodology tags. (vi) video presentations from researchers about their research translated into a context that engages other disciplines (ideally very brief) and (vii) information about upcoming conferences, meetings, past and ongoing collaborations, upcoming events and job postings etc.

Ongoing Development: Additional planned and ongoing activities to identify website content are aimed at following up on preliminary analysis and integrating feedback from other stake-holders. Specifically, we are evaluating options for conducting (a) ethnographies with few selective but representative participants from the focus groups and (b) evaluation methods for more in-depth insight-mining about the Alliance online platform (e.g., usability, task, and user need analyses). Additionally, we are evaluating technological options for ACE so as to not introduce yet another collaborative framework that duplicates some of the elements of existing platforms such as LinkedIn, Pivot, etc.

CIMMS Task III Project – Coping with Drought: Building Resilience to Drought

Mark Shafer (SCIPP), Kirsten Lackstrom (CISA at University of South Carolina), Kathie Dello (CIRC at Oregon State University), Michael Wolfenbarger (Weather Decision Technologies, Inc.), and Aimee Franklin (OU Department of Political Science)

NOAA Technical Lead: Claudia Nierenberg (CPO)

NOAA Strategic Goal 1 – Climate Adaptation and Mitigation: An Informed Society Anticipating and Responding to Climate and its Impacts

Funding Type: CIMMS Task III

Objectives

This project advances drought coordination at multiple levels through four themes: (1) Coping with Drought RISA Team Meeting; (2) Integrating Drought Condition Reporting into the Drought Monitor; (3) Creating an Inventory of Drought-Related Research; and (4) Developing a Ten-Year Vision of Drought Resilience in the Southern Plains. The RISA Team meeting brings together RISA teams that receive Coping with Drought funding via NIDIS to compare their efforts, assess methodologies used to learn about decision processes related to drought, and coordinate activities within NIDIS and the Drought Early Warning Systems. Integrating Drought Condition Reporting completes development of a mobile drought information and reporting app (developed by WDT) and connects reports from users to the Drought Impacts Reporter at the National Drought Mitigation Center. The Inventory of drought-related research builds a database of Federal grant opportunities and publications for inclusion on the U.S. Drought Portal (<http://www.drought.gov>). The Ten-Year Vision convenes a group of scientists and stakeholders to identify long-term solutions to the challenges of preparing, monitoring, and responding to drought in the Southern Plains.

Accomplishments

Pertaining to each of the four themes:

Coping with Drought RISA Team Meeting. This meeting was conducted in June 2017.

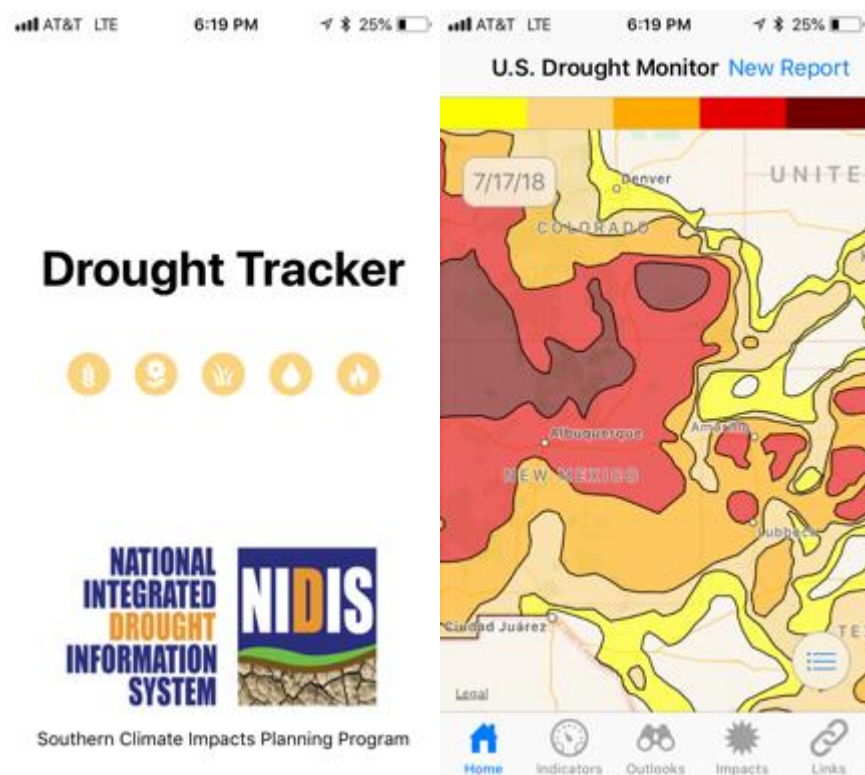
Integrating Drought Condition Reporting into the Drought Monitor. Development on the drought app continued, with work needed on the back-end data management system and drought condition reporting. Information about the app was shared with partners at the National Drought Mitigation Center (NDMC) and National Centers for Environmental Information (NCEI). Condition reports and impact information will be provided to NDMC for integration into the Drought Impact Reporter. Discussions are ongoing with NDMC and NCEI as to a permanent home for the drought app once it is operational. The drought app is expected to become available on the App Store in August 2018 and in Google Play shortly thereafter.

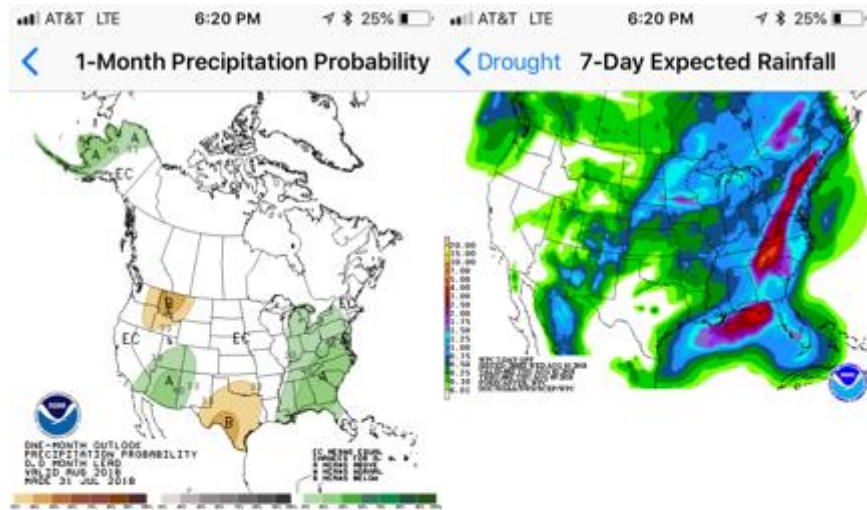
Creating an Inventory of Drought-Related Research. The project, led by Aimee Franklin (University of Oklahoma, Department of Political Science), identified keywords used in drought-related research, searched drought.gov to identify past agency calls for proposals that included those keywords, identified drought-related publications, and identified non-peer-reviewed reports related to drought. The project team built databases of grant opportunities and publications that will be integrated into the research tab on the NIDIS Drought Portal. The databases are currently being updated for delivery to NIDIS.

Developing a Ten-Year Vision of Drought Resilience in the Southern Plains: The panel is charged with examining: impacts of drought sector-by-sector; how long after a drought begins it takes before problems emerge in each sector; monitoring networks and available indices; communication practices; resources and practices available to lessen drought impacts; and resources and practices to lessen risk on a long-term basis. Members to serve on a committee (stakeholders and scientists) were identified but a meeting has not yet occurred. A background questionnaire was developed to solicit information from the committee members prior to an in-person or virtual meeting. Collection of information is currently underway. Following the meeting, a draft report will be developed.

Publications

Franklin, A. L., J. Le, A. Grossman, and M. Shafer, 2017: Efficiently translating research into practice: Oklahoma's contribution through the Southern Climate Impacts Planning Program. *Oklahoma Politics*, **27**, 103-138.





Home Indicators Outlooks Impacts Links

AT&T LTE 6:21 PM 25%

Done New Report Submit

IMPACT TYPE

Water Resources

IMPACT LEVEL

- 1 Reduced stream flow, ponds and lakes low [i](#)
- 2 Ponds and lakes well below normal, recreational impacts [i](#)
- 3 Ponds and lakes nearly empty, fish dying, wells going dry [i](#)
- 4 Lake beds exposed, dry streams, water emergencies [i](#)

REPORT LOCATION

Edit Location

OKLAHOMA

Several screen shots from the Drought Tracker mobile app. The app allows users to access commonly-used information from NOAA and its partners and to contribute condition reports and impact information which is then transmitted to the Drought Impact Reporter archive at the University of Nebraska-Lincoln.

CIMMS Task III Project – Baseline of Public Responsiveness to Uncertainty in Forecasts

Carol Silva, Joseph Ripberger, and Hank Jenkins-Smith (OU Center for Risk & Crisis Management – CRCM)

NOAA Technical Lead: Lans Rothfusz (NSSL)

NOAA Strategic Goal 2 – *Weather Ready Nation: Society is Prepared for and Responds to Weather-Related Events*

Funding Type: CIMMS Task III

Objectives

Identifying valid and reliable indicators of social conditions (such as forecast and warning reception, understanding, and response); creating baseline measures of these indicators under the current forecast and warning system; and designing a protocol that will allow the NWS to track these indicators over time and space so that program managers can empirically detect changes that occur as, when, and where the NWS implements new policies.

Accomplishments

In Year 1 of this project (7/1/15-9/30/16), the University of Oklahoma Center for Risk & Crisis Management (CRCM), began working on item one (valid and reliable indicators) by systematically reviewing previous research on forecast and warning reception, understanding, and response. In this review, we identified indicators that currently exist in the literature and gaps in our understanding. Following this review, we used the Oklahoma M-SISNet (Jenkins-Smith et al. 2017), a panel survey of approximately 2,000 residents of Oklahoma, to validate indicators of new concepts that are not yet addressed in the literature.

In Year 2 of the project (10/1/16-9/30/17), CRCM designed and fielded a nationwide survey on severe weather in the United States. The University of Oklahoma provided funding for all data collection. The Severe Weather and Society Survey (WX17) was fielded June 20-22, 2017 using an online questionnaire that was completed by 2,009 U.S. adults (age 18+) that were recruited from an Internet panel that matches the characteristics of the U.S. population as estimated in the U.S. Census. Pursuant to item two (above), WX17 was designed to establish baseline measures of the extent to which U.S. adults receive, understand, and respond to severe weather forecasts and warnings under the current watch, warning, and advisory (WWA) system. In addition to this set of baseline measures, WX17 measured other social and behavioral factors that the NWS might consider when evaluating performance, including public preferences about tradeoffs during the forecast process (i.e., lead time vs. accuracy/precision of warnings), trust in the NWS (relative to other groups), hazard risk literacy, the relative importance of probability and intensity in risk characterization, and the value of geographically

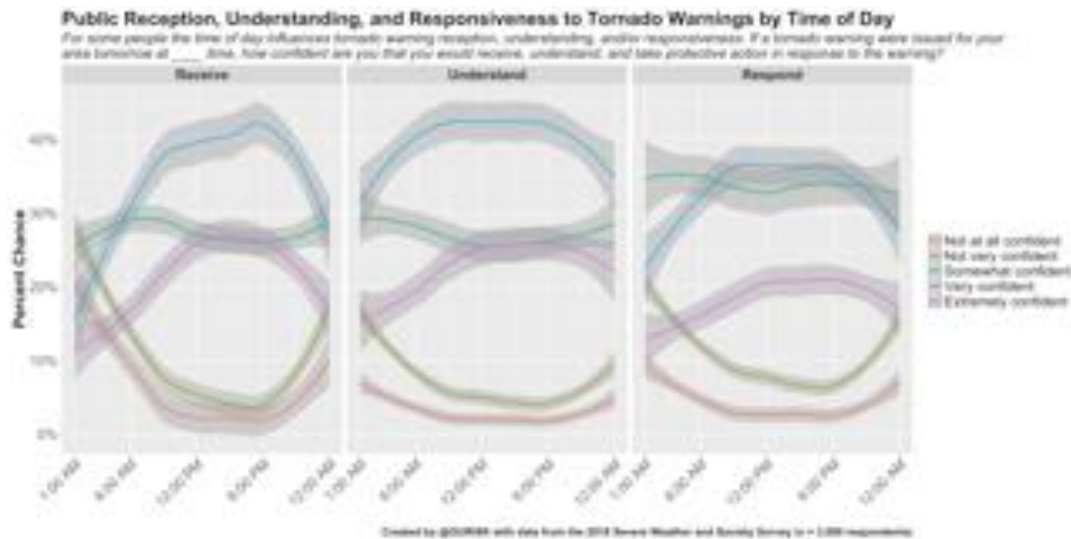
specific and continuous weather warnings, such as those envisioned by the FACETs framework.

In Year 3 of the project (10/1/17-9/30/18), CRCM designed and fielded a nationwide survey on severe weather in the United States. The University of Oklahoma provided funding for all data collection. The Severe Weather and Society Survey (WX18) was fielded July 6-11, 2018 using an online questionnaire that was completed by 3,000 U.S. adults (age 18+) that were recruited from an Internet panel that matches the characteristics of the U.S. population as estimated in the U.S. Census. Pursuant to item three (above) WX18 was designed to move beyond the baseline measures (WX17) of how U.S. adults receive, understand, and respond to severe weather forecasts and warnings under the current watch, warning, and advisory (WWA) system and to begin to implement a protocol where we begin to track these indicators over time and space.

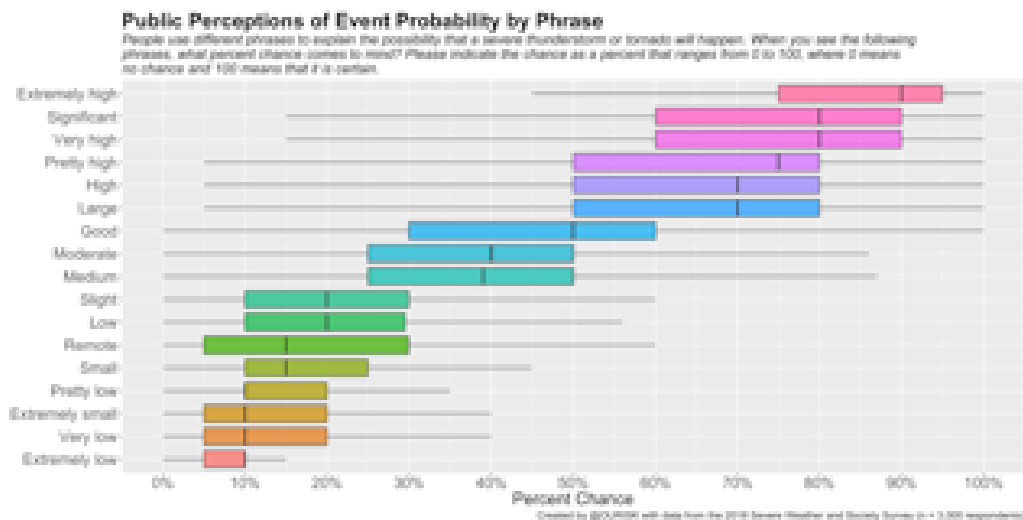
There are several publications and presentations in progress that are designed to highlight the survey results and the time series nature of the data:

- Allan, J., J. Ripberger, V. Ybarra, and E. Cokely, 2017: The Oklahoma Warning Awareness Scale: A Psychometric Analysis of a Brief Self-Report Survey Instrument. *Proceedings of the Human Factors and Ergonomics Society Annual Meeting*.
- Allan, J., J. Ripberger, V. Ybarra, and E. Cokely, 2017: Tornado Risk Literacy: Beliefs, Biases, and Vulnerability. *Proceedings of the International Conference on Naturalistic Decision Making*.
- Robinson, S., J. Pudlo, and W. Wehde. "Threat Intensity and the Public Use of Warning Information: A Quasi-experimental Assessment of Tornado Warnings." R&R at *Public Administration Review*
- Wesley Wehde, Jason Pudlo, and Scott Robinson, "Is Anybody Out There?: Communication of Natural Hazard Warnings at Home and Away," manuscript submitted for review.
- Robinson, S., W. Wehde, and J. Pudlo, "New Ecology of Public Safety Information: Drivers of Redistribution of Tornado Information," manuscript in preparation for submission.
- Ripberger, J., J. Allen, M. Krocak, W. Wehde, H. Jenkins-Smith, and C. Silva, "Tornado Warning Reception, Comprehension, and Response in Contiguous United States," manuscript in preparation for submission.
- 2 Presentations using WX17 data were given at the 2018 Annual AMS meeting:
 - A Difference in the Details: Assessing the Impact of Region on Tornado Threat Awareness and Knowledge
 - Baseline Measures of Reception, Comprehension, and Response to Severe Weather Forecasts and Warnings
- 4 Presentation Proposals using WX17 & WX18 data were submitted to the AMS program committee for presentation at the 2019 Annual AMS meeting:
 - Tornado Warning Reception, Comprehension, and Response across County Warning Areas in United States

- The Geographic Distribution of Extreme Weather and Climate Risk Perceptions in the United States
- How Can You Trust What You Don't Use?: Measuring Patterns of Individual's Weather Information Source Reliance and Trust
- The Waiting Game: The Impact of Lead Time on Protective Action in Response to Tornadoes
- Ripberger, J., C. Silva, and H. Jenkins-Smith have submitted a paper proposal to the Society for Risk Analysis Annual 2019 Conference titled, "The Geographic Distribution of Extreme Weather and Climate Risk Perceptions in the United States"



The Influence of Time of Day on Public Reception, Understanding, and Responsiveness to Tornado Warnings.



Public Perceptions of Probability Phrases in Severe Thunderstorm and Tornado Forecasts.

Public Affairs and Outreach

NOAA Partners and CIMMS Communications, Public Affairs, and Outreach

NOAA Technical Lead: Lans Rothfusz (NSSL)

NOAA Engagement Enterprise – *An Engaged and Educated Public with an Improved Capacity to Make Scientifically Informed Environmental Decisions*

Funding Type: CIMMS Task II

Objectives

Communicate CIMMS and NSSL research and news to OU, OAR, NOAA, and Department of Commerce leadership, the U.S. Congress, decision makers, partners, collaborators, the public, and media.

Accomplishments

1. Data Calls and Monthly Updates - Emily Summars (CIMMS at NSSL)

- Report significant papers: Alert NOAA leadership to published papers determined to be significant by NSSL and CIMMS leadership, add such papers to the OAR Weekly Report and publish in OAR Hot Items. Reports include a summary of each significant paper.
 - CIMMS reported 49 significant papers in FY2018.
- Provide report numbers for Quarterly Education performance taskers to NSSL leadership and CIMMS leadership as needed.
- Fact check total publication numbers against NOAA HQ's for accuracy.
- Provide monthly social media updates, story progress updates and project updates via email and at weekly NSSL Managers Meetings.
- Provide and gather information for the OAR Weekly Report focusing on NSSL and CIMMS activities, research and updates while tying such items significance to the Weather Act and DOC's Blue Economy priorities.
 - From the OAR Weekly Report the Department of Commerce Secretary's Weekly Report is gathered. Work with Headquarters to ensure the accuracy of any CIMMS or NSSL items included in the Secretary's report, add details, photos and other items as requested by OAR leadership

2. NOAA, OAR and CIMMS Communications – Emily Summars (CIMMS at NSSL) and Keli Pirtle (NOAA)

- **OAR Hot Items:** Describe new research, activities and publications. Hot items are posted on the OAR Hub, where internal OAR entities and employees may review the post. **Twenty** Hot Items were submitted on behalf of NSSL and CIMMS in FY2018, including several topics like a stream radar project, VORTEX-Southeast and experiments in NOAA's Hazardous Weather Testbed.

- Participate in weekly and monthly OAR Communications team calls to coordinate releases and important events, such as former EPA Administrator Scott Pruitt's visit to the National Weather Center to view CIMMS and NSSL offices.

3. Research Projects – James Murnan (ACE) and Emily Summars (CIMMS at NSSL)

- Accompany researchers to video, conduct interviews, and take photos during research projects. Examples included VORTEX-Southeast, ANCHOR and NOAA Hazardous Weather Testbed experiments. Provide social media updates while in the field to provide an “in-that-moment” view for followers. The final result from time in the field includes story(s), video, social media updates, and a Flickr photo album. Results from time spent in the field are later used for NSSL and CIMMS outreach materials such as fact sheets, b-roll video and/or Bite-Sized Science videos.



Automated NonContact Hydrologic Observations in Rivers, or ANCHOR, will demonstrate the use of remote-sensing technology for better flood detection and improve downstream predictions by models. OU CIMMS Research Scientists Jorge Duarte Garcia and Danny Wasielewski install devices for the radar to stay hoisted above the stream.

4. Fact Sheets – Emily Summars (CIMMS at NSSL)

- Fact Sheets are 1-2 page handouts on NSSL/CIMMS projects used to give visitors and guests a “take-away” message and call them to action. Four Fact Sheets involving CIMMS were designed, written, and edited in FY2017, including fact sheets for VORTEX-Southeast media day and Congressional fact sheets while the main NSSL and CIMMS Fact Sheets were redesigned and updated.

5. CIMMS on Social Media – Emily Summars (CIMMS at NSSL)

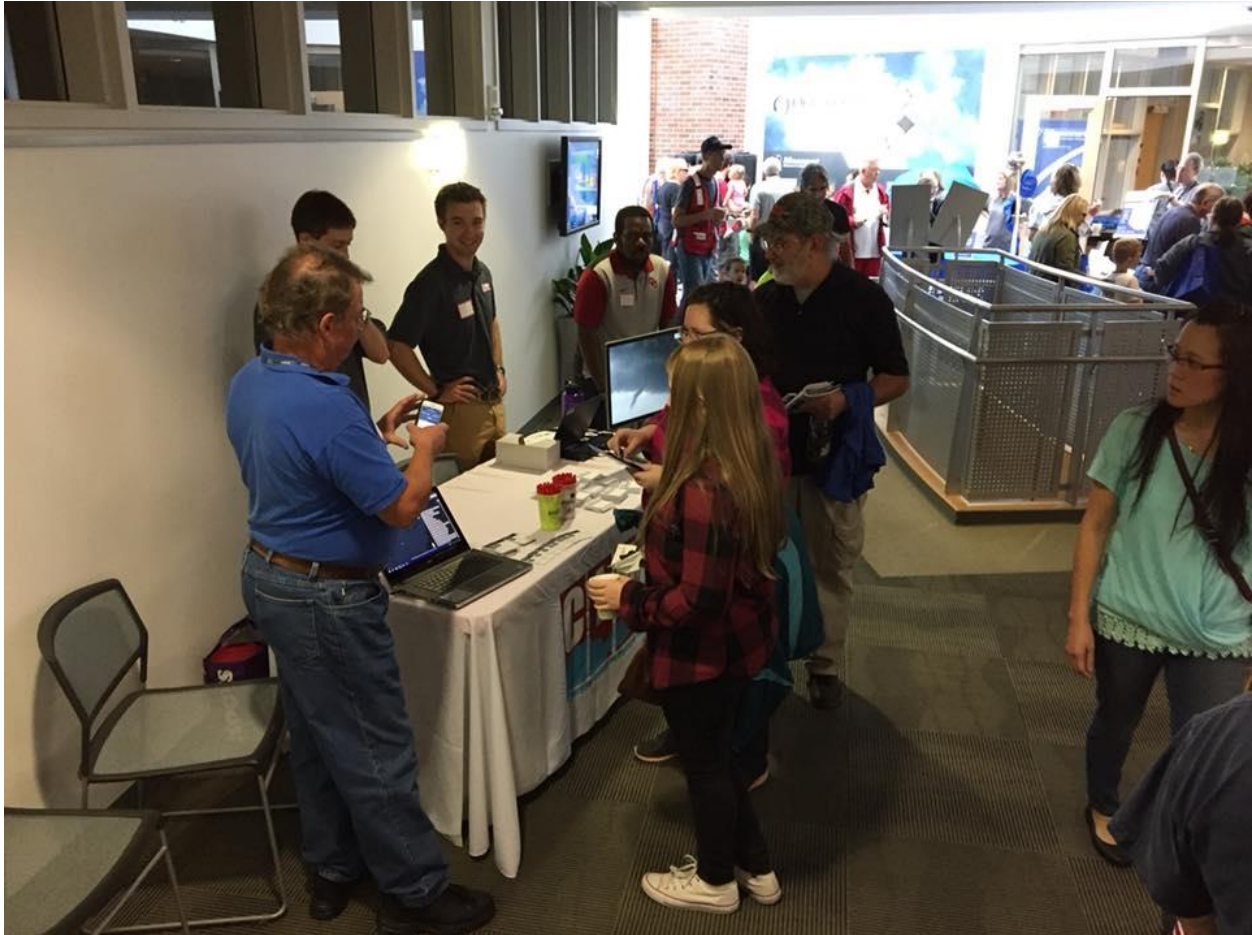
- CIMMS’s Facebook and Twitter accounts are growing in popularity. New content is published weekly based on monthly or daily themes. Partner posts are shared as appropriate. Project photos from researchers, days in the field and media days are shared on NSSL’s Flickr and Instagram accounts. Updated Facebook and Twitter photos, along with header photos as appropriate. Monitor comments and remove comments using inappropriate language, targeting other individuals or impersonating NSSL or CIMMS personnel in the field.
 - CIMMS Facebook “likes”
 - 2018: 846
 - 2017: 780
 - 2016: 613
 - 2015: 375
 - CIMMS Twitter “follows”
 - 2018: 803
 - 2017: 642
 - 2016: 512
 - 2015: 282

6. CIMMS Outreach – Emily Summars (CIMMS at NSSL)

- CIMMS created the first CIMMS Newsletter, highlighting work in the lab, CIMMS’ mission and future focus. The newsletter is used to provide a snapshot of lab happenings for outside visitors, speakers and as a way to publicize internal events.
- CIMMS and NSSL outreach materials were created, including “we’re hiring” business cards and “mPING” trading cards, to provide at events like the National Weather Festival, AMS, public outreach events and other conferences. Several slideshows and short videos were developed highlighting NSSL and CIMMS projects for large television screens at event like AMS’ Annual Meeting, AGU’s Annual Meeting, National Weather Festival and events hosted by OU highlighting severe weather research.
- The public submits questions to CIMMS via the CIMMS Outreach email account.
- The account added to OU CIMMS website and social media in FY2017. In FY2018 CIMMS responded to four outreach questions sent via email.
- Staff outreach:
 - Send reminders about NSSL and OU CIMMS internal Gab at the Lab.
 - Work closely with the College of Atmospheric and Geographic Sciences and the university to ensure all students, faculty and staff are recognized

properly in CIMMS related publications and releases and included in outreach efforts.

- Share stories and social media posts involving students with the College and university to ensure collaborative efforts.



CIMMS Researchers participated in the National Weather Festival outreach event in October 2017 at the National Weather Center. They answered questions about research, projects and the organization.

7. CIMMS Website – Vicki Farmer (ACE) and Emily Summars (CIMMS at NSSL)

- Review, update and post content to the CIMMS website weekly.
- Redesign certain products to create a cohesive brand.
- Track awards, accomplishments and publications then post items considered of interest.
- Google Analytics was created for cimms.ou.edu in FY2018. Since Google Analytics was set up for CIMMS website — cimms.ou.edu — received almost 19,500 page views with the top two page visits being the homepage and job postings.

8. Back-up NOAA Weather Partners Public Affairs – Keli Pirtle (NOAA Weather Partners) and Emily Summars (CIMMS at NSSL)

- Help Keli Pirtle and other NOAA partners field media calls pertaining to CIMMS.
- Provide additional information on projects involving CIMMS researchers.
- Ensure CIMMS researchers are mentioned properly in news and other media articles.

9. Public Education and Outreach – Patrick Hyland (OU College of Atmospheric and Geographic Sciences)

- Lead tour program of the National Weather Center, including NOAA.
- Plan and organize National Weather Festival activities.
- Facilitate educational outreach opportunities.
- Collaborate with NOAA and CIMMS public relations office on requests that require crossover into both the university and NOAA.

CIMMS Staff Outreach at WDTD

Alyssa Bates, Jill Hardy, Austin Harris, Eric Jacobsen, Dale Morris, Stephen Mullens, Chris Spannagle, Nathan Ware, Andrew Wood, Brad Workman, and Alex Zwink (CIMMS at WDTD)

CIMMS staff at WDTD regularly engaged in various outreach activities during the past year. Most of the activities involved partnerships with other organizations in the National Weather Center, while others were outside of the building supporting the local community. These outreach activities included:

- Working support “shifts” at the NWS Norman Weather Forecast Office (WFO) during severe weather events;
- Planning and participating in the hands-on “Issue Your Own Warning” activity at the National Weather Festival and Aircraft Owners and Pilots Association (AOPA) Fly-In;
- Volunteering with other National Weather Center organizations during the Norman United Way Day of Caring;
- Organizing and instructing mini-workshops for OU School of Meteorology students on warning fundamentals;
- Hosting a WDTD booth at the 2018 AMS Boundary Layer conference;
- Volunteered for the National Weather Association (NWA) Foundation WeatherReady Fest teaching children about meteorology through hands-on activities during NWA Annual Meeting at a science museum in Anaheim, CA;
- Hosting a local high school student for a job shadowing opportunity; and
- Leading a hands-on lab session on issuing weather warnings to high school students for Oklahoma Mesonet’s Regents Camp.



CIMMS instructors during the 2017 National Weather Festival showing the public how National Weather Service forecasters issue severe weather warnings.

Appendix A

AWARDS AND HONORS

The following awards or other notable achievements occurred during the fiscal year were received by CIMMS staff and students:

AMS Fellow – **Alexander Ryzhkov**

Mercator Fellowship (Germany) – **Alexander Ryzhkov**

OAR Distinguished Career Award Recipient – **Allen Zahrai**

National Weather Association Special Lifetime Achievement Award – **Stephen Corfidi**

NOAA Bronze Medal – **OPG Team Award**

Larry R. Johnson Special Award from the National Weather Association – **OPG Team Award**

NOAA Team Member of the Month for August 2017 – **Dale Morris**

NOAA Team Member of the Month for April 2018 – **Megan Taylor**

Certified Project Management Professional – **Katie Vigil**

Dean's Award for Excellence in Teaching – College of Atmospheric and Geographic Sciences – **Randy Peppler**

Dean's Award for Outstanding Service – College of Atmospheric and Geographic Sciences – **Randy Peppler**

1st Place Oral Presentation Student Competition – 8th Symposium on Transition from Research to Operations (AMS) – **Makenzie Krocak**

1st Place Oral Presentation Student Competition – 13th Symposium on Societal Applications: Policy, Research and Practice (AMS) – **David Harrison**

1st Place Poster Presentation Student Competition – 29th Conference on Weather Analysis and Forecasting/25th Conference on Numerical Weather Prediction (AMS) – **David Harrison**

1st place Poster Presentation Student Competition: PECAN Symposium (AMS) – **Hristo Chipilski**

1st Place Student Presentation Competition – 34th Conference on Environmental Information Processing Techniques (AMS) – **Andrew Mahre**

2nd Place Oral Presentation Student Competition: 17th Conference on Mesoscale Processes (AMS) – **Hristo Chipilski**

2nd Place Oral Presentation Student Competition: 17th Conference on Artificial and Computational Intelligence and its Applications to the Environmental Sciences (AMS) – **David Harrison**

2nd Place in the Student Paper Award Contest – 2018 IEEE International Symposium on Antennas and Propagation and USNC-URSI Radio Science Meeting (IEEE) – **Mirhamed Mirmozafari**

William H. Barkow Scholarship for Electrical and Computer Engineering students for the 2018-19 academic year – **Mohammad Golbon**

Featured in the journal *Electronics Letters* April 2018 issue for the paper, "Highly Isolated Crossed Dipole Antenna with Matched Copolar Beams" – **Mirhamed Mirmozafari**

"Apparatus and Method for Wet Radome Characterization and Radar Calibration.", U.S. Provisional Patent 62488301, submitted April 21, 2017 – **Jorge L. Salazar-Cerreno, Alessio Mancini and Boon Leng Cheong**

Appendix B

PUBLICATION SUMMARY*

	CIMMS Lead Author				NOAA Lead Author				Other Lead Author			
	2010-11	2011-12	2012-13	2013-14	2010-11	2011-12	2012-13	2013-14	2010-11	2011-12	2012-13	2013-14
Peer Reviewed	28	31	32	57	32	13	8	9	44	35	45	44

	CIMMS Lead Author				NOAA Lead Author				Other Lead Author			
	2014-15	2015-16	2016-17	2017-18	2014-15	2015-16	2016-17	2017-18	2014-15	2015-16	2016-17	2017-18
Peer Reviewed	60	62	45	45	7	5	5	9	40	52	44	34

**Publication numbers are approximate. Numbers are slightly lower this year as they are strictly fiscal year.*

Appendix C

PERSONNEL SUMMARY – NOAA FUNDED RESEARCH ONLY

Category	Number	B.S.	M.S.	Ph.D.
Research Scientist	95	1	47	47
Visiting Scientist	1			1
Postdoctoral Fellow	20			20
Research Support Staff	19	3	14	
Administrative	4	2	1	
Total (>50% support)	139	6	62	67
Undergraduate Students	23			
Graduate Students (current degree)	41	18	23	
Employees that receive <50% NOAA Funding (not including students)	33	5	5	21
Located at Lab	NSSL-91, WDTD-17, ROC-8, SPC-6, NWSTC-5, ARL-3, OUN-1			
Obtained NOAA employment within the last year	9			

Appendix D

COMPILATION OF CIMMS-RELATED PUBLICATION – FY 2018

Publications compiled here were reported for projects funded under Cooperative Agreement NA16OAR4320115.

Peer-Reviewed Journal Articles, Books, and Book Chapters *Published* and in *Early Online Release*

- Belik, P., D. P. Dokken, C. K. Potvin, K. Scholz, and M. M. Shvartsman, 2017: Applications of vortex gas models to tornadogenesis and maintenance. *Open Journal of Fluid Dynamics*, **7**, 596–622.
- Bluestein, H. B., Z. B. Wienhoff, D. D. Turner, D. W. Reif, J. C. Snyder, K. J. Thiem, and J. B. Houser, 2017: A comparison of the finescale structures of a prefrontal wind-shift line and a strong cold front in the southern plains of the United States. *Monthly Weather Review*, **145**, 3307–3330.
- Bluestein, H. B., K. J. Thiem, J. C. Snyder, and J. B. Houser, 2018: The multiple-vortex structure of the El Reno, Oklahoma tornado on 31 May 2013. *Monthly Weather Review*, **146**, 2486–2502.
- Blumberg, W. G., K. T. Halbert, T. A. Supinie, P. T. Marsh, R. L. Thompson, and J. A. Hart, 2017: SHARPy: An open-source sounding analysis toolkit for the atmospheric sciences. *Bulletin of the American Meteorological Society*, **98**, 1625–1636.
- Blumberg, W. G., T. J. Wagner, D. D. Turner, and J. Correia, Jr., 2017: Quantifying the accuracy and uncertainty of diurnal thermodynamic profiles and convection indices derived from the atmospheric emitted radiance interferometer. *Journal of Applied Meteorology and Climatology*, **56**, 2747–2766.
- Bukovcic, P., A. Ryzhkov, D. Zrnica, and G. Zhang, 2018: Polarimetric radar relations for quantification of snow based on disdrometer data. *Journal of Applied Meteorology and Climatology*, **57**, 103–120.
- Campbell, M. A., A. E. Cohen, M. C. Coniglio, A. R. Dean, S. F. Corfidi, and C. M. Mead, 2017: Structure and motion of severe-wind-producing mesoscale convective systems and derechos in relation to the mean wind. *Weather and Forecasting*, **32**, 423–439.
- Carlin, J. T., J. Gao, J. C. Snyder, and A. V. Ryzhkov, 2017: Assimilation of ZDR columns for improving the spinup and forecast of convective storms in storm-scale models: Proof-of-concept experiments. *Monthly Weather Review*, **145**, 5033–5057.
- Clark, A. J., I. L. Jirak, S. R. Dembek, G. J. Creager, F. Kong, K. W. Thomas, K. H. Knopfmeier, B. T. Gallo, C. J. Melick, M. Xue, K. A. Brewster, Y. Jung, A. Kennedy, X. Dong, J. Markel, M. Gilmore, G. S. Gilmore, K. R. Fossell, R. A. Sobash, J. R. Carley, B. S. Ferrier, M. Pyle, C. R. Alexander, S. J. Weiss, J. S. Kain, L. J. Wicker, G. Thompson, R. D. Adams-Selin, and D. A. Imy, 2018: The Community Leveraged Unified Ensemble (CLUE) in the 2016 NOAA/Hazardous Weather Testbed Spring Forecasting Experiment. *Bulletin of the American Meteorological Society*, **99**, 1433–1448.
- Clark III, R. A., Z. L. Flamig, H. Vergara, Y. Hong, J. J. Gourley, D. J. Mandl, S. Frye, M. Handy, and M. Patterson, 2017: Hydrological modeling and capacity building in the Republic of Namibia. *Bulletin of the American Meteorological Society*, **98**, 1697–1715.

- Corfidi, S., 2017: Forecasting Severe Convective Storms. In *Oxford Research Encyclopedia of Climate Science*, Oxford University Press.
- Curtis, C. D., and S. M. Torres, 2017: Adaptive range oversampling processing for nontraditional radar-variable estimators. *Journal of Atmospheric and Oceanic Technology*, **34**, 1607–1623.
- Dafis, S., A. O. Fierro, T. M. Giannaros, V. Kotroni, K. Lavougadros, and E. R. Mansell, 2018: Evaluation of an explicit lightning forecast system. *Journal of Geophysical Research*, **123**, 5130–5148.
- Dokken, D., P. Belik, C. K. Potvin, K. Scholz, and M. Shvartsman, 2017: Applications of vortex gas models to tornadogenesis and maintenance. *Open Journal of Fluid Dynamics*, **7**, 596–622.
- Erlingis, J. M., J. J. Gourley, P. E. Kirstetter, E. N. Anagnostou, J. Kalogiros, M. N. Anagnostou, and W. A. Petersen, 2018: Evaluation of operational and experimental precipitation algorithms and microphysical insights during IPHEX. *Journal of Hydrometeorology*, **19**, 113–125.
- Fierro, A. O., and E. R. Mansell, 2017: Electrification and lightning in idealized simulations of a hurricane-like vortex subject to wind shear and sea surface temperature cooling. *Journal of the Atmospheric Sciences*, **74**, 2023–2041.
- Fierro, A. O., and E. R. Mansell, 2018: Relationships between electrification and storm-scale properties based on idealized simulations of an intensifying hurricane-like vortex. *Journal of the Atmospheric Sciences*, **75**, 657–674.
- Fierro, A. O., S. N. Stevenson, and R. M. Rabin, 2018: Evolution of GLM-observed total lightning in Hurricane Maria (2017) during the period of maximum intensity. *Monthly Weather Review*, **146**, 1641–1666.
- Fierro, A. O., G. Zhao, S. Liu, Y. Wang, J. Gao, K. Calhoun, C. L. Ziegler, E. R. Mansell, and D. R. MacGorman, 2018: Assimilation of total lightning with GSI and NEWS3DVAR to improve short-term forecasts of high impact weather events at cloud resolving scales. *JCSDA Quarterly Newsletter*, No. 58, Winter 2018, 5–12.
- Flora, M. L., C. K. Potvin, and L. J. Wicker, 2018: Practical predictability of supercells: Exploring ensemble forecast sensitivity to initial condition spread. *Monthly Weather Review*, **146**, 2361–2379.
- Franklin, A. L., J. Le, A. Grossman, and M. Shafer, 2017: Efficiently translating research into practice: Oklahoma’s contribution through the Southern Climate Impacts Planning Program. *Oklahoma Politics*, **27**, 103–138.
- Fu, C., J. Gao, Y. Wang, J. Tang, C. Zhou, C. Ye, Z. Zhuang, 2018: Applications of a realtime weather-adaptive 3DVAR analysis system in tornado related severe weather detections and warning. *Advances in Meteorological Science and Technology*, **8**, 19–37.
- Gallo, B. T., A. J. Clark, I. Jirak, J. S. Kain, S. J. Weiss, M. Coniglio, K. Knopfmeier, J. Correia Jr., C. J. Melick, C. D. Karstens, E. Iyer, A. R. Dean, M. Xue, F. Kong, Y. Jung, F. Shen, K. W. Thomas, K. Brewster, D. Stratman, G. W. Carbin, W. Line, R. Adams-Selin, and S. Willington, 2017: Breaking new ground in severe weather prediction: The 2015 NOAA/Hazardous Weather Testbed Spring Forecasting Experiment. *Weather and Forecasting*, **32**, 1541–1568.
- Gallo, B. T., A. J. Clark, B. T. Smith, R. L. Thompson, I. Jirak, and S. R. Dembek, 2018: Blended probabilistic tornado forecasts: Combining climatological frequencies with NSSL-WRF ensemble forecasts. *Weather and Forecasting*, **33**, 443–460.

- Golbon-Haghighi, M.-H., H. Saeidi-Manesh, G. Zhang, and Y. Zhang, 2018: Pattern synthesis for the Cylindrical Polarimetric Phased Array Radar (CPPAR). *Progress in Electromagnetics Research M*, **66**, 87-98.
- Gou, Y., Y. Ma, H. Chen, and Y. Wen, 2018: Radar-derived quantitative precipitation estimation in complex terrain over the eastern Tibetan Plateau. *Atmospheric Research*, **203**, 286–297.
- Greene, B. R., A. R. Segales, S. Waugh, S. Duthoit, and P. B. Chilson, 2018: Considerations for temperature sensor placement on rotary-wing unmanned aircraft systems. *Atmospheric Measurement Technology*, Early Online Release.
- Griffin, C. B., C. C. Weiss, A. E. Reinhart, J. C. Snyder, H. B. Bluestein, J. Wurman, and K. A. Kosiba, 2018: In situ and radar observations of the low reflectivity ribbon in supercells during VORTEX2. *Monthly Weather Review*, **146**, 307-327.
- Griffin, E. M., T. J. Schuur, and A. V. Ryzhkov, 2018: A polarimetric analysis of ice microphysical processes in snow using quasi-vertical profiles. *Journal of Applied Meteorology and Climatology*, **57**, 31–50.
- Hwang, Y., T-Y Yu, V. Lakshmanan, D. M. Kingfield, D-I Lee, and C-H You, 2017: Neuro-fuzzy gust front detection algorithm with S-band polarimetric radar. *IEEE Transactions on Geoscience and Remote Sensing*, **55**, 1618-1628.
- Iltoviz, E., A. Khain, A. Ryzhkov, and J. Snyder, 2018: Relationship between aerosols, hail microphysics, and Zdr columns. *Journal of the Atmospheric Sciences*, **75**, 1755–1781.
- Ivić, I. R., 2017: An approach to simulate the effects of antenna patterns on polarimetric variable estimates. *Journal of Atmospheric and Oceanic Technology*, **34**, 1907–1934.
- Ivić, I. R., 2018: Effects of phase coding on Doppler spectra in PPAR weather radar. *IEEE Transactions on Geoscience and Remote Sensing*, **56**, 2043–2065.
- Johnson, M., Y. Jung, D. Dawson, T. Supinie, M. Xue, J. Park, and Y.-H. Lee, 2018: Evaluation of unified model microphysics in high-resolution NWP simulations using polarimetric radar observations. *Advances in Atmospheric Science*, **35**, 771–784.
- Jones, T. A., and C. Nixon, 2017: Short-term forecasts of left-moving supercells from an experimental Warn-on-Forecast system. *Journal of Operational Meteorology*, **5**, 151–160.
- Jones, T. A., X. Wang, P. Skinner, A. Johnson, and Y. Wang, 2018: Assimilation of GOES-13 imager clear-sky water vapor (6.5 mm) radiances into a Warn-on-Forecast system. *Monthly Weather Review*, **146**, 1077–1107.
- Karstens, C. D., J. Correia, D. S. LaDue, J. Wolfe, T. C. Meyer, D. R. Harrison, J. L. Cintineo, K. M. Calhoun, T. M. Smith, A. E. Gerard, and L. P. Rothfus, 2018: Development of a human–machine mix for forecasting severe convective events. *Weather and Forecasting*, **33**, 715–737.
- Keul, A. G., B. Brunner, J. Allen, K. A. Wilson, M. Taszarek, C. Price, G. Soleiman, S. Sharma, P. Roy, M. Aini, A. Elistina, M. Kadir, and C. Gomes, 2018: Multi-hazard weather risk perception and preparedness in eight countries. *Weather, Climate, and Society*, In Print.
- Kingfield, D. M., and K. M. de Beurs, 2017: Landsat identification of tornado damage by land cover and an evaluation of damage recovery in forests. *Journal of Applied Meteorology and Climatology*, **56**, 965-987.

- Kingfield, D. M., K. M. Calhoun, K. M. de Beurs, and G. M. Henebry, 2018: Effects of city size on thunderstorm evolution revealed through a multiradar climatology of the central United States. *Journal of Applied Meteorology and Climatology*, **57**, 295–317.
- Kirstetter, P.E., N. Karbalaee, K. Hsu, and Y. Hong, 2018: Probabilistic precipitation rate estimates with space-based infrared sensors. *Quarterly Journal of the Royal Meteorological Society*, **144**, 1–15.
- Kong, R., M. Xue, and C. Liu, 2018: Development of a hybrid en3DVar data assimilation system and comparisons with 3DVar and EnKF for radar data assimilation with observing system simulation experiments. *Monthly Weather Review*, **146**, 175–198.
- Krocak, M. J., and H. E. Brooks, 2018: Climatological estimates of hourly tornado probability for the United States. *Weather and Forecasting*, **33**, 59–69.
- Kuster, C. M., P. L. Heinselman, J. C. Snyder, K. A. Wilson, D. A. Speheger, and J. E. Hocker, 2017: An evaluation of radar-based tornado track estimation products by Oklahoma public safety officials. *Weather and Forecasting*, **32**, 1711–1726.
- Lagerquist, R., A. McGovern, and T. Smith, 2017: Machine learning for real-time prediction of damaging straight-line convective wind. *Weather and Forecasting*, **32**, 2175–2193.
- Lawson, J. R., J. S. Kain, N. Yussouf, D. C. Dowell, D. M. Wheatley, K. H. Knopfmeier, and T. A. Jones, 2018: Advancing from convection-allowing NWP to Warn-on-Forecast: evidence of progress. *Weather and Forecasting*, **33**, 599–607.
- Lee, T. R., M. Buban, E. Dumas, and C. B. Baker, 2017: A new technique to estimate sensible heat fluxes around micrometeorological towers using small unmanned aircraft systems. *Journal of Atmospheric and Oceanic Technology*, **34**, 2103–2112.
- Lee, T. R., M. Buban, M. A. Palecki, R. D. Leeper, H. J. Diamond, E. Dumas, T. P. Meyers, and C. B. Baker, 2018: Great American Eclipse data may fine-tune weather forecasts. *Eos*, **99**.
- Li, Y., K. E. Pickering, D. Allen, M. C. Barth, M. M. Bela, K. A. Cummings, L. Carey, R. Mecikalski, A. O. Fierro, T. Campos, A. Weinheimer, T. Ryerson, and G. S. Diskin, 2017: Evaluation of deep convective transport in storms from different convective regimes during the DC3 field campaign using WRF-Chem with lightning data assimilation. *Journal of Geophysical Research*, **122**, 7140–7163.
- Loken, E. D., A. J. Clark, M. Xue, and F. Kong, 2017: Comparison of next-day probabilistic severe weather forecasts from coarse and fine-resolution CAMs and a convection-allowing ensemble. *Weather and Forecasting*, **32**, 1403–1421.
- Mancini, A., J. L. Salazar, R. M. Lebrón, and B. L. Cheong, 2018: A novel instrument for real-time measurement of attenuation of weather radar radome including its outer surface. Part I: The concept. *Journal of Atmospheric and Oceanic Technology*, **35**, 953–973.
- Mancini, A., J. L. Salazar, R. M. Lebrón, and B. L. Cheong, 2018: A novel instrument for real-time measurement of attenuation of weather radar radome including its outer surface. Part II: Applications. *Journal of Atmospheric and Oceanic Technology*, **35**, 975–991.
- Martinaitis, S. M., H. M. Grams, C. Langston, J. Zhang, and K. Howard, 2018: A real-time evaporation correction scheme for radar-derived mosaicked precipitation estimations. *Journal of Hydrometeorology*, **19**, 87–111.

- McGovern, A., C. K. Potvin, and R. A. Brown, 2017: Using large-scale machine learning to improve our understanding of the formation of tornadoes. In *Large-scale Machine Learning in the Earth Sciences*, A. N. Srivastava, R. Nemani, K. Steinhäuser, eds. CRC Press, pp. 95–112.
- McGovern, A., K. L. Elmore, D. J. Gagne, S. E. Haupt, C. D. Karstens, R. Lagerquist, T. Smith, and J. K. Williams, 2017: Using artificial intelligence to improve real-time decision-making for high-impact weather. *Bulletin of the American Meteorological Society*, **98**, 2073–2090.
- Melnikov, V., and D. Zrnic, 2017: Observations of convective thermals with weather radar. *Journal of Atmospheric and Oceanic Technology*, **34**, 1585–1590.
- Mirmozafari, M., and G. Zhang, 2018: On sidelobe problem of configured array antennas. *IEEE Transactions on Antennas and Propagation*, **66**, 3475–3481.
- Mirmozafari, M., S. Saeedi, and G. Zhang, 2018: Highly isolated crossed dipole antenna with matched copolar beams. *Electronics Letters*, **54**, 470–471.
- North, K. W., M. Oue, P. Kollias, S. E. Giangrande, S. M. Collis, and C. K. Potvin, 2017: Vertical air motion retrievals in deep convective clouds using the ARM scanning radar network in Oklahoma during MC3E. *Atmospheric Measurement Techniques*, **10**, 2785–2806.
- Ortega, K. L., 2018: Evaluating multi-radar, multi-sensor products for surface hailfall diagnosis. *Electronic Journal of Severe Storms Meteorology*, **13**, 1–36.
- Osman, M. K., D. D. Turner, T. Heus, and R. Newsom, 2018: Characteristics of water vapor turbulence profiles in convective boundary layers during the dry and wet seasons over Darwin. *Journal of Geophysical Research*, **123**, 4818–4836.
- Oue, M., P. Kollias, A. Ryzhkov, and E. Luke, 2018: Toward exploring the synergy between cloud radar polarimetry and Doppler spectral analysis in deep cold precipitating systems in the Arctic. *Journal of Geophysical Research*, **123**, 2797–2815.
- Pan, S., J. Gao, D. J. Stensrud, X. Wang, and T. A. Jones, 2017: Assimilation of radar radial velocity and reflectivity, satellite cloud water path, and total precipitable water for convective-scale NWP in OSSEs. *Journal of Atmospheric and Oceanic Technology*, **34**, 67–89.
- Peppler, R. A., K. E. Klockow, and R. D. Smith, 2018: Hazardscapes: Perceptions of tornado risk and the role of place in central Oklahoma. In *Explorations in Place Attachment*, J. S. Smith, ed. London: Routledge, pp. 33–45.
- Rosenow, A. A., R. M. Rauber, B. F. Jewett, G. M. McFarquhar, and J. M. Keeler, 2018: Elevated potential instability in the comma head: Distribution and development. *Monthly Weather Review*, **146**, 1259–1278.
- Rosenow, A. A., K. Howard, and J. Meitin, 2018: Gap-filling mobile radar observations of a snow squall in the San Luis Valley. *Monthly Weather Review*, **146**, 2469–2481.
- Rothfus, L. P., R. Schneider, D. Novak, K. Klockow, A. E. Gerard, C. Karstens, G. J. Stumpf, and T. M. Smith, 2018: FACETs: A proposed next-generation paradigm for high-impact weather forecasting. *Bulletin of the American Meteorological Society*, Early Online Release.
- Saeedi, S., and H. H. Sigmarsson, 2018: Miniaturized evanescent-mode cavity SIW bandpass filter with spurious suppression, *IEEE Radio and Wireless Week (RWW)*, January.

- Saeidi-Manesh, H., M. Mirmozafari, G. Zhang, 2017: Low cross-polarisation high-isolation frequency scanning aperture coupled microstrip patch antenna array with matched dual-polarisation radiation patterns. *Electronics Letters*, **53**, 901-902.
- Saeidi-Manesh, H., S. Karimkashi, G. Zhang, and R. J. Doviak, 2017: High-isolation low cross-polarization phased-array antenna for MPAR application. *Radio Science*, **52**, 1544-1557.
- Skinner, P. S., D. M. Wheatley, K. H. Knopfmeier, A. E. Reinhart, J. J. Choate, T. A. Jones, G. J. Creager, D. C. Dowell, C. R. Alexander, T. T. Ladwig, L. J. Wicker, P. L. Heinselman, P. Minnis, and R. Palikonda, 2018: Object-based verification of a prototype Warn-on-Forecast system. *Weather and Forecasting*, **33**, 1225-1250.
- Stratman, D. R., C. K. Potvin, and L. J. Wicker, 2018: Correcting storm displacement errors in ensembles using the feature alignment technique (FAT). *Monthly Weather Review*, **146**, 2125–2145.
- Supinie, T. A., N. Yussouf, J. Cheng, Y. Jung, M. Xue, and S. Wang, 2017: Comparison of the analyses and forecasts of a tornadic supercell storm from assimilating phased array radar and WSR-88D observations. *Weather and Forecasting*, **32**, 1379-1401.
- Wade, A. R., M. C. Coniglio, and C. L. Ziegler, 2018: Comparison of near- and far-field supercell inflow environments using radiosonde observations. *Monthly Weather Review*, **146**, 2403–2415.
- Wang, H., Y. Liu, W. Y. Y. Cheng, T. Zhao, M. Xu, S. Shen, K. M. Calhoun, and A. O. Fierro, 2017: Improving lightning and precipitation prediction of severe convection using lightning data assimilation with NCAR WRF-RTFDDA. *Journal of Geophysical Research*, **122**, 12296–12136.
- Wang, H., Y. Liu, T. Zhao, M. Xu, F. Guo, S. Shen, W. Y. Y. Cheng, E. R. Mansell, and A. O. Fierro, 2018: Incorporating geostationary lightning data into a radar reflectivity based hydrometeor retrieval method: An Observing System Simulation Experiment. *Atmospheric Research*, **209**, 1–13.
- Warde, D. A., and S. M. Torres, 2017: Spectrum width estimation using matched autocorrelations. *IEEE Geoscience and Remote Sensing Letters*, **14**, 1661–1664.
- Waugh, S. M., and T. J. Schuur, 2018: On the use of radiosondes in freezing precipitation. *Journal of Atmospheric and Oceanic Technology*, **35**, 459–472.
- Weiss, S. A., D. R. MacGorman, E. C. Bruning, and V. C. Chmielewski, 2018: Two methods for correcting range-dependent limitations of lightning mapping arrays. *Journal of Atmospheric and Oceanic Technology*, **35**, 1273–1282.
- Wen, Y., A. Behrangi, H. Chen, and B. Lambrigtsen, 2018, How well were early 2017 California atmospheric river precipitation events captured by satellite products and ground weather radars? *Quarterly Journal of the Royal Meteorological Society*, **2018**, 1–16.
- Wienhoff, Z., H. B. Bluestein, L. J. Wicker, J. C. Snyder, A. Shapiro, C. K. Potvin, J. B. Houser, and D. W. Reif, 2018: Applications of a spatially variable advection correction technique for temporal correction of dual-Doppler analyses of tornadic supercells. *Monthly Weather Review*, **146**, 2949–2971.
- Wilson, K. A., P. L. Heinselman, and C. M. Kuster, 2017: Considerations for phased-array radar data use within the National Weather Service. *Weather and Forecasting*, **32**, 1959–1965.
- Wilson, K. A., P. L. Heinselman, and Z. Kang, 2018: Comparing forecaster eye movements during the warning decision process. *Weather and Forecasting*, **33**, 501–521.

- Witt, A., D. W. Burgess, A. Seimon, J. T. Allen, J. C. Snyder, and H. B. Bluestein, 2018: Rapid-scan radar observations of an Oklahoma tornadic hailstorm producing extremely large hail. *Weather and Forecasting*, **33**, 1263-1282.
- Weber, M. E., J. Y. Cho, and H. G. Thomas, 2017: Command and control for multifunction phased array radar. *IEEE Transactions on Geoscience and Remote Sensing*, **55**, 5899–5912.
- Wulfmeyer V., D. D. Turner, B. Baker, R. Banta, A. Behrendt, T. Bonin, W. A. Brewer, M. Buba, A. Choukulkar, E. Dumas, R. M. Hardesty, T. Heus, D. Lange, T. R. Lee, S. Metzendorf, T. Meyers, R. Newsom, M. Osman, S. Raasch, J. Santanello, C. Senff, F. Späth, T. Wagner, and T. Weckwerth, 2018: A new research approach for observing and characterizing land-atmosphere feedback. *Bulletin of the American Meteorological Society*, **99**, 1639-1667.
- Xu, Q., L. Wei, and K. Nai, 2017: A three-step method for estimating vortex center locations in four-dimensional space from radar observed tornadic mesocyclones. *Journal of Atmospheric and Oceanic Technology*, **34**, 2275–2281.
- Xu, Q., and L. Wei, 2018: Formulations for estimating spatial variations of analysis error variance to improve multiscale and multistep variational data assimilation. *Advances in Meteorology*, **2018**, 1–17.

Appendix E

NOAA COMPETITIVE AWARD RECIPIENT REPORTS

and

NOAA HURRICANE SANDY COMPETITIVE AWARD RECIPIENT REPORTS

*These reports are presented in the format provided by the respective PIs directly to their NOAA Program Managers. **They appear in a separate file to this document.***